R-05-17

Hydrogeochemical evaluation

Preliminary site description Forsmark area – version 1.2

Svensk Kärnbränslehantering AB

March 2005

Svensk Kärnbränslehantering AB
Swedish Nuclear Fuel
and Waste Management Co
Box 5864
SE-102 40 Stockholm Sweden
Tel 08-459 84 00
+46 8 459 84 00
Fax 08-661 57 19
+46 8 661 57 19

ISSN 1402-3091
SKB Rapport R-05-17

Hydrogeochemical evaluation

Preliminary site description
Forsmark area – version 1.2

Svensk Kärnbränslehantering AB

March 2005

Preface

This work forms part of the Initial Site Investigation (ISI) stage of the hydrogeochemical evaluation carried out at the Forsmark site leading to a hydrogeochemical site descriptive model (v. 1.2). SKB's HAG (Hydrogeochemical Analysis Group) personnel consisting of independent consultants and university personnel, carried out the modelling during the period July 2004 to December 2004. Where possible, the INSITE and SIERG review comments on the Forsmark 1.1 version were considered in this work. Several groups within HAG were involved and the evaluation was conducted independently using different approaches ranging from expert knowledge to geochemical and mathematical modelling including also transport modelling. During regular HAG meetings the results were presented and discussed. The HAG members contributing to this report where (in alphabetic order):

Luis Auqué, University of Zaragoza, Appendix#3

María Gimeno, University of Zaragoza, Appendix#3

Javier Gómez, University of Zaragoza, Appendix#3

Ioana Gurban, 3D-Terra, Montreal, Appenix#4

Lotta Hallbeck, Vita vegrandis, Göteborg, Appendix#2

Marcus Laaksoharju, Geopoint AB, Stockholm, Appendix#4

Jorge Molinero, University of Santiago de Compostela, Appendix#5

Juan Raposo, University of Santiago de Compostela, Appendix#5

John Smellie, Conterra AB, Stockholm, Appendix#1

Eva-Lena Tullborg, Terralogica AB, Gråbo, Appendix#1

The different modelling approaches applied on the same data set and the similarities in the results gave added confidence to the modelling results presented in this report.

Marcus Laaksoharju

HAG project leader and editor

Summary

Siting studies for SKB's programme of deep geological disposal of nuclear fuel waste currently involves the investigation of two locations, Forsmark and Laxemar-Simpevarp, on the eastern coast of Sweden to determine their geological, hydrogeochemical and hydrogeological characteristics. Present work completed has resulted in Model version 1.2 which represents the second evaluation of the available Forsmark groundwater analytical data collected up to June, 2004 (i.e. the second "data freeze" of the site). The Hydrochemical Analytical Group (HAG) had access to data where a total of 1,131 water samples had been collected from the surface and sub-surface environment (e.g. soil pipes in the overburden, streams and lakes); 252 samples were collected from drilled boreholes. The deepest fracture groundwater samples with sufficient analytical data reflected depths down to 1 km. Most of the waters sampled (66%) lacked crucial analytical information that restricted the evaluation. Model version 1.2 focuses on geochemical and mixing processes affecting the groundwater composition in the uppermost part of the bedrock, down to repository levels, and eventually extending to 1,000 m depth.

The complex groundwater evolution and patterns at Forsmark are a result of many factors such as: a) the present-day topography and proximity to the Baltic Sea, b) past changes in hydrogeology related to glaciation/deglaciation, land uplift and repeated marine/lake water regressions/ transgressions, and c) organic or inorganic alteration of the groundwater composition caused by microbial processes or water/rock interactions. The sampled groundwaters reflect to various degrees processes relating to modern or ancient water/rock interactions and mixing.

The groundwater flow regimes at Forsmark are considered local and extend down to depths of around 600 m depending on hydraulic conditions. Close to the Baltic Sea coastline where topographical variation is even less, groundwater flow penetration to depth will subsequently be less marked and such areas will tend to be characterised by groundwater discharge.

Four main groundwater types are present. In addition to the recent to young Na-HCO_3 type groundwaters and old Na-Ca Cl(SO_4) type groundwaters (with a Littorina Sea and glacial signature), there exist at greater depths (KFM03A; 645 m) an older meteoric Na-Ca-Cl type groundwater (~ 16 pmC) with a small glacial component ($\delta^{18}O$ = –11.6‰ SMOW; δD = –84.3‰ SMOW). At still greater depth (KFM03A: 990 m) the groundwater changes to a higher saline Ca-Na-Cl type characterised by an even greater glacial signature ($\delta^{18}O$ = –13.6‰ SMOW; δD = –98.5‰ SMOW). Although only one deep sample exists, the A2 gently dipping deformation zone appears to form the boundary between the Na-Ca-Cl and Ca-Na-Cl groundwater types were borehole KFM03A is drilled.

The near-surface Na-HCO_3 groundwaters form a distinctive horizon at the centre of the transect which lenses out towards the SE Baltic Coast where discharge of deeper groundwater probably occurs. From Bolundsfjärden to the NW a less marked horizon is indicated but data are few. In addition, the influence of the deformation zone A2 on the groundwater chemistry is not clear at this near-surface locality.

Bordering the shallow Na-HCO_3 groundwaters, and extending from close to the surface (near the SE coast) to depths of around 500 m (along the gently dipping deformation zone A2), are the Littorina Sea type groundwaters. The upward (discharging) movement of these Littorina Sea type groundwaters below Bolundsfjärden Lake is supported by the soil pipe groundwater sample SFM0023 collected under the lake and showing increased Mg and SO_4. The Bolundsfjärden Lake discharge area may correspond to the intersection of steeply dipping deformation zones further connected to the gently dipping deformation A2 zone.

Most lines of evidence support that the sulphur system, microbiologically mediated, is the main redox controller in the deepest and most saline groundwaters. On the other hand, Littorina-rich brackish groundwaters show variable and very high iron contents, in agreement with what has been observed in similar groundwaters elsewhere. The microbial analyses only found trace amounts of sulphate reducing bacteria (SRB) in these samples, but very high numbers of iron-reducing bacteria (IRB). However, there is no correlation between Fe^{2+} concentration and the number of IRB in these groundwaters. Moreover, they show very low but detectable contents of dissolved S^{2-} and the $\delta^{34}S$

values are very homogeneous (around 25‰) and clearly higher than in the present Baltic Sea, indicating that sulphate reduction has operated. These observations could support the existence of an iron-sulphide precipitation process during the Littorina Sea phase of these groundwaters but not intense enough to effectively limit Fe^{2+} solubility.

A modelling approach was used to simulate the obtained groundwater in the Forsmark area by introducing Littorina Sea water. These results indicate that re-equilibrium reaction processes are important in the control of some parameters such as pH (as well as Eh, and some minor-trace elements), moving the waters towards the adularia-albite boundary. However, the main compositional changes, and even the extent of re-equilibration processes, are controlled by the extent of the mixing process.

Coupled transport modelling was used to model the measured water conservative elements, tritium contents and the water recharge into the granitic bedrock. The simulations indicate that quaternary sediments may play a significant role since most of the infiltrated water could flow through the conductive layers in the sediment to discharge zones, mainly associated with lakes and the Baltic Sea coast line. Based on this hypothesis, the effective recharge into the granitic bedrock is estimated to be less than in other investigated sites such as Simpevarp and Laxemar, where the presence of Quaternary overburden is less important. The hydrogeologic behaviour of the Quaternary overburden in Forsmark provides a plausible explanation for the preservation of Littorina Sea signatures found in several groundwater samples, even at very shallow depths. Other (and complementary) explanations can be related with the flat topography, as well as with the fact that the Forsmark site has emerged over the sea level more recently than other investigated sites.

The modelling indicates also that the groundwater composition at repository depths is such that the representative samples from KFM02A: 509–516 m and KFM03A: 448–453 m can meet the SKB chemical stability criteria for Eh, pH, TDS, DOC and Ca+Mg.

In this evaluation the groundwater flow model has been updated, the salinity distribution, mixing processes and the major reactions altering the groundwaters have been modelled down to a depth of 1,000 m, and an updated Hydrogeochemical site descriptive model version 1.2 has been produced. More groundwater and isotopic data, together with microbial information, colloids and gases, provided additional site descriptive information. Finally, the introduction of coupled modelling provided further possibilities to address independently the various processes in question.

Contents

1 Introduction

1.1 Background

SKB is conducting thorough investigations at two candidate sites for the eventual disposal of spent nuclear fuel. These sites are located in the municipalities of Forsmark and Simpevarp/Laxemar and the main objective is aimed at providing detailed proposals of how a deep repository can be constructed and operated. The investigations at Forsmark commenced in 2002 and will take between four and eight years to complete.

The site selection and investigation phases encompass a sufficiently large scale in terms of time, space and content to make a breakdown into different stages necessary. During the initial selection phase the site that is considered most suitable for a deep repository is chosen. A few boreholes are drilled as part of an Initial Site Investigation (ISI) stage and the data they generate enables a decision to be made as to whether the site is still deemed suitable. The site and its immediate surroundings should cover an area of 5–10 km^2 in areal extent.

Provided that the preconditions established are still good, a Complete Site Investigation (CSI) stage follows. The main aim is to collect sufficient knowledge about the rock and its properties to enable SKB to produce both a site description and a construction plant description, and also to conduct a safety analysis.

The surface/near-surface hydrological and groundwater chemistry studies include charting water courses, measuring the discharge and taking water samples. Drilling is the most extensive activity conducted where some 10–20 percussion boreholes will be made to a maximum depth of 200 m and an equal number of cored boreholes to depths of 500–1,000 m in depth. An extensive hydrochemistry programme together with other investigation programmes will be conducted during and after the drilling work.

1.2 Scope and objectives

The aim of the site modelling is to develop a hydrogeochemical site descriptive model according to the strategy for the development of a hydrogeochemical site descriptive model /Smellie et al. 2002/. The first such model for Forsmark was the “version 0” model /SKB, 2002/ followed by the 1.1 version of Forsmark /Laaksoharju et al. 2004a/.

The model presented in this report is model version 1.2 which represents the second evaluation of the available Forsmark groundwater analytical data collected up to June, 2004 (i.e. the so called “data freeze”). The Hydrochemical Analytical Group (HAG) had access to water samples collected from the surface and sub-surface environment (e.g. soil pipes in the overburden, streams and lakes); together with samples collected from drilled boreholes. The deepest samples from Forsmark reflected conditions down to about 1,000 m. When modelled, many of the samples either lacked important analytical information that restricted their evaluation or the sampling or analytical quality was in question. Model version 1.2 focusses on the processes taking place in the deeper part of the bedrock down to 1,000 m and with a first evaluation of groundwater conditions at the repository level.

The work presented here forms part of the Initial Site Investigation (ISI) stage and the derived model represents the second and final ISI model based on measured data from the site investigation programme. As the investigations progress over the next few years, several updated models (version 2.1 and 2.2 within the CSI program) will be derived based on supplementary analytical data and groundwater samples from new boreholes at Forsmark site and repeated sampling from existing boreholes.

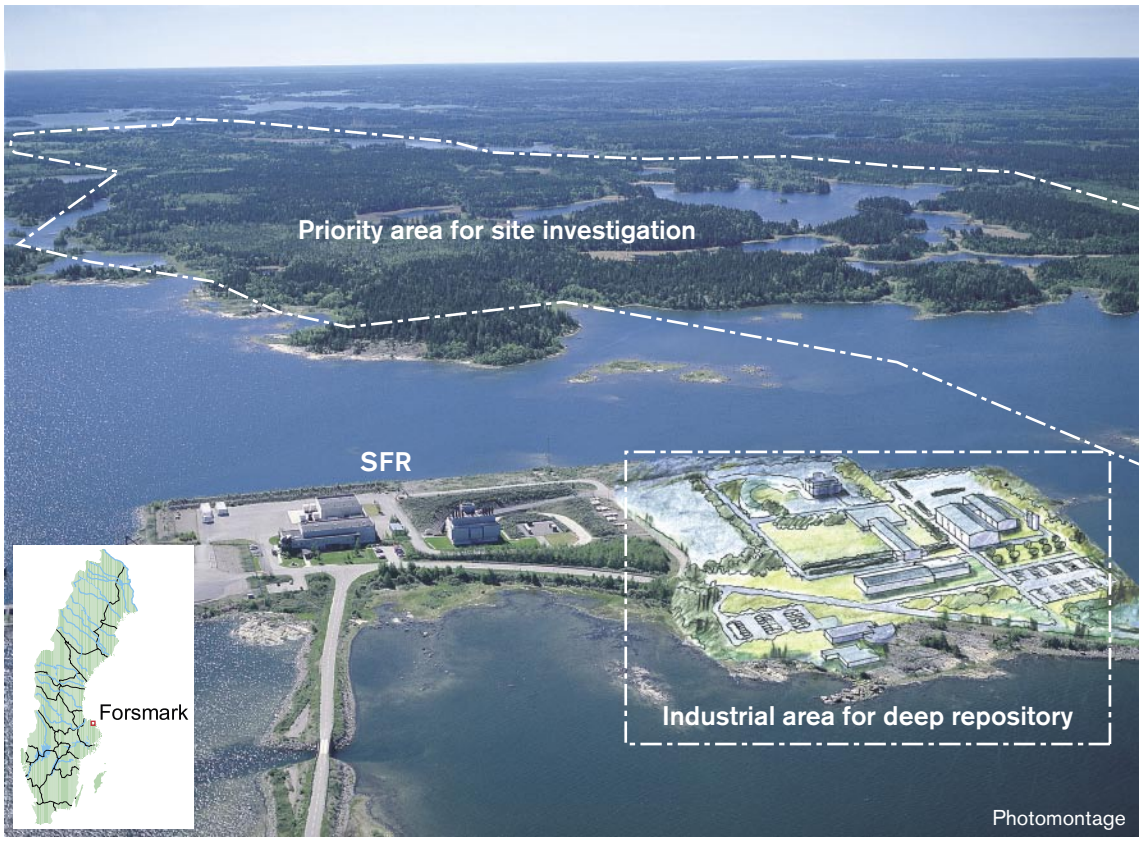

Figure 1-1. *Location and overview of the Forsmark area showing the candidate area for site investigation (dotted area) and the SFR.*

1.3 Setting

The Forsmark site is situated about 150 km north of Stockholm and is located within the confines of the Forsmark nuclear power plant facility. Located in the same area is the world's first underground storage (SFR) for low and medium active radioactive wastes. The facility was constructed by SKB 50 m below the seafloor in crystalline bedrock during 1983–1988, and has a storage capacity of 63,000 m^3. The waste is from the nuclear power plants, from industrial and research applications of radioactive materials and from hospitals. The candidate area selected for the site investigations is located close to SFR and is shown in Figure 1-1 and in Figure 4-2.

1.4 Methodology and organisation of work

1.4.1 Methodology

The main objectives of the hydrogeochemical site descriptive model for the Forsmark site are to describe the chemistry and distribution of the groundwater in the bedrock and overburden and the processes involved in its origin and evolution. The SKB hydrogeochemistry programme /Smellie et al. 2002/ is intended to fulfil two basic requirements: 1) to provide representative and quality assured data for use as input parameter values in calculating long-term repository safety, and 2) to understand the present undisturbed hydrogeochemical conditions and how these conditions will change in the future. Parameter values for safety analysis include pH, Eh, S, SO_4, HCO_3, PO_4 and TDS (mainly cations), together with colloids, fulvic and humic acids, other organics, bacteria and dissolved gases. These values will be used to characterise the groundwater environment at, above and below repository depths. When the hydrogeochemical environment has been fully characterised, this knowledge, together with an understanding of the past and present groundwater evolution,

should provide the basis for predicting future changes. The site investigations will therefore provide important source material for safety analyses and the environmental impact assessment of the Simpevarp area.

1.5 This report

Chapters 1–6 of this report summarise the hydrogeochemical results collated and interpreted by HAG. These results will serve as input for the final site descriptive model report which will integrate collectively the results from all the geoscientific disciplines. The format and structure of this present report follows that established for the final report.

The main aim of this report is to attempt to integrate the different approaches of the HAG groups to arrive at an overall interpretation of the presently available Forsmark hydrogeochemical data. Chapter 2 presents an overview of available information used in the modelling. Chapter 3 describes the present ideas concerning the palaeoevolution of the Forsmark region. Chapter 4 covers the integrated evaluation of the primary hydrogeochemical data and the quantitative modelling covering the different modelling approaches attempted, the assumptions made, an evaluation of the uncertainties involved, and how such modelled results can best be visually presented. Chapter 5 summarises the hydrogeochemical description of the Forsmark area and Chapter 6 presents the main conclusions.

The detailed contributions of the three HAG modelling groups are presented in Appendices 1–5. Appendix 6 lists all the groundwater analytical data available at the ‘data freeze’ point. Appendix 7 lists the Nordic data used as background information for the modelling. Appendix 8 shows how the HAG modelling groups utilised the Forsmark data.

2 Investigations, available data and other prerequisites for the modelling

2.1 Overview

The evaluation of the hydrogeochemical data has been carried out by considering not only the samples from the Forsmark site, but also including data from the nearby boreholes in SFR and other Swedish sites (e.g. Finnsjön, Äspö, Simpevarp and Laxemar) and in some cases also to the whole Fennoscandian hydrochemical dataset. An example of this is selecting the water end members describing other Fennoscandian sites in order to see how well they compare with the general Forsmark trend and whether or not Forsmark can be interpreted as part of the regional hydrogeochemical system. Consequently, information from hydrogeochemical model versions based on previously investigated sites in Sweden and elsewhere, and information from ongoing geological and hydrogeological modelling at Forsmark, where included in the evaluation when possible.

2.1.1 Investigations and primary data aquired up to data freeze 1.1

The dataset available for the 1.1 version consisted in total of 456 water samples /Laaksoharju et al. 2004a/. Samples reflecting the surface/near-surface conditions (precipitation, streams, lakes, sea water and shallow soil pipe waters) comprised a total of 422 samples. Of the remainder, 21 samples were from percussion drilled boreholes and 13 samples from core drilled boreholes; some of these borehole samples represented repeated sampling from the same isolated location. In conclusion, there was a heavy bias at this stage in the site characterisation of water samples from the surface and near-surface environments. Consequently, hydrochemical evaluation at greater depths was restricted to only a few borehole sampling points which did not achieve expected repository levels.

In the total dataset only 112 surface samples, 5 percussion borehole samples and 2 core-drilled samples were at the time of the “data freeze” analysed for all the major elements, stable isotopes and tritium. This meant that 26% of the samples could be used for more detailed evaluation concerning the origin of the water.

2.1.2 Data freeze 1.2 – investigations performed and data acuired

In Table 2-1 the Forsmark data collected for the data freeze 1.2 are listed. Data used for comparison from the Swedish sites including the Nordic sites are listed in Appendix 7.

Table 2-1. Samples included in the Forsmark data freeze 1.2.

Type of Water	Type of sampling	ID code	Dates	Depths	Number of Samples Total (Data Freeze 1.2)	With Major Elements (ME)	With ME & Stable isotopes	With ME & Stable isotopes	Repre-sentative
Ground Water	Packered	HFM01	2002	0-200	22 (1M)	4	2	2	1
		HFM02	2002	0-100	2	2	0	0	1
		HFM03	2002	0-26	2	1	1	1	1
		HFM04	2002	30-222	3	3	3	3	1
		HFM05	2002,03	0-200	8 (1M)	7	7	7	1
		HFM06	2003	0-111	4	4	4	4	1
		HFM08	2003	0-144	3	3	3	3	2
		HFM09	2003,04	0-50	4	4	2	2	1
		HFM10	2003,04	0-150	7 (1M)	5	4	4	1
		HFM11	2003	0-182	3	3	3	3	1
		HFM12	2003	0-210	3	3	3	3	1
		HFM13	2003,04	0-176	5	3	3	3	1
		HFM14	2003	0-151	3	3	3	3	1
		HFM15	2003	0-200	3	3	3	3	1
		HFM16	2003	0-133	3	3	1	1	1
		HFM17	2004	0-203	3	3	1	1	1
		HFM18	2004	0-173	3	3	1	1	1
		HFM19	2004	0-173	3	3	1	1	1
	Packered		2002	0-101	1	0	0	0	0
			2003	110-121	8 (1M,1C)	7	6	6	1
		KFM01A	2003	177-184	10 (1G,1C)	9	9	9	1
	Packered		2003	1-100	1	1	0	0	0
			2002	18-100	2	2	2	2	1
			2003	107-127	3	3	3	3	1
			2003	105-159	1	1	0	0	0
			2003	250-291	1	1	0	0	0
			2003	249-396	1	1	0	0	0
			2003	417-426	3	0	0	0	0
			2004	414-434	3	2	2	2	1
			2003	505-520	28	0	0	0	0
			2003	509-516	16 (2G,1M,1C)	11	3	3	1
	Tube	KFM02	2003	100-1000	16	8	0	0	0
	Packered	KFM03	2003	347-394	1	0	0	0	0
			2003	386-391	4	4	3	3	1
			2003,04	488-456	4 (1G,1M,1C)	4	2	2	1
			2004	639-646	6 (1G,1M,1C)	5	5	5	1
			2004	940-947	8 (1G,1M,1C)	7	0	0	0
			2003	980-1001	8 (1G,1M,1C)	8	8	8	1
	Tube		2003	0-996	17	9	5	5	0
			2004	231-238	7	6	6	6	1
	Packered		2004	354-361	4	0	0	0	1
	Tube	KFM04	2003	0-995	17	9	3	3	0

Type of Water	Type of sampling	ID code	Dates	Depths	Number of Samples Total (Data Freeze 1.2)	With Major Elements (ME)	With ME & Stable isotopes	With ME & Stable isotopes	Repre-sentative
Shallow Ground-water	Private Wells	PFM***	2003		9	9	9	9	6
	Soil Pipes	SFM0001	2002,03,04	05-apr	8	7	7	7	1
		SFM0002	2002,03,04	05-apr	8	7	7	7	1
		SFM0003	2002,03,04	11-sep	8	7	7	7	1
		SFM0005	2002,03,04	02-jan	6	3	3	3	1
		SFM0006	2003,04	04-mar	5	3	3	3	1
		SFM0007	2003		1	0	0	0	0
		SFM0008	2003,04	06-maj	5	4	4	4	1
		SFM0009	2003,04	03-feb	5	5	4	4	1
		SFM0010	2003	02-jan	1	0	0	0	0
		SFM0011	2003	04-mar	1	1	1	1	0
		SFM0012	2003,04	05-apr	6	6	5	5	1
		SFM0013	2003	05-apr	1	1	1	1	1
		SFM0014	2003	02-jan	1	1	1	1	0
		SFM0015	2003,04	07-jun	6	5	5	5	1
		SFM0016	2003	08-jul	1	1	1	1	0
		SFM0017	2003	04-mar	1	1	1	1	0
		SFM0018	2003	05-apr	1	1	1	1	0
		SFM0019	2003	04-mar	1	1	1	1	0
		SFM0020	2003	03-feb	1	1	1	1	0
		SFM0021	2003	02-jan	0	0	0	0	0
		SFM0023	2003,04	04-mar	5	4	4	4	1
		SFM0024	2003	02-feb	3	3	3	3	1
		SFM0025	2003,04	06-maj	5	4	4	4	0
		SFM0026	2003	15-16	1	1	1	1	0
		SFM0027	2003,04	07-jun	5	4	4	4	1
		SFM0028	2003	07-jun	1	1	1	1	0
		SFM0029	2003,04	07-jun	4	3	3	3	1
		SFM0030	2003	04-mar	1	1	1	1	0
		SFM0031	2003,04	04-mar	4	4	3	3	1
		SFM0032	2003,04	03-feb	5	4	4	4	1
		SFM0034	2003	02-jan	1	1	1	1	0
		SFM0035	2003,04	02-jan	3	0	0	0	0
		SFM0036	2003	02-jan	1	1	1	1	0
		SFM0037	2003,04	02-jan	4	3	3	3	1
		SFM0049	2003	04-mar	1	1	1	1	0
		SFM0051	2003,04		4	3	3	3	1
		SFM0053	2003,04		4	3	3	3	1
		SFM0056	2003,04		4	3	3	3	1
		SFM0057	2003,04		4	3	2	2	1
		SFM0060	2004		1	1	1	1	1
		SFM0074	2004		7	0	0	0	0

Type of Water	Type of sampling	ID code	Dates	Depths	Number of Samples Total (Data Freeze 1.2)	With Major Elements (ME)	With ME & Stable isotopes	With ME & Stable isotopes	Repre-sentative
Sea Water		PFM000062	2002,03,04		45	43	10	10	9
		PFM000063	2002,03,04		56	55	13	13	10
		PFM000064	2002,03,04		51	50	11	11	0
		PFM000065	2002,03,04		31	31	9	8	0
		PFM000082	2002,03,04		17	17	4	4	0
		PFM000083	2002,03		7	7	2	2	0
		PFM000084	2002,03		9	9	2	2	0
		PFM000153	2002		2	2	0	0	0
Running Water		PFM000066	2002,03,04		29	28	8	8	8
		PFM000067	2002,03,04		39	38	11	9	9
		PFM000068	2002,03,04		36	35	9	9	9
		PFM000069	2002,03,04		36	36	6	6	6
		PFM000070	2002,03,04		30	29	9	7	7
		PFM000071	2002,03,04		27	26	4	3	3
		PFM000072	2002,03,04		34	33	9	9	9
		PFM000073	2002,03,04		18	18	3	3	3
Lake Water		PFM000074	2002,03,04		30	30	9	8	8
		PFM000086	2002		1	1	0	0	0
		PFM000087	2002,03,04		57	57	15	15	13
		PFM000097	2002,03,04		31	31	8	7	7
		PFM000107	2002,03,04		53	51	12	12	12
		PFM000117	2002,03,04		54	53	14	12	9
		PFM000127	2002,03		23	23	6	6	5
		PFM000135	2002,03,04		10	10	2	2	2
		PFM000151	2002		4	3	1	1	0
Precipitation		PFM002457	2002,03		5	4	4	4	0
Groundwaters		*Deep GW*	Percussion B.		84	60	45	45	19
			Cored B.	Packered	118	77	49	49	12
				Tube	50	26	8	8	0
		Shallow GW			144	112	108	108	22
Total Groundwaters					396	275	210	210	53
Surface waters		Sea Water			218	214	51	50	19
		Running Water			249	243	59	54	54
		Lake Water			263	236	67	63	56
		Precipitation			5	4	4	4	0
Total Surface waters					735	697	181	171	129
TOTAL					1131	972	391	381	182

* (G) sample with dissolved gasses.

* (M) sample with microbial analysis.

* (C) sample with colloids.

2.2 Geographical data

The co-ordinates used and made available for the data freeze are listed in Appendix 6. These data were used in the visualisation work.

2.3 Surface investigations

Available QA data describing the composition of the surface water sampled from lakes, streams, Baltic Sea and soil pipes are listed in Appendix 7.

2.4 Borehole investigations

Available QA data describing the composition of the groundwater sampled from percussion and core drilled boreholes are listed in Appendix 6.

2.5 Other data sources

Available QA data from the SICADA database of groundwater conditions at nearby locations such as SFR and other Swedish sites including data from Finland /e.g. Pitkänen et al. 1999/, were used as background information in the modelling exercises (cf. Appendix 7).

2.6 Databases

The use of the data in the different modelling work is listed in Appendix 8.

2.7 Model volumes

2.7.1 Regional model volume

The regional model area (Figure 2-1) forms an area 15 km long and 11 km wide (165 km²) extending in a NE-SW direction. Around 100 km², or 60% of the area, is covered by the Baltic Sea. This regional model area is considered to capture both the upstream and downstream hydrogeological conditions. A geological description of the Forsmark site can be found in Appendix 1.

2.7.2 Local model volume

The local model area and the candidate area for site investigation are shown in Figure 2-1. The motivation for selection of the local model area is described by /Andersson et al. 2002/.

2.7.3 Model areas

For the model 1.2 work the focus was on data from the Forsmark site but data from other Swedish and Nordic sites were also included in the comparison and evaluation.

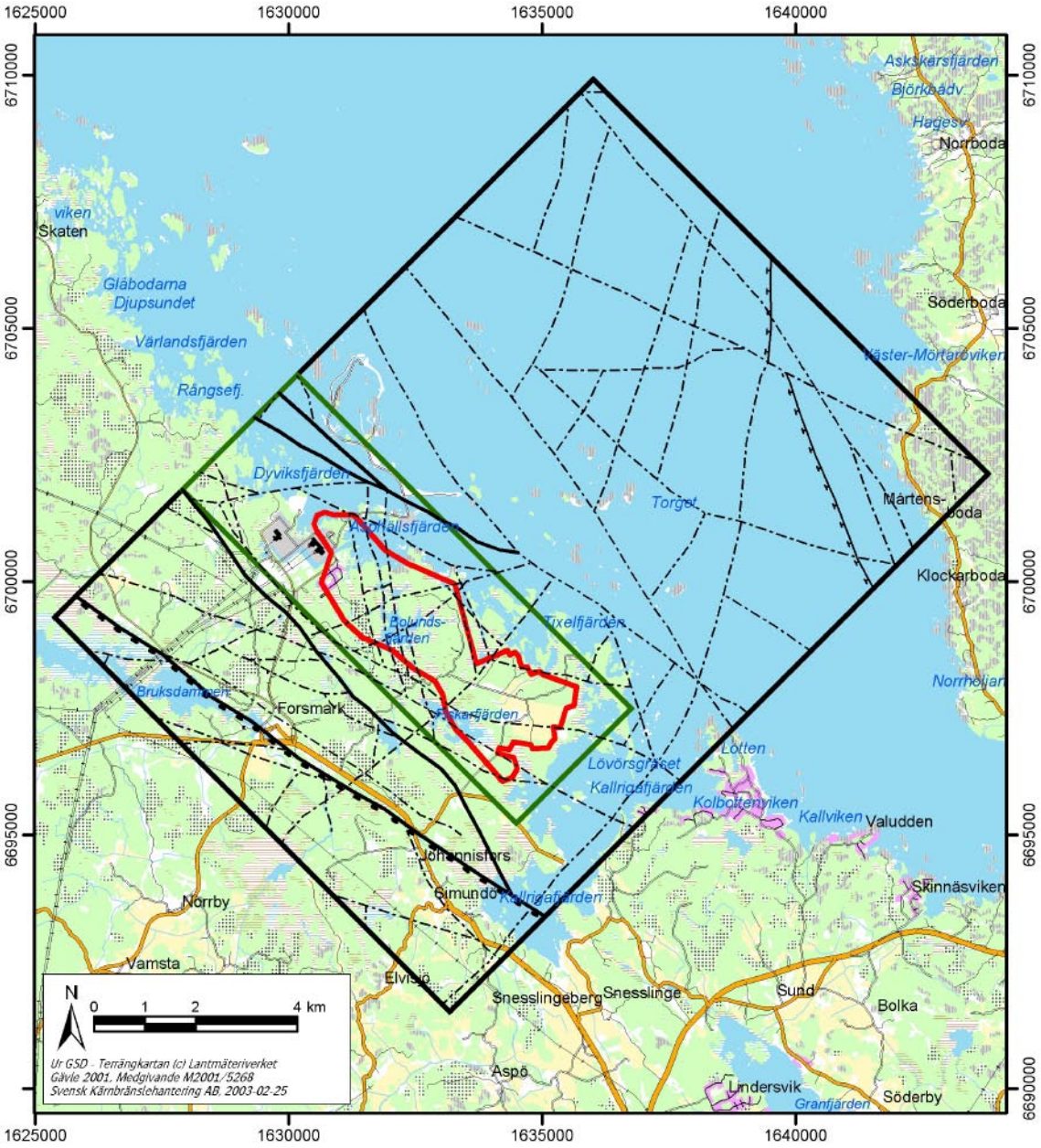

Figure 2-1. *Diagram showing the Forsmark regional model area (in black), the local model area (in green) and the candidate area for site investigations (in red).*

3 Evolutionary aspects of the Forsmark site

3.1 Premises for surface and groundwater evolution

The first step in the groundwater evaluation is to construct a conceptual postglacial scenario model for the site (Figure 3-1) based largely on known palaeohydrogeological events from Quaternary geological investigations. This model can be helpful when evaluating data since it provides constraints on the possible groundwater types that may occur. Interpretation of the glacial/postglacial events that might have affected the Forsmark site is based on information from various sources including /Fredén, 2002; Påsse, 2001; Westman et al. 1999; SKB, 2002; Hedenström and Risberg, 2003/. This recent literature provides background information which is combined with more than 10 years of studies of groundwater chemical and isotopic information from sites in Sweden and Finland in combination with various hydrogeological modelling exercises of the postglacial hydrogeological events /Laaksoharju and Wallin, 1997; Pitkänen et al. 1998; Svensson, 1996/. The presented model is therefore based on Quaternary geology, fracture mineralogical investigations and groundwater observations. These facts have been used to describe possible palaeo events that may have affected the groundwater composition in the bedrock.

3.1.1 Development of permafrost and saline water

When the continental ice sheet was formed at about 100,000 BP permafrost formation ahead of the advancing ice sheet probably extended to depths of several hundred metres. According to /Bein and Arad, 1992/ the formation of permafrost in a brackish lake or sea environment (e.g. similar to the Baltic Sea) produced a layer of highly concentrated salinity ahead of the advancing freezing front. Since this saline water would be of high density, it would subsequently sink to lower depths and potentially penetrate into the bedrock where it would eventually mix with formational groundwaters of similar density. Where the bedrock was not covered by brackish lake or sea water similar freeze-out processes would occur on a smaller scale within the hydraulically active fractures and fracture zones, again resulting in formation of a higher density saline component which would gradually sink and eventually mix with existing saline groundwaters. Whether the volume of high salinity water produced from brackish waters by this freeze-out process would be adequate to produce such widespread effects is presently under debate.

With continued evolution and movement of the ice sheet, areas previously subject to permafrost would be eventually covered by ice accompanied by a rise in temperature at the base of the ice sheet and slow decay of the underlying permafrost layer. Hydrogeochemically, this decay may have resulted in distinctive signatures being imparted to the groundwater and fracture minerals.

3.1.2 Deglaciation and flushing by meltwater

During subsequent melting and retreat of the ice sheet the following sequence of events is thought to have influenced the Forsmark site (see, Figure 3-1).

When the continental ice melted and retreated, glacial meltwater was hydraulically injected under considerable head pressure into the bedrock (> 11,500 BP) close to the ice margin. The exact penetration depth is still unknown, but depths exceeding several hundred metres are possible according to hydrodynamic modelling /e.g. Svensson, 1996/. Some of the permafrost decay groundwater signatures may have been disturbed or destroyed during this stage.

Different non-saline and brackish lake/sea stages then transgressed the Forsmark site during the period ca. 11,000–500 BP. Of these, two periods with brackish water can be recognised; Yoldia Sea (11,500 to 10,800 BP) and Littorina Sea (9,500–2,000 BP (continuing to the present)), with Baltic Sea from 2,000 to the present. The Yoldia period has probably resulted in only minor contributions to the subsurface groundwater since the water was very dilute to brackish in type from the large volumes of glacial meltwater it contained. Furthermore this period lasted only for 700 years. The Littorina Sea period in contrast had a salinity maximum of about twice the present Baltic Sea and this maximum prevailed at least from 6,500 to 5,000 BP; during the last 2,000 years the salinity

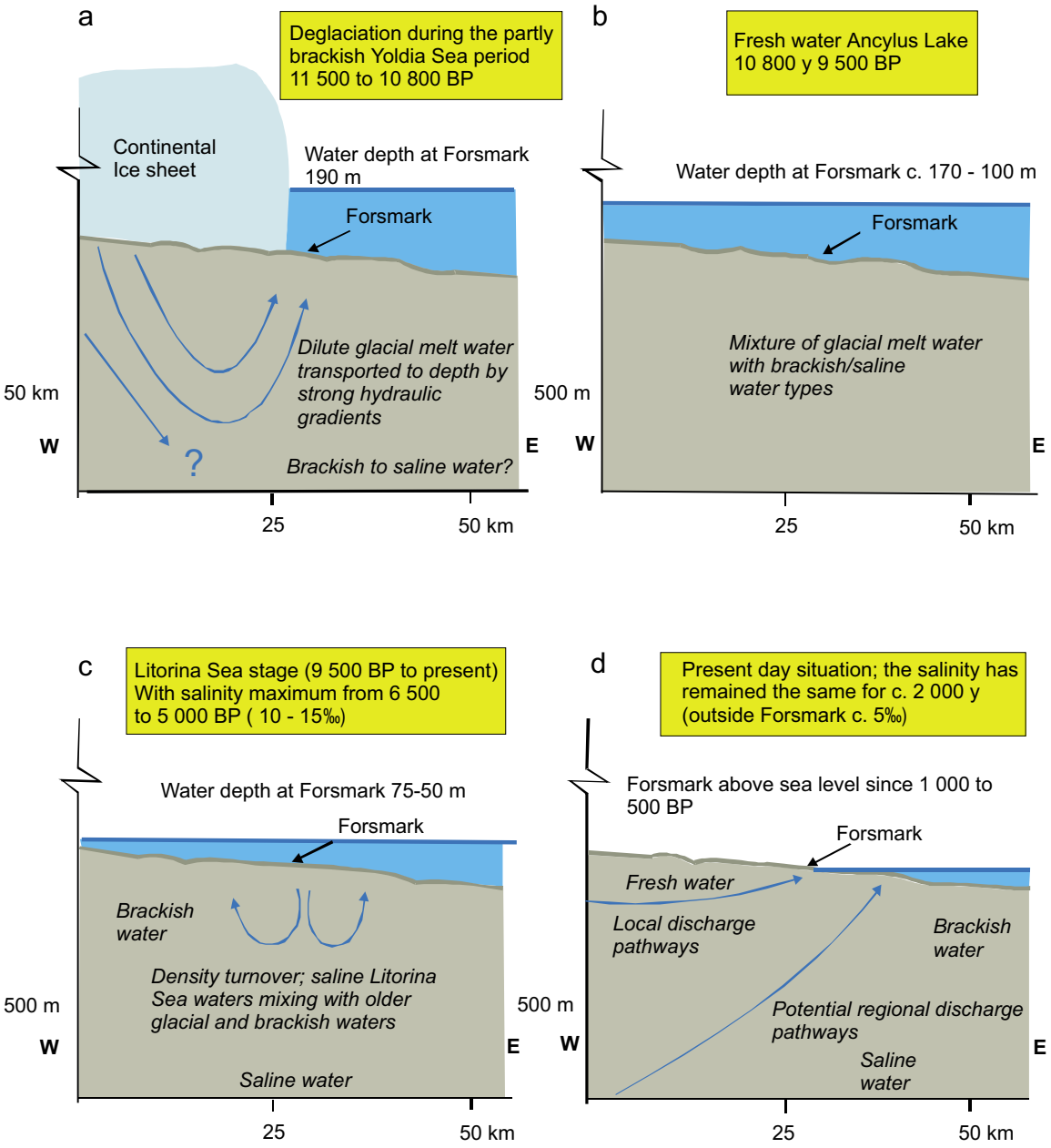

Figure 3-1. *Conceptual postglacial scenario model for the Forsmark area. The figures show possible flow lines, density driven turnover events and non-saline, brackish and saline water interfaces. Possible relation to different known postglacial stages such as land uplift which may have affected the hydrochemical evolution of the site is shown: a) deglaciation of the continental ice, b) Ancylus Lake stage, c) Littorina Sea stage, and d) present day Baltic Sea stage. From this conceptual model it is expected that glacial meltwater and deep and marine water of various salinities have affected the present groundwater. (Based on the shoreline displacement curve compiled by /Påsse, 2001/ and information from /Fredén, 2002; Westman et al. 1999; SKB, 2002; Hedenström and Risberg, 2003/).*

has remained almost equal to the present Baltic Sea values (/Westman et al. 1999/ and references therein). Dense brackish seawater such as the Littorina Sea water was able to penetrate the bedrock resulting in a density turnover which affected the groundwater in the more conductive parts of the bedrock. The density of the intruding seawater in relation to the density of the groundwater determined the final penetration depth. As the Littorina Sea stage contained the most saline groundwater, it is assumed to have had the deepest penetration depth eventually mixing with the glacial /brine groundwater mixtures already present in the bedrock.

When the Forsmark region was subsequently raised above sea level 1,000 to 500 years ago, fresh meteoric recharge water formed a lens on top of the saline water because of its low density. As the present topography of the Forsmark area is flat and the time elapsed since the area was raised above sea level is short, the out flushing of saline water has been limited and the freshwater lens remains at shallow depths (from the surface down to 25–100 m depending on hydraulic conditions).

Many of the natural events described above may be repeated during the lifespan of a repository (thousands to hundreds of thousands of years). As a result of the described sequence of events, brine, glacial, marine and meteoric waters are expected to be mixed in a complex manner at various levels in the bedrock, depending on the hydraulic character of the fracture zones, groundwater density variations and borehole activities prior to groundwater sampling. For the modelling exercise which is based on the conceptual model of the site, groundwater end-members reflecting, for example, Glacial meltwater and Littorina Sea water composition, were added to the data set (cf. Appendix 4).

The uncertainty of the updated conceptual model increases with modelled time. The largest uncertainties are therefore associated with the stage showing the flushing of glacial melt water. The driving mechanism behind the flow lines in Figure 3-1 is the shore level displacement due to the land uplift.

4 Bedrock hydrogeochemistry

The data evaluation and modelling becomes a complex and time-consuming process when the information has to be decoded. Manual evaluation, expert judgment and mathematical modelling must be combined when evaluating groundwater information. The methodology applied in this report is described in detail by /Smellie et al. 2002/. The outcome of the hydrogeochemical modelling is used in e.g. in the hydrogeological modelling, transport modelling and safety assessment modelling. The results of the detailed hydrogeochemical modelling are used to produce a hydrogeochemical site descriptive model.

4.1 State of knowledge at previous model version

The first model of the Forsmark area was the site descriptive hydrogeochemical model version 0 /SKB, 2002/. Although there were few data from the Forsmark area to support a detailed hydrogeochemical site descriptive model, postglacial events believed to have affected the groundwater evolution and chemistry at Forsmark were described in a conceptual model.

The model version 1.1 /Laaksoharju et al. 2004a/ represented the first evaluation of the available Forsmark groundwater analytical data. The complex groundwater evolution and patterns at Forsmark were modelled to be a result of many factors such as: a) the flat topography and proximity to the Baltic Sea, b) past changes in hydrogeology related to glaciation/deglaciation and land uplift associated with repeated marine/lake water regressions/transgressions, and c) organic or inorganic alteration of the groundwater composition caused by microbial processes or water/rock interactions. The sampled groundwaters reflected various degrees of modern or ancient water/rock interactions and mixing processes.

Based on the general geochemical character and the apparent age two major water types were identified in Forsmark: fresh-meteoric waters with a bicarbonate imprint and low residence times (tritium values above detection limit), and brackish-marine waters with Cl contents up to 6,000 mg/L and longer residence times (tritium values below detection limit). The meteoric water was found at the surface and at shallow depths and the marine water was found closer to the coast and at depths affected by Baltic Sea water and probably old Littorina Sea water (see Figure 4-1).

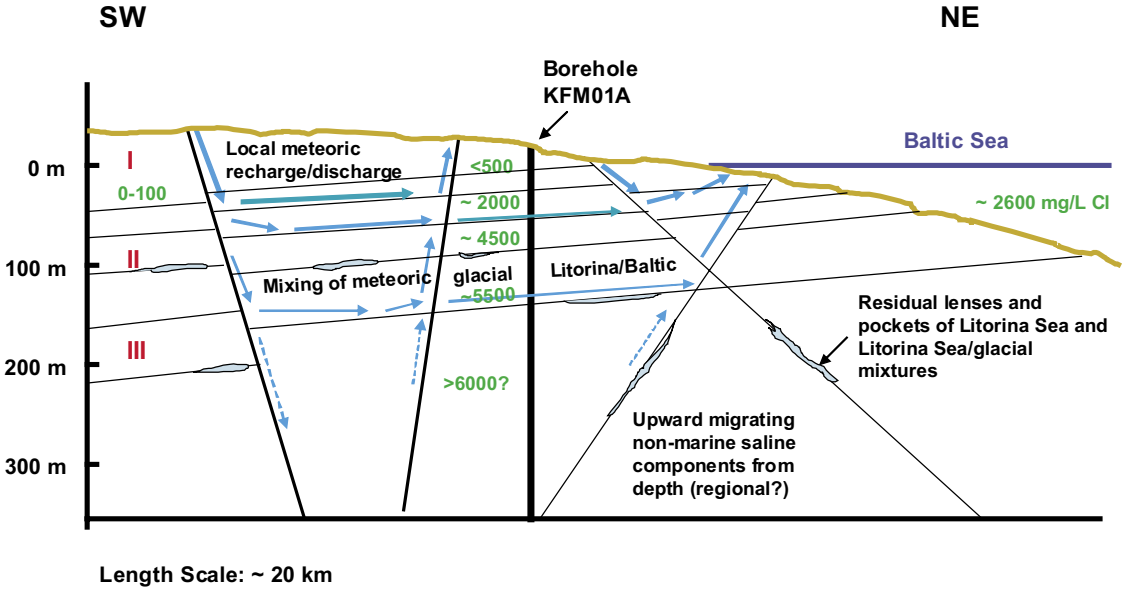

Figure 4-1. *Conceptual model version 1.1 of the Forsmark area /Laaksoharju et al. 2004a/.*

The 1.1 model version knowledge of the reactive system was that the main water-rock interaction processes influencing the chemistry in the fresh meteoric waters were: 1) decomposition of organic matter, 2) calcite, plagioclase, biotite and sulphide dissolution, 3) Na-Ca ion exchange, and 4) phyllosilicate precipitation (probably extremely slow in the present environment). For the brackish–saline groundwaters in contrast, the water/rock interaction processes seemed to be less important although this was not established because of a lack of data. Multiple end-member mixing between especially marine water, glacial meltwater and a deeper saline water was believed to play a significant role.

4.2 Evaluation of primary data

This section describes the evaluation of the primary hydrogeochemical data. Most of these data are from waters sampled at various surface locations and groundwaters in a few boreholes. The evaluation essentially aims at identifying representative datasets which are used for further analysis and eventually providing a first conceptualisation of the origin and evolution of the Forsmark groundwaters.

4.2.1 Hydrogeochemical data evaluation

The Forsmark hydrogeochemical data used in Model v. 1.2 are listed in Appendix 6. Data from other Fennoscandian sites such as Simpevarp, Finnsjön, SFR and Olkiluoto were compiled in the 'Nordic Table' and these data also have been evaluated with respect to properties and representativeness (cf. Appendix 7).

The Forsmark 1.2 dataset consists of 1,131 water samples. Samples reflecting surface conditions (precipitation, streams, lakes and sea water) comprise a total of 735 samples. Of the remaining 396 samples, 84 samples are from percussion-drilled boreholes, 168 from core-drilled boreholes and 144 from shallow soil pipes; some of these borehole samples represent repeated sampling from the same isolated packed-off location or samples from open boreholes (50 tube samples).

From the total dataset only 171 surface water samples and 210 groundwater samples were analysed for all major elements, stable isotopes and tritium at the time of the Data Freeze 1.2. There are some samples with additional information, mainly on colloids, dissolved gases and microbes, which are also listed in Appendix 6. This means that 33.7% of the samples could be used for a detailed evaluation concerning the origin of the waters. The other samples are not necessary rejected from the modelling exercise and are used for background and comparison purposes and may play an important role in the understanding of the variability of the samples.

The detailed representativity check of the samples (Appendix 1) show that only 182 out of 381 samples with complete chemical data have been considered representative. The representative data are labelled in Appendix 6. How this dataset has been used in the different models is listed in Appendix 8.

Analysed data include the same set of parameters as in the previous stages (cf. Appendix 6). The pH and electrical conductivity values used in the evaluation were those determined in the laboratory. There are no data for Eh and temperature for the surface waters but data do exist from some continuous logging of Eh, pH and temperature from several boreholes at different depths. The selected Eh, pH and temperature values are included in the table of the chemical analysis.

Groundwater chemistry data sampled in boreholes

The main focus of this Forsmark v.1.2 evaluation is on boreholes KFM01A, KFM02A, KFM03A and KFM04A systematically drilled to provide a good coverage of the geology and hydrogeology of the candidate site. The borehole sampling locations are shown in Figure 4-2. Of the percussion boreholes indicated, borehole HFM01 supplied flushing water to the drilling of borehole KFM01A, HFM05 for borehole KFM02A, HFM06 for borehole KFM03A, and HFM10 for borehole KFM04A. The remaining percussion boreholes were used mainly for hydraulic (e.g. groundwater flow monitoring) and hydrochemical information and structural (e.g. lineaments; fracture zones) confirmation and identification.

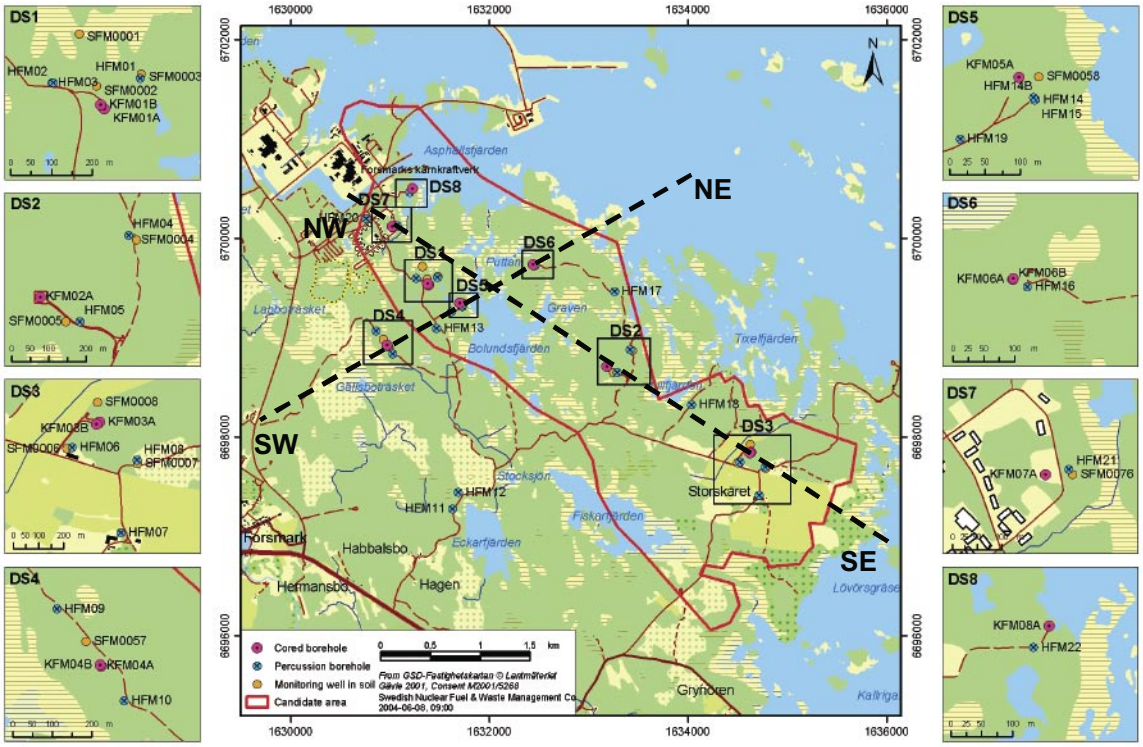

Figure 4-2. *The groundwater sampling locations at Forsmark. The dotted lines indicate the orientation of the cutting planes (NW-SE and NE-SW) used for the visualisations.*

The sampling and analytical data have been reported for the groundwaters by /Nilsson et al. 2003; Nilsson, 2003a,b; Berg and Nilsson, 2004/ and draft versions of P-reports (Nilsson, pers. comm. 2004) were available at the time for the data freeze. The analytical programme included: major cations and anions (Na, K, Ca, Mg, Si, Cl, HCO_3^- SO_4^{2-}, S^{2-}), trace elements (Br, F, Fe, Mn, Li, Sr, DOC, N, PO_4^{3-}, U, Th, Sc, Rb, In, Cs, Ba, Tl, Y and REEs) and stable (^{18}O, ^{2}H, ^{13}C, ^{37}Cl, ^{10}B, ^{34}S) and radioactive-radiogenic (^{3}H, ^{226}Ra, ^{228}Ra, ^{222}Rn, ^{238}U, ^{235}U, ^{234}U, ^{232}Th, ^{230}Th and ^{228}Th) isotopes, microbes, gases and colloids. (cf. Appendix 6).

The different analytical results obtained using contrasting analytical techniques for Fe and S have been confirmed with speciation-solubility calculations and checking their effects on the charge balance. The values selected for modelling were those obtained by ion chromatography (SO_4^{2-}) and spectrophotometry (Fe) assuming no colloidal contribution. The selected pH and Eh values correspond to available downhole data (cf. Appendix 6).

Representativeness of the data

By definition, a high quality sample is considered to be that which best reflects the undisturbed hydrological and geochemical in-situ conditions for the sampled section. A low quality sample may contain in-situ, on-line, at-line, on-site or off-site errors such as contamination from tubes of varying compositions, air contamination, losses or uptake of CO_2, long storage times prior to analysis, analytical errors etc. The quality may also be influenced by the rationale in locating the borehole and selecting the sampling points. Some errors are easily avoided, others are difficult or impossible to avoid. Furthermore, chemical responses to these influences are sometimes, but not always, apparent.

Forsmark site

The Forsmark groundwater analytical data compiled in the SICADA database, which form the basis to the hydrochemical evaluation, will have already undergone an initial screening process by field and laboratory personnel based on sampling, sample preparation and analytical criteria. The next stage in the hydrogeochemical site descriptive process, the focus of this report, is to assess these screened data in more detail to derive a standard set of representative groundwater data for hydrogeochemical modelling purposes.

For this assessment the initial most important stage is to check for groundwater contamination. To accomplish this stage an intimate knowledge of the borehole site is required which entails borehole geology and hydrogeology and a detailed log of borehole activities. These latter activities are a major source of groundwater contamination and include:

- drilling and borehole cleaning,
- open hole effects,
- downhole geophysical/geochemical logging,
- downhole hydraulic logging/testing/pumping, and
- downhole sampling of groundwaters.

In Appendix 1 in this report these potential sources of contamination have been addressed and documented systematically for each borehole drilled and for each borehole section sampled. The degree of contamination has been judged, for example, by plotting tritium against percentage drilling water and using measured values with specifically defined limits, i.e. charge balance (±5%) and drilling water component (< 1%), and supported qualitatively by expert judgement based on detailed studies of the distribution and behaviour of the major ions and isotopes. The final selection of data which best represents the sampled borehole section is based on identifying as near as possible a complete set of major ion and isotope (particularly tritium, ^{18}O and deuterium) analytical data. This is not always the case, however, and a degree of flexibility is necessary in order to achieve an adequate dataset to work with. For example:

A charge balance of ±5% was considered acceptable. In some cases groundwaters exceeding this range were chosen to provide a more representative selection of groundwaters. These groundwaters should therefore be treated with some caution when used in the modelling exercises.

In many cases the drilling water content was either not recorded or not measured. Less than 1% drilling water was considered acceptable. In some cases groundwaters were chosen when exceeding this range to provide a more representative selection of groundwaters. These groundwaters also should be treated with some caution when used in the modelling exercises.

Some of the older tritium data were analysed with a higher detection limit of 8 TU; the detection limit lies around 0.02 TU for recent analyses. For some groundwaters an approximate tritium value is suggested where no recorded value is available. This value is selected normally from the same borehole section but representing an earlier or later sample.

Resulting from this assessment, two groundwater sample types are highlighted in the Appendix 6: one type considered representative, the other type less representative but suitable when used with caution.

The drilling event is considered to be the major source for contamination of the formation groundwater. During drilling large hydraulic pressure differences can occur due to uplifting/ lowering of the equipment, pumping and injection of drilling fluids. These events can facilitate unwanted mixing and contamination of the groundwater in the fractures, or the cutting at the drilling head itself can change the hydraulic properties of the borehole fractures. It is therefore of major importance to analyse the drilling events in detail. From this information not only the uranine spiked drilling water can be traced, but also the major risk of contamination and disturbances from foreign water volumes can be directly identified. Insufficient or excessive extraction of water from a fracture zone prior to sampling can be calculated by applying the DIS (Drilling Impact Study) modelling /Gurban and Laaksoharju, 2002/.

A hydraulically active fracture zone in one isolated section in borehole KFM02A: 509–516 m was the subject of the DIS modelling. The modelling carried out for this fracture zone was based on the DIFF (differential flow meter logging) measurements and the main aim was to model the amount of the contamination for this particular fracture zone (cf. Appendix 4). The result from the sampling shows 22% remaining drilling water in the first chemical sample after pumping a volume of 3.8 m^3, and 6% remaining drilling water in the last sample after pumping an additional 205 m^3. The duration of the pumping, with some interruptions, was approximately 130 days. The amount of drilling water

removed is approximately 22 m^3. The DIS calculations show that pumping should have continued further in order to remove the additional 12.6 m^3. The study identified that there are uncertainties in the dosing and control of the uranine during the drilling process.

One fundamental question in modelling is whether the uncertainties lead to a risk of misunderstanding the information in the data. Generally the uncertainties from the analytical measurements are lower than the uncertainties caused by the modelling but the variability during sampling is generally higher than the model uncertainties.

Nordic sites

The Nordic sites, in addition to Forsmark, comprise Laxemar and Simpevarp and all remaining Swedish sites studied over the last 20–25 years; Olkiluoto in Finland is also included (for more information see, Appendix 1). Most of these sites have undergone earlier detailed assessments as to groundwater quality and representativeness, e.g. Gideå, Kamlunge, Klipperås, Fjällveden, Svartboberget, Finnsjön /Smellie et al. 1985, 1987; Smellie and Wikberg, 1989/, Lansjärv /Bäckblom and Stanfors, 1989/ and Olkiluoto /Pitkänen et al. 1999, 2004/. Based on this information the Nordic Table has been highlighted with respect to representative and less representative groundwater samples (Appendix 7) The 'less' representative groundwaters do not meet all of the criteria for representativeness but are sufficiently important to be included. The importance of early or 'First Strike' samples is emphasised in the evaluation discussed in Appendix 1 and listed in Appendix 7. These are coloured green in the Nordic Table and involve one or more of the following deviations from being considered 'representative':

- lack of important ions – especially Br,
- lack of ^{18}O and deuterium data,
- variation in salinity during the time-series measurements, and
- few or an absence of time-series measurements.

The representative groundwaters are highlighted in the Nordic Table in orange (Appendix 7).

Explorative analysis

A commonly used approach in groundwater modelling is to start the evaluation by explorative analysis of different groundwater variables and properties. The degree of mixing, the type of reactions and the origin and evolution of the groundwater can be indicated by applying such analyses. Also of major importance is to relate, as much as possible, the groundwaters sampled to the near-vicinity geology and hydrogeology.

Borehole properties

Figure 4-3, Figure 4-4, Figure 4-5 and Figure 4-6 show a schematic representation of boreholes KFM01A, KFM02, KFM03A and KFM04A and the intercepted structures and their hydraulic conductivities; groundwater sampling locations are indicated and the sampled chloride contents are shown. The results from drillcore mapping, BIPS measurements, differential flow measurements and electric conductivities, together with groundwater quality and representativeness of the samples, are discussed in detail for all investigated boreholes in Appendix 1.

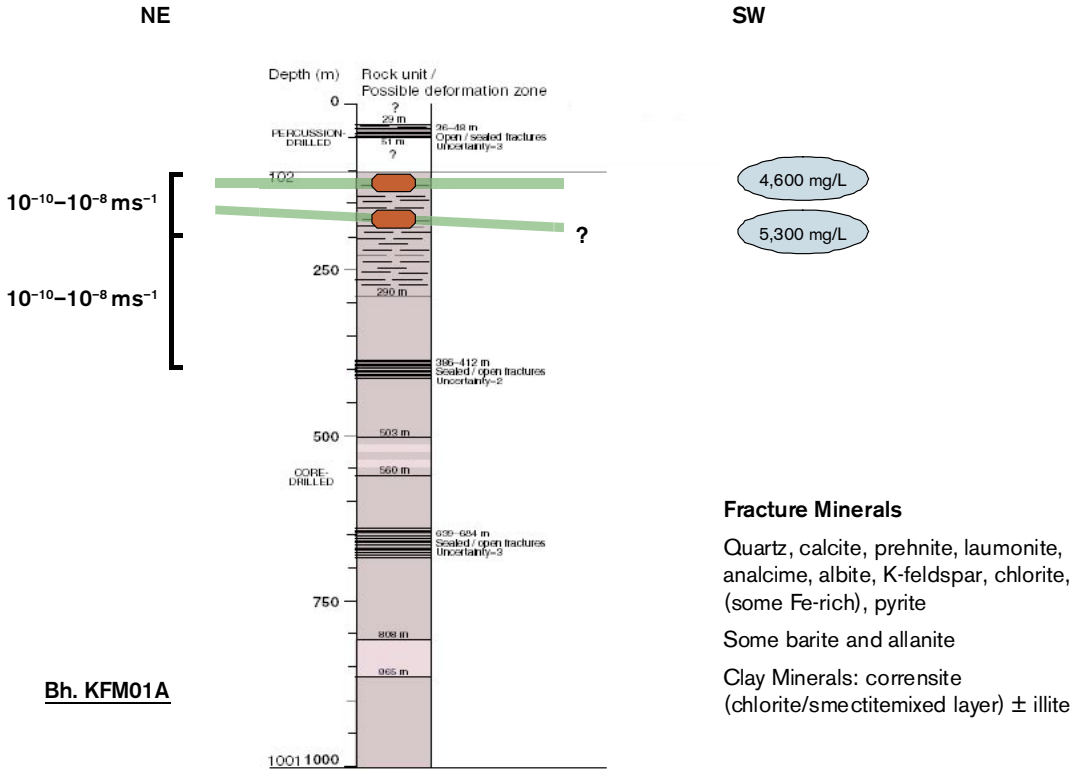

Figure 4-3. *Relation of borehole KFM01A to the identified sampled fracture zones (in green) and hydraulic parameters; groundwater sampling locations are indicated (in red) with the mg/L chloride content (in blue). (Based on M. Stephens, A. Simeonov, written comm. 2004).*

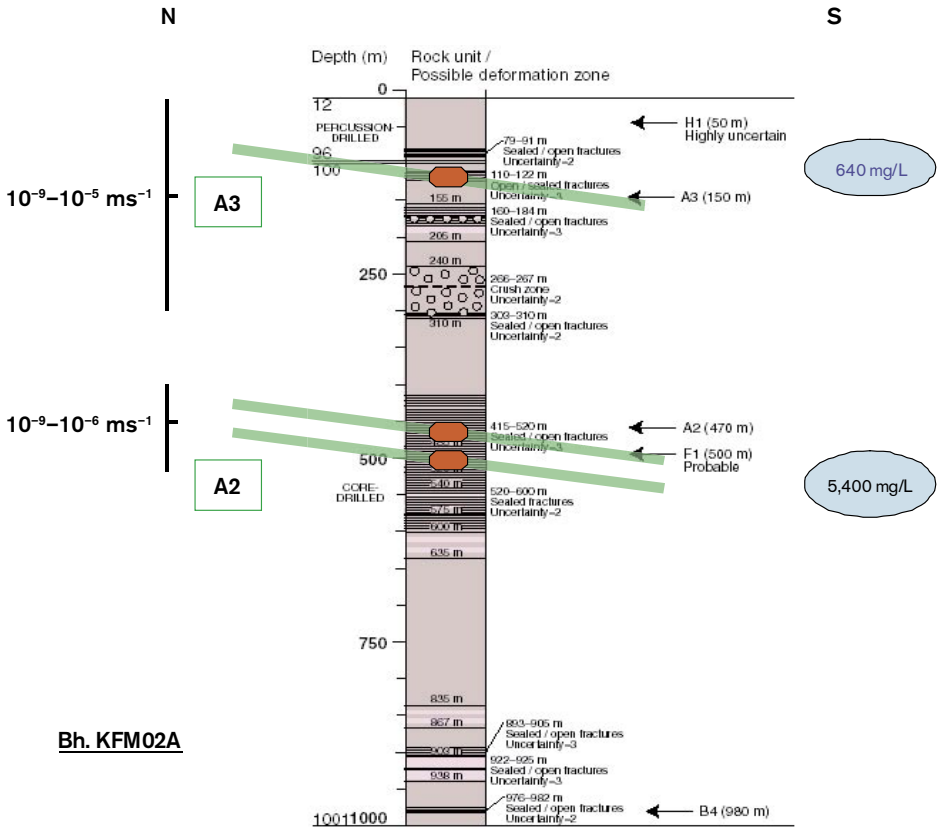

Figure 4-4. *Relation of Borehole KFM02A to the known major structures (A2 and A3 in green) and hydraulic parameters; groundwater sampling locations are indicated in red with the mg/L chloride contents in blue. (Based on M. Stephens, A. Simeonov, written comm. 2004).*

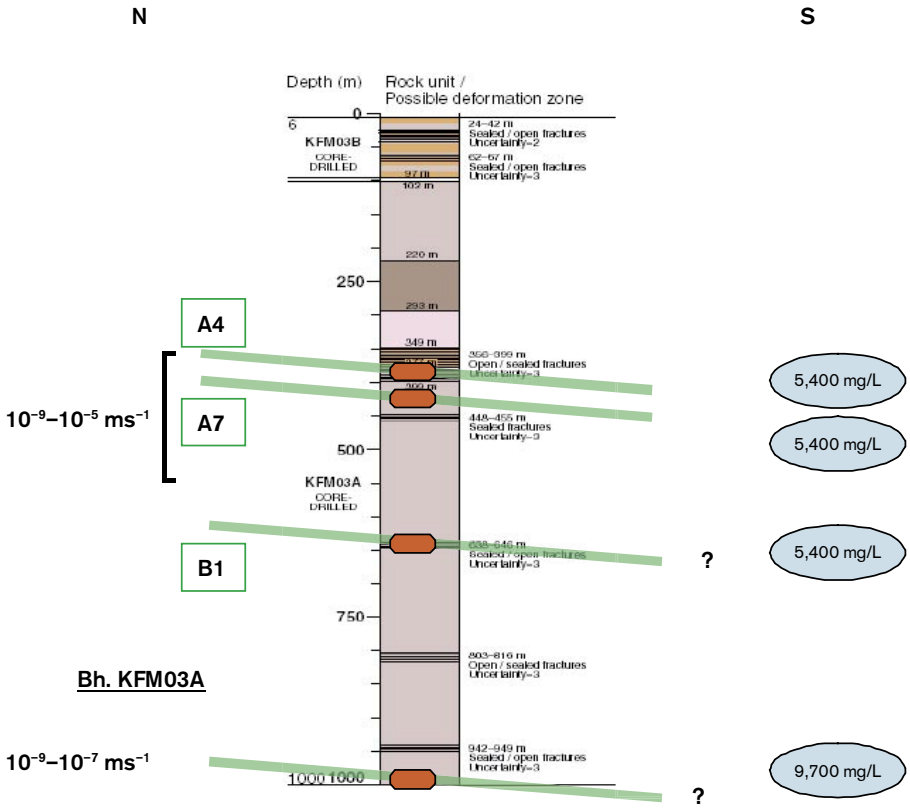

Figure 4-5. *Relation of Borehole KFM03A to the known major structures (in green) and hydraulic parameters; groundwater sampling locations are indicated (in red) with the mg/L chloride contents (in blue). (Based on M. Stephens, A. Simeonov, written comm. 2004).*

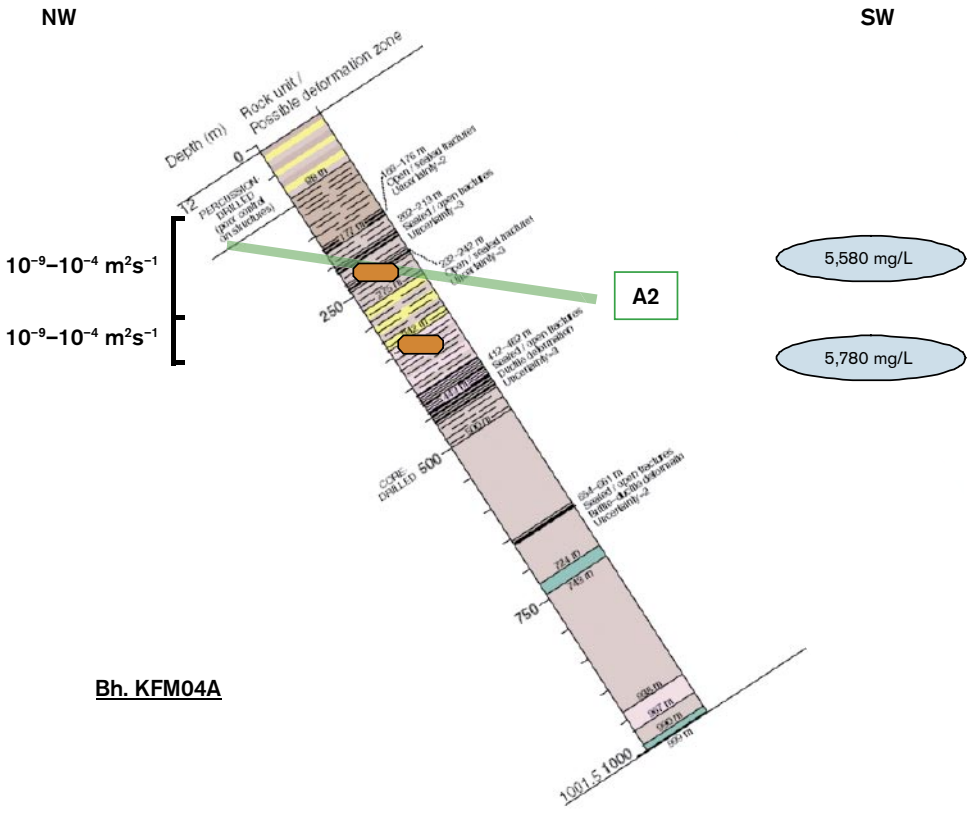

Figure 4-6. *Relation Relation of borehole KFM04A to the known major structures (in green) and hydraulic parameters; groundwater sampling locations are indicated (in red) with mg/L chloride contents in blue). (Based on M. Stephens, A. Simeonov, written comm. 2004).*

Evaluation of scatter plots

The hydrochemical data have been expressed in several X-Y plots to derive trends that may facilitate interpretation. Since chloride is generally conservative in normal groundwater systems its use is appropriate to study hydrochemical evolution trends when coupled to ions, ranging from conservative and non-conservative, to provide information on mixing, dilution, sources/sinks etc. Many of the X-Y plots therefore involve chloride as one of the variables.

The hydrogeochemical evaluation presented below follows a systematic approach /see Smellie et al. 2002/ commencing with traditional plots (e.g. Piper Plots) to group the main groundwater types characterising the Forsmark site and to identify general evolutionary or reaction trends. Comparisons are made with hydrochemical information from other Swedish and Nordic the sites. Importantly, the hydrogeochemistry is related also to the regional and local geology and hydrogeology in order to understand the overall (i.e. large- and small-scale) dynamics and evolution of the groundwater systems which characterise the Forsmark site. A more detailed evaluation of the major components and isotopes can be found in Appendicies 1 and 3. Discussion of many of the reactive elements is presented in the modelling part of this report and also in Appendix 3.

Piper Plot

Water classification is presented in Appendicies 1 and 4. The main groundwater groups characterising Forsmark are: a) shallow (< 200 m) Na-HCO_3 to Na-HCO_3(SO_4) to Na(Ca)-HCO_3 to Na(Ca)- HCO_3-Cl(SO_4) to Na(Ca)-Cl- SO_4(HCO_3) to Na(Ca, Mg)-Cl-SO_4(HCO_3) types, b) intermediate (approx. 200–600 m) Na(Ca, Mg)-Cl(SO_4) to Na-Ca(Mg)-Cl(SO_4) types, and c) deep (> 600 m) Na-Ca-Cl to Ca-Na-Cl types. The variation in compositions, especially in the upper 200 m of the bedrock, is due to local hydrodynamic flow conditions leading to mixing of varying proportions. Microbially mediated reactions are also important influencing both HCO_3 and SO_4, especially in the upper 600 m, as well as ion exchange reactions.

The Piper and Langelier Ludwig plots from the Forsmark site shown in Figure 4-7 emphasise distinct groupings representing: a) the deeper cored borehole groundwaters, b) the shallow cored borehole and percussion borehole groundwaters, and c) the Baltic Sea waters. There is an overall lack of distinction between the Lake and Stream waters and many of the shallow Soil Pipe groundwaters, although most represent more dilute water types. There is some overlapping (i.e. mixing trends) between the main Baltic Sea cluster and some of the percussion borehole groundwaters and, as mentioned above, widespread overlapping between the surface and near-surface Lake and Stream waters and some of the shallow Soil Pipe groundwaters.

General comparison of Cl vs depth with other sites

Comparison of the Forsmark chloride data with some of the other Fennoscandian sites is shown in Figure 4-8. These Fennoscandian sites, i.e. Finnsjön, SFR and Olkiluoto, provide excellent comparisons since both Finnsjön and SFR are close to the Forsmark site and Olkiluoto is the Finnish counterpart to Forsmark in terms of palaeoevolution (coastal location) and also in terms of geological and present-day climatic conditions.

Figure 4-8 for all sites show a similar transition from dilute groundwaters (< 1,000 mg/L Cl) to brackish groundwaters (~ 5,000–6,000 mg/L Cl) at slightly varying depths ranging from 50–200 m. Finnsjön also indicates bedrock areas were local hydrodynamics appear to have transported dilute groundwaters to around 500–550 m although some contamination cannot be ruled out.

The transition from brackish to more saline groundwaters differs between the sites. At Forsmark (represented by KFM03A) this transition to saline appears to occur at depths greater than 650 m. At Olkiluoto it is clearly at around 500 m below which the salinity increases dramatically to a maximum of > 40,000 mg/L Cl at approx. 850 m, whereas at Forsmark the salinity only increases to ~ 10,000 mg/L Cl at 1,000 m. Both the Finnsjön and SFR sites lack groundwater data from great depth.

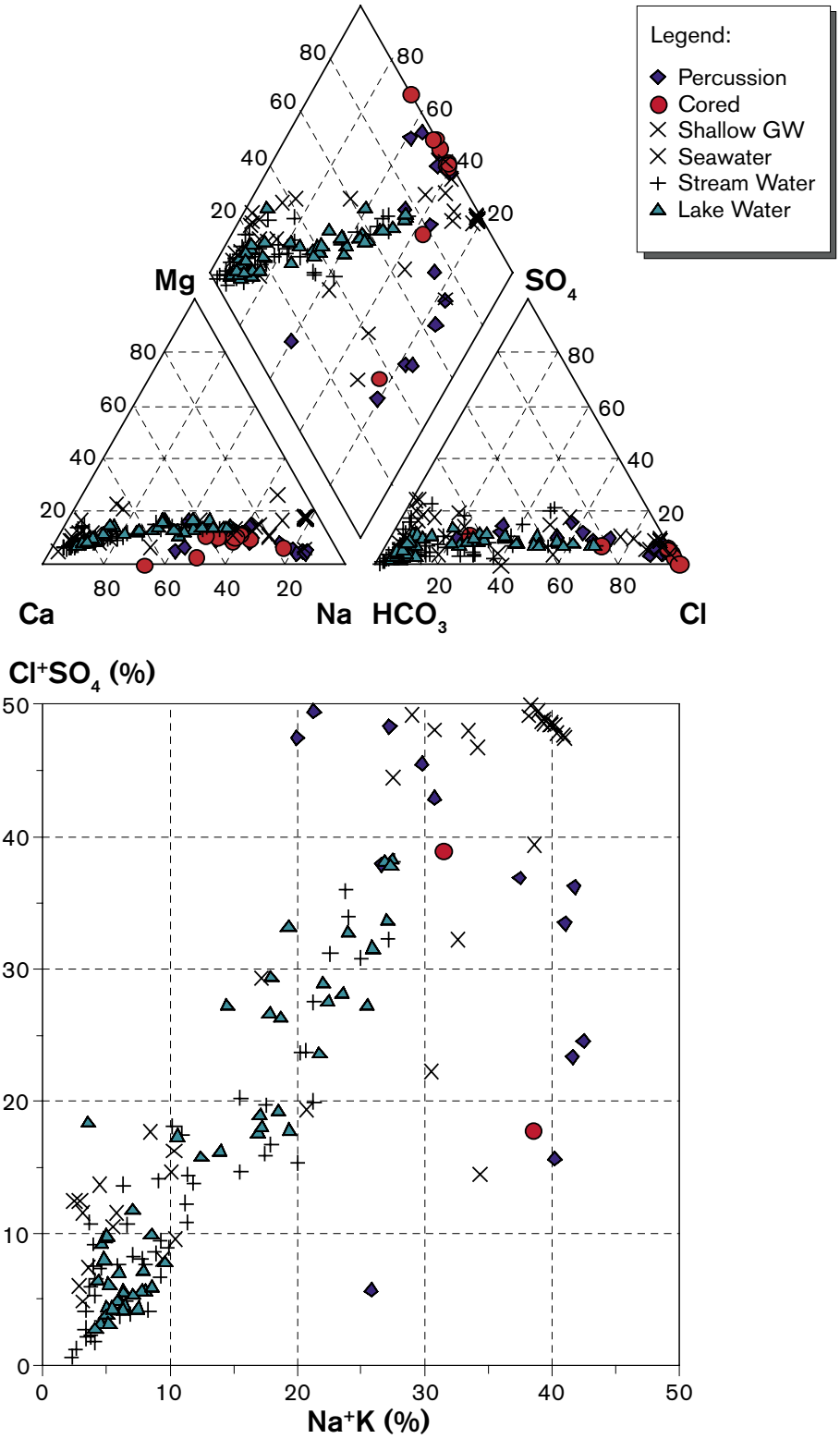

Figure 4-7. *Piper and Ludwig-Langelier plots of surface, near-surface and groundwaters from Forsmark.*

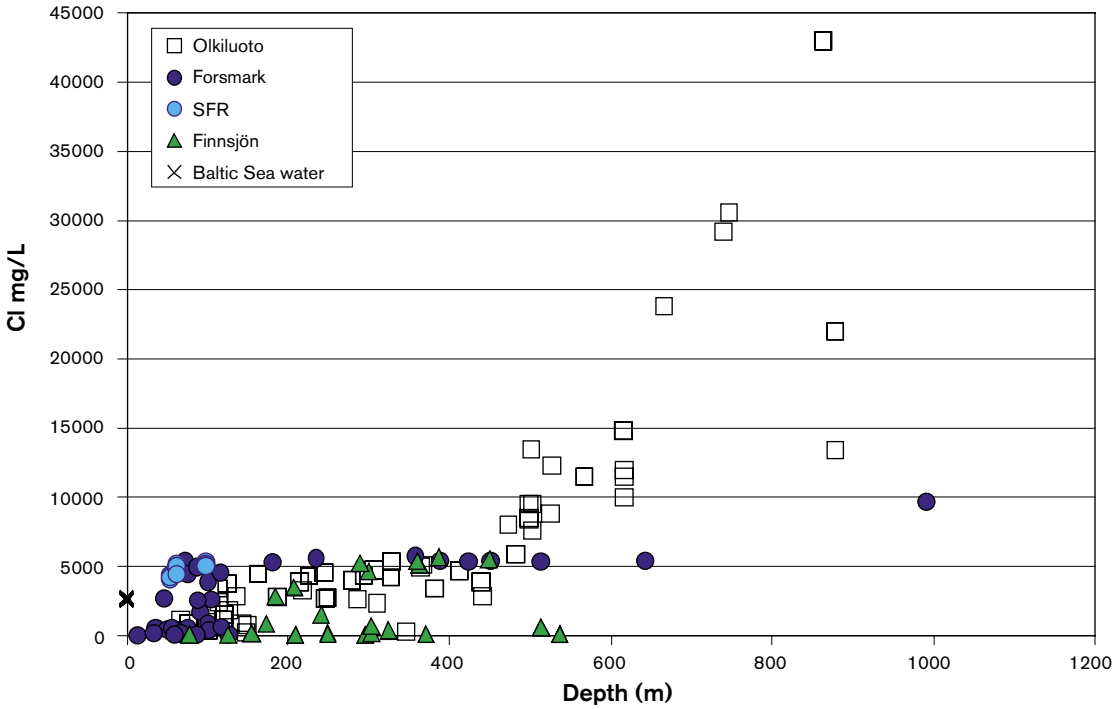

Figure 4-8. *Depth comparison of chloride with other Fennoscandian sites.*

Tritium

Tritium produced by the bomb tests during the early 1960's is a good tracer for waters recharged within the past four decades. As part of an international monitoring campaign, peak values between 1,000 and 4,300 TU were recorded at Huddinge near Stockholm in the years 1963–1964 and values reaching almost 6,000 TU were recorded at Arjeplog and Kiruna in northern Sweden (IAEA database). Due to decay (half life of 12 years) and dispersion, in addition to a cessation of the nuclear bomb tests, precipitation tritium values decreased so that measurements carried out at Huddinge during 1969 showed that values had dropped to between 74 and 240 TU.

Present day surface waters from the Simpevarp and Forsmarks sites show values of 7–20 TU with exceptions of a few Lake and Stream water samples from Forsmark (Figure 4-9). Generally, the Baltic Sea samples (10.3–19.3 TU) show somewhat higher values compared to the meteoric surface waters (7.8–15 TU) for precipitation. The Forsmark Baltic Sea samples show some values that are higher than the Simpevarp Baltic Sea samples but the spread is large for both sites. The successive lowering of tritium contents versus time elapsed since the bomb tests may explain the higher values in the Baltic Sea (due to reservoir effects) compared with precipitation. The difference between the Simpevarp and Forsmark Baltic Sea samples can be a north-south effect, with higher tritium values in the north compared to the south. However this is not demonstrated by the precipitation values (Figure 4-9). Moreover, the ^{14}C content in the Baltic Sea water is relatively similar between the two sites (Figure 4-10).

The measured tritium contents in the precipitation and Baltic Sea water at each site may also contain some tritium locally produced by the nuclear power plants, i.e. that emitted both as vapour to the atmosphere and that contained in the cooling water discharged to the Baltic sea. This contribution is probably very low but the possibility should not be completely ruled out at the moment until background environmental tritium data become available. It should be emphasised that the precipitation values are very few, show a large variation in tritium and therefore are not considered very conclusive. Continued systematic sampling of precipitation (rain and snow) for tritium analysis therefore is encouraged.

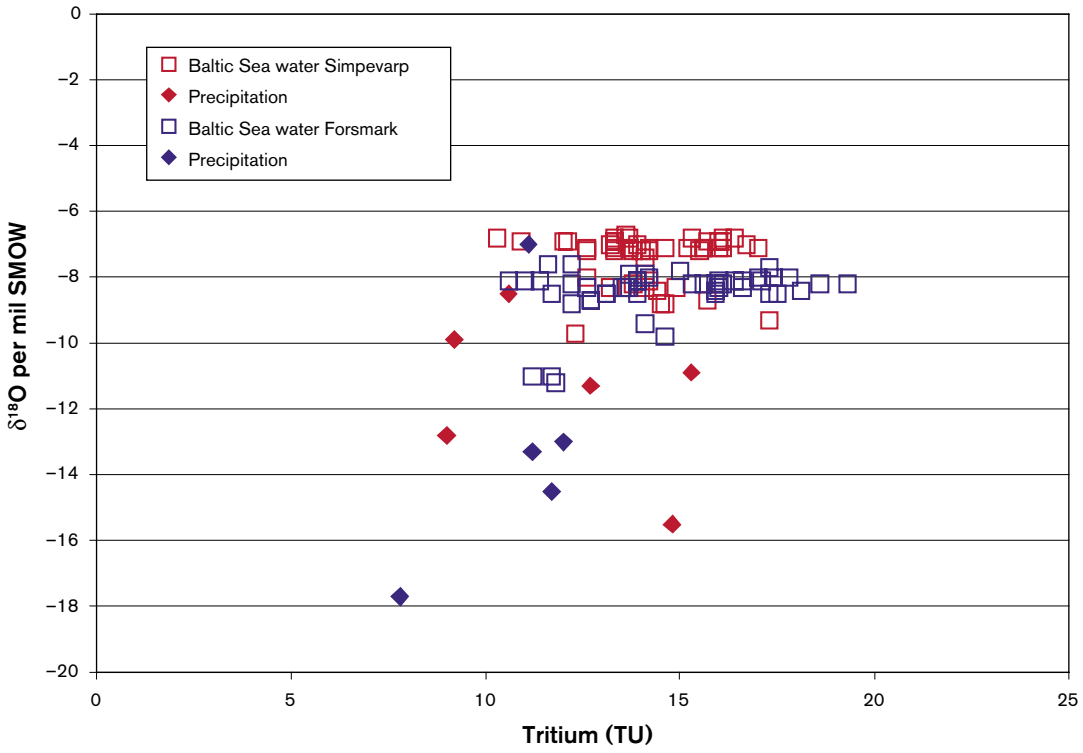

Figure 4-9. *Plot of $\delta^{18}O$ versus tritium in surface water samples from the Forsmark and Simpevarp sites.*

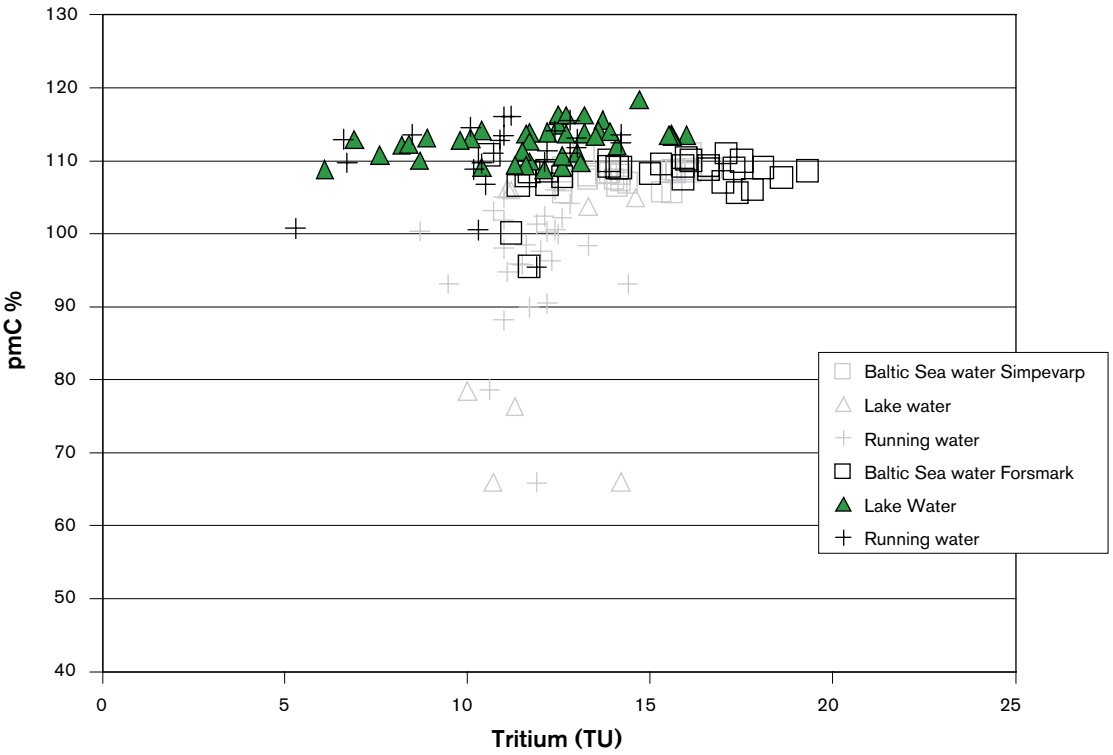

Figure 4-10. *^{14}C content, given as percentage modern carbon (pmC %) versus tritium content for surface waters from Forsmark.*

One problem in using tritium for the interpretation of near-surface recharge/discharge is, as mentioned above, the variation in content in recharge water over time. This implies that near-surface groundwaters with values around 15 TU can be 100% recent, or a mixture of old meteoric (tritium free) water, and also a small portion (10%) of water from the sixties at the height of the atmospheric nuclear bomb tests.

The plot of tritium vs. ^{14}C for surface waters from Forsmark and Simpevarp shows large differences concerning the lake and stream waters of the two sites (Figure 4-10). In Simpevarp the lake and stream waters show a distinct decrease in ^{14}C content whereas the tritium values remain the same or show a small decrease. This may be explained by the addition to the waters of HCO_3 that originates either from calcites devoid of ^{14}C, or, due to microbial oxidation of organic material with lower (or no) ^{14}C. This is the pattern expected for near-surface waters. In Forsmark, in contrast, most lake and stream waters have higher ^{14}C values compared with Baltic Sea waters, whereas the tritium values range from 5–15 TU for all three water sources. Since tritium contents are naturally largely variable and sometimes close to detection, the analytical data used in groundwater modelling have to be carefully scrutinised for any signs of contamination. Since it can be concluded that subsurface in-situ production of tritium is expected to be negligible in the Forsmark granitoids, the major sources of contamination will be related to drilling waters or surface waters that may have entered the borehole.

Figure 4-11 shows tritium vs. percentage drilling water content in the cored boreholes from Forsmark. The drilling water used from the percussion boreholes varied in tritium content from a minimum of 1.9 TU for HFM10 to a maximum of 5.7 TU for HFM06. However, there is no correlation between percentage drilling water and tritium values in the sampled representative groundwaters which indicate that the drilling water was successfully removed prior to sampling.

All available tritium values from groundwaters (percussion boreholes, cored boreholes and soil pipes) are plotted versus depth in Figure 4-12. In the cored boreholes the tritium content decreases significantly in the upper 200 metres but varies considerably in the percussion boreholes. Tritium free groundwater was collected in HFM05 (25–200 m), HFM08 (0–144 m), HFM12 (0–210 m) and HFM14 (0–151 m).

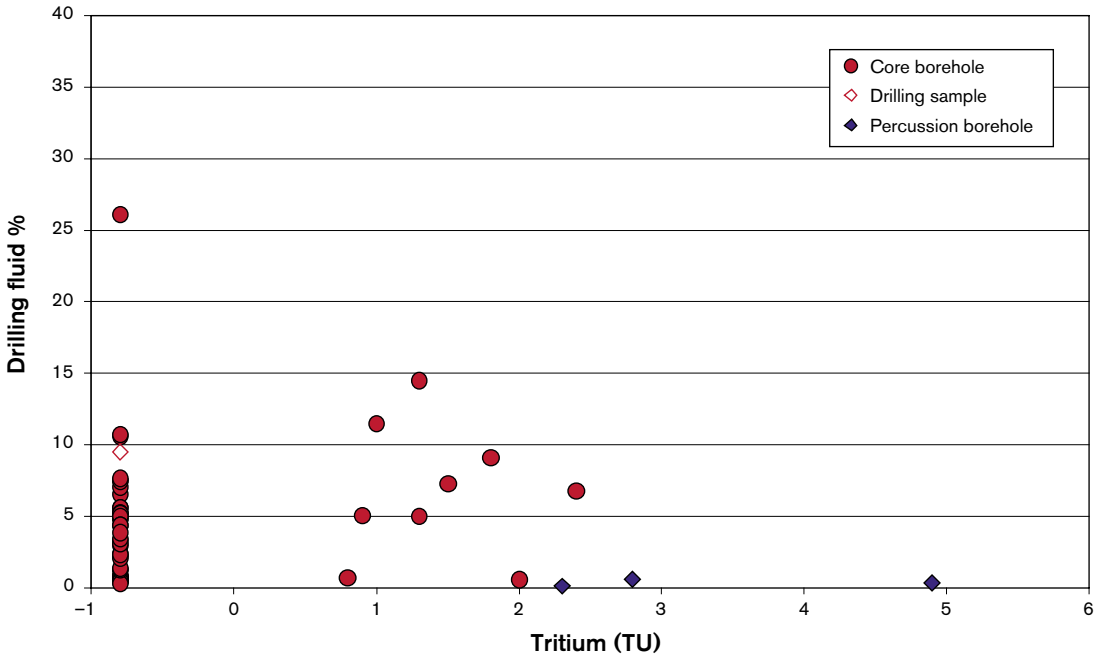

Figure 4-11. *Tritium (TU) versus drilling fluid (%) for boreholes HFM05, KFM01A, KFM02A, KFM03A and KFM04A.*

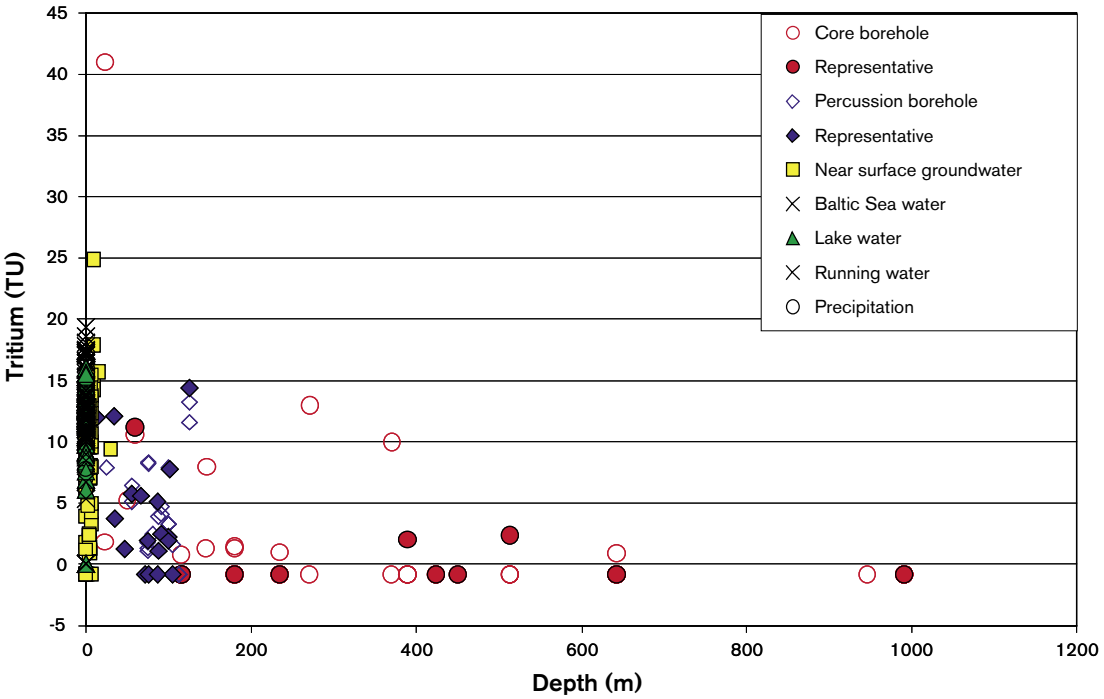

Figure 4-12. *Tritium (TU) versus depth (m) for a) groundwaters from cored boreholes, percussion boreholes and soil pipes, b) Baltic Sea, Lake and Stream waters, and c) precipitation.*

Below 200 m depth tritium values under 3 TU are detected for all samples. For the sections sampled below 300 m the groundwaters systematically collected from each section generally show no detectable tritium. In two cases, however, a few tritium units have been measured in the last sample in the sequence collected which for other reasons has been selected as most representative. Since at the moment it not clear why these water samples show detectable tritium contents, it is suggested that these values are used with some caution until more analyses become available.

One of the near-surface samples KFM03A (0–46 m) shows a very high tritium content of 41 TU indicative of a significant portion of recharge from the sixties or seventies when the recharge tritium contents were much higher than at present. There is therefore the possibility that the observed tritium values in some of the sampled borehole sections reflect some contamination by these tritium-enhanced waters entering into water-conducting fracture systems during open hole borehole activities. This would help to explain the presence of low tritium values and an absence of drilling water.

Tracing the Littorina Sea signature with Mg, Br, and $\delta^{18}O$

The Littorina stage in the postglacial evolution of the Baltic Sea commenced when the passage to the Atlantic Ocean opened through Öresund in the southern part of the Baltic Sea. The relatively high sea level together with the early stages of isostatic land uplift led to a successively increasing inflow of marine water into the Baltic Sea. Salinities twice as high as modern Baltic Sea have been estimated for a time period of about 2,000 years starting some 7,000 years ago (cf. Chapter 3). Based on shore displacement curves it is clear that the Forsmark area has been covered by the Littorina Sea for a long period of time (8,000 to 9,000 years) and the low topography implies that it reached several tens of kilometres further inland for a considerable part of that time. The present meteoric recharge stage following uplift and emergence has only prevailed for less than 1,000 years such that any flushing out of the Littorina Sea component is relatively limited. Strong evidence of a Littorina Sea water signature can therefore be expected in groundwaters at Forsmark which is also confirmed by the hydrochemical interpretations.

The Simpevarp/Laxemar area, in contrast, was only partly covered by the Littorina Sea. Due to the topography of the area and the on-going isotstatic land uplift, the Laxemar area was probably influenced only to a small degree, whereas the Simpevarp peninsula was covered for several thousands of years until eventual emergence during uplift initiated a recharge meteoric water system some 4,000 to 5,000 years ago. This recharge system effectively flushed out much of the Littorina Sea water.

Comparison of Forsmark data with the Simpevarp area (i.e. Äspö, Laxemar and Oskarshamn sites) indicates large differences in the character and origin of the groundwaters, especially for brackish groundwaters with chloride contents of around 4,000–6,000 mg/L Cl. This is exemplified in three plots showing chloride versus magnesium, bromide and $\delta^{18}O$ (Figure 4-13, Figure 4-14 and Figure 4-15). For a more detailed discussion and plots showing individual boreholes see Appendix 1.

The magnesium versus chloride plot (Figure 4-13) clearly shows the difference between the Forsmark and Simpevarp groundwaters characterised by chloride contents up to 5,500 mg/L Cl; characteristically the Forsmark samples closely follow the modern marine (Baltic Sea) trend. Those few groundwaters that plot within the Simpevarp area group are from greater depths in the bedrock and, as such, have been influenced by mixing with deeper non-marine saline groundwaters. A few samples from Äspö (KAS06 and HAS02; Figure 4-13) also show relatively high Mg contents, although not as high as in the Forsmark groundwaters with similar chloride contents. Most of the Simpevarp area groundwaters show low Mg values although small increases are observed for samples in the chloride interval 4,000–6,300 mg/L.

The bromide versus chloride plot (Figure 4-14) underlines the marine signature for most of the Forsmark groundwaters with salinities up to brackish values (~ 5,500 mg/L), with the exception of sample KFM03A: 638–644 m which shows a mixed origin (already commented upon in previous sections), whereas marine signatures only are obtained in a few of the Oskarshamn sub-area groundwaters. This observation is strengthened in the $\delta^{18}O$ versus chloride plot (Figure 4-15) which shows deviating groundwater trends for Forsmark and Simpevarp.

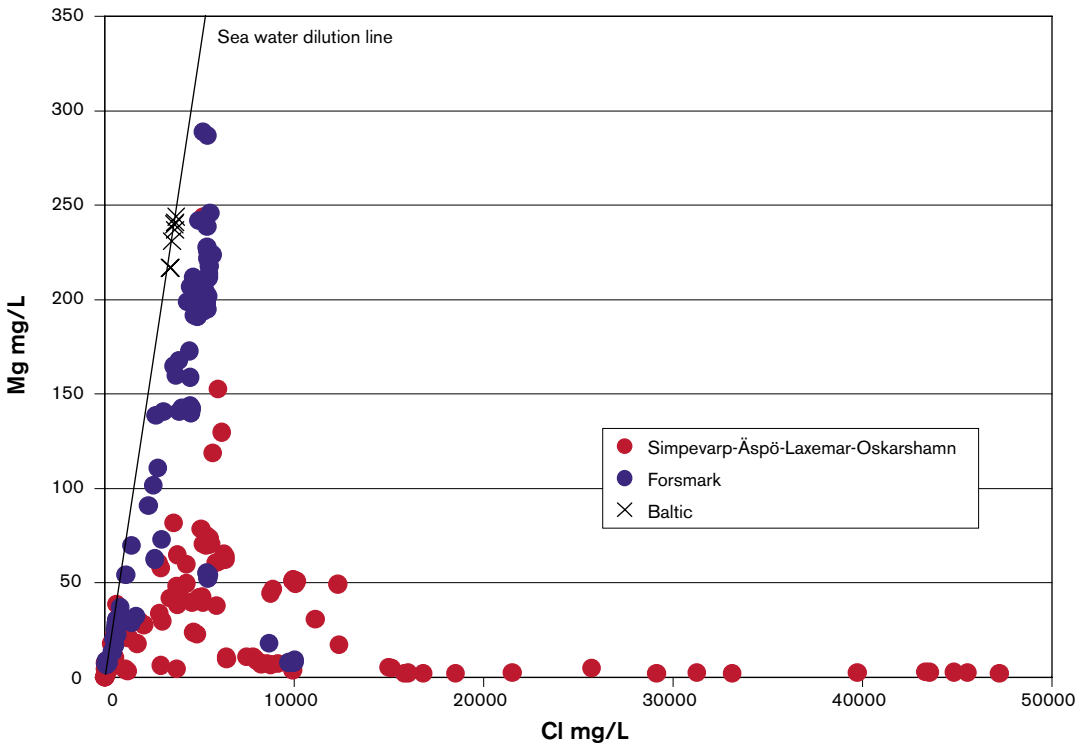

Figure 4-13. *Mg versus Cl for groundwaters from Forsmark and the Simpevarp area (Simpevarp-Äspö-Laxemar-Oskarshamn (KOV01)). Baltic Sea waters from Simpevarp and Forsmark are included for reference.*

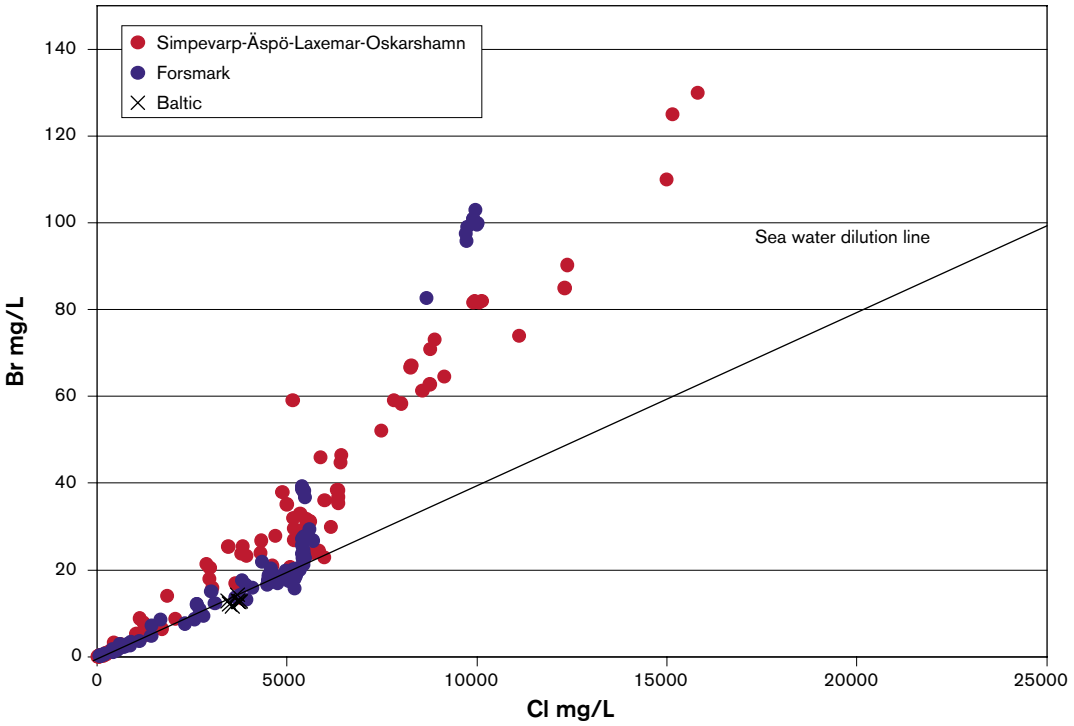

Figure 4-14. *Br versus Cl for groundwater samples from Forsmark and the Simpevarp area (Simpevarp-Äspö-Laxemar-Oskarshamn (KOV01)). Baltic Sea waters from Forsmark and Simpevarp are included for reference.*

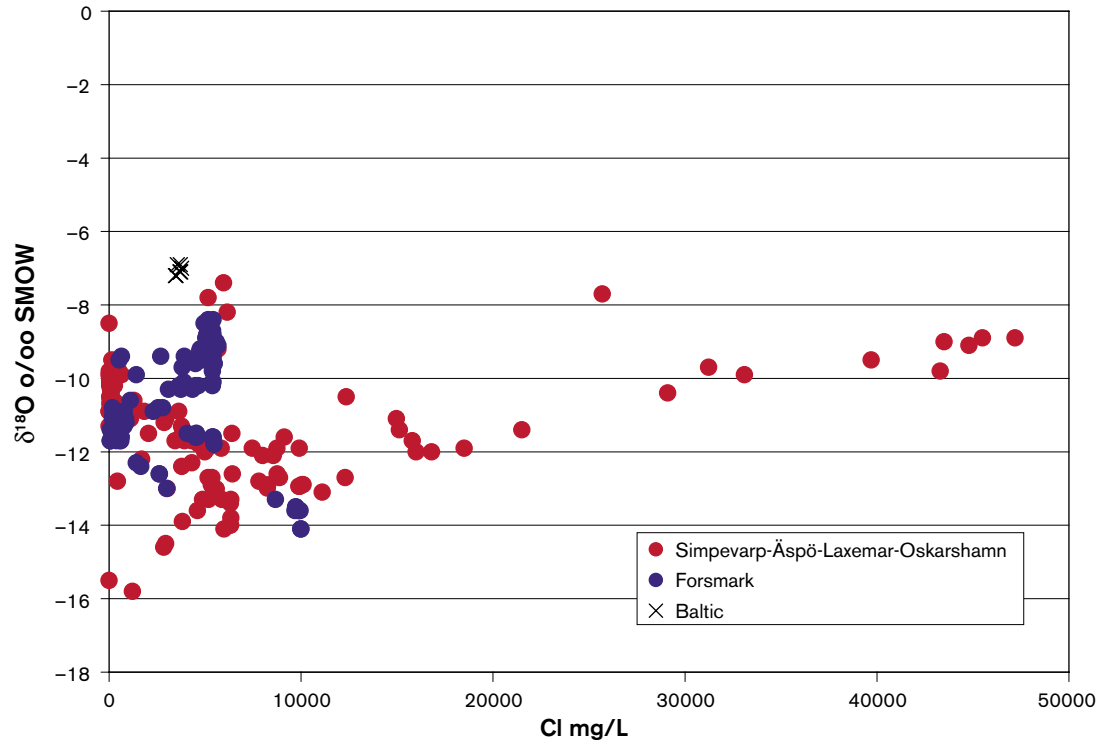

Figure 4-15. *$\delta^{18}O$ versus Cl for groundwaters from Forsmark and the Simpevarp area (Simpevarp-Äspö-Laxemar-Oskarshamn (KOV01)). Baltic Sea waters from Simpevarp are included for reference.*

Generally, with a few exceptions, the brackish groundwaters up to 5,500 mg/L Cl at Forsmark show indications of a marine origin in terms of: a) Br/Cl ratios, b) Mg values ≥100 mg/L, and c) $\delta^{18}O$ values higher than meteoric waters (due to in-mixing of marine waters). In contrast, for the Äspö-Simpevarp-Laxemar samples these criteria are only fulfilled in samples from KAS06 and one sample in KSH03A. In both cases the groundwater samples have been collected from fracture zones outcropping close to the shoreline or under the Baltic Sea.

The chloride content and $\delta^{18}O$ value for the Littorina Sea at maximum salinity is difficult to determine precisely. Interpretations of salinities based on fossil fauna together with $\delta^{18}O$ analyses of the fossils has resulted in suggested salinities around 6,500 mg/L Cl and $\delta^{18}O$ values ~ –4.5‰ SMOW /Donner et al. 1994; Pitkänen et al. 2004/. In Figure 4-16 (Cl versus $\delta^{18}O$) groundwaters from the Forsmark, SFR and Simpevarp areas show Br/Cl ratios < 0.0045 and magnesium values > 100 mg/L. For comparison data from Olkiluoto /Pitkänen et al. 2004/ are included. The top three mixing lines in Figure 4-16 represent Oceanic/Littorina/meteoric, Oceanic/Baltic (Simpevarp)/meteoric and Oceanic/Baltic (Forsmark)/meteoric. The sub-vertical mixing line represents Littorina/glacial. Most of the plotted groundwaters reflect mixtures of varying proportions comprising the four end-members: Glacial, Littorina Sea, Baltic Sea and Meteoric waters.

Assuming that the suggested Littorina Sea water is the product of simple mixing between Ocean Sea water and a meteoric component, then this meteoric water had heavier $\delta^{18}O$ values than present-day mixing processes that have given rise to the Baltic Sea close to Forsmark and Simpevarp (Figure 4-16). It is well known that climatic conditions were warmer during parts of the Littorina Sea period and therefore heavier $\delta^{18}O$ signatures in the meteoric water during that stage were probably the case. However, it is probable that both the salinity and $\delta^{18}O$ were variable during the entire Littorina Sea period such that none of the sampled groundwaters at any of the sites studied achieved a proper estimate of the Littorina Sea composition.

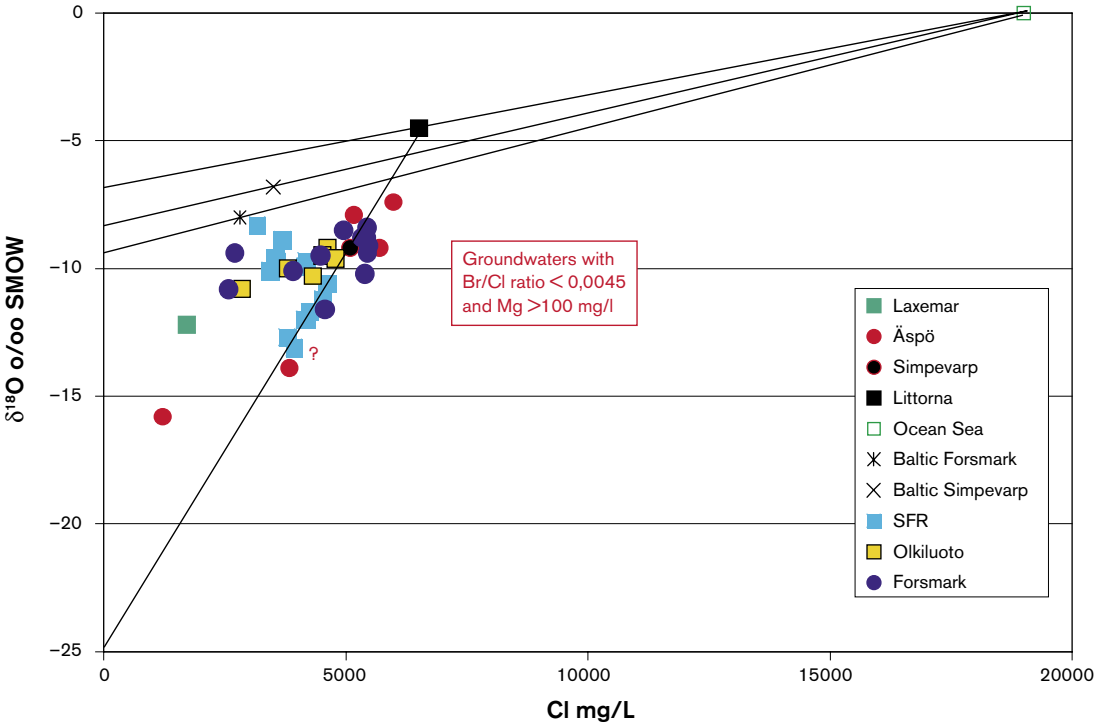

Figure 4-16. *$\delta^{18}O$ versus chloride content for potential marine groundwaters from Simpevarp, Äspö, Forsmark and Olkiluoto, the latter from /Pitkänen et al. 2004/. The top three mixing lines represent Oceanic/Littorina/meteoric, Oceanic/Baltic (Simpevarp)/meteoric and Oceanic/Baltic (Forsmark)/meteoric. The sub-vertical mixing line represents Littorina/glacial. Most of the plotted groundwaters reflect mixtures of varying proportions comprising the four end-members: Glacial, Littorina Sea, Baltic Sea and Meteoric waters.*

Based on the post-glacial scenario a successive replacement of the glacial water by the denser Littorina Sea water has occurred giving rise to the sub-vertical Littorina/glacial mixing line in Figure 4-16. As can be seen a number of waters from Forsmark and SFR cluster along this mixing line together with samples representing the brackish SO_4 type water from Olkiluoto, interpreted by /Pitkänen at al. 2004/ to represent large portions of Littorina water.

From the Simpevarp area there are samples from KAS06 and also one sample from KSH03 that show a large component of Littorina Sea water. Weaker indications are also found in a KAS02 sample from 200 m depth were the magnesium content is low but the Br/Cl ratio is marine.

From Figure 4-16: 1) The uppermost heavier $\delta^{18}O$ values plot along the Oceanic Sea mixing line joining the Littorina Sea with precipitation values at that time of ~ 7‰ SMOW, and 2) The Littorina Sea water subsequently mixed with the older, dilute glacial meltwaters as it slowly descended into the bedrock. This has given rise to 'Littorina Sea' waters of varying chemical and isotopic composition. One such example is the narrow range of composition that characterises many of the SFR groundwaters which plot along the present-data mixing line shown in Figure 4-16.

In conclusion, of the groundwaters sampled in the cored boreholes KFM01A, KFM02A, KFM03A and KFM04A at the Forsmark area, six out of ten sampled sections plot along the Littorina/glacial mixing line. These waters represent depths ranging from 110 m in borehole KFM01A to 520 m in borehole KFM02A. Section 640 m in borehole KFM03A indicates a mixed origin comprising a Littorina/glacial and a deep saline component. Also the groundwaters sampled from KFM04A show inmixing of a deeper saline component based on the Br/Cl ratio, even though a large portion of Littorina Sea is present. Of the 17 percussion boreholes where chemical data are available, three show values that plot along the Littorina Sea mixing line; HFM08 (0–144 m), HFM 10 (0–150 m) and HFM19 (0–173 m). The others show inmixing of today's meteoric and/or modern Baltic Sea to various degrees with the Littorina Sea/glacial mixture. This is also the case for part of the SFR groundwaters; a number of these are approaching Baltic Sea values (Figure 4-16).

If applying simple regularity for the mixing between the glacial and Littorina Sea waters (and assuming that the suggested Littorina Sea and glacial end member values are at least approximately correct) than the glacial components in the Forsmark samples vary from 18 to 33%, and the highest portion of glacial water at 42% is found in the SFR groundwaters. This only concerns the glacial-Littorina mixing; the deep saline/glacial mixing which precedes this event is not addressed here.

Redox indicators

Manganese (Mn^{2+}), one of the potential redox indicators in groundwater systems, is mainly produced by microbes during the oxidation of organic material under anaerobic conditions (cf. Appendix 2). It should be emphasised, however, that the presence of Mn^{2+} is a strong indicator of reducing conditions but its absence (or very low content) in deep groundwaters cannot be taken as an indicator of oxidising conditions.

Figure 4-17 plots all available data against depth. The manganese values vary from very low contents up to 1 mg/L in the surface and near-surface waters and also in the groundwaters sampled down to approx. 100 m depth. This indicates various redox conditions and also different intensities in activity of the Mn-reducing bacteria. In the brackish groundwaters characterised with a marine signature sampled between 150 and 550 m depth, the manganese values are in the range of 1 to 3 mg/L. The deeper groundwaters show lower values (< 0.5 mg/L), which indicate a smaller contribution of microbially reduced manganese to these waters. Collectively, these data once again support the interpretation of a more active groundwater system down to approx. 600 m depth.

The Mn-reducing bacteria do not only produce Mn^{2+} but at the same time also HCO_3 due to oxidation of organic material. The plot of Mn versus HCO_3 in the analysed waters shows, however, no specific trend (Figure 4-18). The surface waters and near-surface groundwaters which have the highest bicarbonte contents (up to 800 mg/L) show Mn values < 1 mg/L suggesting that Mn-reducing bacteria are not the main contributors to HCO_3 production in these waters. In the deeper groundwaters, in contrast, there are higher manganese values in the waters where HCO_3 contents range between 90 to 125 mg/L.

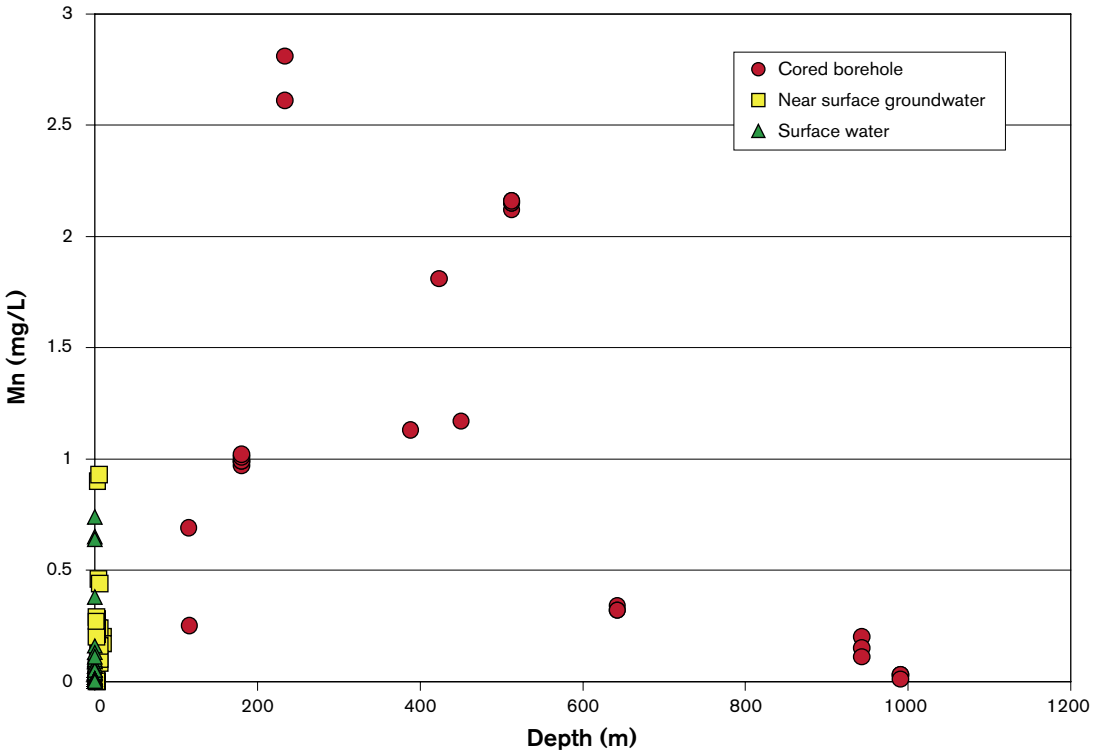

Figure 4-17. *Mn versus depth in surface waters, near-surface groundwaters and groundwaters from cored boreholes in the Forsmark area.*

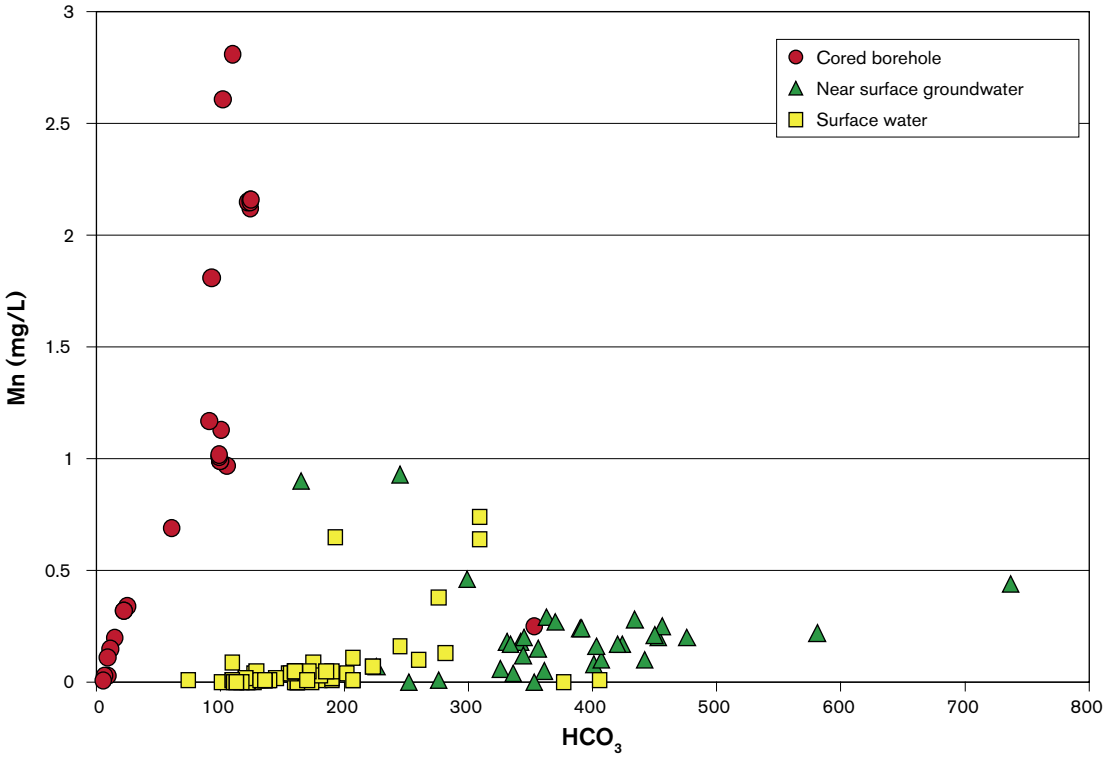

Figure 4-18. *Mn versus HCO_3 in surface waters, near-surface groundwaters and groundwaters from cored boreholes in the Forsmark area.*

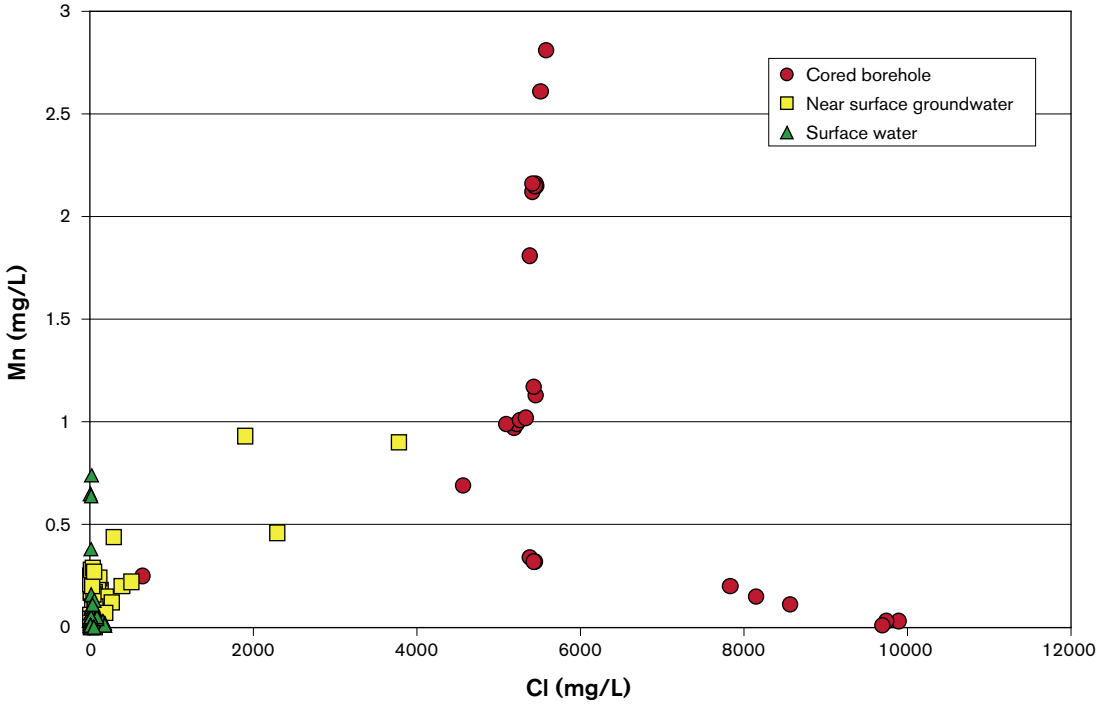

Figure 4-19. *Mn versus Cl in surface waters, near-surface groundwaters and deeper groundwaters from cored boreholes in the Forsmark area.*

As indicated in the plot of Mn versus Cl (Figure 4-19) the highest manganese values are found in waters where chloride contents are between 1,500 to 6,000 mg/L, i.e. those brackish groundwaters with a significant Littorina Sea component. With respect to uranium (cf. discussion below and Appendix 1), high amounts are found in groundwaters where manganese contents exceed 1 mg/L, thus supporting the reducing conditions in these brackish groundwaters.

Uraninum

Uranium contents have been analysed in surface waters (Lake and Stream waters), in near-surface groundwaters from Soil Pipes and in groundwaters from the percussion and cored boreholes. The surface and near-surface waters are characterised by values between 0.05 and 28 µg/L (Figure 4-20). Large variations in uranium content in surface waters are common and are usually ascribed to various redox states (oxidation will facilitate mobilisation of uranium) and various contents of complexing agents, normally bicarbonate (which will keep the uranium mobile). The plot of uranium versus bicarbonate for the waters (Figure 4-21) shows no clear trend although there is a tendency of higher uranium contents in the surface and near-surface groundwaters associated with increasing bicarbonate up to 400 mg/L. For the few near-surface waters with higher bicarbonate contents the uranium tends to decrease, which may be due to very low redox potentials in these waters caused by the microbial reactions producing the bicarbonate (probably to large extent sulphate reducers).

Lower uranium content with depth is expected due to decreasing redox potential and decreasing HCO_3. The groundwaters sampled in the cored boreholes, in contrast, show no such depth trend. Instead, most of the groundwaters show high values (< 30 µg/L) at depths between 200 m and 600 m (Figure 4-21). Groundwaters with high uranium content have bicarbonate contents around 100–125 mg/L with the exception of three samples which all originate from borehole section 639–646 m in KFM03A. This borehole section indicates a mixed groundwater origin (marine and deep saline; cf. discussion in Appendix 1).

Uranium versus chloride (Figure 4-22), shows that the highest uranium contents are found in the waters with chloride values around 5,000–5,500 mg/L, i.e. the brackish groundwaters dominated by a Littorina Sea water component.

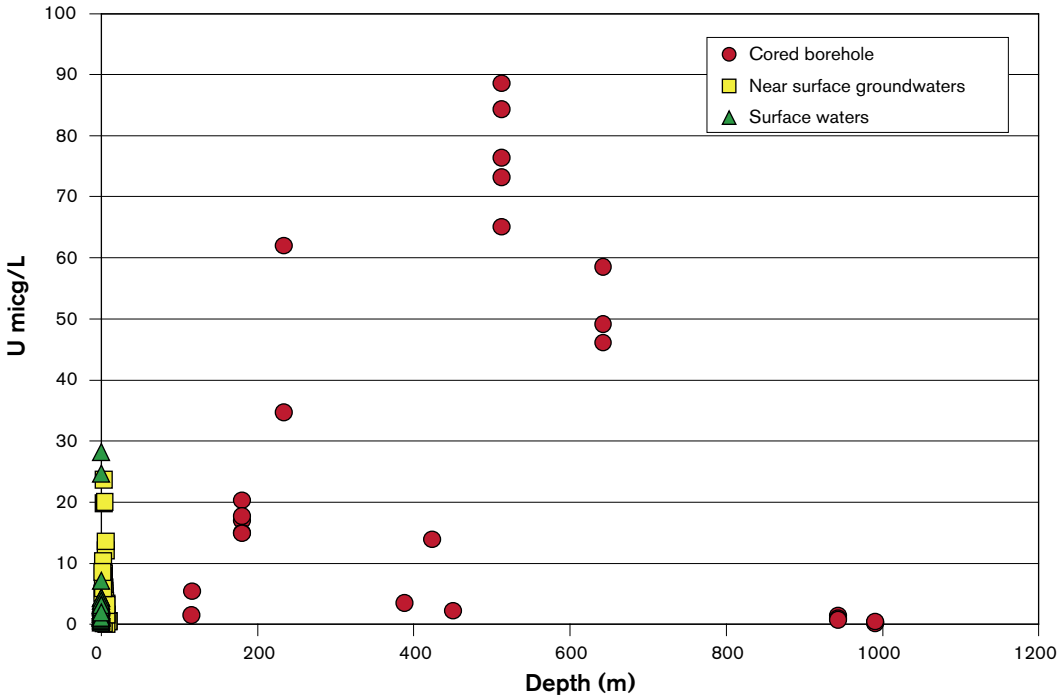

Figure 4-20. *Uranium content (µg/L) in surface and groundwaters from the Forsmark area.*

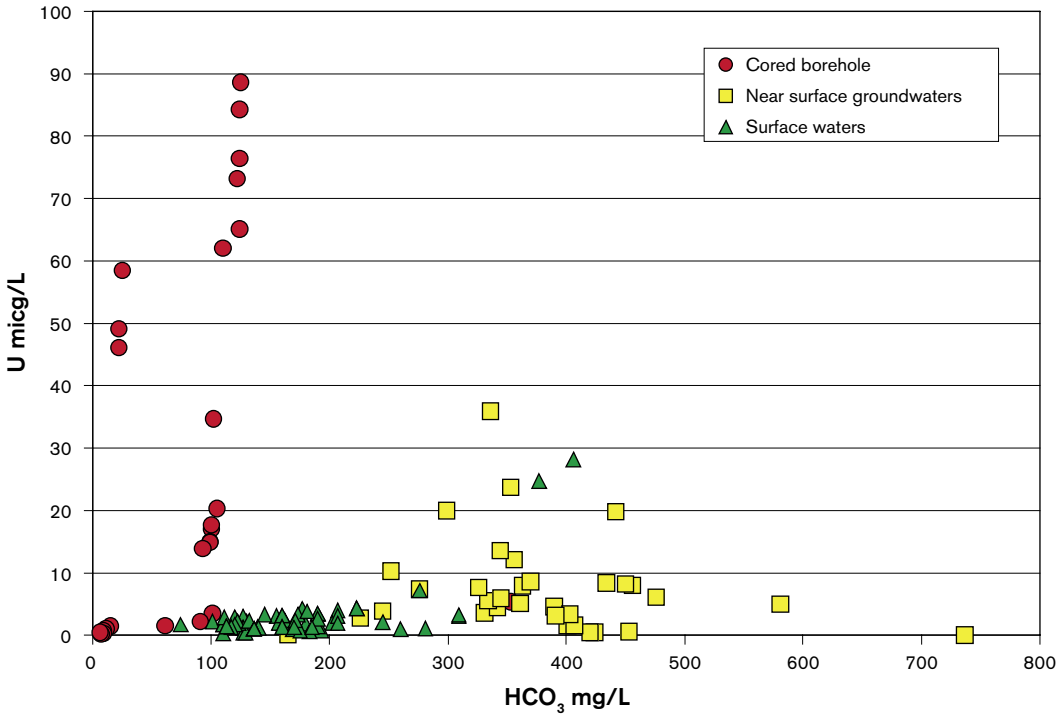

Figure 4-21. *Uranium (µg/L) versus HCO_3 (mg/L) in surface and groundwaters from the Forsmark area.*

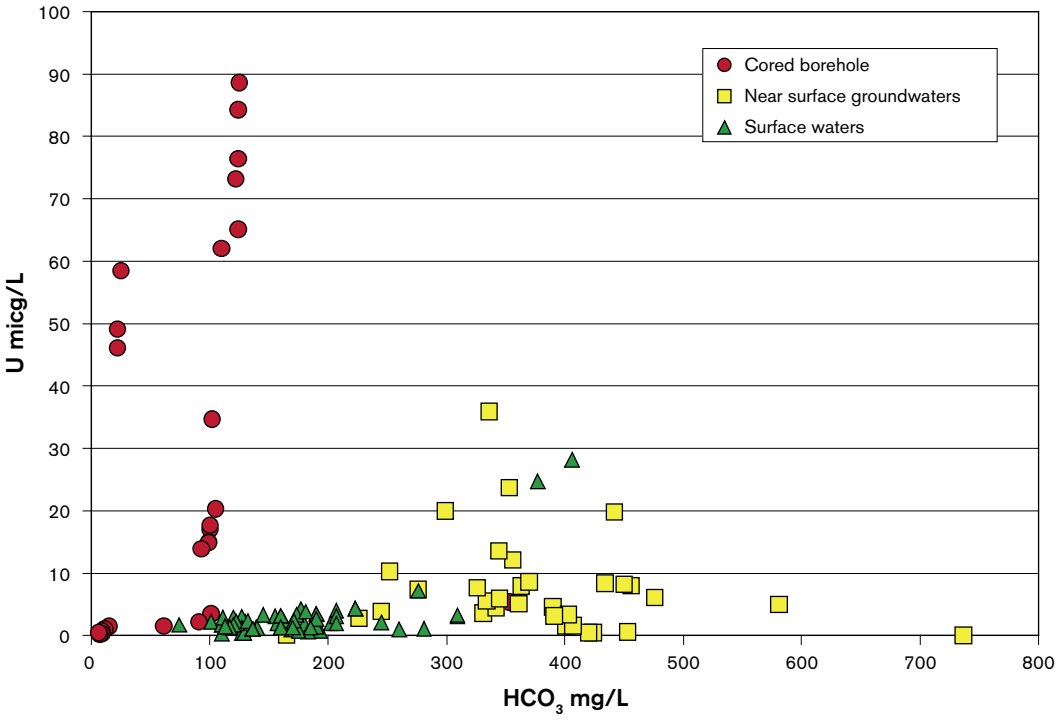

Figure 4-22. *Uranium (µg/L) versus Cl (mg/L) in surface and groundwaters from the Forsmark area.*

Uranium isotope measurements have been carried out in a number of groundwater samples from Forsmark but the reported values are questionable. To resolve this issue an interlaboratory study of reference samples has been initiated and no uranium isotope data will be evaluated in this Forsmark v. 1.2 reporting stage. However, a few measurements carried out at Glasgow University indicate that the uranium $^{234}U/^{238}U$ activity ratios are within the range of 2 to 4, which conform with groundwaters from other sites.

Carbon isotopes

The stable carbon isotope ratios, expressed as $\delta^{13}C$‰ PDB, radiocarbon contents (^{14}C) expressed as pmC (percentage modern carbon), and HCO_3^-, have been analysed from surface waters and groundwaters (cf. Figure 4-23 and Figure 4-24). The tritium versus ^{14}C for surface waters has been discussed already.

Baltic Sea waters have ^{14}C values around 110 pmC and $\delta^{13}C$ values mostly between –2 and –7‰ produced by equilibria with atmospheric CO_2. The lake and stream waters show increasing input of biogenic carbon seen as increased HCO_3 contents, decreased $\delta^{13}C$ values and, somewhat surprisingly, a small increase in ^{14}C (110–120 pmC are measured in many of the lake and stream waters). The stable carbon isotopes indicate exchange with biogenic CO_2 and it is therefore reasonable to assume that breakdown of ^{14}C-enriched organic material has contributed to the somewhat higher values. Several reasons for the ^{14}C enrichments in the organic material at Forsmark are possible, but the main candidate is uptake of radioactive CO_2 emitted into the atmosphere by the nearby nuclear power plant /cf. Eriksson, 2004/. Part of this radioactive CO_2 is incorporated in plants (due to photosyntesis), and successive microbial breakdown of this material will contribute ^{14}C-rich CO_2 to the lake and stream waters.

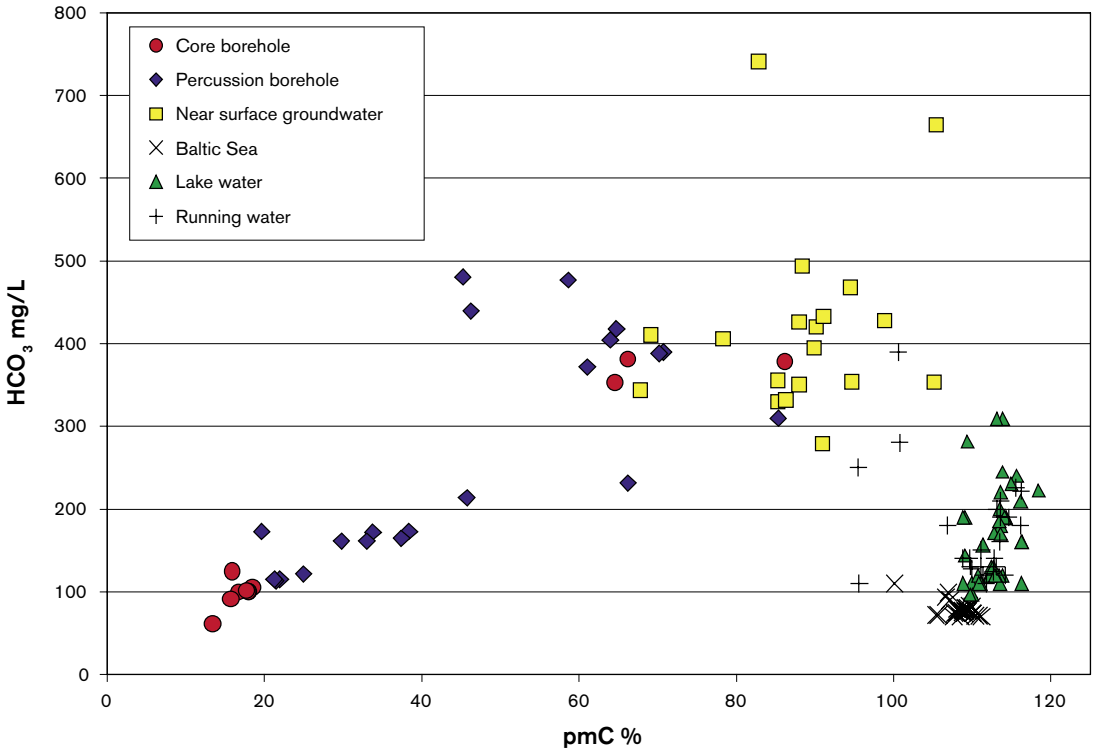

Figure 4-23. *pmC (HCO_3) versus HCO_3 in surface and groundwaters from the Forsmark area.*

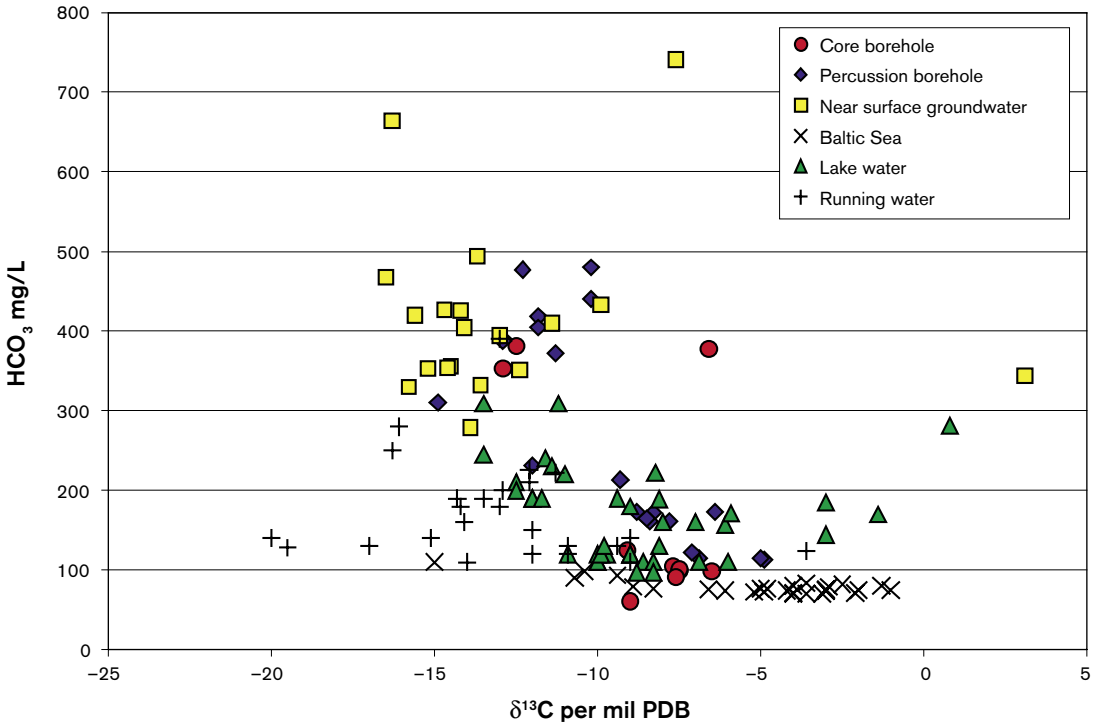

Figure 4-24. *$\delta^{13}C$ (HCO_3) versus HCO_3 in surface and groundwaters from the Forsmark area.*

The highest HCO_3 values are produced in the near-surface groundwaters and in some of the percussion boreholes (cf. Figure 4-24). HCO_3 contents between 300 and 500 mg/L are common in these waters and the $\delta^{13}C$ values are generally between –10 to –17‰ indicating a dominantly biogenic carbon source. However, the ^{14}C contents in these waters are lower, ranging from 80–100 pmC for most surface waters and 60–80 pmC for the high bicarbonate waters sampled in the percussion boreholes. Also, a few shallow samples from the cored boreholes are included in this group. Most of the high bicarbonate waters have detectable tritium values (cf. Figure 4-25) and ^{14}C decay effects are therefore regarded as insignificant. Instead, breakdown of older organic material or contribution of dissolved carbonate minerals (with no ^{14}C) is suggested.

The tritium-free groundwaters from Forsmark show ^{14}C values in the range 14–25 pmC and these waters have generally low HCO_3 contents (< 150 mg/L) and $\delta^{13}C$ values between –10 and –5‰. Figure 4-26 of ^{14}C (expressed as pmC) versus $\delta^{13}C$‰, shows that groundwaters from the percussion and cored boreholes indicate a mixing trend between: a) HCO_3-rich waters with low $\delta^{13}C$ and high ^{14}C content, and b) deeper groundwaters with lower HCO_3 contents, higher $\delta^{13}C$ values and lower ^{14}C. To date there are no groundwaters analysed from below depths of 550 m.

The groundwaters showing the lowest ^{14}C values have chloride contents ranging from 4,500–5,500 mg/L (Figure 4-27); these indicate marine signatures, i.e. they represent waters with a dominant Littorina Sea component. In terms of 'relative age', the measured pmC values indicate 11,000–16,000 years which is significantly older than the Littorina Sea period. This can be explained by an addition of older bicarbonate, probably by dissolution of older carbonate and/or mixing by glacial water (supported by low $\delta^{18}O$ in at least some of these groundwaters).

The plot of ^{14}C content versus depth (Figure 4-28) shows, as expected, a decreasing trend with depth. All groundwaters deeper than 200 m show values below 20 pmC. Together, the distribution of ^{14}C and tritium versus depth supports the occurrence of an upper 100–200 m hydraulically dynamic section and a significantly less dynamic situation at greater depth. This is further supported by the major ion chemistry.

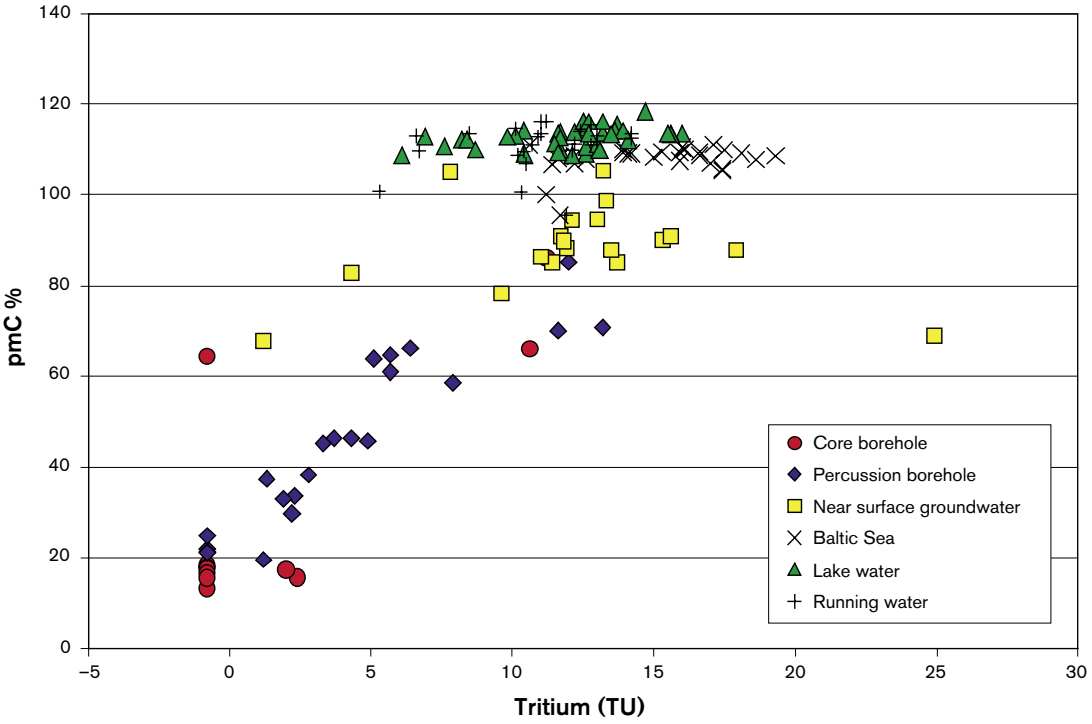

Figure 4-25. *pmC (HCO_3) versus tritium in surface and groundwaters from the Forsmark area.*

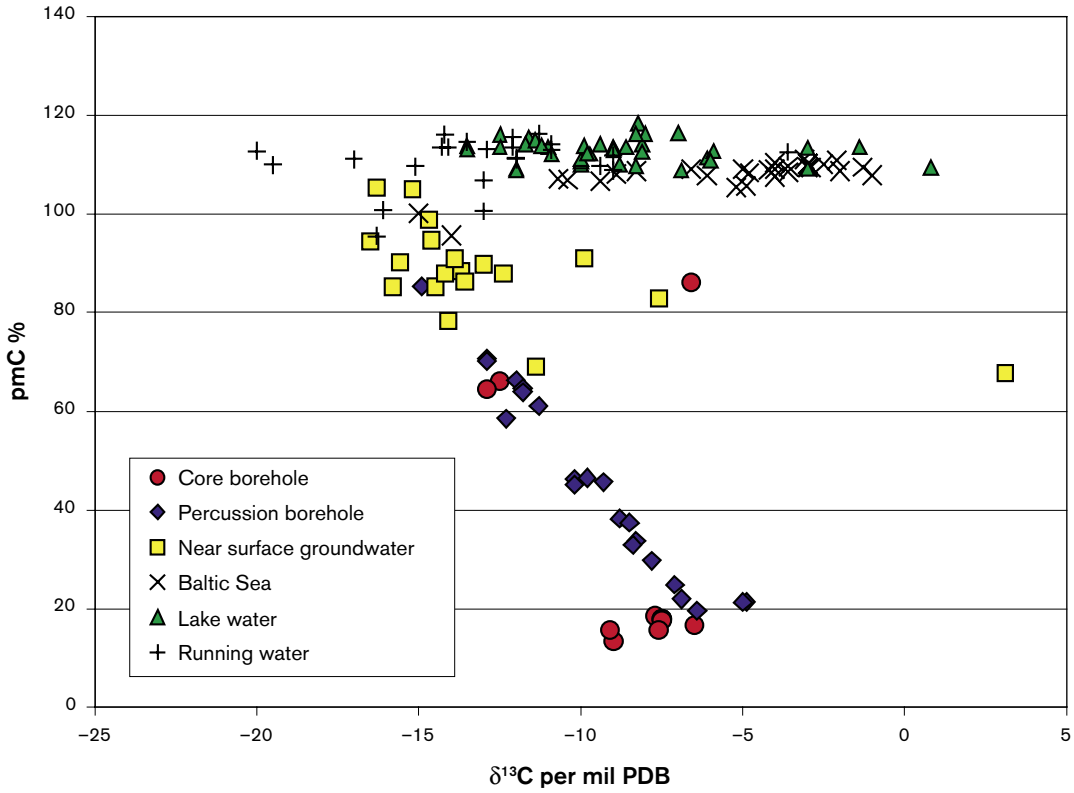

Figure 4-26. *$\delta^{13}C$ versus ^{14}C (pmC) in bicarbonates in surface and groundwaters from the Forsmark area.*

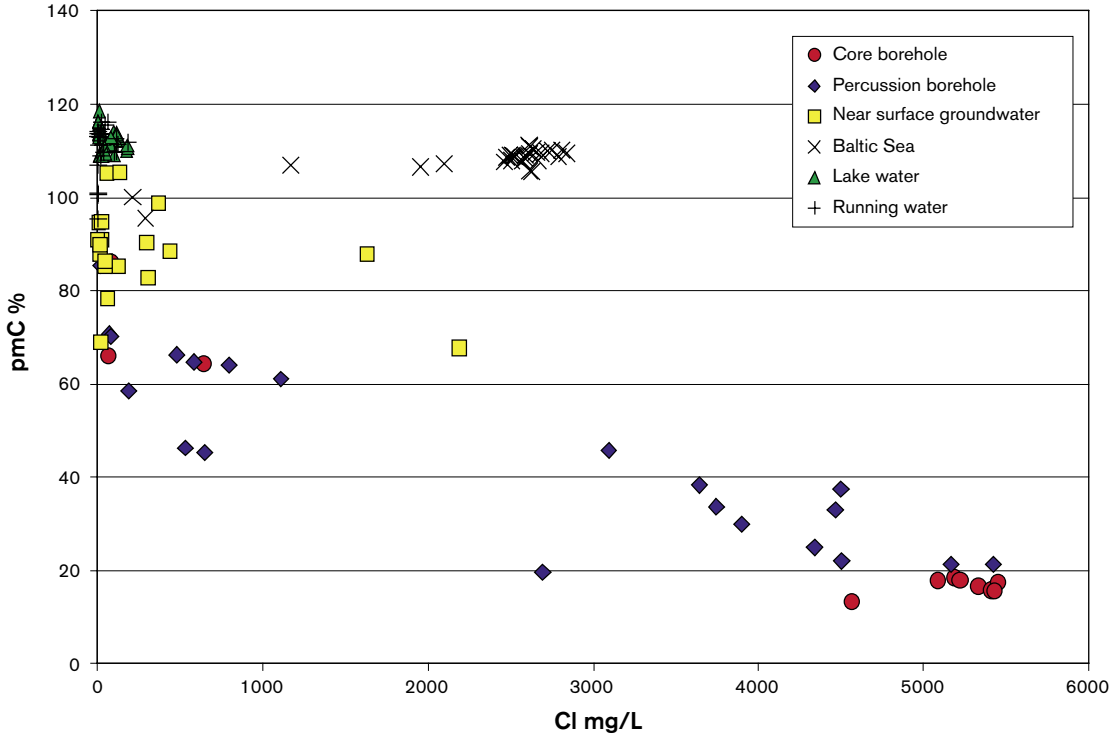

Figure 4-27. *$^{14}C(HCO_3)$ versus Cl in surface and groundwaters from the Forsmark area.*

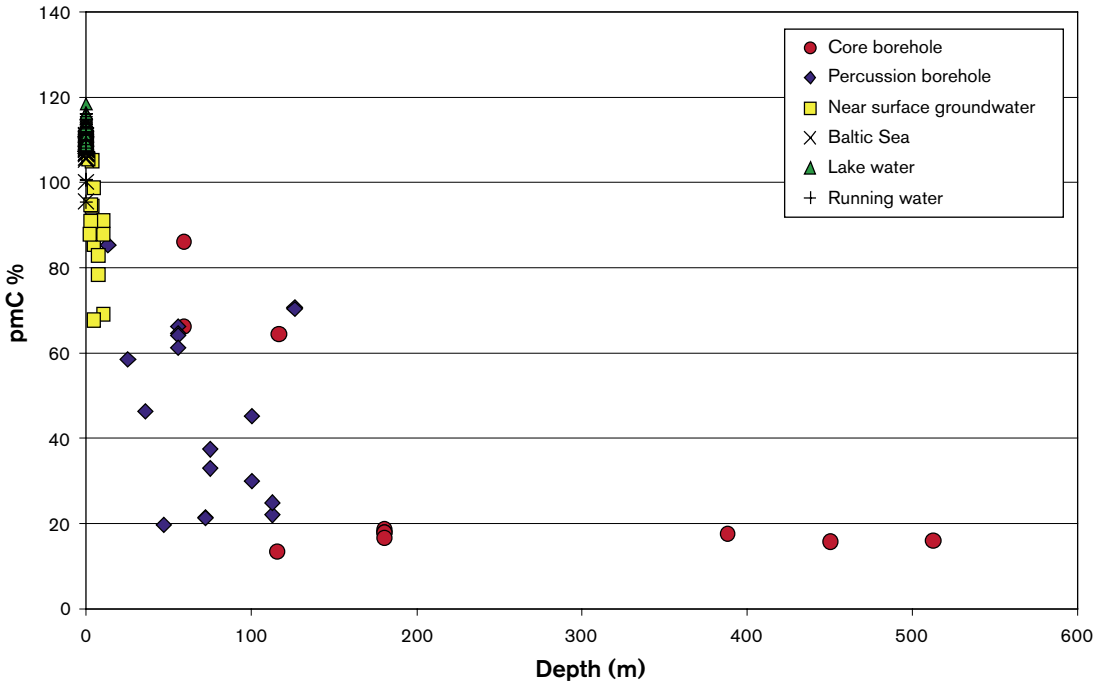

Figure 4-28. *$^{14}C(HCO_3)$ versus depth in surface and groundwaters from the Forsmark area.*

Two organic material samples from KFM01A (110 m and 177 m) have been analysed for ^{14}C resulting in values of 53.20 and 46.4 pmC respectively. These values are much higher when compared with those measured on HCO_3 samples from the same sampled borehole sections, i.e. 13.4 and 16.7 pmC respectively. Earlier interpretation of these waters as being mainly mixtures of glacial and Littorina Sea water is not contradicted by these results, but indicate also the possibility of a Littorina Sea origin for the organic material and support of a more mixed origin for the bicarbonate.

Sulphur isotopes

Sulphur isotope ratios, expressed as $\delta^{34}S$‰ CDT, have been measured in dissolved sulphate in groundwaters,, surface Lake and Stream waters and Baltic Sea waters from the Forsmark area. Some 73 analyses have been performed of which 33 are groundwaters from cored and percussion boreholes. The isotope results are plotted against SO_4 (Figure 4-29) and Cl (Figure 4-30).

The recorded values (Figure 4-29) vary within a wide range (–11 to +30‰ CDT) indicating different sulphur sources for the dissolved SO_4^{2-}. For the surface waters (lake and stream waters) the SO_4 content is usually below 35 mg/L and the $\delta^{34}S$ is relatively low but variable (–1 to +11‰ CDT) with most of the samples in the range 2 to 8‰ CDT. These relatively low values indicate atmospheric deposition and oxidation of sulphides in the overburden as being the origin for the SO_4. Unfortunately there are no isotopic analyses of sulphides in the overburden, but a few (6) $\delta^{34}S$ values of pyrites in fracture coatings have been analysed and show a large spread in values (5.4 to 31.5‰ CDT; /Sandström et al. 2004/). The Baltic Sea samples cluster around 20‰ CDT with some less saline Baltic samples showing lower $\delta^{34}S$ values resulting from inmixing of surface water.

As discussed in Appendix 1, the deeper groundwaters show $\delta^{34}S$ values in the range +12 to +26‰ CDT where all samples with SO_4 contents greater than 250 mg/L show $\delta^{34}S$ values higher than +20‰ CDT. Such values are usually interpreted to result from sulphate-reducing bacterial (SRB) activity in the bedrock aquifer. The Cl versus $\delta^{34}S$ plot (Figure 4-30) shows a clear trend with higher $\delta^{34}S$ values for groundwaters with higher salinities than present Baltic Sea waters (2,800 mg/L Cl). If the $\delta^{34}S$ values in the marine groundwaters are modified by SRB during closed conditions then a clear trend of more positive $\delta^{34}S$ values with decreasing sulphate content should be the result.

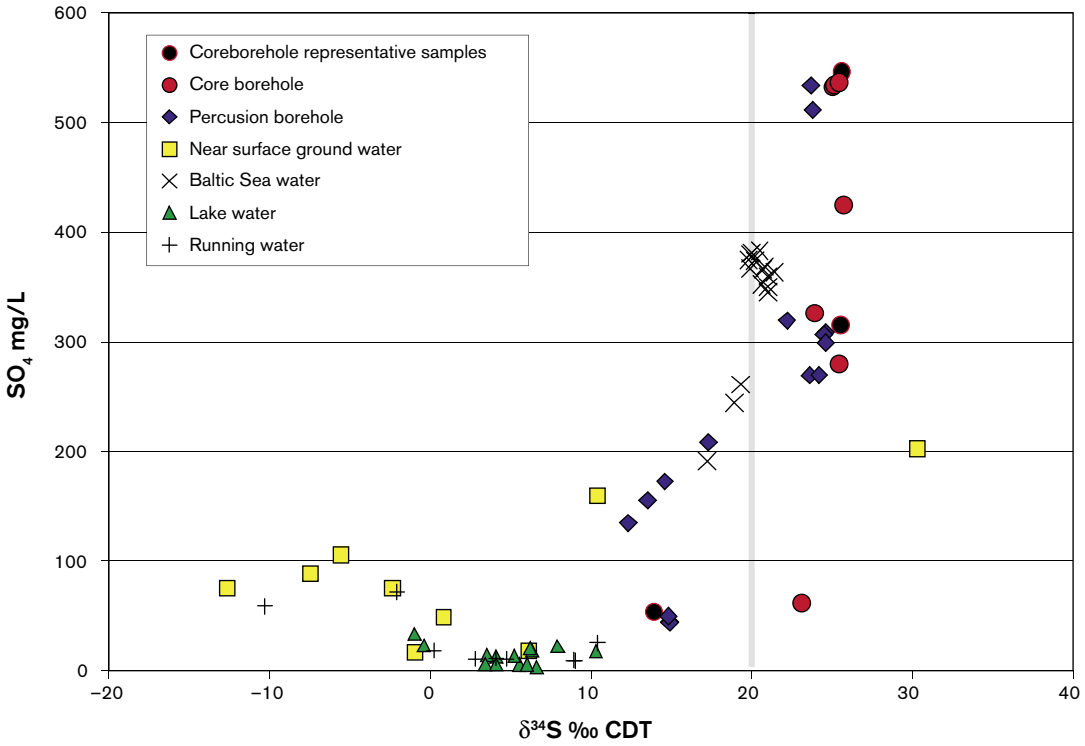

Figure 4-29. *Plot of $\delta^{34}S$ (‰ CDT) versus SO_4^{2-} content for groundwaters and surface waters from the Forsmark area. The grey line indicates the marine median value at around 20‰ CDT.*

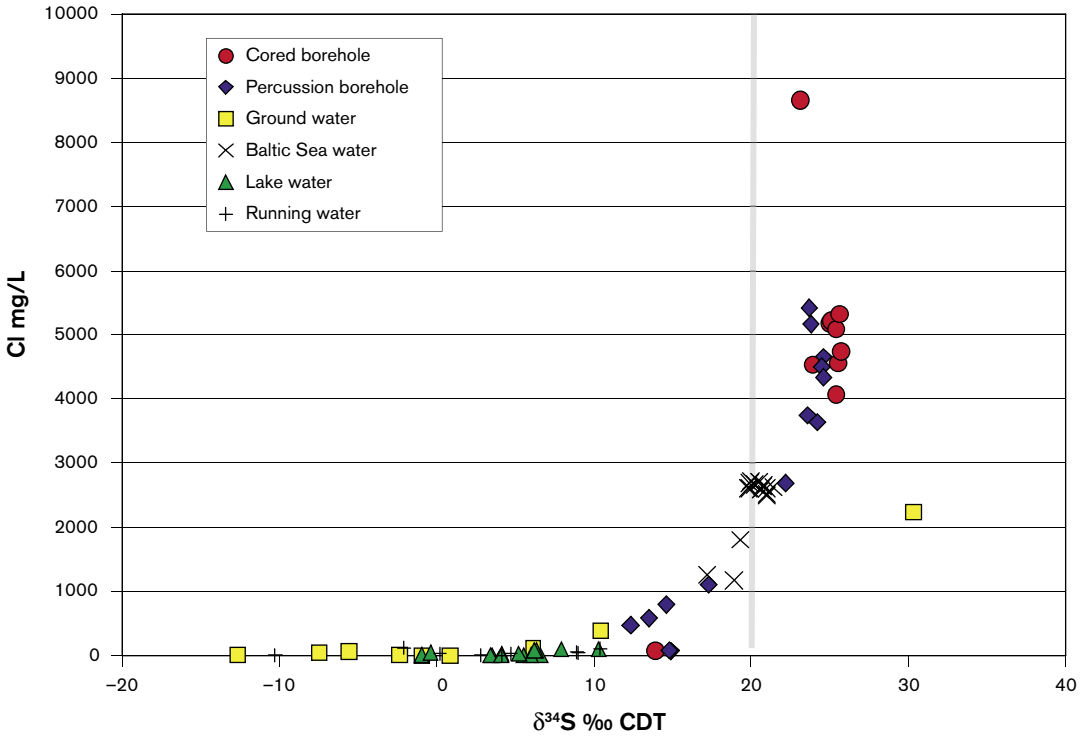

Figure 4-30. *Plot of $\delta^{34}S$ (‰ CDT) versus Cl in surface waters and groundwaters from the Forsmark area. The grey line indicates the marine value at around 20‰ CDT.*

This is not seen and therefore several processes need to be considered. The groundwater with the highest salinity showed a relatively low sulphate content (64 mg/L) and a $\delta^{34}S$ value of +23‰ CDT. However, this was a tube sample (not plotted) and is probably the product of mixing. The only identified sulphate minerals so far are minute grains of barite found in a few fracture coatings /Sandström et al. 2004/.

Amongst the Soil Pipe near-surface groundwaters, one more brackish sample (2,200 mg/L Cl) showed a relatively high $\delta^{34}S$ value (+30‰ CDT). This originates from Bolundsfjärden (sample 0012) which is believed to have a typical discharge character. Other near-surface groundwater samples showed values similar in range, or even lower, than surface waters. The cause of these very low values is not fully understood at the moment.

Strontium isotopes

Strontium isotope ratios ($^{87}Sr/^{86}Sr$) have been measured in surface waters and groundwater samples from the Forsmark area and these are plotted against Sr content in Figure 4-25. The surface waters and especially the near-surface groundwaters show large variation in Sr isotope ratios. Most of the samples show values within the range 0.718 to 0.729 whereas a few near-surface groundwaters have lower values indicating mixing with marine water and a few have significantly higher values indicating local exchange with Rb-rich minerals. The groundwaters sampled in the percussion and cored boreholes show Sr isotope ratios varying within a more narrow range (0.717 to 0.721). Some of these higher values relate to the group of four brackish groundwaters of low strontium values (cf. Figure 4-31) associated with Littorina Sea signatures.

A common way to evaluate mixing between different strontium origins is to plot 1/Sr versus $^{87}Sr/^{86}Sr$ (Figure 4-32); no significant trends can be observed. It should, however, be pointed out that relatively few deep sections have been analysed so far. The groundwaters sampled from borehole KFM01A (110–121 and 177–184 m) show somewhat higher Sr isotope ratios than the other groundwater samples which probably relates to the mineralogical compositions along the pathways. Since many of the groundwaters have dominant portions of a marine origin (i.e. Littorina Sea component), a marine input could have been expected. However, this is not recognised in the plot.

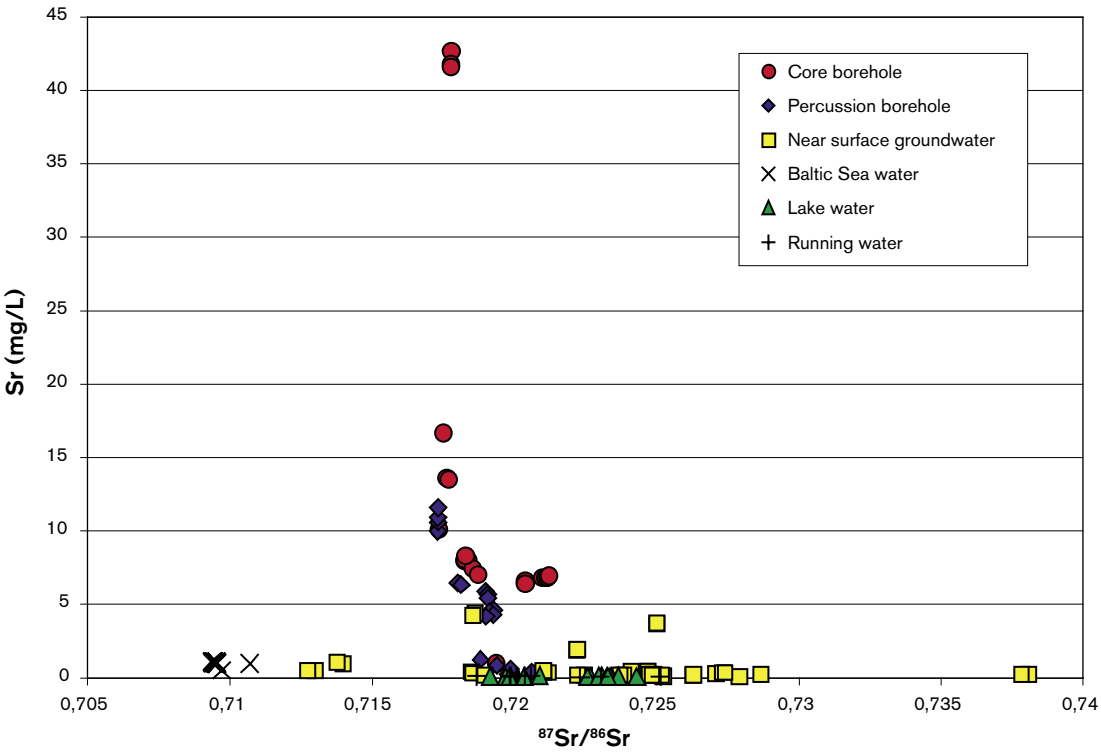

Figure 4-31. *Plot of $^{87}Sr/^{86}Sr$ ratios versus Sr for Baltic Sea waters, surface waters and groundwater samples from the Forsmark area.*

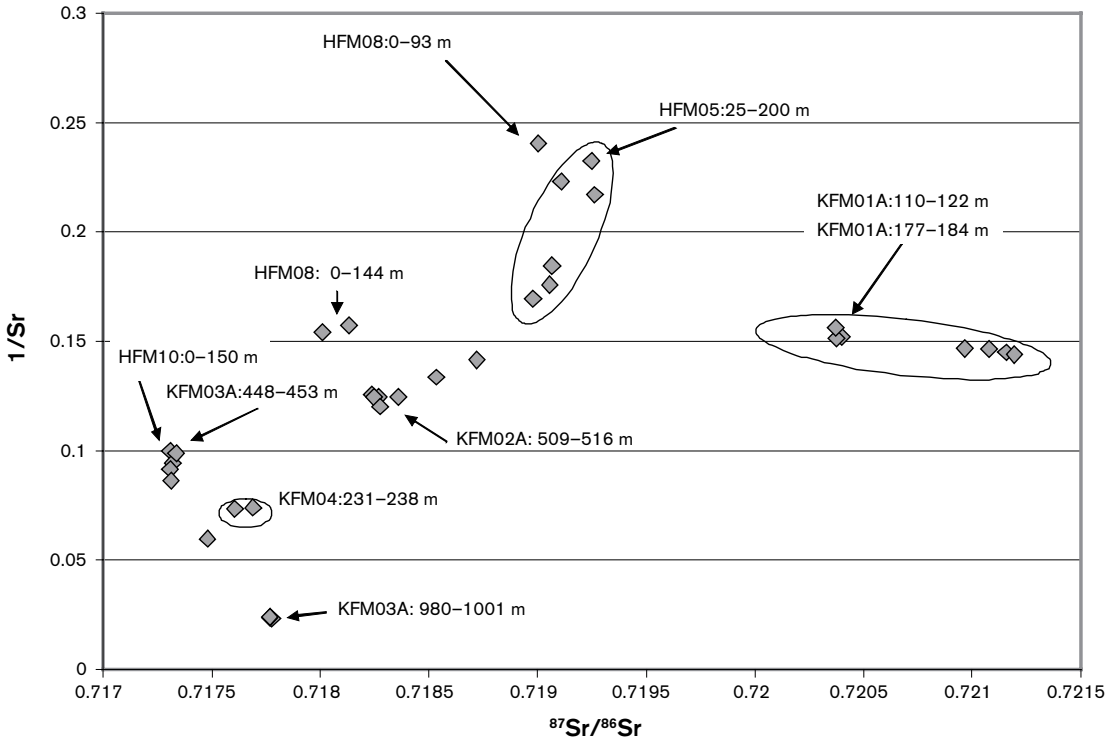

Figure 4-32. *$^{87}Sr/^{86}Sr$ ratio plotted versus 1/Sr in groundwater samples from the Forsmark area.*

From the calcium versus strontium diagram for the groundwater samples (Figure 4-33), calcium and strontium correlate and both have been added to the original Na-Cl dominated water so that the original Sr content (~ 2 mg/L, i.e. twice the values measured in present day Baltic Sea) has increased to 6–10 mg/L Sr. Leaching of minerals and ion exchange are the reason for this.

In conclusion, the strontium isotope values of surface and near-surface waters show relatively large variations in isotope ratios whereas the deeper groundwaters vary within a more limited range. All the isotope values deviate from those measured in the Baltic Sea samples in that they have higher radiogenic strontium which in turn is due to water/rock interaction, probably to a large part ion exchange processes.

The relatively few fracture calcites so far analysed for Sr-isotopes show values below 0.718 supporting that they are not precipitated from today's groundwater and that calcite dissolution has had little influence on the Sr-isotope ratios in the groundwater. Other minerals are more important and analysis of fracture minerals and host rock samples is recommended to achieve a better understanding of the Sr (and Ca) system.

Figure 4-34 compares the Forsmark site with the Simpevarp, Laxemar and Ävrö sites, together with modern Baltic Sea waters. The relatively small variation in Sr-isotope ratios within each area suggests that ion exchange with clay minerals along the flow paths is an important process. For the Laxemar-Simpevarp sites there is a tendency towards higher contents of radiogenic Sr in the groundwaters with highest salinities (and thus highest Sr content). It is not, however, possible from the few data available to give any explanation for this. There seems not to be any major change in mineralogy that can explain a shift, but one possibility may be the increased residence times for these waters leading to more extensive mineral/water interactions. The higher $^{87}Sr/^{86}Sr$ ratios in the Forsmark samples are most probably due to differences in the composition of the bedrock and fracture minerals compared to Simpevarp. The possibility of tracing marine components using Sr-isotopes is often discussed; however clay minerals in the fractures may question such interpretations. For example, the strong Littorina Sea imprint in the Forsmarks waters has not resulted in any detectable marine Sr isotope values in the groundwaters. Instead, modification of the Sr isotope values probably by ion exchange has taken place.

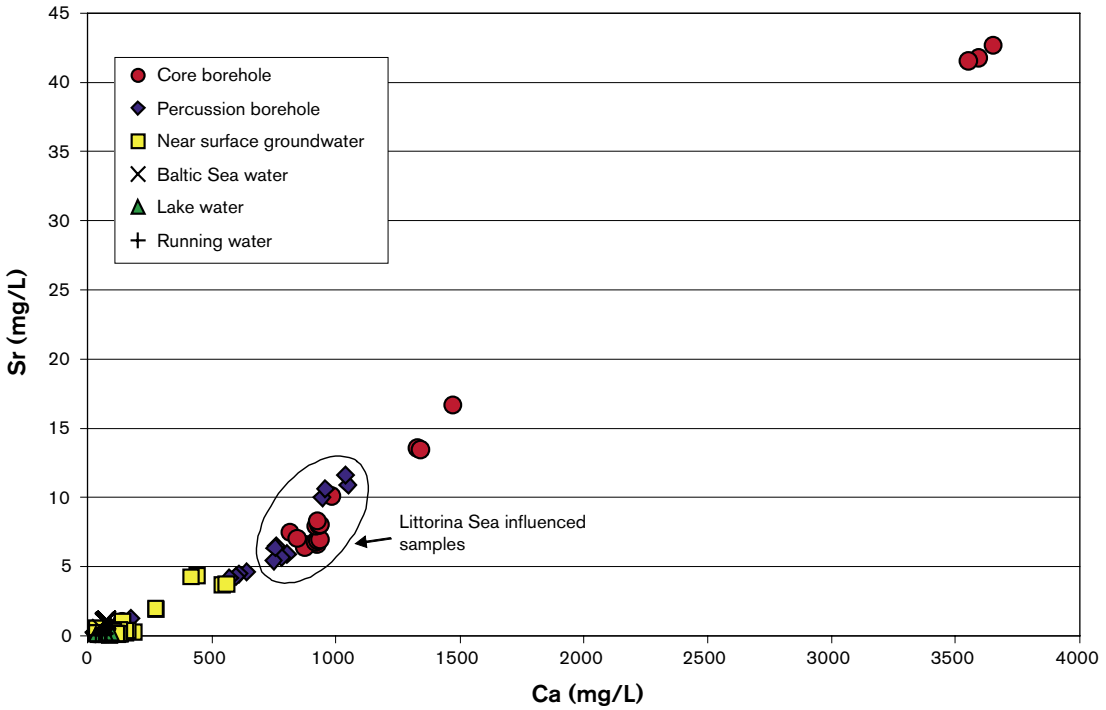

Figure 4-33. *Sr versus Ca in surface waters, Baltic sea waters and groundwaters from the Forsmark area.*

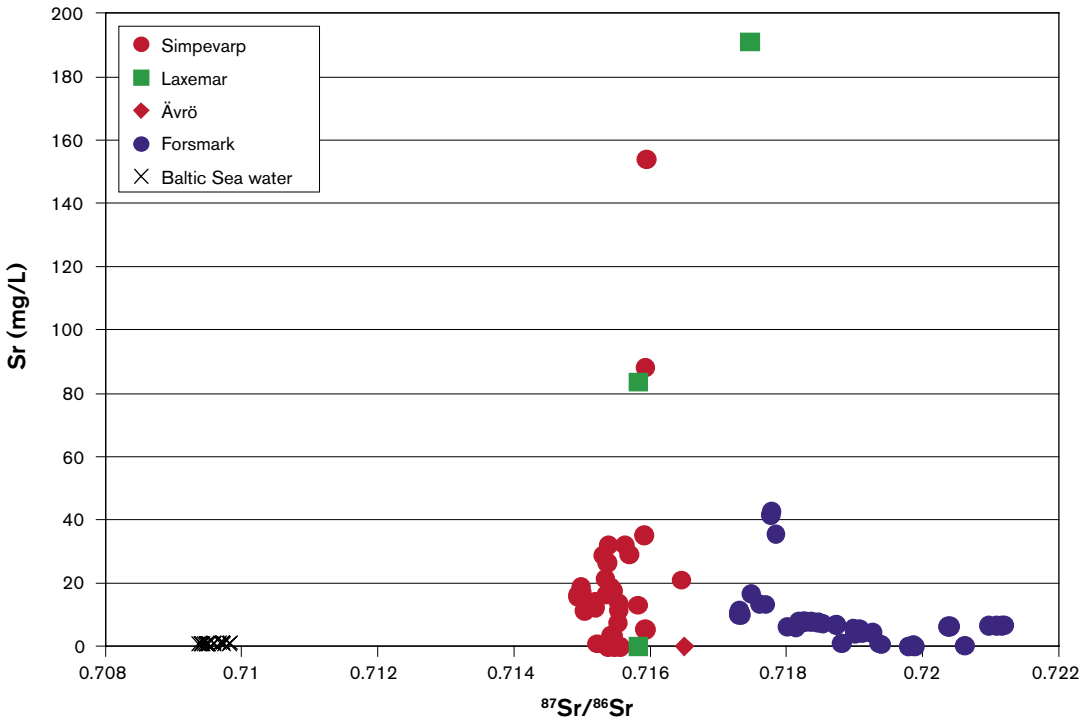

Figure 4-34. *$^{87}Sr/^{86}Sr$ versus Sr for groundwaters from Forsmark, Simpevarp, Laxemar and Ävrö. Baltic Sea waters sampled from the Forsmark and Laxemar/Simpevarp sites are also plotted.*

Chlorine isotopes

Stable chlorine isotopes have been analysed in waters from the Forsmark area and the results are plotted against chloride Figure 4-35. This shows that most of the surface and Baltic Sea waters have values within the range –0.28 to +0.34‰ SMOC. The surface waters and the near-surface groundwaters have the greatest spread (–06 to +2‰ SMOC) where most of the samples are within the interval –0.2 to +05‰ SMOC. The majority of the Baltic Sea samples values are close to 0‰ SMOC or slightly higher (up to +0.3‰ SMOC), a few samples show also lower values down to –0.6‰ SMOC.

Waters from the cored and percussion boreholes are between –0.2 to +0.6‰ SMOC and demonstrate no relation with increasing chloride content. Given the analytical uncertainty of around ±2‰ SMOC /Frape et al. 1996/, the groundwater values correspond to a slight emphasis on a water/rock origin.

The $\delta^{37}Cl$ values in groundwaters from Forsmark and Laxemar/Simpevarp have been compared with chloride (Figure 4-36) together with additional Baltic Sea samples from the Simpevarp area. For brackish groundwaters with chloride contents around 5,000 mg/L there is a large variation in $\delta^{37}Cl$ values; most of the Forsmark samples have slightly negative values whereas the Simpevarp samples have values on the positive side. In groundwaters with higher chloride contents (> 6,000 mg/L) the Simpevarp and Laxemar samples have values higher than 0.3‰ SMOC. The Forsmark sample (only one available so far) shows 0.09‰ SMOC.

Br/Cl versus $\delta^{37}Cl$ (Figure 4-37) show that waters significantly enriched in bromide compared to marine waters display positive $\delta^{37}Cl$ values. The groundwaters at Forsmark, characterised by marine Br/Cl ratios, also cluster around 0‰ SMOC, although a similar spread is also shown by the Baltic Sea samples.

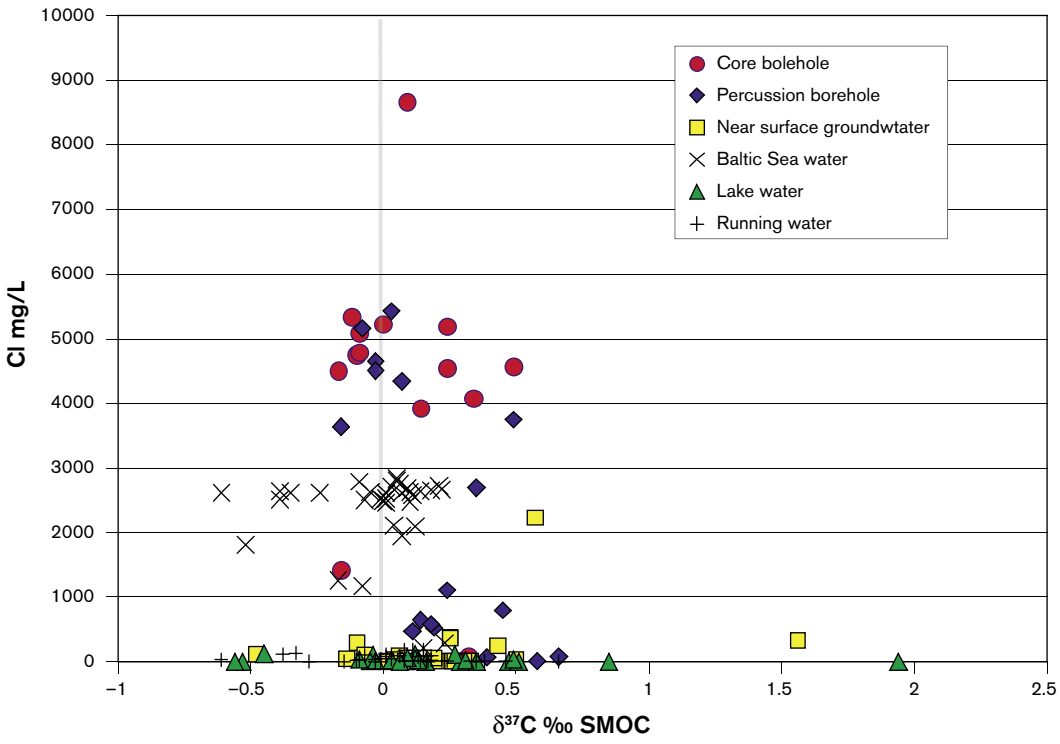

Figure 4-35. *$\delta^{37}Cl$ (expressed as per mille deviation from the standard SMOC) versus Cl in surface waters, groundwaters and Baltic Sea waters from Forsmark.*

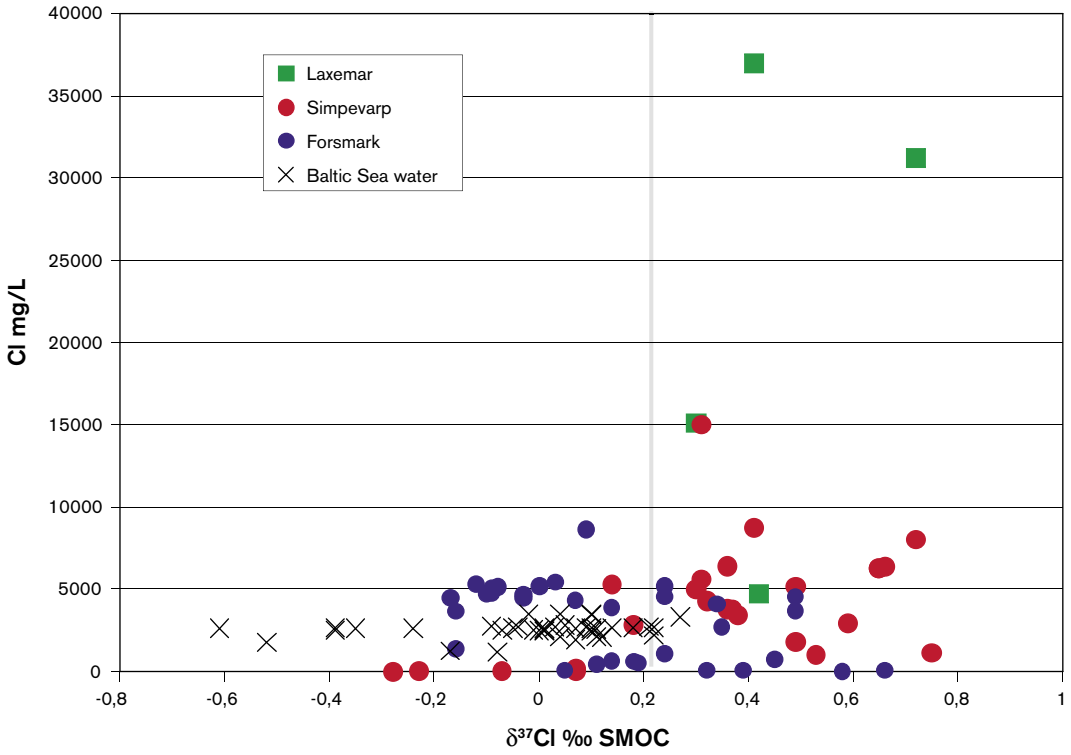

Figure 4-36. *$\delta^{37}Cl$ versus Cl in groundwaters from Forsmark and Laxemar/Simpevarp and Baltic Sea waters from Simpevarp and Forsmark.*

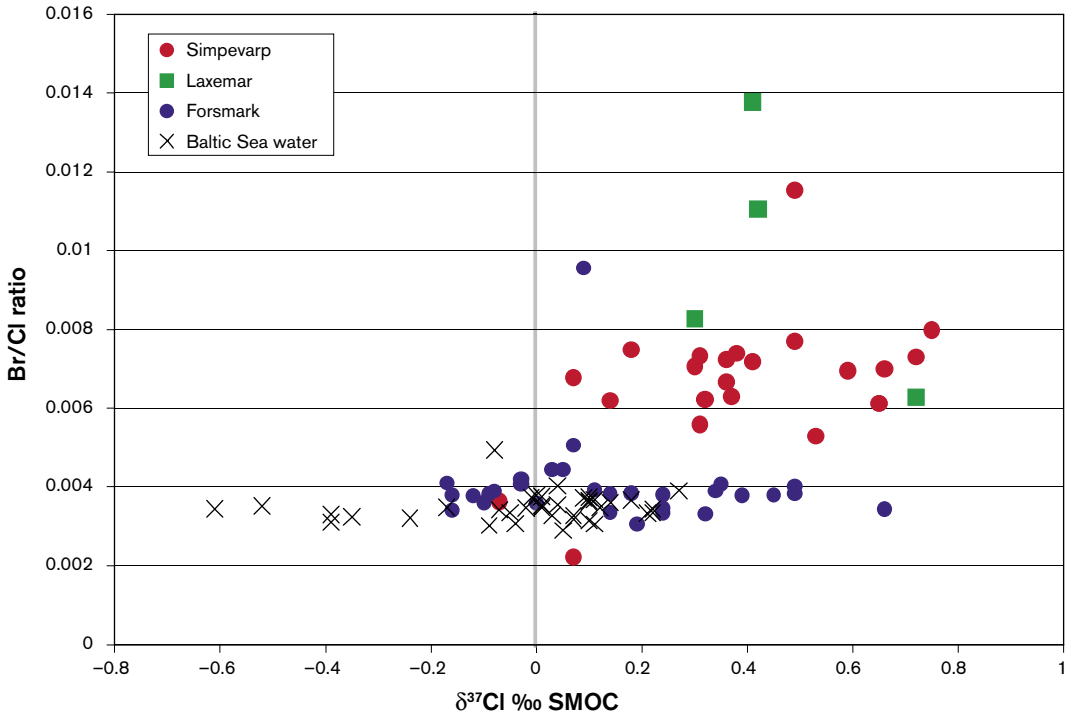

Figure 4-37. *$\delta^{37}Cl$ versus Br/Cl in groundwaters from Forsmark and Laxemar/Simpevarp and Baltic Sea waters from Simpevarp and Forsmark.*

Trace elements

Only a few data exist for the majority of groundwaters and even some of these are incomplete (cf. Appendix 1). The following was concluded from the evaluation:

Li, Rb and Cs (and to a lesser extent Y) from the cored and percussion boreholes show a sharp increase from low values (shallow surface to near-surface waters) to high values at approx. 100 m depth. This is followed by a levelling off (i.e. in the brackish groundwaters) until around 500 m when a decrease to moderate values occurs. Strontium, whilst reflecting a similar trend for the upper 500 m, increases significantly towards depth.

La and Ce from the cored and percussion boreholes are close to detection apart from approx. 400–500 m depth when a significant peak can be observed.

Shallow groundwaters from the Soil Pipes show a wide range of values for Ce, La and Y.

Calcites

In order to sort out different calcite generations and to provide palaeohydrogeological information 54 samples have been analysed for $\delta^{13}C$/ $\delta^{18}O$, of which 16 were selected for $^{87}Sr/^{86}Sr$ and a smaller set (7 samples) analysed for chemical composition. The calcites represent examples from both sealed and open fractures. In some of the latter it has been possible to sample calcites formed in open spaces and showing euhedral crystal forms. When possible, observations have been noted on crystal morphology since a correlation has been demonstrated between calcite morphology (long and short C-axis) and groundwater salinity. Most of the Forsmark calcites (from depths between 0–500 m) show short C-axis and equant crystal forms, indicating fresh or brackish water precipitates.

A sequence of at least three different calcite generations, which can be correlated to the fracture mineralogical subdivision, has been documented. These are:

Hydrothermal calcites with mostly low $\delta^{18}O$-values (down to –18‰) and high $\delta^{13}C$ (–5 to –2‰). These calcites are found together with prehnite and laumontite and thereby support a close relationship between these two generations (Generation 2 and 3). Support that these two generations form part of the same prolonged event is indicated by the tailing in $\delta^{18}O$ from –18 to at least –14‰. This may be due to precipitation from a hydrothermal fluid during decreasing temperatures and/or changes in water-rock ratio during a hydrothermal event. The connection between the calcite in the prehnite and laumontite generations are in accordance with earlier observations from Finnsjön.

Calcites with extremely low $\delta^{13}C$ values (down to –36‰) and $\delta^{18}O$ values of around –12‰. These are found together with quartz fracture coatings (Generation 4). These mineralisations must have been precipitated during lower temperatures than the preceding laumontite formation, although it is reasonable to assume that it was still hydrothermal (< 200°C is suggested). The very low $\delta^{13}C$ values are usually interpreted as due to in-situ microbial activity which implies that the temperature was not significantly above 100°C when the carbon isotope signature was modified. However, the temperature evolution during this period of fracture mineralisation is not yet known. Based on Sr-isotope values this period is clearly separated from the prehnite-laumontite formation, either in time (the radiogenic ^{87}Sr is much higher in the latter generation), or the chemistry of the hydrothermal fluid was significantly different and preferred dissolution of K-Rb minerals occurred.

Euhedral calcites formed possibly as the latest phase on the quartz adularia coatings; usually found together with pyrite (Generation 5). $\delta^{18}O$ values range from –11 to –10‰ and the $\delta^{13}C$-values are in the range of –18 to –20‰.

It has not been possible yet to relate several calcite precipitates to any specific fracture mineralisation event. For example, a group of calcites from borehole KFM02A (110–118 m) shows significantly positive $\delta^{13}C$ values (+6 to +8‰) and $\delta^{18}O$ values of –8 to –11‰. There is also a cluster of samples that may include relatively late (Quaternary) fresh water precipitates. More analyses are therefore needed in order to better identify this group. For further discussion see Appendix 1.

Microbes

Microbes have been evaluated from the Forsmark site (Appendix 2) and Figure 4-38 shows the distribution of the different microbial groups found at the six sampled levels in Forsmark and the measured intervals of redox potentials. The redox potentials varied from –140 to –250 mV but there is no obvious connection between these values and depth within the dataset.

To the right in Figure 4-38 is a so-called redox ladder with different microbial respiration redox couples placed at their respective E_0' intervals. The vertical red line in this figure marks the redox interval measured at Forsmark. These redox values coincide with the positions where iron-, manganese- and sulphate-reducers, together with methanogens and acetogens, can be found. They correlate very well with the most probable number (MPN) results for this area.

Figure 4-39 shows also the MPN numbers but in relation to depth. Here it can be seen that iron- and manganese reducers only are present at shallow depth, above 300 metres. These groups are absent at greater depth where methanogens, acetogens and SRB dominate. However it must be remembered that there are no data of methanogens available from KFM01A, 115.4 and 180.4 m. The overall picture of the distribution with depth is therefore incomplete.

Figure 4-40 shows a schematic representation of the biogeochemical redox variation related to the 6 groundwater sampling levels in boreholes KFM01A, KFM02A and KFM03A. In the shallow levels represented by KFM01A, the iron- and manganese-reducing bacteria dominate and this correlates well with the measured redox values at this depth. Here the sulphate-reducing bacteria (SRB) were absent.

Sulphate-reducing bacteria, on the other hand dominate at the deepest levels, represented by KFM03A, together with acetogens. These two groups could have established a relation where SRBs utilise acetic acid produced by the acetogens. The same kind of relationship has been suggested by /Pitkänen et al. 2004/ to exist in deep groundwaters at Olkiluoto but for methanogens and SRB. That sulphate-reducing bacteria can oxidise methane anaerobically with sulphate as electron acceptor has still to be proved, but environmental studies suggest that this microbial reaction really does exist.

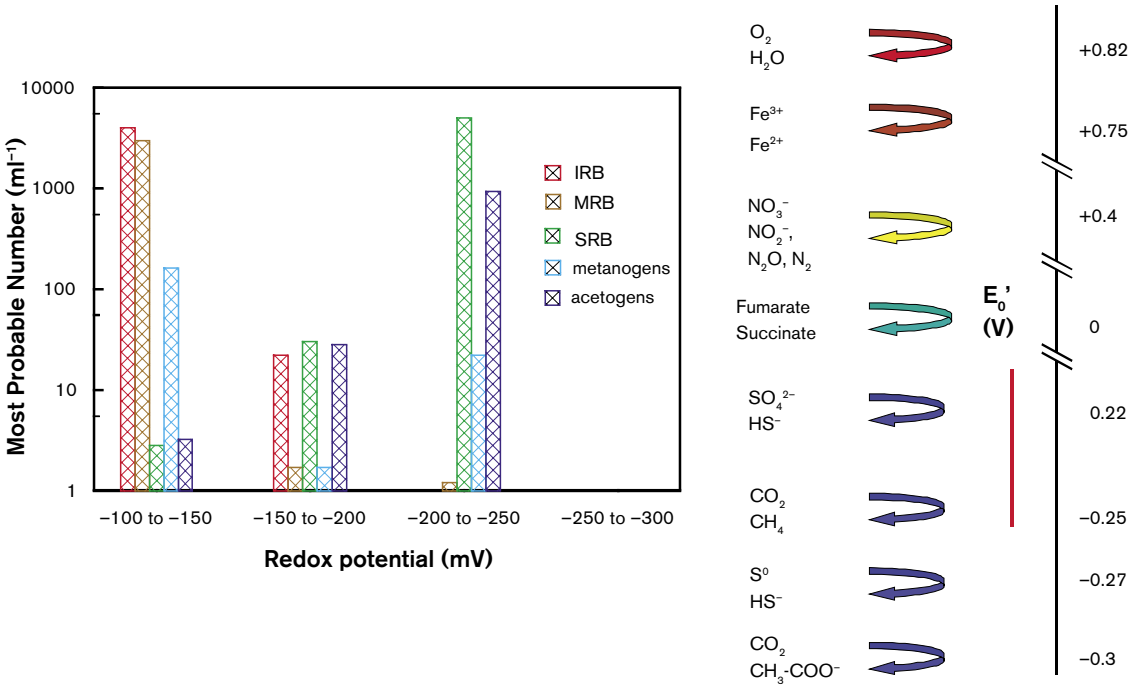

Figure 4-38. *The sums of the most probable number (MPN) of microorganisms versus intervals of redox values in borehole groundwaters from the Forsmark area.*

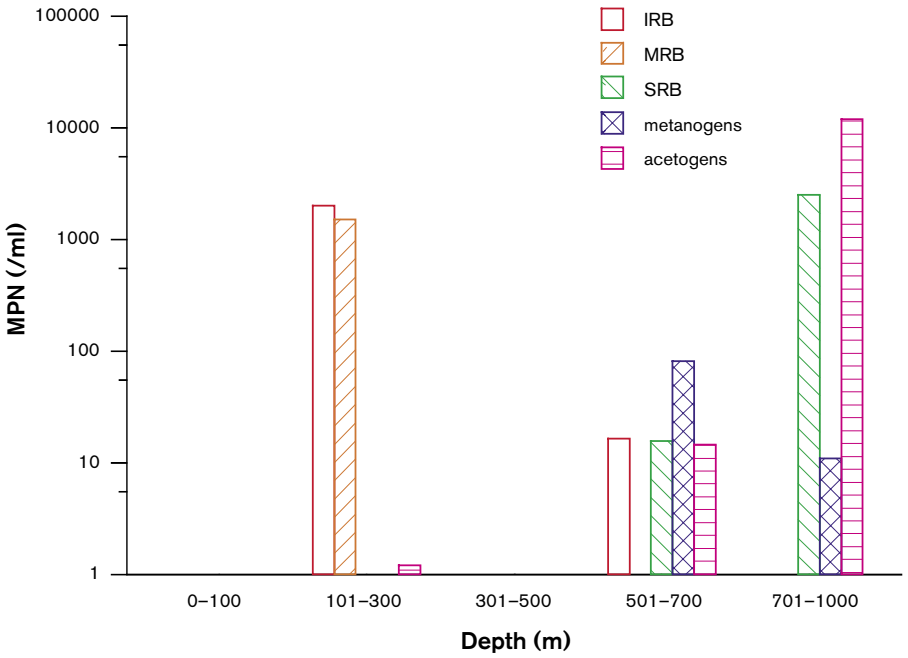

Figure 4-39. *The sums of the most probable number (MPN) of microorganisms versus depth interval in borehole groundwaters from the Forsmark area.*

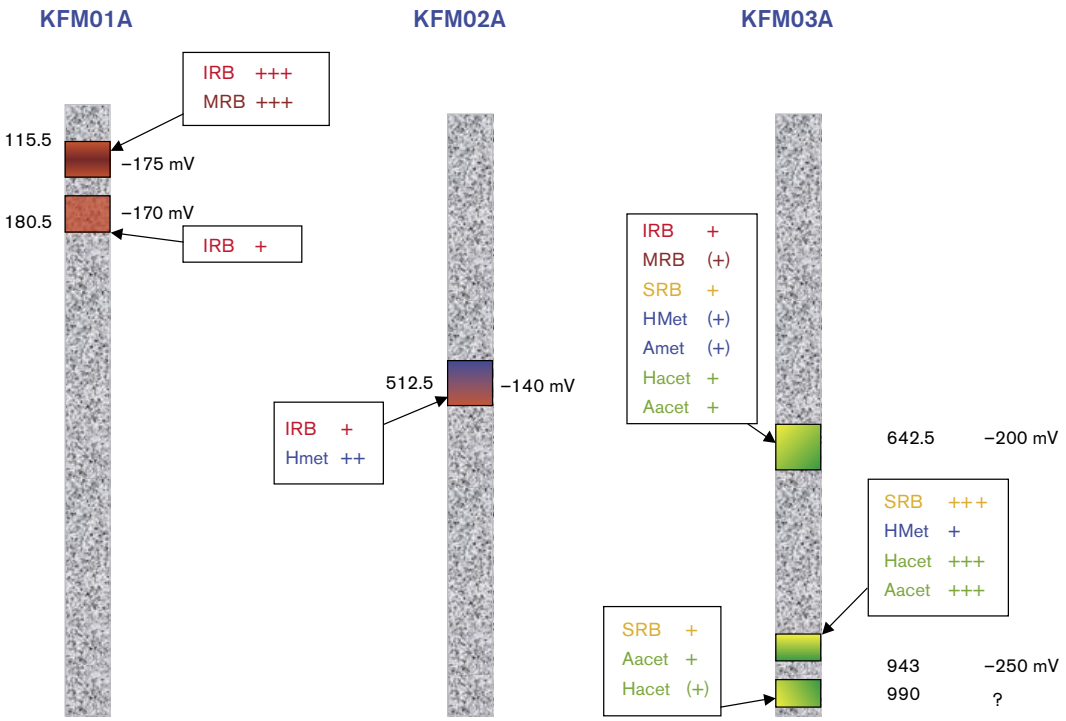

Figure 4-40. *Schematic representation of the biogeochemical redox variation related to the 6 groundwater sampling levels from three boreholes in the Forsmark area.*

At intermediate levels (i.e. KFM02A, 512.5 m and KFM03A, 642.5 m) the microbial populations seem to be more diverse and not dominated by any special group or groups. If the flow in these sections is low and no mixing of groundwater occurs the beneficial electrochemical gradients will not be establish and therefore the activity of certain microbial groups will be less.

Colloids

Colloid compositional data have been evaluated from the Forsmark site (Appendix 2). Figure 4-41 shows the composition of the colloids sampled from different depths in the three boreholes; sulphur is shown also. No data from KFM02A are shown because of broken filters. In Figure 4-42 the sulphur values have been omitted and in both figures the calcite is omitted since it is considered as an artefact due to pressure changes during sampling.

In Figure 4-41 and Figure 4-42 it can be seen that manganese oxides are very rare in all of the three boreholes; small amounts were found in KFM03A only. Significant iron oxides were found in KFM01A and aluminium, here represented as K-Mg-Illite, was present at all sampling depths although this may also be an artefact from borehole drilling. The amount of calcium is not high in any of the samples.

The filtration data available seems to agree with the numbers of colloids earlier reported from Äspö and Bangombé in Gabon /Laaksoharju et al. 1995; Pedersen, 1996/. The new sampling and filtering methods seem to have worked well since the amounts of calcium carbonates were very low. This suggests a rethinking of the sulphur colloids since they might have initially existed as colloids present in the groundwater and then probably as iron sulphides. The silicon values from KFM01A, 115.4 m most likely represent sampling artefacts.

The fractionation data show that there should not be any colloids in the size range < 1,000 D but < 5,000 D. Although this is in contradiction to the filtration results, they could be closer to the truth. There are no sulphur values reported from this method; it would be interesting to carry out a comparison with the filtration method since the presence of iron sulphides could be one explanation for the low sulphide values found in groundwater, even if SRBs were present (cf. Appendix 2).

Data for the numbers of particles could increase the value of colloid analyses by making it possible to calculate the number of binding sites for radionuclides in the different colloid fractions.

Comparison of the two methods, filtration and fractionation, needs to be further evaluated (cf. Appendix 2).

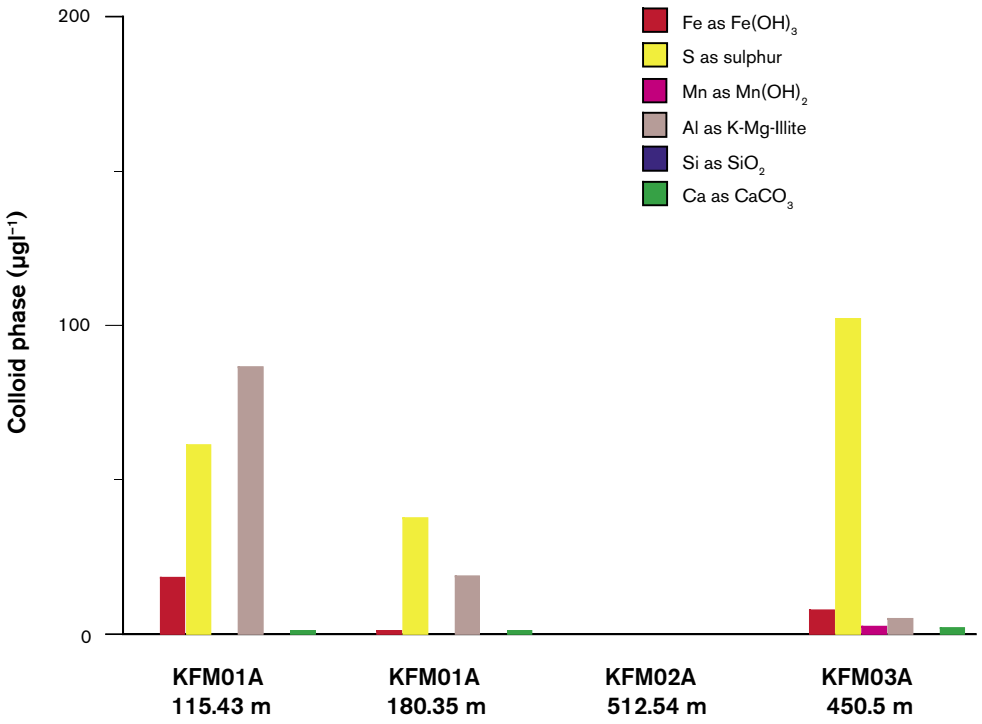

Figure 4-41. *The composition of colloids sampled from boreholes KFM01A, KFM02A and KFM03A in the Forsmark area. Calcite is omitted in this figure and also the values of silica in borehole KFM01A, 115.4 m.*

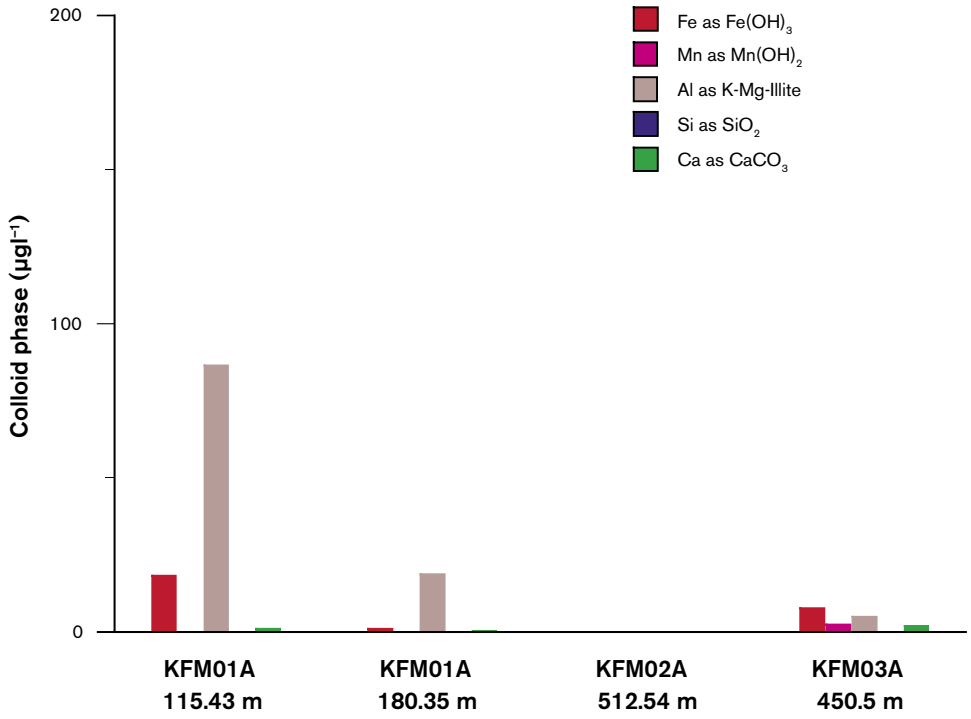

Figure 4-42. *The composition of colloids sampled from boreholes KFM01A, KFM02A and KFM03A in the Forsmark area. Calcite sulphur values are omitted and also the values of silica in borehole KFM01A, 115.4 m.*

Gas

The gas contents were analysed in groundwaters sampled from 5 depths in boreholes KFM01A, KFM02A and KFM03A (Appendix 2). Up to 12 gases were analysed: helium, argon, nitrogen, carbon dioxide, methane, carbon monoxide, oxygen, hydrogen, ethyne, ethene, ethane and propane. Figure 4-43 shows the total volume of gas for all groundwater samples versus depth; a clear linear correlation is indicated. An increasing amount of gas with depth is observed with the greatest volume, 127.5 ml l^{-1}, originating from the deepest level at 990.6 m in KFM03A. In comparison, the shallowest groundwater recorded 57.8 ml l^{-1} gas.

As an example Figure 4-44 shows that the amount of nitrogen, the dominating gas in all the groundwaters, increases with depth reflecting the overall total gas distribution. This corresponds to the gas content in groundwaters recorded from Olkiluoto, Finland, which also showed an increasing trend with depth down to 1,100 m /Pitkänen et al. 2004/. The highest nitrogen concentration measured at Forsmark was 4.7 mM (KFM03A: 990.5 m) and the lowest was 2.4 mM (KFM01A: 180.4 m).

Helium concentrations in the Forsmark area showed similar depth trends to nitrogen, varying between 460 µM and 924 µM , a trend also reflected at Olkiluoto. The origin of nitrogen and helium in the groundwaters is considered to result from crustal degassing of the bedrock; helium ca also be produced by radioactive decay in the bedrock. For more details see Appendix 2.

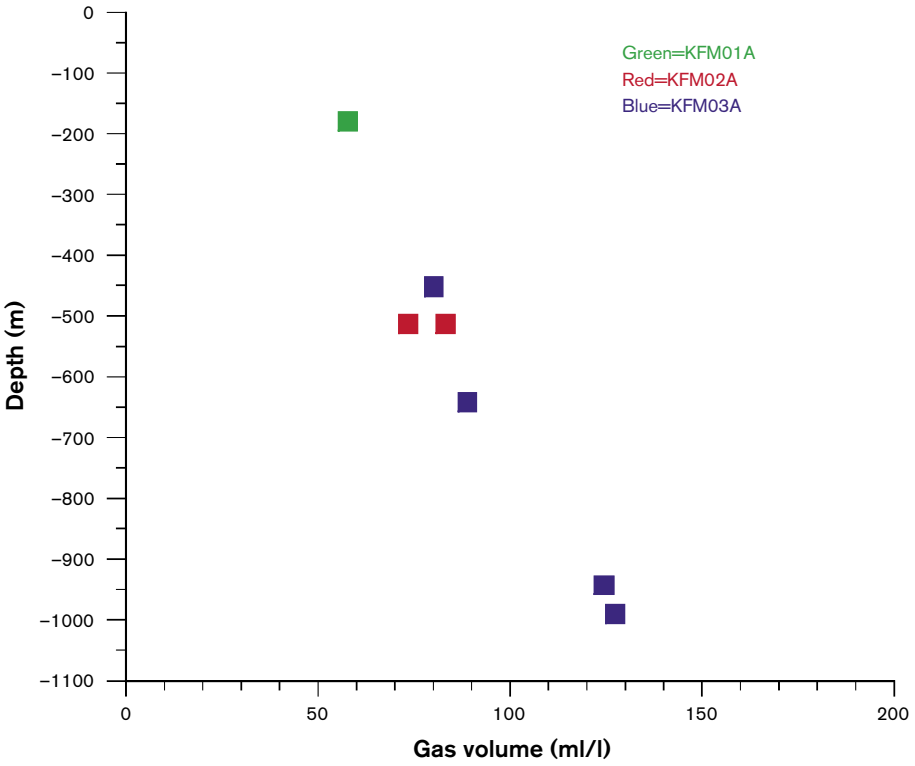

Figure 4-43. *Total volume of gas for samples from groundwaters in the Forsmark area.*

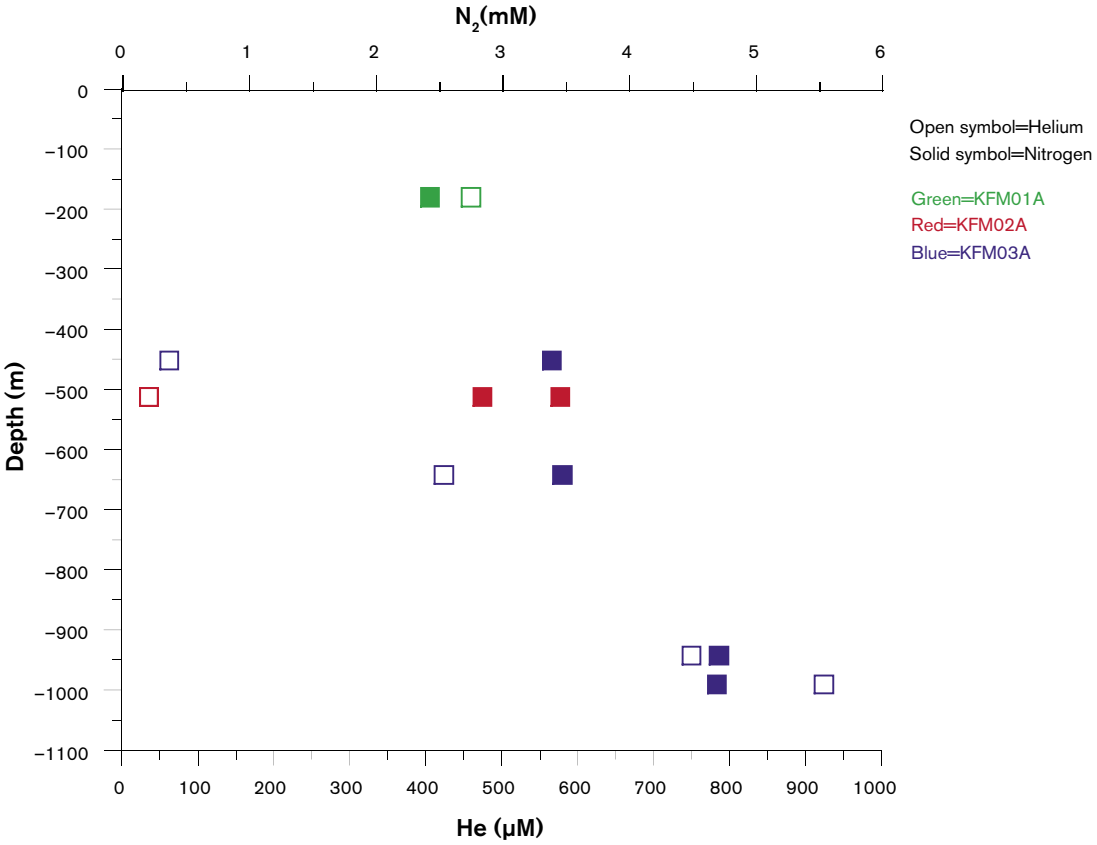

Figure 4-44. *Nitrogen and helium versus depth in groundwater samples from boreholes in the Forsmark area.*

4.3 Modelling assumptions and input from other disciplines

The main modelling assumption is that the obtained groundwater compositions are a result of mixing and reactions including different water types. The water types are a result of palaeohydrogeological events and modern hydrodynamic conditions (see Figure 3-1). A schematic presentation of how a site evaluation/modelling is performed, its components, and the interaction with other geo-scientific disciplines, is shown in Figure 4-45. The methodology applied in this report is described in detail by /Smellie et al. 2002/.

For the groundwater chemical calculations and simulations the following standard modelling tools were used:

For evaluation and explorative analyses of the groundwater:

- AquaChem: Aqueous geochemical data analysis, plotting and modelling tool (Waterloo Hydrogeologic).

Mathematical simulation tools:

- PHREEQC with the database WATEQ4F: Chemical speciation and saturation index calculations, reaction path, advective-transport and inverse modelling /Parkhurst and Appelo, 1999/.
- M3: Mixing and Massbalance Modelling /Laaksoharju et al. 1999/.
- Flow and reactive transport simulations: CORE^{2D} /Samper et al. 2000/.

Visualisation/animation:

- TECPLOT: 2D/3D interpolation, visualisation and animation tool (Amtec Engineering Inc.)

Hydrogeochemical modelling involves the integration of different geoscientific disciplines such as geology and hydrogeology. This information is used as background information, supportive information or as independent information when models are constructed or compared (cf. Appendix 5).

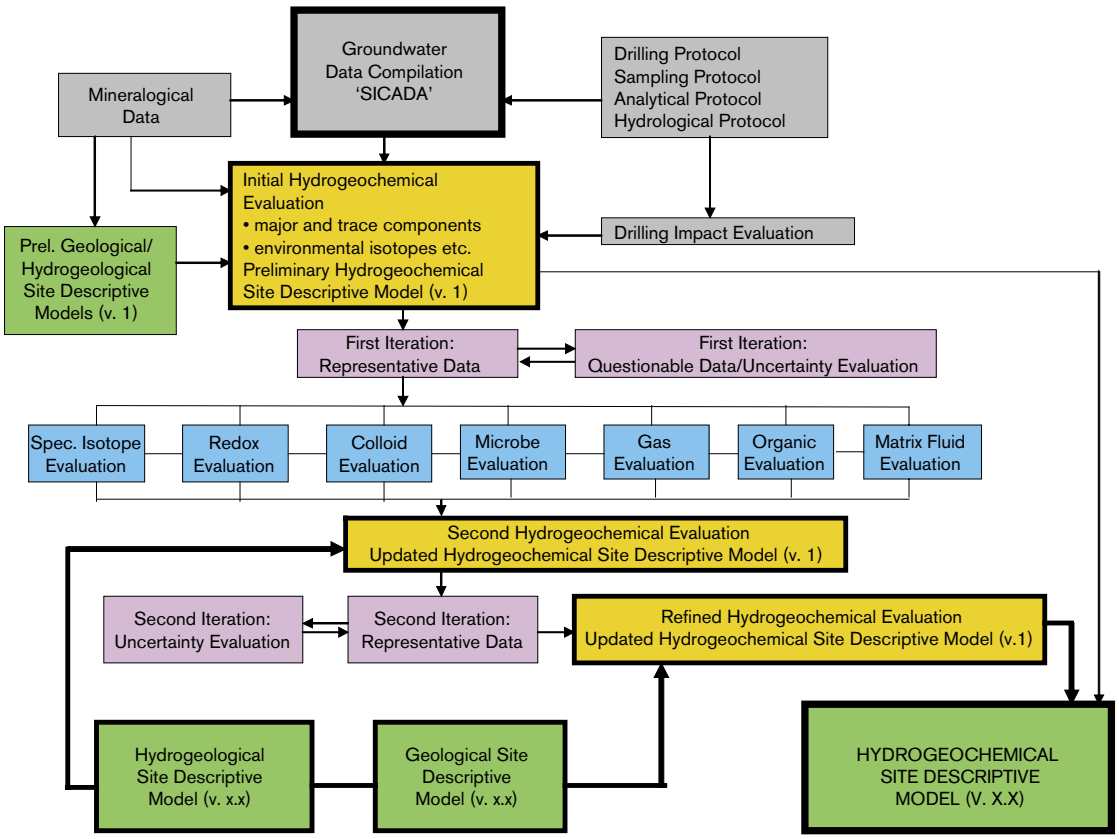

Figure 4-45. *The evaluation and modelling steps used in this report /after Smellie et al. 2002/.*

Geological information is used in hydrogeochemical modelling as direct input in mass-balance modelling but also to judge the feasibility of the results from, for example, saturation index modelling. For this particular modelling exercise geological data were summarised, the information was reviewed and the relevant rock types, fracture minerals and mineral alterations were identified (cf. Appendix 1 and 3).

The underlying geostructural model provides important information of water-conducting fractures used for the understanding and modelling of the hydrodynamics. The cross section used for visualisation of groundwater properties is generally selected with respect to the geological model and the hydrogeological simulations (cf. Appendix 1 and 4). The available hydrogeological information and the results from hydrogeological modelling are directly used in the coupled flow and transport modelling (cf. Appendix 5). The measured values of Cl, ^{18}O, ^{2}H, ^{14}C and the results from the M3 mixing calculations were provided as input data for hydrodynamic modelling simulations (cf. Appendix 4).

4.4 Conceptual model with potential alternatives

The alternative conceptual models tested included different reference waters and local and regional models and different mathematical solutions to calculate the mixing proportions (cf. Appendix 4); various modelling tools and approaches were applied on the data set. In addition, the concept where the obtained water composition is modelled by using PHREEQC and the M4 approach, is discussed in Appendix 3.

4.5 Hydrogeochemical modelling, mass-balance and coupled modelling

4.5.1 Hydrogeochemical modelling

Hydrogeochemical modelling has been carried out with PHREEQC /Parkhurst and Appelo, 1999/ using the WATEQ4F thermodynamic database. The modelling focussed on speciation-solubility calculations (carbonate, silica and sulphate systems), mass balance and mixing calculations, reaction path modelling (for the aluminosilicate system) and redox system analysis. These calculations were used to investigate the processes that control water composition at Forsmark. A detailed description of the modelling performed can be found in Appendix 3.

Calcium carbonate system

Under this heading the evaluation of the main parameters controlling the carbonate system (pH, alkalinity, CO_2 and calcium) is included. Some PHREEQC modelling results (saturation indexes and pCO_2 values) are also included here in order to simplify the description and make the interpretation clearer.

Superficial fresh waters show a wide range of pH values as a consequence of their multiple origin (Figure 4-47a). The lowest values are associated with waters with a marked influence of atmospheric and biogenic CO_2; the highest values (up to 8.5 pH units) are associated with the most diluted groundwater. Overall this gives a decreasing trend with chloride when the rest of the groundwater samples are taken into account, although this trend inverts at depth, so that the more saline groundwaters have slightly higher values. Nevertheless, all these values are affected by uncertainties in pH measurements in the laboratory and there are not enough data from continuous logging pH measurements (apart from the analysis reported in Forsmark phase 1.1) to check them.

Broadly speaking, the main features of the pH trend can be correlated with other Scandinavian sites with similar waters (e.g. Simpevarp area and Olkiluoto; /Laaksoharju et al. 2004b; Pitkänen et al. 1999/ and also affected by uncertainties in pH.

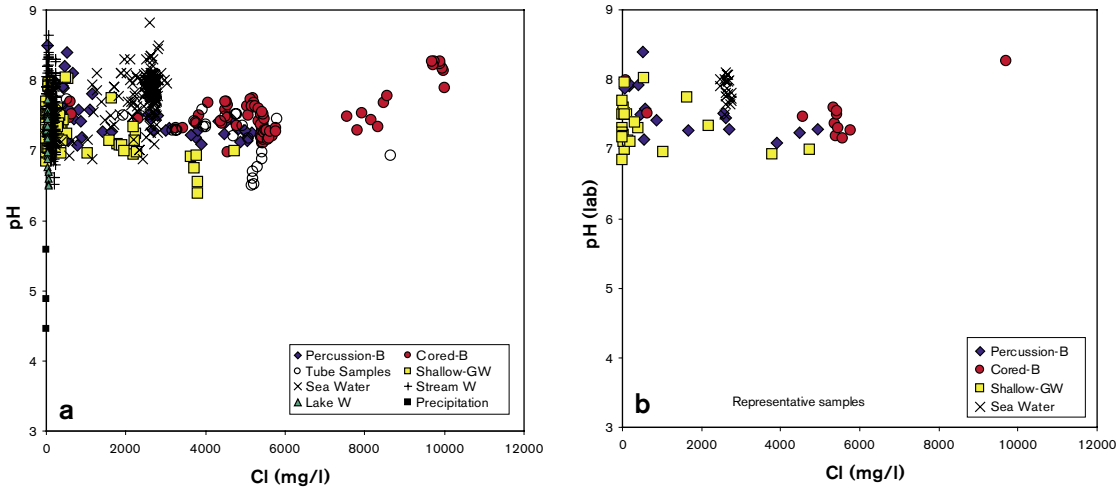

Figure 4-46. *pH versus chloride content in mg/L (increasing with depth) in Forsmark waters. (a) All samples. (b) Representative samples.*

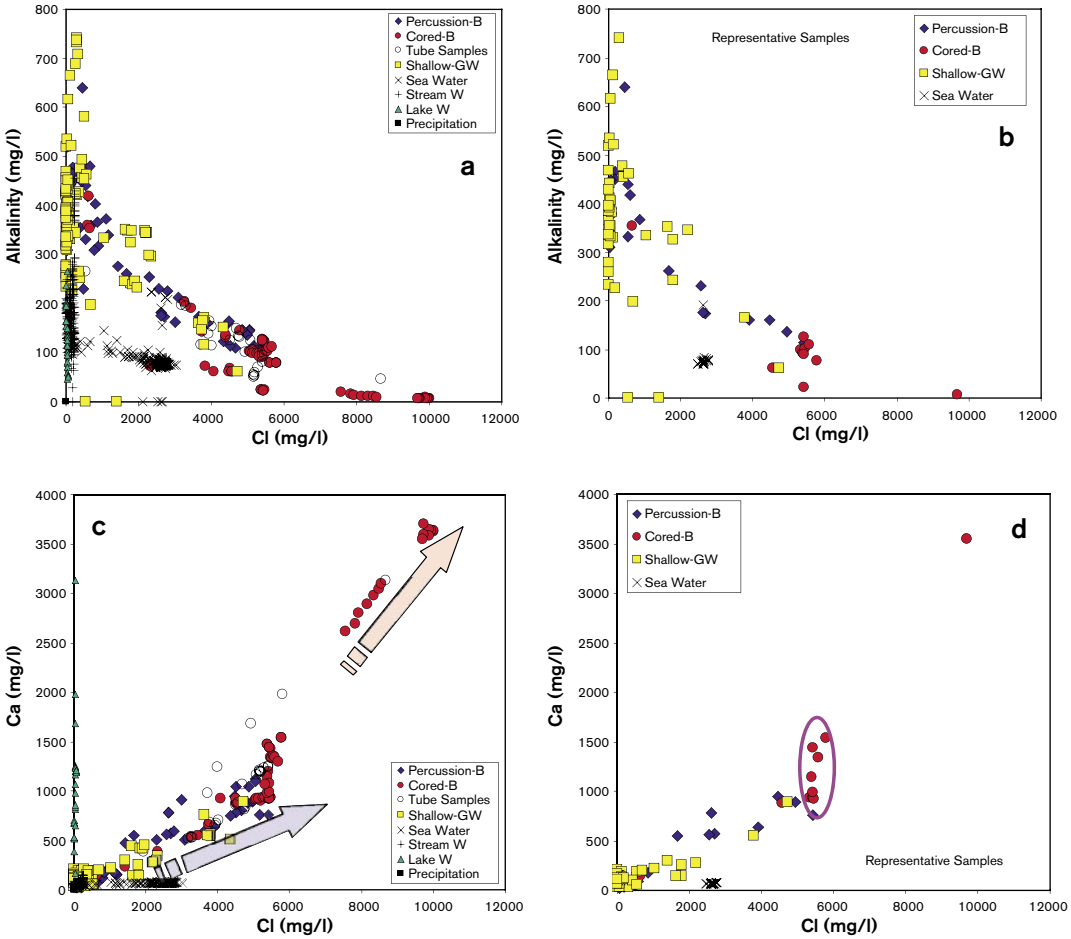

Figure 4-47. *Alkalinity and calcium versus Cl in waters from the Forsmark area. (a) Alkalinity evolution in all waters. (b) Alkalinity evolution in the representative waters. (c) Calcium content in all waters. (d) Calcium content in the representative waters.*

Alkalinity (HCO_3^-) is, together with chloride and sulphate, the third major anion in the system, and is the most abundant in the non-saline waters. Its concentration increases in the shallower groundwaters (Figure 4-48a, b) as a result of atmospheric and biogenic CO_2 influence and/or calcite dissolution. The alkalinity content reaches equilibrium (or oversaturation) with calcite in the fresh waters (Figure 4-48a, b) and then decreases dramatically with depth as it is consumed by calcite precipitation, whereas calcium continues to increase as a result of mixing (Figure 4-48c, d).

As can be seen in Figure 4-48c,d, calcium shows the same two trends (one with an important Littorina Sea component, and the other with a higher contribution of a brine component) as the rest of the cations. In general, it shows a good positive correlation with increasing chloride content, mainly in the most saline groundwaters, suggesting that mixing is the main process controlling the concentration of this element in the Forsmark waters. In spite of the extent of reequilibrium with calcite affecting Ca, the high Ca content of the mixed waters (coming from saline end members) obliterates the effects of mass transfer with respect to this mineral. This fact justifies the quasi-conservative behaviour of calcium, at least in groundwaters with chloride contents higher than 5,000 mg/L. Simple theoretical simulations of mixing between a brine end member and a dilute water, with and without calcite equilibrium, have shown the negligible influence of reequilibrium on the final dissolved calcium contents /Laaksoharju et al. 2004a/.

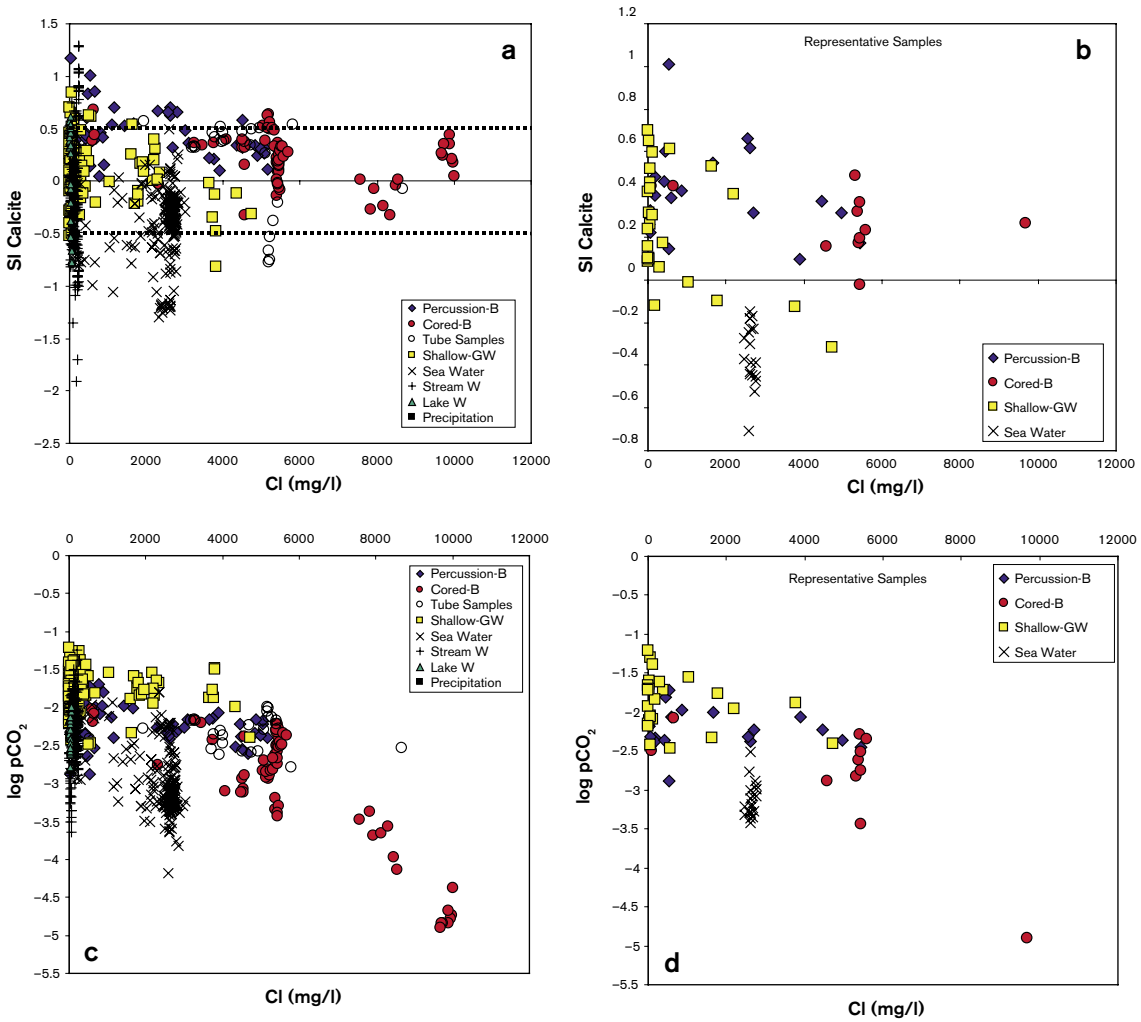

Figure 4-48. *Calculated calcite saturation indexes and partial pressure of CO_2 versus chloride for waters from the Forsmark area. The dashed lines represent the uncertainty associated with SI calculations.(a) and (b) Calcite SI in all waters and in representative waters, respectively. (c) and (d) log pCO_2 in all waters and in the representative waters, respectively.*

Figure 4-49 shows the calcite saturation index in the Forsmark waters. The alkalinity trend described above can be readily explained by this plot. The uncertainty associated with the saturation index calculation (±0.5) is higher than that usually considered (±0.3). This is due to problems during the laboratory measurements of pH (CO_2 outgassing and ingassing), as described in Forsmark v. 1.1 /Laaksoharju et al. 2004a/ and also in Simpevarp 1.2 /SKB, 2004/.

As for CO_2, Figure 4-49c and d shows the trend of decreasing partial pressure with increasing depth reaching values well below atmospheric in the more saline groundwaters.

Silica system

The content of dissolved SiO_2 in surface waters indicates a typical trend of weathering, while in groundwaters it has a narrower range of variation indicative of partial reequilibrium (Figure 4-49a,b). Also in this case, the brackish groundwaters (Cl ~ 5,500 mg/L) show different silica contents for the same chloride concentration. The general process evolves from an increase in dissolved SiO_2 by dissolution of silicates in surface waters and shallow groundwaters to a progressive decrease related to the participation of silica polymorphs and aluminosilicates which control dissolved silica as the residence time of the waters increases. This can be clearly seen in Figure 4-49c,d.

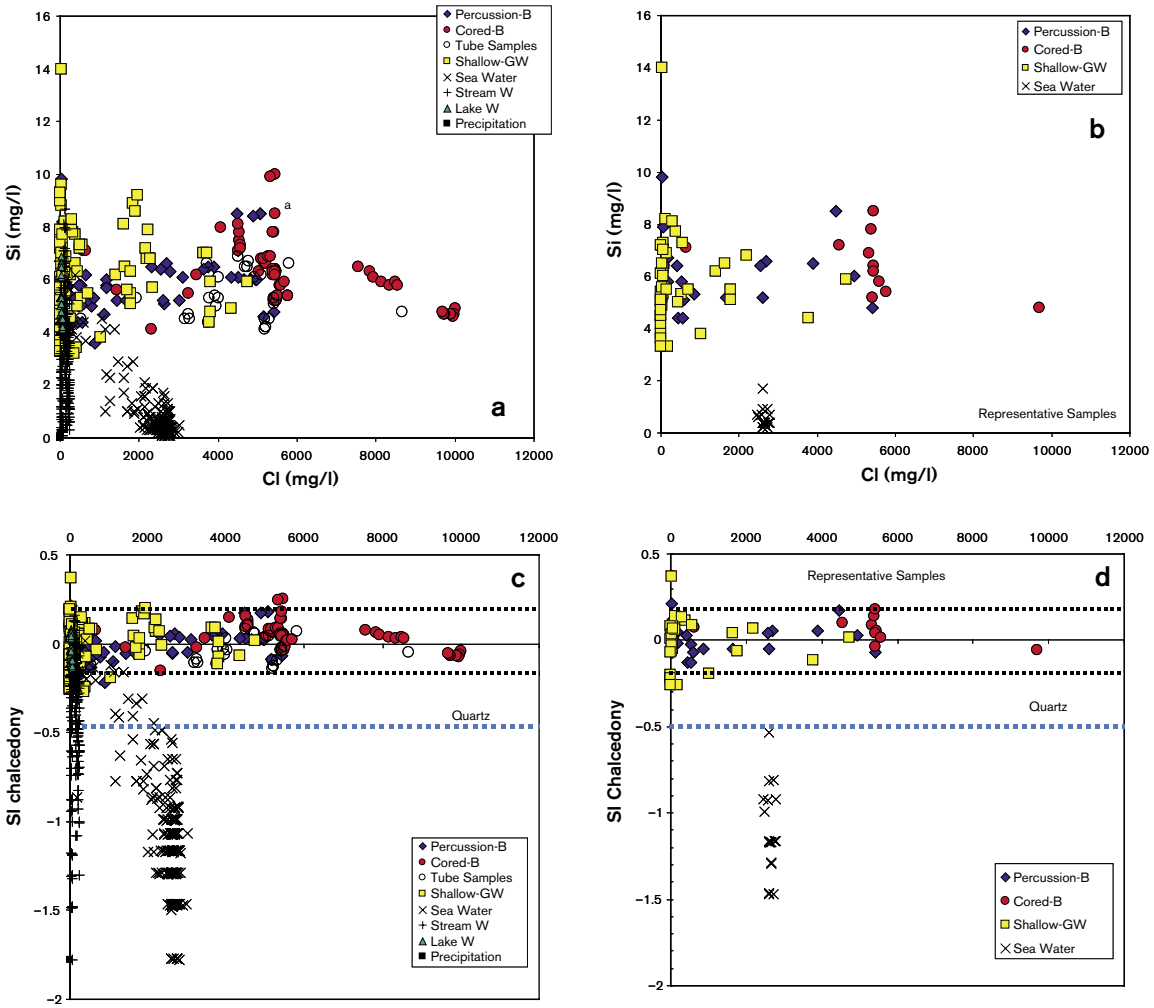

Figure 4-49. *(a) Plot of SiO_2 versus Cl for all Forsmark waters and for the representative waters (b). (c) Saturation indexes of chalcedony and quartz as a function of Cl in all Forsmark waters and in the representative waters (d). The dashed lines represent the uncertainty associated with SI calculations /Deutsch et al. 1982/.*

The weathering of rock-forming minerals is the main source of dissolved silica. Superficial waters have a variable degree of saturation with respect to silica phases (quartz and chalcedony), compatible with the weathering hypothesis, and a rather unclear control by secondary phases. This is a rough generalisation, useful for this general description but it should be noted that surface waters come from diverse systems (streams, lakes and soil zones) involving contrasting processes (evaporation, biological uptake, etc; /Laaksoharju et al. 2004b/ that affect silica concentrations.

Groundwaters are oversaturated with respect to quartz and close to equilibrium with chalcedony (Figure 4-49c,d). Saturation indices are relatively constant and independent of chloride content; this suggests that the groundwater has already reached, at least, an apparent equilibrium state associated with the formation of aluminosilicates or secondary siliceous phases like chalcedony, which seems to be controlling dissolved silica.

Sulphate system

Figure 4-50a, showing SO_4 versus Cl, suggests three possible trends:

a) An obvious modern Baltic Sea water dilution line, including sea water samples and some shallow groundwaters (soil pipes and percussion boreholes).

b) A borehole brackish groundwater dilution trend moving away from (a) towards very high sulphate values, suggesting, as in the previous phase, some Littorina Sea influence /Laaksoharju et al. 2004a/. Some shallow groundwaters (soil pipe samples) are also included in this trend.

c) A decreasing SO_4 trend as chloride increases from 6,000 mg/L to more saline values. In general, these groundwater data lend support to the absence of a significant postglacial marine component, suggesting instead a mixing with deeper, more saline waters of non-marine origin.

There is even an additional low chloride-low sulphate dilution trend incorporating some shallow groundwaters and some Lake/Stream waters. The greater scatter of sulphate at lower chloride levels may partly reflect some modern Baltic Sea water influence, some near-surface oxidation of sulphides, and also the variable effects of microbially mediated reactions (e.g. effect of sulphate-reducing bacteria) below and above the geosphere/biosphere interface.

Perhaps the most interesting aspect of the Forsmark waters is their different evolution, as shown by the sulphate content, with respect to sulphate behaviour in the Simpevarp area /SKB, 2004/. Figure 4-50e shows the sulphate contents in waters from Simpevarp and Olkiluoto. The Forsmark data are more limited in salinity than the Olkiluoto data, but they appear to be following the same trend. In both cases, after an initial increase in sulphate (reaching the maximum values when salinity is around 5,000–6,000 mg/L of Cl) there is a clear decrease towards zero. On the contrary, for the same chloride content, sulphate concentration in the Simpevarp area is clearly higher (Figure 4-50e).

This contrasting behaviour must be related to the process controlling sulphate content in these waters. Analysing the saturation state of the groundwaters with respect to gypsum some conclusions can be drawn. This analysis was also carried out for Simpevarp and included in Simpevarp 1.2 report /SKB, 2004/. In both cases (Simpevarp 1.2 and Forsmark 1.2) the range of salinity in the samples has increased since the previous data freeze, and a more complete evolution can be observed.

The Forsmark groundwaters are undersaturated with respect to gypsum but they evolve towards equilibrium with gypsum as chloride increases to 6,000 mg/L (Figure 4-50c, d). Then, the more saline groundwaters evolve towards an even more undersaturated state than the shallow groundwaters. The same behaviour can be seen in the Olkiluoto groundwaters. However, in the Simpevarp groundwaters the gypsum SI trend indicates a clear evolution towards equilibrium (Figure 4-50f) which is reached at chloride values of 10,000 mg/L and maintained even in the most saline groundwaters /Laaksoharju et al. 2004b/.

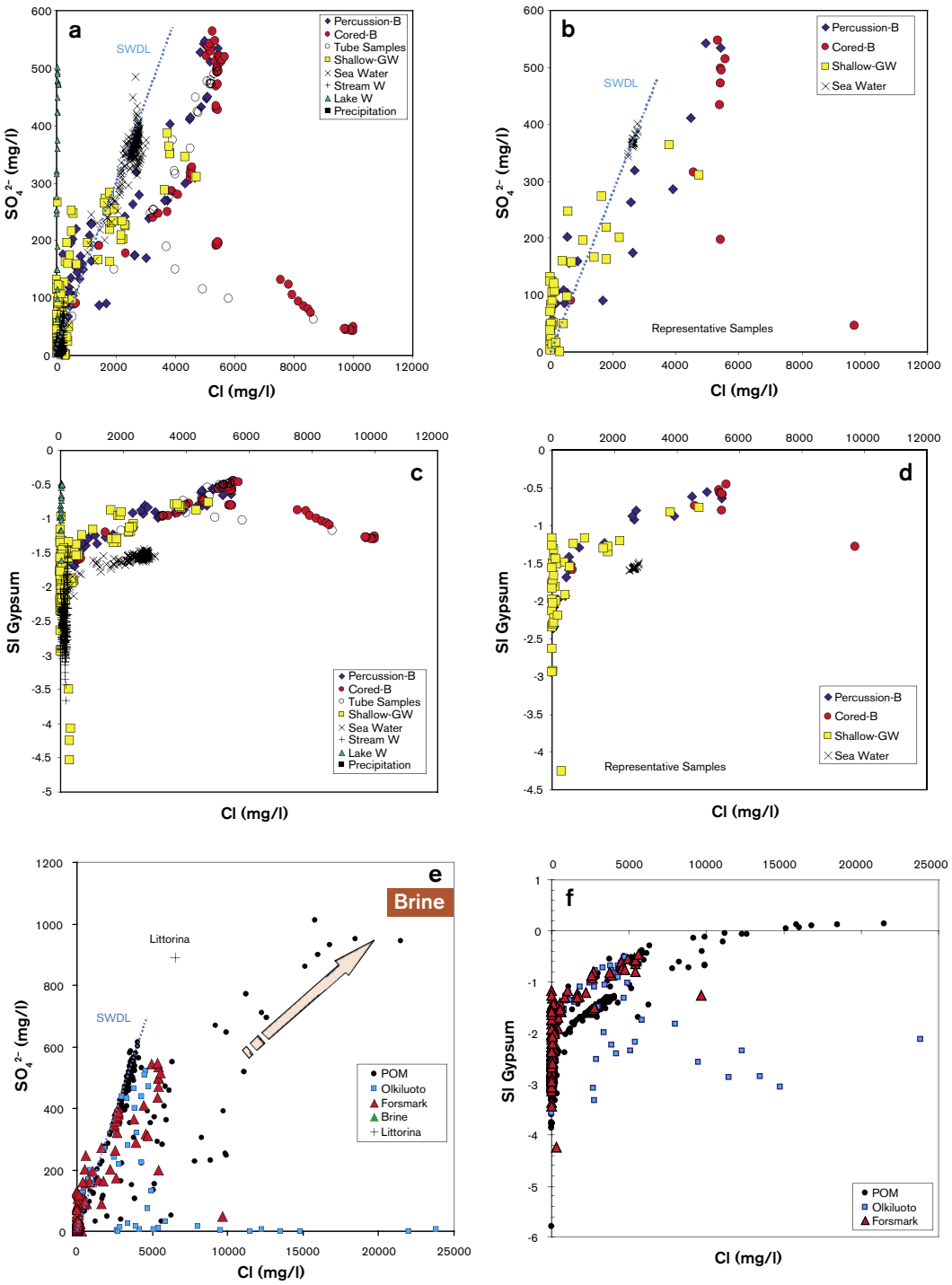

Figure 4-50. *(a) and (b) SO_4 versus Cl for all Forsmark waters and for the representative ones, respectively. (c) and (d) Gypsum saturation index (SI) versus Cl for all Forsmark waters and the representative ones, respectively. (e) and (f) SO_4 and Gipsum SI versus Cl comparing Forsmark data with samples from the Simpevarp area and Olkiluoto.*

Massbalance and mixing calculations using PHREEQC and M4

In the previous evaluation of the Forsmark groundwaters, presented in Chapter 2, two different trends were identified and ascribed to two representative mixing processes: the first one giving rise to Littorina-rich waters (already identified in Forsmark 1.1; /Laaksoharju et al. 2004a/), and the second producing waters with an important participation of a brine end member. Besides, the presence of very shallow groundwaters with compositional features representative of discharge zones of old groundwaters has now been identified as a separate group.

These three groups of samples have been processed through the mass balance capabilities of PHREEQC in order to check the hypothesis advanced above on the influence of the different end members on their chemistry[1]. Additionally, mixing proportions obtained by PHREEQC for selected samples have been compared with the results obtained with a modified version of M3, called M4, developed by the University of Zaragoza team, in order to validate the code. Some additional comparisons between M3 and M4 are presented later in this report (cf. Appendix 4). Appendix 3 gives a summary of the code, together with a sensitivity analysis carried out with both synthetic and real samples (Appendix C in Appendix 3). The methodology used for inverse modelling is described in Appendix 3.

Table 4-1 summarises the PHREEQC and M4 results, showing good agreement between both approaches (see also Appendix C in Appendix 3 for an in-depth validation of M4). PHREEQC results give the maximum and minimum values among all the successful mixing models for each sample.

Samples of Group 1 have Littorina proportions ranging from 35 to 51% (only the two samples with the most extreme Littorina mixing proportions are shown in the table: 4538 and 8016). In detail, the sample with the lowest chloride content (4,538 mg/L) has a similar proportion of Littorina and Glacial end-members, while the other samples (represented in Table 4-1 by sample #8016) have a higher Littorina proportion (50%) and a much lower Glacial proportion. Brine percent is consistently low (< 5%) and Precipitation is in the range 20–23%. Therefore, this set of samples shows a clear Littorina contribution but, in some cases, Glacial proportions can also be important.

The only sample representative of Group 2 (the most saline groundwaters found in Forsmark, #8152), reveals an important Brine contribution (16.02%; cf. < 5% in Group 1 samples) and a lower (or null) participation of Littorina (< 9%). The most important contribution comes from the Glacial end member (48%). These values are consistent with the results obtained for other groundwaters at similar depths elsewhere in Sweden /SKB, 2004/ and correspond to waters representative of old (> 10,800 BP) mixing events with Brine and Glacial end-member waters, with little modification by more recent mixing processes.

Finally, Group 3 samples (shallow groundwaters in discharge zones, #8078 and 8252) are characterized by a high Littorina percentage, similar in general to the value reported for Group 1 samples. The other end-members have also similar contributions to the ones in Group 1. Therefore, they could represent genuine discharge zones of old, deep groundwaters.

Table 4-1. PHREEQC and M4 results for the groundwaters representative of three different trends in the Forsmark area.

	Sample	Code	Brine	Littorina	Glacial	Precipitation
Brackish-saline	4538	PHREEQC	3.8–5.1	27.9–35.2	27.8–31.6	29.4–39.0
	Cl = 4,563 mg/L Depth: 115 m	M4	2.6	35.7	40.8	20.8
	8016	PHREEQC	3.3–4.3	50–54	12.2–14.3	28.6–33.5
	Cl = 5,410 mg/L Depth: 512 m	M4	1.6	50.8	24.4	23.2
Saline	8152	PHREEQC	17.5–19.5	0–15	34–42	24–42
	Cl = 9,690 mg/L Depth: 990 m	M4	16.02	9.2	47.9	26.9
Discharge	8078	PHREEQC	3.5–4.8	30.5–38.5	27.2–32	28.2–33.5
	Cl = 4,730 mg/L Depth: 3 m	M4	2.7	39	39.4	18.9
	8252	PHREEQC	1.3–2.4	50.9–55	11.6–15.9	27.2–34
	Cl = 3,780 mg/L Depth: 3.8 m	M4	0	51.4	26.3	22.4

[1] This group of fresh non-saline waters was already identified and analysed in the previous phase (Forsmark 1.1; /Laaksoharju et al. 2004a/) and will not be presented here.

The main reaction processes associated to these mixing models include decomposition of organic matter; dissolution of plagioclase, biotite and $Fe(OH)_3$; precipitation of calcite, K- and Mg-phyllosilicates, silica (chalcedony), and sulphides; and ionic exchange between Na and Ca. Mass transfers associated with dissolution-precipitation reactions are small (< 0.1 mmol) and slightly higher for cation exchange processes (in the range of 1 mmol), especially for groundwaters with high Littorina Sea signature.

Reactions involving redox species are not well constrained in these types of calculations because the end members lack a proper redox characterisation. Nevertheless, most of the models obtained for Group 2 groundwaters predict a significant precipitation of sulphides (mass transfer rates similar to non-redox minerals). This result is consistent with the redox and microbiological character of these waters as discussed in Section 3.3.

In conclusion, brackish groundwaters (with chloride around 5,000 mg/L) show an important Littorina Sea signature, usually being the dominant end member, with mixing proportions around 45–50%. Locally, the Littorina contribution is lower (35%) and then the Glacial end member becomes dominant (40%). These groups of groundwaters are scattered in depth, from 100 to 500 m, and therefore deeper than previously assumed in Forsmark 1.1 iteration /Laaksoharju et al. 2004a/. At depths below 200 m, these brackish groundwaters are located at the same level as the fresh-non saline groundwaters found in other boreholes. In fact, some soil pipe samples (Group 3 samples, < 3 m depth) show the same compositional characteristics and mixing proportions as the deeper brackish groundwaters, suggesting the existence in the system of discharge zones for these old, Littorina-dominated groundwaters.

The deepest saline groundwaters (1,000 m depth) show a clear Brine signature, a low (or null) Littorina Sea contribution and a dominance of the Glacial end-member. These Group 2 groundwaters represent the remnant of a very old mixing process (Baltic Ice Lake Stage, > 10,800 BP) when glacial melt water flushed the bedrock and mixed with ancient Brine groundwaters. It can then be concluded that the forced introduction of glacial melt water in Forsmark reached at least a depth of 1,000 m.

Reaction-path modelling

As it has been commented on above, the mineralogical study of boreholes KFM01B, KFM02A, KFM03A and KFM04A have demonstrated the presence of a complex sequence of fracture fillings. Besides the granite rock-forming minerals, most fracture filling phases are aluminosilicate minerals with which waters have been in contact during their geochemical evolution. Therefore, they are important water-rock interaction phases. However, as already pointed out, the lack of aluminium data for Forsmark groundwaters precludes a speciation-solubility analysis, limiting the analysis to a graphical representation of stability diagrams.

The accuracy of the stability diagrams depends on pH and is therefore affected by uncertainties in its value. Uncertainties in the equilibrium constants of the aluminosilicates (especially the phyllosilicates) also affect the conclusions drawn from these diagrams and from the ensuing theoretical models based on them /e.g. Laaksoharju and Wallin, 1997; Trotignon et al. 1997, 1999/. As a consequence, the study of aluminosilicate phases has been restricted to those with low uncertainties, using thermodynamic data already tested and verified in comparable systems. That means that the "aluminosilicate system" as defined here reduces to the set adularia, albite, kaolinite, laumontite, prenhite and chlorite. The selected thermodynamic data are taken from /Grimaud et al. 1990/ at 15ºC in their study of Stripa groundwaters.

The following description includes a general evaluation of Forsmark groundwaters from their position in the stability diagrams and a discussion on the effects of mixing and reaction on the chemistry[2] of the groundwater. This discussion is illustrated by means of a theoretical equilibrium modelling. The origin of the saline groundwaters (Littorina Sea and/or Brine end members) is not discussed here, and the model just assumes that they are already in the system, participating in the mixing process. Nevertheless, in the Simpevarp 1.2 report, the potential use of this modelling approach to predict the chemical characteristic of these old saline groundwaters is indicated.

[2] In this section different diagrams and computer simulations for Forsmark waters are presented, in some of the cases together with other sites (Stripa, Olkiluoto and Simpevarp area).

Stability diagrams

Following the same procedure developed for Simpevarp 1.2 phase /SKB, 2004/, the Forsmark waters have been plotted in different stability diagrams (see Appendix D in Appendix 3). The set of thermodynamic data utilised to construct the stability diagrams was calibrated for Stripa groundwaters /Grimaud et al. 1990/, and the presentation and explanation of the original diagrams can be found in /SKB, 2004/.

The analysis of Forsmark waters uses the kaolinite-albite-adularia stability diagram because it is the most suitable for discriminating waters that have undergone mixing, and because many Fenoscandian groundwaters plot near the albite-adularia boundary line, suggesting a true or apparent equilibrium with both phases.

Figure 4-51 shows the kaolinite-albite-adularia diagram for the Forsmark waters. Green and blue arrows mark the two main trends that can be distinguished. *The first trend* (green arrows) starts inside the kaolinite stability field and evolves towards the kaolinite-adularia boundary. This trend is defined by modern surface waters and shallow groundwaters with low chloride contents and whose geochemical evolution is mainly the result of water-rock interaction.

The evolution path of these waters in the kaolinite field has a slope of around 2, similar to other weathering/alteration processes in granitic materials and represents the effects of a progressive dissolution of the rock forming minerals calcite, biotite, plagioclase, K-feldspars, etc. Along this process, partial reequilibria with phyllosilicates (represented by, e.g. kaolinite) can be reached. Ionic exchange and, in later stages, calcite precipitation can also take place. Waters close to or on the kaolinite-adularia boundary would correspond to the most evolved samples in this water-rock interaction process.

Some shallow groundwaters (soil pipes) and lake waters from Forsmark do not plot inside the kaolinite field, as expected, but inside the adularia stability field instead. Some of these samples (samples close to the adularia-albite limit, see below) show clear evidence of mixing with modern Baltic Sea, and even with another older marine (Littorina Sea) and saline (non marine) end members. Therefore, they could be waters whose chemistry is not only controlled by water-rock interaction and plot together with groundwaters characterised by mixing. The rest of the soil pipe and lake samples plot in the adularia field further away from the adularia-albite limit. They have low chloride contents but anomalously high K, Mg, SO_4^{2-}, etc. These samples could be the result of water-rock interaction

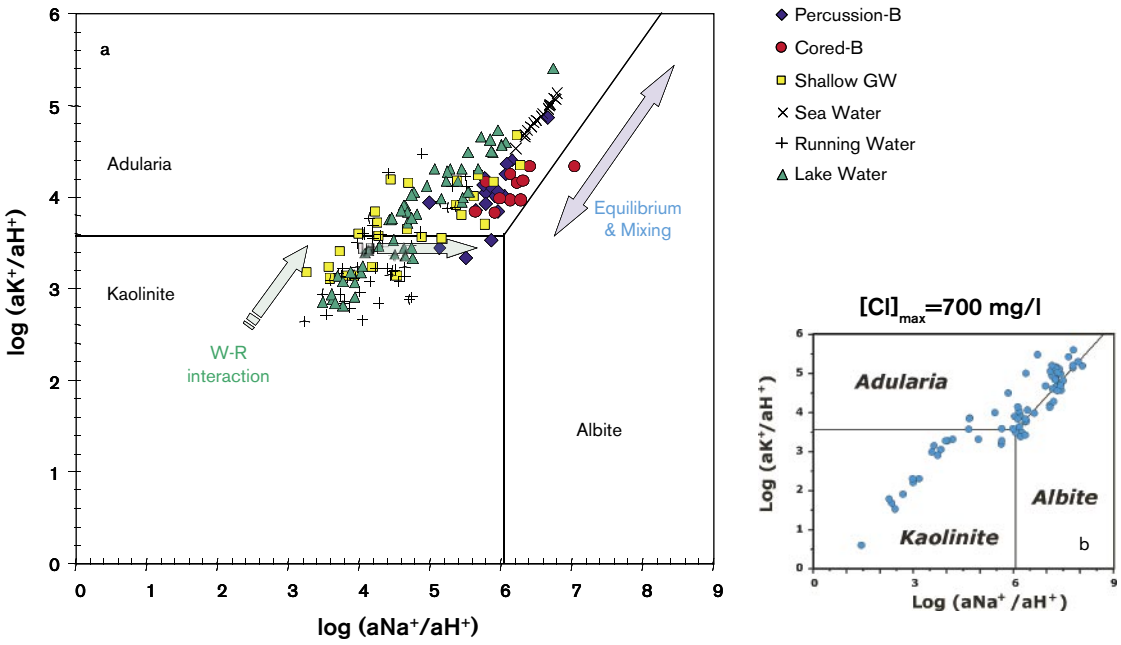

Figure 4-51. *Kaolinite-adularia-albite stability diagram for Forsmark representative surface and groundwaters (a) and for Stripa groundwaters (b).*

in the detritic overburden or could even represent some kind of contribution from an old marine component, as they are geographically associated to what seems to be discharge zones in the system. More data would be needed to determine the origin of these waters.

The second trend (blue arrow), followed by all Forsmark brackish and saline groundwaters, runs parallel to the adularia-albite limit, indicating an equilibrium (or near equilibrium) situation. This result is very similar to that of Stripa (compare the figures and the scale) but with an important difference: the maximum chloride content in Stripa reaches only 700 mg/L, whereas Forsmark groundwaters, plotted in the same position, have Cl contents up to 10,000 mg/L. The residence time of Stripa groundwaters has been estimated at roughly 100,000 years /Fontes et al. 1989/, meaning that water-rock interaction processes can only provide up to 700 mg/L of chloride in such a large time span. It is clear, therefore, that an additional source of salinity is needed to justify the existence of much younger waters with much higher chloride concentrations in Forsmark. This source of chlorine comes from mixing with a saline component of marine and/or non marine origin. This points again to mixing as the key process controlling the chemistry of these waters, as it has been repeatedly reported in previous works /Laaksoharju and Wallin, 1997; Laaksoharju et al. 1999, 2004b/.

In Figure 4-52 the Forsmark samples have been plotted together with those of Olkiluoto /Pitkänen et al. 2004/ and of the Simpevarp area /SKB, 2004/. The Olkiluoto waters occupy, in general, the same position as the Forsmark waters[3]. The Olkiluoto samples in the kaolinite stability field and on the kaolinite-adularia boundary correspond to subsurface or shallow groundwaters whose chemistry is controlled by water-rock interaction. Samples located on the adularia-albite boundary correspond to brackish and saline groundwaters characterised by having undergone complex mixing processes (between Meteoric, Littorina, Glacial and Saline end members, /Pitkänen et al. 2004/. Results for Simpevarp groundwaters are similar, although in this case the number of samples in the adularia stability field is smaller than is the cases for Forsmark and Olkiluoto.

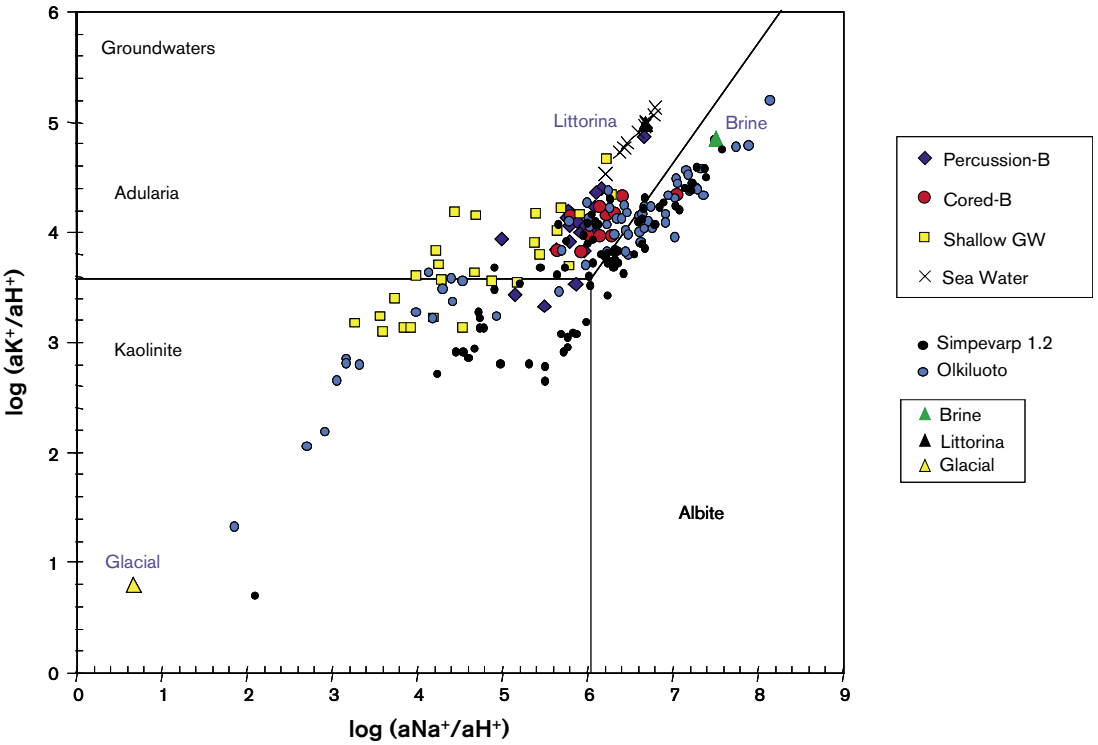

Figure 4-52. *Kaolinite-adularia-albite stability diagram. Together with the Forsmark representative groundwaters, the Olkiluoto /Pitkänen et al. 2004/ and Simpevarp area groundwaters, and also the theoretical end members (Brine, Littorina and Glacial), have been plotted in this diagram.*

[3] Although not presented in the Appendix D, the same match is observed in diagrams AD-1 and AD-2.

The position of the theoretical end members is also shown in Figure 4-52 (Brine, Littorina Sea and Glacial; Meteoric is close to Glacial). It is fairly clear that the evolution path of these waters is the result of: (a) reaction between the rock and diluted waters (surface and shallow groundwaters), (b) mixing in depth with more saline groundwaters in different proportions, as a function of location and residence time, and (c) the simultaneous interaction of these deep waters with the rock.

An identical result has been found in Simpevarp 1.2 /SKB, 2004/. However, in this case there is an important number of samples located close to the adularia-albite boundary but inside the adularia field, showing a clear trend towards the Littorina Sea end member. The uncertainty of the modelling is discussed in Appendix 3.

Simulating the obtained water composition

As shown above, the Forsmark, Simpevarp area and Olkiluto groundwaters on the adularia-albite boundary and inside the adularia stability field but close to the boundary include samples of broadly different salinities, chemical contents and depths, but reflecting an apparently similar equilibrium situation. In a first approximation, they could be interpreted as the result of different mixing episodes between different end members at different times during the site evolution. Alongside this main process, there would be re-equilibration periods (reaction with the rock) following the disequilibrium created by the successive mixing episodes.

The chemistry of the groundwaters is then the result of a complex sequence of mixing and reaction. Following the procedure developed in the Simpevarp 1.2 report, a direct mixing and reaction calculation has been chosen in order to evaluate the relative contribution of the two processes.

The modelling performed in Simpevarp 1.2 was focussed on the assessment of the oldest mixing episode between the saline and glacial end members (8,000–10,000 BC) and is entirely valid as an explanation of the more saline waters in Forsmark (see a detailed description in /Laaksoharju et al. 2004b/, and also Figure 3-4). Therefore, in this report the simulations will be focussed on the next mixing episode, involving the previously mixed waters and a certain amount of Littorina Sea water end member.

The simulation flow chart is shown in Figure 4-53. From previously calculated (Simpevarp 1.2) mixing proportions between Brine and Glacial (the two extreme cases analysed: 63% Brine and 37% Glacial, 5% Brine and 95% Glacial), equilibrium with different mineral assemblages was imposed ("Reaction" in Figure 3-3). Equilibrium with calcite, chalcedony, albite, and adularia has been chosen here only as an example, but models with other mineral assemblages have also been run. The resulting water (final solutions 1 and 2 in Figure 4-53) was mixed with different proportions of Littorina (between two extreme cases: 10% and 70%). The new mixed waters are named Mix 1, 2, 3 and 4. The final step consists of imposing again an equilibrium with different mineral assemblages. The equilibria with calcite-chalcedony and calcite-chalcedony-albite-kaolinite have been chosen here as mere examples.

Figure 4-54 shows the location of final solutions 1 and 2 after mixing with Brine and Glacial and in equilibrium with the selected minerals (black squares and orange diamonds). They plot on the adularia-albite boundary very close together. They represent the final result of the simulations performed in Simpevarp 1.2 and the starting point of this new calculation.

The next modelling step is a mixing calculation. Each of the already calculated final solutions was mixed with the Littorina Sea end member in two different proportions: 10% and 70%.The position of these mixed waters is plotted in the stability diagrams (cf. Appendix 3). After mixing, the equilibrium of the mixed waters with different combinations of calcite, chalcedony, albite, adularia and kaolinite was simulated in order to measure its effects on the final composition of the waters. Detailed description of the modelling and its uncertainties can be found in Appendix 3. Examples of the calculated mass transfers are listed in Table 4-2.

As a summary, these results indicate that re-equilibrium reaction processes are important in the control of some parameters such as pH (as well as Eh, and some minor-trace elements), moving the waters towards the adularia-albite boundary. However, the main compositional changes, and even the extent of re-equilibration processes[4], are controlled by the extent of the mixing process.

[4] Calculated mass transfers for the same equilibrium situation change in more than one order of magnitude depending on the considered mixing proportions (Table 3-2).

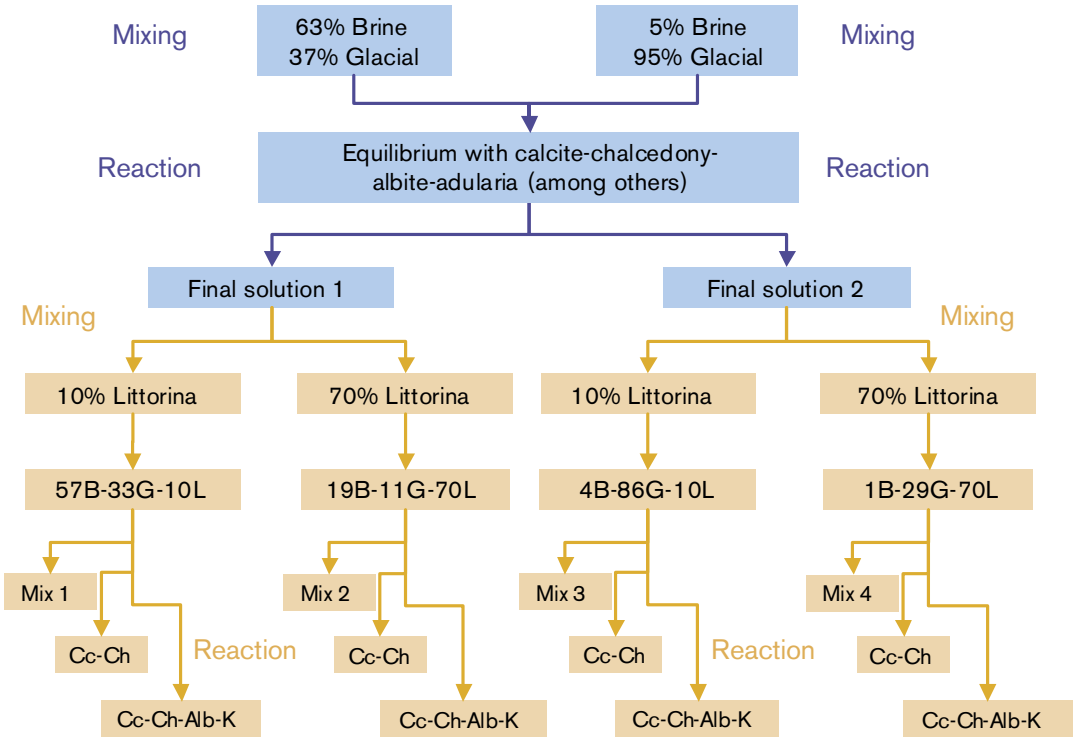

Figure 4-53. *Simulation procedure for the assessment of the mixing episode between Littorina Sea and a saline groundwater (result of a previous mixing process between Brine and Glacial end members and the equilibrium with a mineral assemblage).*

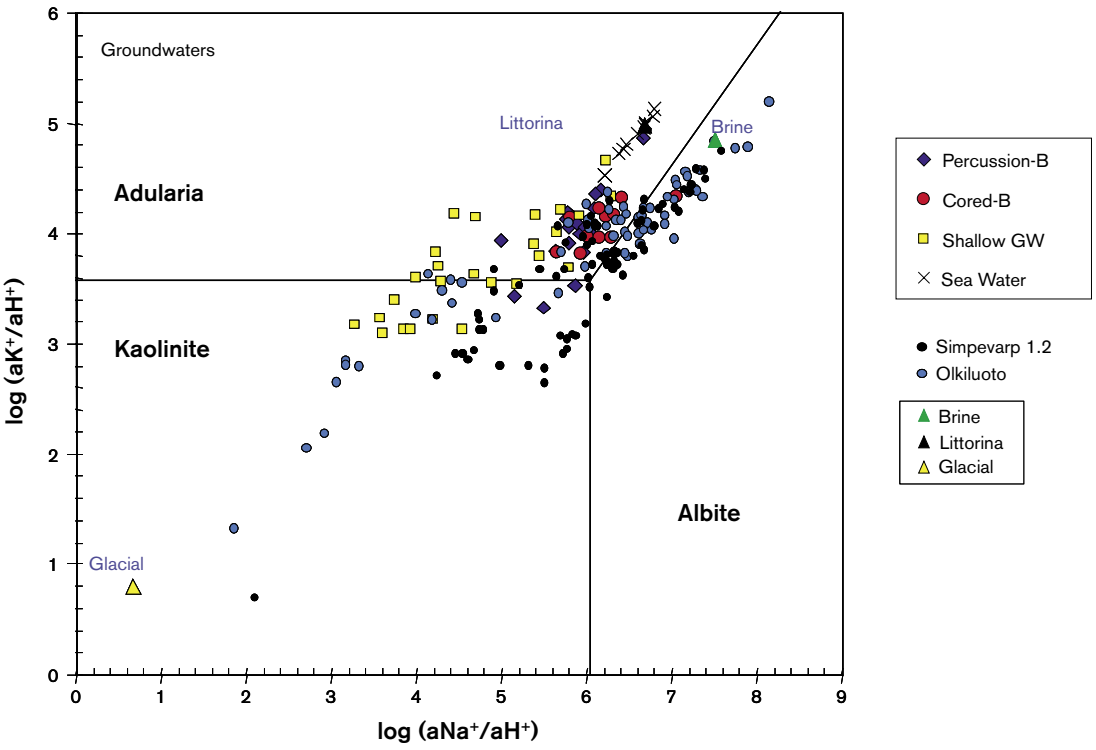

Figure 4-54. *Starting point for the simulation of the mixing episode between Littorina Sea and a saline groundwater result of a previous mixing process between Brine and Glacial end members (Mix points in the plot), and the equilibrium with a mineral assemblage (C_Ch_Alb_Adu in the plot).*

Table 4-2. Calculated mass transfers (mol/L) in the four mixing proportions as discussed above. Only two examples are shown here: the equilibrium with calcite (Cc) and chalcedony (Ch), and the equilibrium with calcite, chalcedony, kaolinite (Kaol) and albite (Alb).

Mass Transfers	90% (63Brine – 37Glacial) 10%Litt.		30% (63Brine – 37Glacial) 70%Litt.		90% (5Brine – 95Glacial) 10%Litt.		30% (5Brine – 95Glacial) 70%Litt	
	57B+33G+10L		19B+11G+70L		4B+86G+10L		1B+29G+70L	
	Cc-Ch	Cc-Ch-Kaol-Alb	Cc-Ch	Cc-Ch-Kaol-Alb	Cc-Ch	Cc-Ch-Kaol-Alb	Cc-Ch	Cc-Ch-Kaol-Alb
Calcite (C)	6.6·10–6	2.2·10–4	1.1·10–4	4.7·10–4	4.3·10–6	1.1·10–4	5.6·10–6	1.4·10–3
Chalcedony (Ch)	8.1·10–6	5.1·10–4	6.0·10–5	8.2·10–4	5.3·10–6	2.5·10–4	6.0·10–5	3.3·10–3
Kaolinite (K)		1.3·10–4		2.2·10–4		6.1·10–5		8.1·10–4
Albite (Alb)		2.5·10–4		4.4·10–4		1.2·10–4		1.6·10–3

Redox modelling

In this section the results from the modelling of the redox state in the Forsmark area are presented (cf. Appendix 3 for more details and methodology). For Forsmark 1.2, the amount of suitable data for a redox study is slightly greater than for Forsmark 1.1 and, therefore, this study is somehow more complete. The two possibilities suggested in previous studies about the redox state of the groundwaters have been revisited, namely: (a) the iron system controls the redox state /Grenthe et al. 1992/; and (b) the sulphur system controls the redox state /e.g. Nordstrom and Puigdomenech, 1986/.

For this modelling exercise, only samples with enough redox data were selected. This includes Eh and pH[5] data from continuous logging, concentrations of Fe^{2+}, S^{2-} and CH_4, and microbiological information. The selection criteria have drastically reduced the number of suitable samples for the redox characterisation of the system. In spite of this, the selected samples cover a wide range of depths (115 to 990 m; Figure 4-55) in three boreholes KFM01, KFM02 and KFM03. Moreover, they all have continuous Eh logging, redox pair concentrations and even microbiological information (in some cases) and thus, a combination of these three data sets can be made.

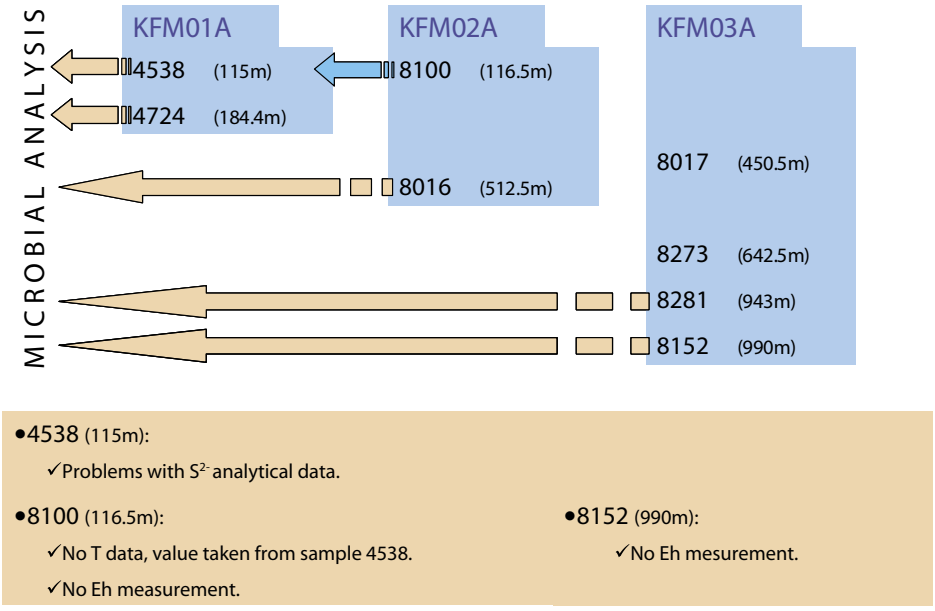

Figure 4-55. *Selected groundwater samples for the redox modelling indicating their depths and the kind of available information. The analytical problems associated with sample 4538 are detailed in Appendix D.*

[5] In order to minimise the pH uncertainty effects on the redox calculations /Laaksoharju et al. 2004a,b; SKB, 2004/.

Redox pair calculations

The results from the redox pair calculations (cf. Appendix 3) are summarised in Figure 4-56 and Figure 4-57. The Eh calculated with the $Fe(OH)_3/Fe^{2+}$ redox pair and Grenthe's calibration agrees reasonably well with the Eh values measured in the deepest samples[6]. The Eh calculated with the same redox pair for microcrystalline $Fe(OH)_3$ is much more oxidant. On the contrary, the microcrystalline phase gives better results in the shallower samples (4538), whereas Grenthe's calibration gives a much more reducing Eh value (Figure 4-57). This observation was already made in the previous phase (Forsmark 1.1, /Laaksoharju et al. 2004a/). In some samples (4724, 8100, 8016) none of the iron calibrations provide good results. This fact suggests that the groundwater redox state can be controlled by iron oxides and oxyhydroxides with different degrees of crystallinity.

Except for a few samples, the different "sulphur system" redox pairs provide Eh values coincident with the potentiometrically measured Eh. The SO_4^{2-}/S^{2-} homogeneous redox pair gives Eh values similar to the ones obtained from the heterogeneous pairs ($Pyrite/SO_4^{2-}$ and FeS/SO_4^{2-}; Figure 4-56 and Figure 4-57) as calculated with WATEQ4F thermodynamic data. A sensitivity analysis carried out comparing these data to /Bruno et al. 1999/ shows only minor differences.

As expected, Eh values obtained with the CH_4/CO_2 pair are very similar to those obtained with the SO_4^{2-}/S^{2-} pair (and to the remaining sulphur redox pairs). Therefore, they also agree well with the potentiometrically measured Eh.

Redox pairs results for samples with noisy Eh measurements (8100 and 8152) are not so easy to interpret, but it seems that the measured Eh in sample 8100 agrees well with the Eh value from the sulphur pairs. However, Eh values from these pairs obtained for sample 8152 agree well with the ones from CH_4/CO_2, but all of them are more reducing than the measured Eh value.

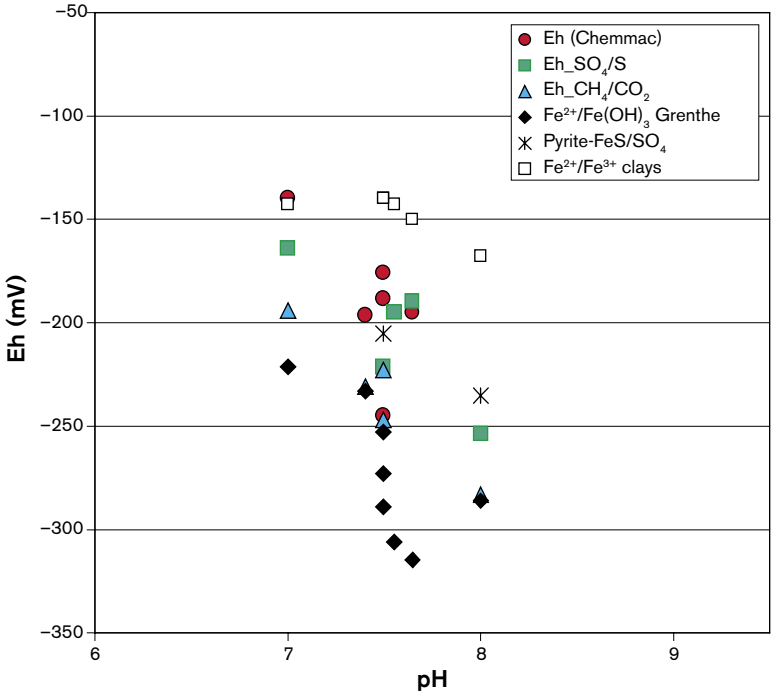

Figure 4-56. *Comparison of redox results for different redox pairs in the Forsmark selected groundwaters.*

[6] In the case of sample 8152, the result must be taken with caution. Fe^{2+} concentration in this sample (0.026 mg/L or $4.6 \cdot 10^{-7}$ mol/L) is below the lower limit (10^{-6} molar) for successful Eh measurements when iron pairs control the redox potential /Grenthe et al. 1992/.

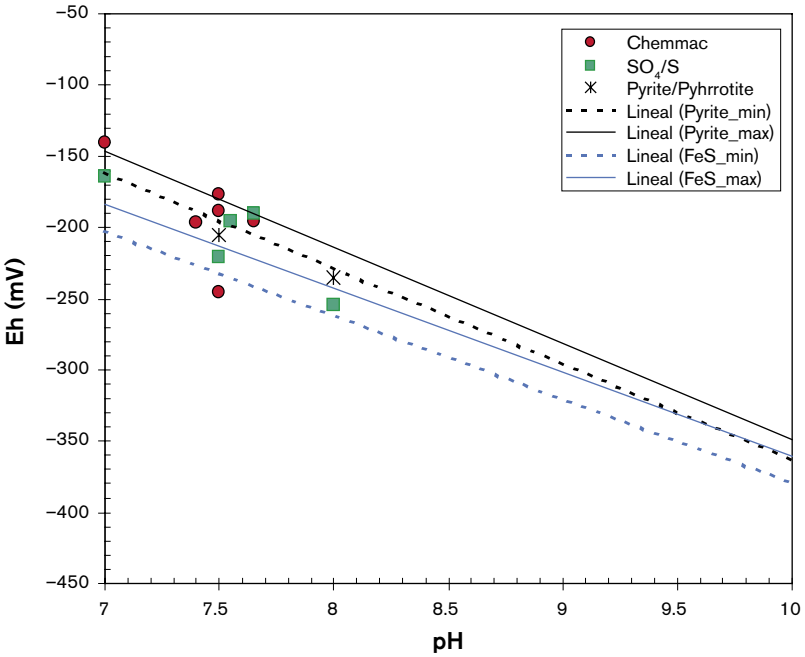

Figure 4-57. *Eh-pH diagram showing the calculated Eh values for the Forsmark samples. Potentionetrically measured values are shown as red circles. The Eh values from the SO_4^{2-}/S^{2-} redox pair are represented with green squares and the values obtained with the pyrite-pyhrrotite/SO_4^{2-} pair, with an asterisk. "Pyrite_min" and "Pyrite max" lines represent the equilibrium situation for the range of SO_4^{2-} and Fe^{2+} concentrations found in Forsmark groundwaters. The same is valid for the FeS/SO_4^{2-} equilibrium.*

There is an overall good agreement between the potentiometrically measured Eh and the values calculated using the heterogeneous sulphur pairs, the homogeneous sulphur pair and the CH_4/CO_2 pair, even taking into account the low concentrations of S^{2-} and CH_4. Grenthe's calibration for $Fe(OH)_3/Fe^{2+}$, provides Eh values in good agreement with the measured Eh for the deepest waters but in the shallowest samples the iron system seems to be controlled by a microcrystalline hydroxide and not by an intermediate phase, as Grenthe's calibration assumes.

This suggests that the sulphur system is the main controller of the groundwater redox state, as reported previously /Nordstrom and Puigdomenech, 1986; Glynn and Voss, 1999; Laaksoharju et al. 2004a,b/, or at least that it is the most suitable (together with the CH_4/CO_2 redox pair) to characterize the redox state of these groundwaters. The variable results obtained with the $Fe(OH)_3/Fe^{2+}$ pair do not mean that the iron system does not participate in the redox control of these waters, but the variable crystallinity of the phases involved hinders a clear and general assessment. The uncertainty of the modelling is discussed in Appendix 3.

Conceptual model for the redox system

Microbial analysis (Appendix 2) of the Forsmark groundwaters has identified Sulphate-reducing Bacteria (SRB) at depths from 642.5 m (sample 8273) to 990 m (sample 8152), and their number is specially high at 943 m, in sample 8281. At these depths the lowest values of SO_4^{2-} and the highest values of S^{2-} from all the analysed waters are found, which is consistent with the metabolic activity of SRB. However, there is no correlation between the number of SRB and dissolved sulphide; moreover, sulphide concentrations (0.03–0.06 mg/L) are too low for the high SRB number found and the expected intensity of the sulphate reduction process.

This fact, together with the low ferrous iron concentration, could indicate the presence of active iron-sulphide precipitation in fractures. This process can maintain dissolved sulphide at the low levels detected, even though sulphate reduction might produce substantial amounts of sulphide. And it can be active if a source of Fe^{2+} (iron oxyhydroxides) exists. This source can explain the low iron concentrations in samples at 642.5 and 943 m depth, but it has apparently been exhausted in the deepest groundwaters (at 990 m).

In summary, most lines of evidence support that the sulphur system, microbiologically mediated, is the main redox controller in the deepest and most saline groundwaters. On the other hand, Littorina-rich brackish groundwaters show variable and very high iron contents, in agreement with what has been observed in similar groundwaters elsewhere (e.g. at Olikiluoto; cf. /Pitkänen et al. 1999/). The microbial analysis only found trace amounts of SRB in samples 4538 and 8016 (115.5 and 512.5 m depth, respectively), but very high numbers of iron-reducing bacteria (IRB), mainly in sample 4538. However, there is no correlation between Fe^{2+} concentration and the number of IRB in these groundwaters. Moreover, they show very low but detectable contents of dissolved S^{2-} and the $\delta^{34}S$ values are very homogeneous (around 25‰) and clearly higher than in present Baltic Sea, indicating that sulphate reduction has operated. These observations could support the existence of an iron-sulphide precipitation process in these groundwaters but not intense enough to effectively limit Fe^{2+} solubility. The question then arises as when did it happen?

The high Fe^{2+} concentration in these groundwaters and the main episode of sulphate reduction could have happened during Littorina Sea water infiltration through sea bottom sediments during the Littorina Sea stage. Sedimentological studies support the existence of sulphate reduction processes at that moment in the organic-rich sediments /e.g. Albi and Winterhalter, 2001/. Later on, the mixing of this Littorina Sea water with pre-Littorina groundwaters was not able to provide enough organic carbon to keep the sulphate reduction process going with the necessary intensity to completely reduce the high Fe^{2+} concentration in these waters /Pitkänen et al. 1999/. At present, sulphate reduction could be limited by the lack of nutrients or by competition with other organisms.

Finally, methanogens were found at 512.5 and 642.5 m depth but not in the deepest samples[7]. Besides, there are no isotopic data for the measured methane (cf. Appendix 2 and, therefore an organic control on the CH_4/CO_2 redox pairs for Forsmark groundwaters cannot be established.

4.5.2 M3 modelling

Introduction

A further modelling approach which is useful in helping judge the origin, mixing and major reactions influencing groundwater samples is the M3 modelling concept (Multivariate Mixing and Mass-balance calculations) detailed in /Laaksoharju et al. 1995; 1999/ and applied on the Forsmark 1.1 data in /Laaksoharju et al. 2004a/.

Model results

The M3 method consists of 4 steps where the first step is a standard principal component analysis (PCA), selection of reference waters, followed by calculations of mixing proportions, and finally mass balance calculations (for more details see Appendix 4).

The reference waters used in the M3 modelling have been identified from: a) previous site investigations (e.g. Äspö and Laxemar), b) evaluation of the Forsmark primary data set, and c) selecting possible compositions of end-members which according to the post glacial conceptual model (Figure 3-1) may have affected the site. The selected reference waters are more extreme than actually present at Forsmark (e.g. Rain-60 or Littorina Sea). Their function is: a) to be able to compare differences/similarities of the Forsmark groundwaters with possible end-members, b) to be available to describe all data used in the local and regional model, and c) to facilitate comparison with the results from the hydrogeological modelling. The analytical composition of the selected reference waters are listed in Appendix 4. The reference waters should not be regarded as point sources of flow but rather as possible contributors to the obtained water type. The reference waters have the following features:

- **Brine water:** Represents the sampled deep brine type (Cl = 47,000 mg/L) of water found in KLX02: 1,631–1,681 m /Laaksoharju et al. 1995/. An old age for the Brine is suggested by the measured ^{36}Cl values indicating a minimum residence time of 1.5 Ma for the Cl component /Laaksoharju and Wallin, 1997/. The sample contains some tritium (TU 4.2) which is believed to be contamination from borehole activities. In the modelling 0 TU were used for this sample.

[7] Unfortunately no data for the shallowest depths are available.

- **Glacial water:** Represents a possible melt-water composition from the last glaciation > 13,000 BP. Modern sampled glacial melt water from Norway was used for the major elements and the $\delta^{18}O$ isotope value (−21‰ SMOW) was based on measured values of $\delta^{18}O$ in calcite surface deposits /Tullborg and Larsson, 1984/. The $\delta^{2}H$ value (−158‰ SMOW) is a calculated value based on the equation ($\delta H = 8 \times \delta^{18}O + 10$) for the global meteoric water line.
- **Littorina Sea:** Represents old marine water and its calculated composition has been based on /Pitkänen et al. 1999/. This water is used for modelling purposes to represent past Baltic Sea water composition.
- **Modified Sea water (Sea sediment):** Represents sea water affected by microbial sulphate reduction.
- **Precipitation:** Corresponds to infiltration of meteoric water (the origin can be rain or snow) from 1960. Sampled modern meteoric water with a modelled high tritium (2,000 TU) content was used to represent precipitation from that period.

The results of the PCA modelling are shown at the regional scale (Forsmark data are compared with Simpevarp data and other Nordic sites data) in Figure 4-58. In Appendix 4 the local scale using only the Simpevarp data is shown also.

The M3 modelling shown in Figure 4-58 indicates that the Forsmark samples are affected by the reference waters: Meteoric, Marine and Glacial. The surface meteoric water types show seasonal variations and closer to the coast the influence of marine water (Baltic Sea) is detected for the shallow samples. Several samples from Forsmark are showing a possible Littorina Sea water influence which is much stronger at Forsmark compared with data from the Simpevarp area. Only a few samples at depth from Forsmark indicate a Glacial-Brine component. The deviation calculations

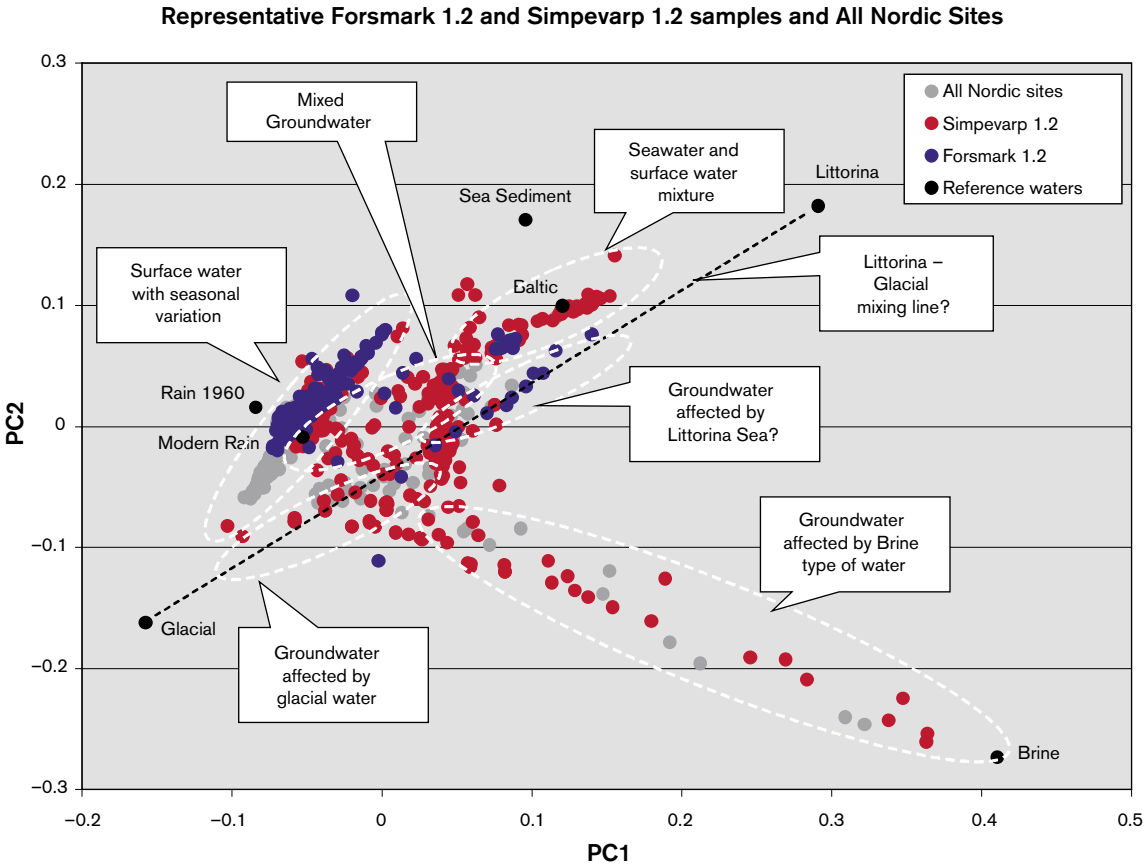

Figure 4-58. *PCA modelling of the representative Forsmark (blue dots), Simpevarp area (red dots) and Nordic data (grey dots). The reference waters used in the modelling are shown and the possible influences from different end-members on the samples are indicated.*

in the M3 mixing calculations show potential for organic decomposition/calcite dissolution in the shallow waters. Indications of ion exchange and sulphate reduction have been modelled. These M3 results support the initial evaluation of primary data and general modelling results described n previous chapters.

4.5.3 Visualisation of the groundwater properties

Measured Cl content and the calculated M3 mixing proportions based on representative samples are shown for two core boreholes within the modelling domain in Figure 4-59. The results for all the boreholes are shown in Appendix 4. The purpose of the plots is to show the water type, changes with depth, and to facilitate comparison of the hydrochemical results with the hydrogeological results. Due to the fact that the hydrogeologists use only 4 reference waters, the marine components (Littorina and Sea Sediment reference waters) were combined and referred to as Marine water.

The 3D/2D visualisation of the Forsmark Cl values was performed using the Tecplot code. Figure 4-60 shows the 3D and the 2D visualisation of Cl in the sampling points for all the samples (both representative and non-representative samples) and for the M3 mixing proportions. The relatively few observations in the 3D space results in uncertainties; only in the near-vicinity of the observations are the uncertainties low. However, the interpolations can still be used to indicate the major occurrence of the different water types at the site. For example: a) Meteoric water is dominating in the north west part and in the central part of the cutting plane, b) Marine water is found towards the coast in the east part of the cutting plane, c) Glacial influences is found in the deeper part of the boreholes KFM02A and KFM03A. The glacial component found in the NW is due to cold water influences in some of the shallow samples, and d) Brine type water component is increasing with depth.

The Figure 4-61 show an example of the comparison between the different mixing proportions calculated with the M3 versus the M4 codes. The M4 calculation code (cf. Appendix 3) performs the mixing calculations in multidimensional space and therefore the uncertainties associated with the mixing proportion calculations can be reduced. For the local PCA model, 295 samples can be calculated with M3 but only 106 samples with M4. A higher accuracy is obtained with the M4 calculation but there is risk of losses of observations. Further comparisons between the codes will be conducted in future phases of the project.

4.5.4 Coupled modelling

A first attempt for combined hydrogeological and hydrochemical analysis of Forsmark is described in Appendix 5. The main objective of this exercise is to develop a framework to integrate available hydrogeological and hydrochemical information, with special emphasis on the consistency assessment between them.

The adopted approach follows a systematic methodology from data analyses to preliminary modelling of groundwater flow and solute transport. These preliminary models must be regarded as a tool for quantitative testing of different hypothesis and/or conditions rather than a accurate descriptions of the site.

A groundwater flow simulation was performed using the boundary conditions and parameters described in Appendix 5. Figure 4-62 shows an example of computed results for conservative dissolved specie such as salinity using recharge flow rates of 1 mm/year and 2 mm/year, respectively.

Figure 4-62 shows that computed results using lower recharge values on the top boundary are more consistent with measured salinity in Forsmark. As expected, the simulated penetration of meteoric water is much shorter when using a recharge value of 1 mm/year (Figure 4-62A). In this scenario, 100% of meteoric water is only computed at very shallow depths under the inland surface close to the water divide (upper-right corner in Figure 4-8a). The rest of shallow granite shows meteoric water proportions between 20% (near the sea) and 100% (Figure 4-62A). Computed results using a recharge value of 2 mm/year shows a greater penetration of meteoric water into the shallow granite, ranging between 40% close to the sea (upper left in Figure 4-62b) to 100% inland.

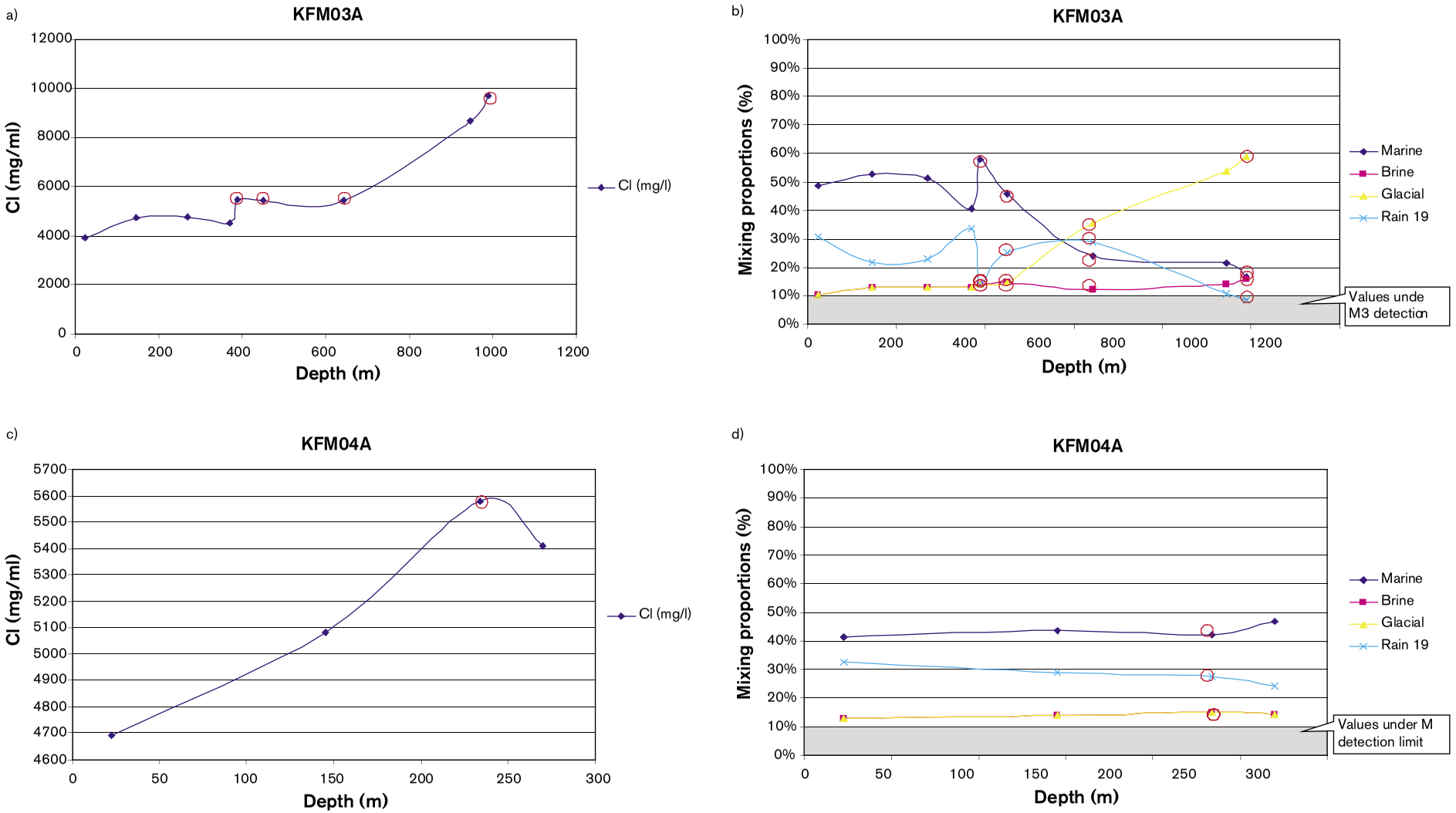

Figure 4-59. *(a) and (b) scatter plots of the Cl content and mixing proportions with depth for borehole KFM03A. (c) and (d) scatter plots of the Cl content and mixing proportions with depth of borehole KFM04. The samples with red circles indicate representative samples. A mixing proportion of less than 10% is regarded as being under the detection limit of the M3 method and is therefore shaded. The mixing proportions have an uncertainty range of ±0.1 mixing units.*

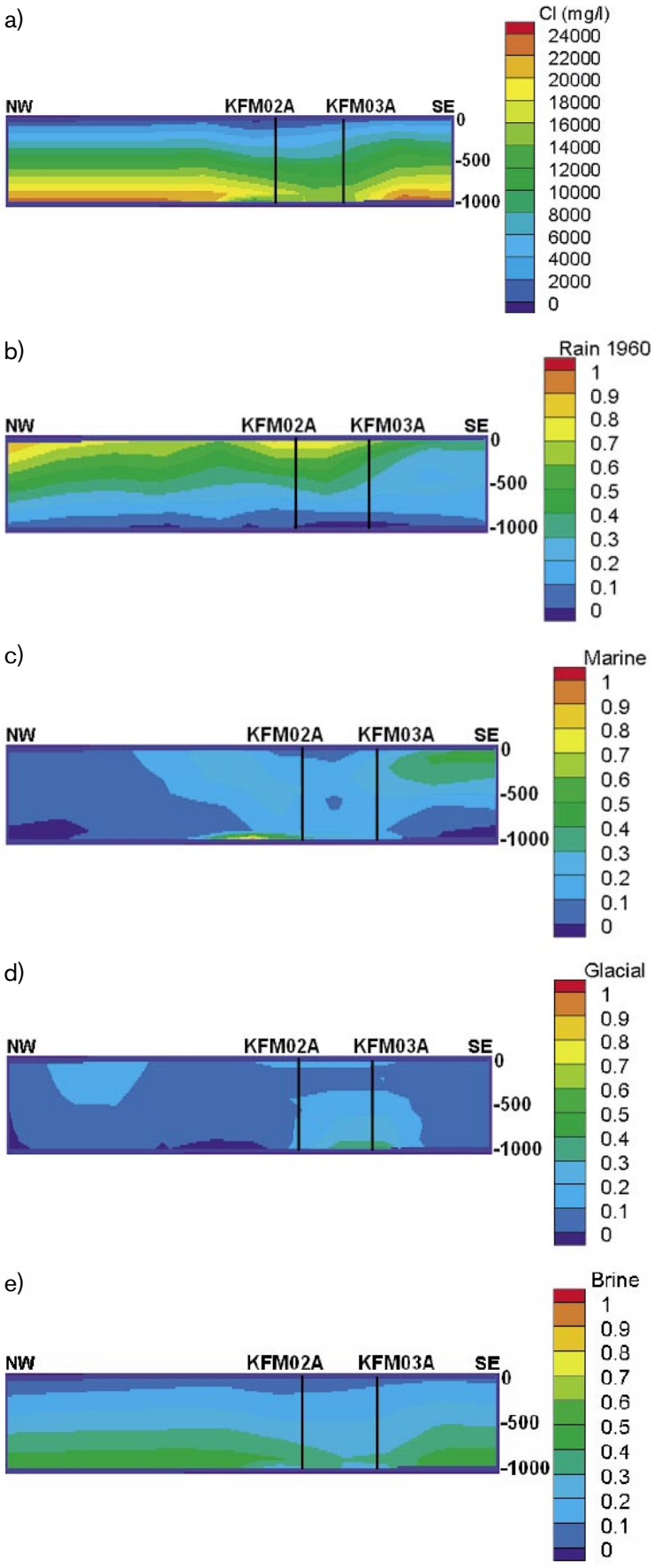

Figure 4-60. *3D interpolation and 2D visualisation of the groundwater properties along the NW-SE cutting plane (for orientation see Figure 4-2). (a) Cl interpolation, Figures b, c, d, and e show the mixing proportions for the water types Rain 1960, Marine, Glacial and Brine. The elevation is in metres.*

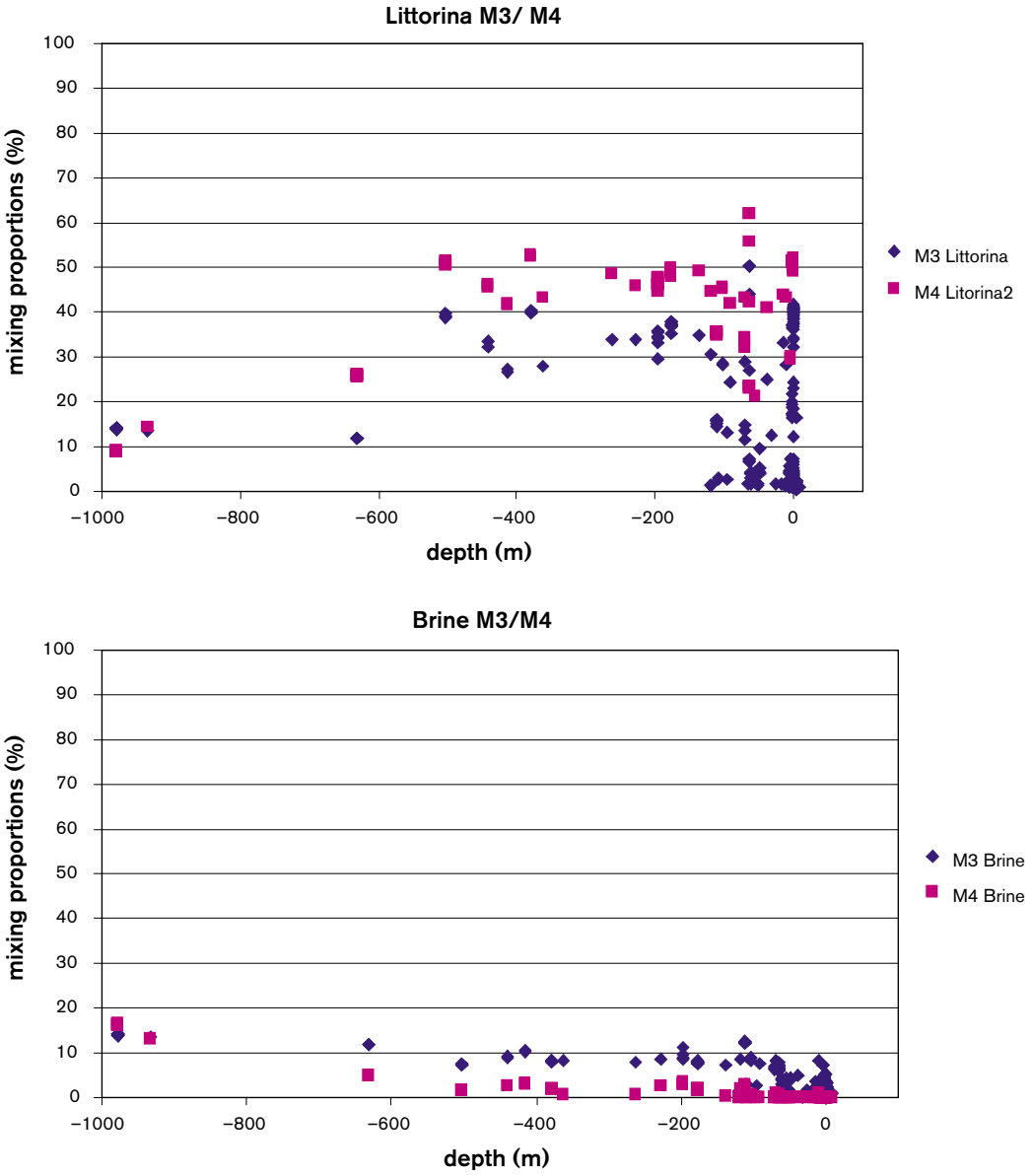

Figure 4-61. *Comparison of the Littorina Sea and Brine mixing proportions obtained with M3 versus M4 codes.*

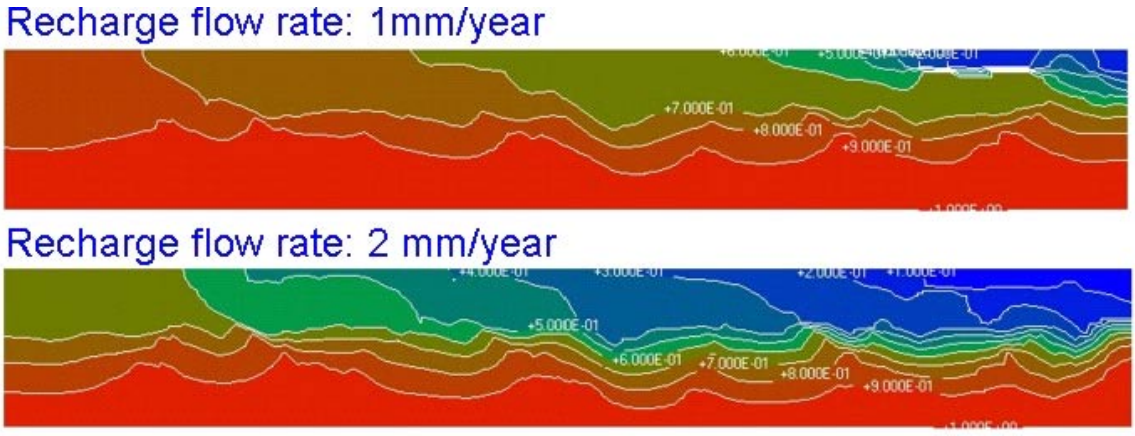

Figure 4-62. *Computed concentrations of a conservative dissolved specie (i.e. salinity) at 500 years using different values of recharge flow rate: a) 1 mm/ year; b) 2 mm/year. The transect coincides with the SW-NE cutting plane shown in Figure 4-1. The depth of the model domain is 1,000 m.*

According to these model results, it seems that the presence of shallow Littorina Sea signatures at Forsmark could be explained by decreasing recharge flow rates in the granitic top surface. The recharge value should be in the order of 5–10 times shorter than the recharge in other Swedish sites such as Simpevarp, Laxemar or Äspö. However, it is worth remarking that comprehensive sensitivity analyses has not been performed at the present stage of the work, so similar fresh water penetration into the bedrock can possibly be reproduced with different combinations of hydrogeologic parameters. This analysis should be performed in future versions of the work. For more details see Appendix 5.

Figure 4-63 shows a comparison of computed tritium contents (at simulated year 2004) using different recharge values on the top boundary. As expected, computed tritium concentrations are also highly sensitive to variations on the recharge flow rate prescribed in the top of the granite.

Computed tritium contents are consistent with previously computed results of salinity. Using a recharge flow rate of 10 mm/year (which is the average accepted value in Laxemar area) leads to a an unrealistic large penetration of meteoric water with high tritium contents. In this case, almost the first 500 m of the model domain contains water with 18–20 TU (Figure 4-63a). It has been already shown that this is not the case for shallow groundwater in Forsmark, where most of the water samples collected in the first 100 m of the bedrock have tritium contents in the range of 2 to 8 TU. It is worth noting that computed tritium contents in the shallow granite (in the equivalent positions to Forsmark site) are in the range of 6 to 14 TU when a recharge flow rate of 2 mm/year is prescribed (Figure 4-63b). Finally, it can be seen that using a recharge value of 1 mm/year leads to computed tritium contents in the range of 2 to 10 TU, which provide a much better agreement with field measurements.

In summary, both measured salinity and tritium contents could be "qualitatively" reproduced by reducing the effective recharge flow rate on the upper boundary of the model. Computed results suggest that effective recharge flow rates on the upper granitic surface of Forsmark could be shorter than expected. The "calibrated" effective recharge is as low as 1 mm/year. For more details see Appendix 5.

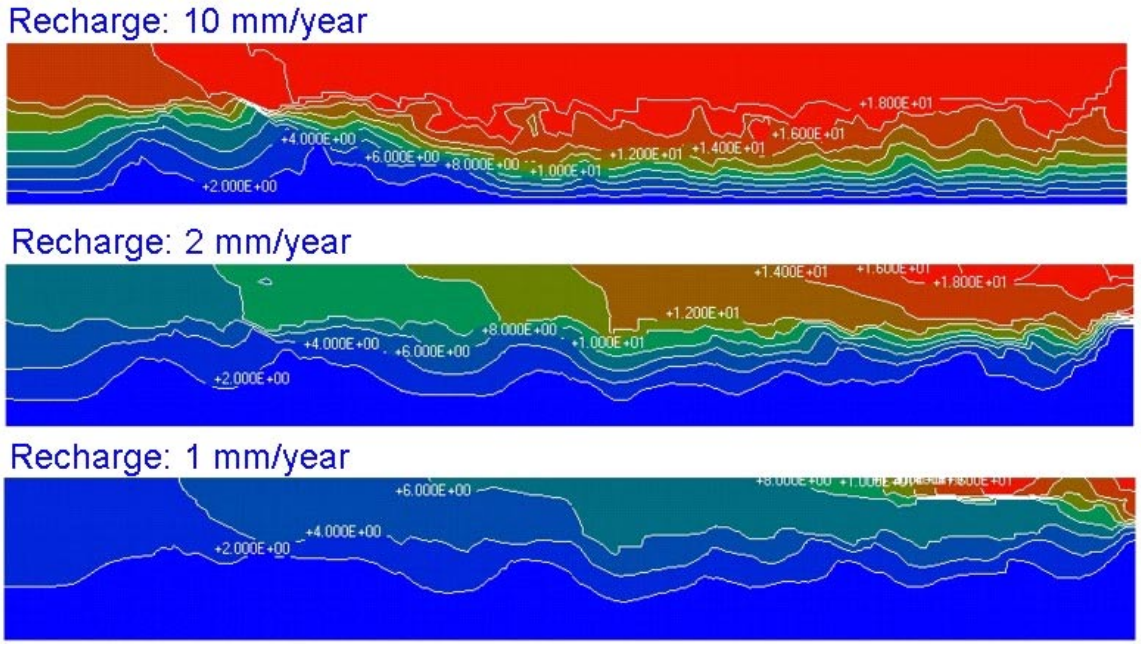

Figure 4-63. *Computed tritium concentrations (simulated year 2004) using different values of recharge flow rate: a) 10 mm/year, b) 2 mm/year, and c) 1 mm/year. The transect coincides with the SW-NE cutting plane shown in Figure 4-2 The depth of the model domain is 1,000 m.*

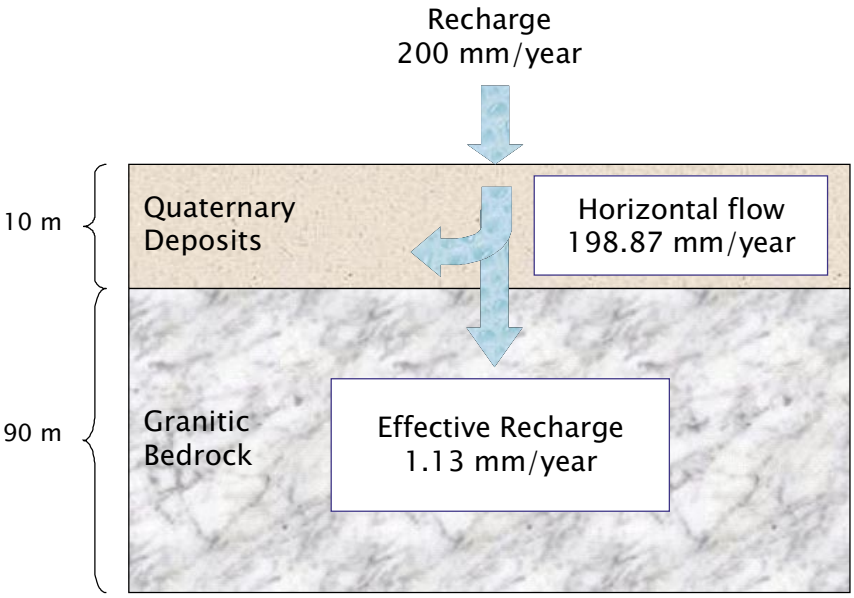

Figure 4-64. *Water budget computed with the base run of the numerical model. Computed effective recharge into the bedrock is about 1 mm/year.*

Water recharge into the granitic bedrock was modelled in Appendix 5. The computed water budget shows that the total amount of water crossing through the Quaternary – bedrock interface is as low as 1 mm/year. The rest of the infiltrated water circulates through the Quaternary deposits. Figure 4-64 illustrates the water budget computed with the numerical model. It is worth remarking that these results have been computed using average hydraulic conductivity values reported in SDM v1.1 /SKB, 2004/. Sensitivity analysis and uncertainty evaluation should be performed in future versions of this modelling approach.

Computed results shown in Figure 4-64 provide quantitative support to the hypothesis of having a very small effective recharge at Forsmark. It is worth remarking that this conclusion has been achieved by two different modelling approaches, but both of them are still affected by uncertainties. The Quaternary deposits of Forsmark are thought to play an important hydrogeologic role by limiting the amount of meteoric water penetration, and thus limiting the flushing of older groundwaters in the shallow bedrock. This hypothesis provides a plausible explanation for the distribution and permanence of Littorina Sea signatures which have been found in several Forsmark groundwater samples, even at shallow depths.

4.6 Evaluation of uncertainties

At every phase of the hydrogeochemical investigation programme – drilling, sampling, analysis, evaluation, modelling – uncertainties are introduced which have to be accounted for, addressed fully and clearly documented to provide confidence in the end result, whether it will be the site descriptive model or repository safety analysis and design /Smellie et al. 2002/. Handling the uncertainties involved in constructing a site descriptive model has been documented in detail by /Andersson et al. 2002/. The uncertainties can be conceptual uncertainties, data uncertainty, spatial variability of data, chosen scale, degree of confidence in the selected model, and error, precision, accuracy and bias in the predictions. Some of the identified uncertainties recognised during the modelling exercise are discussed below.

The following data uncertainties have been estimated, calculated or modelled for the Forsmark data; these are based on models used for the 1.1 model versions and based on the Äspö modelling where similar uncertainties are believed to affect the present modelling:

- disturbances from drilling; may be ± 10–70% (cf. DIS modelling in Appendix 4),
- effects from drilling during sampling; is < 5%,
- sampling; may be ± 10%,
- influence associated with the uplifting of water; may be ± 10%,
- sample handling and preparation; may be ± 5%,
- analytical error associated with laboratory measurements; is ± 5% (the effects on the modelling was tested in Appendix 1),
- mean groundwater variability during groundwater sampling (first/last sample); is about 25%.
- The M3 model uncertainty; is ±0.1units within 90% confidence interval (the effects on the modelling were tested in Appendix 4).

Conceptual errors can occur in, for example, the palaeohydrogeological conceptual model. The influence and occurrences of old water end members in the bedrock can only be indicated by using certain element or isotopic signatures. The uncertainty is therefore generally increasing with the age of the end member. The relevance of an end member participating in the groundwater formation can be tested by introducing alternative end member compositions or by using hydrodynamic modelling to test if old water types can reside in the bedrock during prevailing hydrogeological conditions. In this model version the validation is checked by comparison with hydrogeological simulations.

Uncertainties in the PHREEQC code depend on which code version is being used. Generally the analytical uncertainties and uncertainties concerning the thermodynamic data bases are of importance (in speciation-solubility calculations). Care also is required to select mineral phases which are realistic (even better if they have been positively identified) for the systems being modelled. These errors can be addressed by using sensitivity analyses, alternative models and descriptions. A sensitivity analysis was performed concerning the calculations of activity coefficients in waters with high ionic strength and also the uncertainties of the stability diagrams and redox modelling were discussed in Appendix 3.

The uncertainty due to 3D interpolation and visualisation depends on various issues, i.e. data quality, distribution, model uncertainties, assumptions and limitations introduced. The uncertainties are therefore often site specific and some of them can be tested such as the effect of 2D/3D interpolations. The site specific uncertainties can be tested by using quantified uncertainties, alternative models, and comparison with independent models such as hydrogeological simulations.

Uncertainties in the coupled coupled flow and solute transport modelling are numerous at the present site investigation stage. These uncertainties can be of two main types: (a) conceptual model uncertainties, and (b) parameter uncertainties. Coupled transport modelling is based on version 1.1 hydrogeological and current hydrochemical conceptual models. Thus, possible conceptual uncertainties are directly translated into the reactive transport model results. Conceptual uncertainties are mainly related to the extent and nature of boundary conditions (i.e. dimensions of the model, water recharge values, etc), and the selection of physical-chemical processes included in the calculations. Parameter uncertainties are also present in the model (permeability, porosity, cation exchange capacity, amount of calcite in the granite, etc). However, at present stage a coupled flow and transport model has been used as a tool for testing the consistency (or plausibility) of different assumptions. It is considered that parameter uncertainty is less relevant than conceptual uncertainties at the present stage.

The discrepancies between different modelling approaches can be due to differences in the boundary conditions used in the models or in the assumptions made. The discrepancies between models should be used as an important validation and confidence building opportunity to guide further modelling efforts. In this work the use of different modelling approaches starting from manual evaluation to advanced coupled modelling can be used as a tool for confidence building. The same type of process descriptions independent of the modelling tool or approach increases confidence in the modelling.

4.7 Feedback to other disciplines

4.7.1 Comparison between the hydrogeological and hydrogeochemical models

Since hydrogeology and hydrogeochemistry deal with the same geological and hydrodynamic properties, these two disciplines should be able to complement each other when describing/ modelling the groundwater system. Testing such an integrated modelling approach was the focus of a SKB project (Task 5) based on the Äspö HRL /Wikberg, 1998; Rhén and Smellie, 2003/. The advantages with such an approach were identified as follows:

- Hydrogeological models will be constrained by a new data set. If, as an example, the hydrogeological model, which treats advection and diffusion processes in highly heterogeneous media, cannot produce any Meteoric water at a certain depth and the hydrogeochemical data indicate that there is a certain fraction of this water type at this depth, then the model parameters and/or processes has to be revised.
- Hydrogeological models are fully three dimensional and transient processes such as shoreline displacement and variable-density flow can be treated, which means that the spatial variability of flow related hydrogeochemical processes can be modeled, visualised and communicated. In particular, the role of the nearby borehole hydraulic conditions for the chemical sampling can be described.
- Hydrogeochemical models generally focus on the effects from reactions on the obtained groundwater rather than on the effects from transport. An integrated modelling approach can describe flow directions and hence help to understand the origin of the groundwater. The turn over time of the groundwater system can indicate the age of the groundwater and, knowing the flow rate, can be used to indicate the reaction rate. The obtained groundwater chemistry is a result of reactions and transport, and therefore only an integrated description can be used to correctly describe the measurements.
- By comparing two independent modelling approaches a consistency check can be made. As a result greater confidence in active processes, geometrical description and material properties can be gained.

Major recent developments in hydrogeological modelling of the Simpevarp area (Rhén, pers. comm. 2004) and Forsmark (Follin, pers. comm. 2005) represents further progress since the TASK#5 exercise /Rhén and Smellie, 2003/. The present 1.2 modelling has further developed the comparison and integration between hydrochemistry and hydrogeology. The hydrogeological model can provide predictions of the groundwater components and isotopes such as Cl, ^{18}O and ^{2}H in the connected rock matrix, in the flowing groundwater and for dynamic predictions over time for the different water types (meteoric, marine, glacial and brine). Furthermore, the hydrodynamic model can, independently from chemistry, predict these salinity features at any point within the modelled rock volume, and the predictions can be checked by direct hydrogeochemical measurements or calculations. The mixing proportions from the hydrogeological model can, for example, be directly compared with the mixing calculations from the hydrogeochemical modelling or, conversely, the hydrogeochemical model can be used to predict the chemistry which results only from transport which, in turn, can be compared with that obtained from reactions. Such modelling will increase the understanding of transport, mixing and reactions and will also provide a tool for predicting future chemical changes due to climate changes. The coupled transport modelling presented in Appendix 5 can be used as an independent validity tool to check different processes and transport hypotheses.

5 Resulting description of the Forsmark area

5.1 Bedrock Hydrogeochemical Description

The results of the hydrogeochemical manual and mathematical modelling are used to produce a hydrogeochemical site descripte model. The model consists of a conceptual hydrochemical model of the site and of a descriptive part summarising the most important findings from the modelling.

5.1.1 Site descriptive hydrochemical model

One of the objectives of the Initial Site Investigation (ISI) stage is to produce versions of the hydrogeochemical descriptive model on a site scale. Visualisation of the hydrogeochemical 1.2 evaluation is in the form of two vertical transects through the Forsmark site local model area, one oriented in a SW-NE direction and the other in a NW-SE direction (for orientation see Figure 4-2). Their positions are based on topographical and hydrogeological criteria and the locations of the site characterisation boreholes (Follin, written comm. 2004). The vertical extent of the transects is to approx. 2,000 m to accommodate the known and suspected geological features. The approach to locate and construct the transect is described in Appendix 1. Based on existing geological and hydrogeological information, schematic manual versions of the transects were produced to facilitate illustrating the most important structures/fault zones and their potential hydraulic impact on the groundwater flow (Appendix 1). This hydraulic information was then integrated with the results of the hydrogeochemical evaluation and modelling results to show the vertical and lateral changes in the groundwater chemistry (Figure 5-1 and Figure 5-2).

Figure 5-1 shows the structural features with the main groundwater flow directions and the observed hydrochemistry along the SW-NE transect. Groundwater data are limited to shallow depths (0–350 m). Two major groundwater types are indicated: 1) recent to young (0–5.6 TU) Na-HCO_3 type of meteoric origin ($\delta^{18}O$ = –11 to –9‰ SMOW; δD = –81.9 to –77.5‰ SMOW), and 2) old Na-Ca Cl(SO_4) type (Littorina Sea signature) of marine origin ($\delta^{18}O$ = –9.5 to –8.4‰ SMOW; δD = –84.4 to –66.1‰ SMOW); some inmixing with present meteoric water and/or cold climate (glacial origin) may also be characteristic.

The lateral and vertical spatial extent of the Na-HCO_3 groundwater is uncertain due to a lack of data, but certainly the deeper, older Littorina Sea groundwater type lies close to the surface towards the SW in the near vicinity of the steeply dipping deformation zones NW003A and NW017A. These structures are believed to be discharging. Furthermore, close to Bolundsfjärden Lake the vertical extent of the Na-HCO_3 groundwater may be less than shown since this lake area is considered a zone influenced by discharge.

Figure 5-2 shows the structural features with the main groundwater flow directions and relative velocities and the observed hydrochemistry along the NW-SE transect.

The groundwater flow regimes at Forsmark are considered local and extend down to depths of around 600 m depending on hydraulic conditions. Close to the Baltic Sea coastline where topographical variation is even less, groundwater flow penetration to depth will subsequently be less marked and such areas will tend to be characterised by groundwater discharge.

Four main groundwater types are present. In addition to the recent to young Na-HCO_3 type groundwaters and old Na-Ca Cl(SO_4) type groundwaters (with a Littorina Sea and glacial signature) as already described above, there exist at greater depths (KFM03A; 645 m) an older meteoric Na-Ca-Cl type groundwater (~ 16 pmC) with a small glacial component ($\delta^{18}O$ = –11.6‰ SMOW; δD = –84.3‰ SMOW). At still greater depth (KFM03A: 990 m) the groundwater changes to a higher saline Ca-Na-Cl type characterised by an even greater glacial signature ($\delta^{18}O$ = –13.6‰ SMOW; δD = –98.5‰ SMOW). Although only one deep sample exists, the A2 gently dipping zone appears to form the boundary between the Na-Ca-Cl and Ca-Na-Cl groundwater types were borehole KFM03A is drilled.

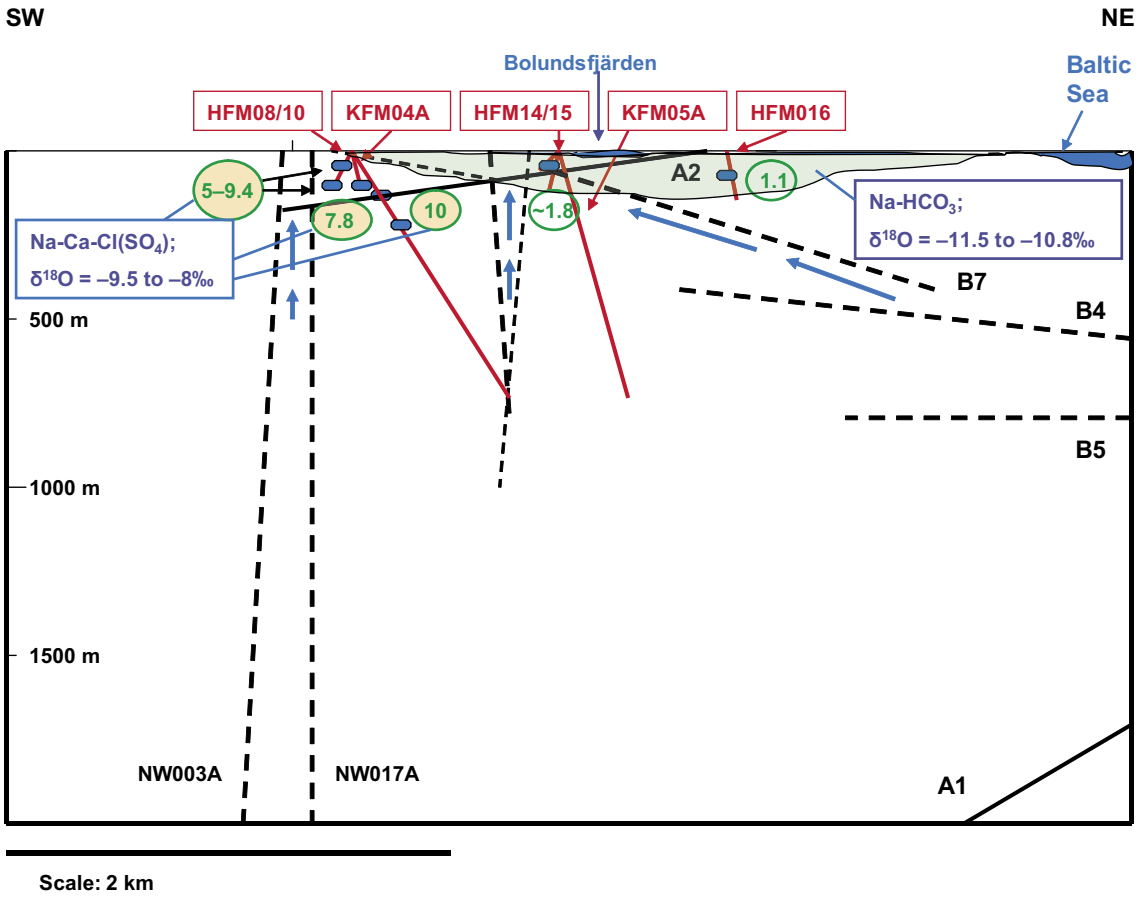

Figure 5-1. *Schematic 2-D model integrating the major structures, the major groundwater flow directions and the different groundwater chemistries. Sampled borehole sections are indicated in blue, circled numbers refer to g/L TDS and the orange infilled circles refer to groundwaters exhibiting a Littorina Sea signature. The blue arrows are estimated groundwater flow directions and their respective lengths reflect relative groundwater flow velocities (short = low flow; longer = greater flow). The 'δ' values refer to 'δ^{18}O = ‰ SMOW'.*

The near-surface Na-HCO_3 groundwaters form a distinctive horizon at the centre of the transect which lenses out towards the SE Baltic Coast where discharge of deeper groundwater probably occurs. From Bolundsfjärden to the NW a less marked horizon is indicated but data are few. In addition the influence of the deformation zone A2 on the groundwater chemistry is not clear at this near-surface locality.

Bordering the shallow Na-HCO_3 groundwaters, and extending from close to the surface (near the SE coast) to depths of around 500 m (along the gently dipping deformation zone A2), are the Littorina Sea type groundwaters. The upward (discharging) movement of these Littorina Sea type groundwaters below Bolundsfjärden Lake is supported by the soil pipe groundwater sample SFM0023 collected under Bolundsfjärden showing increased Mg and SO_4. Therefore, assuming that Bolundsfjärden Lake is a recharge area, which in Figure 1.6 may correspond to the intersection of the illustrated steeply dipping deformation zones (further connected to A2), then the distribution of the near-surface Na-HCO_3 groundwaters may be as indicated although a mixture of Na-HCO_3 and deeper Littorina Sea groundwaters would be more representative in the bedrock under Bolundsfjärden Lake.

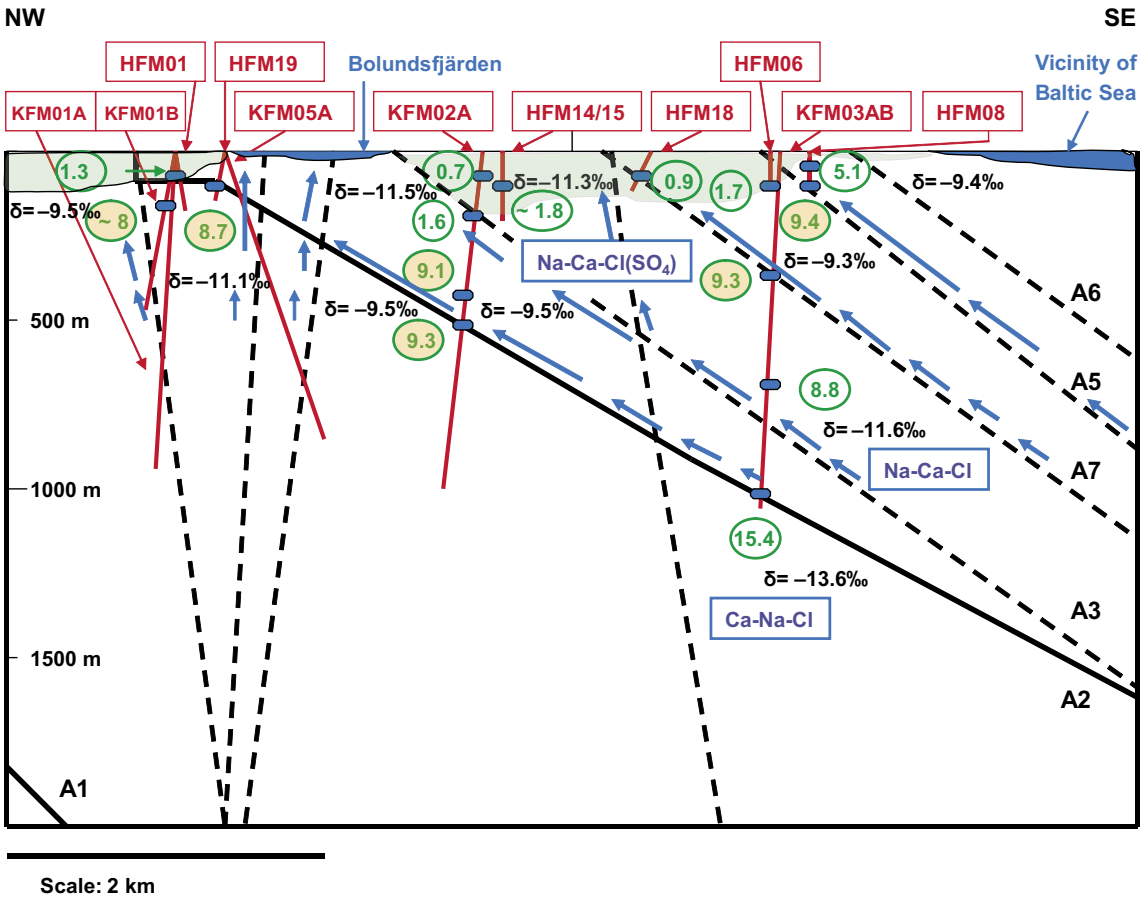

Figure 5-2. *Schematic 2-D model integrating the major structures, the major groundwater flow directions and the variation in groundwater chemistry from the sampled boreholes. Sampled borehole sections are indicated in blue, circled numbers refer to g/L TDS and the orange infilled circles refer to groundwaters exhibiting a Littorina Sea signature. The blue arrows are estimated groundwater flow directions and their respective lengths reflect relative groundwater flow velocities (short = low flow; longer = greater flow).*

5.1.2 Descriptive and modelled features of the site

Descriptive and modelled observations are included in the hydrogeochemical site descriptive model and they are the fundamental behind the overall hydrochemical understanding of the site. The most important features are summarised in the chapters below. The final result of the hydrogeochemical evaluation is to assess that the site meets the SKB hydrogeochemical stability criteria. These parameters are discussed in the last chapter.

Descriptive observations

Main elements

- General depth trends show increasing TDS with depth; in particular the increase in Ca/Na and Br/Cl ratios.
- Three main depth-related hydrochemical subdivisions can be recognised: a) shallow (0–150 m) dilute groundwaters (< 1,000 mg/L Cl), b) intermediate (~ 150–600 m) brackish groundwaters (5,000–6,000 mg/L Cl), and c) deep (> 600 m) saline groundwaters (~ 10,000 mg/L Cl).
- The dilute shallow region is characterised mainly by Na-HCO_3-type groundwaters, but subordinate Na-HCO_3(SO_4) to Na(Ca)- HCO_3-Cl(SO_4) groundwater types also occur.

- The intermediate groundwater region is dominated by Na(Ca, Mg)-Cl(SO_4) to Na-Ca(Mg)-Cl(SO_4) groundwater types. A strong Littorina Sea signature is apparent in this brackish region.
- The deep groundwater region comprises Na-Ca-Cl to Ca-Na-Cl groundwater types.
- The marked deviation of the deep groundwater from all other groundwaters can be explained by increased mixing with an older deep saline component of a non-marine or non-marine/old marine origin. This is clearly shown by the Na/Ca/Mg and Br/Cl ratios versus Cl content. Only one deep groundwater sample so far exists, that from borehole KFM03A at 980–1,001 m. This borehole is characterised by fracture zones A4, A7 and B1 within the depth interval of 350–550 m. It would seem that this structural interval hydraulically separates brackish groundwaters partly of old and/or new marine origin, from deeper increasingly saline groundwaters of non-marine origin.
- Compared to other Fennoscandian sites, Forsmark shows close similarities with the nearby Finnsjön and SFR sites and also to the Olkiluoto site in Finland. The similarity with Olkiluoto, especially down to 500 m, is particularly relevant as the brackish groundwaters at this site also have a strong Littorina Sea signature.
- The Littorina Sea signature at Forsmark is indicated mainly by increases in Mg and SO_4, both of which decease rapidly after 500–600 m depth. A marine origin is further supported by the Br/Cl ratios. Although HCO_3 decreases markedly after 150 m depth, it persists at around the 100 mg/L level within the Littorina-type brackish groundwaters before dropping to very low values at depths greater than 500 m.

Isotopes

- The stable isotope data plot on or close to the Global Meteoric Water Line (GMWL) indicating a meteoric origin for the Forsmark waters. Values range from $\delta^{18}O$ = –13.6 to –8.4‰ SMOW and δD = –98.5 to –66.1‰ SMOW with the most negative isotopic signatures (i.e. cold climate meteoric input) corresponding to the deepest groundwater sampled at 980–1,001 m.
- Plotting oxygen-18 against chloride further details the three distinct groups of groundwaters present at Forsmark: a) shallow, dilute groundwaters with a narrow range of $\delta^{18}O$ (–12 to –10‰ SMOW), close to present day precipitation, b) a wider range of values ($\delta^{18}O$ = –12 to –8‰ SMOW) for the more brackish groundwaters, the large variability in $\delta^{18}O$ is explained by mixing between glacial and Littorina Sea (characterised by heavier isotope values) groundwaters, and c) the deepest outlier ($\delta^{18}O$ = –13.6 SMOW) representing the most saline groundwater.
- One problem in using tritium for the interpretation of near-surface recharge/discharge is its variation in recharge water over time. This implies that near-surface groundwaters with values around 15 TU can be 100% recent, or a mixture of old meteoric (tritium free) water, and also a small portion (10%) of water from the sixties at the height of the atmospheric nuclear bomb tests.
- Below 200 m depth tritium values under 3 TU are detected for all samples. For the borehole sections sampled below 300 m there are samples with no detectable tritium but in two cases a few tritium units have been measured in the last sample collected in the time sequence prior to sampling. One of the near-surface samples KFM03A (0–46 m) shows a very high tritium content of 41 TU indicative of a significant portion of recharge from the sixties or seventies when tritium contents were much higher than at present. There is therefore the possibility that the observed tritium values in some of the deeper sampled borehole sections reflect some contamination by these tritium-enhanced waters entering into water-conducting fracture systems during open hole borehole activities.
- Tritium contents in surface and near-surface waters need to be carefully interpreted. For example, the measured tritium contents in the precipitation and Baltic Sea water at Forsmark may also contain some tritium locally produced by the nuclear power plants, i.e. that emitted as vapour to the atmosphere and that contained in the cooling water discharged to the Baltic Sea.
- The plot of tritium versus ^{14}C for surface waters from Forsmark shows that most Lake and Stream waters have higher ^{14}C values compared with Baltic Sea waters, whereas the tritium values range from 10–15 TU for all three water sources, although generally there is higher tritium in the Baltic Sea waters (due to reservoir effects).

- The tritium-free groundwaters from Forsmark show ^{14}C values in the range 14–25 pmC and these waters have generally low HCO_3 contents (< 150 mg/L) and $\delta^{13}C$ values between –10 and –5‰. A plot of ^{14}C (expressed as pmC) versus $\delta^{13}C$‰, shows that groundwaters from the percussion and cored boreholes indicate a mixing trend between: a) HCO_3-rich waters with low $\delta^{13}C$ and high ^{14}C content, and b) deeper groundwaters with lower HCO_3 contents, higher $\delta^{13}C$ values and lower ^{14}C.
- The groundwaters showing the lowest ^{14}C values have chloride contents ranging from 4,500–5,500 mg/L; these indicate marine signatures, i.e. they represent waters with a dominant Littorina Sea component. (Note: No ^{14}C analyses are available from the deep saline groundwaters). In terms of 'relative age', the measured pmC values indicate 11,000–16,000 years which is significantly older than the Littorina Sea period. This can be explained by an addition of older bicarbonate, probably by dissolution of older carbonate and/or mixing by glacial water (supported by low $\delta^{18}O$ in at least some of these groundwaters).
- The $\delta^{34}S$ data have a wide range (–11 to +30‰ CDT) indicating different sulphur sources for the dissolved SO_4. For the surface waters (Lake and Stream waters) the SO_4 content is usually below 35 mg/L and the $\delta^{34}S$ is relatively low but variable (–1 to +11‰ CDT) with most of the samples in the range 2 to 8‰ CDT. These relatively low values indicate atmospheric deposition and oxidation of sulphides in the overburden as being the origin for the SO_4. The Baltic Sea samples cluster around 20‰ CDT with some less saline Baltic samples showing lower $\delta^{34}S$ values resulting from inmixing of surface water.
- The deeper groundwaters show $\delta^{34}S$ values in the range +12 to +26‰ CDT where all samples with SO_4 contents greater than 250 mg/L show $\delta^{34}S$ values higher than +20‰ CDT. Such values are usually interpreted to result from sulphate-reducing bacterial activity in the bedrock aquifer.
- The Cl versus $\delta^{34}S$ plot shows a clear trend with higher $\delta^{34}S$ values for groundwaters with higher salinities than present Baltic Sea waters (2,800 mg/L Cl). If the $\delta^{34}S$ values in the marine groundwaters are modified by sulphate-reducing bacteria during closed conditions then a clear trend of more positive $\delta^{34}S$ values with decreasing sulphate content should be the result. This is not seen and therefore several processes need to be considered.
- The relatively few fracture calcites so far analysed for Sr-isotopes show values below 0.718 supporting that they are not precipitated from today's groundwater and that calcite dissolution has had little influence on the Sr-isotope ratios in the groundwater.
- Plotting $\delta^{37}Cl$ against chloride shows that most of the surface, near-surface and Baltic Sea waters have values within the range –0.28 to +0.34‰ SMOC. The former waters have the greatest spread (–06 to +2‰ SMOC) where most of the samples are within the interval –0.2 to +05‰ SMOC. The majority of the Baltic Sea samples values are close to 0‰ SMOC or slightly higher (up to +0.3‰ SMOC); a few samples show also lower values down to –0.6‰ SMOC.
- $\delta^{37}Cl$ in groundwaters from the cored and percussion boreholes are between –0.2 to +0.6‰ SMOC and demonstrate no relation with increasing chloride content. Given the analytical uncertainty of around ±2‰ SMOC, the groundwater values correspond to a slight emphasis on a water/rock origin.
- The presence of uranium in surface and near-surface waters is characterised by values between 0.05 and 28 µg/L. Large variations in uranium content in surface waters are common and are usually ascribed to various redox states and various contents of complexing agents, normally bicarbonate.
- Uranium versus bicarbonate for the waters shows no clear trend although there is a tendency of higher uranium contents in the surface and near-surface groundwaters associated with increasing bicarbonate up to 400 mg/L. For the few near-surface waters with higher bicarbonate contents the uranium tends to decrease, which may be due to very low redox potential in these waters caused by the microbial reactions producing the bicarbonate (probably to large extent sulphate reducers).
- Uranium versus chloride shows that the highest uranium contents are found in the waters with chloride values around 5,000–5,500 mg/L, i.e. the brackish groundwaters dominated by a Littorina Sea water component.

- These high but variable uranium contents at Forsmark are accompanied by increased ^{226}Ra and ^{222}Rn indicating that uranium and radium along the fracture pathways have been mobilised to various degrees by the slowly descending Littorina Sea waters. One possible scenario is that the glacial melt water is accompanied by oxidised uranium into the (near-surface?) fracture zones and subsequently easily remobilised by the reducing but bicarbonate (and DOC) rich Littorina Sea water. The mobilised uranium was then transported to greater depths during the density turnover. The reducing character of the Littorina Sea water is supported by, for example, the high Mn^{2+} contents (1–3 mg/L; resulting from Mn-reducing bacteria) recorded for most of the uranium-rich water samples.
- The primary origin of the oxidised and remobilised uranium may have been the uranium mineralisations found at several localites in Uppland. For example, pitchblende vein fillings in skarn have been documented only some kilometres from the Forsmark site.

Microbes, colloids and gases

Three boreholes with six different depths were sampled and the data were used in a two-dimensional descriptive biogeochemical model.

- Redox potentials in the boreholes differed from –140 mV to –250 mV.
- At the shallowest depths with the relatively high redox potential, iron- and manganese-reducing bacteria dominated.
- The number of methanogens was high in KFM02A: 512.5 m.
- Sulphate-reducing bacteria together with acetogens dominated at one of the deep levels (KFM03A: 943 m).
- The abundance and activity of microbial species in the Forsmark boreholes seem to be closely correlated with the redox potential.
- High percentage of cultivable microorganisms with the MPN method was found in KFM01A: 115.4 m (iron-and manganese-reducing bacteria) and in KFM03A: 943 m (sulphate-reducing bacteria and acetogens).
- An explanation for the different amounts of cultivable cells could be differences in flow and mixing of groundwaters at the sampled sites. Thorough mixing of two or more groundwaters resulting in a gradient of different redox pairs would promote growth and activity of microorganisms with a suitable metabolism.
- The filtration data available seems to agree with the numbers of colloids earlier reported from Äspö and Bangombé, Gabon /Laaksoharju et al. 1995; Pedersen, 1996/. The new sampling and filtering methods seemed to work well since the amounts of calcium carbonates were very low. This suggests a rethinking of the sulphur colloids since they might have initially existed as colloids present in the groundwater and then probably as iron sulphides. The silicon values from KFM01A, 115.4 m most likely represent sampling artefacts,
- The fractionation data show that there should not be any colloids in the size range < 1,000 D but rather < 5,000 D. Although this is in contradiction to the filtration results, they could be closer to the truth. There are no sulphur values reported from this method; it would be interesting to carry out a comparison with the filtration method since the presence of iron sulphides could be one explanation for the low sulphide values found in groundwater, even if SRBs (sulphate-reducing bacteria) were present.
- Data for the numbers of particles could increase the value of colloid analyses by making it possible to calculate the number of binding sites for radionuclides in the different colloid fractions.
- Comparison of the two methods, filtration and fractionation, needs to be further evaluated.
- Up to 12 gases were analysed: helium, argon, nitrogen, carbon dioxide, methane, carbon monoxide, oxygen, hydrogen, ethyne, ethene, ethane and propane. So far, the amounts of gas data are limited and exclude any considerable analysis of the impact of gases on geochemistry and microbiology but there is a clear trend with increasing volumes of gas towards depth.

- The available gas data for the Forsmark area show that the gas content is in the same order of magnitude as in most of the Nordic sites studied.
- The gases are probably mostly mantle-generated.
- Gases are probably oversaturated in relation to atmospheric pressure but not at depth.

Modelled observations

PHREEQC modelling

Groundwaters in Forsmark can be divided into three groups based on their salinity:

(1) *Saline groundwaters* with a brine signature (only 1 representative sample: #8152). Mixing between Brine and Glacial end members is responsible, directly or indirectly, for most of their chemical content, especially for Cl concentrations higher than 7,000 mg/L. A Littorina component is absent or in a very low percentage. Their alkalinity is low, and controlled by equilibrium with calcite. pH is controlled by calcite equilibrium and, possibly, by reactions with aluminosilicate minerals. These old mixed waters tend, with time, to re-equilibrate with the complex mineral assemblage identified as fracture fillings in Forsmark. Both mass balance and thermodynamic calculations predict low reaction mass transfers between these waters and the aluminosilicates, although more work is needed due to the wide variety of aluminosilicates detected. Fast cation exchange reactions are also possible but, in groundwaters with long residence times, these exchange processes may cause irreversible changes in the clay minerals /Pitkäanen et al. 1999/, favouring an apparent solubility control.

The redox state is mainly controlled by the sulphur system. The existence of active sulphate-reduction processes and sulphide precipitation is in agreement with the presence of high numbers of sulphate-reduction bacteria (SRB) detected in the microbiological analysis.

Finally, the high contribution of the Glacial end member points to the forced introduction of glacial melt water in Forsmark which reached at least a depth of 1,000 m. This penetration depth is higher than at Olkiluoto, but similar to that reported in other Swedish sites /Puigdomenech, 2001/.

(2) *Brackish groundwaters* with an important and relatively constant Littorina Sea component. They are widely distributed in the Forsmark area, from very shallow levels (discharge areas?) to 500 m depth. A combination of slow and fast chemical reactions have influenced the mixed groundwaters waters. Calcite re-equilibrium and Ca-Na exchange reactions are the kinetically most favoured processes. Re-equilibrium with different aluminosilicates is also possible, although the mass transfers involved are low even when “forcing” pure equilibrium situations.

As in other Littorina-rich groundwaters /Pitkänen et al. 2004/, the iron concentration is variable but usually high, while dissolved sulphide, although detectable, is present in very low concentrations. This suggests that sulphate reduction is of minor importance (in agreement with microbial studies) and that iron does not have a strict solubility limit through sulphide precipitation. In this situation, the good results provided by the sulphur redox pairs in characterising the redox state of these groundwaters deserve further attention.

The penetration depth of Littorina Sea waters (500 m) is higher than presumed in the previous work (Forsmark 1.1; /Laaksoharju et al. 2004a/), and slightly higher than the one deduced for Olkiluoto /Pitkänen et al. 1999, 2004/. However, this penetration depth appears to be similar to that calculated for the Äspö area /Puigdomenech, 2001/.

(3) Non saline dilute groundwaters in Forsmark cover a wide range of chloride concentrations and show different trends (Ca-Na-HCO_3, Na-HCO_3-Cl, Na-Cl-HCO_3, etc). The compositional character of the most diluted groundwaters is controlled by weathering reactions (dissolution of calcite, plagioclase, biotite, sulphides, etc) induced by atmospheric and biologically produced dissolved gasses (CO_2 and O_2). More concentrated waters show an additional and variable mixing contribution with a marine component (some of them with a clear modern Baltic Sea signature) that gradually promotes Na-Ca exchange and the precipitation of calcite.

M3 and DIS modelling

M3 modelling helped to summarise and understand the data in terms of origin, mixing proportions and reactions.

The surface meteoric type waters show seasonal variations and closer to the coast the influence of marine water is indicated. Several samples from Forsmark are showing a possible Littorina Sea water influence; this signature is much clearer at Forsmark compared with the data from the Simpevarp area. Only a few samples at depth from Forsmark indicate a Glacial-Brine component. The deviation calculations in the M3 mixing calculations show the potential for organic decomposition/calcite dissolution in the shallow waters. Indications of ion exchange and sulphate reduction have been modelled. These M3 results support the initial evaluation of primary data and general modelling results.

The 3D/2D visualisations indicate that meteoric water is dominating in the northwest part and in the middle part of the site. Marine water is found towards the coast in the eastern part of the site. Glacial influence is found in the deeper part of the boreholes KFM02A and KFM03A. Brine type water component is increasing with depth.

DIS evaluation can help to judge the representativeness of the sampled data. The section 509–516 m in KFM02A was investigated and the results showed that pumping should have continued further in order to remove the additional 12.6 m^3 water still influenced by flushing water contamination. The study identified that there are uncertainties in the dosing and control of the uranine during the drilling process.

Coupled transport modelling

Well developed Quaternary deposits occupy more than 80% of the emerged lands in Forsmark. These Quaternary deposits can be conceptualised as a 3-layer hydrogeologic domain, with the first and third layer being highly conductive. Quaternary sediments may play a significant role since most of the infiltrated water could flow through the conductive layers to discharge zones, mainly located al lakes and the Baltic coast line. Based on this hypothesis, the effective recharge into the granitic bedrock is estimated to be shorter than in other investigated sites such as Simpevarp and Laxemar, where the presence of Quaternary overburden is less important.

Based on numerical modelling, and using average values of reported hydraulic conductivity, effective recharge actually reaching the granitic bedrock has been estimated to be on the order of 1 mm/year. By using this recharge flow rate, meteoric water penetration and tritium contents can be qualitatively reproduced in larger-scale numerical models.

The hydrogeologic behaviour of the Quaternary overburden in Forsmark provides a plausible explanation for the presence of Littorina Sea signatures found in several groundwater samples, even at very shallow depths. Other (and complementary) explanations can be related with the flat topography, as well as with the fact that the Forsmark site has emerged over the sea level more recently than other investigated sites.

Contrary to what was observed at Simpevarp, near-surface groundwater in Forsmark is at saturation, even over-saturated, with respect to calcite. This provides additional support to the hydrogeologic role of the Quaternary sediments, where large amounts of calcite have been reported (up to 20%).

Hydrochemical and isotopic patterns observed in soil pipe samples are consistent with field data of phreatic level. Water samples collected in recharge zones (with the highest phreatic levels) are Ca-HCO_3 in type, and show high tritium and low $\delta^{18}O$ values compared to water samples collected at discharge zones. The latter are Na-HCO_3-Cl in type and show lower tritium contents and higher $\delta^{18}O$ values. ^{14}C data are also consistent with this trend, with the highest pmC values in the recharge zones and the lowest in the discharge zones. However, hydrochemical and isotopic differences have been detected between the presumed discharge zones.

Shallow groundwaters under Bolundsfjärden show the highest salinity (~ 4,000 mg/L Cl) and low tritium values (~ 2 TU). Whether this indicates the discharge of deeper groundwater should be further investigated. Other explanations are possible such as the presence of “trapped” relict water not yet flushed out (due to low permeability bedrock, quasi-stagnant water pockets, etc).

The rest of the presumably discharge zones seem to display along a theoretical mixing line between Littorina Sea and recent-fresh groundwater. The most relevant ones are a small lake (SFM12), soil pipes under the Baltic Sea (SFM15 and 24) and other soil pipes at (or close to) topographical minima. The convergence of both very local (shallow) and deeper flow lines, in different proportions of flow rates, could explain the different degree of apparent mixing. Again, other explanations are possible and should be investigated in future stages of the site investigation programme.

Eckarfjärden has been also identified as a groundwater discharge zone. However, hydrochemical and isotopic signatures show significant differences compared to the rest of the discharge zones. Groundwater under this lake is diluted and has relatively low tritium values (3–5 TU) but, according to the δ^{18}O-Cl plot, this shallow groundwater is the only one which seems to be out of the theoretical mixing line with Littorina Sea water. It is interesting that this lake is the one located more distant to the coast and close to a pronounced topographical slope-change. The absence of information inland makes it difficult to establish reliable hypotheses to explain the hydrochemistry of this discharge zone.

Down to the Quaternary-bedrock interface groundwater is more saline, with maximum values of about 5,000 mg/L which coincide in the same area to the brackish water in the Quaternary soil pipes, pointing towards the occurrence of deep groundwater discharge in these areas. On the other hand, some local recharge areas of the near-surface groundwater system (Quaternary) are not clearly reflected in the hydrochemical signatures of shallow bedrock groundwater.

Hydrochemical stability criteria

The modelling indicates that the groundwater composition at repository depths is such that the representative sample from KFM02A: 509–516 m and KFM03A: 448–453 m can meet the SKB chemical stability criteria (Table 5-1) for Eh, pH, TDS, DOC and Ca+Mg /see Andersson et al. 2000/.

Table 5-1. The hydrochemical stability criteria defined by SKB are valid for the analysed values of the represenative samples KFM02A: 509–516 m and KFM03A: 448–453 m.

	Eh mV	pH (units)	TDS (g/L)	DOC (mg/L)	Colloids (mg/L)	Ca+Mg (mg/L)
Criterion	< 0	6–10	< 100	< 20	< 0.5	> 4
KFM02A: 509–516 m	–140	7.0	9.2	2.1	< 0.1	1,160
KFM03A: 448–453 m	–250	7.5	9.2	1.2	< 0.1	1,187

NA = Not analysed

5.2 Consistency between bedrock disciplines

The consistency between the hydrochemical and hydrogeological description will be discussed in the integrated site description report.

5.3 Consistency in interface between the surface and bedrock system

The groundwater chemistry description data from surface to depth are used to produce a description at the interface between the surface and bedrock water systems. The coupled modelling in Appendix 5 describes this interaction. A more detailed description will be given in the integrated site description report.

6 Conclusions

6.1 Overall changes since previous model version

In this report the salinity distribution, water type occurrence, mixing processes and the major reactions altering the groundwaters have been modelled in detail to the depth of 1,000 m. A new hydrogeochemical site descriptive model version 1.2 has evolved. The resulting description has improved compared to the 1.1 version by producing a more detailed process modelling, redox description, and microbial description including colloids and gas. The microbial characterisation gives direct support to, for example, the redox modelling. The coupled transport modelling can address processes and questions from a solute transport point of view which is a major improvement.

6.2 Overall understanding of the site

The overall understanding of the site describes the major processes taking place at the surface and to depth which includes expected repository levels. The confidence in this description is relatively high since independent model approaches were utilised in the work. The origin, the postglacial evolution and the major reactions in the waters are fairly well understood. However, confidence concerning the spatial variation is low due to relatively few observations at depth. The continuation of the ongoing sampling programme at Forsmark will provide better spatial information and thus will increase confidence.

6.3 Implication for further modelling

Comparison and integration between geological and hydrogeological models was in this model version restricted to input concerning the structural model, fracture mineralogy, postglacial scenario models, chloride, TDS, oxygen-18, tritium, carbon-14 and mixing proportion calculations.

Future coupled reactive transport modelling should incorporate additional geochemical processes. Further developments could also incorporate geological heterogeneity, as well as the deeper saline groundwater system.

The use of independent modelling approaches within the HAG group provided the possibility to compare the outcome of the different models and to use discrepancies between models to guide further modelling efforts. The many similarities resulting from the HAG modelling gave confidence to the obtained results.

The correct choice of groundwater end members is important for many of the modelling exercises reported. Whilst experience from Äspö and other Fennoscandian sites has contributed to a standard set of groundwater end members, individual sites (at different depths) may lack one or more of these standard end members. This possibility will have to be taken into account. In future versions, end-member variants will be further tested and also alternative models to M3 to calculate the groundwater mixing proportions will be further explored (Gomez, pers. comm. 2004). The general application of alternative models and descriptions should be further developed in future versions together with uncertainty tests of the models applied.

6.4 Implications for the ongoing site investigation programme

From the HAG modelling work the following suggestions have been made for the ongoing site investigation programme ***(the response from the site is indicated in italics)***:

All samples should have x, y, z coordinates in order to be useful in the visualisation work. These coordinates should be listed in SICADA as are the mid section coordinates. Those z coordinates not always available for the surface samples (sea, lake, streams) were estimated to be 0. However,

to the depth of the model (1.1 km) this represents an error of 1–2% in the model. *Coordinates are calculated when data are extracted from SICADA using 'id code' information. X and y coordinates are always available for surface waters but the z-value varies due to water level and sampling depth. It can be calculated from available information (z-coordinate for reference point, water level and sampling depth) but just now it has to be done manually. It is probably possible to make an application for the calculation within SICADA. As explained before, mid section coordinates can easily be calculated within SICADA during extraction of data. The HAG group must specify the need for mid section coordinates when they ask for data. To include coordinates in the actual data tables in SICADA would only introduce a lot of disadvantages and no improvements. The coordinate handling in SICADA is much more advanced and it is working very well.*

It is necessary to know exactly the meaning of each column in the SICADA table including the detection limits (e.g. S^{2-}) of the analytical techniques and the number of significant decimals. *Each data delivery should include a table description with an explanation to the columns. If this description is not included, the HAG group should ask for it. The detection limits, reporting limits and measurement uncertainties are given in the P-reports for example P-04-108 (also S^{2-}). The measurement techniques and sample treatment are also listed there. A lot of efforts is put into producing P-reports and they deserve to be used.*

It is not sufficient to only analyse for ^{10}B; ^{11}B and B are needed also for interpretation. Methane, aluminium, ^{36}Cl and density measurements are needed. *Methane is analysed, aluminium is difficult due to contamination risk, ^{36}Cl has been discussed before (and also mentioned below) and will be done at a few well chosen occasions due to the large costs. Nobody has asked for B before, but it can easily be included. It may be useful to ask for Al results from Oskarshamn (Not in SICADA but available as laboratory reports due to misunderstanding of the SKB class definition) and try to evaluate the data. If these data give the necessary information we can include Al analyses also in Forsmark.*

pH is always measured in the field but the data reported in the SICADA table are laboratory-derived pH values. It is necessary to have access to the field pH and these should be included in the SICADA extraction routines. *It is up to the HAG-group to ask for them. They are in SICADA and can easily be extracted although they do not have sample numbers (measurements are performed at more than one depth and often as profiles).*

The SICADA table, following highlighting of the representative samples, should be checked by the site chemist before finally putting them on the project place. *A need that is recognised at last.*

The in-situ Eh and pH measurements (CHEMMAC) are very useful and efforts should be made to obtain as many measurements as possible. These efforts are always made, but there is only one available set of equipment per site. The investigation programme R 01-10 stipulates complete chemical characterisation in only about 3 boreholes. This demand will be fulfilled easily. When hydraulic test equipment (PSS) has been used for pumping, to allow investigations in two boreholes at a time, it is not possible to measure Eh. This is due to pump and pump string design. Sometimes the measurements fail also with the MFL equipment due to bad measurement conditions in the borehole. *The reality is such and it is not very much to do about it. It is necessary to read the P-reports in order to understand the reasons for missing or unreliable data.*

Drilling data should be made available at an early stage in order to facilitate DIS modelling. Data requirements are: a) the drilling water volume pumped in and out from the borehole, b) the uranine concentration in the drilling water pumped in and out from the borehole, and c) the water pressure and drawdown along the borehole. *The question has arisen before, but it seems to be impossible for the drilling staff to do the reporting during drilling. However, the reporting time was shortened for boreholes KFM05A and 6A and the data have been available some time ago.*

The monitoring equipment should be more reliable concerning, for example: a) the water pressure sensor, and b) the quality of the uranine concentration in the return water. Frequent flow meter malfunctions should be avoided. *Of course, every measure is taken already in order to improve these data and the quality is much better for the boreholes KFM05A, 6A and 7A*

Standard topographical maps in combination with the location of the boreholes are more useful for modelling to make cross-sections, establish hypotheses about recharge or discharge zones etc

compared to colour maps without topographic information. *This point is difficult to understand. It is just to ask the GIS staff for any type of map that is required.*

Absence of deep samples – this is being addressed by the site personnel. Chemistry is prioritised until the amount of deep data is sufficient but water bearing fractures are few at depth. The preliminary flow logging results from KFM07A indicates water at below 900 m depth.

Time to strategically select suitable samples for ^{36}Cl (deepest samples from KFM03A) – however no laboratory identified as yet. *A few samples will be sent, probably from KFM06A 670 m, if possible KFM07A > 900 m and one more section. It is an advantage if the samples are collected from the prioritised part of the candidate area.*

Require more data on the shallow Soil Pipe groundwater samples (i.e. location descriptions; how much contamination during drilling; which groundwater samples can be used? P-reports may be in draft form). *A P-report is being produced.*

Soil Pipe soil profiles – preferably from close to the sampled groundwaters. Soil profiles to be analysed for pore water chemistry and isotopes – tritium palaeoprofiles, stable isotope palaeoprofiles; U-series palaeoprofiles. Sites preferably located within recharge/discharge areas. Important for the surface/near-surface interface studies already planned for Laxemar. *Soil profiles exist. BAT samples can be regarded as some kind of pore water and samples/analyses from three sampling points exist. "Pore" water studies are planned for wet land pipes (also BAT technique).*

Evaluation of tritium from as many different surface sampling locations to evaluate possible contribution from the Forsmark Power Plant. *Existing surface water data should be enough.*

For further interpretation of shallow/near-surface groundwater studies – is there the necessity to resample some of the percussion boreholes in more detail (3 m intervals)? Might be interesting to see if one can differentiate between recent meteoric/Old Baltic Sea/older Littorina Sea etc. *Does 3 m intervals mean each third metre in an open borehole? In that case I can see no use. Sampling must be restricted to water bearing fracture zones and the section lengths are also depending on the length of the fracture zones. The only existing equipment is the HTHB. It will probably be difficult to go back to old boreholes and investigate several packed off sections due to ongoing installation of permanent instrumentation in the boreholes. It may be possible to combine sampling in several sections with hydraulic tests in one of the future boreholes. However, this is a special investigation and not included in the present plans. Further discussions are needed.*

Surface radon survey to locate more accurately areas of discharge – similar to what has been done at the URL site at Whiteshell. *This is a special investigation which is more suitable for the detailed site investigation stage. The survey is not included in the present plans.*

Need for an interlaboratory study of U-decay series analysis on groundwaters. *The U-study is planned during the ongoing investigation in KFM06A.*

Need to investigate the possibilities of determining the oxidation states of U-bearing mineral phases in fractures. *Is this a suggestion for the site? I guess U-minerals can be investigated within fracture mineral activities?*

Uranium analysis on colloids is suggested. Uranium could easily be included. Sulphur and calcium are analysed but not used/calculated. *This will also be changed.*

According to hydrogeological models, it is possible that local flow cells play a significant role in Forsmark area. Then, different local discharge and recharge areas could be present at the investigated area. If this is the case, shallow groundwater should have different hydrochemical and isotopic signatures which could help to support (or not) the existence of these local flow cells. It is recommended to increase the number of soil pipes and/or shallow boreholes, but with special emphasis in all the "possible" discharge zones: (a) lakes (under the bottom sediments) and (b) swamp areas. *Planned.*

New boreholes and sampling inland (as much "inland" as possible) would improve the knowledge about hydrogeological boundary conditions in Forsmark. *Not planned as far as I know, the usefulness needs to be discussed.*

7 Acknowledgements

This study forms part of the SKB site investigation programme, managed and supported by the Swedish Nuclear Fuel and Waste Management Company (SKB), Stockholm. The support and advice from Anders Ström, SKB and Kristina Skagius, Kemakta AB are acknowledged. The helpful comments by the internal reviewers Mel Gascoyne, GGP Inc. and Bill Wallin, Geokema improved the work. The helpful interaction with the site chemist Ann-Chatrin Nilsson, Geosigma AB is acknowledged.

8 References

Albi K, Winterhalter B, 2001. Authigenic mineralisation in the temporally anoxic Gotland Deep, the Baltic Sea. Baltica, 14, 74–83.

Andersson J, Christiansson R, Munier R, 2000. Djupförvarsteknik: Hantering av osäkerheter vid platsbeskrivande modeller. SKB TD-01-40, Svensk Kärnbränslehantering AB.

Andersson J, Berglund J, Follin S, Hakami E, Halvarson J, Hermanson J, Laaksoharju M, Rhén I, Wahlgren C-H, 2002. Testing the methodology for site descriptive modelling, Application for the Laxemar area. SKB TR-02-19, Svensk Kärnbränslehantering AB.

Bein A, Arad A, 1992. Formation of saline groundwaters in the Baltic region through freezing of seawater during glacial periods. Journal of Hydrology, 140, Elsevier Science B.V. pp75–87.

Berg C, Nilsson A-C, 2004. Hydrochemical logging of KFM04A. Forsmark site investigation. SKB P-04-47, Svensk Kärnbränslehantering AB.

Bruno J, Cera E, Grivé M, Rollin C, Ahonen L, Kaija J, Blomqvist R, El Aamrani F Z, Casas I, de Pablo J, 1999. Redox Processes in the Palmottu Uranium Deposit. Redox measurements and redox controls in the Palmottu System. (Technical Report), Quantisci, Barcelona, Spain, 76 p.

Bäckblom G, Stanfors R, 1989. Interdisciplinary study of post-glacial faulting in the Lansjärv area, northern Sweden. SKB TR-89-31, Svensk Kärnbränslehantering AB.

Deutsch W J, Jenne E A, Krupka K M, 1982. Solubility equilibria in basalt aquifers: The Columbia Plateau, Eastern Washington, USA. Chem. Geol. 36, 15–34.

Donner J, Kankainen T, Karhu J A, 1994. Radiocarbon ages and stable isotope composition of Holocene shells in Finland. In T. Andrén (ed), Proceedings of the Conference The Baltic – past, present and future. Stockholm March 14–16, 1994. Stockholm University, Quaternaria A:7, 31–38.

Eriksson L, 2004. Miljörapport 2003. Utsläpp av radioaktiva ämnen. Forsmarks Kraftgrupp. Rep. Nr. FQ-2004-78.

Fontes J-Ch, Louvat D, Michelot J-L, 1989. Some constraints on geochemistry and environmental isotopes for the study of low fracture flows in crystalline rocks – The Stripa case. In: International Atomic Energy Agency (Eds.) Isotopes techniques in the study of the Hydrology of Fractured and Fissured Rocks. IAEA, Vienna, Austria.

Frape S K, Byrant G, Blomqvist R, Ruskeeniemi T, 1996. Evidence from stable chlorine isotopes for multiple sources of chloride in groundwaters from crystalline shield environments. In: Isotopes in Water Resources Management, 1966. IAEA-SM-336/24, Vol. 1, 19–30.

Fredén C, 2002. Berg och Jord, Sveriges Nationalatlas. 208 pp.

Glynn P D, Voss C I, 1999. SITE-94. Geochemical characterization of Simpevarp ground waters near the Äspö Hard Rock laboratory. (Technical Report SKI R 96-29), SKI, Stockholm, Sweden 210 p.

Grenthe I, Stumm W, Laaksoharju M, Nilson A C, Wikberg P, 1992. Redox potentials and redox reactions in deep groundwater systems. Chem. Geol. 98, 131–150.

Grimaud D, Beaucaire C, Michard G, 1990. Modeling of the evolution of ground waters in a granite system at low temperature: the Stripa ground waters, Sweden. Applied Geochemistry, 5, 515–525.

Gurban I, Laaksoharju M, 2002. Drilling Impact Study (DIS); Evaluation of the influences of drilling, in special on the changes on groundwater parameters. SKB PIR-03-02, Svensk Kärnbränslehantering AB.

Hedenström A, Risberg J, 2003. Shore displacement in northern Uppland during the last 6500 calendar years. SKB TR-03-17, Svensk Kärnbränslehantering AB.

Laaksoharju M, Degueldre C, Skårman C, 1995. Studies of colloids and their importance for repository performance assessment SKB TR-95-24, Svensk Kärnbränslehantering AB.

Laaksoharju M, Wallin B, 1997. Evolution of the groundwater chemistry at the Äspö Hard Rock Laboratory. Proceedings of the second Äspö International Geochemistry Workshop, June 6–7, 1995. SKB, International Cooperation Report 97-04.

Laaksoharju M, Skårman C, Skårman E, 1999. Multivariate Mixing and Mass-balance (M3) calculations, a new tool for decoding hydrogeochemical information. Applied Geochemistry Vol. 14, #7, 1999, Elsevier Science Ltd. pp861–871.

Laaksoharju M (ed), Gimeno M, Smellie J, Tullborg E-L, Gurban I, Auqué L, Gómez J, 2004a. Hydrogeochemical evaluation of the Forsmark site, model version 1.1. SKB R-04-05, Svensk Kärnbränslehantering AB.

Laaksoharju M (ed), Smellie J, Gimeno M, Auqué L, Gomez, Tullborg E-L, Gurban I, 2004b. Hydrochemical evaluation of the Simpevarp area, model version 1.1. SKB R 04-16, Svensk Kärnbränslehantering AB.

Nilsson A-C, 2003a. Sampling and analyses of groundwater in percussion drilled boreholes and shallow monitoring wells at drillsite DS1. Results from the percussion boreholes HFM01, HFM02, HFM03, KFM01A (borehole section 0–100 m) and the monitoring wells SFM0001, SFM0002 and SFM0003. Forsmark site investigation. SKB P-03-47, Svensk Kärnbränslehantering AB.

Nilsson A-C, 2003b. Sampling and analyses of groundwater in percussion drilled boreholes and shallow monitoring wells at drillsite DS2. Results from the percussion boreholes HFM04, HFM05, KFM02A (borehole section 0–100 m) and the monitoring wells SFM0004 and SFM0005. Forsmark site investigation. SKB P-03-48, Svensk Kärnbränslehantering AB.

Nilsson A-C, Karlsson S, Borgiel M, 2003. Sampling and analyses of surface waters. Results from sampling in the Forsmark area, March 2002 to March 2003. Forsmark site investigation. SKB P-03-27, Svensk Kärnbränslehantering AB.

Nordstrom D K, Puigdomenech I, 1986. Redox chemistry of deep ground-waters in Sweden. SKB TR 86-03, 30 p, Svensk Kärnbränslehantering AB.

Parkhurst D L, Appelo C A J, 1999. User's Guide to PHREEQC (Version 2), a computer program for speciation, batch-reaction, one-dimensional transport, and inverse geochemical calculations. U.S. Geological Survey Water-Resources Investigations Report 99-4259, 312 p.

Pedersen K (ed), 1996. Bacteria, colloids and organic carbon in groundwater at the Bangombé site in the Oklo area. SKB TR-96-01, Svensk Kärnbränslehantering AB.

Pitkänen P, Luukkonen A, Ruotsalainen P, Leino-Forsman H, Vuorinen U, 1998. Geochemical modelling of groundwater evolution and residence time at the Kivetty site. POSIVA Report 98-07, Helsinki, Finland, 139 p.

Pitkänen P, Luukkonen A, Ruotsalainen P, Leino-Forsman H, Vuorinen U, 1999. Geochemical modelling of groundwater evolution and residence time at the Olkilouto site. POSIVA Report 98-10, Helsinki, Finland, 184 p.

Pitkänen P, Partamies S, Luukkonen A, 2004. Hydrogeochemical interpretation of baseline groundwater conditions at the Olkiluoto Site. (Technical Report POSIVA 2003-07), POSIVA, Helsinki, Finland, 159 p.

Puigdomenech I (ed), 2001. Hydrochemical stability of groundwaters sourrunding a spent nuclear fuel repository in a 100000 year perspective. SKB TR 01-28, 83 p, Svensk Kärnbränslehantering AB.

Påsse T, 2001. An empirical model of glacio-isostatic movements and shore level displacement in Fennoscandia. SKB R-01-41, 1–59, Svensk Kärnbränslehantering AB.

Rhén I, Smellie J, 2003. Task force modelling of groundwater flow and transport of solutes. Task 5 summary report. SKB TR-03-01, Svensk Kärnbränslehantering AB. (ISSN 1404-0344).

Samper J, Delgado J, Juncosa R, Montenegro L, 2000. CORE2D v 2.0: A Code for non-isothermal water flow and reactive solute transport. User's manual.ENRESA Technical report 06/2000.

Sandström B, Savolainen M, Tullborg E-L, 2004. Fracture mineralogy. Results from fracture minerals and wall rock alteration in boreholes KFM01A, KFM02A, KFM03A and KFM03B (In press).

SKB, 2002. Forsmark – site descriptive model version 2002. SKB R-02-32, Svensk Kärnbränslehantering AB.

SKB, 2004. Preliminary site description. Forsmark area – version 1.1. SKB R-04-15, Svensk Kärnbränslehantering AB.

Smellie J A T, Larsson N-Å, Wikberg P, Carlsson L, 1985. Hydrochemical investigations in crystalline bedrock in relation to existing hydraulic conditions: Experience from the SKB test-sites in Sweden. SKB TR-85-11, Svensk Kärnbränslehantering AB.

Smellie J A T, Larsson N-Å, Wikberg P, Puigdomenech I, Tullborg E-L, 1987. Hydrochemical investigations in crystalline bedrock in relation to existing hydraulic conditions: Klipperås test-site, Småland, southern Sweden. SKB TR-87-21, Svensk Kärnbränslehantering AB.

Smellie J A T, Wikberg P, 1989. Hydrochemical investigations at the Finnsjön site, central Sweden. J. Hydrol. 126, 147–169.

Smellie J, Laaksoharju M, Tullborg E-L, 2002. Hydrochemical site descriptive model – a stategy for the model development during site investigation. SKB R-02-49, Svensk Kärnbränslehantering AB.

Svensson U, 1996. SKB Palaeohydrogeological programme. Regional groundwater flow due to advancing and retreating glacier-scoping calculations. In: SKB Project Report U 96-35, Svensk Kärnbränslehantering AB.

Trotignon L, Beaucaire C, Louvat D, Aranyossy J F, 1997. Equilibrium geochemical modelling of Äspö groundwaters: a sensitivity study to model parameters. In: Laaksoharju M and Wallin B (eds.) Evolution of the groundwater chemistry at the Äspö Hard Rock Laboratory. SKB 97-04, Svensk Kärnbränslehantering AB.

Trotignon L, Beaucaire C, Louvat D, Aranyossy J F, 1999. Equilibrium geochemical modelling of Äspö groundwaters: a sensitivity study of thermodynamic equilibrium constants. Appl. Geochem. 14, 907–916.

Tullborg E-L, Larson S Å, 1984. δ18O and δ13C for limestones, calcite fissure infillings and calcite precipitates from Sweden. Geologiska föreningens i Stockholm förhandlingar 106(2).

Westman P, Wastegård S, Schoning K, Gustafsson B, 1999. Salinity change in the Baltic Sea during the last 8,500 years: evidence, causes and models. SKB TR 99-38. Svensk Kärnbränslehantering AB.

Wikberg P, 1998. Äspö Task Force on modelling of groundwater flow and transport of solutes. SKB progress report HRL-98-07.

Appendix 1

Explorative analysis and expert judgement of major components and isotopes

Contribution to the model version 1.2

John Smellie, Conterra AB, Stockholm

Eva-Lena Tullborg, Terralogica AB, Göteborg

December 2004

Contents

1 Geological and hydrogeological setting

1.1 Regional geology

The Forsmark site is located NE of Forsmark village at the Baltic coast in an area bounded by two major regional deformation zones (Singö and Eckarfjärden) striking NW-SE (Figures 1-1, 1-2). In places outcrops are few, especially away from the coastal margins. The main rock type is a meta-granitoid of Svecofennian age; subordinate rock types include metamorphosed sediments, volcanics and gabbros. Widespread plastic deformation occurred during the Svecofennian (~ 1,870 Ma), when temperatures exceeded 500°C, to around 1,800 Ma ago when subsequent cooling to less than 500°C occurred. Such deformation zones border the selected candidate site (Figure 1-2).

The site is traversed by local steeply dipping deformation zones mainly trending NE-SW and ENE-WSW with a weaker fracture group mostly trending approximately N-S and NW-SE (Figure 1-3). The Eckarfjärden deformation zone effectively truncates these former fracture zones; the 1.2 modelled structural interrelationships are presented in Figure 1-4.

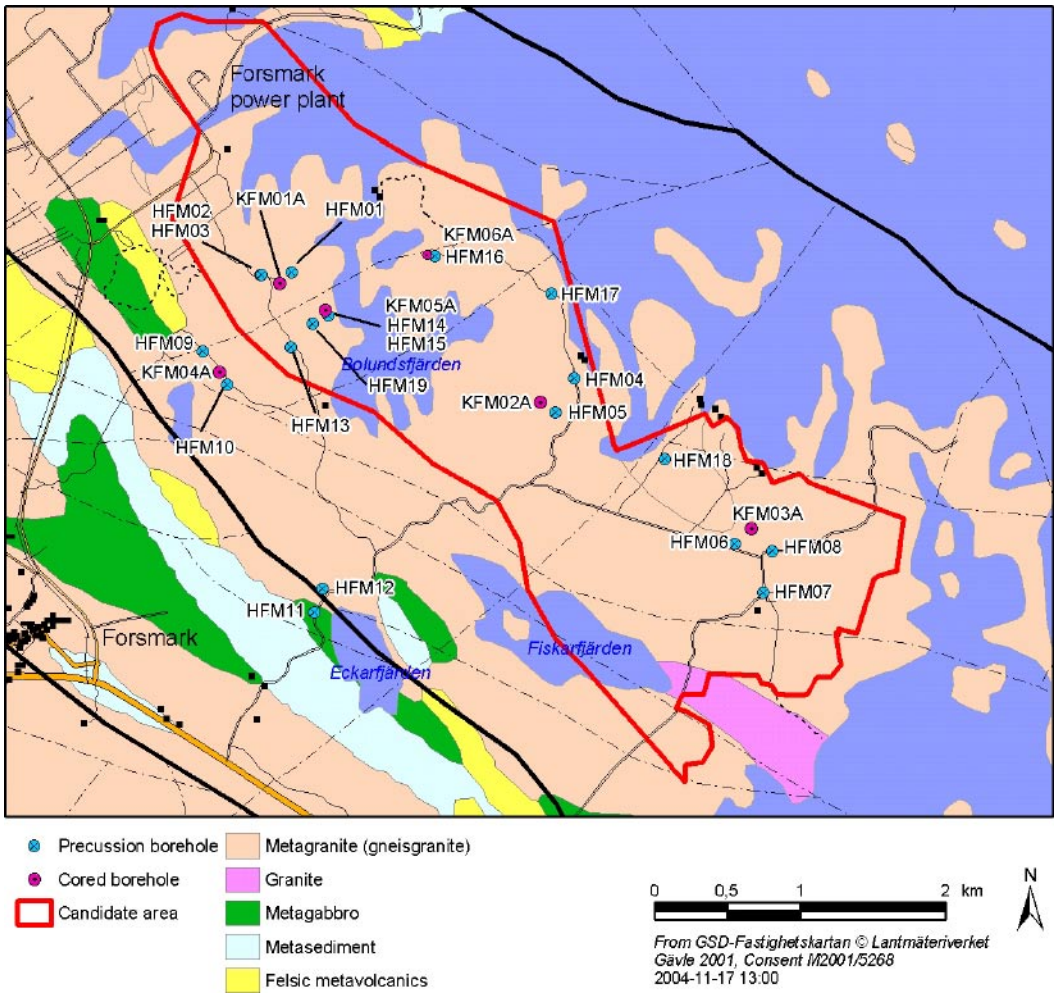

Figure 1-1. *Geology of the Forsmark site showing the location of the evaluated boreholes KFM01A–KFM04A. Bounding NW-SE regional deformation zones are in black.*

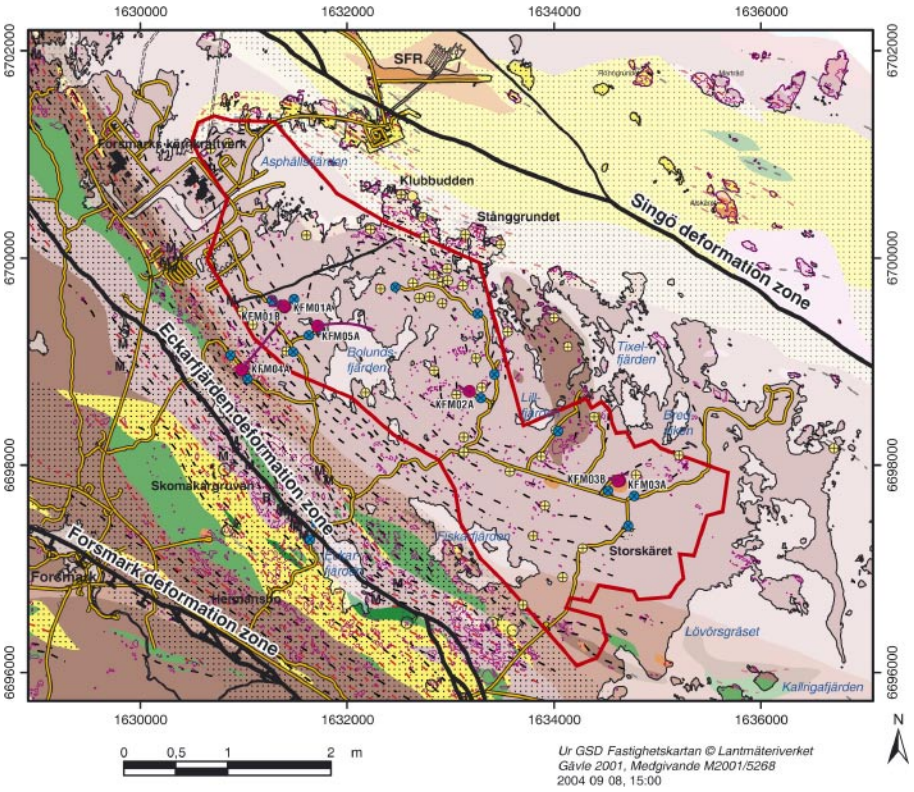

Figure 1-2 *Detailed geology of the Forsmark area. Plastic deformation zones are indicated by hatched lines along and beyond the west (strongly deformed) and east (less deformed) boundaries of the demarcated candidate site. (M. Stephens, A. Simeonov, written comm., 2004).*

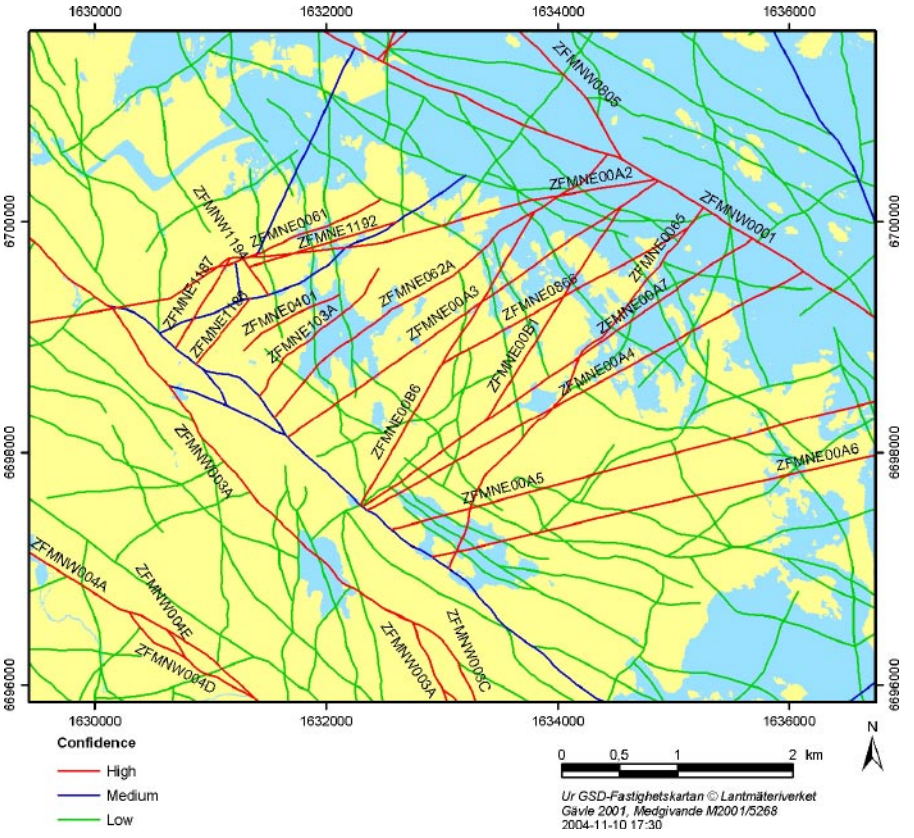

Figure 1-3. *Structural patterns in the Forsmark area. Large-scale deformation zones (shown in blue) truncate to the west steeply dipping deformation fracture zones (shown in red) mostly trending NE-SW/ ENE-WSW. Weaker, steeply dipping deformation zones trending NW-SE and sometimes N-S are shown in green. (M. Stephens, A. Simeonov, written comm., 2004).*

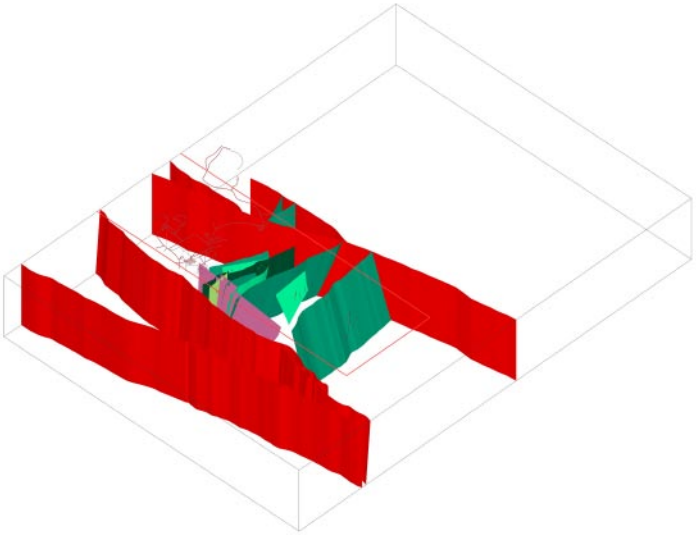

Figure 1-4a. *Structural 1.2 model showing high confidence steeply dipping deformation structures. Indicated are the major bounding vertical deformation zones in red (Singö, Eckartfjärden, Forsmark; Figure 1-2), the NE-SW striking steeply dipping deformation zones in green and the approx. NW-SE deformation zones in purple. Note that the set of gently dipping deformation NE striking zones is not included on this figure, but instead is shown in Figure 1-4b. (M. Stephens, A. Simeonov, written comm., 2004).*

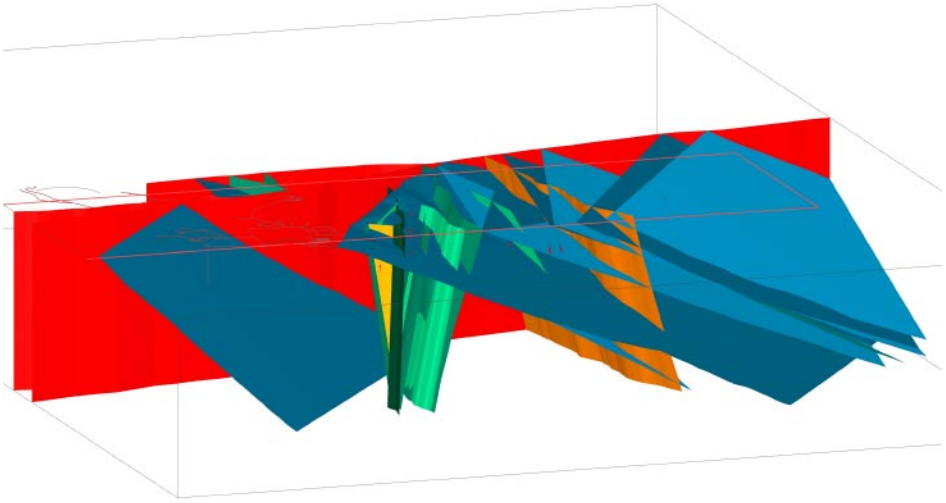

Figure 1-4b. *Structural 1.2 model showing high confidence steeply dipping deformation structures. Details shown include the Singö lineament (in red) and the gently dipping deformation zones in blue. (M. Stephens, A. Simeonov, written comm., 2004).*

Gently dipping deformation zones exist, but since their presence can only be confirmed by a systematic drilling campaign, they tend to be under-represented from surface bedrock investigations. The location and lateral extent of these gently dipping deformation zones are still a focus of study but have been identified with confidence in the vicinity of the SFR repository site to the NW, including part of the candidate site (Figure 1-5). These gently dipping deformation zones may be highly transmissive; for example the H2 zone indicated has indicated hydraulic connections over a distance of 1.3 km (Sven Follin, pers. comm. 2005).

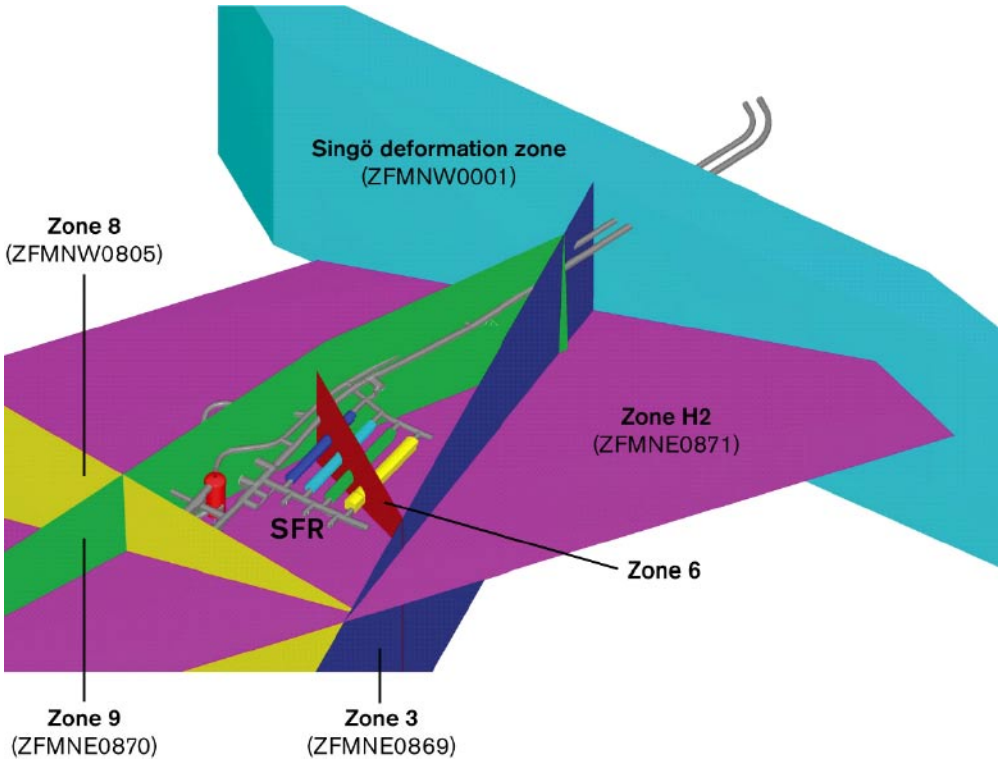

Figure 1-5. *Gently dipping deformation zones in the Forsmark area (i.e. H2) in the vicinity of the SFR repository. (M. Stephens, A. Simeonov, written comm., 2004).*

1.2 Regional hydrogeology

The Forsmark area is characterised by a low relief with small-scale topography and relatively shallow Quaternary deposits /SKB, 2004/. The region therefore consists of small catchment areas characterised by localised shallow groundwater flow systems. Whilst the vertical extent of these systems will be dependent on the topography, they will be influenced also by the presence of sub-horizontal fracture zones at varying depths. Large-scale regional groundwater flow systems are not considered important at Forsmark. Regionally, infiltration in recharge areas is considered equivalent to the specific discharge which is estimated to be approx. 200 mm/year.

Groundwater levels are shallow and unsaturated overburden is uncommon. In areas of recharge the groundwater level is commonly less than 3 m below the surface and in discharge areas less than 1 m; annual fluctuations are 2–3 m and less than 1 m respectively. Fluctuations in sea-level may have a major influence on groundwater levels in the low-lying parts of the candidate site.

The overburden consists of Quaternary till deposits less than 20 m thick and rock outcrops are common. Hydraulic conductivities vary within these deposits with the upper 1 m characterised by high values (10^{-5}–10^{-4} ms^{-1}) and also the sediments in contact with the underlying bedrock (~ 10^{-5} ms^{-1}). Below 1 m the hydraulic conductivity decreases significantly to 10^{-8}–10^{-6} ms^{-1} where the clay content increases. This effectively means that with abundant recharge the groundwater levels will quickly rise resulting in lateral flow and surface water discharge.

The lakes and streams are assumed to be important channels of discharge; marshes and wetlands in hydraulic contact with the groundwater zone may also contribute.

In conclusion, and important for this present hydrogeochemical evaluation, is that only a very small fraction of the total groundwater discharge from the overburden (< 10%) will eventually reach the uppermost permeable part of the bedrock.

Not a great deal is known about the deep regional hydrogeology of the region hosting the Forsmark site. Being a coastal area an upward discharge of regional groundwater may be expected, driven by high recharge gradients driven from the western Swedish and central Norwegian upland areas. If this simple recharge/discharge mechanism describes the regional pattern, then old, deep basement saline groundwaters might be expected to be located reasonably close to the surface at the coast (500–1,000 m).

1.3 Borehole locations and drilling

The borehole locations are shown in Figure 1-1 but in more detail in Figure 1-6. The main focus of this Forsmark v.1.2 evaluation are boreholes KFM01A, KFM02A, KFM03A and KFM04A systematically drilled to provide a good coverage of the geology and hydrogeology of the candidate site.

Of the percussion boreholes indicated in Figure 1-6, HFM01 supplied flushing water to the drilling of borehole KFM01A, HFM05 for borehole KFM02A, HFM06 for borehole KFM03A, and HFM10 for borehole KFM04A. The remaining percussion boreholes were used mainly for hydraulic (e.g. groundwater flow monitoring) and hydrochemical information and structural (e.g. lineaments; fracture zones) confirmation and identification.

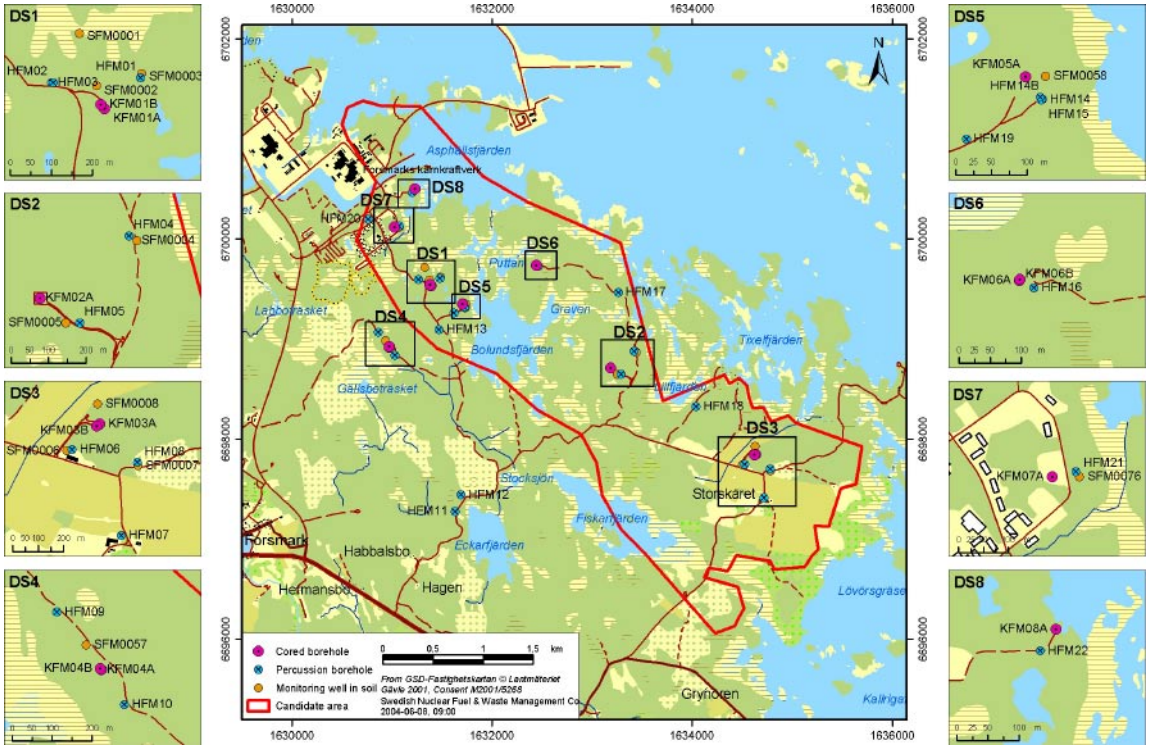

Figure 1-6. *Core drilled borehole locations at the Forsmark site; boreholes KFM01A, KFM02A, KFM03A and KFM04A are the focus of the model 1.2 evaluation.*

1.4 Borehole KFM01A

Borehole KFM01A was core drilled to 1,001.49 m at an inclination of 4.2° to the vertical. The first 100.52 m were percussion drilled and cased to 100.43 m.

1.4.1 Geological and hydrogeological character

Borehole KFM01A is dominated by the metagranitoid rock unit (medium-grained granite to granodiorite) with minor lenses/bands of amphibolite, pegmatite and fine-grained granitoid (Figure 1-7). Amphibolite is more common in the upper 150–250 m in association with increased fracture frequency. The pegmatites and fine-grained granitoid occur mostly below 500 m with the greatest thickness of fine-grained granitoid occurring between 800–900 m depth.

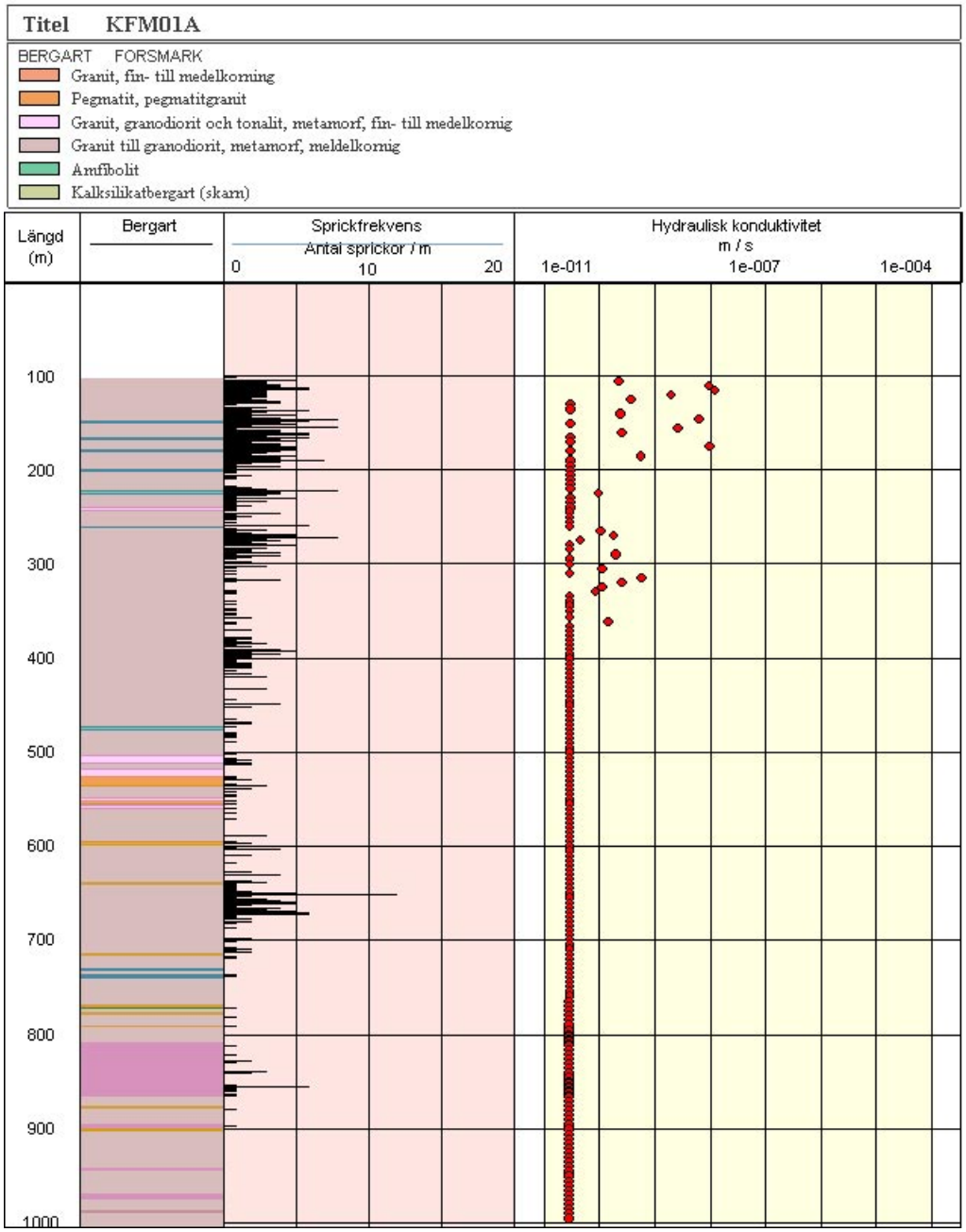

Figure 1-7. *Integrated geology, fracture frequency and hydraulic conductivity along borehole KFM01A.*

The fracture frequency is considered normal (2–5 fractures/m) to around 300 m. Below this depth the number of fractures decrease markedly with only two exceptions at approximately 400 m and 650 m.

The hydraulic character of the bedrock (Figure 1-7) indicates relatively high hydraulic conductivity (10^{-10}–10^{-8} ms^{-1}) down to 200 m coinciding with the increased fracture frequency. Otherwise from 200–400 m values are very low (to 10^{-9} ms^{-1}) and at greater depths at or below the measurement limit of 10^{-11} ms^{-1}.

Figure 1-8 illustrates the major fractures intercepted by borehole KFM01A as derived from downhole BIPS-imaging and drillcore mapping. Sub-horizontal fractures are especially frequent in the upper 350 m of the borehole showing variable dips and strikes and with hydraulic conductivities (cf. Figure 1-7) ranging from 10^{-10}–10^{-8} ms^{-1} in the upper 200 m to 10^{-10}–10^{-9} ms^{-1} from 200–350 m. From 350 m to the borehole bottom at 1,001.5 m there is only one major sub-horizontal fracture at around 700 m; hydraulic conductivities through this hydraulically tight bedrock length are at or below the limit of measurement at $10^{-10.5}$ ms^{-1}. The fracture zones sampled for groundwater in the borehole do not represent any of the major structures in the site area, but may well be connected to one in the close vicinity.

As a cautionary note, observations from borehole KFM02A (cf. section 1.5) suggest that the paucity of fractures below 200–300 m indicated in KFM01A may not be fully representative of the site area.

Groundwater samples were collected from 110–120.77 m and 176.8–183.9 m with salinities of 4,600 mg/L Cl and 5,300 mg/L Cl respectively.

Borehole KFM01A is cased to 100 m depth which excludes BIPS and Differential Flow Meter data from this borehole length; Figure 1-9 shows BIPS-images from selected open fractures which have contributed to the collected groundwater samples.

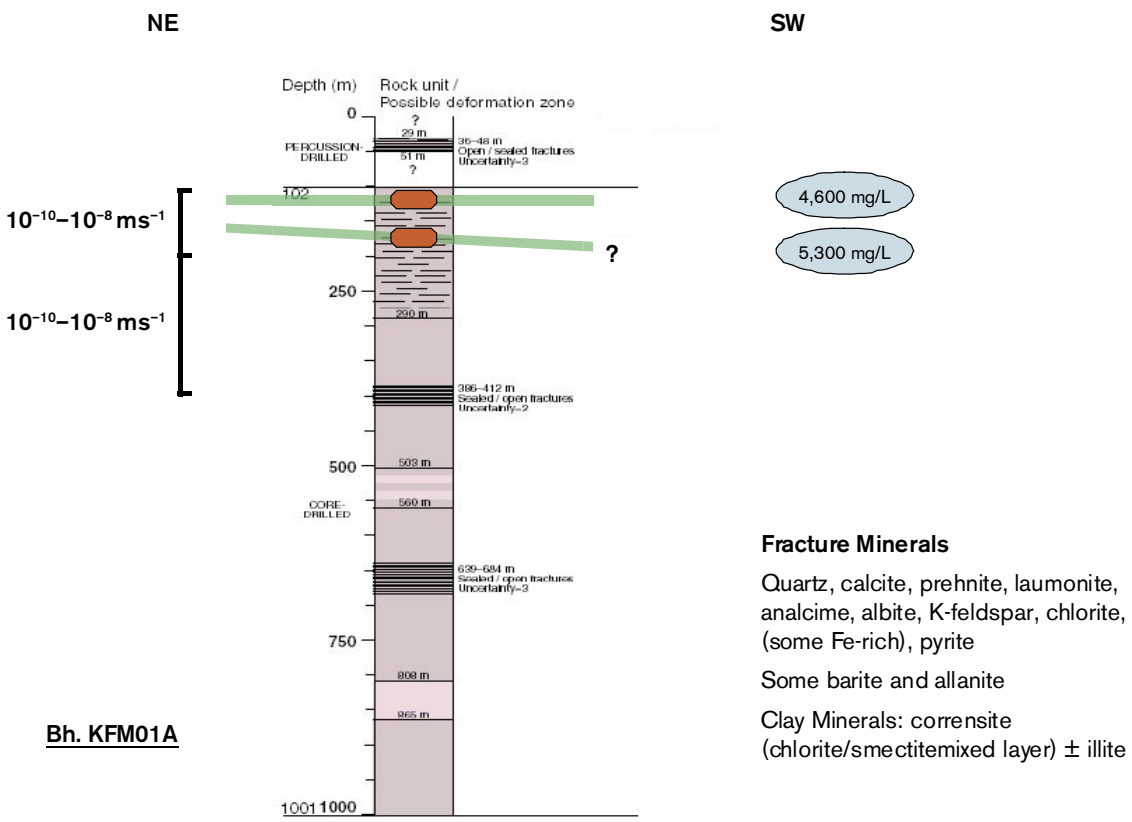

Figure 1-8. *Relation of borehole KFM01A to the identified sampled fracture zones (in green) and hydraulic parameters; groundwater sampling locations are indicated (in red) with the mg/L chloride content (in blue). (Based on M. Stephens, A. Simeonov, written comm., 2004).*

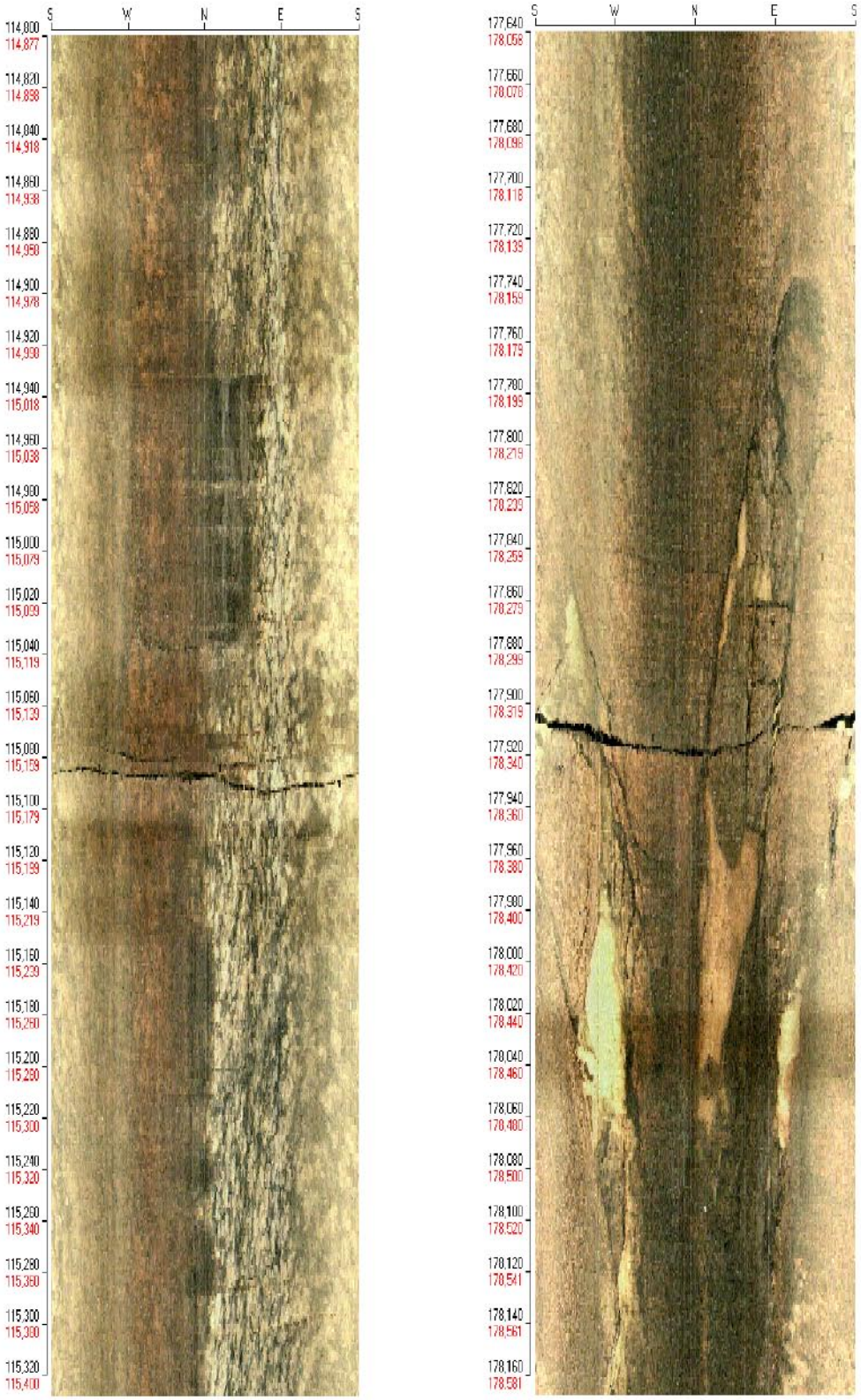

Figure 1-9. *BIPS-images from KFM01A showing the probable main water-conducting open fractures from borehole sections 110–120.77 m and 176.8–183.9 m.*

The recorded rates of groundwater flow under 'natural' hydraulic conditions (i.e. no pumping) via fractures into the borehole from the surrounding bedrock, and conversely from the borehole into the bedrock, indicate, with only one exception at approx. 150 m, that water movement is mostly into the borehole (Figure 1-10). During pumping all movement of formational groundwater is into the borehole. Under open hole conditions, therefore, formation groundwater would be expected to enter into the borehole with the most hydraulically conducting fractures contributing the greatest volume. Since only at the 150 m level is there a possibility that water is moving from the borehole into the bedrock, any groundwater circulatory movement along the borehole length during open hole conditions would be driven mainly by density differences reflecting different sources (i.e. depths) from the surrounding bedrock.

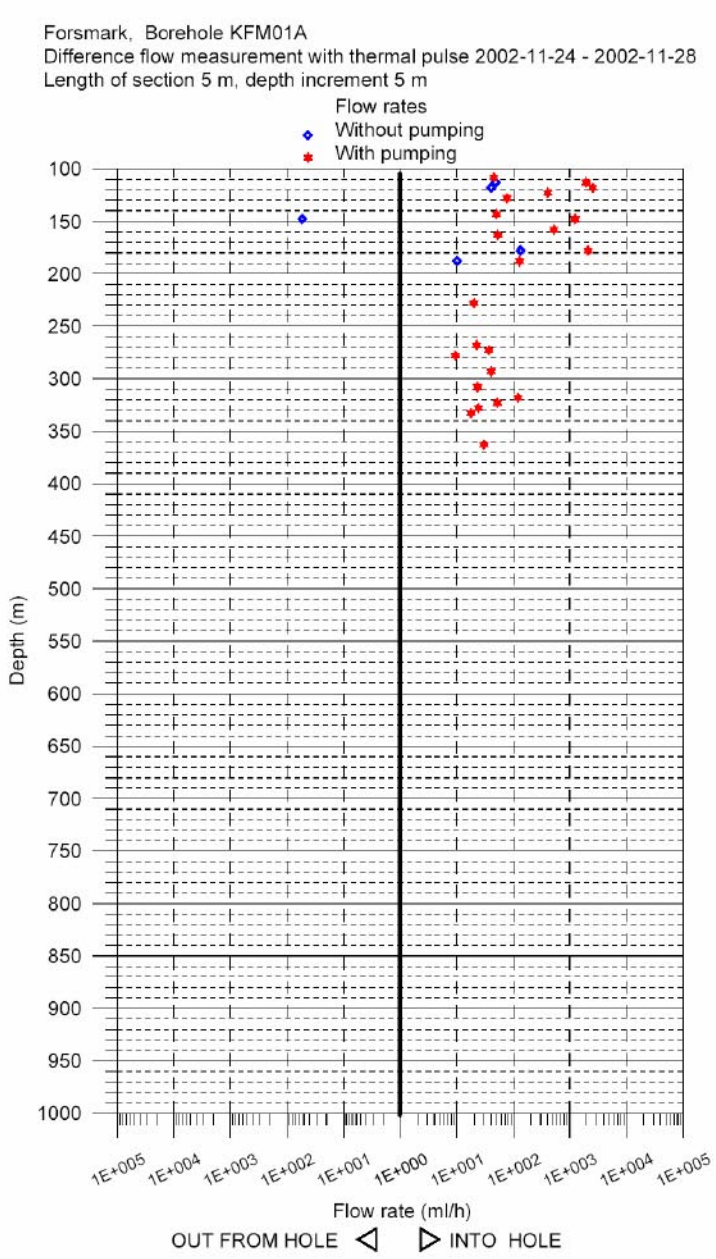

Figure 1-10. *Downhole differential flow measurements along borehole KFM01A (105–1,000 m) showing groundwater flow rate (mL/h) into and out of the borehole (P-03-28).*

Figure 1-11 shows an electric conductivity log of borehole KFM01A during open hole conditions prior to groundwater sampling; differences in salinity trends obtained before and during pumping are very small. The profile shows a high salinity increase between 50–200 m depth corresponding to the most hydraulically conductive part of the borehole. From 200 m to the borehole bottom there is a fairly rapid decrease to below 0.5 S/m at 500 m which continues to 1,000 m. As shown by the low hydraulic conductivity values, little water is entering the borehole over this length. This suggests strongly that the water in the borehole from around 200 m to 1,000 m is mostly residual flushing water taken from percussion borehole HFM01 for drilling purposes. Analysis of the flushing water from HFM01 during a 7 week period following the drilling and sampling of borehole KFM01A showed a variation in electric conductivity from 0.075–0.320 S/m, equivalent to 9–651 mg/L Cl.

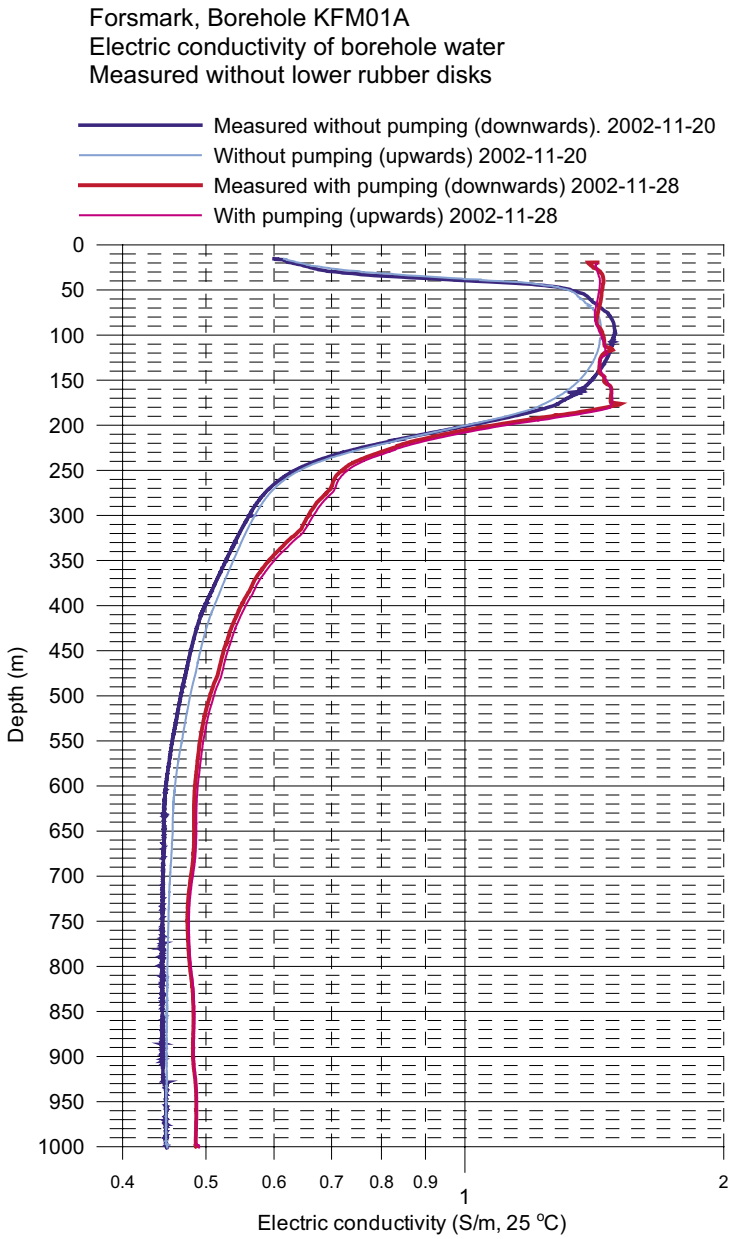

Figure 1-11. *Electric conductivity log for borehole KFM01A during open hole conditions (P-03-28).*

1.5 Borehole KFM02A

Borehole KFM02A was core drilled to1,002.5 m depth at an inclination of 4.6° to the vertical. The first 100.40 m were percussion drilled and cased to approx. 100 m.

1.5.1 Geological and hydrogeological character

The bedrock intercepted is dominated by metagranitoid with sporadic subordinate lenses/bands of amphibolite, pegmatite and fine-grained granite/granodiorite. These lenses/bands appear to be distributed relatively uniformly throughout the borehole with no apparent association with zones of increased fracturing (Figure 1-12). At approx. 280 m there is a distinctive horizon of porous metagranitoid believed to be the result of early hydrothermal leaching.

The fracture frequency is considered normal (i.e. 2–5 fractures/m) to around 400 m (compared to 200 m in KFM01A) but higher (up to an average 10 fractures/m) from approx. 400–530 m. From 530 m to the borehole bottom the fracture frequency is low apart from individual (?) fractures at 800 m and 900 m. Localised fractures also occur at approx. 115 m and 165 m.

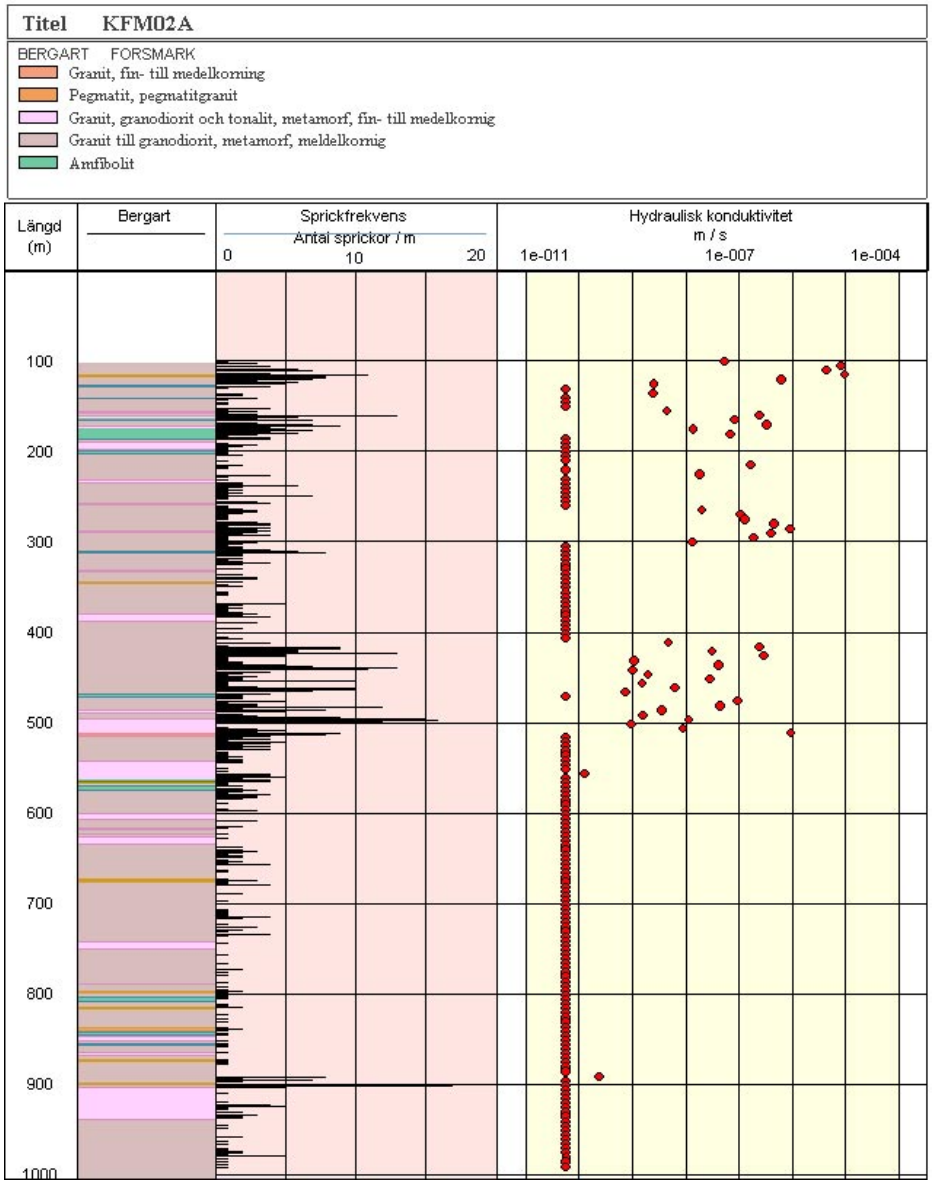

Figure 1-12. *Integrated geology, fracture frequency and hydraulic conductivity along borehole KFM02A.*

Downhole hydraulic measurements (Figure 1-12) reveal two sections of high hydraulic conductivity: a) 100–300 m (10^{-9}–10^{-5} ms^{-1}), and b) 400–520 m (10^{-9}–10^{-6} ms^{-1}); a weak increase is observed associated with the fracture zone at approx. 900 m. Otherwise the rest of the borehole is characterised by very low hydraulic conductivity, at or below the measurement limit at just under 10^{-10} ms^{-1}.

Figure 1-13 shows the relationship of borehole KFM02A to the major structures and the location of the groundwater sampling points. The groundwaters were taken from structures A2 and A3 at depths of 106.5–126.5 m (A3) and 413.5–433.5 m and 509.1–516.1 m (A2) respectively. Salinities increased from 640 mg/L Cl at approx. 110–120 m depth to 5,400 mg/L Cl between 400–500 m depth.

Borehole KFM01A is cased to 100 m depth which excludes BIPS and differential flow measurement data from this borehole length; Figure 1-14 shows BIPS-images from selected open fractures which have contributed to the collected groundwater samples.

The recorded rates of groundwater flow under 'natural' hydraulic conditions (i.e. no pumping) via fractures into the borehole from the surrounding bedrock, and conversely from the borehole into the bedrock, mainly indicate that groundwater movement is mostly into the borehole (Figure 1-15). Exceptions occur at shallow depths, i.e. 100–130 m and 230–240 m. During pumping all movement of formational groundwater is into the borehole. Under open hole conditions, therefore, formation groundwater would be expected to enter into the borehole with the most hydraulically conducting fractures contributing the greatest volume. In common with KFM01A, since only at the 100–150 m level is there a possibility that water is moving from the borehole into the bedrock, any groundwater circulatory movement along the borehole length during open hole conditions would be driven mainly by density differences reflecting different sources (i.e. depths) from the surrounding bedrock.

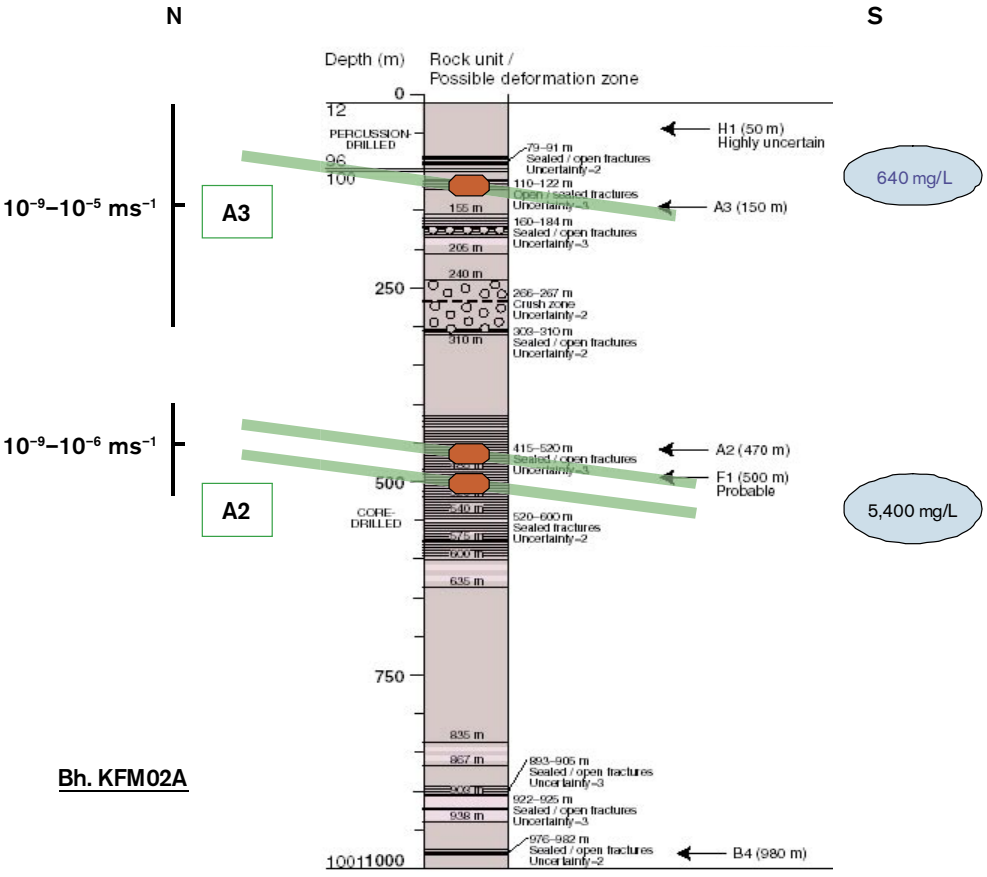

Figure 1-13. *Relation of Borehole KFM02A to the known major structures (A2 and A3 in green) and hydraulic parameters; groundwater sampling locations are indicated in red with the mg/L chloride contents in blue. (Based on M. Stephens, A. Simeonov, written comm., 2004).*

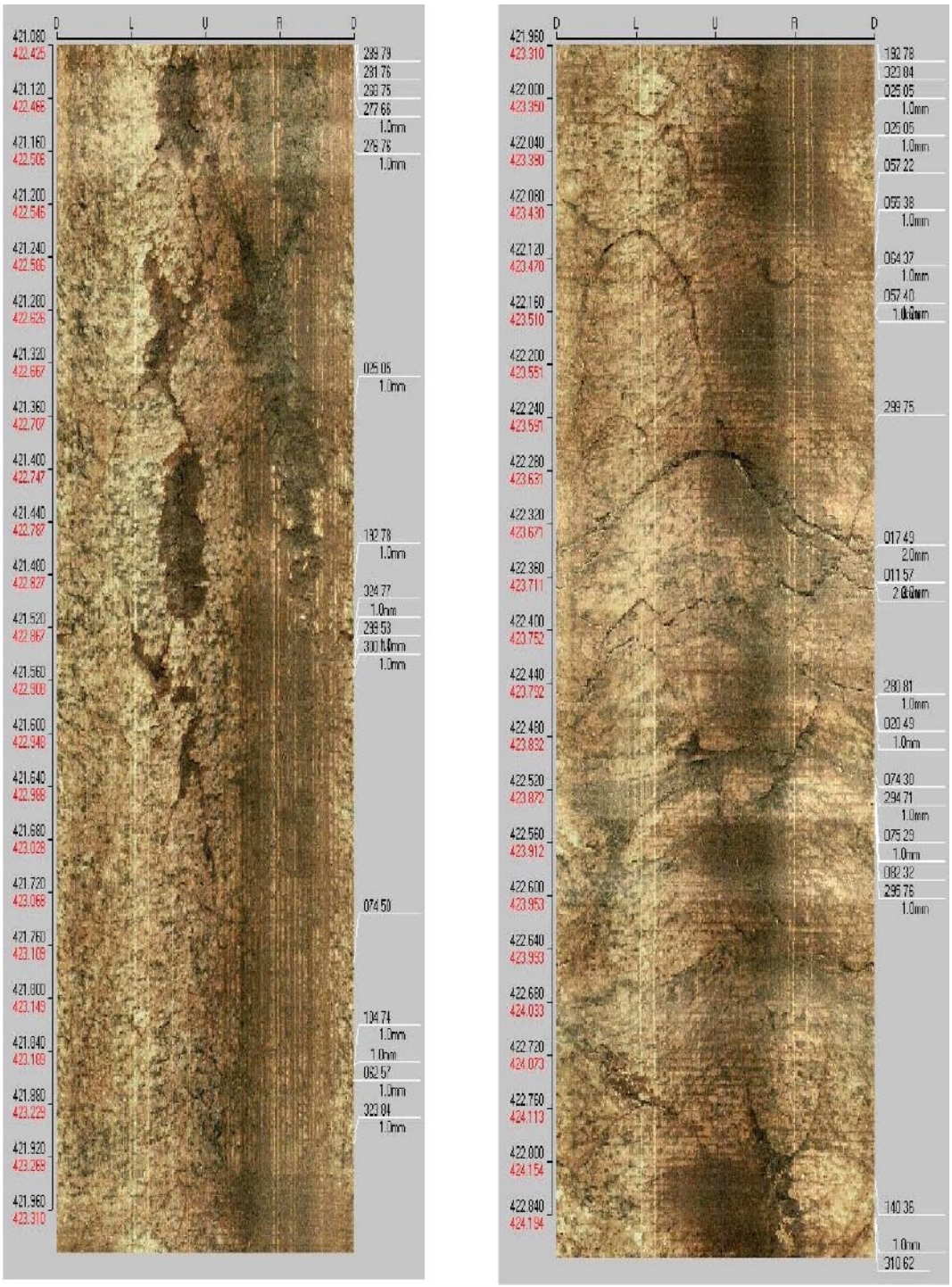

Figure 1-14. *BIPS-images from KFM02A showing the probable main water-conducting open fractures sampled from borehole section 413.5–433.5 m.*

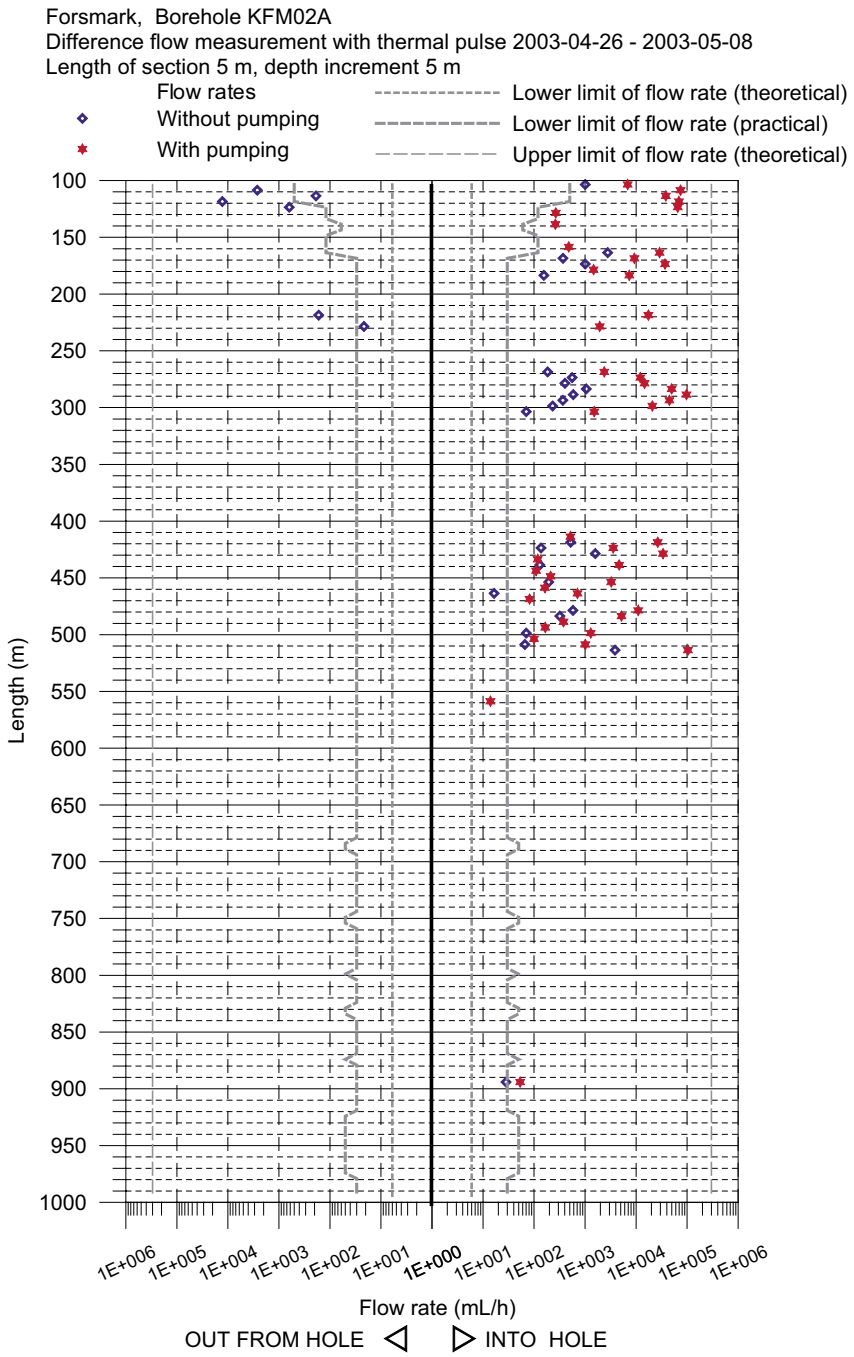

Figure 1-15. *Downhole differential flow measurements along borehole KFM02A (100–1,002.5 m) showing groundwater flow rate (mL/h) into and out of the borehole (SKB P-04-188).*

Figure 1-16 shows the variation of electric conductivity with depth in borehole KFM02A; note the first 100 m is cased. Comparing with and without pumping little difference is observed. Below the casing there is a rapid increase in salinity to around 1.5 S/m and this level is maintained increasing slightly until 520 m. Here there is a gradual decrease to approx. 1.0 S/m at 650 m and this continues until the bottom of the borehole. The borehole is therefore characterised by saline groundwater which can probably be explained by flushing water from HFM05 which is brackish (~ 4,500 mg/L Cl) and of saline/meteoric origin; tritium is below detection (< 0.8 TU). This is further discussed in section 3.3.2.

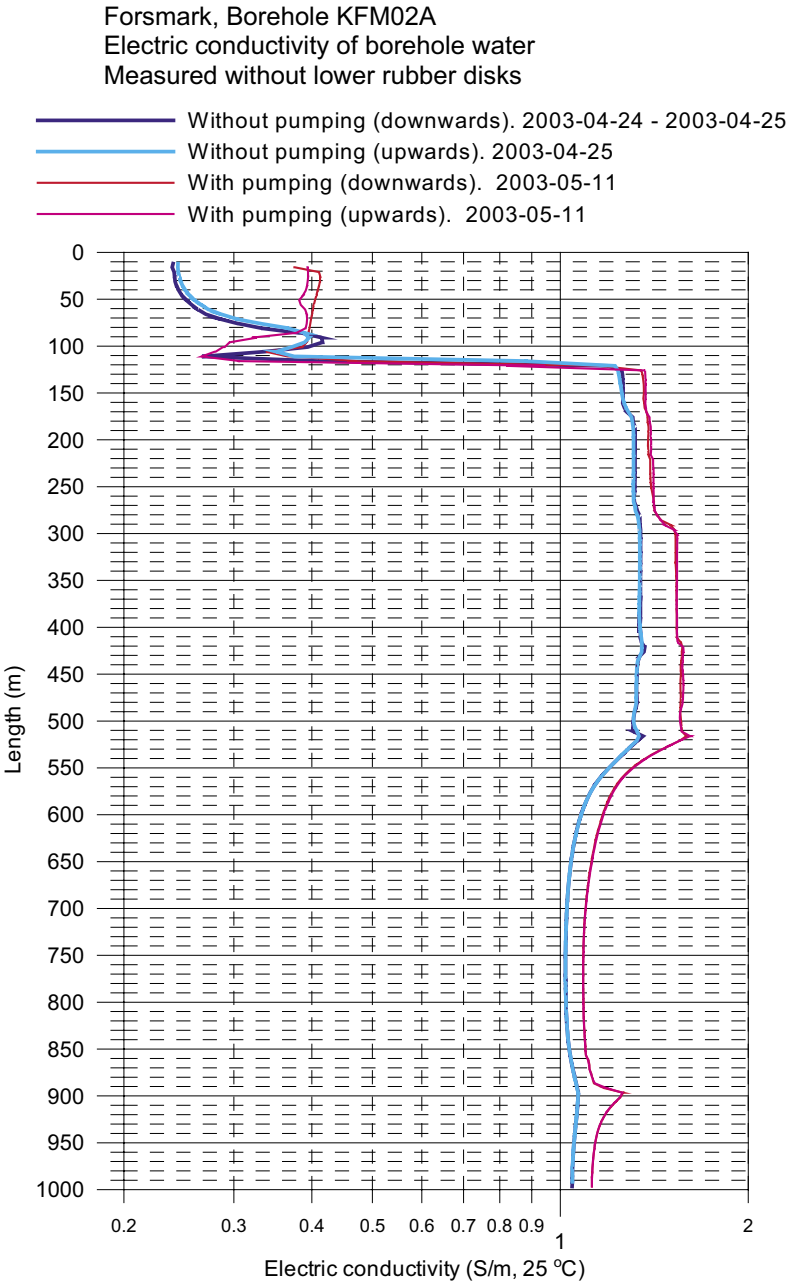

Figure 1-16. *Electric conductivity log for borehole KFM02A during open hole conditions (SKB P-04-188).*

1.6 Borehole KFM03A

Borehole KFM03A was core drilled to 1,001.9 m depth at an inclination of 4.2° to the vertical. The first 100 m were percussion drilled and cased to approx. 100 m.

1.6.1 Geological and hydrogeological character

The bedrock intercepted is dominated by metagranitoid containing sporadic subordinate lenses/bands of amphibolite and pegmatite occurring throughout. The exception is between 200–400 m where alternations of fine-grained granite/granodiorite and tonalite are dominant (Figure 1-17).

The fracture frequency is low (i.e. 2–3 fractures/m) to around 370 m where an increase in frequency occurs to 400 m; this is thought to reflect the intersection of a major fracture zone. Below 400 m the fracture frequency is low with only isolated individual(?) fractures occurring, particularly at around 800 m and 1,000 m.

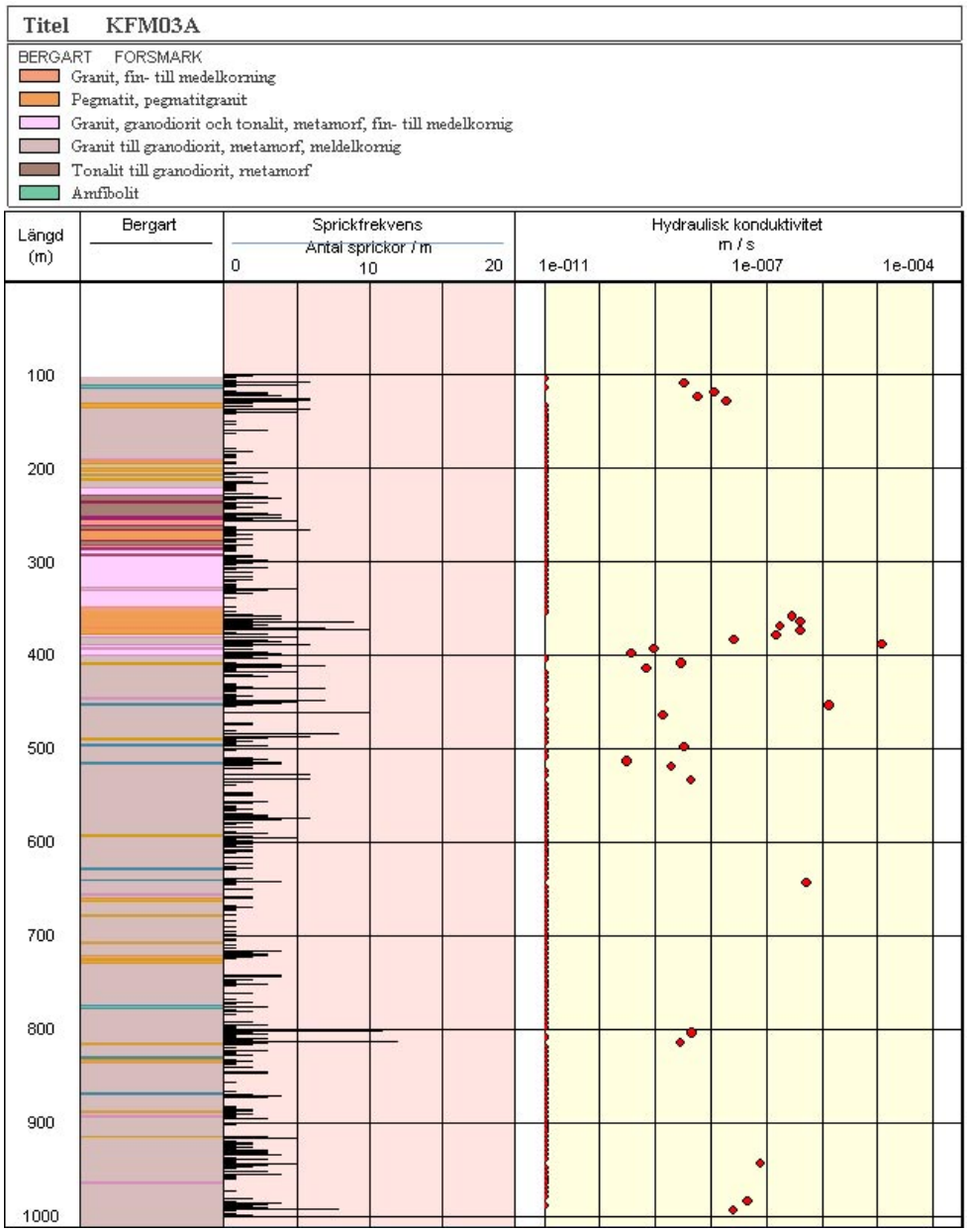

Figure 1-17. *Integrated geology, fracture frequency and hydraulic conductivity along borehole KFM03A.*

Figure 1-17 also shows the variation in hydraulic conductivity. The highest values range from 10^{-9}–10^{-5} ms^{-1} at a depth of 350–550 m, coinciding with the greatest frequency of fractures. Other enhanced sections include approximately 120 m (~ 10^{-6} ms^{-1}) and approximately 800 m and 1,000 m (10^{-9}–10^{-7} ms^{-1}). Otherwise the rest of the borehole is characterised by very low hydraulic conductivity, at or below the measurement limit at just under 10^{-8} ms^{-1}.

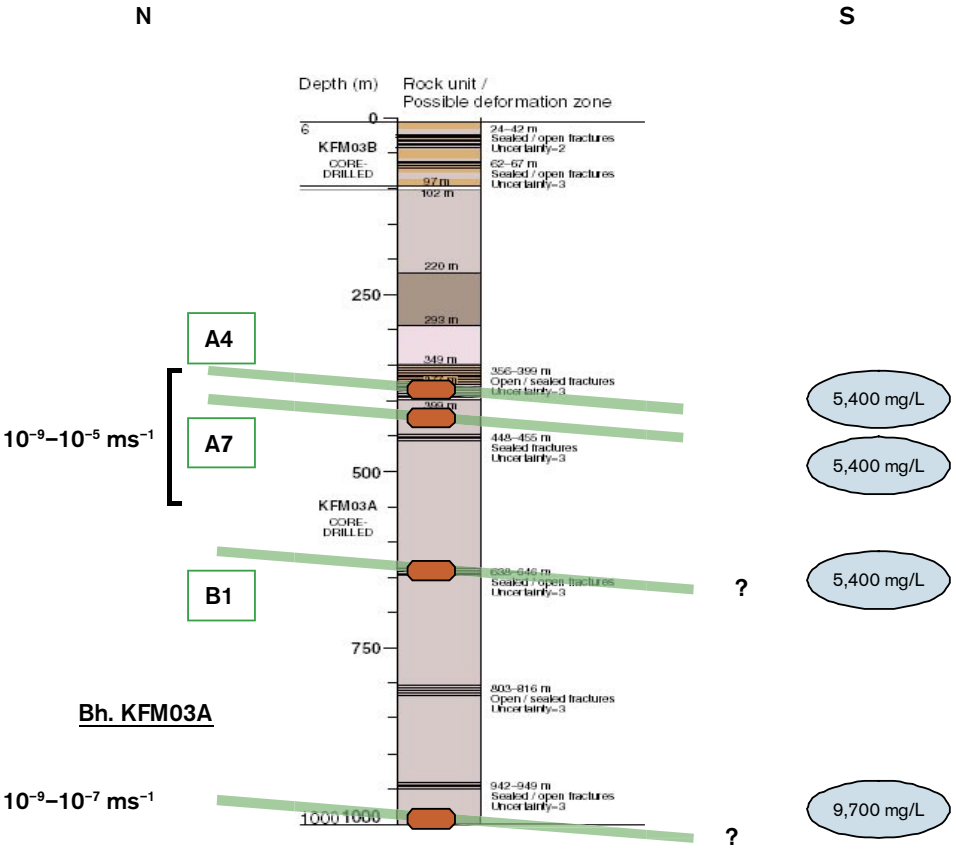

Figure 1-18. *Relation of Borehole KFM03A to the known major structures (in green) and hydraulic parameters; groundwater sampling locations are indicated (in red) with the mg/L chloride contents (in blue). (Based on M. Stephens, A. Simeonov, written comm., 2004).*

Figure 1-18 shows the relationship of borehole KFM03A to the major structures and the location of the groundwater sampling points. The groundwaters were taken from structures A4, A7 and B1 at depths of 386–391 m, 448–456 m and 639–646 m (Figure 1-19) respectively. Salinities are identical (5,400 mg/L Cl) from structures A4, A7 and B1 over a depth interval of 250 m; this might suggest some short-circuiting between these fractures and also between the fractures and the packed-off borehole sections sampled. At the deepest sampled location (980–1,001 m; Figure 1-19), which so far does not belong to any major structure in the area, the salinity reaches 9,700 mg/L Cl.

The recorded rates of groundwater flow under ‘natural’ hydraulic conditions (i.e. no pumping) via fractures into the borehole from the surrounding bedrock, and conversely from the borehole into the bedrock, indicate (with only one exception) that groundwater movement is dominantly from the borehole into the bedrock (Figure 1-20). During pumping all movement of formational groundwater is into the borehole. Under open hole conditions, therefore, any formation groundwater entering into the borehole (i.e. mainly shallow meteoric waters) will tend to migrate out into the bedrock via the major fracture zones located between 300–550 m depth and described above (cf. Figures 1-17 and 1-18). Below 550 m it is unlikely that any significant groundwater movement will occur and this borehole section will probably consist of meteoric groundwaters which have entered directly into the borehole at shallow depths (0–150 m) and of residual shallow groundwaters used as flushing water during drilling.

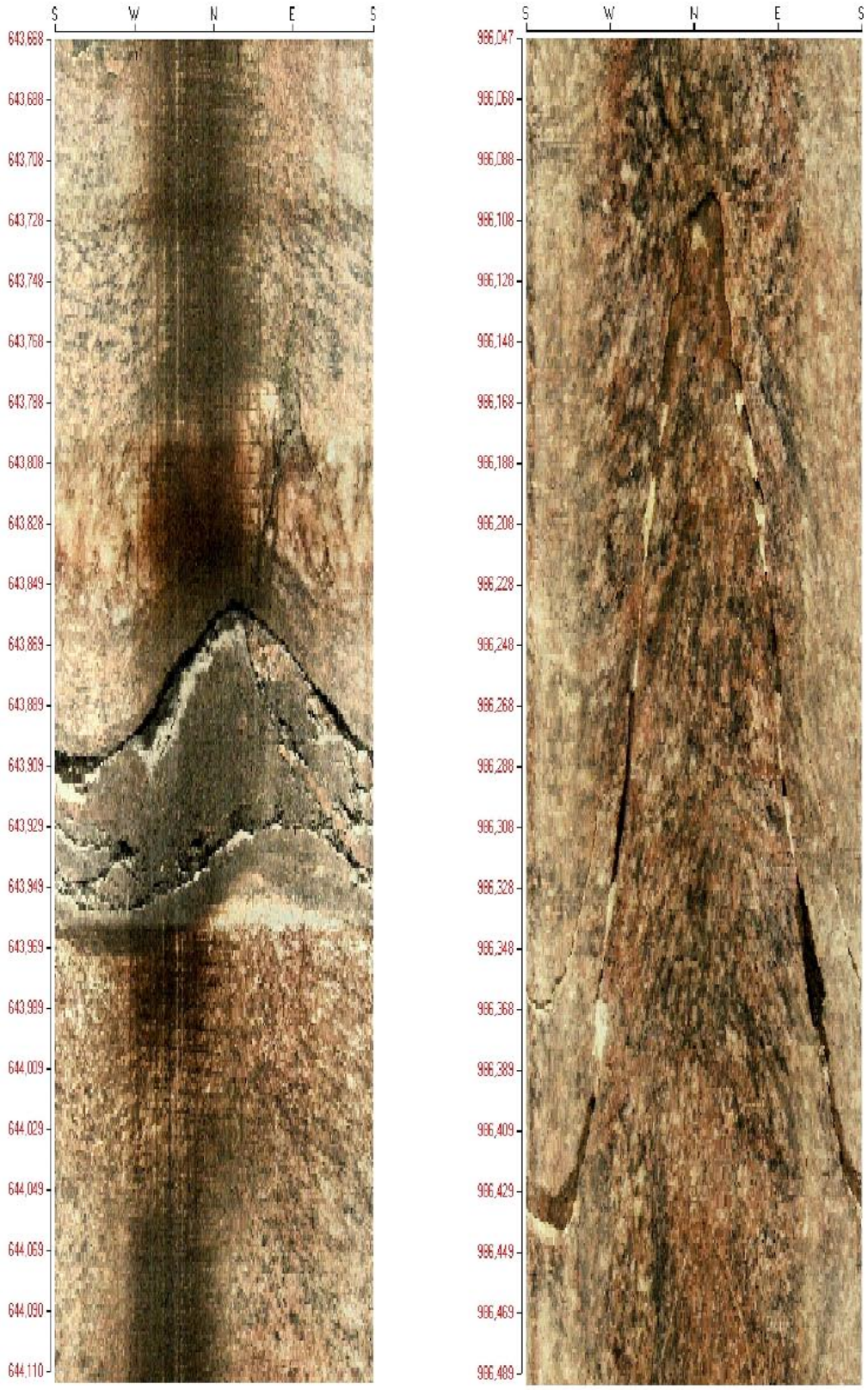

Figure 1-19. *BIPS-images from KFM03A showing the probable main water-conducting open fractures sampled from borehole sections 639–646 m and 980–1,001 m.*

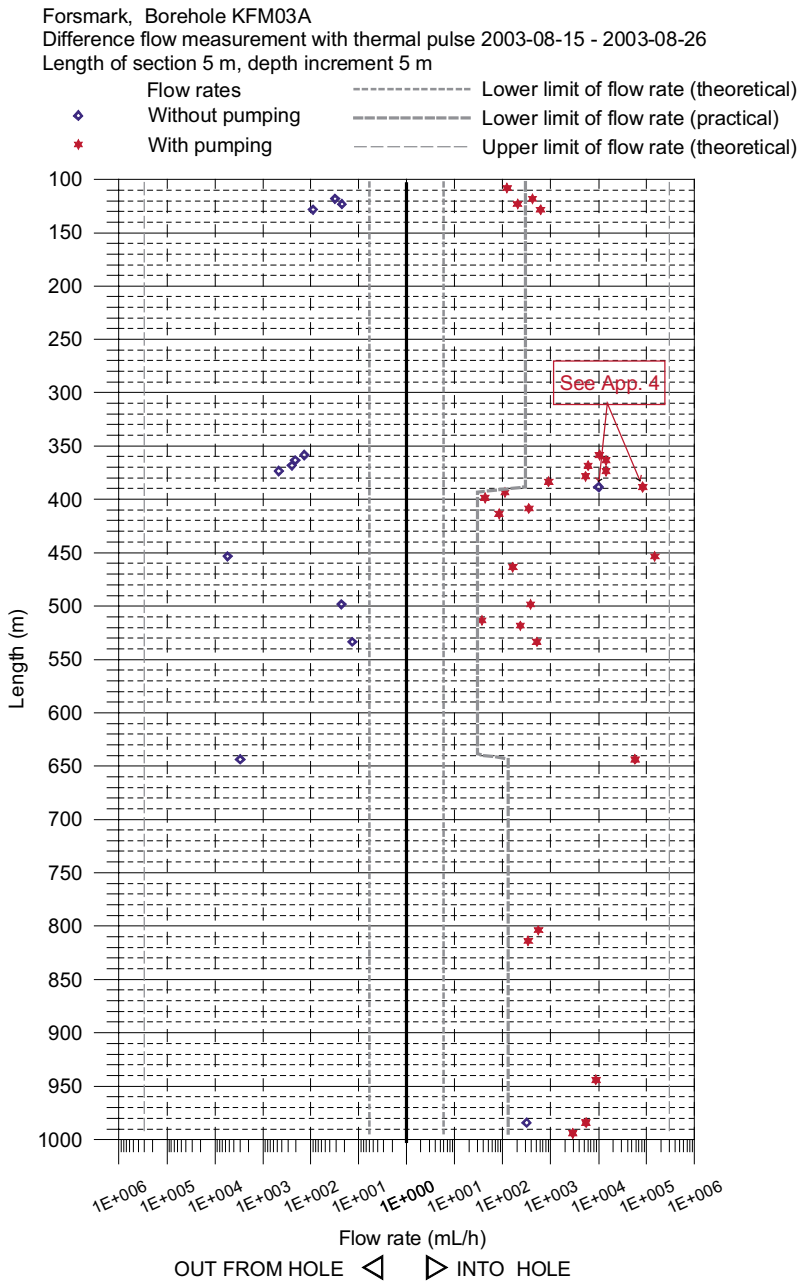

Figure 1-20. *Downhole differential flow measurements along borehole KFM03A (100–1,001.9 m) showing groundwater flow rate (mL/h) into and out of the borehole (SKB P-04-189).*

Figure 1-21 shows the variation of electric conductivity with depth in borehole KFM03A; note the first 100 m is cased. The borehole has been logged on two occasions, in 2003-08-14/15 and 2004-05-05/6. Taking the earlier log without pumping, there is a constant salinity level (approx. 2.6 S/m) from 100–650 m where it increases slightly to around 3.5 S/m and continues to the bottom of the borehole where 4 S/m is reached. After a lapse of almost 9 months the salinity log has maintained its overall profile but shows a small decrease. The only significant change is the downward movement of a less saline front to 300 m, due probably to the recharge of shallow meteoric waters into the borehole.

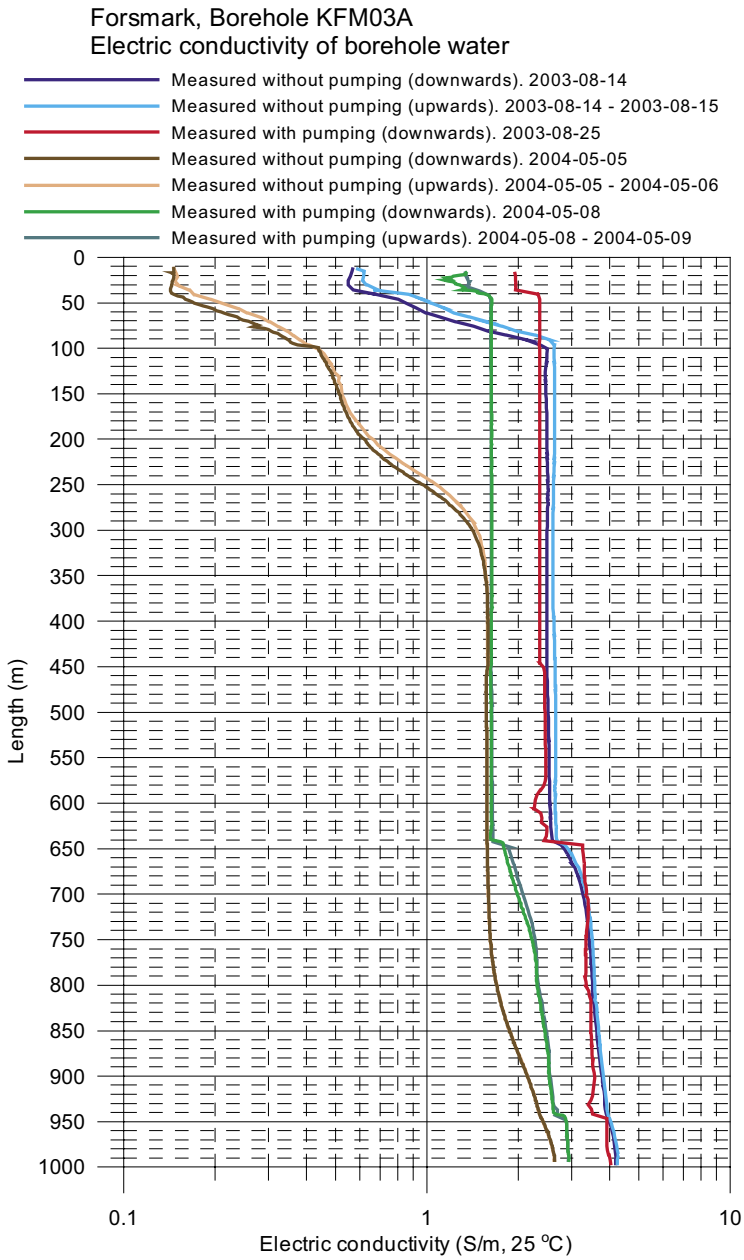

Figure 1-21. *Electric conductivity log for borehole KFM03A during open hole conditions (SKB P-04-189).*

1.7 Borehole KFM04A

Borehole KFM04A was core drilled to 1,001.42 m at an angle of 40° to the vertical. The first 107.42 m were percussion drilled and cased to this length.

1.7.1 Geological and hydrogeological character

The upper 500 m of the bedrock is dominated by metagranitoid with sporadic lenses/bands of amphibolite, pegmatite and fine-grained granite/granodiorite. From 500 m to the bottom of the borehole the fine-grained granite/granodiorite becomes dominant. Sporadic lenses/bands of pegmatite and amphibolite continue throughout; a small thickness of tonalite occurs around 950–970 m depth (Figure 1-22).

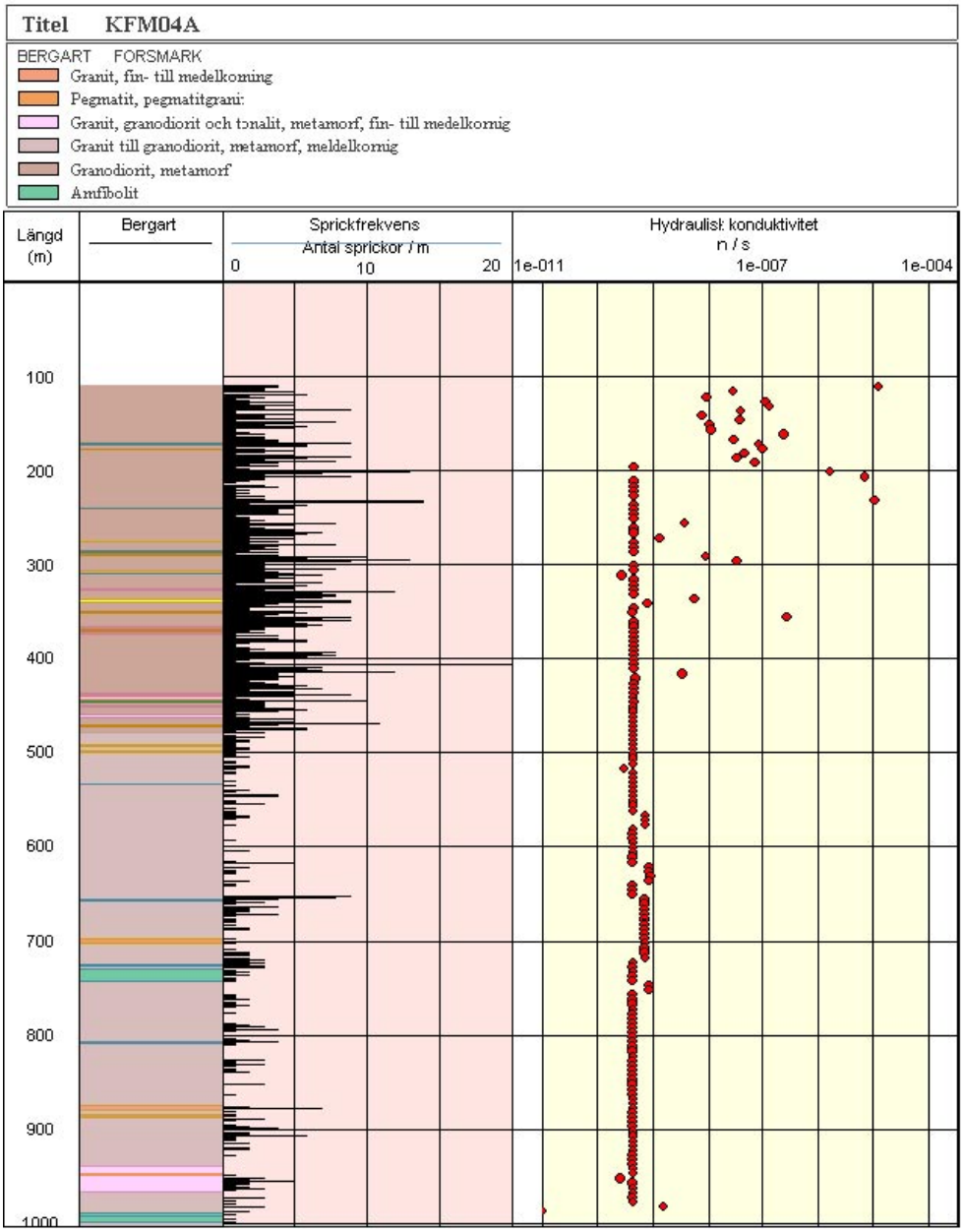

Figure 1-22. *Integrated geology, fracture frequency and hydraulic conductivity along borehole KFM04A.*

The fracture frequency along the borehole length to around 500 m is considered above normal (i.e. 2–7 fractures/m), with up to 20 fractures/m at about 400 m. This 100–500 m interval represents a steeply dipping NW striking major deformation zone. From 500 m to the borehole bottom the fracture frequency is low apart from individual (?) fractures at approx. 540 m, 670 m and a small increase around 900 m.

Downhole hydraulic measurements (Figure 1-22) reveal a major section of concentrated high transmissivity from 100–250 m (10^{-9}–10^{-4} m^2s^{-1}) and a second lower transmissive section (10^{-9}–10^{-6} m^2s^{-1}) from 250–360 m. Otherwise the rest of the borehole is characterised by very low hydraulic conductivity, at or below the measurement limit at just under $10^{-9.5}$ m^2s^{-1}. Weak indications are observed at 420 m, 520 m and 950 m.

Figure 1-23 shows the relationship of borehole KFM03A to the major structures and the location of the groundwater sampling points. The groundwaters were taken from structure A2 at 231–238 m borehole length and one other location at 354–361 m borehole length (Figure 1-24). Salinities are identical (~ 5,800 mg/L Cl) from both locations and may suggest some short-circuiting between these fractures and also between the fractures and the packed-off borehole sections sampled.

The recorded rates of groundwater flow under 'natural' hydraulic conditions (i.e. no pumping) via fractures into the borehole from the surrounding bedrock occur at approx. 210 m and 290–360 m (Figure 1-25). Conversely at 110–180 m and at 230 m groundwater flow is from the borehole into the bedrock. Under open hole conditions, therefore, formation groundwater would be expected to circulate into and out from the borehole from 100–350 m. Below 350 m static hydraulic conditions prevail and any groundwater circulatory movement would be driven mainly by density differences responding to small inputs of groundwaters from different sources (i.e. depths) in the surrounding bedrock.

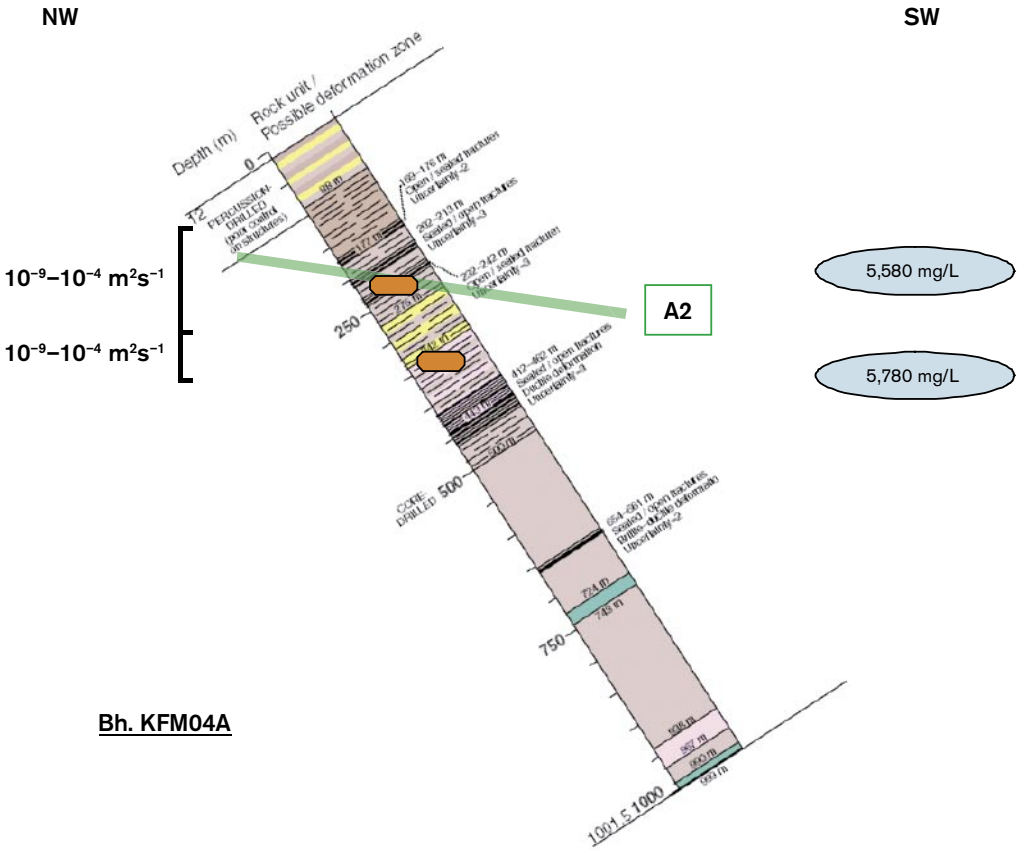

Figure 1-23. *Relation of borehole KFM04A to the known major structures (in green) and hydraulic parameters; groundwater sampling locations are indicated (in red) with mg/L chloride contents in blue). (Based on M. Stephens, A. Simeonov, written comm., 2004).*

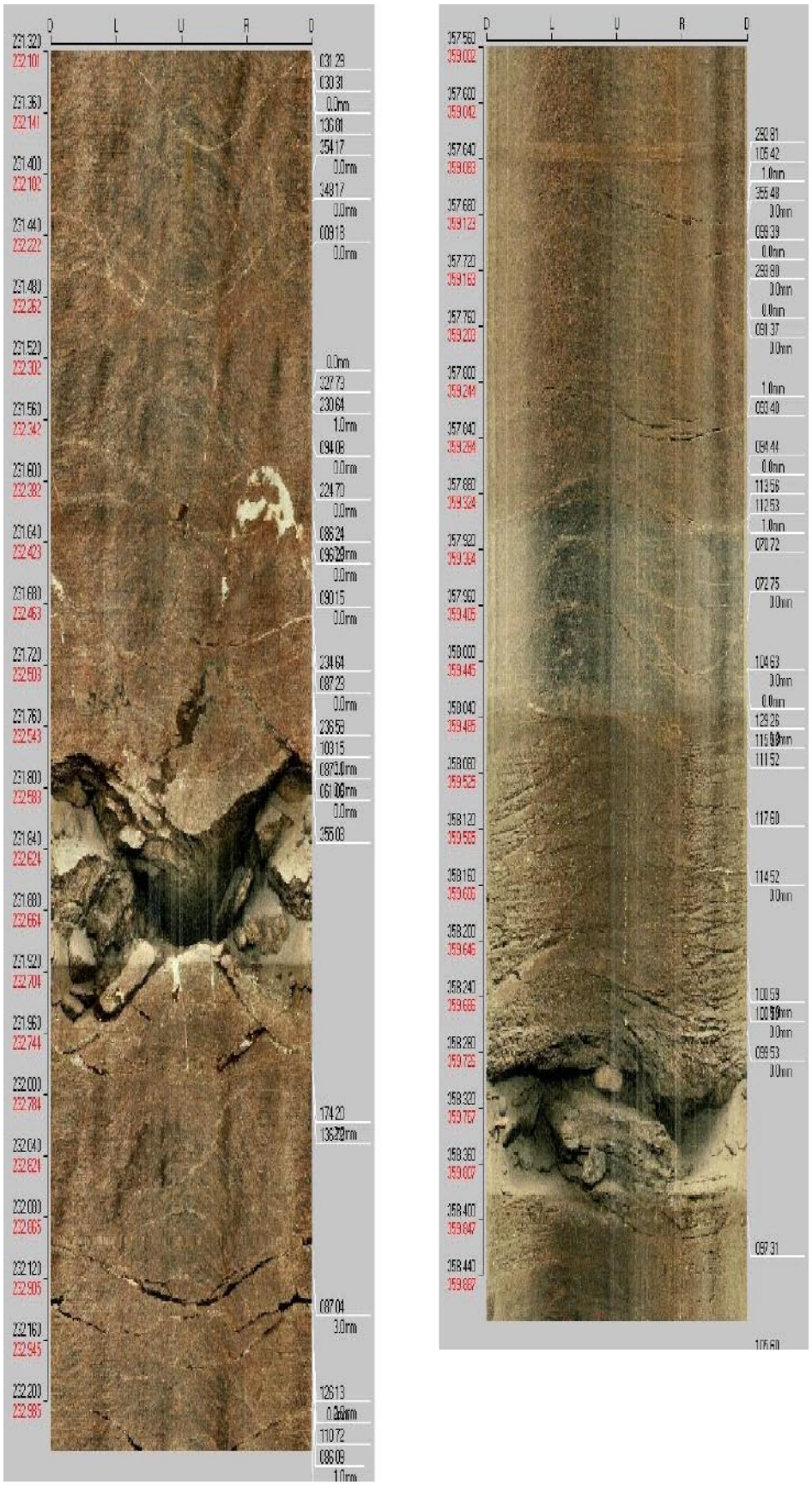

Figure 1-24. *BIPS-images from KFM04A showing the probable main water-conducting open fractures sampled from borehole sections 231–238 m and 354–361 m.*

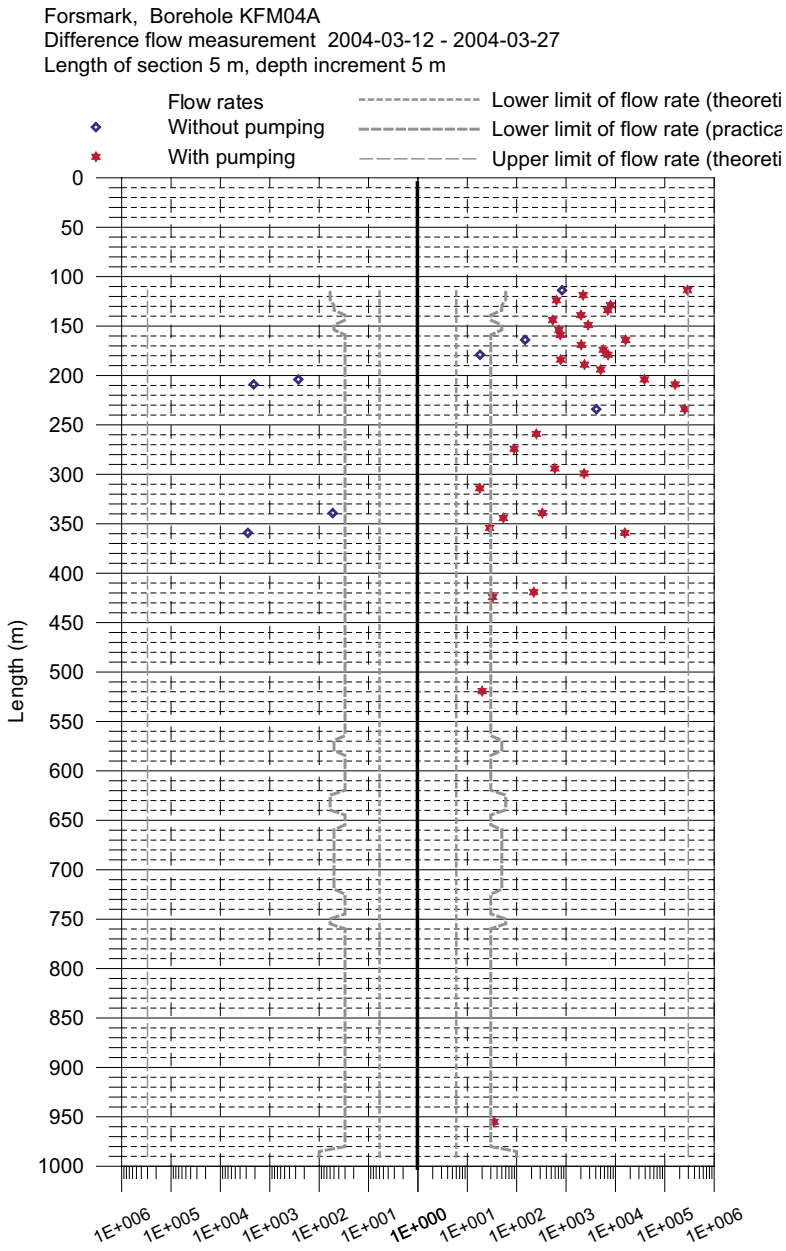

Figure 1-25. *Downhole differential flow measurements along borehole KFM04A (107.42–1,001.42 m) showing groundwater flow rate (mL/h) into and out of the borehole (SKB P-03-84).*

Figure 1-26 shows the variation of electric conductivity with depth in borehole KFM04A; note the first 107.42 m is cased. Comparing with and without pumping there is little difference in the shape of salinity profiles observed, just a slightly higher salinity recorded during the absence of pumping. Basically there is no variation in salinity with depth. The borehole is therefore characterised by saline groundwater which may be explained by: a) flushing water from borehole HFM10 (0–150 m) which is typically brackish (~ 5,000 mg/L Cl) with a small modern component (1.1–1.25 TU), and/or b) borehole KFM04A is drilled into the same reservoir of formation water as pumped from HFM10. This is further discussed in section 3.3.2.

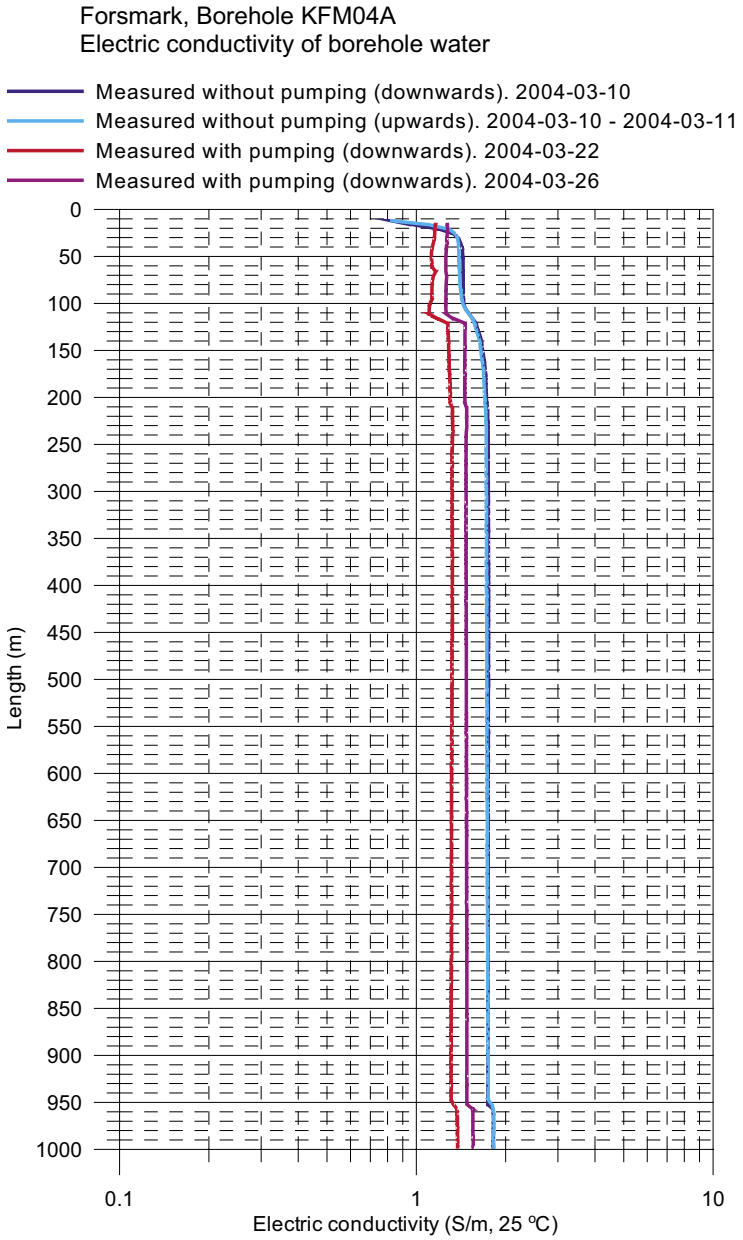

Figure 1-26. *Electric conductivity log for borehole KFM04A during open hole conditions (SKB P-03-84).*

1.8 Shallow Soil Pipes

Data exist for 22 groundwaters collected from the overburden by means of sunken soil pipes to depths ranging from 1–11 m (Figure 1-27). Numbered are several soil pipes including four with enhanced salinities; these are discussed in Chapter 4.

Some of the soil pipes have been drilled in locations to monitor changes in the near-surface groundwater chemistry during percussion and core drilling of nearby deep boreholes. The remaining soil pipes have been located solely to monitor the natural undisturbed near-surface groundwater system.

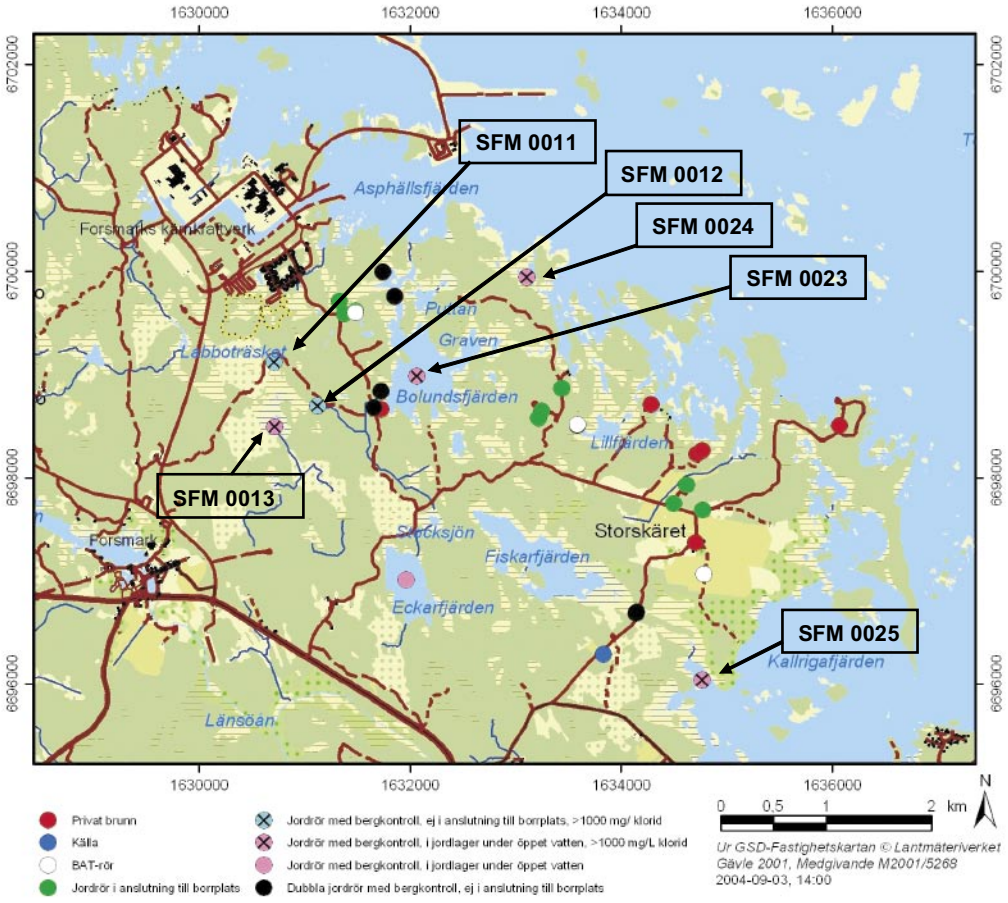

Figure 1-27. *Location of the shallow Soil Pipes for overburden groundwater extraction. Marked are those with enhanced salinities (SFM0012, 13, 23 and 24).*

1.9 Fracture filling studies

The mineralogy and the geochemical composition of the fracture minerals are of importance for the understanding and interpretation of past and present groundwater systems. The issues of importance include groundwater/mineral equilibrium/near-equilibrium during present conditions and the influence of changing groundwater chemistries (e.g. external effects such as glaciations) on the type and chemistry of the fracture fillings.

Fracture minerals are initially documented during mapping of the drillcore which forms an integral part of the bore map system used in the site characterisation protocol. Based on this information, fracture filling phases are further selected for more detailed study which involves:

- X-ray diffractometry; especially used for identification of clay minerals and gouge material. A total of approx. 46 samples from boreholes KFM01A, KFM02A and KFM03A have been analysed by XRD /Petersson et al. 2004/.
- Microscopy of fracture fillings; around 50 fractures from boreholes KFM01A, KFM02A and KFM03A have been sampled and 40 thin sections and 11 fracture surfaces have been studied by SEM. /Sandström et al. 2004/.
- ICP analyses of fracture fillings from boreholes KFM01A and KFM02A have been carried out and are documented in /Petersson et al. 2004/.
- Isotopic analyses ($\delta^{13}C$ and $\delta^{18}O$) of fracture calcites sampled from the same three boreholes also have been carried out /Sandström et al. 2004/.

Quartz, chlorite and calcite occur in several different varieties of fractures, being particularly common in open fractures (Figure 1-28). Adularia (low temperature K-feldspar) also is found in several fracture types of which one is the sealed variety containing haematite (Figure 1-29). Other common minerals are epidote, prehnite, laumontite, (low-temperature K-feldspar), analcime, haematite and pyrite. Apophyllite more rarely has been identified. Black organic precipitates of asphaltite have been found in some fractures in the upper 150 m (Figure 1-30).

Clay minerals identified, in addition to chlorite, comprise: a) corrensite (Figure 1-28); mixed layer chlorite/smectite or chlorite/vermiculite clay; the smectite or vermiculite layer is characterised by swelling properties), b) illite, c) mixed-layer illite/smectite (swelling), and d) a few observations of smectites. Of these minerals corrensite is the one most frequently found. Results from the XRD analysis are shown in Appendix 1.

The fracture mineralogy as revealed in drillcores KFM01A, KFM02A and KFM03A shows a paragenesis of mineralisation that can be summarised as follows:

Generation 1: The initial generation in the fracture mineral history includes epidote, quartz and chlorite formation during semi-ductile to brittle greenschist facies conditions. Only very thin mylonites are present whereas cataclasites are more frequent in the three boreholes investigated to date (KFM01A, KFM02A and KFM03A+B).

Generation 2 and **Generation 3** probably represent the same prolonged hydrothermal period which has first precipitated the brick red adularia followed by prehnite and thereafter laumonitite (Generation 3). In addition, calcite as well as chlorite/corrensite, adularia and quartz have been precipitated during this event. The interpretation is that the minerlisations resulting in generations 2 and 3 took place during brittle conditions and changing P-T conditions. This resulted in a change from prehnite-pumpellyite phases to upper zeolite phases. Generations 2 and 3 represent a clearly distinct stress regime as compared to Generation 1. There is a clear dominance of steep NE-oriented fractures which have truncated the foliation during Generation 3. Furthermore, this period seems to represent a new fracturing event characterised initially by laumontite coatings.

Generation 4: This phase starts with dissolution along older laumontite/prehnite sealed fractures causing cavities to form in the fractures and to a lesser extent in the adjacent host rock; new fractures have also been formed during this period. Subsequent temperature decrease has caused precipitation of quartz covering fracture surfaces and coating voids. Adularia, chlorite/corrensite and calcite are also precipitated during this period (Figure 1-28). Many of the hydraulically conductive fracture reflect this paragenesis.

Generation 5 probably represents a late-stage phase of Generation 4 when analcime, pyrite and calcite have been produced. A common origin for generations 4 and 5 is supported by, for example, the stable isotope results from the respective calcites characterising these generations.

Generation 6 includes the precipitates found as a top-layer on the fractures. Precipitates include calcite, clay minerals such as illite, mixed-layer clays and smectites. Asphaltite may also belong to this generation, but further analyses are needed for confirmation. It is probable that continued fracture mineral studies will provide further subdivision of the formation of this mineral assemblage which probably extends from the pre-Cambrian until the Quaternary.

The hydraulically conductive fractures in the cored borehole sections sampled for hydrochemical characterisation show mostly coatings of quartz, adularia, calcite, chlorite and corrensite ±albite. Section 100–120 m in drillcore KFM02A deviates in having a mixed layer illite/smectite clay. In section 386–391 m in drillcore KFM03A smectite has been identified and section 639–634 m shows the presence of haematite.

The locations of the hydraulically conductive fractures in the upper 100 metres (samples close to the percussion boreholes) are often associated with loose material which consists of crushed rock fragments rich in quartz, K-feldspar and clay minerals. This material has only been possible to sample in some of the ‘B’ boreholes (0–100 m) drilled from the surface, whereas the ‘A’ boreholes only commence at 100 m. It has been difficult to obtain undisturbed samples from these zones so far, but ongoing analyses indicate that they are more rich in illite and mixed –layer clays compared with the deeper section based on one sample from KFM03B (/Petersson et al. 2004/, and ongoing investigations of KFM01B).

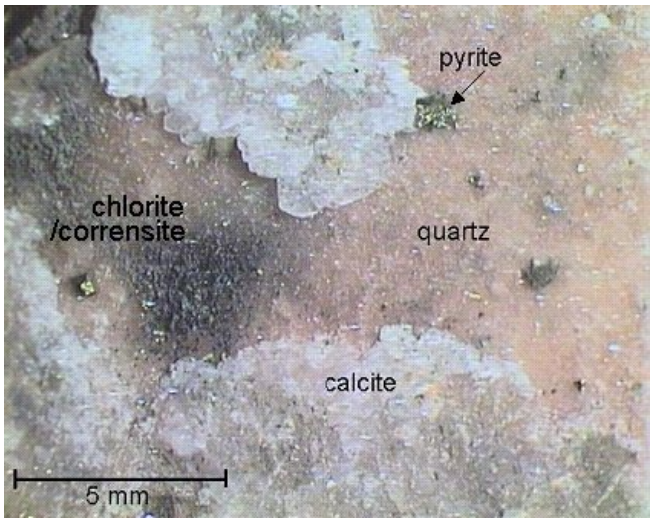

Figure 1-28. *Open fracture covered with quartz crystals, calcite and pyrite (KFM04A: 298.6 m).*

Figure 1-29. *Fracture filled with adularia that is brick coloured due to micrograins of haematite. Some calcite is also present in the fracture. The diameter of the drill-core is approx. 5 cm. (KFM03A: 184.34–184.50 m).*

Figure 1-30. *Drillcore with quartz and containing large voids partly filled with asphaltite (KFM01B: 2.97–23.05 m).*

2 Groundwater quality and representativeness

2.1 Background

Prior to any hydrochemical evaluation is the necessity to judge the quality and the representativeness of the groundwater data derived from the site characterisation in question. The thoroughness of this exercise may vary depending on the eventual use of the data, for example, high quality groundwater data are required for geochemical equilibrium reaction modelling, whilst semi-quantitative data may suffice to model large-scale variations in groundwater chemistry or distinguish time-series chemical trends. The hydrogeochemical evaluation approach used at Forsmark and the uncertainties involved are based on the methodology outlined in SKB R-02-49.

Evaluation of the Forsmark hydrogeochemical data in Model v. 1.2 entails comparison with other geographically located sites in its near-vicinity, i.e. Finnsjön and SFR, and also other Fennoscandian sites such as Simpevarp and Olkiluoto in Finland. Groundwater data from all these sites are compiled in the 'Nordic Table' and these data also have been evaluated with respect to representativeness. This was carried out in parallel to the Simpevarp and Forsmark v. 1.2 data evaluations and documented in the Simpevarp evaluation report (Simpevarp Site: Hydrogeochemical Evaluation (Model 1.2 stage); submitted October, 2004).

2.2 Forsmark site

The Forsmark groundwater analytical data compiled in the SICADA database, which form the basis to the hydrochemical evaluation, will have already undergone an initial screening process by field and laboratory personnel based on sampling, sample preparation and analytical criteria. The next stage in the hydrogeochemical site descriptive process, the focus of this report, is to assess these screened data in more detail to derive a standard set of representative groundwater data for hydrogeochemical modelling purposes.

To carry out this assessment the initial most important stage is to check for groundwater contamination. For this to be accomplished an intimate knowledge of the borehole site is required which entails borehole geology and hydrogeology and a detailed log of borehole activities. These latter activities are a major source of groundwater contamination and include:

- drilling and borehole cleaning,
- open hole effects,
- downhole geophysical/geochemical logging,
- downhole hydraulic logging/testing/pumping, and
- downhole sampling of groundwaters.

In Chapter 3 in this report these potential sources of contamination have been addressed and documented systematically for each borehole drilled and for each borehole section sampled. Where applicable, use has been made of results from the Drilling Impact Study (DIS). The degree of contamination can be judged, for example, by plotting tritium against percentage drilling water, and using measured values with specifically defined limits, i.e. charge balance (±5%) and drilling water component (< 1%), and supported qualitatively by expert judgement based on detailed studies of the distribution and behaviour of the major ions and isotopes.

The final selection of data which best represents the sampled borehole section is based on identifying as near as possible a complete set of major ion and isotope (particularly tritium, ^{18}O and deuterium) analytical data. This is not always the case, however, and a degree of flexibility is necessary in order to achieve an adequate dataset to work with. For example:

- A charge balance of ±5% was considered acceptable. In some cases groundwaters were chosen when exceeding this range to provide a more representative selection of groundwaters. These groundwaters should therefore be treated with some caution when used in the modelling exercises.
- In many cases the drilling water content was either not recorded or not measured. Less than 1% drilling water was considered acceptable. In some cases groundwaters were chosen when exceeding this range to provide a more representative selection of groundwaters. These groundwaters also should be treated with some caution when used in the modelling exercises.
- Some of the older tritium data were analysed with a higher detection limit of 8 TU; the detection limit lies around 0.02 TU for recent anlayses. For some groundwaters an approximate tritium value is suggested where no recorded value is available. This value is selected normally from the same borehole section but representing an earlier or later sample.

Resulting from this assessment, two groundwater sample types are highlighted in the SICADA database: one type considered representative, the other type less representative but suitable when used with caution.

2.3 Nordic sites

The Nordic sites, in addition to Forsmark and the near-vicinity Finnsjön and SFR sites, comprise Simpevarp and all remaining Swedish sites studied over the last 20–25 years; Olkiluoto in Finland is also included. Most of these sites have undergone earlier detailed assessments as to groundwater quality and representativeness, e.g. Gideå, Kamlunge, Klipperås, Fjällveden, Svartboberget, Finnsjön /Smellie et al. 1985, 1987; Smellie and Wikberg, 1989/, Lansjärv /Bäckblom and Stanfors, 1989/ and Olkiluoto /Pitkänen et al. 1999, 2004/. Based on this information the Nordic Table has been highlighted with respect to representative and less representative groundwater samples, similar to the Finnsjön and SFR sites referred to above in section 2.1.

The ‘less’ representative groundwaters do not meet all of the criteria for representativeness but are sufficiently important to be included (Simpevarp v. 1.2 Report, Appendix 3). The importance of early or ‘First Strike’ samples is emphasised in this evaluation. These are coloured green in the Nordic Table and involve one or more of the following deviations from being considered ‘representative’:

- lack of important ions – especially Br,
- lack of ^{18}O and deuterium data,
- variation in salinity during the time-series measurements, and
- few or an absence of time-series measurements.

The representative groundwaters are highlighted in the Nordic Table in orange. Some, however, lack bromine data, and these are highlighted (see Simpevarp v. 1.2 Report, Appendix 3) also using orange font.

3 Evaluation of groundwater representativeness

3.1 Sources addressed

Major groundwater sources addressed include: a) groundwaters from four deep cored boreholes (to approx. 1,000 m) sampled for complete chemical characterisation and representing hydrochemical bedrock conditions to repository depths (KFM01A–KFM04A), and b) groundwaters from 18 shallow percussion boreholes (HFM01–HFM06; HFM08–HFM19) which, in cases, provide sources of flushing water for the drilling of the cored boreholes and, in general, provide a spatial distribution of groundwater chemistry in the demarcated site area between 50–250 m depth.

Intermediate groundwater sources addressed involve soil pipe samples (1–16 m depth) of near-surface and ground waters (SFM0001–8, SFM0057/58) important because of their potential influence on recharge water chemistry percolating into the bedrock.

Other water sources addressed include Sea Water, running Stream Water and Lake Water; Stream and Lake waters may provide surface indications of active areas of regional/local groundwater recharge/discharge.

3.2 Shallow percussion boreholes

Out of a total of 19 percussion drilled boreholes, groundwater chemical data are available for all with the exception of HFM07; sources include P-reports for HFM01–HFM06 and HFM08 (P-03-47/48/49). Hydraulic data for HFM01–19 include P-reports: P-03-33/34/36 and P-04-34/64/65/71/72/74. Drilling and geological information for HFM01–19 include P-reports: P-03-30/51/58 and P-04-76/85/94/106. Groundwater samples for hydrochemical classification were generally collected in connection with hydraulic testing.

3.2.1 Available data

Available data include:

- Geological and drilling information.
- Single hole pumping tests to determine the position and size of inflow sections in the boreholes.
- Flow logging (flow rate, temperature and electric conductivity) to determine the transmissivity of flow anomalies in the boreholes.
- Groundwater chemistry either from the complete borehole or from packed off sections.

To facilitate the descriptions presented below reference is made to the relative age and composition of the sampled groundwaters. These refer to:

Approximate Groundwater Age		Groundwater Salinity (mg/L)	
Old	> 10,000 years	Dilute	< 500
Recent	< 10,000–50 years	Low salinity	500–2,000
Modern	< 50 years	Moderate salinity	2,000–4,000
		Brackish	~ 5,000–6,000

3.2.2 Borehole HFM01

Borehole HFM01 inclined at 22.5° to the vertical was drilled to 200.2 m (cased to 31.93 m) at the DS1 site with the primary purpose of supplying flushing water to drill borehole KFM01A. Drilling of HFM01 was completed in 2002-05-03.

Hydraulics

Four groundwater inflow sections were identified at 34.5–43 m ($T = 4.5 \times 10^{-4}$ m^2s^{-1}), 48–50 m ($T = 5 \times 10^{-4}$ m^2s^{-1}), 60.5–63.5 m ($T = 2.5 \times 10^{-4}$ m^2s^{-1}) and 64–64.5 m ($T = 1.1 \times 10^{-5}$ m^2s^{-1}); below 65.5 m flow into the borehole was below the limit of measurement. See /Ludvigson et al. 2003a/ for further details.

Chemistry

Groundwater samples for Class 3 analysis were collected from 0–71 m (1 sample), 0–200 m (4 samples) and 70–200 m (sequence of 3 samples). The first sample was taken on 2002-05-16 and the final sample on 2002-06-25; the sequence of 3 was taken on 2002-05-14. Since all the major inflow sections occur within the 0–70 m borehole length sampled initially, this would be the obvious choice of the most representative sample. This is supported by the sequence of 3 samples taken from 70–200 m which show an increase in salinity. The samples taken from 0–200 m therefore represent groundwater dominated by the 0–70 m section, but probably contain a very small saline component from depth. The 0–70 m groundwater is low in salinity (500–600 mg/L Cl), recent to modern in age (45 pmC; 3–4 TU) and originates from a mixture of modern meteoric and older brackish groundwaters. Charge balance is acceptable. See /Nilsson, 2003a/ for further details.

Representativeness

The initial sample from 0–70 m is considered to best represent ‘undisturbed’ in-situ groundwater conditions for this depth.

3.2.3 Borehole HFM02

Borehole HFM02 inclined at approx. 12° to the vertical was drilled to 100 m (cased to 25.4 m) at the DS1 site with the primary purpose of groundwater flow monitoring. Drilling was completed in 2002-05-21.

Hydraulics

One groundwater inflow section was identified at 42–44.5 m ($T = 5.9 \times 10^{-4}$ m^2s^{-1}); below 45 m flow into the borehole was below the limit of measurement. See /Ludvigson et al. 2003a for further details.

Chemistry

Groundwater samples for Class 3 analysis were collected from 0–100 m (sequence of 2 samples on 2002-06-04); this was carried out 13 days after borehole completion. The first sample indicated greater salinity which decreased to near HFM01 levels during the second sampling on the same day. This is taken to indicate that higher saline contamination from deeper in the borehole during the first sampling has been removed and replaced by groundwater from the dominant inflow at 42–44.5 m during the later sampling. The second sample taken from 0–100 m therefore represents groundwater dominated by the 42–44.5 m section, but probably contains a very small saline component from depth. The dominant groundwater is low in salinity (400–500 mg/L Cl); no isotopic data are available but in common with HFM01 (to which there is a hydraulic connection via a subhorizontal fracture) it probably represents a near-surface meteoric origin. See /Nilsson, 2003a; Ludvigson et al. 2003a/ for further details.

Representativeness

The second sample from 44–42.5 m is considered to best represent 'undisturbed' in-situ groundwater conditions at this depth even though the charge balance is ~ 14%, probably due to the dilute nature of the groundwater sample.

3.2.4 Borehole HFM03

Borehole HFM03 inclined at approx. 12.5° to the vertical was drilled to 26 m (cased to 13.1 m) at the DS1 site with the primary purpose of groundwater flow monitoring. Drilling was completed in 2002-05-28.

Hydraulics

One groundwater inflow section was identified at 42–44.5 m ($T = 5.9 \times 10^{-4}$ m^2s^{-1}); below 45 m flow into the borehole was below the limit of measurement. See /Ludvigson et al. 2003a/ for further details.

Chemistry

Groundwater samples for Class 3 analysis were collected from 0–26 m (sequence of 2 samples on 2002-05-29); this was carried out approx. 1 month after borehole completion. There is little difference in the groundwater chemistries. The groundwater is dilute (12–16 mg/L Cl), recent to modern in age (85.3 pmC, 12 TU) and near-surface meteoric in origin. See /Nilsson, 2003a/ for further details.

Representativeness

The second sample from 0–26 m has been selected to best represent 'undisturbed' in-situ groundwater conditions by virtue of having a more complete analytical dataset even though the charge balance is ~ 10%.

3.2.5 Borehole HFM04

Borehole HFM04 inclined at 5.5° to the vertical was drilled to 221.7 m (cased to 12 m) at the DS2 site with the primary purpose of groundwater monitoring and hydrochemical characterisation. Drilling was completed in 2002-12-03.

Hydraulics

One dominant groundwater inflow section was identified at 60–63.5 m ($T = 7.87 \times 10^{-5}$ m^2s^{-1}); below 63 m flow into the borehole was below the limit of measurement. See /Ludvigson et al. 2003b/ for further details.

Chemistry

Groundwater samples for Class 3 analysis were collected from 30.0–221.7 m (sequence of 3 samples on 2002-12-10); this was carried out 3 days after borehole completion. Major ion chemistry and isotopic signatures differed little between the samples except for a small systematic increase in salinity (72–82 mg/L Cl) and decrease in tritium during the sampling period. The groundwater is therefore dilute, recent to modern in age (~ 70 pmC; ~ 12 TU) and near-surface meteoric in origin. Charge balance is acceptable. See /Nilsson, 2003b/ for further details.

Representativeness

Because of the small but significant change in groundwater chemistry during the sampling sequence, the first sample collected is considered to best represent 'undisturbed' in-situ groundwater conditions. This is in agreement with /Nilsson, 2003b/.

3.2.6 Borehole HFM05

Borehole HFM05 inclined at approx. 5° to the vertical was drilled to 200.10 m (cased to 12 m) at the DS2 site with the primary purpose of providing flushing water to drill borehole KFM02A and for groundwater monitoring and hydrochemical characterisation. Drilling of HFM05 was completed in 2002-12-16.

Hydraulics

One dominant groundwater inflow section was identified at 150.5–156.5 m ($T = 3.96 \times 10^{-4}$ m^2s^{-1}); below 156 m flow into the borehole was below the limit of measurement. See /Ludvigson et al. 2003b/ for further details.

Chemistry

Groundwater samples for Class 3 analysis were collected from 25–200 m (sequence of 3 samples on 2002-12-19); this was carried out 3 days after borehole completion. At a later stage a single sample was taken from 0–200 m on 2003-08-20. Major ion chemistry and isotopic signatures of the first 3 groundwaters differed little. Furthermore, there was no marked difference between the sample collected some 9 months later although slightly less salinity and significant tritium (2.2 TU) indicates some contamination/mixing of a younger, shallower groundwater component. The dominant groundwater is brackish (~ 4,500 mg/L Cl), old (22–25 pmC) and originates from a mixture of meteoric and older brackish groundwaters (Littorina signature?); tritium was below detection (< 0.8 TU). Charge balance is acceptable. See /Nilsson, 2003b/ for further details.

Representativeness

Because of the small but significant change in groundwater chemistry during the sampling sequence, the first sample collected is considered to best represent 'undisturbed' in-situ groundwater conditions. This is in agreement with /Nilsson, 2003b/.

3.2.7 Borehole HFM06

Borehole HFM06 inclined at approx. 5.5° to the vertical was drilled to 110.7 m (cased to 12 m) at the DS3 site with the primary purpose of providing flushing water to drill borehole KFM03A and for groundwater monitoring and hydrochemical characterisation. Drilling of HFM06 was completed in 2003-01-14.

Hydraulics

Four groundwater inflow sections were identified at 20.5–23.0 m ($T = 5.0 \times 10^{-5}$ m^2s^{-1}), 42.5–44.0 m ($T = 5.3 \times 10^{-5}$ m^2s^{-1}), 60–64 m ($T = 4.4 \times 10^{-5}$ m^2s^{-1}) and 69–71 m ($T = 1.8 \times 10^{-4}$ m^2s^{-1}); below 71 m flow into the borehole was below the limit of measurement. See /Källgården et al. 2003/ for further details.

Chemistry

Groundwater samples for Class 3 analysis were collected from 0–111 m (sequence of 4 samples on 2003-01-21); this was carried out 7 days after borehole completion. Major ion chemistry shows an increase in salinity (476–1,108 mg/L Cl) and suggestion of an older water component (66–61 pmC) beginning to appear during the sampling period; tritium remained relatively stable. Generally the groundwater is of low salinity (~ 1,000 mg/L Cl), recent to modern (~ 65 pmC; ~ 5.5 TU) and originates from a mixture of modern meteoric and older brackish groundwaters. Charge balance is acceptable. See /Nilsson, 2003c/ for further details.

Representativeness

Because of the significant change in groundwater chemistry during the sampling sequence, and based on the flow log/electric conductivity log /Källgården et al. 2003/ the second sample from 42.5–44.0 m depth seems to represent the main groundwater input into the borehole and is therefore assumed to best represent 'undisturbed' in-situ groundwater conditions at this depth.

Note: This borehole appears to illustrate well the horizontal stratification of groundwater salinity over 111 m depth.

3.2.8 Borehole HFM07

Borehole HFM07 inclined at 5.5° to the vertical was drilled to 122.50 m (cased to 18 m) at the DS2 site with the primary purpose of groundwater monitoring and hydrochemical characterisation. Drilling was completed in 2003-01-28.

Hydraulics

Due to the minor groundwater inflow into HFM07 no hydraulic tests could be performed. See /Källgården et al. 2003/ for further details.

Chemistry

Due to the minor groundwater inflow into HFM07 no sampling could be carried out.

Representativeness

Absence of hydraulic and hydrochemical data.

3.2.9 Borehole HFM08

Borehole HFM06 inclined at approx, 5.5° to the vertical was drilled to 143.5 m (cased to 12 m) at the DS3 site with the primary purpose for groundwater monitoring and hydrochemical characterisation. Drilling of HFM08 was completed in 2003-02-12.

Hydraulics

Two groundwater inflow sections were identified at 89.5–90.0 m ($T = 5.7 \times 10^{-5}$ m^2s^{-1}) and 137.5–139.5 m ($T = 1.2 \times 10^{-3}$ m^2s^{-1}); below 139 m flow into the borehole was below the limit of measurement. See /Källgården et al. 2003/ for further details.

Chemistry

Groundwater samples for Class 3 analysis were collected from 0–93 m (1 sample on 2003-03-20) and 0–144 m (1 sample on 2003-02-18 and 1 on 2003-03-18); the first sampling was carried out 36 days after borehole completion. Major ion chemistry and isotopic signatures show an increase in salinity (2,694 vs 5,421 mg/L Cl) and decrease in tritium (1.2 TU vs below detection) when comparing the two sampled borehole lengths. This underlines the stratigraphic variation with depth of the groundwater chemistry represented by the 89.5–90.0 m inflow point and that from the deeper 137.5–139.5 m inflow point.

Length 0–90 m: Moderately saline (2,694 mg/L Cl) groundwater, old (~ 20 pmC) with a very small modern component (1.2 TU), and originates from a mixture of meteoric and older brackish groundwaters. Charge balance is acceptable.

Length 0–144 m: Brackish (~ 5,200 mg/L Cl), old (~ 20 pmC) and meteoric/saline in origin (Littorina signature?) with a tritium content under detection. There is a small increase in salinity between the two samplings which are one month apart. Charge balance is acceptable. See /Nilsson, 2003c/ for further details.

Representativeness

Because of the significant change in groundwater chemistry between the two borehole lengths, two compositions can be considered representative, each reflecting the two major inflow points into the borehole. The 0–90 m chemistry is assumed to best represent 'undisturbed' in-situ groundwater conditions down to 144 m. However, even though less favourable since it represents the mixing of both inflow points, the 0–144 m length has been included because of its importance of indicating a Littorina Sea signature.

Note: This borehole appears to illustrate well the horizontal stratification of groundwater salinity over 111 m depth.

3.2.10 Borehole HFM09

Borehole HFM09 at an inclination of approx. 20° to the vertical was drilled to 50.25 m (cased to 17.02 m) at the DS4 site with the purpose of groundwater flow monitoring and potentially for some structural evidence. Drilling was completed in 2003-06-30.

Hydraulics

Two groundwater inflow sections were identified at 22–29 m ($T = 3.26 \times 10^{-4}$ m^2s^{-1}) and 46.5–49 m ($T = 4.67 \times 10^{-5}$ m^2s^{-1}); below 46.5 m flow into the borehole was below the limit of measurement. See /Ludvigson et al. 2004d/ for further details.

Chemistry

Groundwater samples for Class 3 analysis were collected from 0–50 m (1 sample on 2003-08-13) and 17–50 m (sequence of 3 samples on 2004-02-18). Despite an interval of approx. 7 months from drilling to taking the first sample (2003-08-13) and a further approx. 6 months to taking the sequence of 3 samples (2004-02-18), the overall chemistry of the groundwaters varied little despite the different section sampled. The groundwater is typically dilute (160–190 mg/L), recent to modern (~ 60 pmC; ~ 10 TU) and near-surface meteoric in origin. Charge balance is acceptable. See /Nilsson, 2004/ for further details.

Representativeness

Although all four samples can be considered representative, the last sample in the sequence of 3 probably best represents 'undisturbed' in-situ groundwater conditions. This is in agreement with /Nilsson, 2004/.

3.2.11 Borehole HFM10

Borehole HFM10 at an inclination of approx. 22° to the vertical was drilled to 150.0 m (cased to 11.8 m) at the DS4 site with the purpose of providing flushing water to drill KFM04A and for groundwater flow monitoring. Drilling of HFM10 was completed in 2003-08-20.

Hydraulics

One groundwater inflow section was identified at 114.5–121 m ($T = 3.11 \times 10^{-4}$ m^2s^{-1}); below 117.5 m flow into the borehole was below the limit of measurement. See /Ludvigson et al. 2004d/ for further details.

Chemistry

Groundwater samples for Class 3 analysis were collected from 0–150 m (4 samples following drilling; 1 in 2003-08-21, 2 in 2003-09-18 and 1 in 2003-10-21) and later from 12–150 m (sequence of 3 samples in 2004-02-25). Despite an interval of approx. 4 months from taking the last of the initial 4 samples at 0–150 m and taking the later sequence of 3 samples at 12–150 m (2004-02-25),

the chemistry of the groundwaters varied little although a marginal increase in salinity is observed for the more recent sampling campaign. The groundwater is typically brackish (~ 5,000 mg/L Cl), recent (~ 35 pmC) with a small modern component (1.1–1.25 TU) and probably originates from a mixture of meteoric and older brackish groundwaters (Littorina signature?). Charge balance is acceptable. See /Nilsson, 2004/ for further details.

Representativeness

Although all seven samples can be considered representative, the first sample taken following drilling probably best represents 'undisturbed' in-situ groundwater conditions at that depth. The last sample selected was preferred by /Nilsson, 2004/.

3.2.12 Borehole HFM11

Borehole HFM11 at an inclination of approx. 41° to the vertical was drilled to 182.35 m (cased to 12 m) approx. 2 km south of the DS4 site with the purpose of providing hydraulic and hydrochemical information on the Eckarfjärd regional fracture zone /Ludvigson et al. 2004a; Claesson and Nilsson, P-04-106/. Drilling was completed in 2003-08-21.

Hydraulics

Six significant groundwater inflow points were identified: 37.7–38.7 m ($T = 7.27 \times 10^{-6}$ m^2s^{-1}), 40.7–43.7 m ($T = 1.521 \times 10^{-5}$ m^2s^{-1}), 108.2–110.2 m ($T = 1.03 \times 10^{-5}$ m^2s^{-1}), 135.7–136.7 m ($T = 2.91 \times 10^{-6}$ m^2s^{-1}), 141.2–143.7 m ($T = 1.02 \times 10^{-5}$ m^2s^{-1}) and 146.2–147.3 m ($T = 4.57 \times 10^{-6}$ m^2s^{-1}); below 146.2 m flow into the borehole was below the limit of measurement. These high transmissive zones are narrow (1–3 m). See /Ludvigson et al. 2004a/ for further details.

Chemistry

Groundwater samples for Class 3 analysis were collected from 0–182 m (sequence of 3 samples in 2003-10-02); this was carried out 2 months following completion of drilling. The chemistry of the groundwaters showed a significant increase in salinity between the first and second sampling (390–1,420 mg/L Cl) and a smaller increase during the third sampling (1,650 mg/l Cl), although the question remains whether this trend would have continued to increase with further pumping. The average groundwater therefore is of low salinity, contains a small modern component (2.5 TU) and probably originates from a mixture of modern meteoric and older brackish groundwaters. Charge balance is acceptable. No P-report available.

Representativeness

The final sample taken probably best represents 'undisturbed' in-situ groundwater conditions.

3.2.13 Borehole HFM12

Borehole HFM12 at an inclination of 41° was drilled to 209.50 m (cased to 14.9 m) at approx. 2 km south of the DS4 site with the purpose of providing hydraulic and hydrochemical information on the Eckarfjärd regional fracture zone /Ludvigson et al. 2004a; Claesson and Nilsson, P-04-106/. Drilling was completed in 2002-09-16.

Hydraulics

Two significant groundwater inflow points were identified: 110.2–111.2 m ($T = 1.36 \times 10^{-6}$ m^2s^{-1}) and 123.3–123.8 m ($T = 6.51 \times 10^{-6}$ m^2s^{-1}); below 123.2 m flow into the borehole was below the limit of measurement. These high transmissive zones are narrow (0.6–2.0 m). See /Ludvigson et al. 2004a/ for further details.

Chemistry

Groundwater samples for Class 3 analysis were collected from 0–210 m (sequence of 3 samples on 2003-09-26); this was carried out 10 days following completion of drilling. The chemistry of the groundwaters showed a slight decrease in salinity between the first and the subsequent two samplings (3,000–2,600 mg/L Cl); the last two samples show similar compositional ranges. Taking the second and third samples, the average groundwater is of low to moderate salinity, contains very little modern component (< 1.6 TU) and probably originates from a mixture of meteoric and older brackish groundwaters. Charge balance is acceptable. No P-report available.

Representativeness

The final sample taken probably best represents 'undisturbed' in-situ groundwater conditions.

3.2.14 Borehole HFM13

Borehole HFM13 at an inclination of approx. 31° to the vertical was drilled to 175.60 m (cased to 14.9 m) at the DS5 site with the purpose of providing hydraulic and hydrochemical information and lineament identification. Drilling was completed in 2003-10-02.

Hydraulics

Two significant groundwater inflow points were identified: 105.5–106.0 m ($T = 2.11 \times 10^{-5}$ m^2s^{-1}) and 162.5–163.5 m ($T = 2.91 \times 10^{-4}$ m^2s^{-1}); below 163 m flow into the borehole was below the limit of measurement. These high transmissive zones are narrow (1.0–1.5 m). See /Ludvigson et al. 2004c/ for further details.

Chemistry

Groundwater samples for Class 3 analysis were collected from 0–176 m (sequence of 3 samples in 2003-11-17); this was carried out 38 days following completion. A further sample was collected after approx. 3 months (2004-02-25) and one more 1 month later (2004-03-24). The chemistry of the first sequence of 3 samples show no significant variation; a small increase in salinity (2,500–3,800 mg/l Cl) and tritium (1.1–3.9 TU) is apparent after the lapse of 3–4 months before the next sampling. Taking the initial samples, the average groundwater is of low to moderate salinity (~ 2,500 mg/l Cl), contains an insignificant modern component (~ 1.0 TU) and probably originates from a mixture of meteoric and older brackish groundwaters. Charge balance is acceptable. No P-report available.

Representativeness

The initial 3 samples appear to be representative; the second sample has been chosen to represent 'undisturbed' in-situ groundwater conditions.

3.2.15 Borehole HFM14

Borehole HFM14 at an inclination of approx. 30° to the vertical was drilled to 150.50 m (cased to 3.1 m) at the DS5 site with the purpose of providing hydraulic and hydrochemical information. Drilling was completed in 2003-10-09.

Hydraulics

Due to cavities and fractures in the borehole the downhole equipment could not be utilised; no hydraulic data therefore are available. See /Ludvigson et al. 2004c/ for further details.

Chemistry

Groundwater samples for Class 3 analysis were collected from 0–151 m (sequence of 3 samples in 2003-11-05); this was carried out 33 days after borehole completion. The chemistry of the 3 samples shows a significant systematic decrease in salinity (887–545 mg/L Cl) and tritium (8.3 TU – below

detection) with time. The question is whether continued pumping would have produced an even more dilute sample. Taking the final sample, the average groundwater is of low salinity (545 mg/l Cl), contains no modern component (below detection TU) and probably originates from a mixture of meteoric and a component of older brackish groundwaters. Charge balance is acceptable. No P-report is available.

Representativeness

The last sample taken may (?) best represent 'undisturbed' in-situ groundwater conditions.

3.2.16 Borehole HFM15

Borehole HFM15 at an inclination of approx. 46° to the vertical was drilled to 99.50 m (cased to 6.0 m) at the DS5 site with the purpose of providing hydraulic and hydrochemical information and structural identification. Drilling was completed in 2003-10-15.

Hydraulics

Four significant groundwater inflow points were identified: 22.9–24.5 m ($T = 6.88 \times 10^{-5}$ m^2s^{-1}), 67–68.5 m ($T = 8.24 \times 10^{-5}$ m^2s^{-1}), 71.9–74.5 m ($T = 6.58 \times 10^{-5}$ m^2s^{-1}) and 88.0–89.0 m ($T = 1.024 \times 10^{-4}$ m^2s^{-1}); below 89 m flow into the borehole was below the limit of measurement. These high transmissive zones are narrow (0.5–1.0 m). See /Ludvigson et al. 2004c/ for further details.

Chemistry

Groundwater samples for Class 3 analysis were collected from 0–200 m (sequence of 3 samples in 2003-11-12); this was carried out approx. 1 month following borehole completion. The chemistry of the 3 samples shows a significant systematic increase in salinity (57–857 mg/L Cl) and decrease in tritium (3.3–1.9.8 TU) with time. The question is whether continued pumping would have produced an even more saline sample. Taking the final sample, the average groundwater is of low salinity (857 mg/l Cl), contains a small modern component (1.9 TU) and probably originates from a mixture of meteoric and older brackish groundwaters. Charge balance is acceptable. No P-report available.

Representativeness

The last sample taken may (?) best represent the 'undisturbed' in-situ groundwater conditions.

3.2.17 Borehole HFM16

Borehole HFM16 at an inclination of approx. 6° to the vertical was drilled to 132.50 m (cased to 6.0 m) at the DS6 site with the purpose of providing flushing water to drill KFM06A, for groundwater flow monitoring and to investigate a lineament north of the drilling site. Drilling of HFM16 was completed in 2003-11-11.

Hydraulics

Four significant groundwater inflow points were identified: 41.0–41.5 m ($T = 1.18 \times 10^{-4}$ m^2s^{-1}), 56.0–56.5 m ($T = 4.08 \times 10^{-5}$ m^2s^{-1}), 58.5–59.5 m ($T = 3.10 \times 10^{-4}$ m^2s^{-1}) and 69.0–69.5 m ($T = 5.724 \times 10^{-5}$ m^2s^{-1}); below 69 m flow into the borehole was below the limit of measurement. See /Ludvigson et al. 2004b/ for further details.

Chemistry

Groundwater samples for Class 3 analysis were collected from 0–133 m (sequence of 3 samples on 2003-11-12), this was carried out one day after borehole completion. The chemistry of the 3 samples shows a small increase in salinity between the first and second sampling; this appears to stabilise

with the third sampling. Taking the final sample, the average groundwater is dilute (~ 170 mg/l Cl), contains a modern component (5.6 TU) and is near-surface meteoric in origin. Charge balance is acceptable. No P-report is available.

Representativeness

The last sample has been taken to best represent the 'undisturbed' in-situ groundwater conditions.

3.2.18 Borehole HFM17

Borehole HFM17 at an inclination of approx. 6° to the vertical was drilled to 210.65 m (cased to 8.0 m) at the DS2/DS6 site with the purpose of providing hydraulic and hydrochemical information and lineament identification. Drilling was completed in 2003-12-08.

Hydraulics

One significant groundwater inflow point was identified at 30–32.5 m ($T = 3.93 \times 10^{-5}$ m^2s^{-1}); below 32 m flow into the borehole was below the limit of measurement. See /Ludvigson et al. 2004c/ for further details.

Chemistry

Groundwater samples for Class 3 analysis were collected from 0–203 m (sequence of 3 samples on 2003-12-05); this was carried out 3 days after borehole completion. The chemistry of the 3 samples shows no significant variation during the sampling period. The groundwater is dilute (~ 415 mg/l Cl), contains a modern component (7.8 TU) and is near-surface meteoric in origin. Charge balance is acceptable. No P-report is available.

Representativeness

All samples are representative; the first sample has been taken to represent the 'undisturbed' in-situ groundwater conditions as the analyses are more complete.

3.2.19 Borehole HFM18

Borehole HFM18 at an inclination of 31° to the vertical was drilled to 180.65 m (cased to 9.0 m) at the DS5 site with the purpose of providing hydraulic and hydrochemical information and lineament identification. Drilling was completed in 2003-12-16.

Hydraulics

Four significant groundwater inflow points were identified: 36.5–38.0 m ($T = 7.78 \times 10^{-5}$ m^2s^{-1}), 46.0–46.5 m ($T = 5.91 \times 10^{-5}$ m^2s^{-1}) and 48.0–48.5 m ($T = 2.49 \times 10^{-5}$ m^2s^{-1}); below 48 m flow into the borehole was below the limit of measurement. See /Ludvigson et al. 2004c/ for further details.

Chemistry

Groundwater samples for Class 3 analysis were collected from 0–173 m (sequence of 3 samples on 2004-02-10); this was carried out approx. 2 months after borehole completion. The chemistry of the 3 samples shows a small decrease in salinity between the first and second sampling; this appears to stabilise with the third sampling. Taking the final sample, the average groundwater is dilute (56.5 mg/l Cl), contains a modern component (5.1 TU) and is near-surface meteoric in origin. Charge balance is acceptable. No P-report is available.

Representativeness

The second and third samples are representative; the last sample has been taken to represent the 'undisturbed' in-situ groundwater conditions (NB. Use isotopic data from first sample as highlighted in the Table).

3.2.20 Borehole HFM19

Borehole HFM19 at an inclination of 32° to the vertical was drilled to 185.20 m (cased to 6.0 m) at the DS5 site with the purpose of providing hydraulic and hydrochemical information and lineament identification. Drilling was completed in 2003-12-18.

Hydraulics

Four significant groundwater inflow points were identified: 100–102 m ($T = 4.02 \times 10^{-5}$ m^2s^{-1}), 148–150 m ($T = 1.55 \times 10^{-5}$ m^2s^{-1}), 160–163 m ($T = 6.18 \times 10^{-6}$ m^2s^{-1}) and 170–182.5 m ($T = 2.75 \times 10^{-4}$ m^2s^{-1}); most of the inflow into the borehole occurs below 170 m. See /Ludvigson et al. 2004c/ for further details.

Chemistry

Groundwater samples for Class 3 analysis were collected from 0–173 m (sequence of 3 samples on 2004-02-03); this was carried out approx. 2.5 months after borehole completion. The chemistry of the 3 samples shows no significant variation during the sampling period. The groundwater is brackish (~ 4,900 mg/l Cl), contains no modern component (below detection TU) and probably originates from a mixture of meteoric and older brackish groundwaters (Littorina signature?). Charge balance is acceptable. No P-report available.

Representativeness

All samples are representative; the first sample has been taken to represent the 'undisturbed' in-situ groundwater conditions as the analyses are more complete.

3.3 Cored boreholes

3.3.1 Available data

Available data included:

- Borehole activity logs in various reports – *(KFM01; KFM02; KFM03; KFM04)*.
- Groundwater chemistry from open hole tube sampling – *(KFM02A; KFM03A; KFM04A)*.
- Groundwater chemistry from isolated borehole sections – *(KFM01A; KFM02A; KFM03A; KFM04A)*.
- Chemmac log data (pH, Eh, Temp., Dissolved oxygen) and electric conductivity are available for KFM01A, KFM02A, KFM03A and KFM04A.

3.3.2 Tube sampling

Open hole tube sampling was carried out and documented for boreholes KFM02A (P-03-95), KFM03A (P-03-96) and KFM04A (P-04-47).

Borehole KFM02A

Percussion borehole HFM05 (0–200.10 m; Section 2.6) is the source of flushing water for the drilling of KFM02A. The dominant groundwater is brackish (~ 4,500 mg/L Cl), old (22–25 pmC) and probably originates from a mixture of meteoric and older brackish groundwaters (Littorina

signature?); tritium was below detection (< 0.8 TU). This contrasts with the groundwaters collected from the percussion drilled part of KFM02A (18–100.4 m) which was dilute (~ 70 mg/L Cl), modern to recent (~ 11 TU; ~ 75 pmC) and near-surface meteoric in origin; the main source of the groundwater was from 79.5–81.5 m depth ($T = 3.98 \times 10^{-4}$ m^2s^{-1}; P-03-34).

Following characterisation of the KFM02A percussion borehole casing was installed to approx. 100 m thus cutting off the main source of groundwater inflow. Cored drilling of KFM02A commenced and when completed two attempts were made to clear the borehole from accumulated residual flushing water and groundwaters from various sources during drilling. Mammoth pumping was carried out following drilling (128 m^3) and just prior to the Tube Sampling (164 m^3).

In an open borehole situation, for example borehole KFM02A where hydraulic conductivities are mostly within the range of 10^{-9}–10^{-7} ms^{-1} and water-conducting fracture zones below 100 m are rare, the flushing water might be expected to dominate, especially at greater depths. This is especially true with KFM02A where most of the significant water producing fracture zones are located in the upper 400 m of the borehole (10^{-7}–10^{-6} ms^{-1}). This pattern was reflected by the Tube Sampling subsequently carried out despite the attempts to clean the borehole. /Wacker and Nilsson, 2003/ show high to very high flushing water contents along the complete borehole (35–79%) apart from the shallowest sample with 11%. Since this contamination did not improve significantly with further attempts to clean the borehole, it was concluded that these open hole tube samples should be disregarded from the hydrochemical evaluation and modelling.

Representativeness

No samples can be considered representative.

Borehole KFM03A

Percussion borehole HFM06 (0–110.7 m; Section 2.7) is the source of flushing water for the drilling of KFM03A. Generally the groundwater is of low salinity (~ 1,000 mg/L Cl), relatively recent to modern (~ 65 pmC; ~ 5.5 TU) and probably originates from a mixture of modern meteoric and older brackish groundwaters. Because of the low overall transmissivity of the borehole, retention of the flushing water might be expected.

The Tube Sampling carried out in borehole KFM03A has been described and discussed by /Wacker and Nilsson, 2003/. They found that in the first 300 m of the open hole the flushing water was low (5.5–8%) and dominated by brackish groundwater (~ 4,800 mg/L Cl). The deeper part (400–800 m) had high flushing water contents (16–53.5%) with slightly less salinity (3,710–5,000 mg/L Cl) to 700 m, before increasing to around 6,000 mg/L Cl and slightly lower flushing water content (44.5%) at 850 m. The deepest sample is characterised by low flushing water (9%) and only slightly higher salinity at 8,663 mg/L Cl. Tritium values are widely variable with the deepest sample indicating below detection (< 0.8 TU) and the shallowest sample at 0–46 m indicating the highest value of 41 TU (fall-out influence?). From 100–300 m the Cl and Mg contents suggest a Littorina Sea signature, and from 900–1,000 m a deep saline (probably non-marine) component is present.

Representativeness

Because of the obvious mixing of groundwaters from different origins (flushing water, brackish and deep saline) none of the analysed samples can be considered representative.

Borehole KFM04A

Percussion borehole HFM10 (0–150 m; Section 2.11) is the source of flushing water for the drilling of KFM04A. The groundwater is typically brackish (~ 5,000 mg/L Cl), recent (~ 35 pmC) with a small modern component (1.1–1.25 TU) and probably originates from a mixture of meteoric and older brackish groundwaters (Littorina signature?). Because of the low overall transmissivity of the borehole, retention of the flushing water might be expected.

The Tube Sampling carried out in borehole KFM04A has been described and discussed by /Berg and Nilsson, 2004/. They found a general increase in flushing water from 10% in the near-surface sample, to 40% at 500 m and 53% close to 1,000 m depth. Because of the high flushing water content, from 300–1,000 m the major ion data are incomplete and no isotopic data are available. The interesting feature is the uniformity of the salinity along the borehole (in contrast to KFM03A for example) ranging from 4,690–5,410 mg/L Cl; the highest values occur from about 300–700 m with the deepest sample recording 5,170 mg/L Cl. Available isotopic data indicate tritium to be low to below detection (1.8–< 0.8 TU) and the single carbon isotope data point from 95–195 m indicates an old groundwater (22.5 pmC).

Representativeness

Because of the relative uniform chemistry along the borehole and its similarity in chemistry to the HFM10 flushing water, the indication is that: a) borehole KFM04A is dominated by flushing water, and/or b) borehole KFM04A is drilled into the same reservoir of formation water as pumped from HFM10. However, because of the obvious mixing of different groundwaters (even if comprising similar groundwaters from different locations), none of the analysed samples can be considered representative.

3.3.3 Isolated borehole sections

Groundwater samples from isolated borehole sections have been collected during drilling (where conditions allowed) and following borehole completion.

Borehole KFM01A

Borehole KFM01A was core drilled to 1,001.49 m at an inclination of 4.3° to the vertical. The first 100.52 m were percussion drilled and cased to 100.43 m. Relevant reports include: P-03-28, P-03-32, P-03-33, P-03-39, P-03-45, P-03-47 and P-03-94.

Downhole activity log

The downhole activity log for borehole KFM01A, relating to potential groundwater disturbances, is given below. Samples highlighted by red font were taken from predetermined borehole sections following borehole completion and the green font represents open hole Tube Sampling. During drilling some samples have been hoisted directly from borehole sections using the wireline (i.e. denoted by ‘wireline’). Some groundwater samples are referred to as ‘unclassified’, i.e. presumably not falling within the range of Class 1 to 5 in the analytical protocol.

Activity	Date	Comments
Percussion drilling	2002-05-07 to 2002-06-10	0–100.52
PLU pump tests	2002-05-24 to 2002-05-27	29.4–100.5 m
Water sampling	2002-05-25	Class 3 (29.40–100.57 m)
Radar/BIPS logging	2002-05-28	30.00–47.50 m (no BIPS possible)
Casing installed	2002-06-10	Cased to 100.43 m
Core drilling	2002-06-25 to 2002-10-28	100.52–1,001.49 m
Flow meter logging	2002-11-18 to 2002-11-30	100–1,000 m
BIPS logging	2002-12-11	100–1,000 m
Water sampling	2003-01-17 to 2003-02-24	Class 2–5 (110–120.77 m)
Colloid sampling	2003-02-25	110–121 m
Microbe sampling	2003-02-25	110–121 m
Water sampling	2003-03-27 to 2003-03-31	Class 4–5 (176.8–183.9 m)
Colloid sampling	2003-04-01 to 2003-04-07	176.8–183.9 m

Percussion borehole samples

Only one sample representing the percussion drilled section was collected; there are indications of a significant groundwater inflow to the borehole at 48–52 m depth. Based on details from the surrounding percussion boreholes HFM01, HFM02 and HFM03 described in Chapter 2, the groundwater sample from the percussion borehole probably represents a mixture of modern, dilute, near-surface derived groundwater and deeper more brackish and potentially older groundwaters.

Representativeness: Because of the mixing, the percussion borehole sample is not considered representative.

Samples collected during drilling

There is no record of samples collected during drilling because of the generally very small groundwater inflow to the borehole.

Samples collected following borehole completion

Two samples were collected from different borehole levels: 110–120.77 m and 176.8–183.9 m. A description of the hydrochemistry is given in P-03-94 and a detailed evaluation of the representativeness of groundwaters from borehole section 110–120.77 m is presented by Smellie and Tullborg (Forsmark v.1.1; ProjectPlace).

Borehole section: 110–120.77 m

As mentioned this section has already been evaluated and reported in Smellie and Tullborg (Forsmark v. 1.1, ProjectPlace).

Representativeness: Although the majority of the samples can be considered representative, the final sample in the series of groundwaters collected has been chosen because of more complete analytical data.

Borehole section: 176.8–183.9 m

A series of 10 samples were collected over a period of 32 days from section 176.8–183.9 m which has a transmissivity of around 10^{-8} m^2s^{-1}, compared to a background value of around 10^{-10} m^2s^{-1} (P-03-28). Due to the high flushing water pressure during drilling, and based on similar hydraulic considerations discussed for section 110–127.77 m, flushing water might be expected to have accumulated within section 176.8–183.9 m and consequently a component may be expected in the sampled groundwaters. The analytical data indicate some 17.84% flushing water for the first sample; this was reduced to 7.26% some 4 days later when the second sample was collected. For the rest of the sampling series the flushing water decreased to around 5% and remained at this level until the final groundwater was sampled.

The Chemmac monitoring data (pH, dissolved oxygen and redox potential measurements), and surface electric conductivity measurements, when stabilised after the initial stages, showed excellent consistency during the remainder of the sampling period. This has enabled the evaluation of reliable values for these parameters to be used in the modelling exercises: Electric Conductivity (1,548±20 mSm^{-1}), pH-surface (7.41±0.25), pH-borehole (7.41±0.18), Eh-borehole (–188±16 mV) and dissolved oxygen (0.00±0.01 mg/L) /Wacker et al. 2003/.

The analytical data are almost complete and generally indicate a consistent increase in salinity (5,044–5,335 mg/L) and relative age (18.53–16.68 pmC) during the sampling period. Since more saline groundwaters are known to exist at greater depths, these data therefore may indicate some hydraulic connection and thus the groundwaters collected may not be totally representative of the depth sampled. In general, the groundwaters brackish (~ 5,200 mg/L Cl), old (~ 18 pmC) and probably originates from a mixture of meteoric and older brackish groundwaters (Littorina signature?); tritium was below detection (< 0.8 TU) for all but for two samples (1.3–1.5 TU). The charge balance is acceptable.

***Representativeness**:* Because of the persistent flushing water component (~ 5%) and the small gradual increase in salinity with sampling time, caution should be exercised when using these data. The composition of the flushing water is dilute (500–600 mg/L Cl) and recent to modern when compared to the sampled groundwaters (see Section 2.2 and borehole HFM01). The final groundwater taken has been chosen as being representative because of more complete analytical data.

Borehole KFM02A

Borehole KFM02A was core drilled to 1,002.5 m depth at an inclination of 4.6° to the vertical. The first 100.40 m were percussion drilled and cased to approx. 100 m. Relevant reports include: P-03-34, P-03-48, P-03-53, P-03-95 and P-04-40.

Downhole activity log

The downhole activity log for borehole KFM02A, relating to potential groundwater disturbances, is given below. Samples highlighted by red font were taken from predetermined borehole sections following borehole completion and the green font represents open hole Tube Sampling. During drilling some samples have been hoisted directly from borehole sections using the wireline (i.e. denoted by 'wireline'). Some groundwater samples are referred to as 'unclassified', i.e. presumably not falling within the range of Class 1 to 5 in the analytical protocol.

Activity	Date	Comments
Percussion drilling	2002-11-20 to 2002-11-26	0–100.40 m
PLU pump tests	2002-11-29 to 2003-12-02	12–100.40 m
PLU pump tests	2002-11-29 to 2003-11-29	22–100.40 m
Water sampling	2002-11-29	Class 3 (18–100.4 m)
Geophysical logging	2002-12-03	0–100 m
Casing installed	2002-12-10	0–100 m
Core drilling	200?-??-?? to 2003-03-12	100–1,002.50 m
Water during drilling	2003-01-12	105–159 m (Wireline; unclassified)
Water during drilling	2003-01-27	250–290 m (Wireline, unclassified)
Water during drilling	2003-01-29	249–396 m (Wireline; unclassified)
BIPS logging	2003-02-13	101–635 m
Geophysical logging	2003-02-14	100–634 m
Tube sampling	2003-03-31	Class 3 (0–994 m)
BIPS logging	2003-04-15	101–999 m
Flow meter logging	2003-05-08	101–997 m
Water sampling	2003-06-04 to 2003-06-12	Class 2 (417–426 m)
Water sampling	2003-07-07 to 2003-08-24	Class 2 (505–520 m)
Water sampling	2003-06-13 to 2003-09-02	Class 2 (509.1–516.1 m)
Water sampling	2003-09-04 to 2003-10-20	Class 4–5 (509.1–516.1 m)
Water sampling	2003-10-24	Colloids (509.1–516.1 m)
Water sampling	2003-10-27	Microbes (509.1–516.1 m)
Water sampling	2003-11-07 to 2003-11-18	Class 4–5 (106.5–126.5 m)
Water sampling	2004-02-05 to 2004-02-23	Class 4–5 (413.5–433.5 m)

Percussion borehole samples

The upper percussion part of KFM02A was drilled to 100.40 m. As mentioned in Section 3.2.1, hydraulic tests showed a significant groundwater inflow to the borehole at 79.5–81.5 m ($T = 3.98 \times 10^{-4}$ m^2s^{-1}), a source which has probably dominated the groundwater sample taken from the open borehole for analysis. Two samples were collected on the same day from 18–100 m

(2002-11-29) and were typical of groundwaters of a dilute (~ 70 mg/L Cl), modern to recent (~ 11 TU; ~ 75 pmC) near-surface meteoric in origin. At a later stage, when cored drilling of KFM02A was completed and just prior to the Tube Sampling (2003-03-31), a groundwater sample from 0–100 m showed a more saline (3,256 mg/L Cl) chemistry more in common with the composition of the flushing water.

***Representativeness**:* Both samples can be considered representative; the second groundwater taken has been chosen because of more complete analytical data.

Samples collected during drilling

Three unclassified samples were collected by wireline during drilling: 105–159 m, 250–290 m and 249–396 m. The only data indicated are those quoted by /Wacker et al. 2004a/ which refer to the flushing water contents of 43%, 20% and 89% respectively.

***Representativeness**:* Although inadequate data available, the flushing water contamination exclude these samples as being representative.

Samples collected following borehole completion

Sampling centred on three main locations identified during drilling and confirmed from the Flow Meter log (P-report P-03-84 not yet available on the Web): 106.5–126.5 m, 417–426/413.5–433.5 m and 505–520/509–516.6 m. A description of the sampling and hydrochemistry is given by /Wacker et al. 2004a/.

Borehole section: 106.5–126.5 m

Section 106.5–126.5 m has a transmissivity of 1.1×10^{-4} m^2s^{-1} (optimal value in the near-vicinity of 10^{-6} m^2s^{-1}) and a series of three samples were collected over a period of 11 days. No flushing contents are quoted for this section in the SICADA Table but /Wacker et al. 2004a/ refer to this section being within the upper limit of 1%.

The Chemmac monitoring for Eh never quite stabilised and showed a small, but consistent increase with time when the groundwater samples were being collected; this casts some doubt as to whether stable values were, or would have been achieved. No electric conductivity or dissolved oxygen data were available due to equipment malfunctions.

The chemical analyses indicate a groundwater of low salinity (~ 600 mg/L Cl), recent (64.5 pmC) and near-surface and meteoric in origin; tritium was below detection (< 0.8 TU). The charge balance is acceptable. Although only a time series of 3 samples are available, there is a small but significant increase in salinity over the 11 day period. More saline groundwaters are known to exist at greater depths and the data therefore may indicate some hydraulic connection.

***Representativeness**:* The recorded changes in groundwater chemistry, although real, do not exclude the groundwaters from being considered generally representative of the depth sampled. Similar dilute chemistries have been documented from shallow bedrock depths in the area. The final groundwater taken has been chosen because of more complete analytical data.

Borehole section: 413.5–433.5 m

This borehole section was initially sampled approx. 8 months earlier (see activity log: section 417–426 m), but was only subject to a Class 2 analytical protocol since the flushing water contents were steady at approx. 35% over an 8 day sampling period. Consequently only the later sampling will be referred to below.

Section 413.5–433.5 m has a transmissivity of 2.7×10^{-6} m^2s^{-1} and a series of 3 samples were collected over a period of 18 days. Flushing water contents for this period exceeded the upper 1% limit ranging from 3.27–2.18%, although decreasing with sampling time.

No Chemmac and other probe monitoring data are available because of equipment malfunction.

The groundwater analytical data are incomplete for the three samples collected in series over the 18 day period. The general groundwater is brackish (~ 5,400 mg/L Cl), probably old (no pmC data but in common with other similar groundwaters) and of a saline/meteoric origin (Littorina signature?); tritium was below detection (< 0.8 TU). The charge balance is acceptable. Insufficient time series data are available, but there is no suggestion from the major ion chemistry of any consistent fluctuation with time.

***Representativeness**:* Despite the slightly over limit content of flushing water, these groundwaters are considered representative for the depth sampled. The presence of flushing water is not a concern since the composition of the groundwaters from this section is almost similar (only somewhat more saline) to that of the flushing water itself (see Section 2.6 and borehole HFM05). The final groundwater taken has been chosen because of more complete analytical data.

Borehole section: 509.1–516.1 m

This borehole section was sampled at different occasions, at different positions, for different time periods and for different analytical Class protocols. The borehole activity log separates:

- Class 2 analyses (section at 505–520 m: sampled 2003-07-07 to 2003-08-24).
- Class 2 analyses (section at 519.1–516.1 m: sampled 2003-07-07 to 2003-09-02).
- Class 4/5 analyses (section at 519.1–516.1 m: sampled 2003-09-04 to 2003-10-20).

The Class 2 analytical protocol for section 505–520 m appears to be devoid of any groundwater analytical data in the SICADA Table. The Class 2 protocol for section 519.1–516.1 m appears to be restricted to pH (surface Chemmac), electric conductivity and the downhole Chemmac monitoring data on pH, Eh, dissolved oxygen and temperature.

The Class 4/5 analytical protocol provides almost complete data relating to section 509.1–516.1 m. This section has a transmissivity of 3.9×10^{-6} m^2s^{-1} (optimum range 10^{-8}–10^{-6} m^2s^{-1}) and a series of 11 samples were collected over a period of 36 days.

The collected groundwaters show a uniform level of flushing water contamination (variation of 5.78–7.49%) over the sampling period, significantly exceeding the upper limit of 1%.

Chemmac monitoring data (pH, Eh, Dissolved oxygen and Temperature) and electric conductivity are available from 2003-09-01 to 2003-10-21. From 2003-10-17 to 2003-10-21 the readings were stabilised enough to be used to evaluate ‘representative’ values to be used in the modelling exercises /Wacker et al. 2004a/: El. Cond. (1,613±20 mSm), pH-surface (6.93±0.24), pH-borehole (6.83±0.15), Eh-borehole (–143±30 mV) and dissolved oxygen (0.01±0.01 mg/L).

The analytical data are almost complete and indicate a brackish groundwater (~ 5,400 mg/L Cl), old (15.8 pmC) and of a saline/meteoric origin (Littorina signature?); tritium was below detection (< 0.8 TU) apart from the final sample which had 2.4 TU. The charge balance is acceptable. There is no suggestion from the major and trace ion chemistry of any consistent variation with time. The main difference between this groundwater and that from section 413.5–433.5 m is a slightly higher mineralisation (TDS) for most of the major and trace ion chemistry; however chloride remains at similar levels.

***Representativeness**:* Low levels of flushing water contamination are a concern. However, as mentioned for section 413.5–433.5 m the composition of the groundwaters is similar (only somewhat more mineralised) to that of the flushing water itself (see Section 2.6 and borehole HFM05), and the contaminating effect therefore may not be so detrimental. Consequently, with caution, the final groundwater taken has been chosen to be ‘representative’ because of more complete analytical data even though a small modern component (2.4 TU) has been detected in this sample.

Borehole KFM03A

Borehole KFM03A was core drilled to 1,001.9 m depth at an inclination of 4.2° to the vertical. The first 100 m were percussion drilled and cased to approx. 100 m. Relevant reports include: P-03-12, P-03-36, P-04-41 and P-04-108 (not yet on the Web).

Downhole activity log

The downhole activity log for borehole KFM03A, relating to potential groundwater disturbances, is given below. Samples highlighted by red font were taken from predetermined borehole sections following borehole completion and the green font represents open hole Tube Sampling. During drilling some samples have been hoisted directly from borehole sections using the wireline (i.e. denoted by 'wireline').

Percussion borehole samples

The upper percussion part of KFM03A was drilled to 100.34 m. No hydraulic tests were conducted because of very low groundwater yields (P-03-36) and, therefore, no groundwater samples were taken. Evidence from the Tube Sampling (see Section 3.2.2) infers a brackish water type at the shallowest levels with excessively high tritium.

***Representativeness**:* No samples to evaluate.

Activity	Date	Comments
Percussion drilling	2003-03-24 to 2003-03-28	0–100.34 m
Casing installed	2003-03-25	1–12 m
BIPS logging	2003-03-26	0–100 m
Core drilling	200?-??-?? to 2003-06-23	100.34–1,001.19 m
Water during drilling	2003-05-06	347–394 m (Wireline; Class 3)
Mammoth pumping	2003-06-23	0–1,001.19 m
Tube sampling	2003-06-30	Class 3 (101–994 m)
BIPS logging	2003-08-03	101–999.5 m
Flow meter logging	2003-08-26	101–1,001.9 m
BIPS logging	2003-09-01	101–981.7 m
Water sampling	2003-09-16 to 2003-10-06	Class 4–5 (386–391)
Water sampling	2003-10-17 to 2003-10-24	Class 4–5 (448–453 m)
Water sampling	2003-11-06 to 2003-12-03	Class 4–5 (980–1,001 m)
Microbe/Colloid/Gas	2003-12-08	980.00–1,001.19 m
Water sampling	2004-02-04 to 2004-02-23	Class 2–5 (639–646 m)
Colloid sampling	2004-02-23	939.50–946.62 m
Microbe/Gas sampling	2004-02-23	939.50–946.62 m
Water sampling	2004-04-15 to 2004-04-27	Class 5 (448–456 m)
Colloid sampling	2004-04-27	448.50–455.62 m
Microbe/Gas sampling	2004-04-28	448.50–455.62 m

Samples collected during drilling

Only one sample was collected.

Borehole section: 347–394 m

One sample was collected during drilling, at 347–394 m, and registered 9.5% flushing water content; in contrast tritium was below detection (< 0.8 TU). For confirmation, a further sample from the same location was collected 55 days later and this is described below in section 3.3.3.4.

***Representativeness**:* Taking into consideration the duplicate sample discussed in section 3.3.3.4, this sample collected during drilling is probably more representative. However, the lack of a time series of samples for comparison plus the significant flushing water content render this sample as doubtful.

Samples collected following borehole completion

Borehole section: 346–396 m

A single duplicate sample was collected from the same section. Compared to the initial sample (described above) this duplicate sample had a lower salinity and a substantial tritium content (10 TU) after a lapse of 55 days. The indication is that a modern, near-surface derived water has entered the fracture zone during the period between sampling, and mixed with existing water mixtures.

***Representativeness**:* Not considered representative.

Borehole section: 386–391 m

Section 386–391 m records transmissivities of 2×10^{-4}–3×10^{-4} m^2s^{-1} and sampled groundwaters show a range of flushing water content consistently under the upper limit of 1% for 4 samples over a period of 17 days. The charge balance is acceptable.

Due to malfunctioning, the Chemmac monitoring equipment could be used only to measure pH. Electric conductivity data are available which show excellent stability for the full period of measurement, i.e. 22 days.

The chemical analytical data for the 4 samples show stability over the sampling period. The groundwater sampled is brackish (~ 5,400 mg/L Cl), old (17.6 pmC) and probably originates from a mixture of meteoric and older brackish groundwaters (Littorina signature?); tritium was below detection (< 0.8 TU) except for the final sample at 2 TU. The charge balance is acceptable.

***Note*:** /Wacker et al. 2004b/ point out that the iron analyses showed low Fe(II) concentrations compared to the total iron. It is unlikely that these represent the Fe(III) concentrations of the groundwater due to the possibility of air entering the water sampling line causing oxidation of Fe(II) prior to, or at the time of sampling.

***Representativeness**:* Although all the samples can be considered representative, the final sample in the series of groundwaters collected has been chosen because of more complete analytical data.

Borehole sections: 448–453 and 448–455.6 m

This section has been sampled on two different occasions some 6 months apart and two samples were taken on each occasion. It has a transmissivity of 7×10^{-8} m^2s^{-1} and on both sampling periods the upper limit of 1% flushing water was not exceeded.

The Chemmac and other probe monitoring were carried out at the second sampling period and, although some equipment malfunctioning occurred, the measured parameters when stability was achieved indicated uniform values during sampling. These data have been evaluated to derive representative values for modelling purposes /Wacker et al. 2004b/. The following values have been presented: Electric conductivity 1,571±20 mSm), pH-surface (7.27±0.42), pH-borehole (7.29±0.14), Eh-surface (–176±10 mV) and dissolved oxygen (0.00±0.01 mg/L).

The chemical analytical data for both pairs of samples show close similarity despite a lapse of 6 months; a minor increase in TDS is observed in the second sampling. The groundwater sampled is brackish (~ 5,400 mg/L Cl), old (15.7 pmC) and probably originates from a mixture of meteoric and older brackish groundwaters (Littorina signature?); tritium was below detection (< 0.8 TU).

Note. /Wacker et al. 2004b/ point out that the iron analyses showed low Fe(II) concentrations compared to the total iron. It is unlikely that these represent the Fe(III) concentrations of the groundwater due to the possibility of air entering the water sampling line causing oxidation of Fe(II) prior to, or at the time of sampling.

Representativeness: Although all the samples can be considered representative, the second sample of the first two groundwaters collected has been chosen because of more complete analytical data.

Borehole section: 639–646 m

This section has a transmissivity of 2.5×10^{-6} m^2s^{-1} and a series of 6 groundwaters were sampled over a period of 19 days. During this time the flushing water content remained significant (4.35–5.05%) and constant.

The Chemmac and other probe monitoring showed a constant increase in electric conductivity and increase in negative redox potential during the initial sampling period, but stabilisation of the parameters was achieved prior to collection of the last three samples. After /Wacker et al. 2004b/ the following values have been derived for modelling purposes: Electric conductivity 1,529±20 mSm), pH-surface (7.48±0.32), pH-borehole (7.38±0.12), Eh-surface (–196±12 mV) and dissolved oxygen (0.00±0.01 mg/L).

The chemical analytical data reflect the monitoring data in that the final three samples show stable values. The groundwater is brackish (~ 5,440 mg/L Cl), probably old (no isotopic data but based on the shallower levels described) and probably originates from a mixture of meteoric and older brackish groundwaters; tritium is consistently below detection (< 0.8 TU). The charge balance is acceptable. The major difference between this water and the other brackish varieties described at higher levels is the lower contents of Mg (~ 53 vs ~ 220 mg/L), Na (~ 1,650 vs ~ 200 mg/L) and SO_4 (~ 195 vs ~ 480 mg/L), and a higher content of Ca (~ 1,440 vs ~ 950 mg/L). The first water sampled in the series had 199 mg/L Mg but this quickly fell to around 50 mg/L Mg in the second sample collected 2 days later; this probably indicated the removal of residual groundwater which had penetrated the fracture from higher levels. This may indicate that somewhere between the 450–650 m level exists the limit of the Littorina Sea component.

Representativeness*:* Apart from the significant flushing water component, the final three groundwater samples collected are representative for the depth sampled. Because of the dilute nature of the flushing water and the absence of tritium in the sampled groundwaters, these three samples are considered close to being representative but caution should be employed. The final sample has been highlighted.

Borehole section: 939.5–946.6 m

This section has a transmissivity of 3.3×10^{-7} m^2s^{-1} and a series of 8 groundwaters were collected over a time period 31 days. Flushing water contents were significant (9–13.3%) and constant throughout this period.

Chemmac and other probe monitoring data show a gradual increase in electric conductivity and negative redox potential with time and stabilisation is never quite achieved. Despite this, /Wacker et al. 2004b/ have derived useful representative values for modelling purposes: Electric conductivity 2,205±20 mSm), pH-surface (7.53±0.12), pH-borehole (7.32±0.15), Eh-surface (–245±12 mV) and dissolved oxygen (0.00±0.01 mg/L).

The chemical analytical data reflect the monitoring trends with, for example, an increase in salinity from 7,560–8,560 mg/L Cl and corresponding decrease in Mg (37.3–17.9 mg/L) during the sampling period. The data indicate that an increasingly deep saline component is characterising the bedrock system which is reflected from the Tube Sampling (see Section 3.2.2). Generally, the groundwater is highly saline, presumably old (no isotopic data available) and is probably not marine or meteoric in origin (no isotopic data available). The charge balance is acceptable.

Representativeness*:* The presence of significant flushing water, the instability of the chemical parameters during the sampling period (suggesting hydraulic connection with deeper levels) and the absence of isotopic data render this groundwater only of qualtitative use and should be treated with caution. No highlight has been made.

Borehole section: 980–1,001.2 m

This section has a transmissivity of 3.1×10^{-7} m^2s^{-1} and a series of 8 groundwaters were collected over a time period of 32 days. Flushing water contents were low but exceeded the upper limit if 1%; interestingly a gradual increase from 1.25% to 3.85% occurred throughout this sampling period suggesting a hydraulic connection with a source of contaminated groundwater.

The Chemmac and other probe monitoring data showed, during a period of 19 days, relative electric conductivity stability (2,600–2,553 mSm) although it was decreasing with time, and an absence of redox potential stability which showed increasingly negative values. This contributed to the rejection of the Chemmac pH and Eh measurements by /Wacker et al. 2004b/ who limited their evaluation parameters to Electric conductivity 2,547±20 mSm), pH-surface (7.97±0.46) and dissolved oxygen (0.00±0.01 mg/L).

The chemical analytical data support the change in monitoring parameters with sampling time by indicating a decrease in salinity from 10,000–9,690 mg/L Cl. The groundwaters are generally highly saline, presumably old (no isotopic data available) and not marine or meteoric in origin; tritium was consistently below detection (< 0.8 TU). The charge balance is acceptable.

***Representativeness**:* Low levels of flushing water, relative stability of major parameters and the fact that it is from the deepest level, make this groundwater important in the overall hydrochemical evaluation. Unfortunately the isotopic data are incomplete. The final sample has been highlighted because of more complete data.

Borehole KFM04A

Borehole KFM04A was core drilled to 1,001.42 m at an inclination of 40° to the vertical. The first 107.42 m were percussion drilled and cased to its full length. Relevant reports include: P-04-47 and P-04-67.

Downhole activity log

The downhole activity log for borehole KFM04A, relating to potential groundwater disturbances, is given below. Samples highlighted by red font were taken from predetermined borehole sections following borehole completion and the green font represents open hole Tube Sampling.

Activity	Date	Comments
Percussion drilling	2003-0?-?? to 2003-05-27	0–107.42
BIPS logging	2003-06-02	0–100 m
Casing installed	2003-06-10	Cased to 100.43 m
Core drilling	2003-0?-?? to 2003-11-19	107.42–1,001.42 m
Mammonth Pumping	2003-??-??	100–1,000 m
BIPS logging	2003-12-05	100–1,000 m
Radar logging	2003-12-07	101–999.6 m
Tube Sampling	2003-12-08	100–1,000 m
Water sampling	2004-01-16 to 2004-02-12	Class 5 (231–238 m)
BIPS logging	2004-03-09	100–1,000 m
Water sampling	2004-04-20 to 2004-05-10	Class 5 (354–361 m)
BIPS logging	2004-05-12	100–1,000 m

Percussion borehole samples

The upper percussion part of KFM04A was drilled to 107.42 m. No hydraulic tests are reported and no groundwater samples were taken probably because of very low groundwater yields. Evidence from the Tube Sampling (see Section 3.2.3) infers a brackish water type at the shallowest level sampled (0–45 m) with a small tritium content (1.8 TU) and a flushing water content of 9.09%.

***Representativeness**:* No samples were available.

Samples collected during drilling

Borehole section: 231–238 m

No hydraulic information is available. A series of 7 samples were collected over a period of 27 days. Flushing water contents ranged from 11.50–7.05% with the first 3 samples collected ranging from 11.5–10.7% and the second 4 samples from 7.05–7.65%.

No Chemmac or other probe monitoring data are available prior to sampling; surface pH and electric conductivity data are available only during sampling.

The chemical analytical data indicate a slight but consistent increase in salinity during the 27 days of sampling (5,480–5,680 mg/L Cl); tritium is at or below the detection limit. The groundwater is typically brackish (~ 5,500), old (no isotopic data available but based on Tube sample 95–145 m with 22.5 pmC and section 354–361 described below) with no modern component (< 0.8 TU) and probably originates from a mixture of meteoric and older brackish groundwaters (Littorina signature?).

***Representativeness**:* The slight increase in salinity may suggest a continuous removal of flushing water from the isolated fracture zone and/or a weak hydraulic connection with a deeper, more saline groundwater source. There is virtually no difference in major chemistry (and tritium levels) between the flushing water from HFM10 (see Section 2.11) and that sampled from section 231–238 m. There is, therefore, the strong possibility that the same groundwater source has been sampled on both occasions; HFM10 is located only some 100 m from KFM04A.

The highlighted sample was chosen for the most complete analytical data.

Borehole section: 354–361 m

No hydraulic information is available. A series of 4 samples were collected over a period of 20 days. Flushing water contents ranged from 6.15–7.15%.

No Chemmac or other probe monitoring data are available prior to sampling; surface pH and electric conductivity data are available only during sampling.

The chemical analytical data indicate a slight increase in salinity during sampling but his appears to have stabilised for the last two samples, although a greater number of samples would be required to confirm this. The groundwater is typically brackish (~ 5,700), old (26.5 pmC) with no modern component (1–< 0.8 TU) and probably originates from a mixture of meteoric and older brackish groundwaters (Littorina signature?).

***Representativeness**:* Apart from a small increase in salinity and, for example, a decrease in Mg, there is an overall similarity with section 231–238 m and the HFM10 flushing water. The suggestion is, therefore, that at this level the major formation groundwater source is the same for all three sampling locations. The final sample collected was highlighted.

3.4 Shallow soil pipe samples

This involved 134 near-surface or ground water samples with the prefix ‘SFM’ collected from 42 borehole localities. The evaluation approach entailed the following approach.

Some of the soil pipes have been drilled in locations to monitor changes in the near-surface groundwater chemistry during percussion and core drilling of nearby deep boreholes. The remaining soil pipes have been located solely to monitor the natural undisturbed near-surface groundwater system. In both cases, however, it is important to select, if possible, the earliest (i.e. First-Strike’) uncontaminated samples collected because:

During nearby drilling operations the natural groundwater system may be disturbed, and

The natural groundwater system may show variations in groundwater chemistry due to perturbations such as periodic sampling of groundwater from the soil pipe which may deplete the surrounding sediments causing movement of other water types to fill the voids, and also seasonal variations.

The sampled shallow soil pipe waters were first screened by the filed personnel based on observations during drilling. Some of the initial samples collected were too contaminated by soil/ organic particles and these have been excluded. Of those samples remaining, an attempt has been made to select early or 'First-Strike' samples provided that there are adequate analytical data and that the charge balance is within the ± 5% range. The analytical data considered most important are the major ions and the environmental isotopes: tritium, ^{14}C (pmC), ^{18}O and deuterium. These parameters are also important for M3 calculations.

In addition, when a time-series of samples are available from a location and show no systematic variation in chemistry, the most suitable sample is selected with respect to analytical data. When only a single sample is available, this is chosen if the analytical data listed above are complete.

3.5 Shallow well groundwater samples

This involved 2 groundwater samples with the prefix 'PFM' collected from private well localities (PFM002942; PFM004778). These were not considered representative due to the possible mixing of groundwaters from different sources.

3.6 Baltic Sea water samples

There are a large number of samples collected over a period of approx. 11 months. These comprise samples ranging from the open Baltic Sea, to coastal areas comprising bays and coves, some of which border active freshwater drainage discharge areas of varying importance. From a hydrochemical viewpoint, the important criteria are:

- A representative Baltic Sea end-member for the Forsmark latitude which has not been influenced by freshwater discharge
- Representative compositions from coastal Baltic Sea localities which may be in hydraulic contact at depth with the mainland where deep boreholes are located.

Since presently there is inadequate data to select the second type of representative samples, the Baltic Sea Water samples selected in this evaluation relates to the end-member for use in the modelling and evaluation studies. The selected samples have been based on the charge balance (± 5%), chloride content within the range of 2,500–2,700 mg/L (i.e. based on an average of 2,600 mg/L Cl derived for the Forsmark Baltic Sea area after R-04-05) and complete environmental isotopes of tritium, ^{18}O, and deuterium.

3.7 Lake and stream water samples

These surface and near-surface water samples were evaluated based on charge balance (±10%), major ions and isotopic data. In common with the soil pipe groundwaters, these surface/near-surface waters are subject to seasonal fluctuations, complex processes in the biosphere and, for the Lake and Stream waters, potential discharge influences. Consequently, all selected samples are indicated in the database by green font indicating major ion and isotopic data and therefore of limited suitability.

3.8 Precipitation

Five samples are included from one locality; these were collected during a one year period from 2002-11-04 to 2003-11-03. These waters have not undergone any representativity check *senso stricto*. On the other hand, the main intention has been to monitor $\delta^{18}O$, δD and tritium, since these parameters are used to identify modern meteoric groundwater components at depth. Consequently, all the precipitation isotope data available are used for this purpose. Disturbances, such as unpredictable annual and seasonal trends and possible evaporation, have not been evaluated in this present representativity check.

4 Hydrogeochemical evaluation

4.1 General groundwater types and hydrochemical trends

The main groundwater groups characterising Forsmark are: a) shallow (< 200 m) Na-HCO_3 to Na-HCO_3(SO_4) to Na(Ca)-HCO_3 to Na(Ca)- HCO_3-Cl(SO_4) to Na(Ca)-Cl- SO_4(HCO_3) to Na(Ca, Mg)-Cl-SO_4(HCO_3) types, b) intermediate (approx. 200–600 m) Na(Ca, Mg)-Cl(SO_4) to Na-Ca(Mg)-Cl(SO_4) types, and c) deep (> 600 m) Na-Ca-Cl to Ca-Na-Cl types. The variation in compositions, especially in the upper 200 m of the bedrock, is due to local hydrodynamic flow conditions leading to mixing of varying proportions. Microbially mediated reactions are also important influencing both HCO_3 and SO_4, especially in the upper 600 m, as well as ion exchange reactions.

The Piper and Langelier Ludwig plots from the Forsmark site shown in Figure 4-1 emphasise distinct groupings representing: a) the deeper cored borehole groundwaters, b) the shallow cored borehole and percussion borehole groundwaters, and c) the Baltic Sea waters. There is an overall lack of distinction between the Lake and Stream waters and many of the shallow Soil

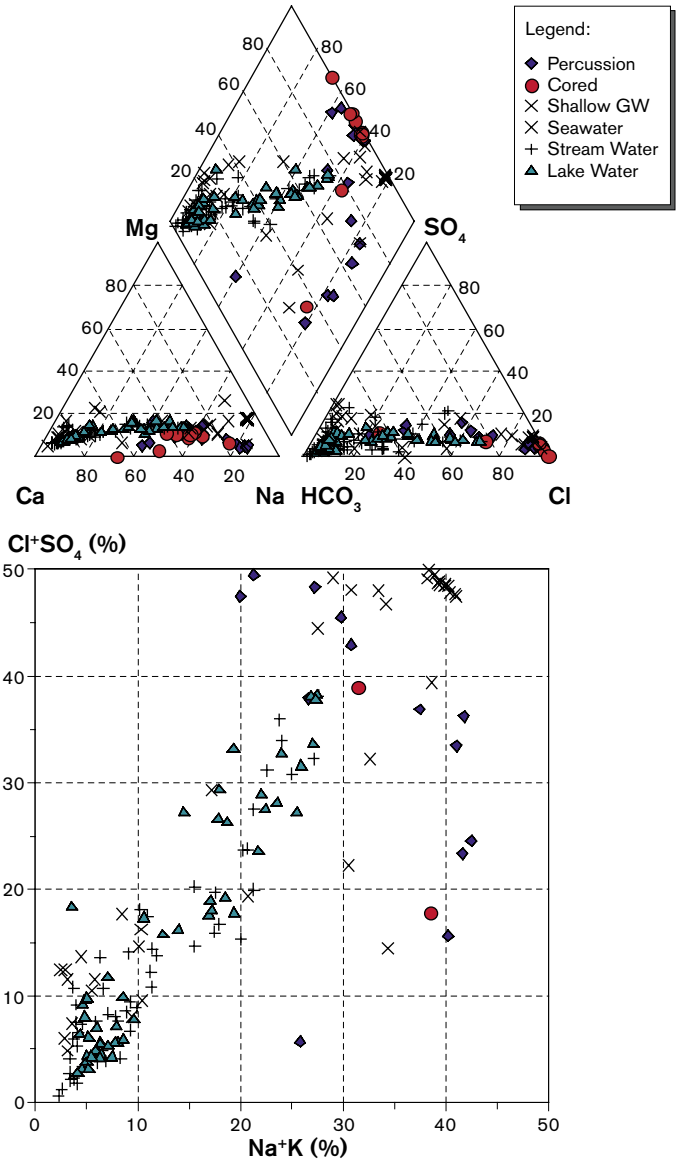

Figure 4-1. *Piper and Langelier Ludwig plots of surface, near-surface and groundwaters from Forsmark.*

Pipe groundwaters, although most represent more dilute water types. There is some overlapping (i.e. mixing trends) between the main Baltic Sea cluster and some of the percussion borehole groundwaters and, as mentioned above, widespread overlapping between the surface and near-surface Lake and Stream waters and some of the shallow Soil Pipe groundwaters.

4.2 Major ion and isotope plots for all Forsmark data and comparison with other Fennoscandian sites

The major ion and isotope contents of the groundwaters are initially described in relation to depth to establish the general stratification trends if present. Since chloride in groundwater systems is considered be conservative, plots of chloride with selected cations and isotopes are then used to help evaluate the major geochemical reaction and mixing processes which characterise the Forsmark site. When appropriate, the Forsmark data are compared to other Fennoscandian localities (i.e. Finnsjön, SFR, Simpevarp and Olkiluoto).

4.2.1 Hydrochemical depth trends

NOTE: Since the groundwaters collected from the percussion boreholes mostly represent the complete vertical borehole lengths, or at least long packed-off section lengths, the depths plotted refer to the maximum depths even though the major groundwater sources may be from shallower levels.

All Forsmark data

pH

The cored borehole groundwaters (Figure 4-2) show an initial decrease in pH (7.99–7.16 units) down to 238 m followed by a steady increase to 8.26 units at 1,000 m; exception is at 512 m in borehole KFM02A where the groundwater pH drops to 7.18 units. The shallow percussion borehole groundwaters (0–200 m) show a similarly wide range of pH as the cored boreholes (7.14–8.4 units) but no distinct trend with depth. However, in general, the overall data suggest more neutral pH at around 100–200 m depth with greater alkalinity at depths both shallower and deeper. In addition, the large variation in pH in the upper 100–200 m suggests groundwater mixing and/or water/rock reactions.

Sodium

Figure 4-3 shows that at shallow depths there is a large variation in sodium reflecting dilute to brackish groundwater types; this heterogeneity is shared by both the percussion and the cored borehole groundwaters and probably results from mixing and/or water/rock reactions of groundwaters, possibly from different sources. At greater depths, as shown by the cored borehole data, the sodium content varies little (1,740–2,110 mg/L) averaging 1,925 mg/L.

Potassium

In common with sodium, potassium (Figure 4-4) shows a wide range of values (5.6–67.8 mg/L) in the upper approx. 200 m of bedrock with higher values corresponding to depths at around 150–200 m. At greater depths the cored borehole groundwaters continue to show a variation to around 500 m (13.8–47.6 mg/L), after which there is a marked decrease to 6.9 mg/L K at 1,000 m.

Calcium

The distribution calcium (Figure 4-5) shows similar general features to sodium apart from a greater jump in concentration between approx. 500 m depth (~ 1,000 mg/L) and the deepest groundwater at 980–1,001 m (3,550 mg/L Ca).

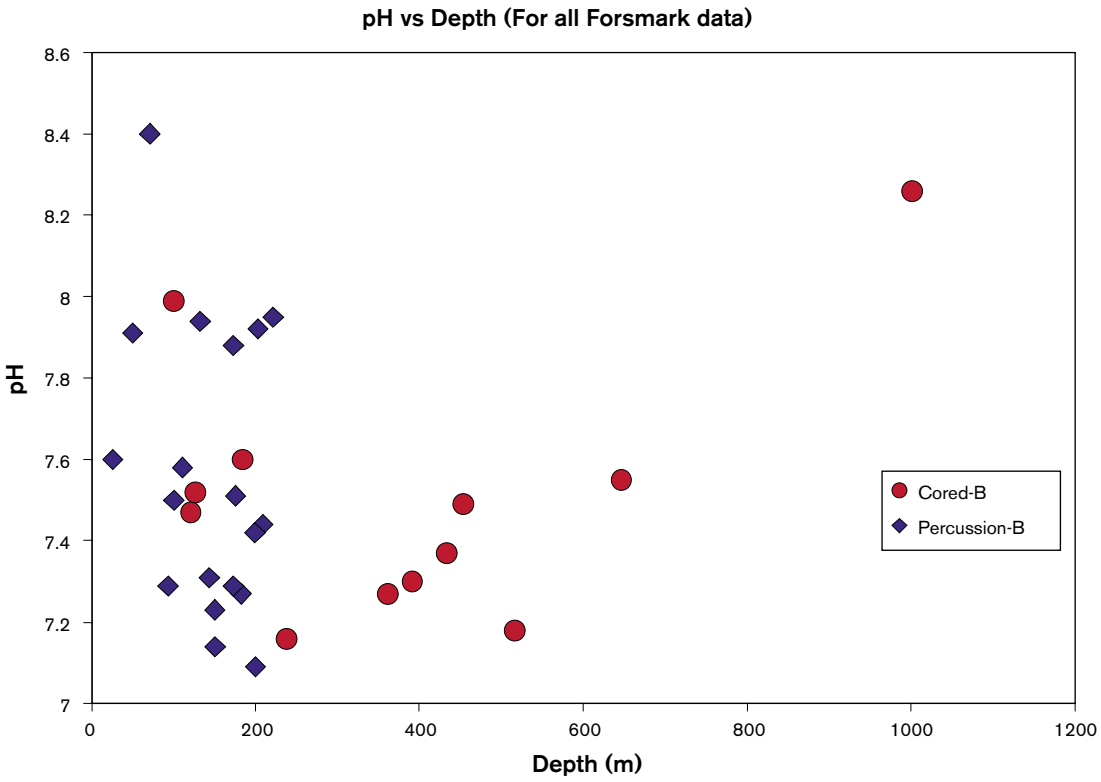

Figure 4-2. *Variation of pH with depth.*

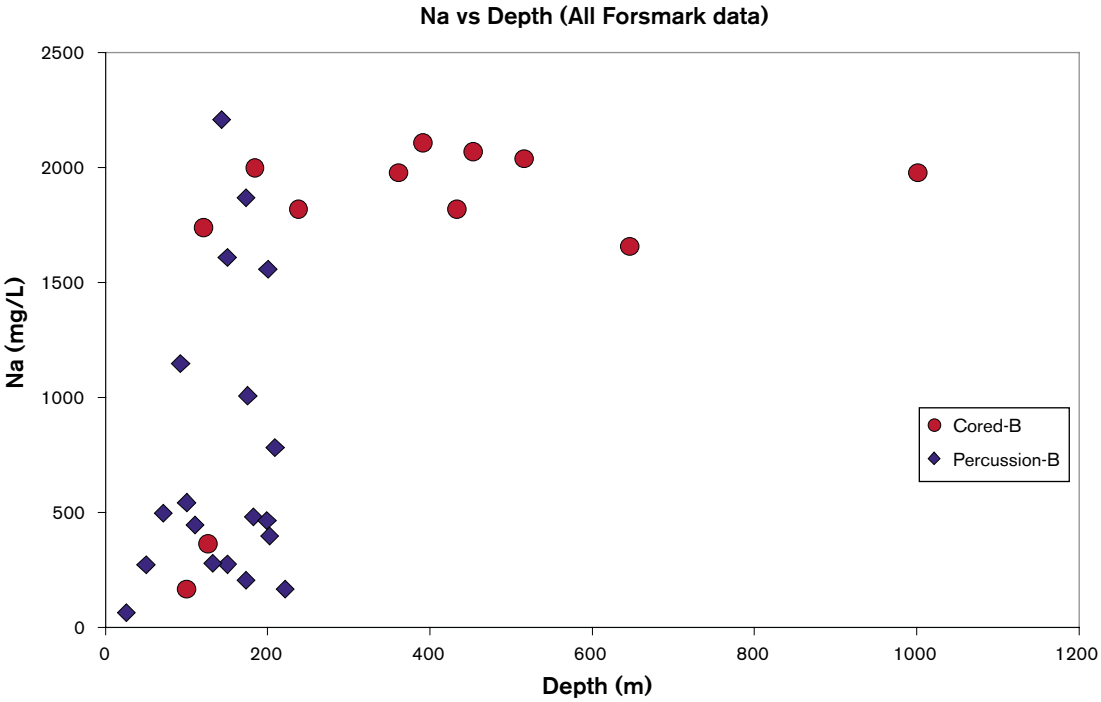

Figure 4-3. *Variation of Na with depth.*

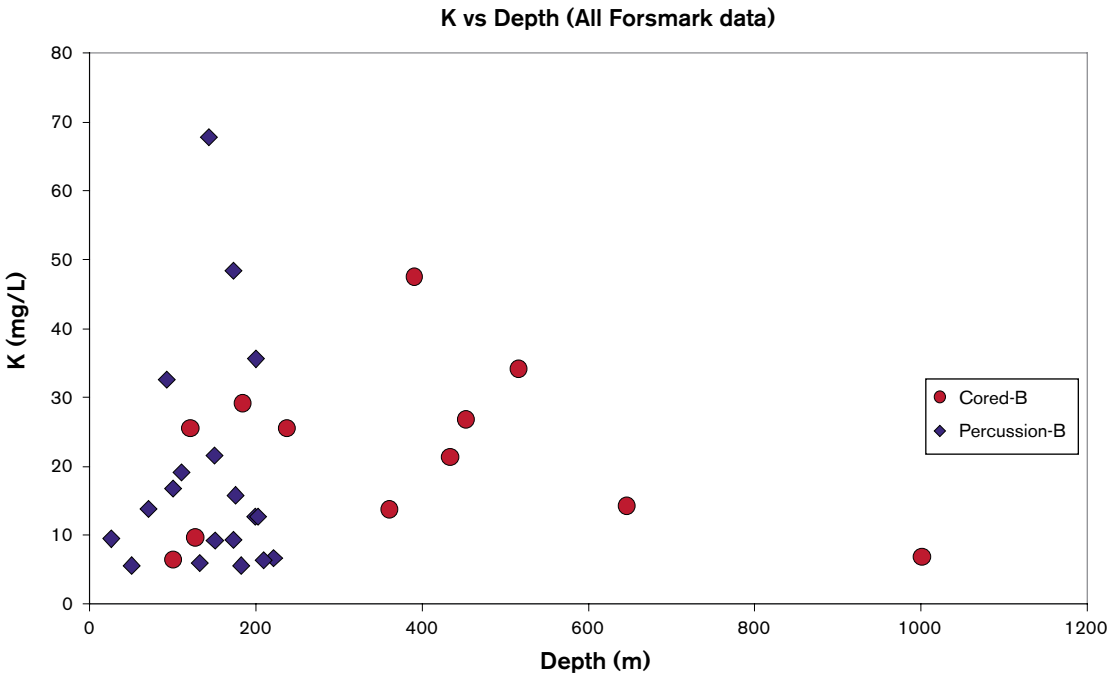

Figure 4-4. *Variation of K with depth.*

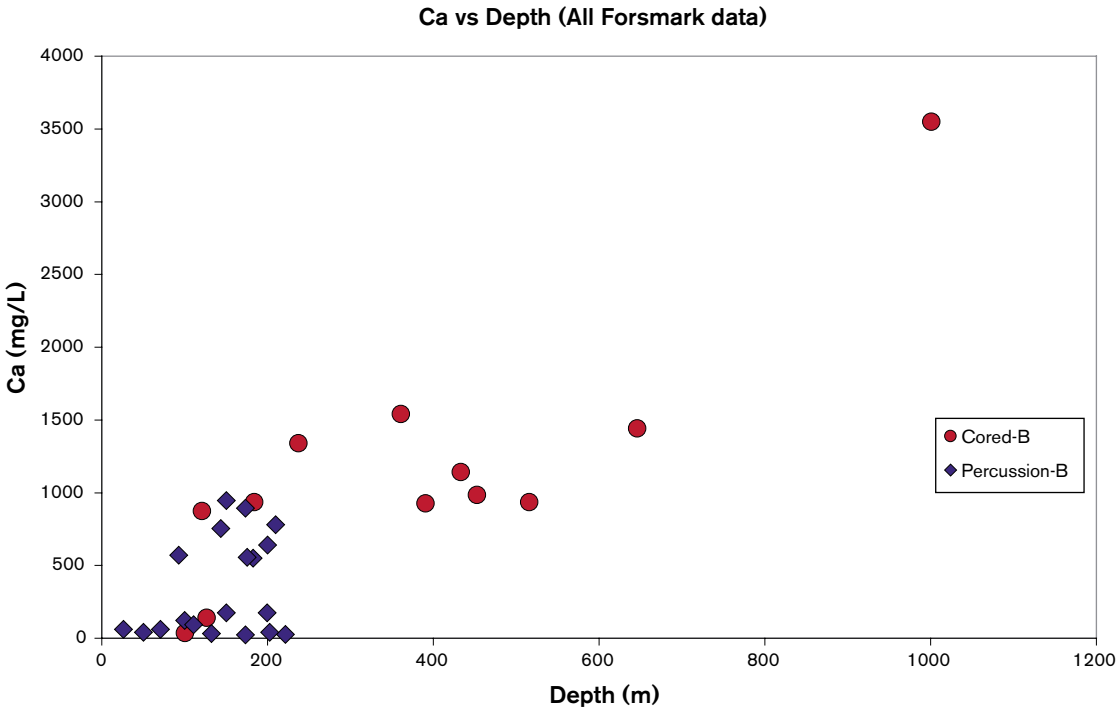

Figure 4-5. *Variation of Ca with depth.*

Magnesium

In the upper 200 m two general features are apparent (Figure 4-6); dilute groundwaters with less than 40 mg/L Mg, and a marked increase in magnesium (to a maximum of 287 mg/L) between approx. 150–200 m. At greater depths in the cored boreholes this magnesium increase continues between (165–234 mg/L) to approx. 500 m when a sharp decrease occurs to a value of 8.1 mg/L at 980–1,001 m. The enhanced magnesium between approx. 150–200 m indicates a marine component; possibilities include present Baltic Sea, old Baltic Sea and Littorina Sea. Higher values at 200–500 m restrict the possibilities to a Littorina Sea component with the added possibility of old Baltic Sea.

Bicarbonate

Figure 4-7 shows a large variation in bicarbonate (61–640 mg/L) in groundwaters prevailing at shallow depths. At increasing depth, to approx. 500 m, lower concentrations (78–125 mg/L HCO_3) persist. At even greater depths the bicarbonate content is consistently low (< 25 mg/L) and with only 6 mg/L recorded at 980–1,001 m.

Chloride

The distribution of chloride (Figure 4-8) clearly shows: a) mainly dilute (< 1,000 mg/L Cl) groundwaters dominating at shallow depths, b) a sharp increase to brackish groundwaters (~ 5,500 mg/L Cl) at around 100–200 m, c) the continuation of brackish groundwater to approx. 700 m, and d) an increase to saline groundwater with a maximum (9,690 mg/L Cl) at 980–1,001 m. Some exceptions occur when more brackish groundwaters exist closer to the surface (100–200). The uniform brackish groundwater composition is significant and may indicate the likely penetration depths of the Littorina Sea water at the Forsmark site locality. Unfortunately only borehole KFM03A.has groundwaters characterised at greater depths to show that deeper groundwaters are more saline. The depth of transition from brackish to saline is therefore still uncertain.

Bromide

Bromide (Figure 4-9), as expected, shows similar behaviour to that of chloride with depth.

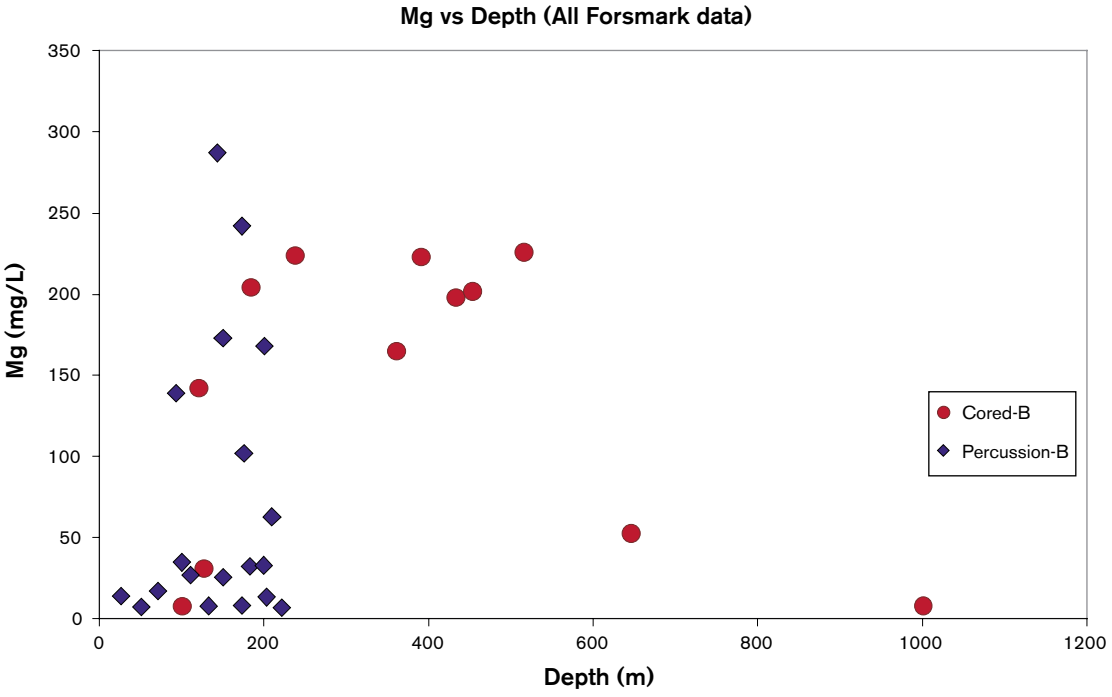

Figure 4-6. *Variation of Mg with depth*

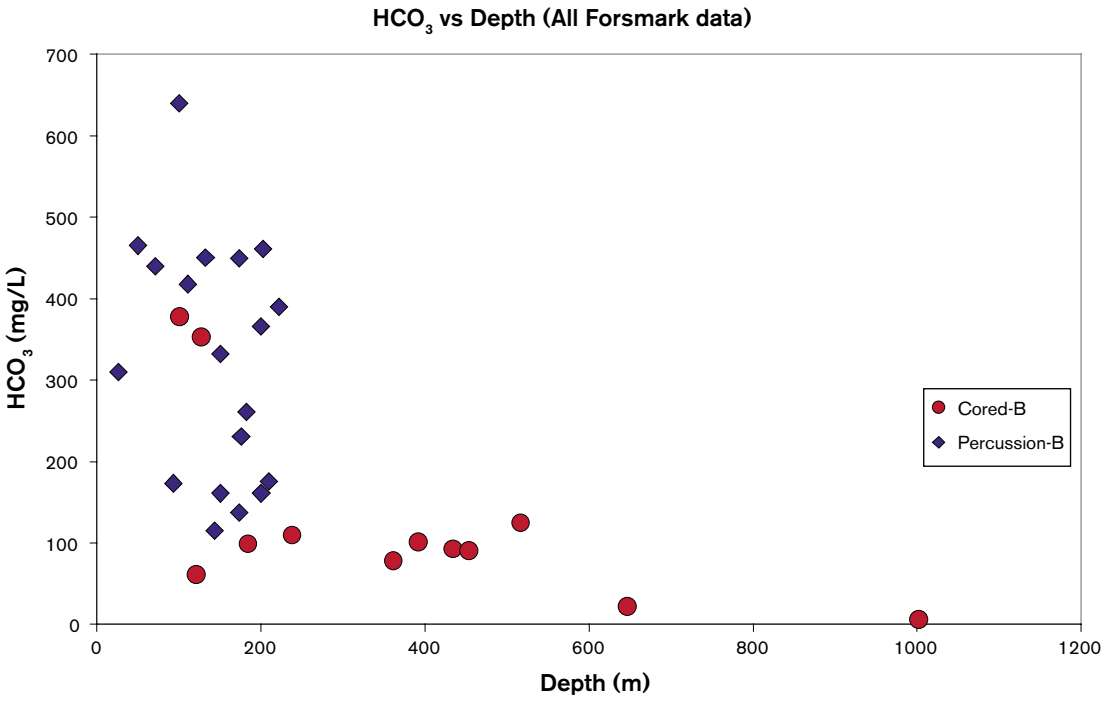

Figure 4-7. *Variation of HCO_3 with depth.*

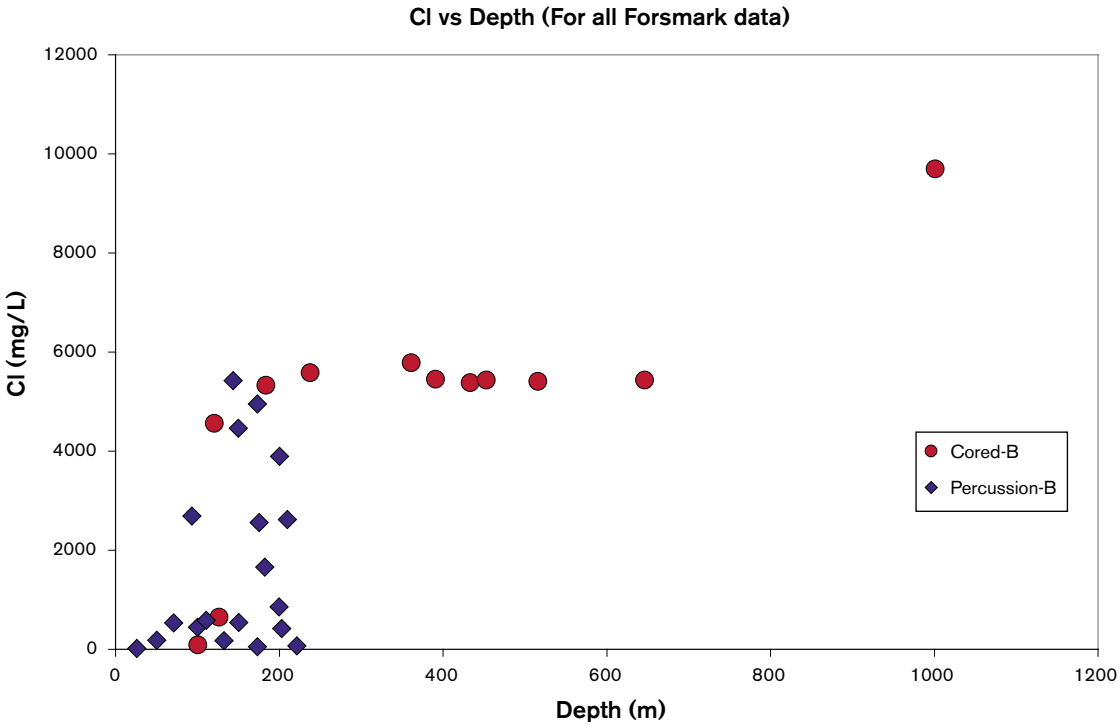

Figure 4-8. *Variation of Cl with depth.*

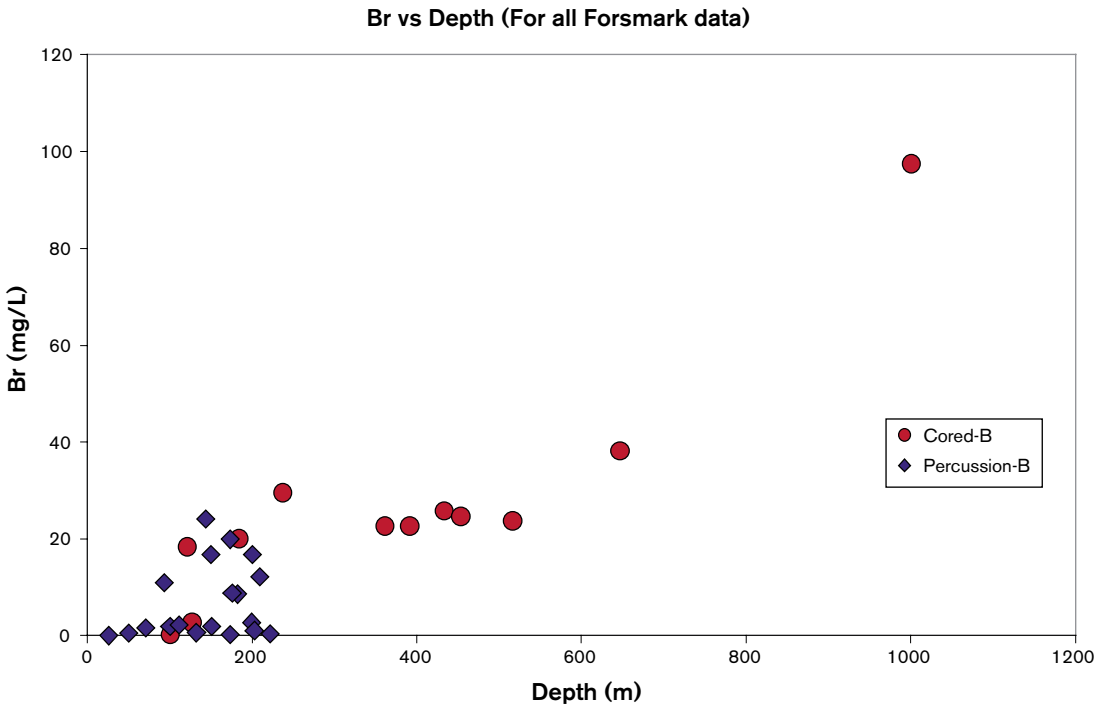

Figure 4-9. *Variation of Br with depth*

Sulphate

Generally, sulphate shows a similar increase to many of the other major ions in the shallow, near-surface groundwaters (Figure 4-10). Furthermore, there is a general levelling out around 500 mg/L SO_4 to about 500 m depth where the sulphate content decreases sharply, finally dropping to 46.7 mg/L SO_4 at the deepest level sampled. The association of enhanced sulphate with the brackish groundwaters is added support for a Littorina Sea component; /Pitkänen et al. 1999/ has estimated 890 mg/L SO_4 for the Littorina Sea.

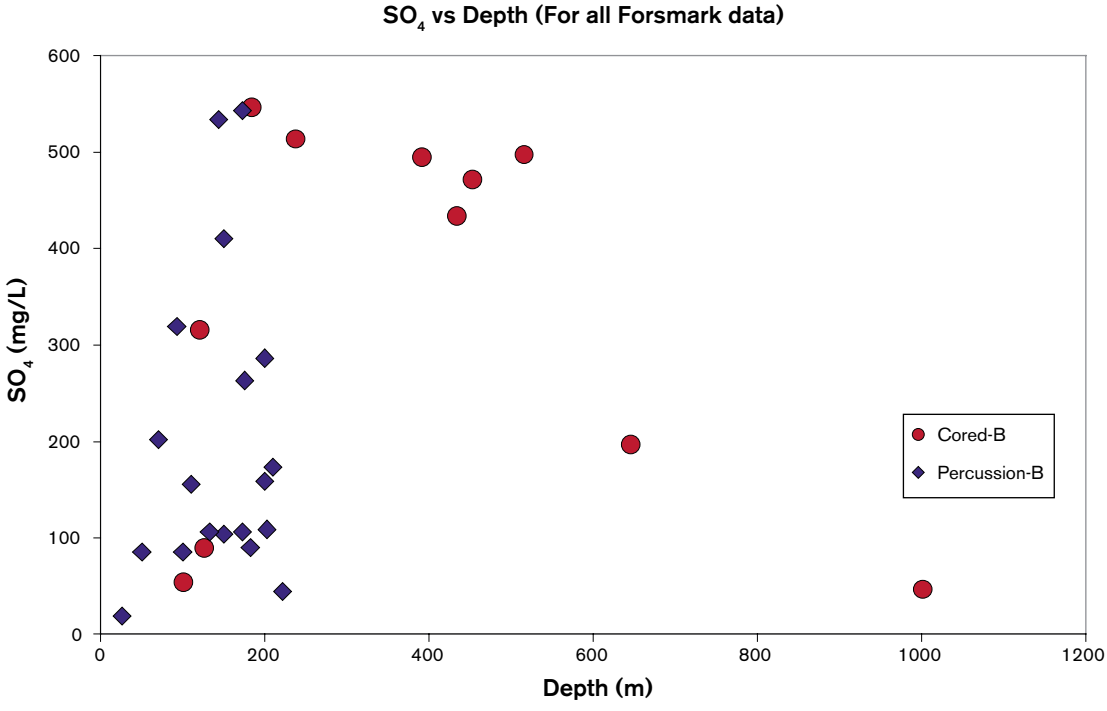

Figure 4-10. *Variation of SO_4 with depth.*

Oxygen-18

Figure 4-11 shows from 200–1,000 m a gradual increase in light $\delta^{18}O$ isotopic values for the cored borehole groundwaters signifying an increase in a cold recharge water component, particularly in the two deepest groundwaters ($\delta^{18}O$ = –13.6 to –11.6‰ SMOW). The other groundwaters, plus most of the percussion boreholes, show typical recent to modern recharge values ($\delta^{18}O$ = –11.5 to –8‰ SMOW.) Two of the percussion groundwaters clearly show some cold climate component (–13 to –12‰ SMOW).

Comparison with other Fennoscandian sites

Chloride

Comparison of the Forsmark chloride data with some of the other Fennoscandian sites is shown in Figure 4-12. These Fennoscandian sites, i.e. Finnsjön, SFR and Olkiluoto, provide excellent comparisons since both Finnsjön and SFR are close to the Forsmark site and Olkiluoto is the Finnish counterpart to Forsmark in terms of palaeoevolution (coastal location) and also in terms of geological and present-day climatic conditions.

Figure 4-12 for all sites show a similar transition from dilute groundwaters (< 1,000 mg/L Cl) to brackish groundwaters (~ 5,000–6,000 mg/L Cl) at slightly varying depths ranging from 50–200 m. Finnsjön also indicates bedrock areas were local hydrodynamics appear to have transported dilute groundwaters to around 500–550 m although contamination cannot be ruled out.

The transition from brackish to more saline groundwaters differs between the sites. At Forsmark (represented by KFM03A) this transition to saline appears to occur at depths greater than 650 m. At Olkiluoto it is clearly at around 500 m below which the salinity increases dramatically to a maximum of > 40,000 mg/L Cl at approx. 850 m, whereas at Forsmark the salinity only increases to ~ 10,000 mg/L Cl at 1,000 m. Both the Finnsjön and SFR sites lack groundwater data from great depth.

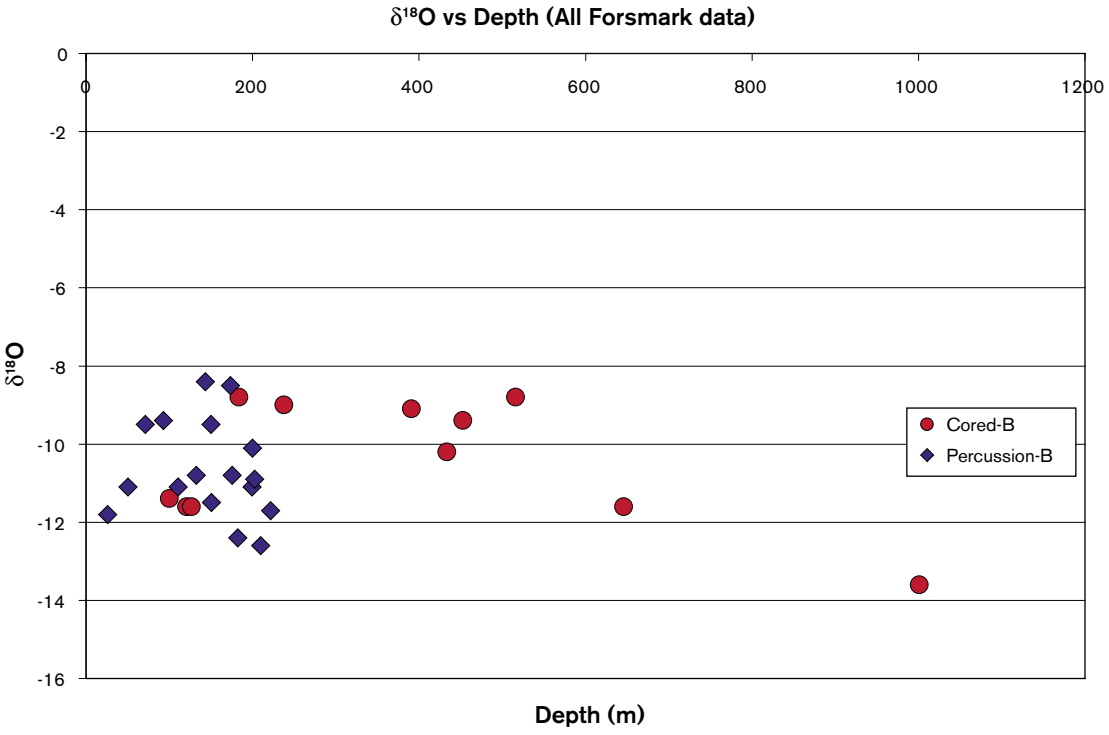

Figure 4-11. *Variation of $\delta^{18}O$ with depth.*

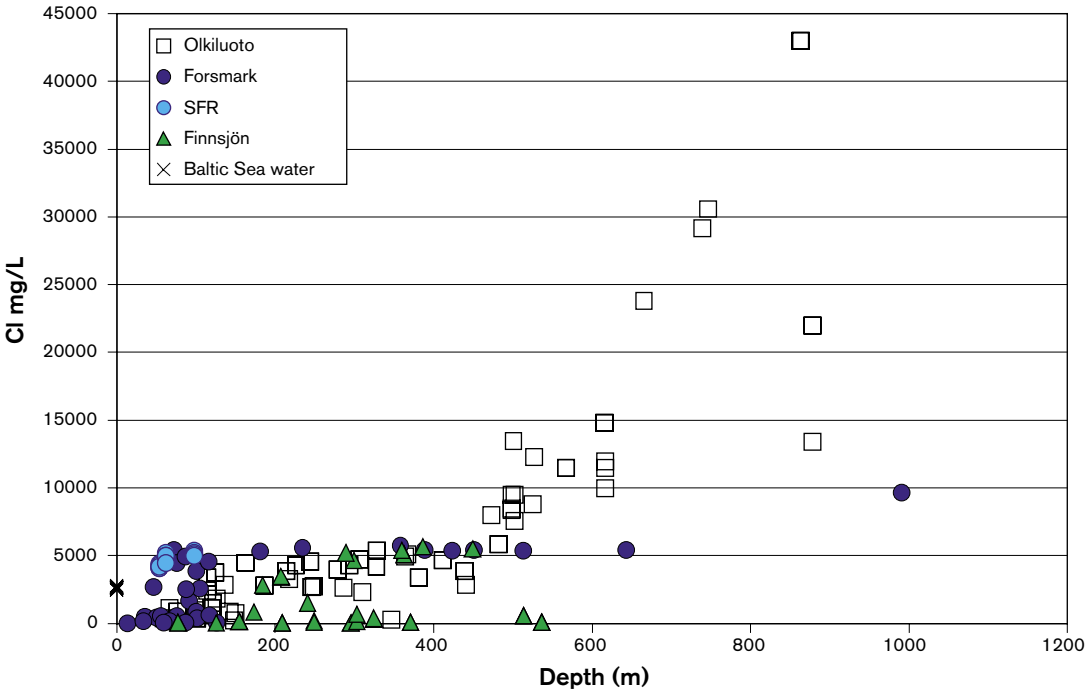

Figure 4-12. *Depth comparison of chloride with other Fennoscandian sites.*

4.2.2 Hydrochemical evolution trends – major ions and stable isotopes

Using data judged to be representative X-Y plots are presented for most of the analysed major ions and isotopes. When appropriate, local scale hydrochemical trends characteristic of the Forsmark site are compared with the nearby Finnsjön and SFR sites and sometimes with other sites in Fennoscandia (e.g. Olkiluoto, Finland) to provide a more regional setting for interpretation.

Plots of sodium versus chloride

All Forsmark data

Figure 4-13 shows a close correlation between Na and Cl. Four features are indicated: a) shallow dilute (> 1,000 mg/L Cl) groundwater trend which closely follows the modern sea water dilution line and represents groundwaters from soil pipes, some of the percussion boreholes and the upper part (18–100 m) of cored borehole KFM02A, b) a clustering of data at brackish groundwater compositions (5,000–6,000 mg/L Cl) mostly representing the cored boreholes and two percussion boreholes; this cluster has deviated from the sea water dilution line and is interpreted as indicating an inmixing of a Littorina Sea component, c) between the dilute and brackish groundwaters several percussion and soil pipe groundwaters plot on or close to the modern Baltic Sea water dilution line and one plots close to a present Baltic Sea composition, and d) the deepest sampled groundwater from KFM03A (980–1,001 m) shows a marked deviation from all other groundwaters and can be explained by increased mixing with an older deep saline component of a non-marine or non-marine/ old marine origin.

The soil pipe shallow groundwaters of higher salinity are anomalous when compared to the majority of the others. There is the possibility that some of these may represent localised discharge areas (cf. Figure 1-27). An exception is groundwater SFM0012 sampled near the coast (and thus influenced by Baltic Sea water) which plots close to the present Baltic Sea average composition.

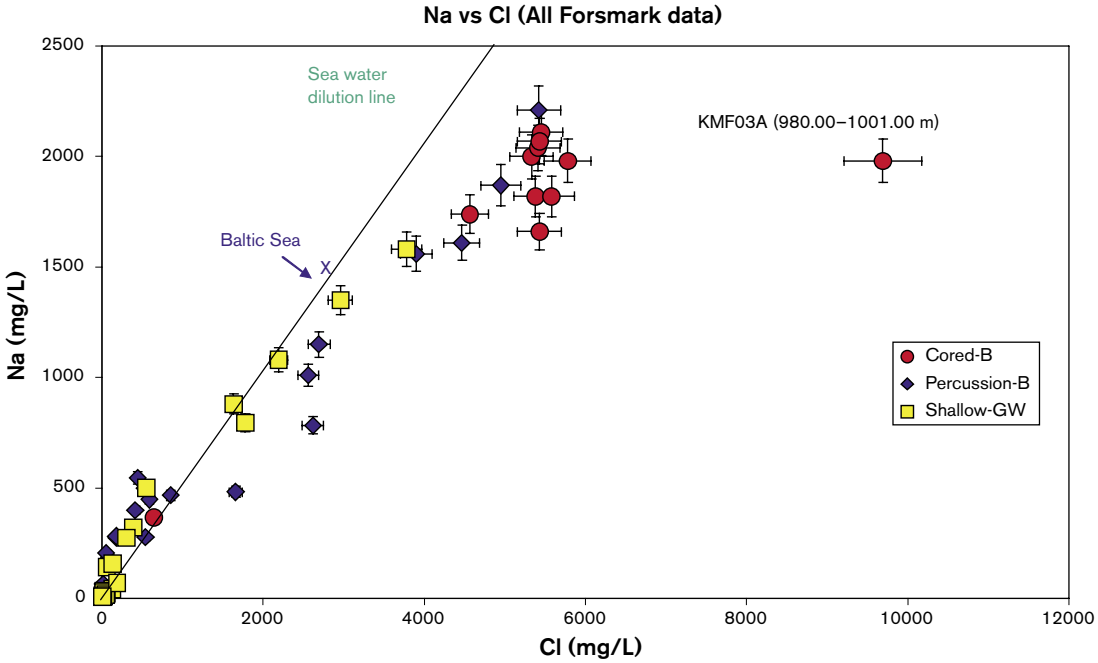

Figure 4-13. *Plot of Na vs Cl for all Forsmark data showing error bars ±5%.*

Comparison with other Fennoscandian sites

Figure 4-14 compares Forsmark with the other Fennoscandian sites. All sites show dilute groundwaters plotting along the modern Baltic Sea dilution line and all sites emphasise to varying degrees the clustering of data around 5,000 mg/L Cl; this deviates from the sea water dilution line. In common with Forsmark, these groundwaters are interpreted as containing an old marine component which may reflect an old Baltic Sea input or an even older Littorina Sea input. At greater depths Olkiluoto in particular shows a marked deviation towards an increasing component of groundwater of non-marine or non-marine/old marine origin. This supports a similar origin for the deepest Forsmark groundwater (KFM03A: 980–1,001 m).

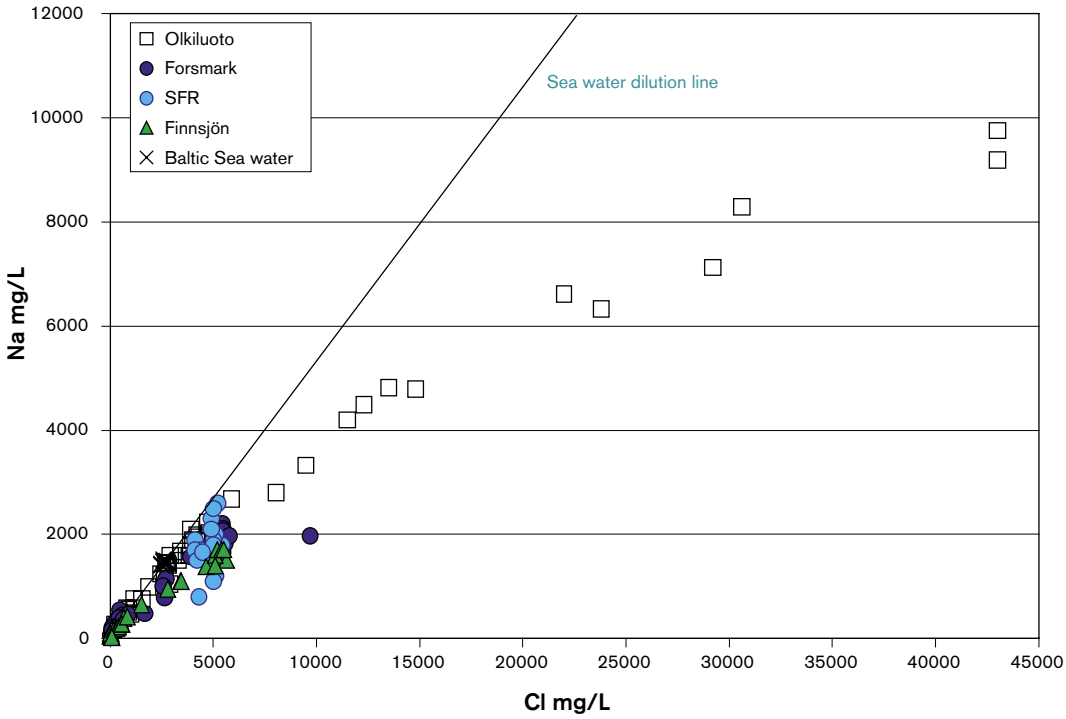

Figure 4-14. *Plot comparing all Forsmark Na vs Cl data with other Fennoscandian sites.*

Plots of potassium versus chloride

Figure 4-15 shows a wide range of potassium values (13.8–67.8 mg/L) associated with the brackish-type groundwaters of around 5,000–6,000 mg/L Cl; this is similar to the magnesium/chloride plot discussed below (Figure 4-16). In common with sodium, some of the soil pipe samples with enhanced salinity and potassium contents plot on or close to the modern sea water dilution line.

Plots of magnesium versus chloride

All Forsmark data

Figure 4-16 shows that the more brackish groundwaters (> 2,000 mg/L Cl) deviate from the modern Baltic Sea water dilution line. Although there is no sharp trend, there is an obvious increase of magnesium with increasing salinity, at least to around 5,000–6,000 mg/L Cl where most of the cored borehole data cluster. Two percussion boreholes (HFM08 and HFM19) plot closely to the cluster and these are significant since they record the highest magnesium contents at 287 and 242 mg/L Mg respectively. At salinities greater than 5,000–6,000 mg/L Cl, represented only by KFM03A (980–1,001 m), magnesium drops to 8.1 mg/L. The other major exception is KFM03A (639–646 m) which is brackish but with a low magnesium content of 52.7 mg/L. In this context borehole KFM03A is characterised by fracture zones A4, A7 and B1 (cf. Figure 1-18) within the depth interval of 350–550 m. It would seem that this structural interval hydraulically separates brackish groundwaters partly of old and/or new marine origin, from deeper increasingly saline groundwaters of non-marine origin.

The cluster of brackish groundwaters characterised by higher magnesium than modern Baltic Sea water are believed to represent components of Littorina Sea water and maybe also of older than recent Baltic Sea water (e.g. > 1,000 yrs). Estimated values for the Littorina Sea composition (Mg ~ 448 mg/L; Cl ~ 6,500 mg/L) have been derived by /Pitkänen et al. 1999/. Of interest is the near inclusion of soil pipe groundwater sample SFM0023 in this cluster. This has been collected under Bolundsfjärden, one of the possible discharge locations (cf. Figure 1-27).

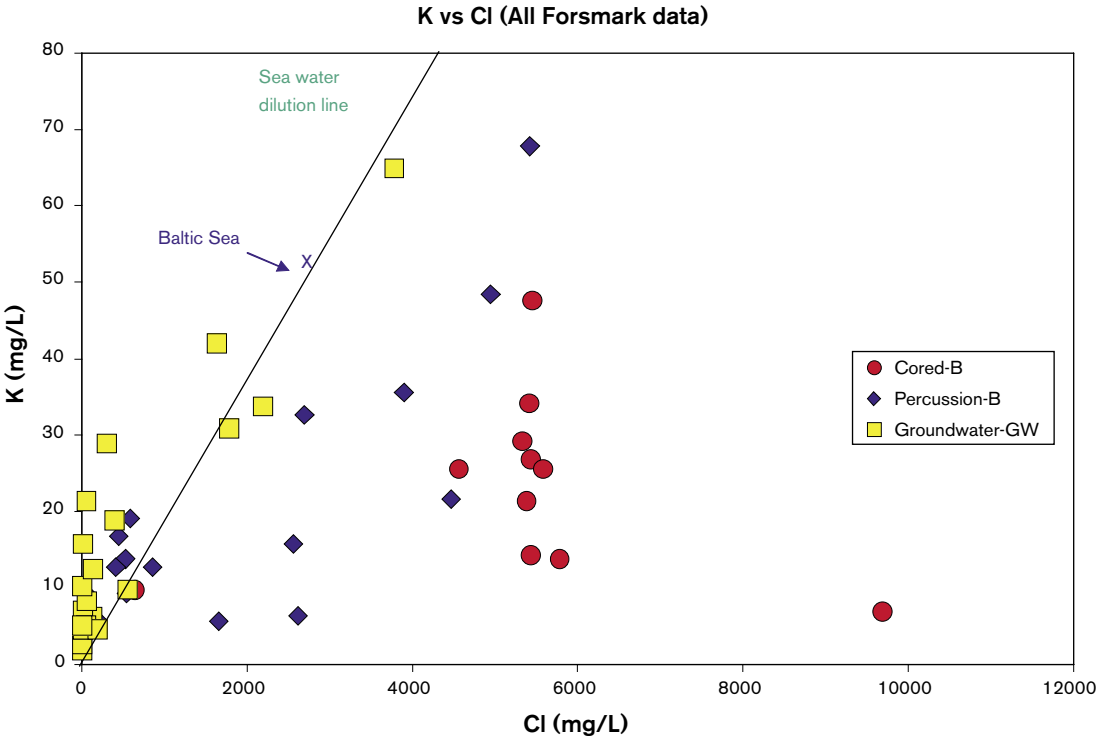

Figure 4-15. *Plot of K vs Cl for all Forsmark data.*

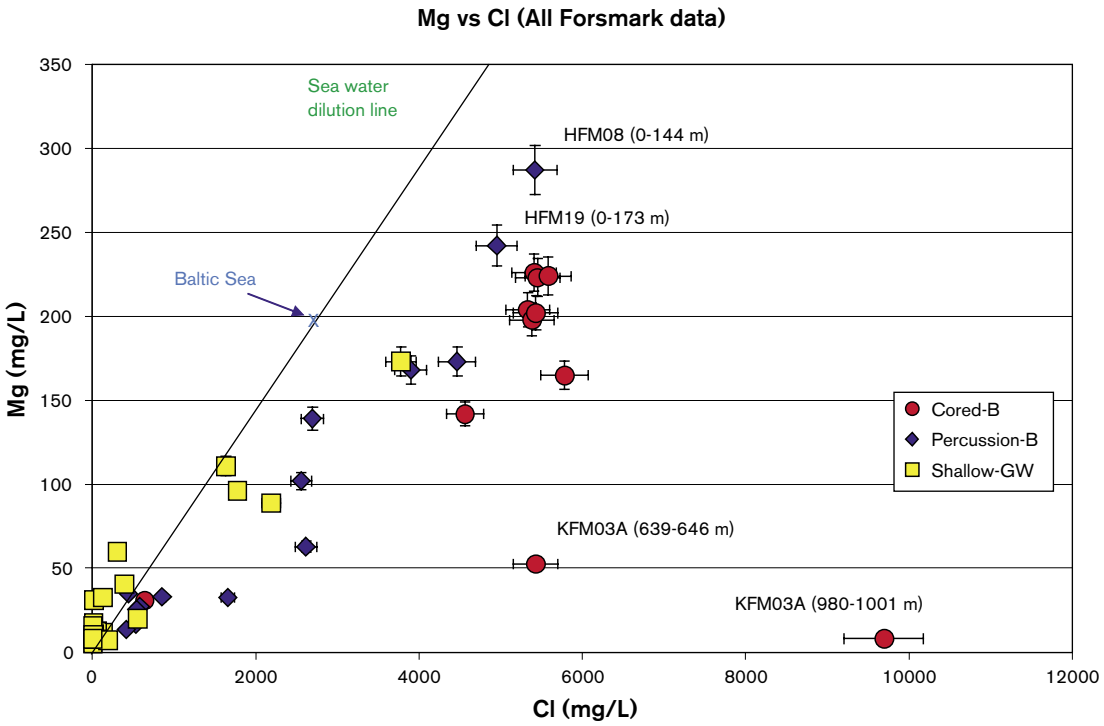

Figure 4-16. *Plot of Mg vs Cl for all Forsmark data showing error bars ±5%.*

Comparison with other Fennoscandian sites

Comparison with other Fennoscandian site data (Figure 4-17) confirms the Forsmark trends; note that some of the SFR groundwaters have even higher magnesium contents. Of particular importance are the groundwaters of brackish composition, plotting close to the red line at around 5,000 mg/L Cl, and their related magnesium contents. The magnesium contents of these groundwaters are widely variable reflecting probable mixing of old marine waters (old Baltic Sea and Littorina Sea) and in some cases modern Baltic Sea water. As will be discussed later, mixing of dilute glacial water is also part of the equation. The transition from brackish to lower magnesium (> 100 mg/L) saline and eventually highly saline groundwaters is indicated convincingly from the figure. As mentioned above, this trend represents an increasing influence of deep, non-marine saline groundwaters, and the sharp interface indicated at Olkiluoto and probably at Forsmark (KFM03A) may suggest some kind of hydrostructural control (sub-horizontal fracture zones?) on the groundwater flow system.

Plots of calcium versus chloride

All Forsmark data

Figure 4-18 shows that all samples, with the exception of the most dilute groundwaters, deviate from the modern sea water dilution line. Two main trends are suggested by the hatched lines, one demarcating a lower chloride brackish group (up to ~ 2,000–5,000 mg/L Cl) where there is some degree of correlation between calcium and chloride, and a higher chloride brackish group (5,000–6,000 mg/L Cl), where there is a narrow salinity range corresponding to a wide calcium range which may be the result of differential ion-exchange and/or mixing processes. Once again these brackish groundwaters may represent a potential site for a residual old marine water (i.e. Littorina Sea) component. The third trend is towards a deeper, more saline and calcium-rich groundwater (KFM03A: 980–1,001 m) which has undergone extensive water/rock interaction.

Comparison with other Fennoscandian sites

Figure 4-19 serves to support the Forsmark trends, once again the cluster of variable concentrations associated with the brackish groundwaters and the increasing non-marine signature of deeper calcium-rich saline groundwaters.

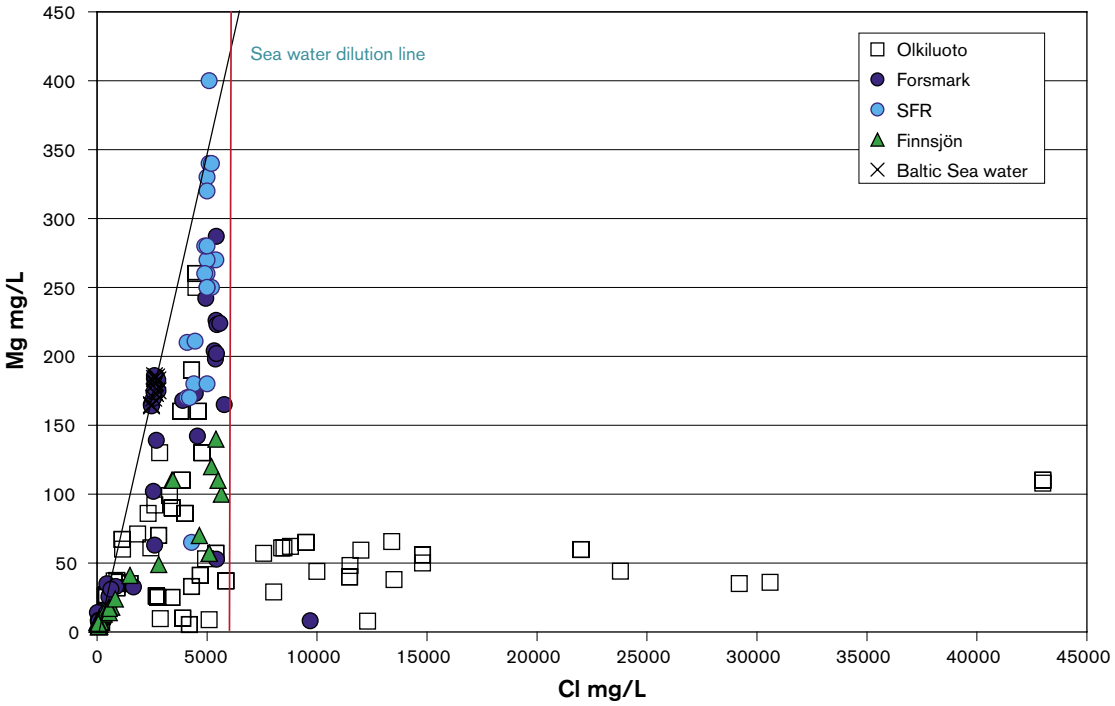

Figure 4-17. *Plot comparing all Forsmark Mg vs Cl data with other Fennoscandian sites.*

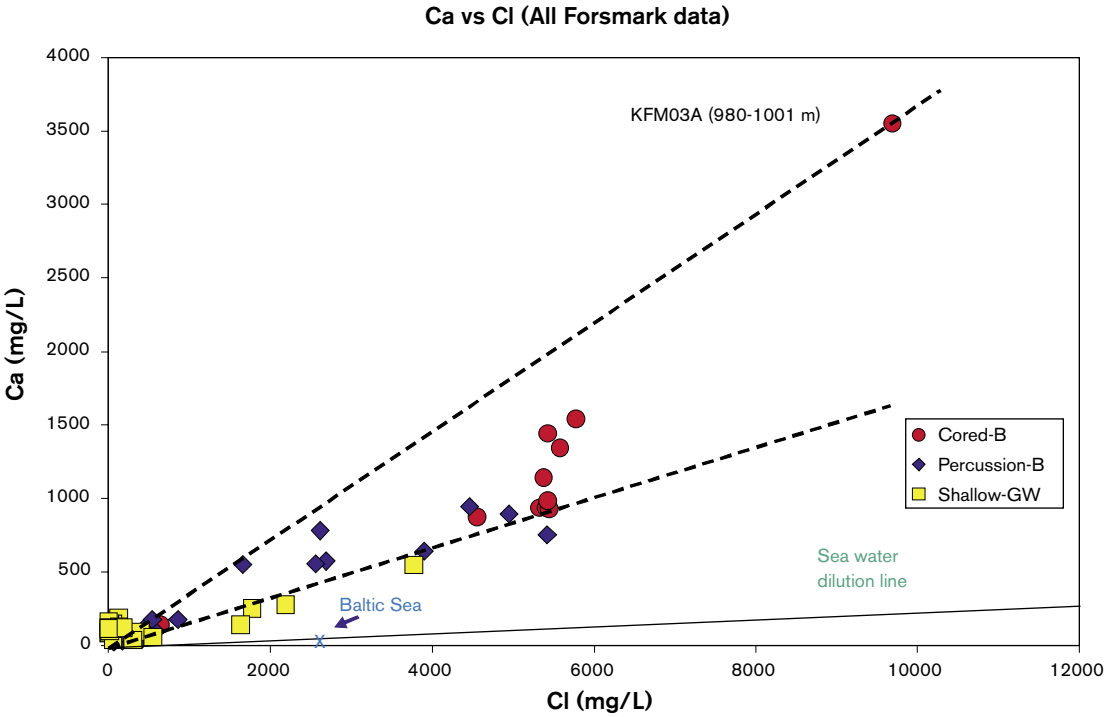

Figure 4-18. *Plot of Ca vs Cl for all Forsmark data (possible trends are indicated by the hatched lines).*

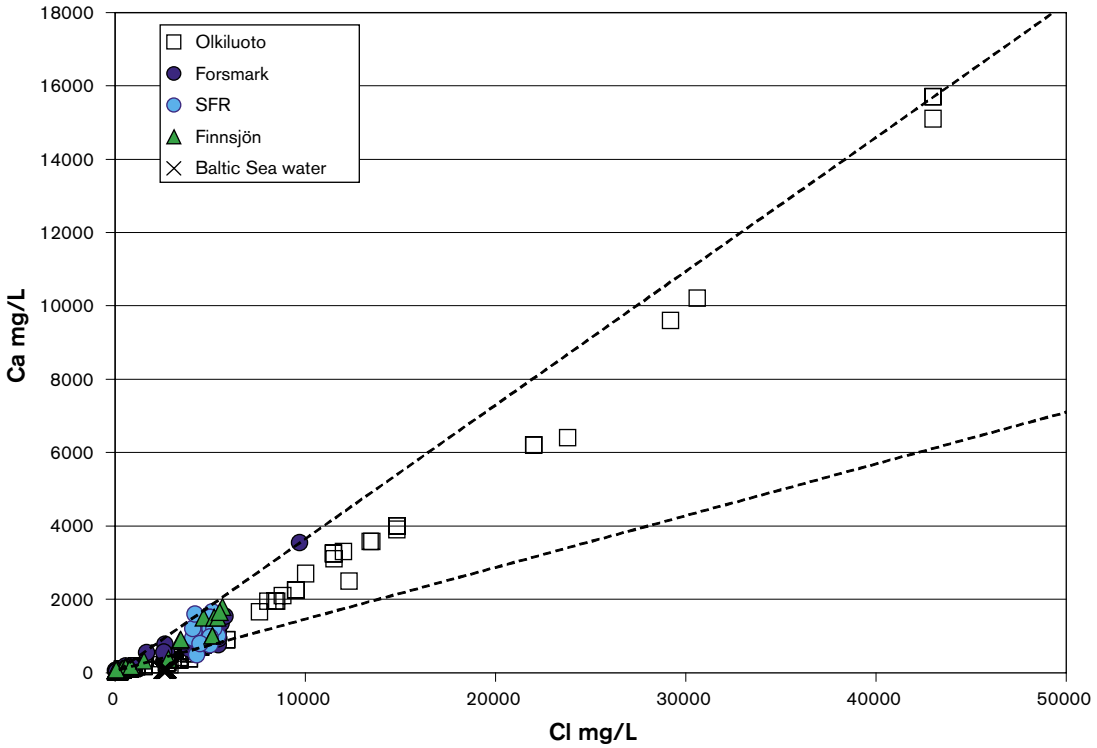

Figure 4-19. *Plot comparing all Forsmark Ca vs Cl data with other Fennoscandian sites.*

Plots of sulphate versus chloride

All Forsmark data

Figure 4-20 shows some similarity to the magnesium plot (Figure 4-16) where there is a weak correlation trend towards the brackish groundwater cluster (5,000–6,000 mg/L Cl) and high magnesium seems to correspond to high sulphate which here ranges from 434–546 mg/L. This is consistent with mixing of an infiltrated Littorina Sea water component, supporting also the interpretation of /Pitkänen et al. 2004/ for the brackish Olkiluoto groundwaters; /Pitkänen et al. 1999/ have estimated an original Littorina Sea composition of 890 mg/L SO_4^{2-}.

The deeper groundwater system represented by KFM03A borehole section 980–1,001 m is once again obvious from the low sulphate concentration (46.7 mg/L SO_4) compared to the brackish groundwater cluster. Similarly low sulphate in increasingly deep saline groundwaters at Olkiluoto has been explained by prevailing methanic redox conditions which reduces SO_4^{2-}.

Borehole KFM03A section 639–646 m records a slightly higher sulphate content suggesting that some inmixing of a Littorina Sea component is present at this depth. Infiltration has probably been weaker due to the decreasing permeability of the bedrock. This is supported by the sulphate distribution illustrated in Figure 4-10 which shows a sharp drop in sulphate just below the 600 m depth. The presence of a structural barrier (e.g. sub-horizontal fracture zone) may also prohibit deeper infiltration of more shallow derived groundwaters.

For the shallow, dilute and bicarbonate enriched groundwaters, the increased sulphate content in many of the Soil Pipe and percussion borehole samples exceed the sea water dilution line. This indicates an additional sulphate source other than sea water.

Comparison with other Fennoscandian sites

Comparison with other Fennoscandian sites (Figure 4-21) reinforces the features described for Forsmark, in particular the significant infiltration and mixing of a Littorina Sea component and the rapid transition from sulphate/magnesium-rich brackish groundwaters to deeper, saline/highly saline and sulphate/magnesium-poor groundwaters.

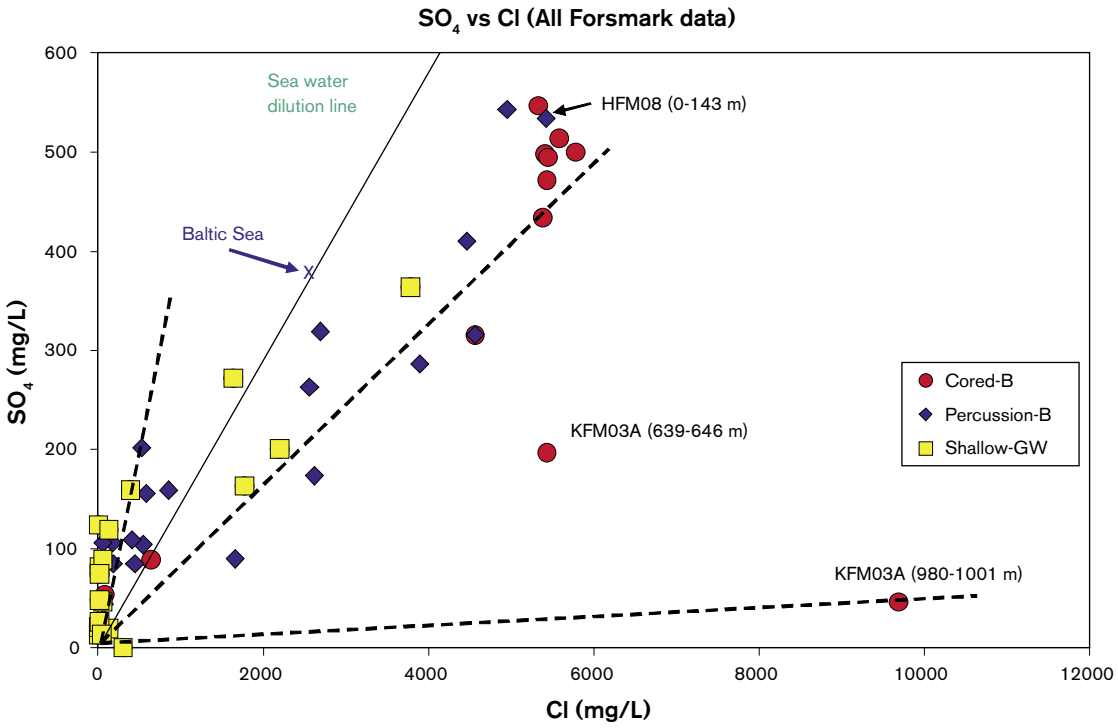

Figure 4-20. *Plot of SO_4^{2-} vs Cl for all Forsmark data (possible trends are indicated by the hatched lines).*

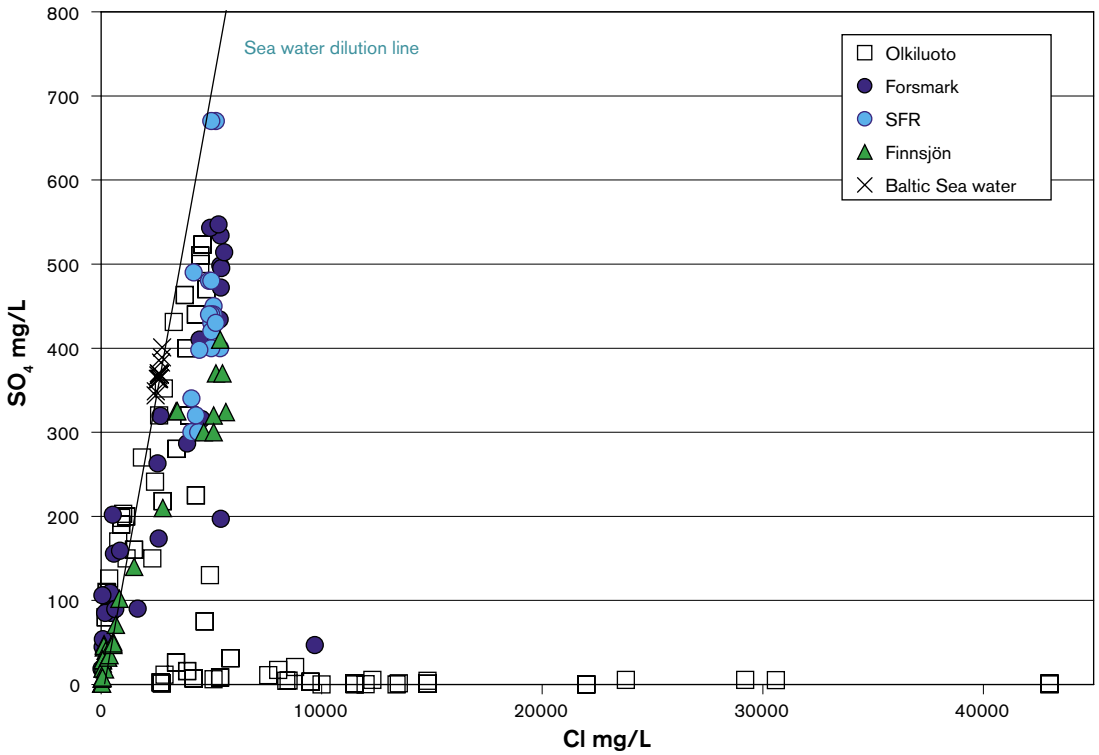

Figure 4-21. *Plot comparing all Forsmark SO_4^{2-} vs Cl data with other Fennoscandian sites.*

Plots of bromide versus chloride

All Forsmark data

Figure 4-22 shows a good correlation between bromide and chloride close to the sea water dilution line to a depth of approx. 500 m. At this depth the brackish cluster (i.e. Littorina Sea-type groundwater) deviates slightly; the somewhat deeper KFM03A (639–646 m) deviates further and the deepest sample KFM03A (980–1,001 m) further still. The enhanced bromide in the brackish cluster is a further indication of an associated Littorina Sea component; /Pitkänen et al. 1999/ estimate a bromide content of 22.2 mg/L Br for the Littorina Sea.

Comparison with other Fennoscandian sites

Comparison with other Fennoscandian sites (Figure 4-23) shows the Forsmark groundwaters plotting along the lower part of a well defined trend of increasing bromide with increasing salinity defined by the Olkiluoto groundwaters. This feature lends further support for a deep, non-marine or non-marine/ old marine mixing origin for the deepest, most saline Forsmark groundwater.

Plots of bicarbonate versus chloride

All Forsmark data

Figure 4-24, combining all Forsmark data, emphasis high bicarbonate contents (200–800 mg/L) present in the shallow, dilute groundwaters, which contrast with low contents (> 125 mg/L) in the brackish groundwaters and very low values in the most saline groundwater (6 mg/L). Soil Pipe sample SFM0023 (cf. Figure 1-27) from under Bolundsfjärden, believed to be a discharge location, shows the lowest bicarbonate content of the soil pipe groundwaters (165 mg/L). This groundwater appears to be more in line with some of the percussion boreholes plotting close to the brackish groundwater cluster, i.e. additional support for a deeper discharge origin to shallow groundwater SFM0023.

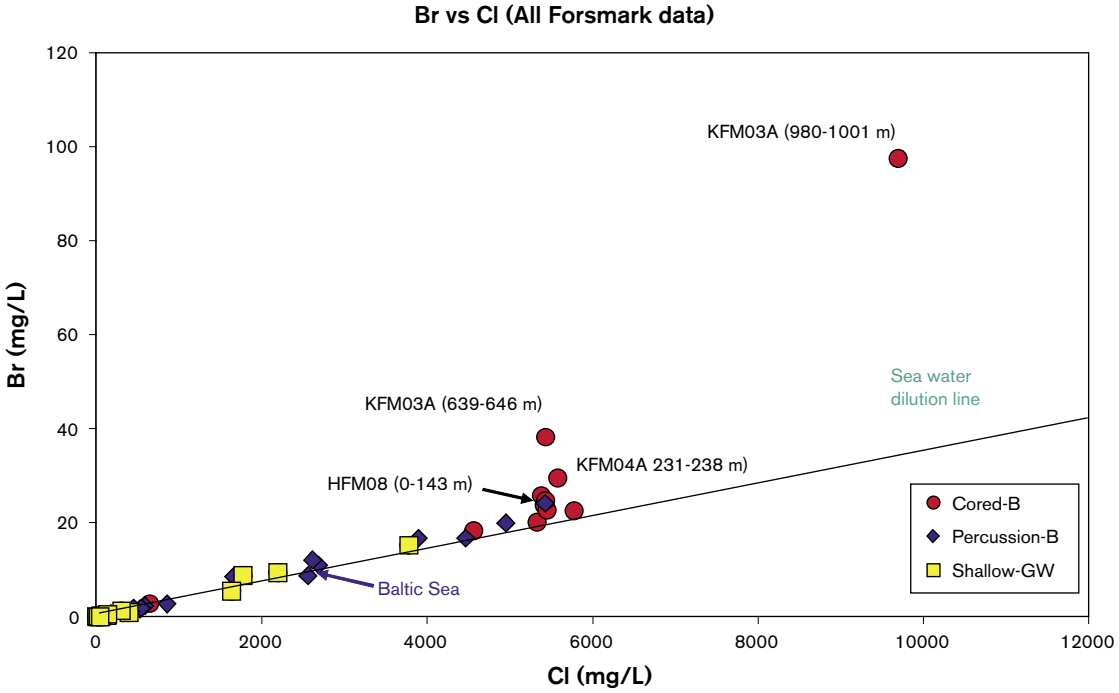

Figure 4-22. *Plot of Br vs Cl for all Forsmark data.*

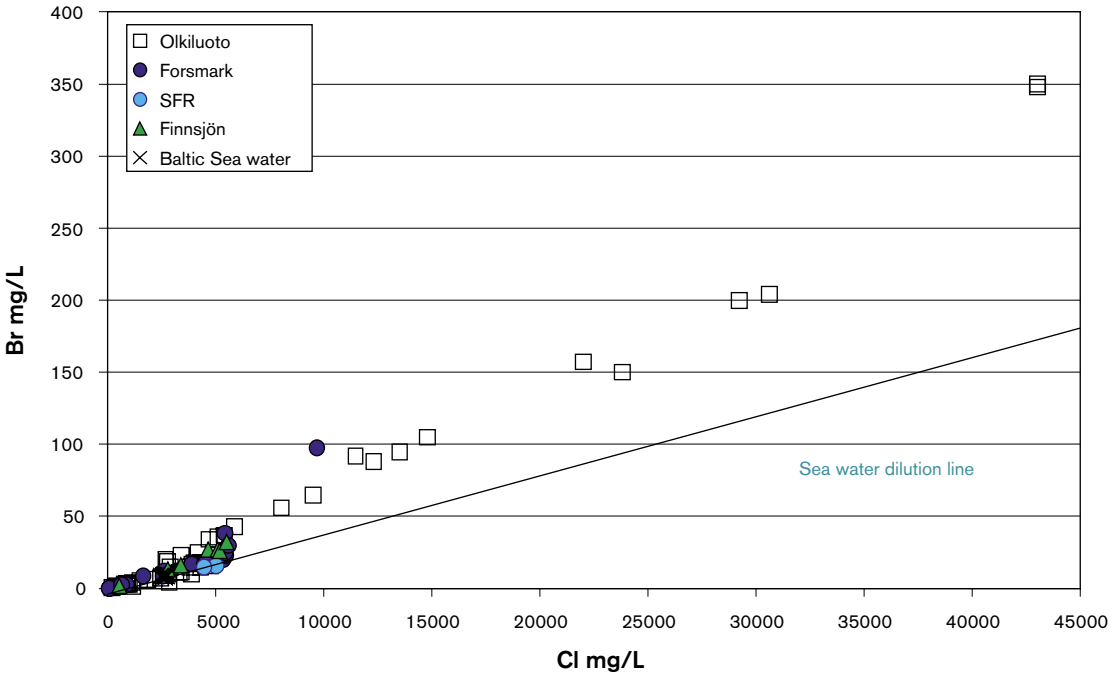

Figure 4-23. *Plot comparing all Forsmark Br vs Cl data with other Fennoscandian sites.*

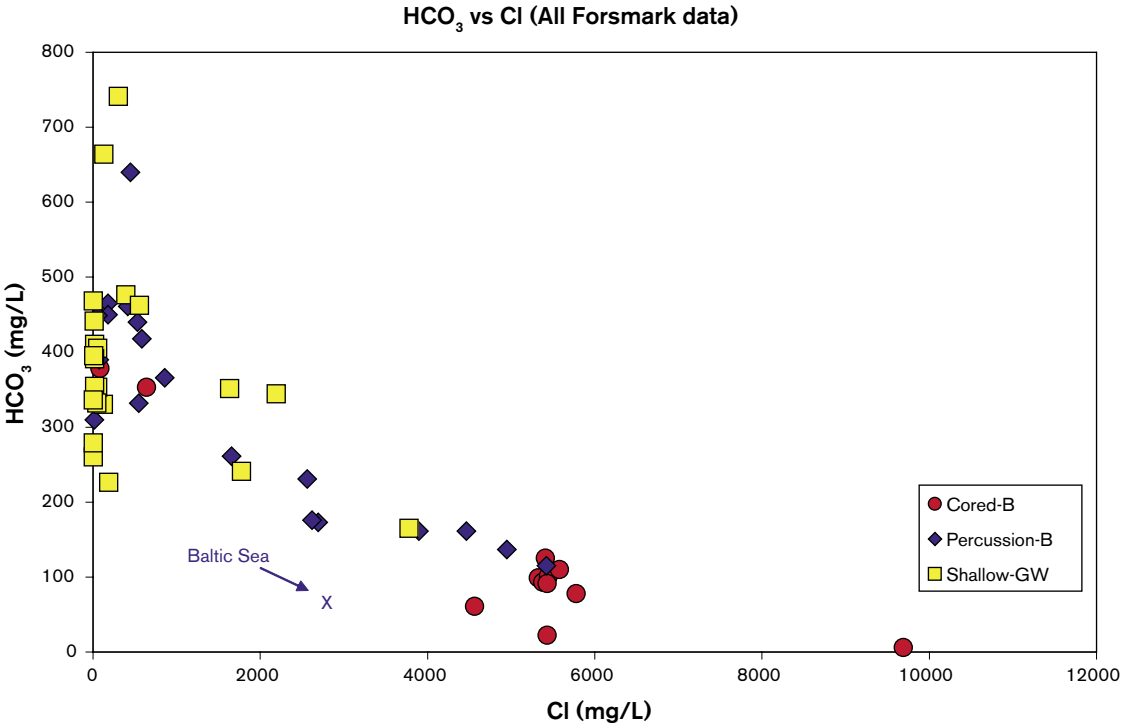

Figure 4-24. *Plot of HCO_3 vs Cl for all Forsmark data.*

Comparison with other Fennoscandian sites (Figure 4-25) further clarifies the sharp transition from high to low bicarbonate where groundwaters are brackish in type, i.e. within the range of 5,000–6,000 mg/L Cl, corresponding to depths of around 200 m at Forsmark (Figure 4-8). The most saline Forsmark groundwater (KFM03A: 980–1,001 m) plots along the trend of the deep saline Olkiluoto groundwaters.

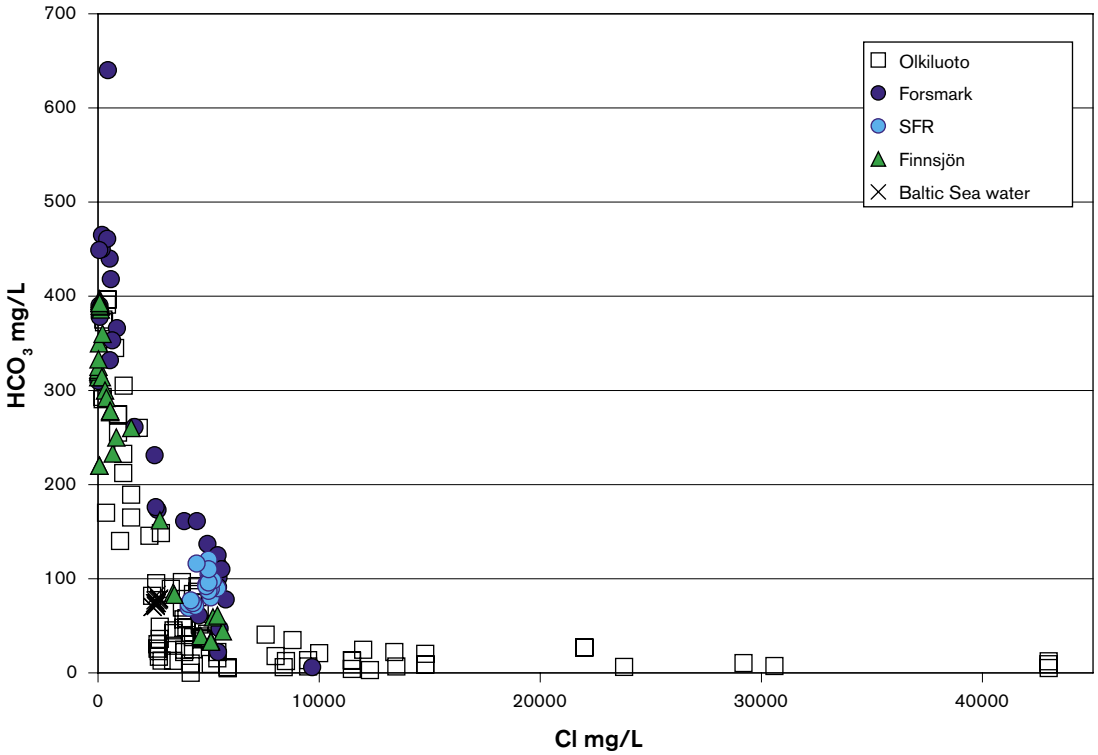

Figure 4-25. *Plot comparing all Forsmark HCO_3 vs Cl data with other Fennoscandian sites.*

Plot of magnesium versus calcium

All Forsmark data

Figure 4-26 shows similarities to the Mg vs Cl plot (Figure 4-16) which reflects the close correlation of high salinity with high calcium content (Figure 4-18). However, ion exchange reactions influencing particularly calcium, but also potentially magnesium, have contributed to the general lack of correlation observed. Further influences have resulted from mixing processes involving old marine waters (i.e. Littorina Sea and old Baltic Sea) and, as will be discussed below, waters of glacial origin.

Comparison with other Fennoscandian sites

This plot reflects that in Figure 4-26 giving further support for. a) one separate trend for the brackish marine water (old Baltic Sea and Littorina Sea), and b) the deep saline waters characterised by lower magnesium and much higher calcium.

Plot of calcium versus sulphate

All Forsmark data

Figure 4-28 shows three trends: a) the more dilute shallow groundwaters plot close to the sea water dilution line, b) there is a weak correlation between increasing sulphate and calcium up to and including the brackish groundwaters, and c) deep groundwater KFM03A (980–1,001 m) is a distinct outlier representing a calcium-rich, sulphate-poor groundwater system. Furthermore, given the sensitivity of calcium to ion exchange processes and the fact that sulphate may be influenced by microbially mediated reactions, this may explain some of the lack of correlation shown by the dilute to brackish groundwaters at shallower depths.

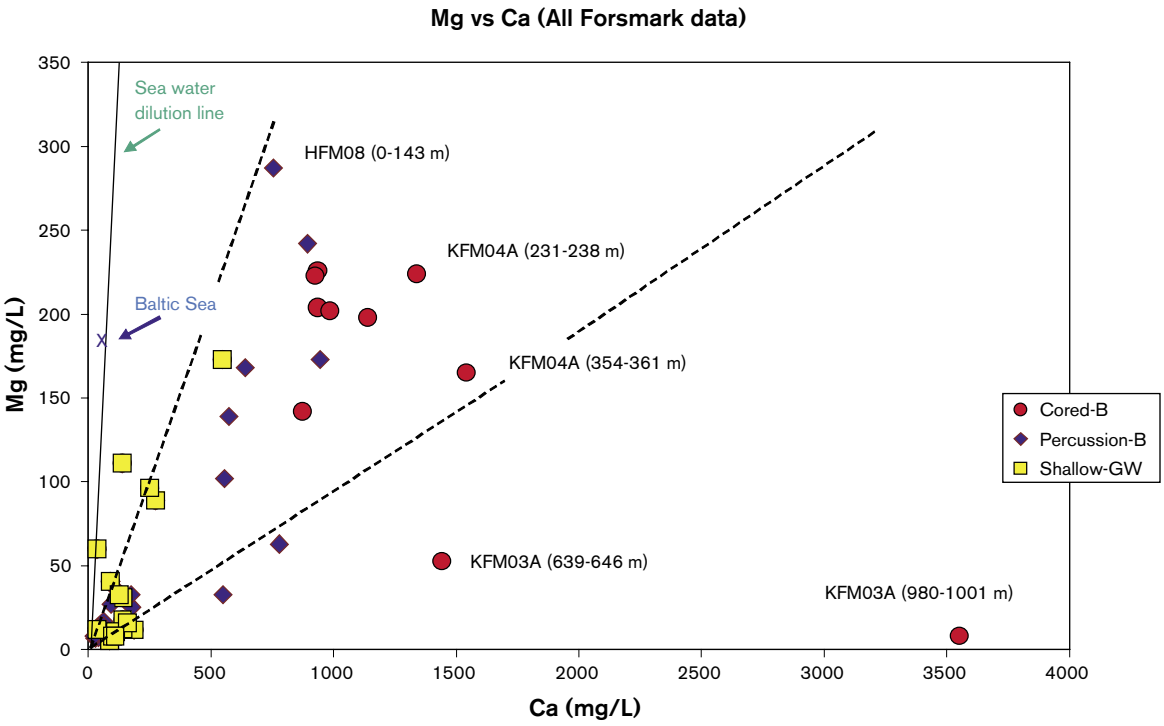

Figure 4-26. *Plot of Mg vs Ca for all Forsmark data (possible trends are indicated by the hatched lines).*

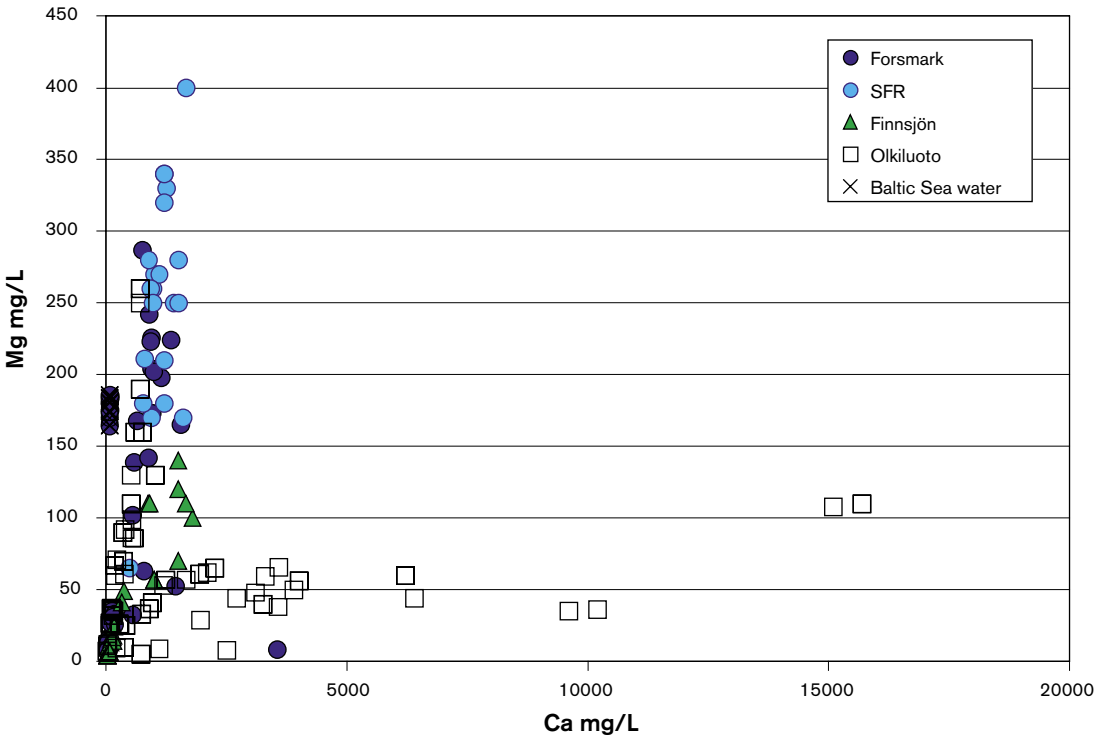

Figure 4-27. *Plot comparing all Forsmark Mg vs Ca data with other Fennoscandian sites.*

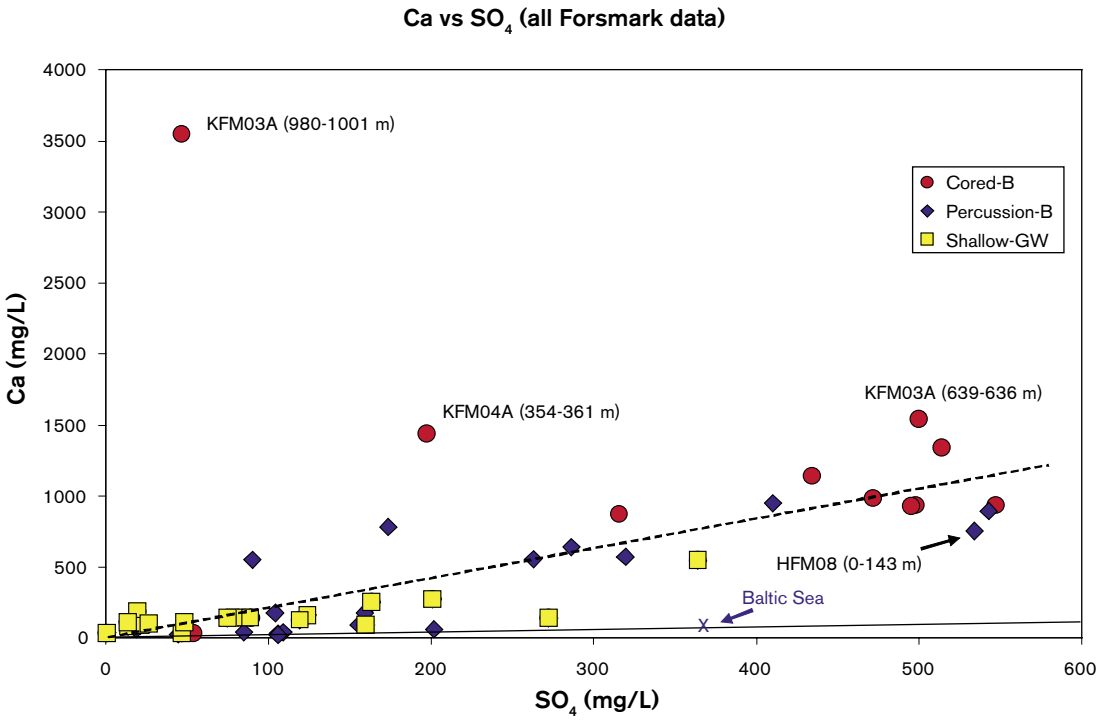

Figure 4-28. *Plot of Ca vs SO_4 for all Forsmark data (possible trend is indicated by the hatched line).*

Comparison with other Fennoscandian sites

Figure 4-29 gives further credibility to the correlation between increasing sulphate and calcium within the dilute to brackish groundwaters, and the strong Olkiluoto deep water trend supports the very low sulphate content in the deep saline groundwater from KFM03A (980–1,001 m).

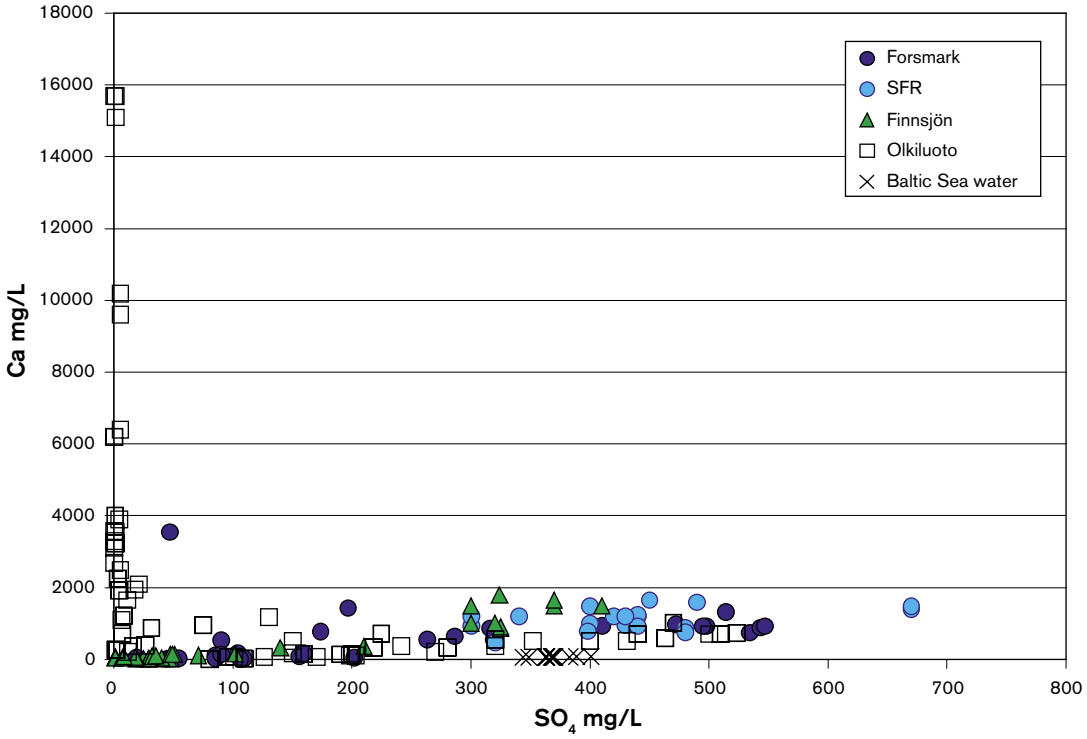

Figure 4-29. *Plot comparing all Forsmark Mg vs Ca data with other Fennoscandian sites.*

Plot of calcium/magnesium versus bromide/chloride

Comparison with other Fennoscandian sites

By plotting Ca/Mg versus Br/Cl, Figure 4-30 provides an opportunity to differentiate between groundwaters of modern marine origin (e.g. present Baltic Sea), of old marine origin (e.g. Littorina Sea and old Baltic Sea) and of non-marine origin. The figure clearly shows the Baltic Sea group of modern marine waters and also the deepest non-marine saline groundwaters from Forsmark (one point) and Olkiluoto. Between these two end-members plot most of the groundwater data. The red arrow shows the direction towards the deep saline non-marine types, and much of the data plotting along this pathway represent groundwaters which contain an increasing component of the deep saline non-marine end-member. Likewise, at the other extreme, some of the plotted data closest to the modern Baltic Sea end-member may well comprise shallow groundwaters (0–100 m depth) which include a modern marine water signature. In addition there is the presence of older marine groundwaters, both Littorina Sea and old Baltic Sea in origin, although it is not possible to differentiate them. These two types are associated with the shallower brackish groundwaters which persist from 100–650 m depth, depending on local hydraulic conditions. These groundwaters are circled in purple and indicate enhancements of, for example, Mg and Br.

Plot of oxygen-18 versus deuterium

All Forsmark data

Figure 4-31 details the stable isotope data which plot on or close to the Global Meteoric Water Line (GMWL) indicating a meteoric origin. Values range from $\delta^{18}O$ = –13.6 to –8.4‰ SMOW and δD = –98.5 to –66.1‰ SMOW with the most negative isotopic signatures (i.e. cold climate meteoric input) corresponding to the deepest groundwater sampled at 980–1,001 m (KFM03A; see also Figure 4-10). There is no evidence of contamination at this depth; the drilling water originated from percussion borehole HFM06 which is slightly saline (~ 1,000 mg/L Cl), recent in origin (5.7 TU) with stable isotope values of $\delta^{18}O$ = –11.1‰ SMOW and δD = –81.2‰ SMOW.

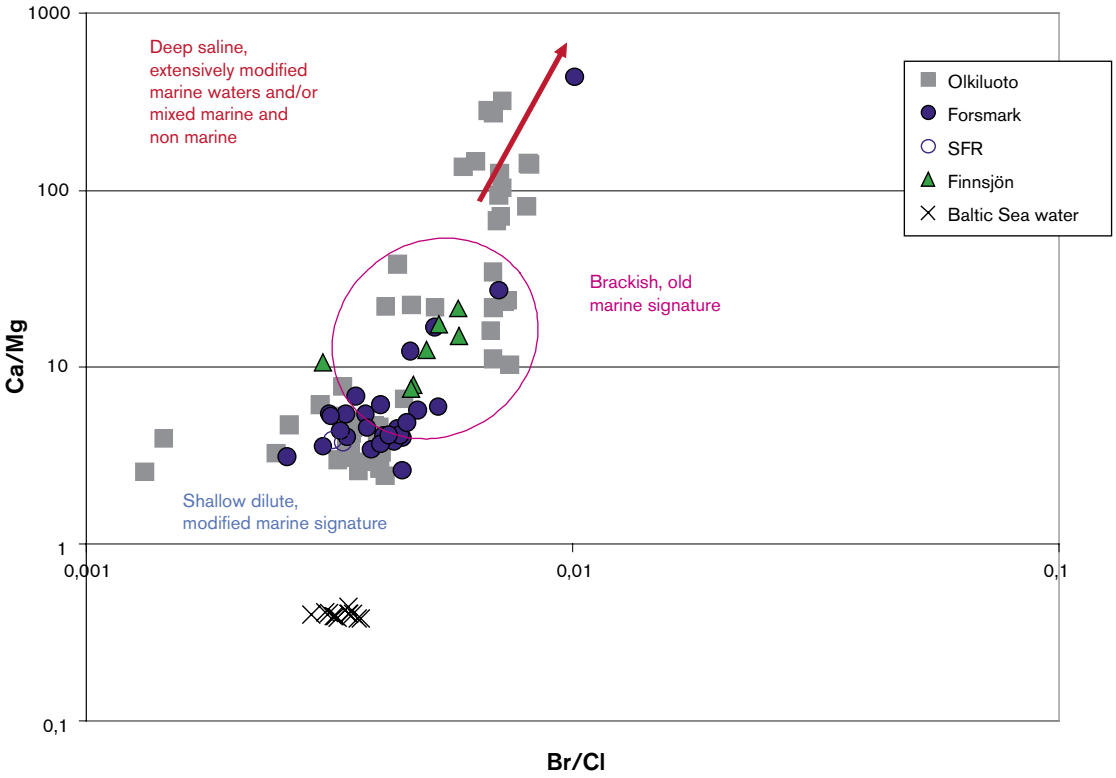

Figure 4-30. *Plot comparing all Forsmark Ca/Mg vs Br/ Cl data with other Fennoscandian sites.*

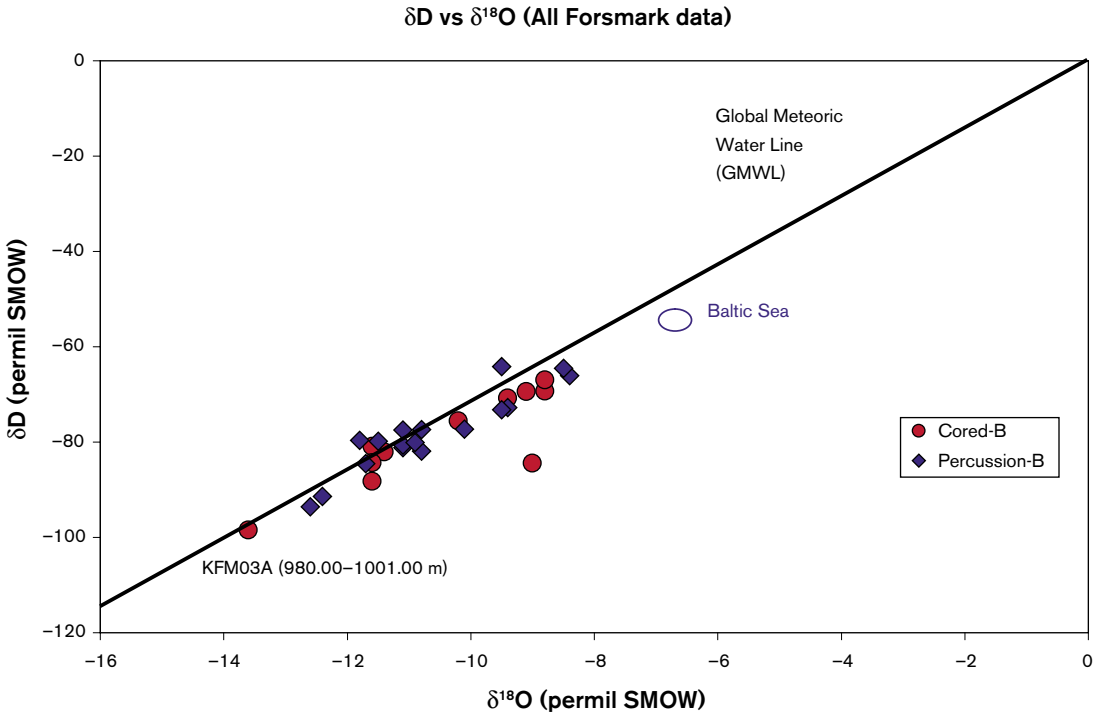

Figure 4-31. *Plot of $\delta^{18}O$ versus δD for all Forsmark data.*

Plot of oxygen-18 versus chloride

All Forsmark data

Figure 4-32 further details the three distinct groups of groundwaters present at Forsmark: a) shallow, dilute groundwaters (< 1,000 mg/L Cl) with a narrow range of $\delta^{18}O$ (–12 to –10‰ SMOW), close to present day precipitation, b) a wider range of values ($\delta^{18}O$ = –12 to –8‰ SMOW) for the more brackish groundwaters including those with Littorina Sea signatures, and c) the deepest outlier ($\delta^{18}O$ = –13.6‰ SMOW) representing the most saline groundwater. The deepest saline groundwater and some of the brackish groundwaters therefore show evidence that cold climate recharge waters have infiltrated and mixed. Later infiltration and mixing of old marine waters (i.e. Littorina Sea and old Baltic Sea) has taken place and appears to have been restricted to the brackish groundwater environment (5,000–6,000 mg/L Cl) to maximum depths of around 600 m. The incursion and mixing of isotopically heavy Littorina Sea water (estimated to –4.7‰ SMOW; /Pitkänen et al. 1999/) has served to produce heavier $\delta^{18}O$ values and this can be clearly seen in Figure 4-32 where there is an isotopically heavier brackish groundwater cluster between –10 to –8‰ SMOW at around 5,500 mg/L Cl. At similar salinities there also exist more negative $\delta^{18}O$ values which suggest that the earlier cold recharge component at these sampling locations may be more dominant.

Cold climate recharge, in contrast to Littorina Sea water, albeit on the basis of one sample, seems to have penetrated to much greater depths (~ 1,000 m). This is also evident at the Simpevarp site.

Comparison with other Fennoscandian sites

Figure 4-33 compares the Forsmark data with other Fennoscandian sites. The figure further emphasis the large range of $\delta^{18}O$ values (and therefore mixing processes) up to and including the brackish groundwaters. The heavier $\delta^{18}O$ isotopic values at these brackish compositions (at approx. 5,000 mg/L Cl), identified from the Forsmark data and interpreted to reflect a Littorina Sea mixing component (discussion above), is further accentuated by the SFR, Finnsjön and Olkiluoto data.

At greater depths and increasing salinity the Olkiluoto groundwaters suggest a possible decrease in both the cold recharge and Littorina Sea components, although the reason for the scatter at higher salinities (> 20,000 mg/L Cl) is unclear /Pitkänen et al. 2004/.

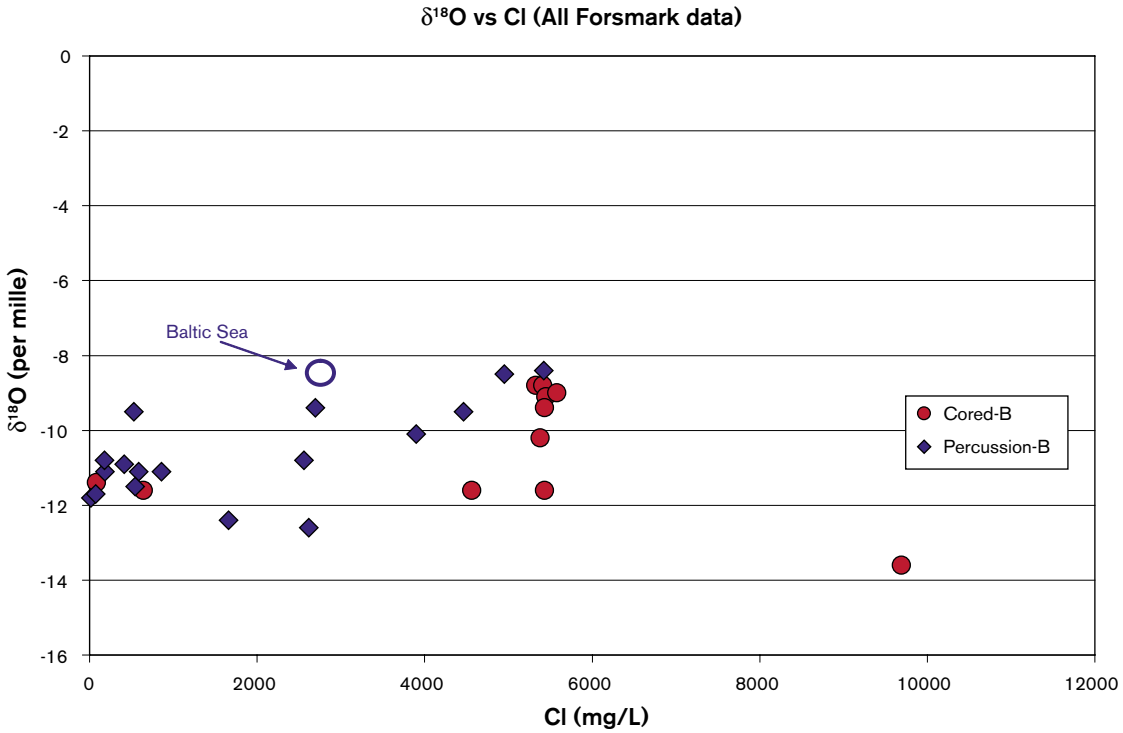

Figure 4-32. *Plot of $\delta^{18}O$ versus Cl for all Forsmark data.*

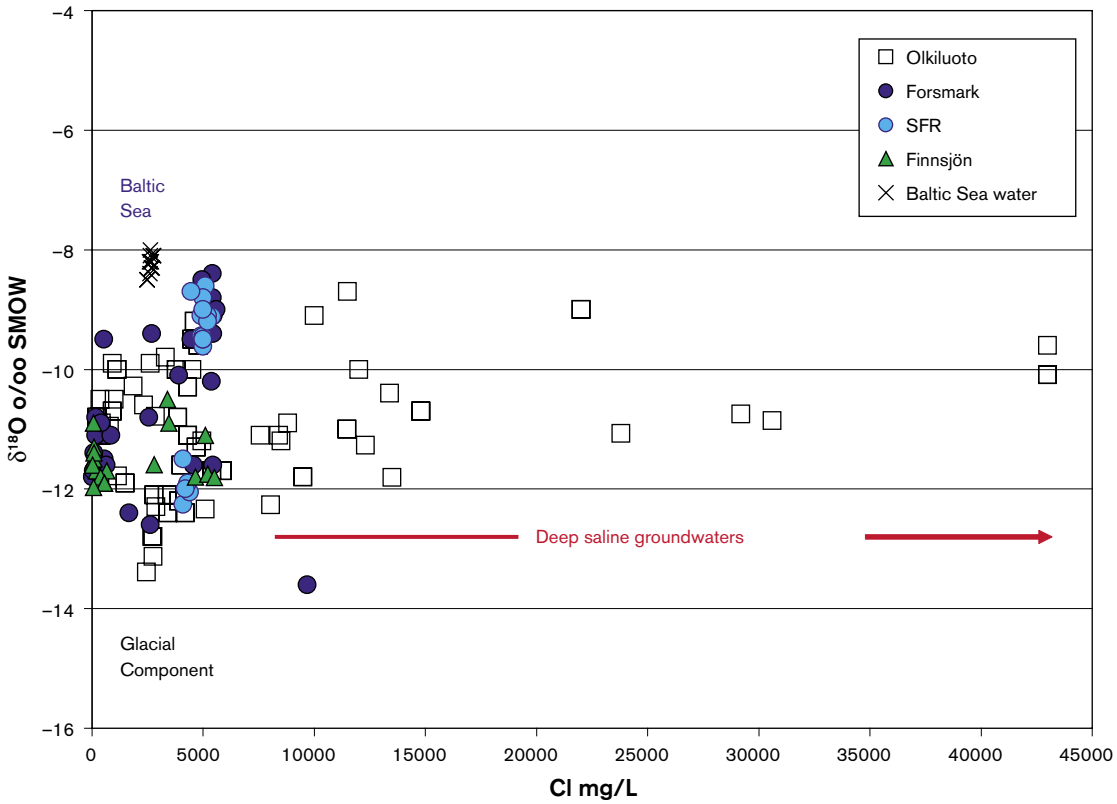

Figure 4-33. *Plot comparing all Forsmark $\delta^{18}O$ versus Cl data with other Fennoscandian sites.*

4.3 Trace element plots for all Forsmark data

This section presents data of available trace element analyses from the cored boreholes. Only a few data exist for the majority of groundwaters and even some of these are incomplete. Plotted below are some examples of trace elements for which there are enough data to indicate depth trends.

4.3.1 Cerium

Figure 4-34 shows two basic features: a) near detection cerium for most of the cored borehole groundwaters apart from those around the 400–550 m depth (i.e. corresponding to the proposed brackish Littorina Sea-type groundwaters), and b) anomalously high cerium values for three of the shallow groundwaters corresponding to SFM0001, SFM0006 and SFM0023.

4.3.2 Lanthanum

Figure 4-35 plots lanthanum against depth which, as expected, shows the same distribution and features as cerium.

4.3.3 Lithium

Figure 4-36 shows a marked increase in lithium peaking at 200 m depth. This is followed by a more gradual but consistent decrease with increasing depth, with a more rapid decrease in lithium from approx. 500 m depth, i.e. the apparent limit of the proposed brackish Littorina Sea-type groundwaters.

4.3.4 Strontium

Strontium is expected to show similarities with calcium and a distinct positive correlation between these elements is seen in Figure 4.2.59.

Strontium (Figure 4-37) shows a clear overall increase with increasing depth for the cored borehole groundwaters, but a group of four brackish groundwaters show a significant decrease from approx. 350–600 m. Also two brackish groundwaters at shallower depths (100–200 m) have similar

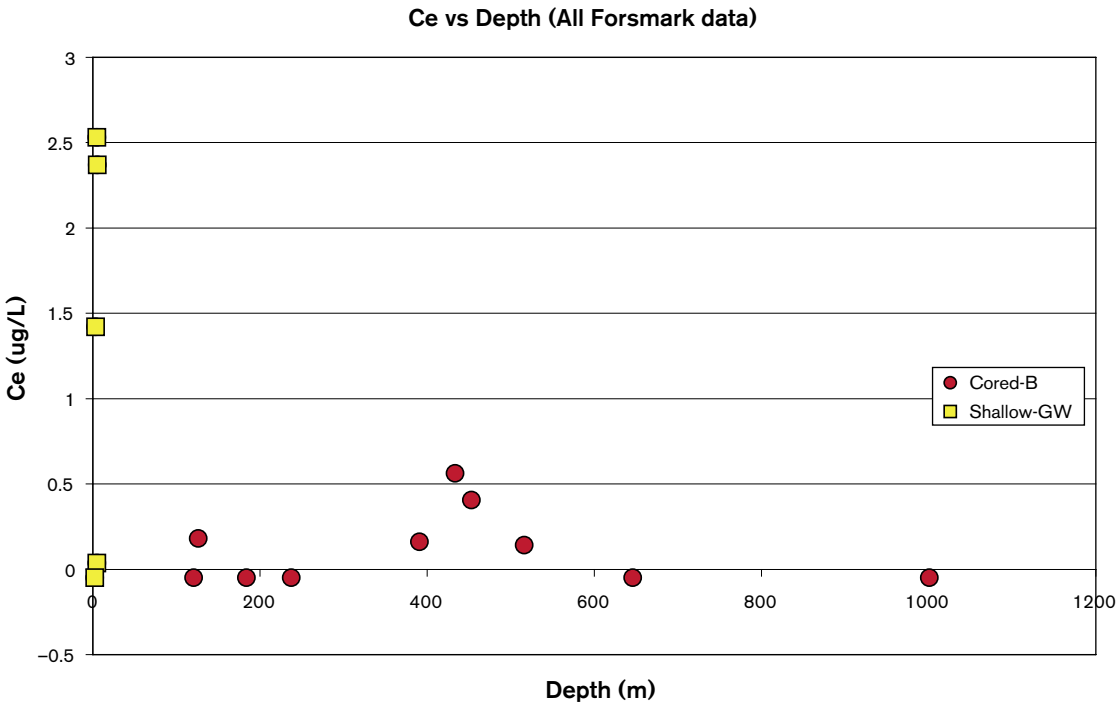

Figure 4-34. *Plot of cerium versus depth.*

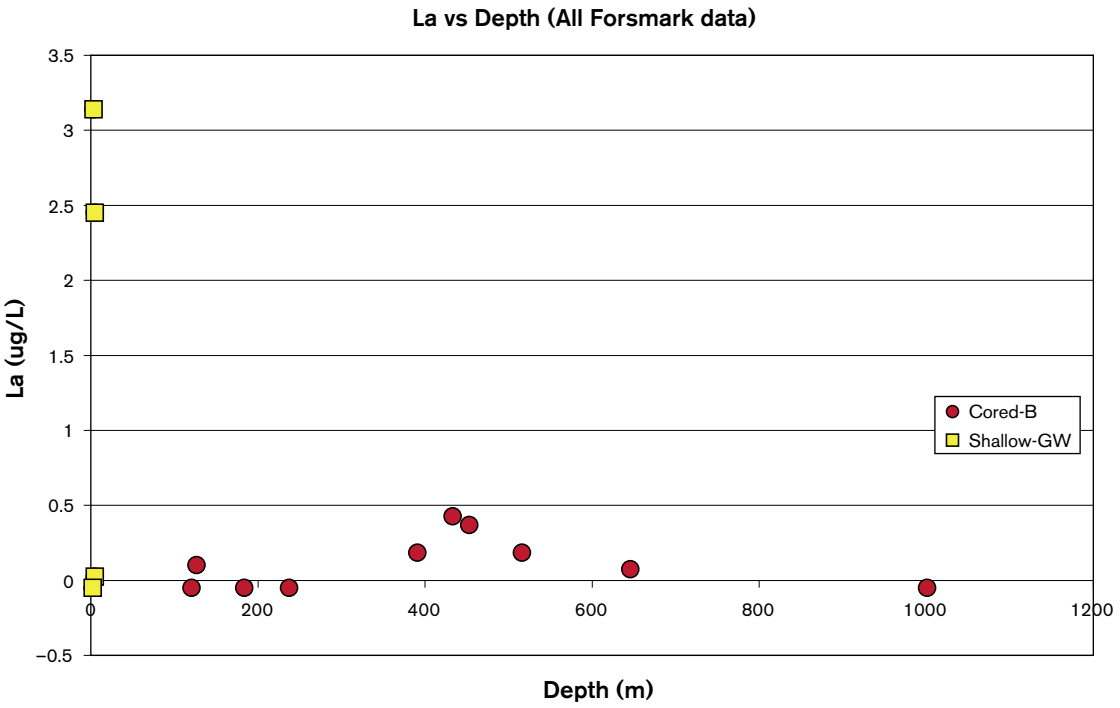

Figure 4-35. *Plot of lanthanum versus depth.*

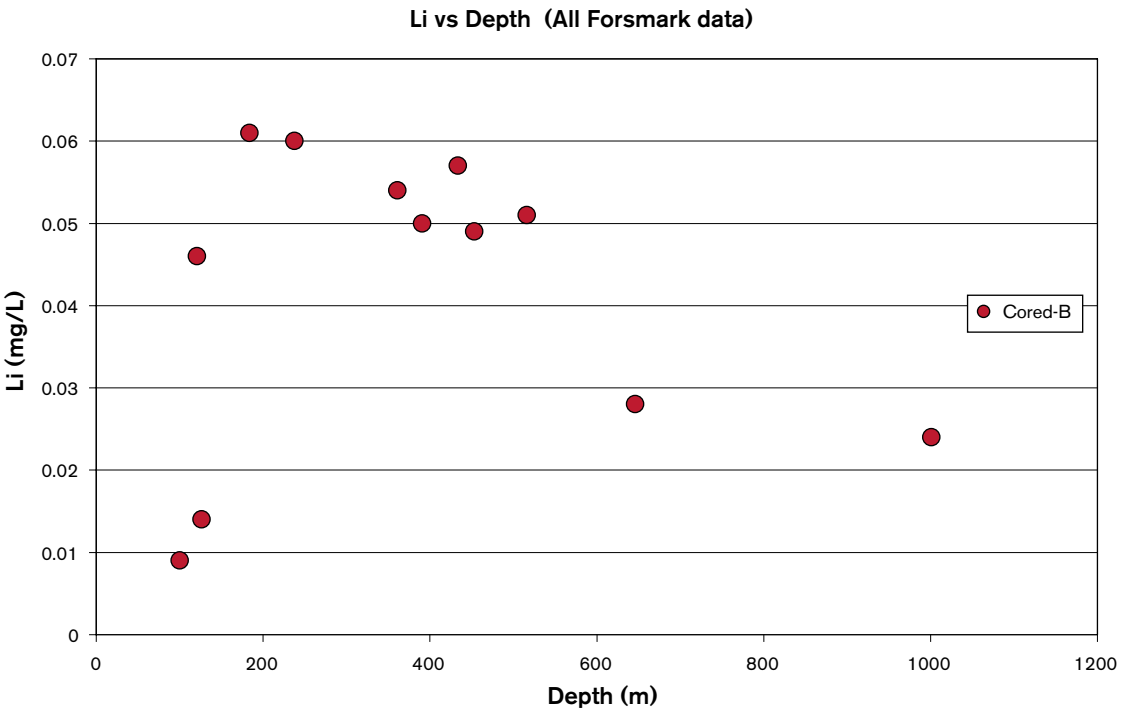

Figure 4-36. *Plot of lithium versus depth.*

strontium contents. The general strontium trend suggests water/rock interaction under increasing residence times at greater depths. The low strontium values for the brackish groundwaters (~ 5,000 mg/L Cl) from approx. 400–550 m may suggest the presence of a Littorina Sea component.

The majority of the shallow percussion borehole groundwaters are near detection, even to over 200 m depth; however exceptions do occur which follow the same increasing trend at shallow depths as the cored boreholes.

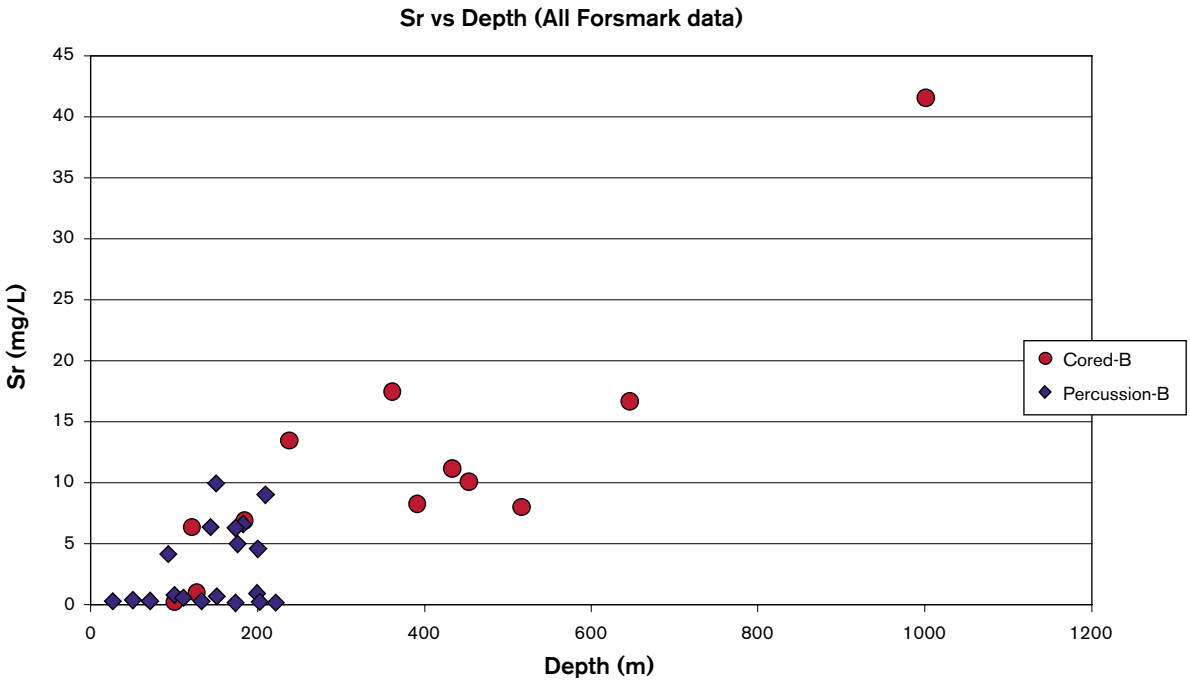

Figure 4-37. Plot of strontium versus depth.

4.3.5 Rubidium and caesium

The rubidium and caesium patterns (Figures 4-38 and 4-39), i.e. reflecting an initial rapid increase over the first 200 m followed by a more gradual decrease with increasing depth, are similar to that described for lithium suggesting a common source for all three trace elements. In these cases, unlike cerium, lanthanum and strontium, the brackish groundwaters are not anomalously high or low.

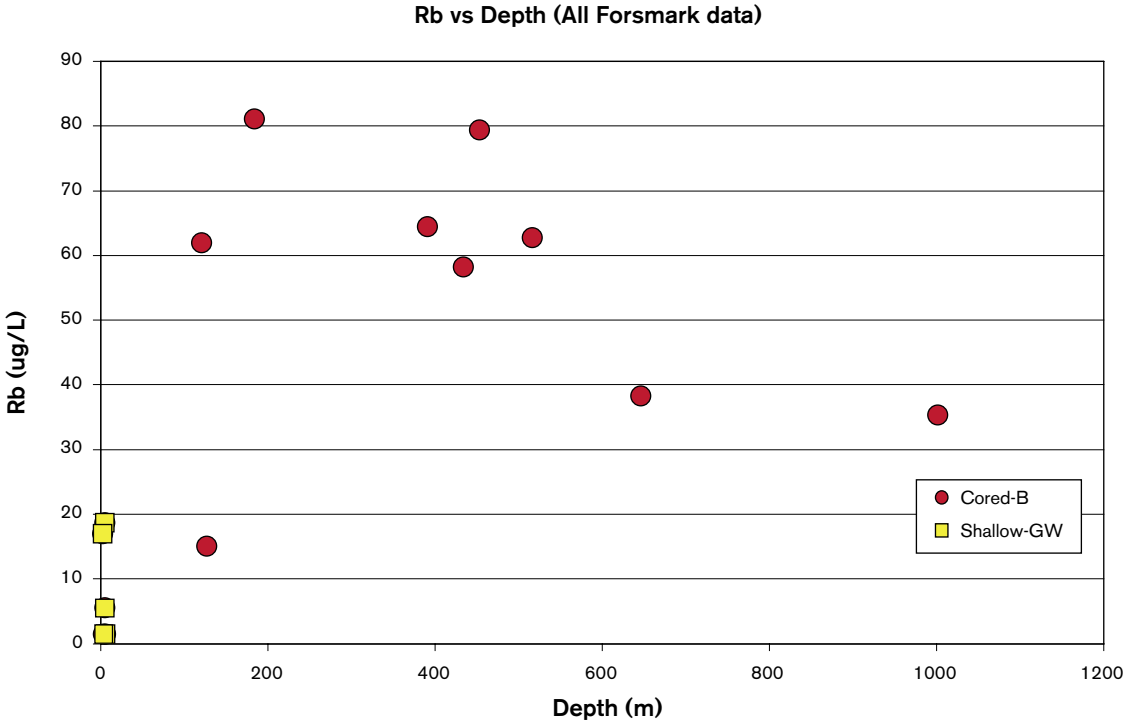

Figure 4-38. Plot of rubidium versus depth.

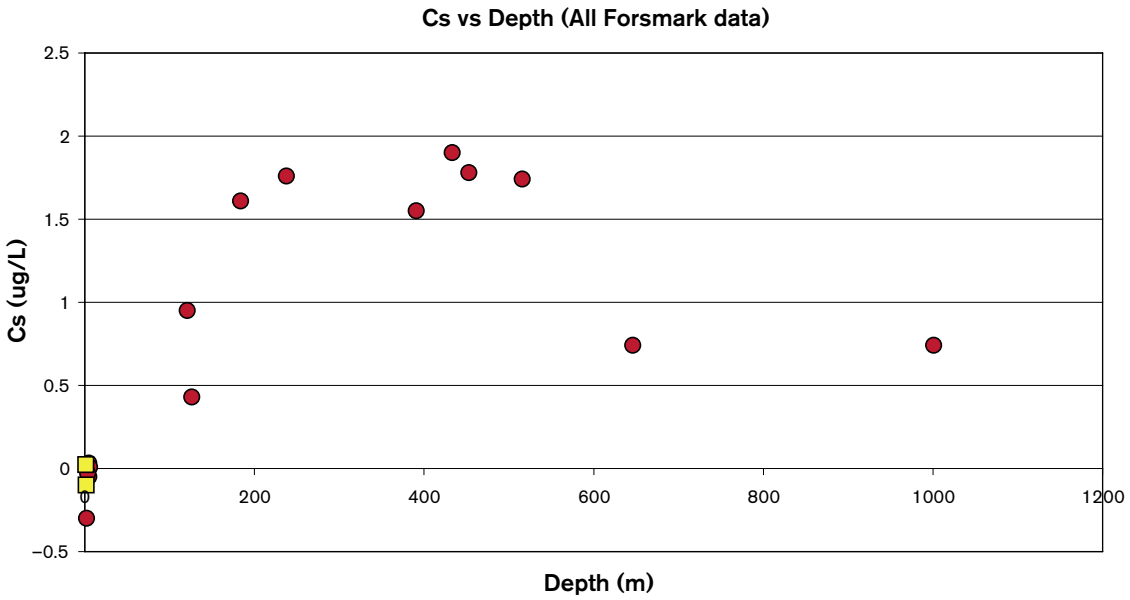

Figure 4-39. *Plot of caesium versus depth.*

4.3.6 Yttrium

Yttrium (Figure 4-40) from the cored borehole groundwaters and most of the shallow groundwaters shows a general scatter from near detection to under 3 µg/L down to approx. 550 m; at greater depths uniformly low values are suggested. Two groundwaters, one cored borehole groundwater and a shallow Soil Pipe groundwater, show anomalously high values.

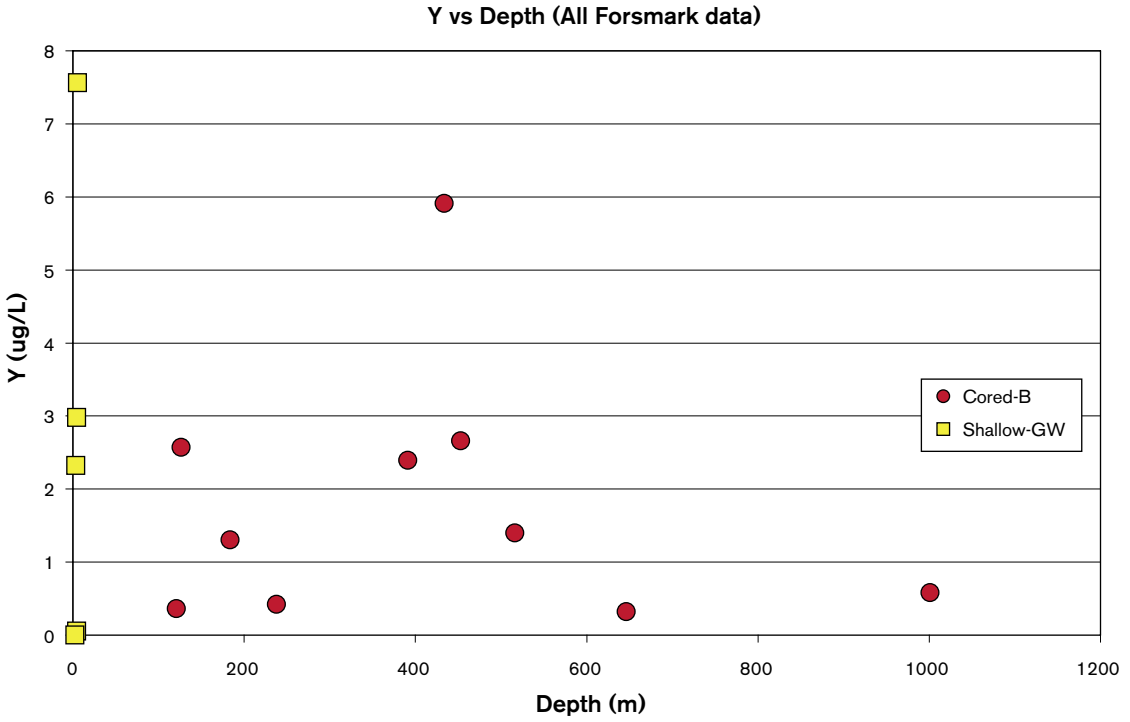

Figure 4-40. *Plot of yttrium versus depth.*

4.4 Isotope data for all Forsmark data and comparison with other fenoscandian sites

This section presents isotope data relating to tritium, carbon-13/14, sulphur-34, chlorine-37 and strontium-86/87; the boron and boron-10/11 data are incomplete and have not been evaluated at this model stage.

4.4.1 Tritium

Tritium produced by the bomb tests during the early 60´s is a good tracer for waters recharged within the past four decades. As part of an international monitoring campaign, peak values between 1,000 and 4,300 TU were recorded at Huddinge near Stockholm in the years 1963–1964 and values reaching almost 6,000 TU were recorded at Arjeplog and Kiruna northern Sweden (IAEA database). Due to decay (half life of 12 y) and dispersion, in addition to a cessation of the nuclear bomb tests, precipitation tritium values decreased so that the 8 measurements carried out at Huddinge during 1969 showed that values had dropped to between 74 and 240 TU.

Present day surface waters from the Simpevarp and Forsmarks sites show values of 7–20 TU with the exception of a few lake and stream water samples from Forsmark (Figure 4-41). Generally, the Baltic Sea samples show somewhat higher values compared to the meteoric surface waters (10.3–19.3 TU for Baltic Sea compared with 7.8–15 TU for precipitation). The Forsmark Baltic Sea samples show some values that are higher than those recorded for the Simpevarp, but the spread is large for both sites. The successive lowering of the tritium contents versus time elapsed since the bomb tests may explain the higher values in the Baltic Sea (due to reservoir effects) compared with precipitation. The difference between the Simpevarp and Forsmark Baltic Sea samples can be a north-south effect, with higher tritium values in the north compared to the south. However this is not demonstrated by the precipitation values (Figure 4-41). Moreover the ^{14}C content in the Baltic Sea water is relatively similar between the two sites (Figure 4-42). The measured tritium contents in the precipitation and Baltic Sea water at each site may also contain some tritium locally produced by the nuclear power plants, i.e. that emitted both as vapour to the atmosphere and that contained in the

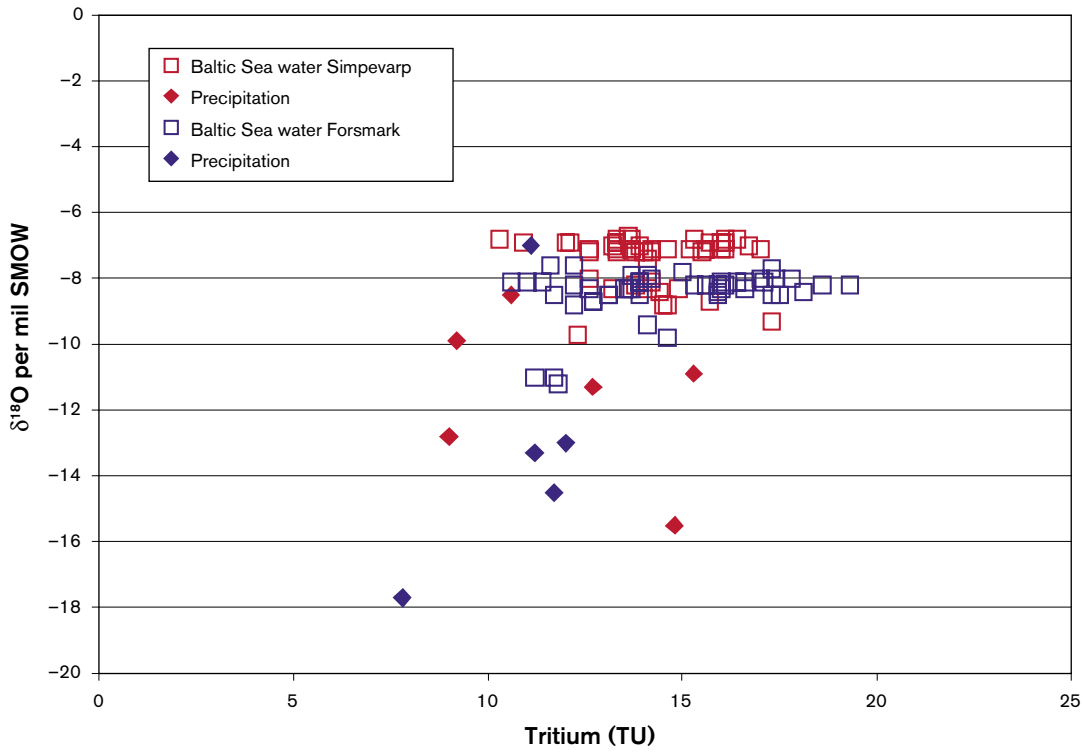

Figure 4-41. *$\delta^{18}O$ versus tritium; tritium values given as TU for Baltic Sea waters and precipitation from the Forsmark and Simpevarp sites.*

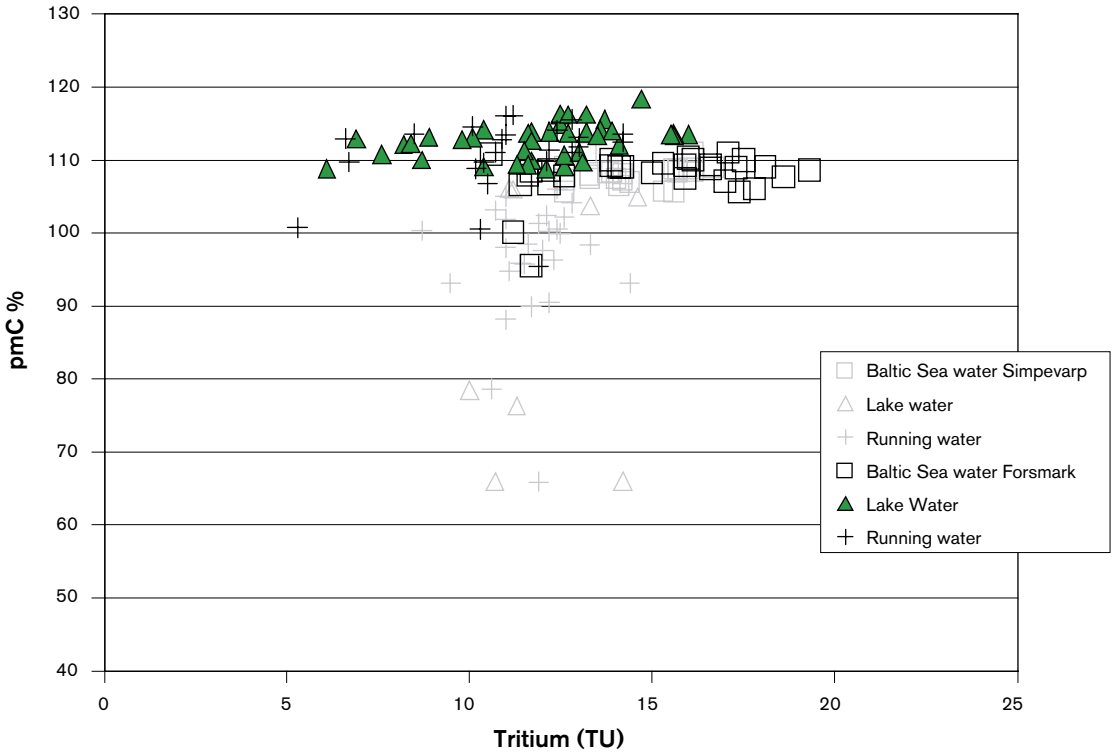

Figure 4-42. *^{14}C as pmC versus tritium for surface waters from the Forsmark area.*

cooling water discharged to the Baltic sea. This contribution is probably very low but the possibility should not be completely ruled out at the moment until background environmental tritium data become available. It should be emphasised that the precipitation values are very few, show a large variation in tritium and therefore are not considered very conclusive. Continued systematic sampling of precipitation (rain and snow) for tritium analysis therefore is encouraged.

One problem in using tritium for the interpretation of near-surface recharge/discharge is, as mentioned above, the variation in content in recharge water over time. This implies that near-surface groundwaters with values around 15 TU can be 100% recent, or a mixture of old meteoric (tritium free) water, and also a small portion (10%) of water from the sixties at the height of the atmospheric nuclear bomb tests.

The plot of tritium vs. ^{14}C for surface waters from Forsmark and Simpevarp shows large differences concerning the lake and stream waters of the two sites (Figure 4-42). In Simpevarp the lake and stream waters show a distinct decrease in ^{14}C content whereas the tritium values remain the same or show a small decrease. This may be explained by the addition to the waters of HCO_3 that originates either from calcites devoid of ^{14}C, or, due to microbial oxidation of organic material with lower (or no) ^{14}C. This is the pattern expected for near-surface waters. In Forsmark, in contrast, most lake and stream waters have higher ^{14}C values compared with Baltic Sea waters, whereas the tritium values range from 5–15 TU for all three water sources.

Since tritium contents are naturally largely variable and sometimes close to detection, the analytical data used in groundwater modelling have to be carefully scrutinised for any signs of contamination. Since it can be concluded that subsurface in-situ production of tritium is expected to be negligible in the Forsmark granitoids, the major sources of contamination will be related to drilling waters or surface waters that may have entered the borehole. Figure 4-43 shows tritium vs. percentage drilling water content in the cored boreholes from Forsmark. The drilling water used from the percussion boreholes varied in tritium content from a minimum of 1.9 TU for HFM10 to a maximum of 5.7 TU for HFM06 (cf. section 3.2). However, there is no correlation between percentage drilling water and tritium values in the sampled representative groundwaters which indicate that the drilling water was successfully removed prior to sampling.

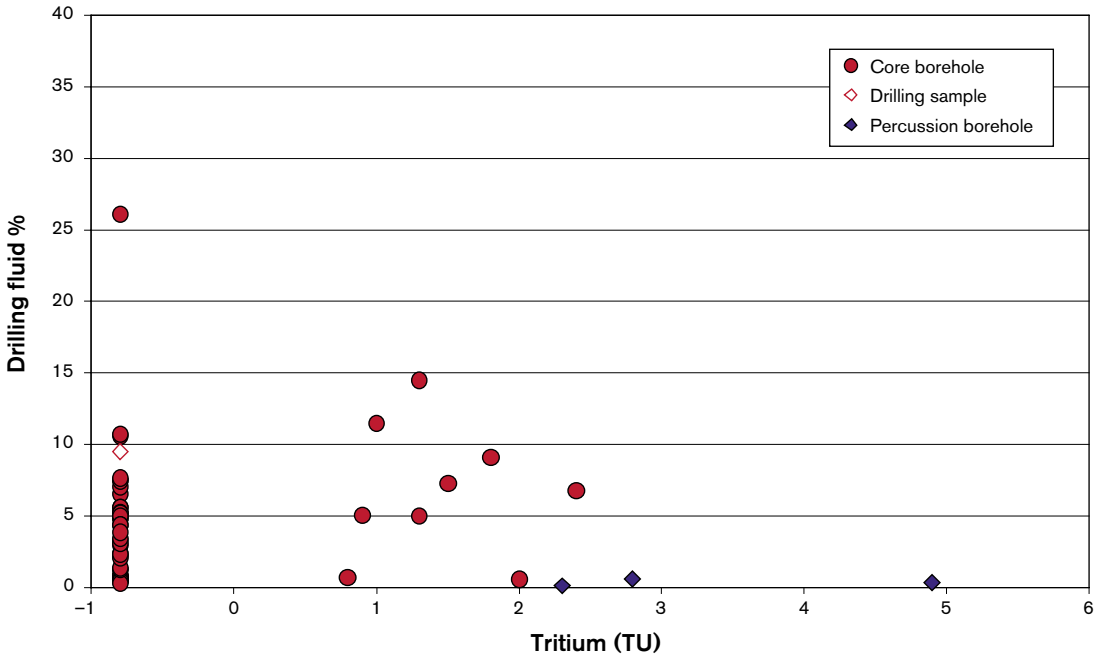

Figure 4-43. *Tritium versus drilling fluid for boreholes HFM05, KFM01A, KFM02A, KFM03A and KFM04A.*

All available tritium values from groundwaters (percussion boreholes, cored boreholes and soil pipes) are plotted versus depth in Figure 4-44. In the cored boreholes the tritium content decreases significantly in the upper 200 metres but varies considerably in the percussion boreholes. Tritium free groundwater was collected in HFM05 (25–200 m), HFM08 (0–144 m), HFM12 (0–210 m) and HFM14 (0–151 m).

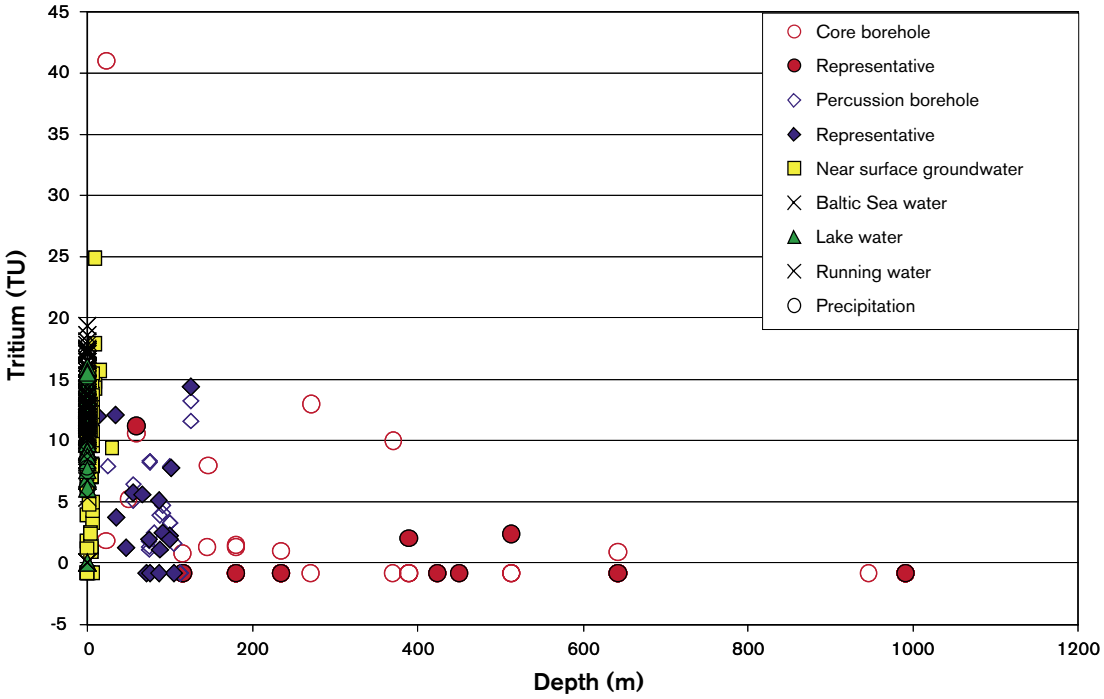

Figure 4-44. *Tritium versus depth for: a) groundwaters from cored boreholes, percussion boreholes and soil pipes, b) Baltic Sea, Lake and Stream waters, and c) precipitation.*

Below 200 m depth tritium values under 3 TU are detected for all samples. For the sections sampled below 300 m the groundwaters systematically collected from each section generally show no detectable tritium. In two cases, however, a few tritium units have been measured in the last sample in the sequence collected which for other reasons has been selected as most representative. Since at the moment it not clear why these water samples show detectable tritium contents, it is suggested that these values are used with some caution until more analyses become available.

One of the near-surface samples KFM03A (0–46 m) shows a very high tritium content of 41 TU indicative of a significant portion of recharge from the sixties or seventies when the recharge tritium contents were much higher than at present. There is therefore the possibility that the observed tritium values in some of the sampled borehole sections reflects some contamination by these tritium-enhanced waters entering into water-conducting fracture systems during open hole borehole activities. This would help to explain the presence of low tritium values and an absence of drilling water.

4.4.2 Carbon

The stable carbon isotope ratios, expressed as $\delta^{13}C$ ‰ PDB and radiocarbon contents (^{14}C) expressed as pmC, have been analysed on dissolved HCO_3 from surface waters and groundwaters (Figures 4-45 and 4-46).

Baltic Sea waters have ^{14}C values around 110 pmC and $\delta^{13}C$ values mostly between –2 and –7‰ produced by equilibria with atmospheric CO_2. The lake and stream waters show increasing input of biogenic carbon seen as increased HCO_3 contents, decreased $\delta^{13}C$ values and, somewhat surprisingly, a small increase in ^{14}C (110–120 pmC are measured in many of the lake and stream waters). The stable carbon isotopes indicate exchange with biogenic CO_2 and it is therefore reasonable to assume that breakdown of ^{14}C-enriched organic material has contributed to the somewhat higher values. Several reasons for the ^{14}C enrichments in the organic material at Forsmark are possible, but the main candidate is uptake of radioactive CO_2 emitted into the atmosphere by the nearby nuclear power plant /cf. Eriksson, 2004/. Part of this radioactive CO_2 is incorporated in plants (due to photosynthesis), and successive microbial breakdown of this material will contribute ^{14}C-rich CO_2 to the lake and stream waters.

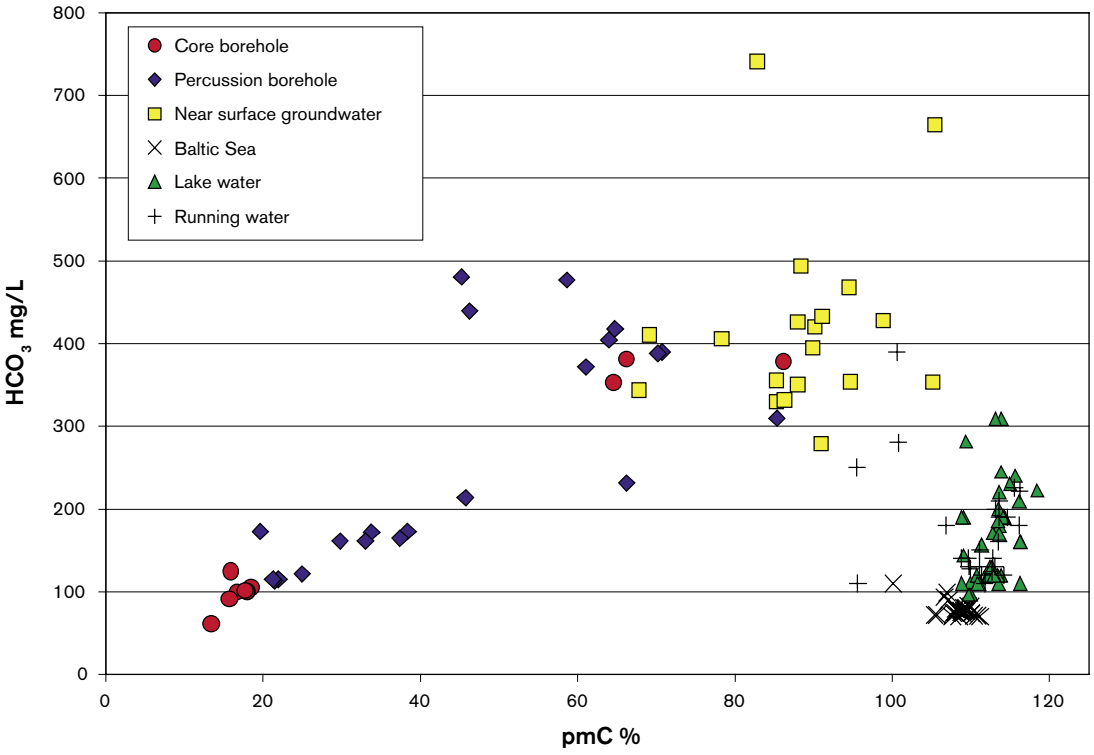

Figure 4-45. *pmC (HCO_3) versus HCO_3 in surface and groundwaters from the Forsmark area.*

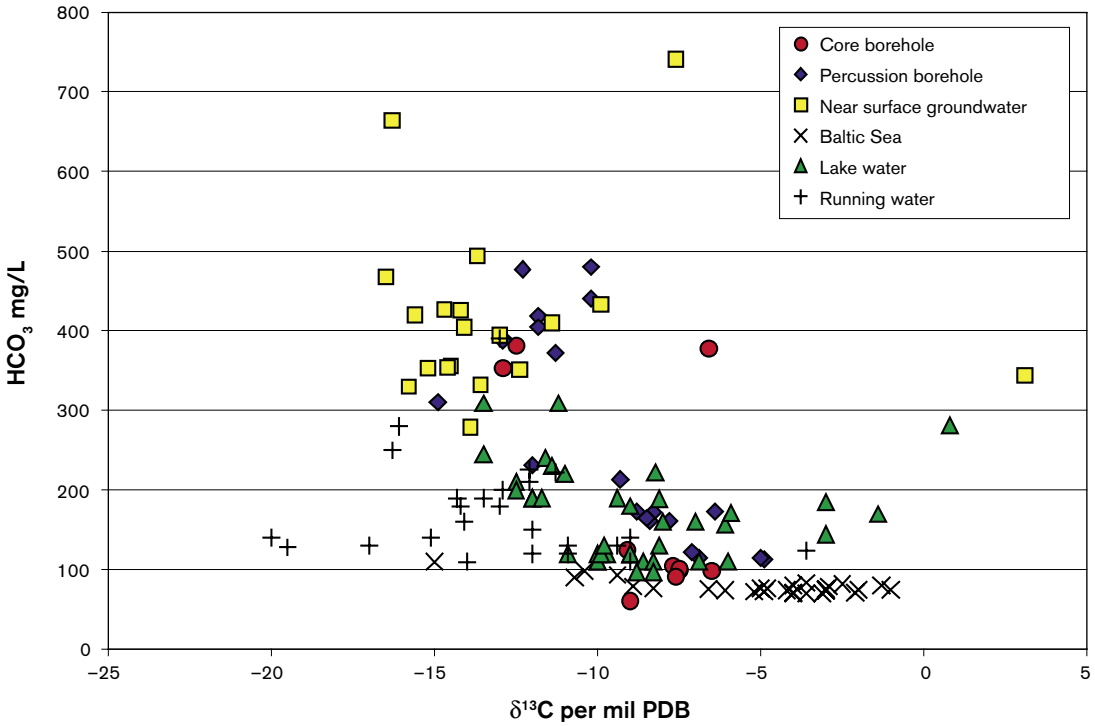

Figure 4-46. *$\delta^{13}C$ (HCO_3) versus HCO_3 in surface and groundwaters from the Forsmark area.*

The highest HCO_3 values are produced in the near-surface groundwaters and in some of the percussion boreholes (cf. Figure 4-7). HCO_3 contents between 300 and 500 mg/L are common in these waters and the $\delta^{13}C$ values are generally between –10 to –17‰ indicating a dominantly biogenic carbon source. However, the ^{14}C contents in these waters are lower, ranging from 80–100 pmC for most surface waters and 60–80 pmC for the high bicarbonate waters sampled in the percussion boreholes. Also, a few shallow samples from the cored boreholes are included in this group. Most of the high bicarbonate waters have detectable tritium values (cf. Figure 4-47) and ^{14}C decay effects are therefore regarded as insignificant. Instead, breakdown of older organic material or contribution of dissolved carbonate minerals (with no ^{14}C) is suggested.

The tritium-free groundwaters from Forsmark show ^{14}C values in the range 14–25 pmC and these waters have generally low HCO_3 contents (< 150 mg/L) and $\delta^{13}C$ values between –10 and –5‰. Figure 4-48 of ^{14}C (expressed as pmC) versus $\delta^{13}C$ ‰, shows that groundwaters from the percussion and cored boreholes indicate a mixing trend between: a) HCO_3-rich waters with low $\delta^{13}C$ and high ^{14}C content, and b) deeper groundwaters with lower $HC0_3$ contents, higher $\delta^{13}C$ values and lower ^{14}C. To date there are no groundwaters analysed from below depths of 550 m.

The groundwaters showing the lowest ^{14}C values have chloride contents ranging from 4,500–5,500 mg/L (Figure 4-49); these indicate marine signatures, i.e. they represent waters with a dominant Littorina Sea component. In terms of ‘relative age’, the measured pmC values indicate 11,000–16,000 years which is significantly older than the Littorina Sea period. This can be explained by an addition of older bicarbonate, probably by dissolution of older carbonate and/or mixing by glacial water (supported by low $\delta^{18}O$ in at least some of these groundwaters).

The plot of ^{14}C content versus depth (Figure 4-50) shows, as expected, a decreasing trend with depth. All groundwaters deeper than 200 m show values below 20 pmC . Together, the distribution of ^{14}C and tritium versus depth supports the occurrence of an upper 100–200 m hydraulically dynamic section and a significantly less dynamic situation at greater depth. This is further supported by the major ion chemistry.

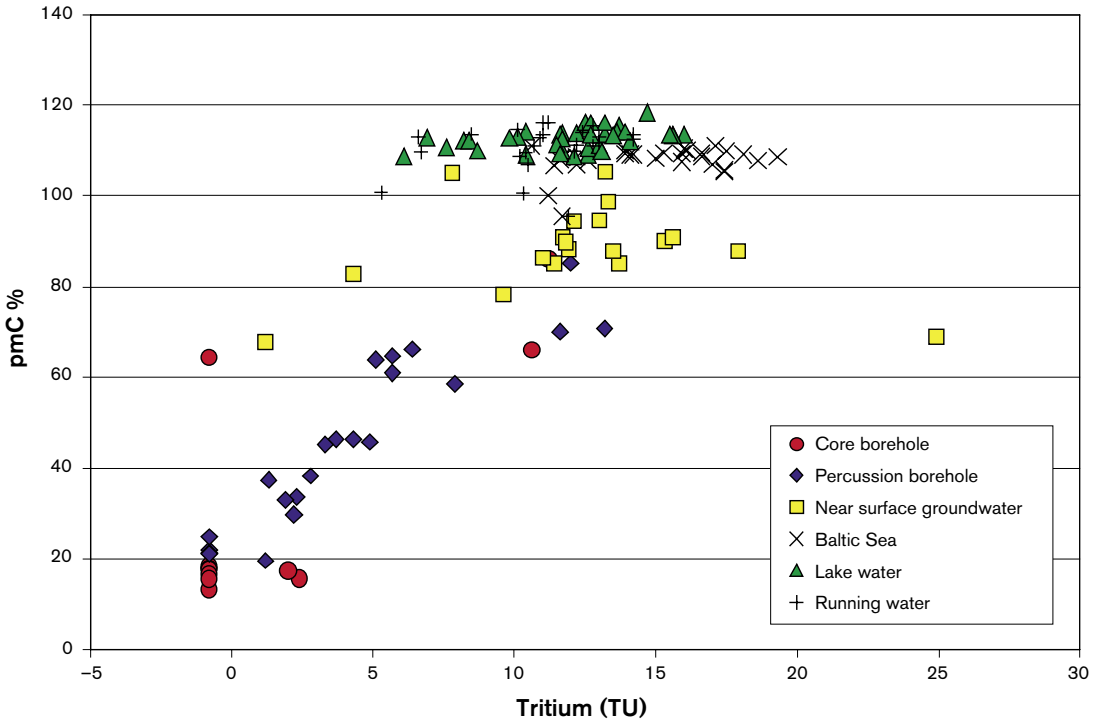

Figure 4-47. *pmC (HCO_3) versus tritium in surface and groundwaters from the Forsmark area.*

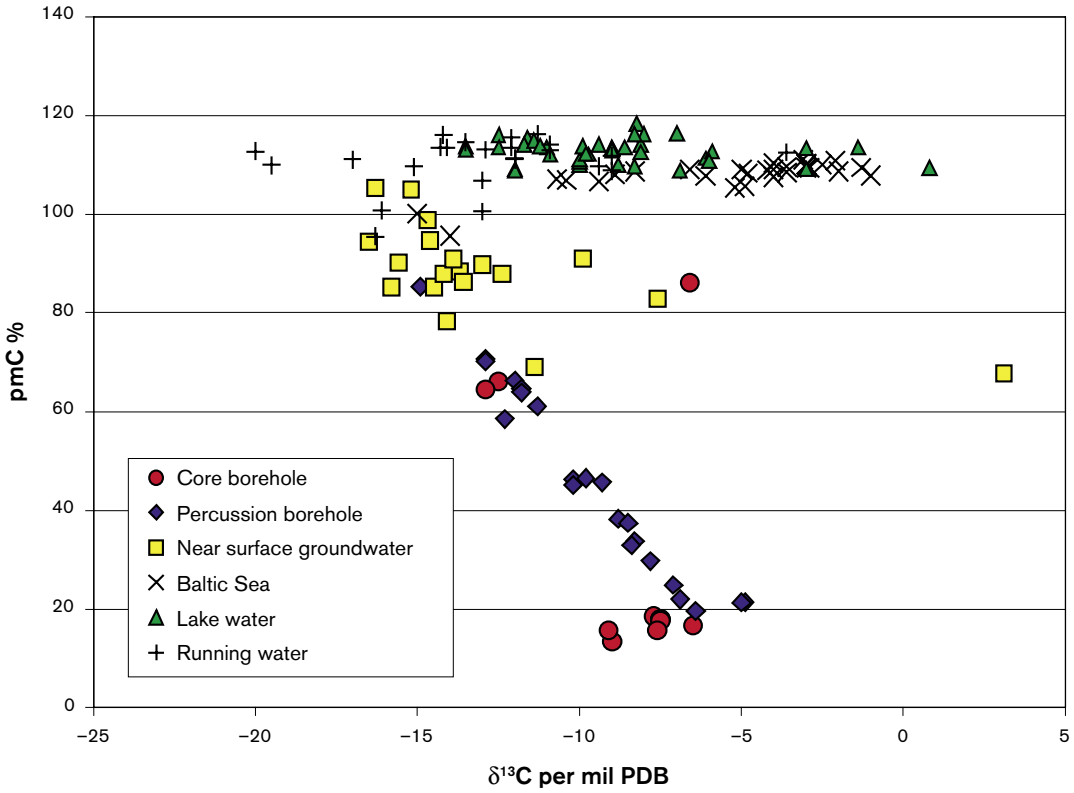

Figure 4-48. *$\delta^{13}C$ versus ^{14}C (pmC) in bicarbonates in surface waters and groundwaters from the Forsmark area.*

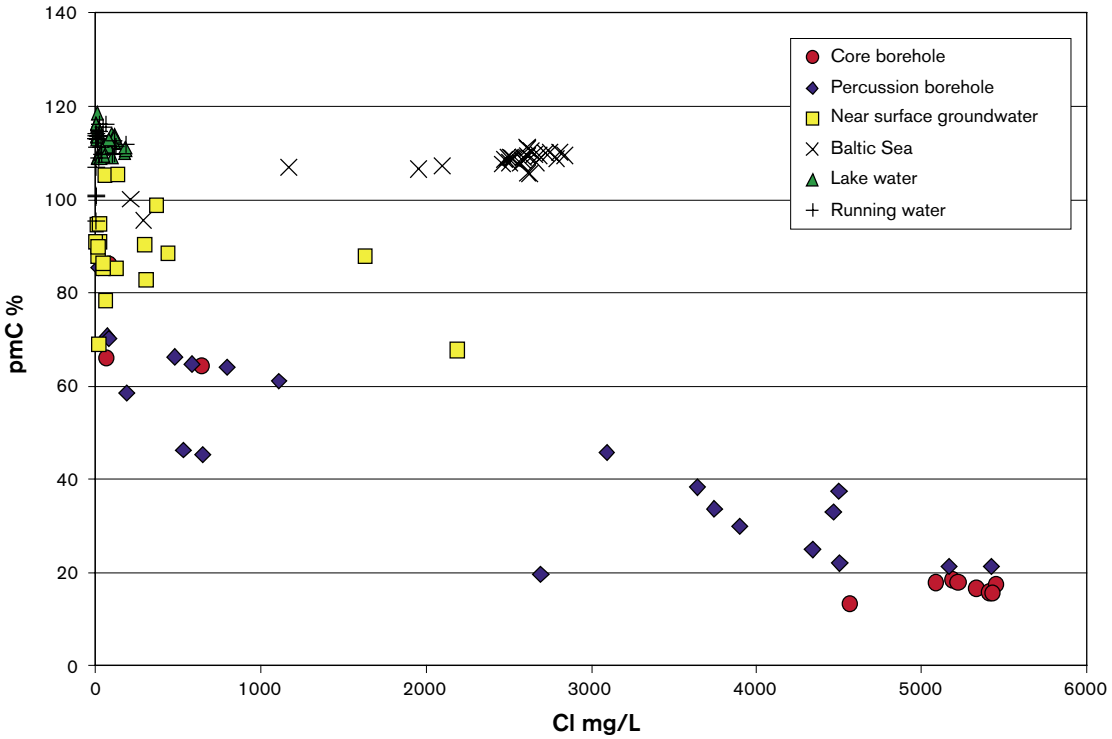

Figure 4-49. *$^{14}C(HCO_3)$ as pmC versus Cl in surface waters and groundwaters from the Forsmark area.*

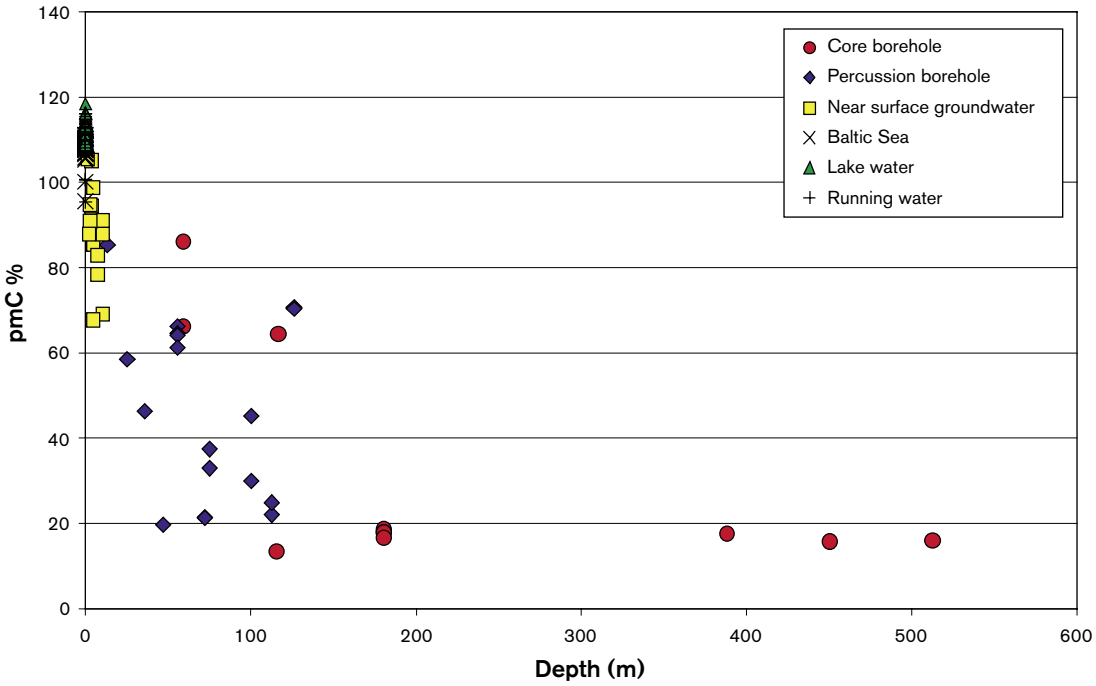

Figure 4-50. *$^{14}C(HCO_3)$ as pmC in surface waters and groundwaters from the Forsmark area.*

Two organic material samples from KFM01A (110 m and 177 m) have been analysed for ^{14}C resulting in values of 53.20 and 46.4 pmC. These values should be compared with those measured on HCO_3 samples from the same sampled borehole sections which show values of 13.4 and 16.7 pmC. Earlier interpretation of these waters as being mainly mixtures of glacial and Littorina Sea water is not contradicted by these results, but indicate also the possibility of a Littorina origin for the organic material and support of a more mixed origin for the bicarbonate.

4.4.3 Sulphur

Sulphur isotope ratios, expressed as $\delta^{34}S$ ‰ CDT, have been measured in dissolved sulphate in groundwaters, surface Lake and Stream waters and Baltic Sea water samples from the Forsmark area. Some 73 analyses have been performed of which 33 are groundwaters from cored and percussion boreholes. The isotope results are plotted against SO_4 (Figure 4-51) and Cl (Figure 4-52).

The recorded values in Figure 4-51 have a wide range (–11 to +30‰ CDT) indicating different sulphur sources for the dissolved SO_4. For the surface waters (lake and stream waters) the SO_4 content is usually below 35 mg/L and the $\delta^{34}S$ is relatively low but variable (–1 to +11‰ CDT) with most of the samples in the range 2 to 8‰ CDT. These relatively low values indicate atmospheric deposition and oxidation of sulphides in the overburden as being the origin for the SO_4. Unfortunately there are no isotopic analyses of sulphides in the overburden, but a few (6) $\delta^{34}S$ values of pyrites in fracture coatings have been analysed and show a large spread in values (5.4 to 31.5‰ CDT; (Sandström et al. in press).

The Baltic Sea samples cluster around 20‰ CDT with some less saline Baltic samples showing lower $\delta^{34}S$ values resulting from inmixing of surface water.

The deeper groundwaters show $\delta^{34}S$ values in the range +12 to +26‰ CDT where all samples with SO_4 contents greater than 250 mg/L show $\delta^{34}S$ values higher than +20‰ CDT. Such values are usually interpreted to result from sulphate-reducing bacterial (SRB) activity in the bedrock aquifer. The Cl versus $\delta^{34}S$ plot (Figure 4-52) shows a clear trend with higher $\delta^{34}S$ values for groundwaters with higher salinities than present Baltic Sea waters (2,800 mg/L Cl). If the $\delta^{34}S$ values in the marine groundwaters are modified by SRB during closed conditions then a clear trend of more positive $\delta^{34}S$ values with decreasing sulphate content should be the result. This is not seen and therefore several processes need to be considered. The groundwater with the highest salinity showed a relatively low sulphate content (64 mg/L) and a $\delta^{34}S$ value of +23‰ CDT. However, this was a tube sample (not plotted) and is probably the product of mixing. The only identified sulphate minerals so far are minute grains of barite found in a few fracture coatings /Sandström et al. 2004/.

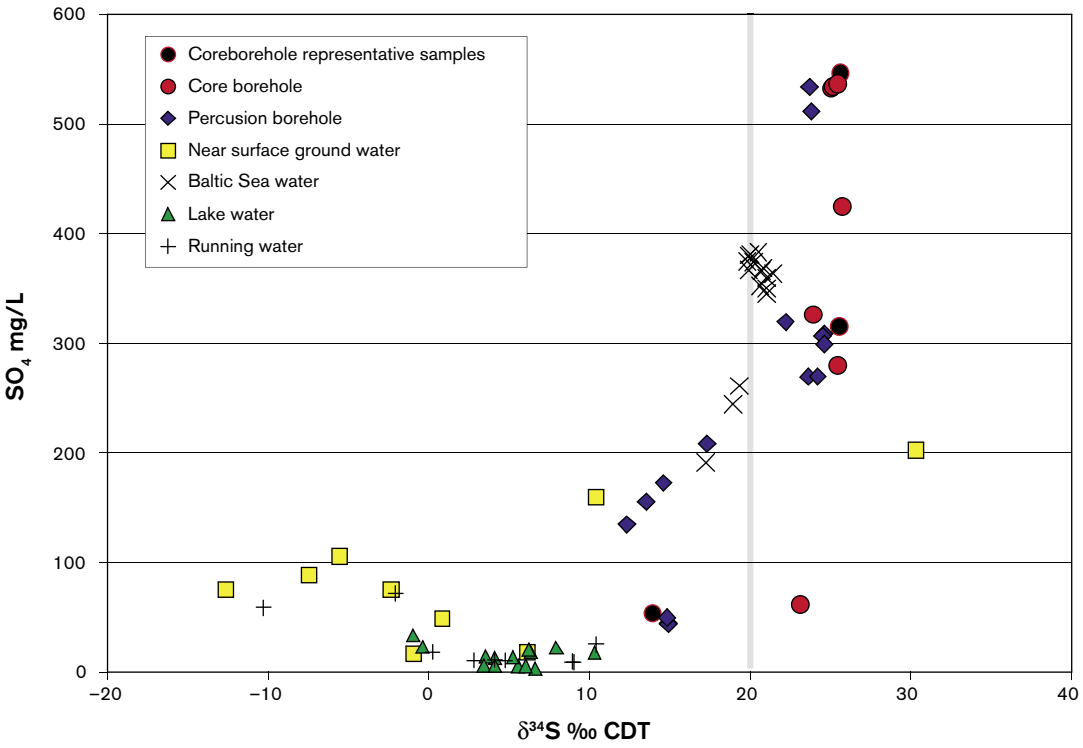

Figure 4-51. *$\delta^{34}S$ versus SO_4 in surface waters and groundwaters from the Forsmark area. The grey line indicates the marine median value around 20‰ CDT.*

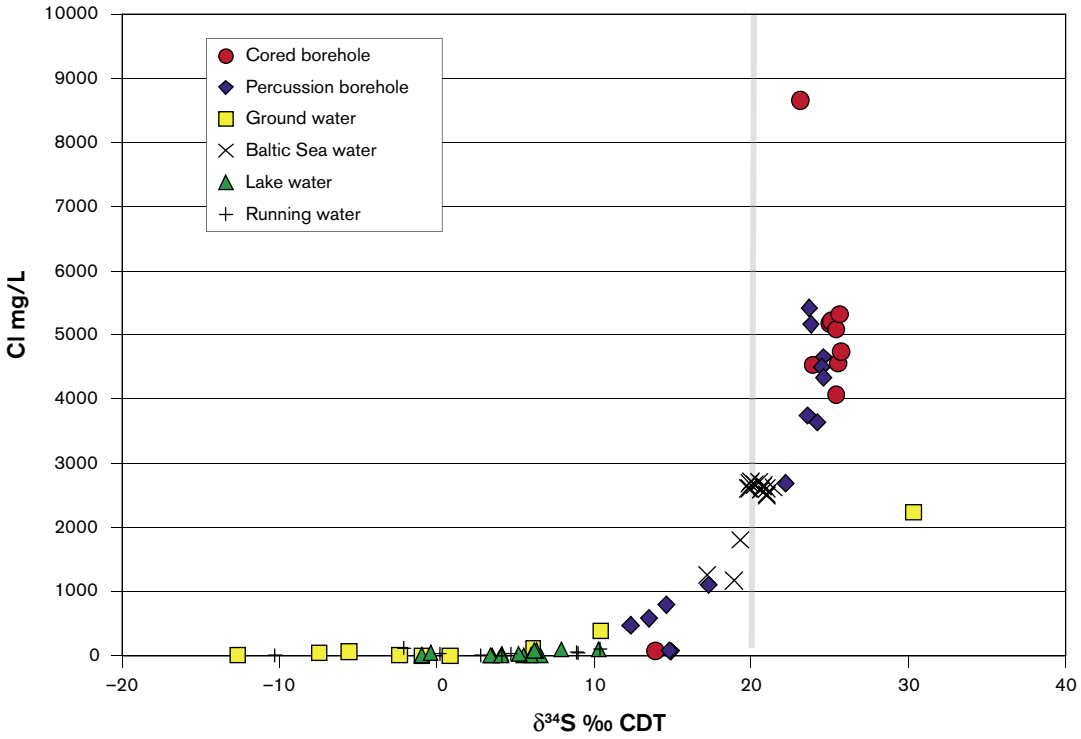

Figure 4-52. *$\delta^{34}S$ versus Cl in surface waters and groundwaters from the Forsmark area. The grey line indicates the marine median value around 20‰ CDT.*

Amongst the Soil Pipe near-surface groundwaters, one smore brackish sample (2,200 mg/L Cl) showed a relatively high $\delta^{34}S$ value (+30‰ CDT). This originates from Bolundsfjärden (Figure 1-27; sample 0012) which is believed to have a typical discharge character. Other near-surface groundwater samples showed values similar in range, or even lower, than surface waters. The cause of these very low values is not fully understood at the moment.

4.4.4 Strontium

^{87}Sr is a radiogenic isotope produced by the decay of ^{87}Rb (half-life 5×10^{10}a). Marine waters show a distinct Sr isotope signature (0.7092) which is very close to the measured values in the Baltic Sea waters, whereas all other waters show higher Sr isotope ratios indicating contributions of radiogenic Sr; this is explained by water-rock interaction processes involving Rb containing minerals.

Strontium isotope ratios ($^{87}Sr/^{86}Sr$) have been measured in surface waters and groundwater samples from the Forsmark area and these are plotted against Sr content in Figure 4-53. The surface waters and especially the near-surface ground waters show large variation in Sr isotope ratios. Most of the samples show values within the range 0.718 to 0.729 whereas a few near-surface groundwaters have lower values indicating mixing with marine water and a few have significantly higher values indicating local exchange with Rb-rich minerals. The groundwaters sampled in the percussion and cored boreholes show Sr isotope ratios varying within a more narrow range (0.717 to 0.721). Some of these higher values relate to the group of four brackish groundwaters of low strontium values (cf. Figure 4-37) associated with Littorina Sea signatures.

A common way to evaluate mixing between different strontium origins is to plot 1/Sr versus $^{87}Sr/^{86}Sr$ (Figure 4-54); no significant trends can be observed. It should, however, be pointed out that relatively few deep sections have been analysed so far. The groundwaters sampled from borehole KFM01A (110–121 and 177–184 m) show somewhat higher Sr isotope ratios than the other groundwater samples which probably relates to the mineralogical compositions along the pathways. Since many of the groundwaters have dominant portions of a marine origin (i.e. Littorina Sea component), a marine input could have been expected. However, this is not recognised in the plot.

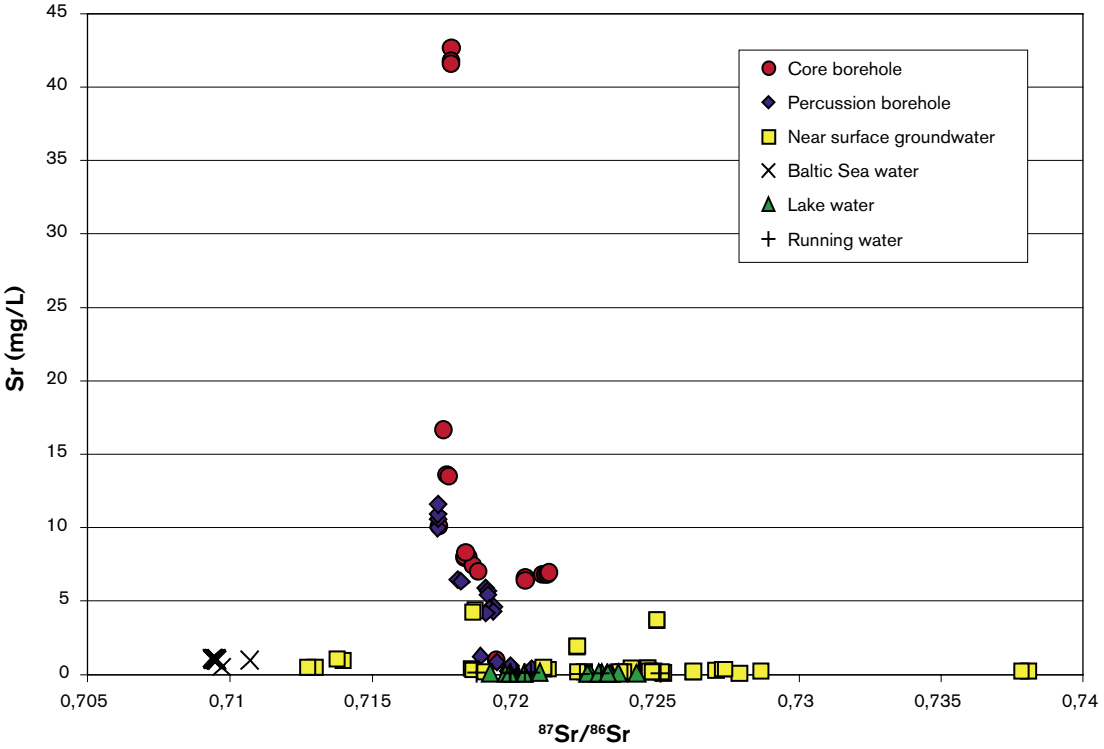

Figure 4-53. *$^{87}Sr/^{86}Sr$ versus Sr for Baltic Sea waters, surface waters and groundwater samples from the Forsmark area.*

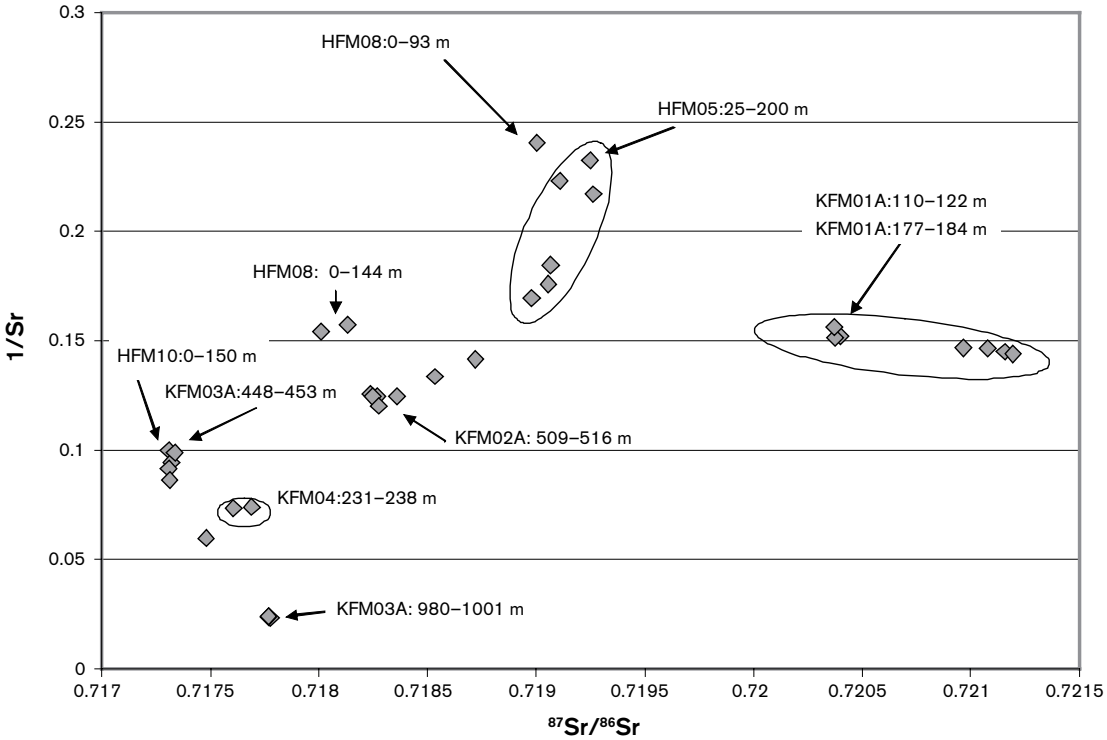

Figure 4-54. *$^{87}Sr/^{86}Sr$ versus 1/Sr in groundwaters from the Forsmark area.*

From the calcium versus strontium diagram for the groundwater samples (Figure 4-55), calcium and strontium correlate and both have been added to the original Na-Cl dominated water so that the original Sr content (~ 2 mg/L, i.e. twice the values measured in present day Baltic Sea) has increased to 6–10 mg/L Sr. Leaching of minerals and ion exchange are the reason for this.

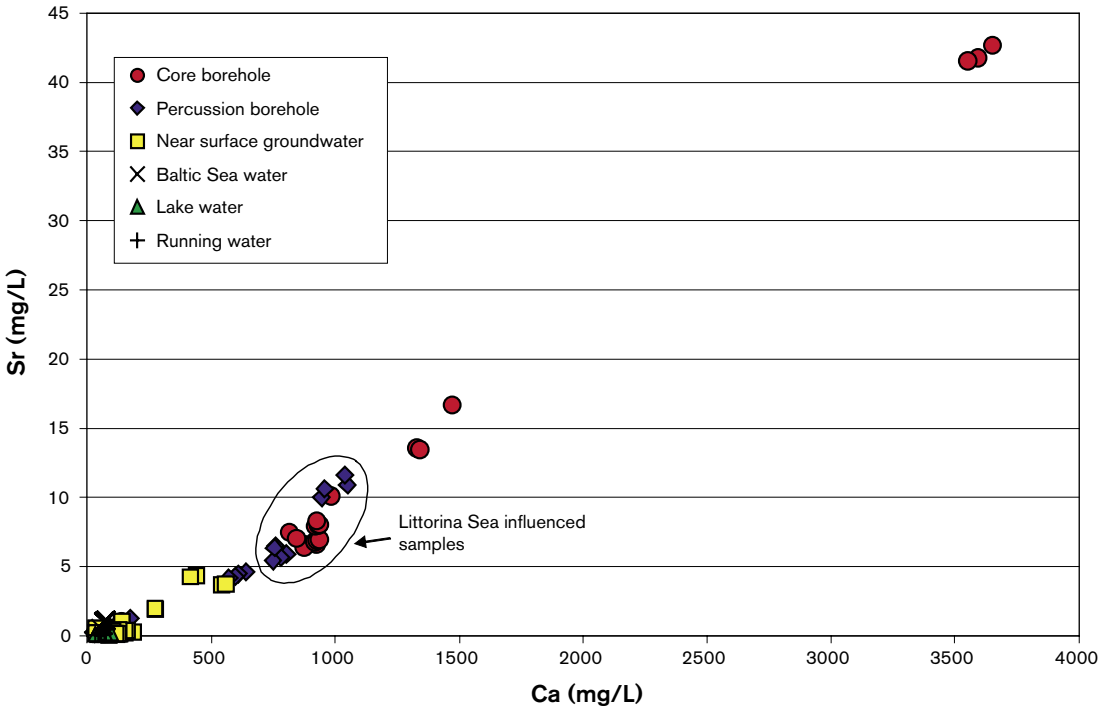

Figure 4-55. *Sr versus Ca in surface waters, Baltic Sea waters and groundwater samples from the Forsmark area.*

In conclusion, the strontium isotope values of surface and near-surface waters show relatively large variations in isotope ratios whereas the deeper groundwaters vary within a more limited range. All the isotope values deviate from those measured in the Baltic Sea samples in that they have higher radiogenic strontium which in turn is due to water/rock interaction, probably to a large part ion exchange processes.

The relatively few fracture calcites so far analysed for Sr-isotopes show values below 0.718 supporting that they are not precipitated from today's groundwater and that calcite dissolution has had little influence on the Sr-isotope ratios in the groundwater. Other minerals are more important and analysis of fracture minerals and host rock samples is recommended to achieve a better understanding of the Sr (and Ca) system.

Figure 4-56 compares the Forsmark site with the Simpevarp, Laxemar and Ävrö sites, together with modern Baltic Sea waters. The relatively small variation in Sr-isotope ratios within each area suggests that ion exchange with clay minerals along the flow paths is an important process. For the Laxemar-Simpevarp sites there is a tendency towards higher contents of radiogenic Sr in the groundwaters with highest salinities (and thus highest Sr content). It is not, however, possible from the few data available to give any explanation for this. There seems not to be any major change in mineralogy that can explain a shift, but one possibility may be the increased residence times for these waters leading to more extensive mineral/water interactions. The higher $^{87}Sr/^{86}Sr$ ratios in the Forsmark samples are most probably due to differences in the composition of the bedrock and fracture minerals compared to Simpevarp. The possibility of tracing marine components using Sr-isotopes is often discussed; however clay minerals in the fractures may question such interpretations. For example, the strong Littorina Sea imprint in the Forsmarks waters has not resulted in any detectable marine Sr isotope values in the groundwaters. Instead, modification of the Sr isotope values probably by ion exchange has taken place.

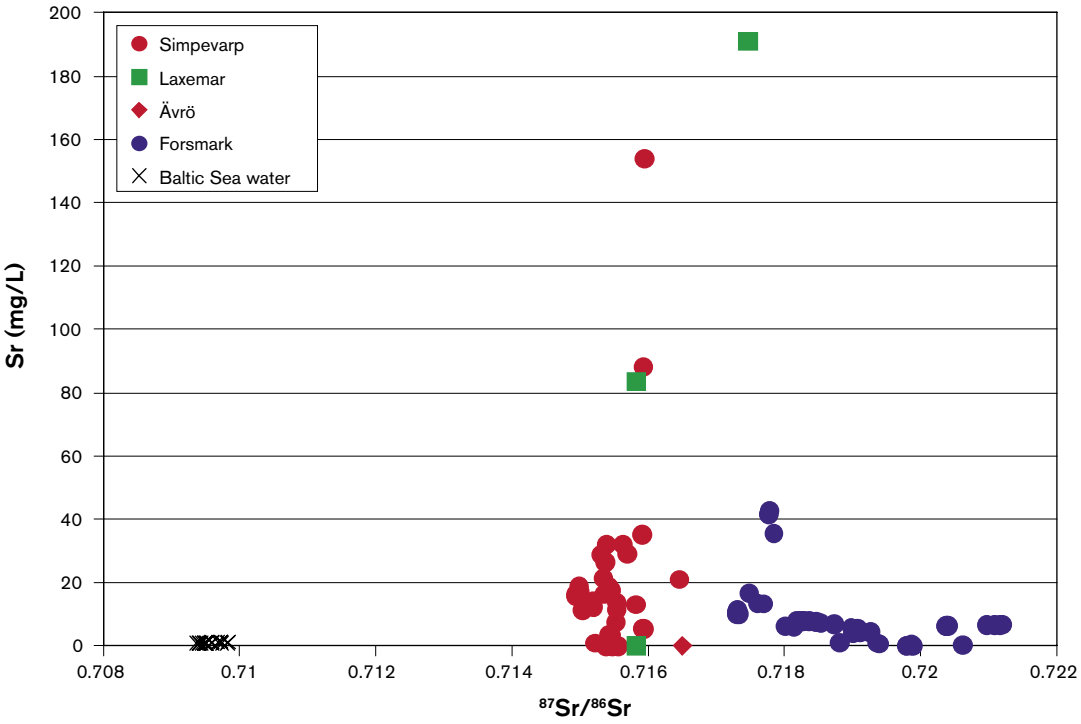

Figure 4-56. *$^{87}Sr/^{86}Sr$ versus Sr in groundwaters from Simpevarp, Laxemar, Ävrö and Forsmark. Baltic Sea waters sampled from the two sites are also plotted.*

4.4.5 Chlorine

Stable chlorine isotopes have been analysed in waters from the Forsmark area and the results are plotted against chloride in Figure 4-57. This shows that most of the surface and Baltic Sea waters have values within the range –0.28 to +0.34‰ SMOC. The surface waters and the near-surface groundwaters have the greatest spread (–06 to +2‰ SMOC) where most of the samples are within the interval –0.2 to +05‰ SMOC. The majority of the Baltic Sea samples values are close to 0‰ SMOC or slightly higher (up to +0.3‰ SMOC), a few samples show also lower values down to –0.6‰ SMOC.

Waters from the cored and percussion boreholes are between –0.2 to +0.6‰ SMOC and demonstrate no relation with increasing chloride content. Given the analytical uncertainty of around ±2‰ SMOC /Frape et al. 1996/, the groundwater values correspond to a slight emphasis on a water/rock origin.

The $\delta^{37}Cl$ values in groundwaters from Forsmark and Laxemar/Simpevarp have been compared with chloride (Figure 4-58) together with additional Baltic Sea samples from the Simpevarp area. For brackish groundwaters with chloride contents around 5,000 mg/L there is a large variation in $\delta^{37}Cl$ values; most of the Forsmark samples have slightly negative values whereas the Simpevarp samples have values on the positive side. In groundwaters with higher chloride contents (> 6,000 mg/L) the Simpevarp and Laxemar samples have values higher than 0.3‰ SMOC. The Forsmark sample (only one available so far) shows 0.09‰ SMOC.

Br/Cl versus $\delta^{37}Cl$ (Figure 4-59) show that waters significantly enriched in bromide compared to marine waters display positive $\delta^{37}Cl$ values. The groundwaters at Forsmark, characterised by marine Br/Cl ratios, also cluster around 0‰ SMOC, although a similar spread is also shown by the Baltic Sea samples.

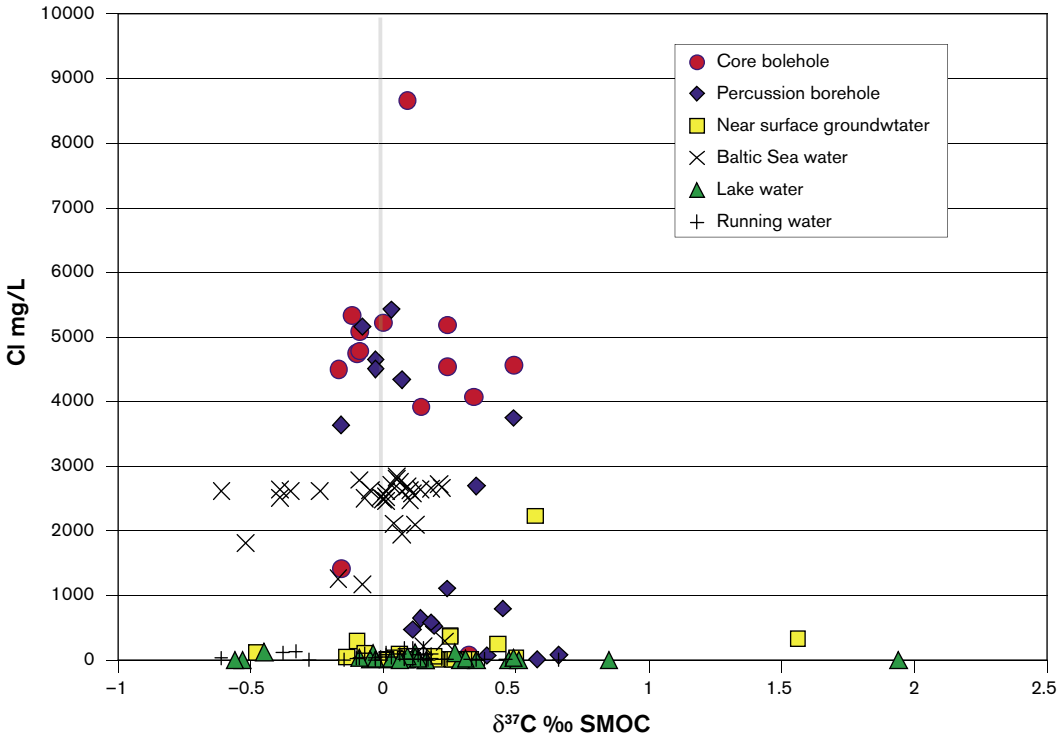

Figure 4-57. *$\delta^{37}Cl$ versus Cl in surface waters, groundwaters and Baltic Sea waters from the Forsmark area.*

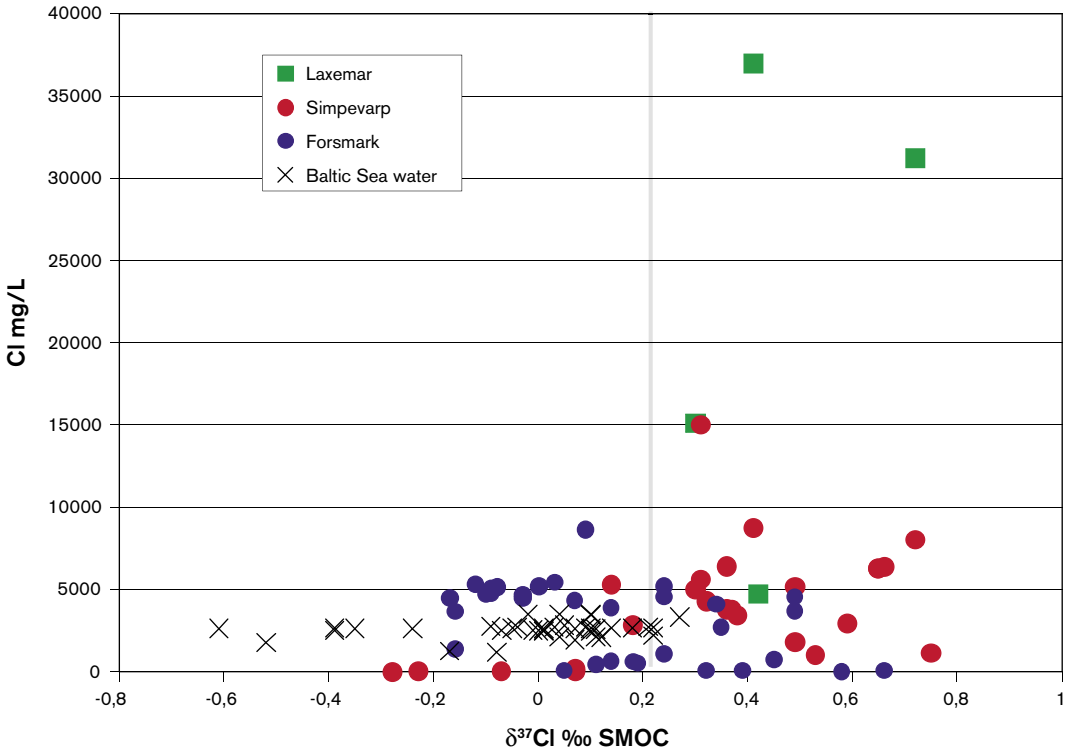

Figure 4-58. *$\delta^{37}Cl$ versus Cl in groundwaters from Forsmark and Laxemar/Simpevarp and Baltic Sea waters from Simpevarp and Forsmark.*

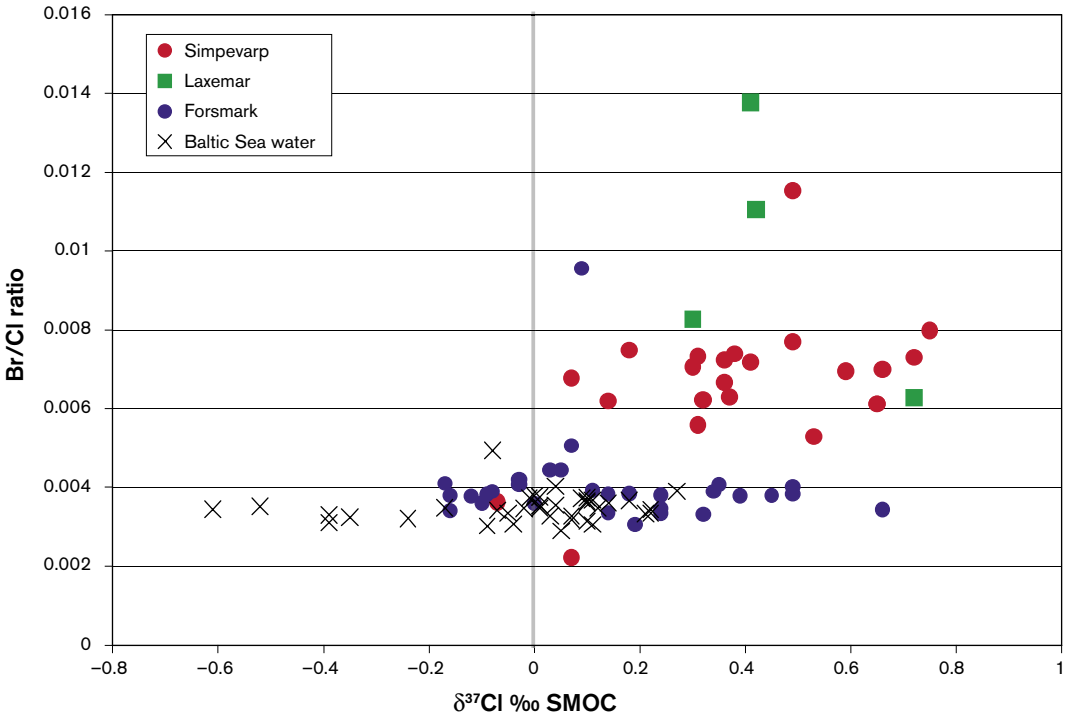

Figure 4-59. *$\delta^{37}Cl$ versus Br/Cl in groundwaters from Forsmark and Laxemar/Simpevarp and Baltic Sea waters from Simpevarp and Forsmark.*

4.4.6 Uranium

Uranium contents have been analysed in surface waters (Lake and Stream waters), in near-surface groundwaters from Soil Pipes and in groundwaters from the percussion and cored boreholes. The surface and near-surface waters are characterised by values between 0.05 and 28 µg/L (Figure 4-60). Large variations in uranium content in surface waters are common and are usually ascribed to various redox states (oxidation will facilitate mobilisation of uranium) and various contents of complexing agents, normally bicarbonate (which will keep the uranium mobile). The plot of uranium versus bicarbonate for the waters (Figure 4-61) shows no clear trend although there is a tendency of higher uranium contents in the surface and near-surface groundwaters associated with increasing bicarbonate up to 400 mg/L. For the few near-surface waters with higher bicarbonate contents the uranium tends to decrease, which may be due to very low redox potential in these waters caused by the microbial reactions producing the bicarbonate (probably to large extent sulphate reducers).

Lower uranium content with depth is expected due to decreasing redox potential and decreasing HCO_3. The groundwaters sampled in the cored boreholes, in contrast, show no such depth trend. Instead, most of the groundwaters show high values (< 30 µg/L) at depths between 200 m and 600 m (Figure 4-61). Groundwaters with high uranium content have bicarbonate contents around 100–125 mg/L with the exception of three samples which all originate from borehole section 639–646 m in KFM03A. This borehole section indicates a mixed groundwater origin (marine and deep saline; cf. e.g. Figure 4-60 and discussion).

Uranium versus chloride (Figure 4-62), shows that the highest uranium contents are found in the waters with chloride values around 5,000–5,500 mg/L, i.e. the brackish groundwaters dominated by a Littorina Sea water component.

Uranium isotope measurements have been carried out in a number of groundwater samples from Forsmark but the reported values are questionable. To resolve this issue an interlaboratory study of reference samples has been initiated and no uranium isotope data will be evaluated in this Forsmark v. 1.2 reporting stage. However, a few measurements carried out at Glasgow University indicate that the uranium $^{234}U/^{238}U$ activity ratios are within the range of 2 to 4, which conform with groundwaters from other sites.

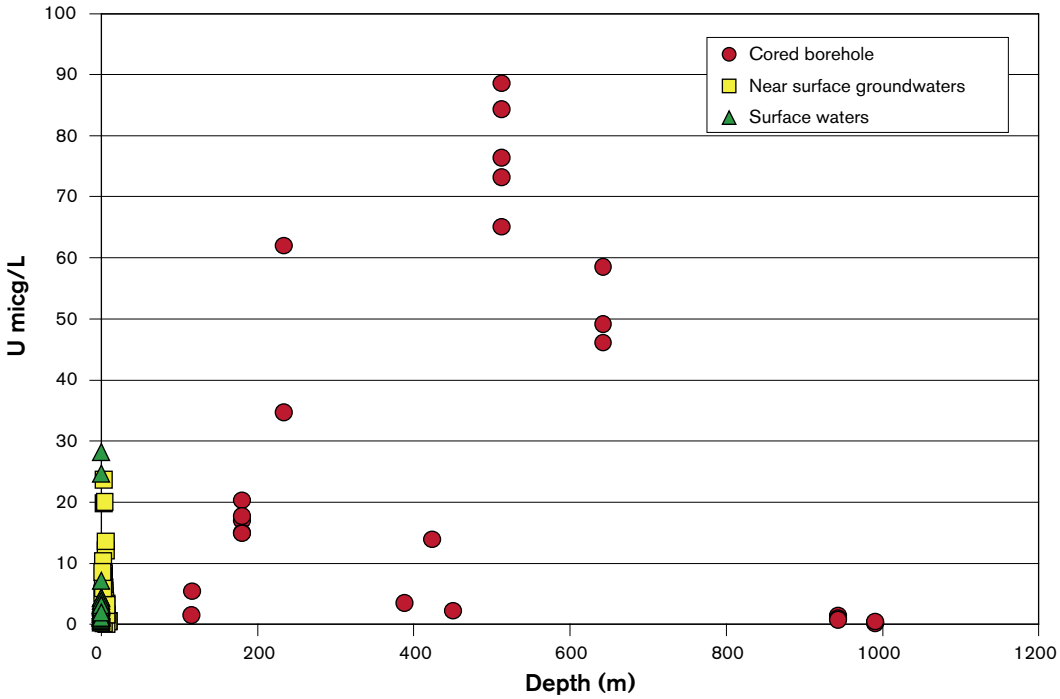

Figure 4-60. *Uranium versus depth in surface and groundwaters from the Forsmark area.*

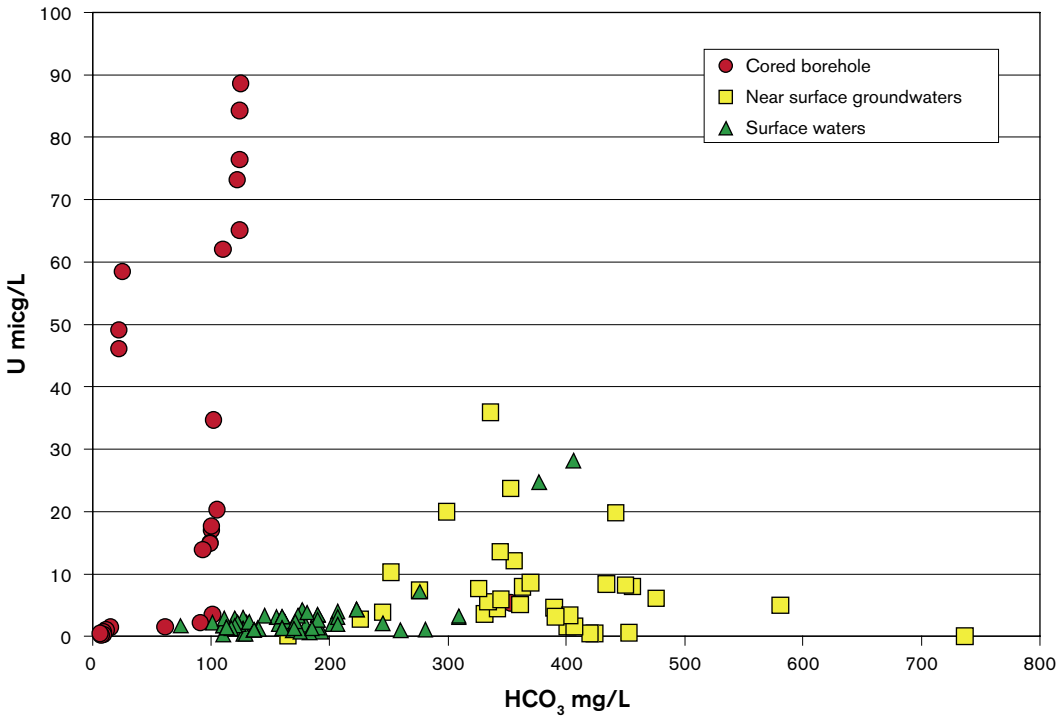

Figure 4-61. *Uranium versus $HC0_3$ in surface and groundwaters from the Forsmark area.*

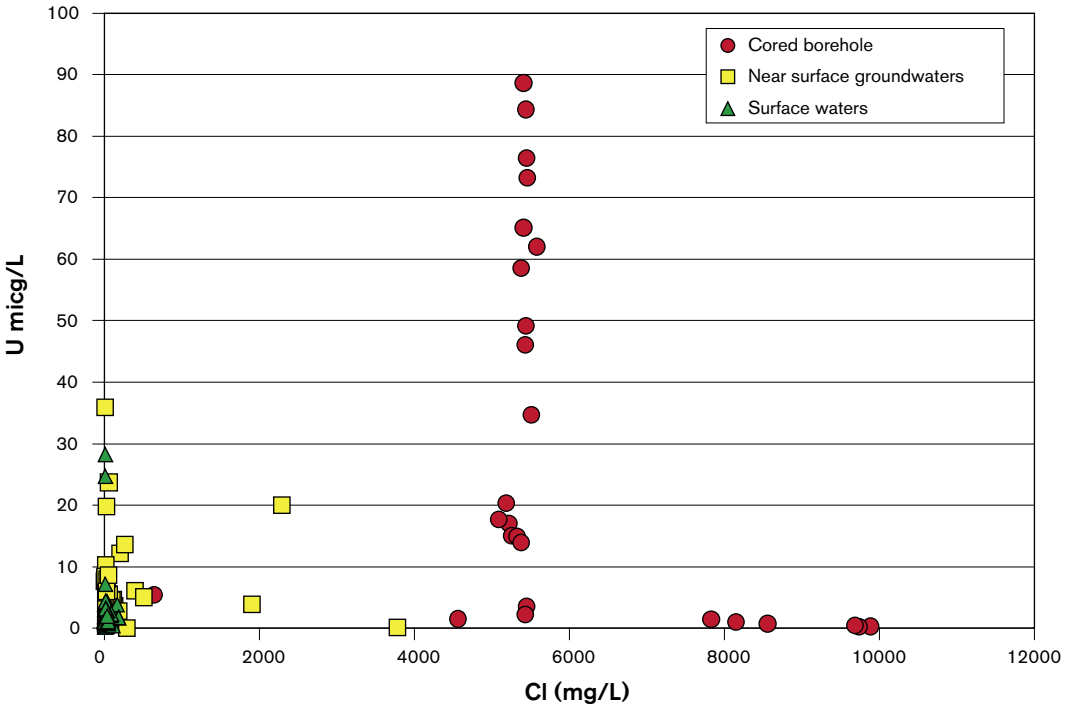

Figure 4-62. *Uranium versus Cl in surface and groundwaters from the Forsmark area.*

4.4.7 Radium and radon

Radium (^{226}Ra) has been measured in groundwaters from 11 near-surface and 9 deep localities; Figures 4-63 and 4-64 show the relationship of radium with chloride and uranium respectively. Higher radium values are common in the deeper, more saline groundwaters (Figure 4-63) which is to be expected since radium largely behaves like, for example, strontium and barium, and at least partly shows a positive correlation with chloride. Figure 4-64 shows that the 3 samples with highest uranium also have the highest radium values. However, the ^{226}Ra activity is in most Forsmark samples significantly higher than the ^{238}U activity (and if a ^{234}U/^{238}U activity ratio of 2–4 is assumed, the ^{226}Ra is also higher than the ^{234}U activity; see above). This implies that the radium in the groundwater can not simply result from the uranium in the water. Instead, both uranium and radium in the groundwaters originate from mineral phases/precipitates locally along the fracture pathways.

Radon (^{222}Rn) has been measured in the same groundwaters analysed for ^{226}Ra.(Figure 4-65). The sample showing the highest ^{226}Ra and ^{222}Rn values is KFM03A: 639–646 m which also contains a relatively high uranium content (46 µg/L). In addition, chemical analyses of fracture coatings in this borehole interval demonstrate significantly enhanced uranium values (2,200 and 2,310 ppm; /Sandström et al. 2004; Petersson et al. 2004/), but it has not been possible to identify the host uranium phase to date. Of the 19 fracture coatings analysed for uranium, those from KFM03A (639–646 m) are extreme when compared with the rest of the fracture coatings which have values below 40 ppm U and most of the samples have values < 16 ppm U. Three fracture samples from the gently dipping NE A2 Zone intersecting borehole KFM01B at 48 m, and borehole KFM03A at 423 m and 516 m, record uranium contents between 20 and 40 ppmU. In contrast, groundwater samples from the A2 zone intersection in borehole KFM03A at 509–516 m show very high uranium values (65 and 88 µg/L) and are also high in ^{226}Ra and ^{222}Rn (Figures 4-64 and 4-65). Obviously the uranium phase contributing to radium and radon to the water was not observed from the mineral analyses, possibly due to removal during drilling.

Generally, radon seems to increase with depth; however, no measurements are available yet from greater than 640 m (Figure 4-66).

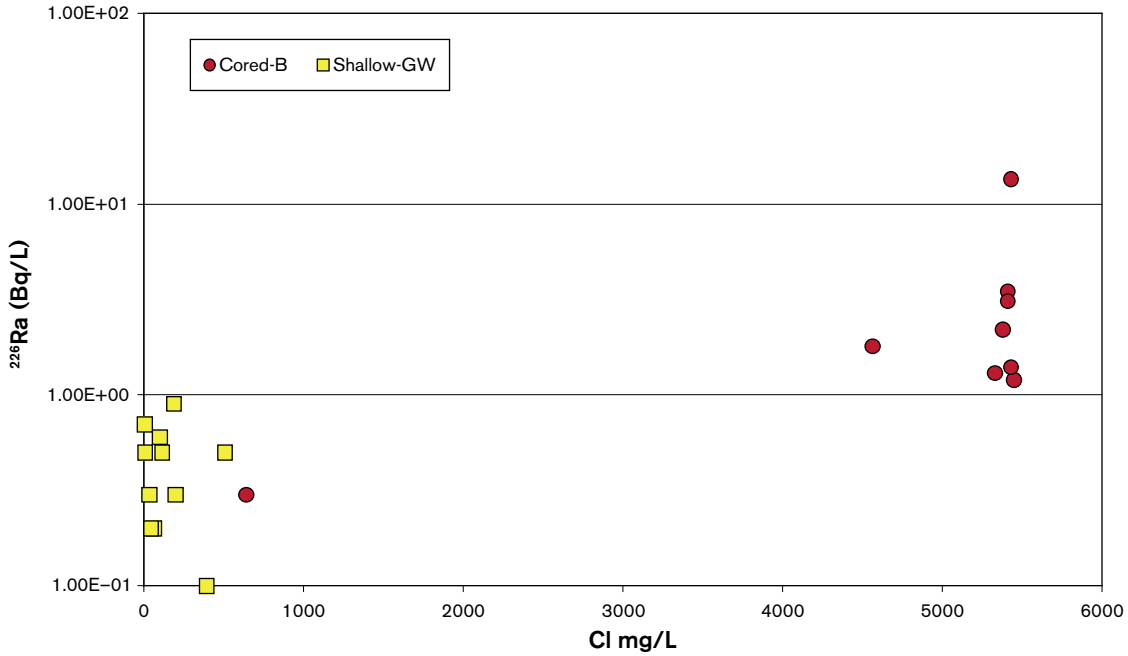

Figure 4-63. *^{226}Ra(Bq/L) versus Cl in shallow and deep groundwaters from the Forsmark area.*

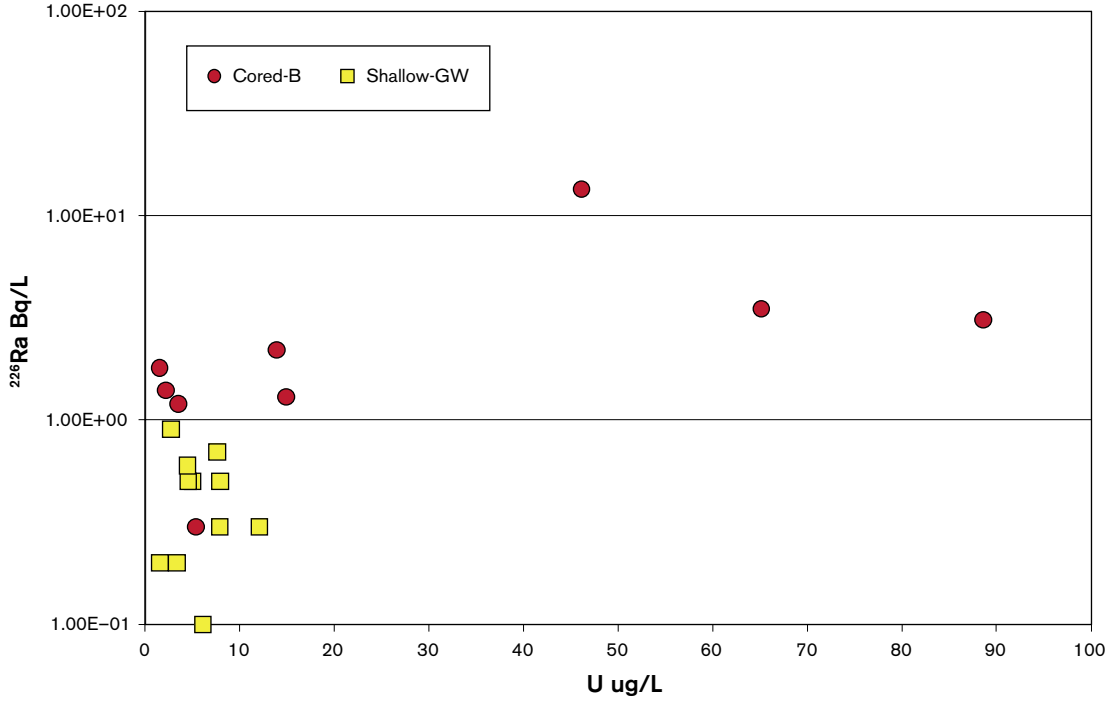

Figure 4-64. *^{226}Ra versus U in shallow and deep groundwaters from the Forsmark area.*

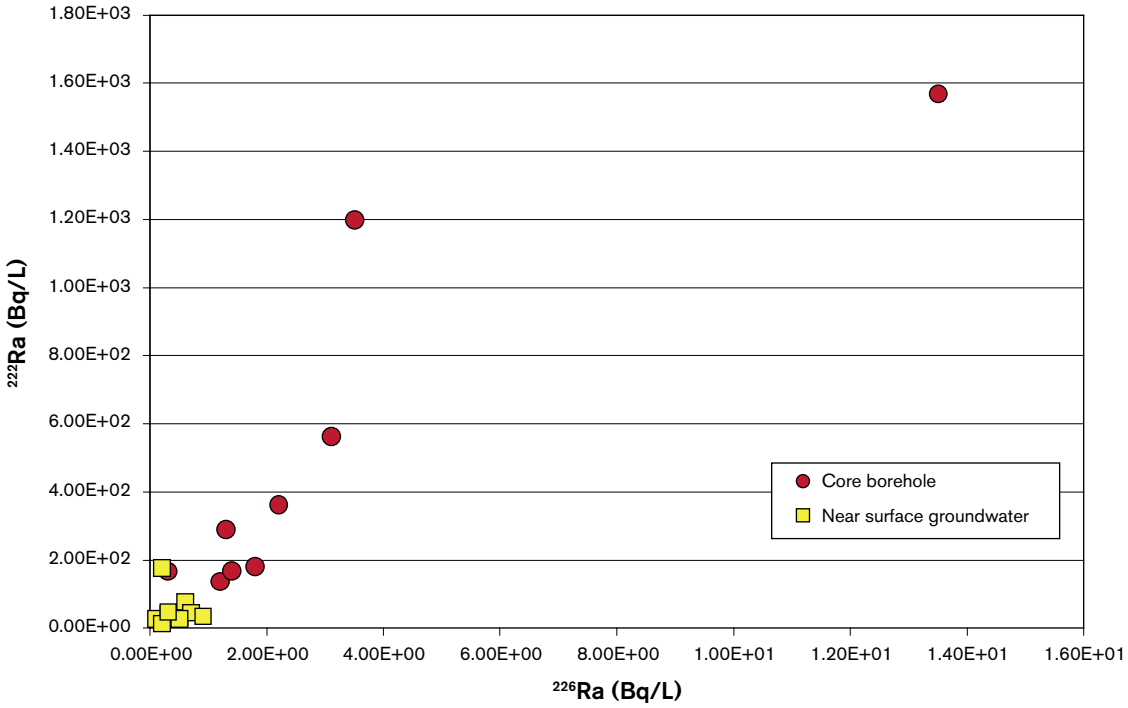

Figure 4-65. *^{222}Rn versus ^{226}Ra in near-surface and deep groundwaters from the Forsmark area.*

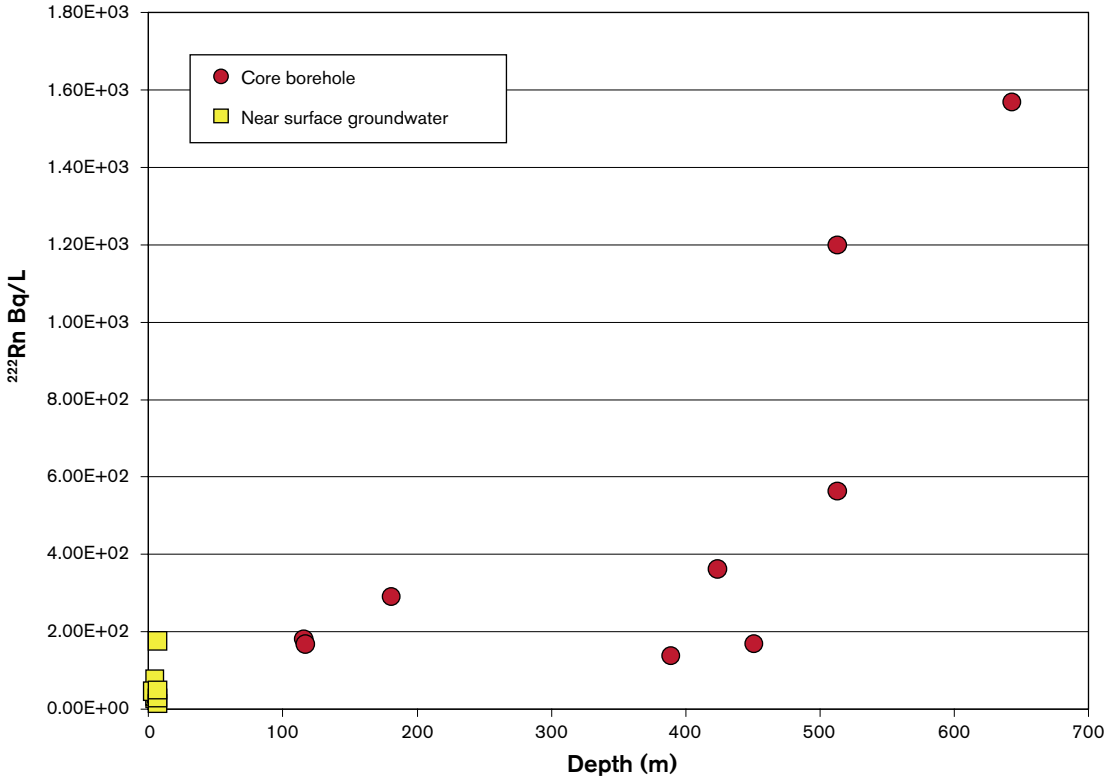

Figure 4-66. *^{222}Rn versus depth in near-surface and deep groundwaters from the Forsmark area.*

In conclusion, the marine (Littorina Sea) groundwaters at Forsmark show high but variable uranium contents. The high uranium is accompanied by increased ^{226}Ra and ^{222}Rn indicating that uranium and radium along the fracture pathways have been mobilised to various degrees by the slowly descending Littorina Sea waters. One possible scenario is that the glacial melt water is accompanied by oxidised uranium into the (near-surface?) fracture zones and subsequently easily remobilised by the reducing but bicarbonate (and DOC) rich Littorina Sea water. The mobilised uranium was then transported to greater depths during the density turnover. The reducing character of the Littorina Sea water is supported by, for example, the high Mn^{2+} contents (1–3 mg/L) recorded for most of the uranium-rich water samples.

The primary origin of the oxidised and remobilised uranium may have been the uranium mineralisations found at several localites in Uppland. For example pitchblende vein fillings in skarn have been documented some kilometres from the site /Welin, 1964/.

It should be pointed out that the activity of radium is usually much higher than the ^{238}U activity in groundwaters. At the Äspö site, /Byegård et al. 2002/ measured $^{226}Ra/^{238}U$ ratios to range from 95–174.

If the uranium contents are recalculated to activity values, $^{226}Ra/^{238}U$ ratios for the Forsmark waters are within the range 1.3–96, with 8 out of 11 samples in the range 2.8 to 27.9. This is significantly lower that the ratios measured at Äspö and indicates the presence of a more mobile uranium phase locally available in some fractures at Forsmark.

4.5 Evidence of redox indicators

Manganese (Mn^{2+}), one of the potential redox indicators in groundwater systems, is mainly produced by microbes during the oxidation of organic material under anaerobic conditions /cf. Hallbeck, 2004/. It should be emphasised, however, that the presence of Mn^{2+} is a strong indicator of reducing conditions but its absence (or very low content) in deep groundwaters cannot be taken as an indicator of oxidising conditions.

Figure 4-67 plots all available data against depth. The manganese values vary from very low contents up to 1 mg/L in the surface and near-surface waters and also in the groundwaters sampled down to approx. 100 m depth. This indicates various redox conditions and also different intensities in activity of the Mn-reducing bacteria. In the brackish groundwaters characterised with a marine signature sampled between 150 and 550 m depths, the manganese values are in the range of 1 to 3 mg/L. The deeper groundwaters show lower values (< 0.5 mg/L), which indicate a smaller contribution of microbially reduced manganese to these waters. Collectively, these data once again support the interpretation of a more active groundwater system down to approx. 600 m depth.

The Mn-reducing bacteria do not only produce Mn^{2+} but at the same time also HCO_3 due to oxidation of organic material. The plot of Mn versus HCO_3 in the analysed waters shows, however, no specific trend (Figure 4-68). The surface waters and near-surface groundwaters which have the highest bicarbonte contents (up to 800 mg/L) show Mn values < 1 mg/L suggesting that Mn-reducing bacteria are not the main contributors to HCO_3 production in these waters. In the deeper groundwaters, in contrast, there are higher manganese values in the waters where HCO_3 contents range between 90 to 125 mg/L.

As indicated in the plot of Mn versus Cl (Figure 4-69) the highest manganese values are found in waters where chloride contents are between 1,500 to 6,000 mg/L, i.e. those brackish groundwaters with a significant Littorina Sea component. With respect to the above discussion of uranium (cf. sections 4.4.6 and 4.4.7) high amounts are found in groundwaters where manganese contents exceed 1 mg/L, thus supporting the reducing conditions in these brackish groundwaters.

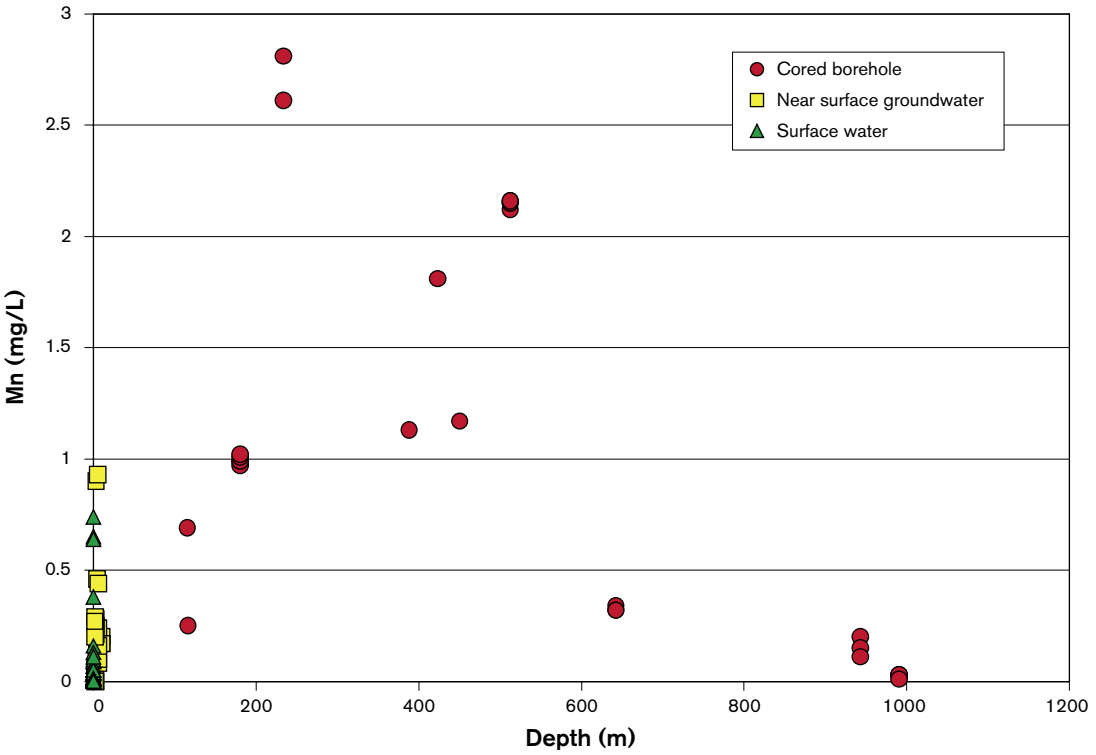

Figure 4-67. *Mn versus depth in surface waters, near-surface groundwaters and groundwaters from cored boreholes in the Forsmark area.*

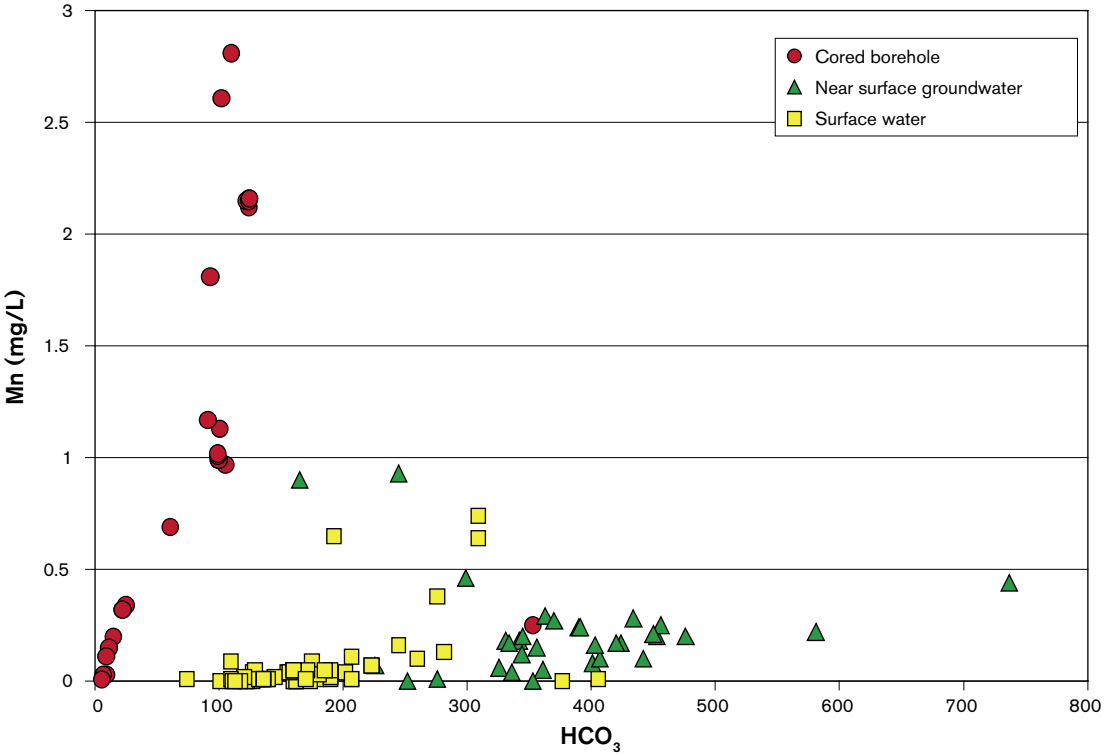

Figure 4-68. *Mn versus $HC0_3$ in surface waters, near-surface groundwaters and groundwaters from cored boreholes in the Forsmark area.*

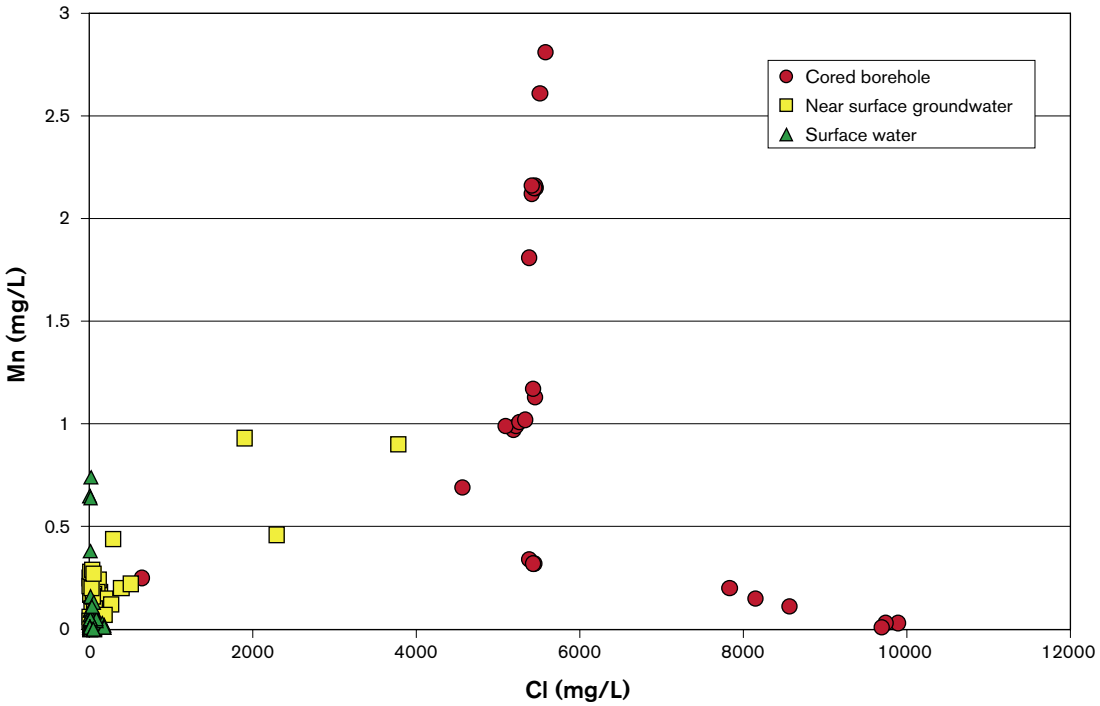

Figure 4-69. *Mn versus Cl in surface waters, near-surface groundwaters and deeper groundwaters from cored boreholes in the Forsmark area.*

4.6 Calcite isotope studies

In order to sort out different calcite generations and to provide palaeohydrogeological information 54 samples have been analysed for $\delta^{13}C$/ $\delta^{18}O$, of which 16 were selected for $^{87}Sr/^{86}Sr$ and a smaller set (7 samples) analysed for chemical composition. The results are presented in /Sandström et al. 2004/. The calcites represent examples from both sealed and open fractures. In some of the latter it has been possible to sample calcites formed in open spaces and showing euhedral crystal forms. When possible, observations have been noted on crystal morphology since a correlation has been demonstrated between calcite morphology (long and short C-axis) and groundwater salinity in fracture mineral studies documented from Sellafield, U.K. by /Milodowski et al. 1998/. The indication from these studies is that fresh water carbonates usually show short C-axis (nailhead shaped crystals), whereas calcite precipitated from saline waters preferably show long C-axis (scaleohedral shapes). Equant crystals are common in transition zones of brackish water. Concerning the Forsmark samples (from depths between 0–500 m) most crystals show short C-axis and equant crystal forms, indicating fresh or brackish water precipitates.

The $\delta^{13}C$/ $\delta^{18}O$ values of calcites from boreholes KFM01A, KFM02A, KFM03A and KFM03B are plotted with previously analysed calcites from the Finnsjön area /Tullborg and Larson, 1982; Figure 4-70/. There is a remarkable similarity between the range of the Forsmark samples and that of the Finnsjön calcites, although the more extreme $\delta^{13}C$ values were not identified in the Finnsjön samples, possibly due to mixing of different generations in this early sampling campaign. The Forsmark calcites show $\delta^{18}O$ values ranging from –7.4 to –18‰ and $\delta^{13}C$ values from –36 to +8‰. The calcites with the lowest $\delta^{18}O$ values have $\delta^{13}C$ typical for hydrothermal calcites without signs of biogenically modified carbon (–7 to –2‰). The calcites with higher $\delta^{18}O$ values (indicating possible precipitates from meteoric or brackish Baltic Sea water based on fractionation fractures by /O´Neil et al. 1969/ and ambient temperatures in the range of 7–15 °C) also show larger variation in their $\delta^{13}C$ carbon isotope values, supporting interaction with biogenic carbon. Extreme $\delta^{13}C$ values are recorded both on the low and high side (< –20‰ and > 0‰). These are interpreted to be the result of in-situ microbial activity (in the bedrock) causing locally extreme enrichment or depletion in ^{13}C in the CO_2-HCO_3^- system which is then inherited by the calcites. It should be noted that the fractionation between HCO_3^- and $CaCO_3$ is only a few per mille and the $\delta^{13}C$ value in the calcite therefore largely reflects the $\delta^{13}C$ value in the bicarbonate at the time of calcite formation.

The calcites with euhedral crystals show $\delta^{18}O$ values between –9 and –12.2‰ and $\delta^{13}C$ values usually within the range of –5 to –20‰, except for the only two samples showing typical elongated scaleohedral shapes. The latter two samples are part of a population of five fracture samples displaying positive $\delta^{13}C$ values (+5 to +8‰), all of which belong to borehole KFM02A and four of them to a fracture zone at approx. 110–118 m depth.

There are no indications of low temperature precipitates from marine Sea water, although a brackish water origin (e.g. similar to Littorina Sea composition) can not be ruled out for a number of samples in the $\delta^{18}O$-interval –7.4‰ to –9.5‰, for example those showing scaleohedral shapes in the KFM02 borehole at 110–118 m depth.

Figure 4-70 plots $\delta^{18}O$ versus $\delta^{13}C$ for the Forsmark samples with the shape of the euhedral calcites distinguished where possible. In some cases, it has been possible to sample two generations of calcites and the arrows in Figure 4-71 indicate the direction of association from the oldest to the youngest generation.

A sequence of at least three different calcite generations, which can be correlated to the fracture mineralogical subdivision, has been documented. These are:

- Hydrothermal calcites with mostly low $\delta^{18}O$-values (down to –18‰) and high $\delta^{13}C$ (–5 to –2‰). These calcites are found together with prehnite and laumontite and thereby support a close relationship between these two generations (Generation 2 and 3).
- Calcites with extremely low $\delta^{13}C$ values (down to –36‰) and $\delta^{18}O$ values of around –12‰. These are found together with quartz fracture coatings (Generation 4).
- Euhedral calcites formed possibly as the latest phase on the quartz adularia coatings; usually found together with pyrite (Generation 5). $\delta^{18}O$ values range from –11 to –10‰ and the $\delta^{13}C$-values are in the range of –18 to –20‰.

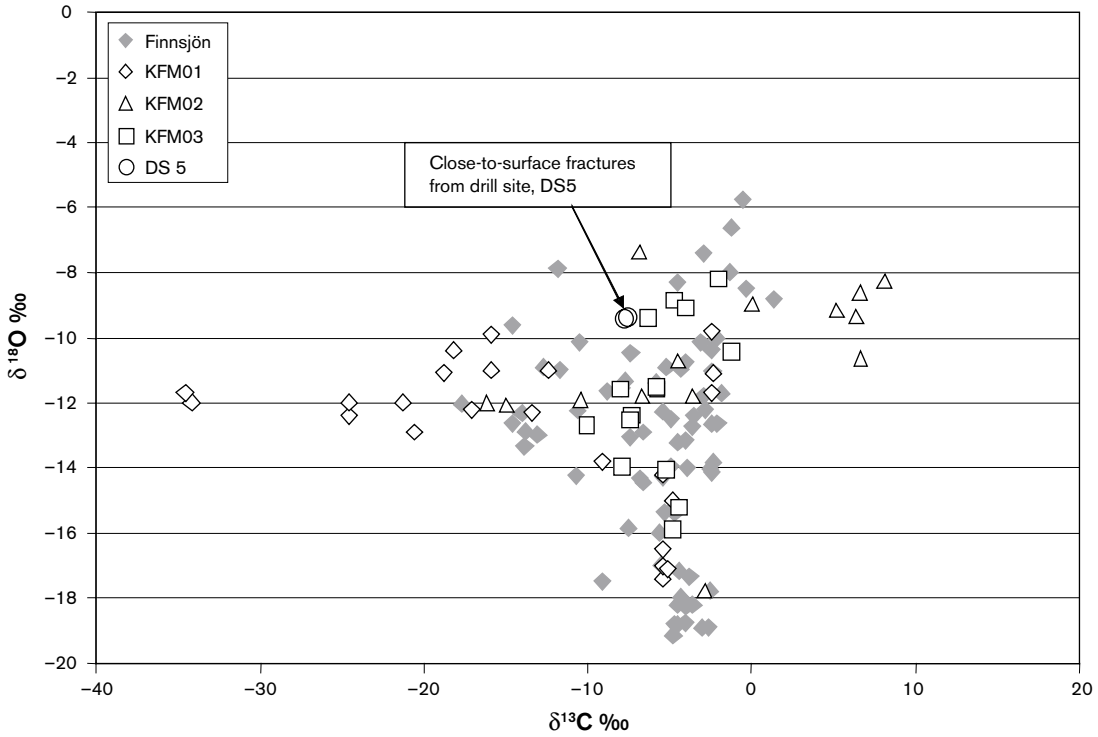

Figure 4-70. *$\delta^{13}C/\delta^{18}O$ values for fracture calcites from boreholes KFM01A, KFM02A, KFM03A, KFM03B and two surface samples from the DS5 site (the drilling site for the fifth deep borehole KFM05A) plotted together with earlier analysed samples from the nearby Finnsjön site /Tullborg and Larson, 1982/.*

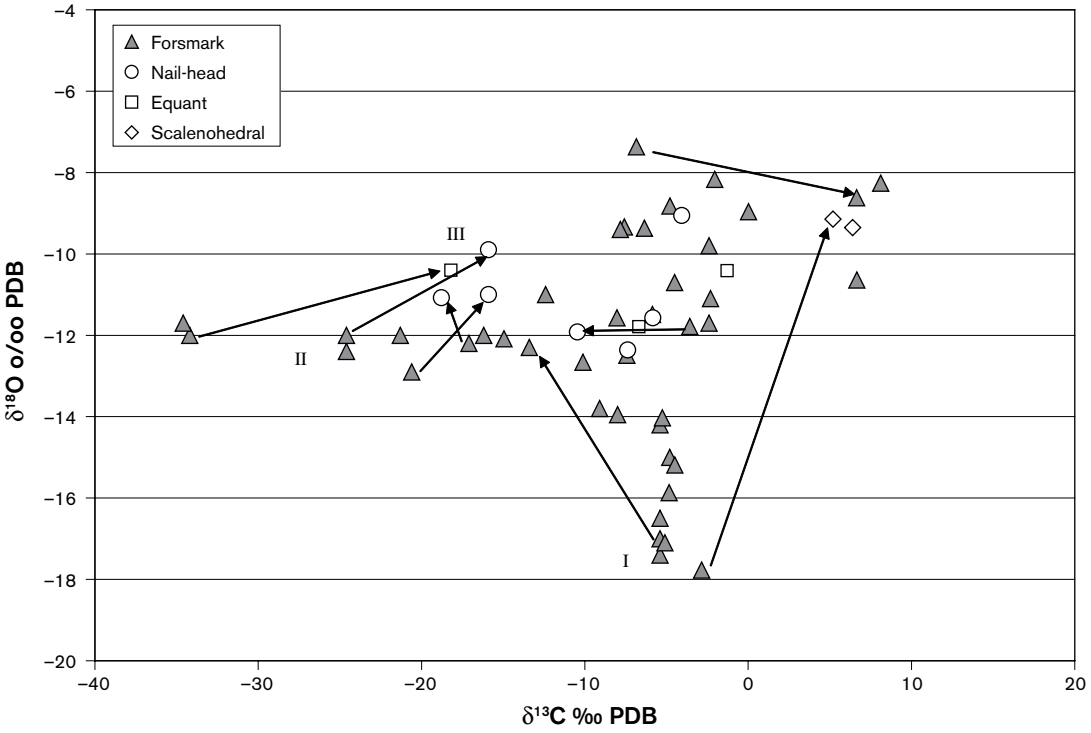

Figure 4-71. *$\delta^{13}C/\delta^{18}O$ values for fracture calcites from boreholes KFM01A, KFM02A, KFM03A, KFM03B and the two from surface samples from the DS5 site. The arrows indicate samples where two calcite generations have been sampled from the same fracture. Directions are from the oldest to the youngest generation. Note that crystal shapes are indicated when possible to distinguish.*

Figures 4-72 and 4-73 show $\delta^{18}O$ and $\delta^{13}C$ plotted against depth for the analysed Forsmark samples. These plots put the focus on the heterogeneous distribution of the samples versus depth. The interval between 100 to 500 m is relatively well represented whereas only four samples are from greater depths than 600 m. In the uppermost 100 m there is only a group of near-surface samples available to date. Note that no samples with a hydrothermal signature have been found in these shallow samples, probably due to dissolution of old calcite.

The Sr isotope values ($^{87}Sr/^{86}Sr$-ratios) have been analysed for 16 of the calcites from borehole KFM01A. The results demonstrate values between 0.707377 and 0.717800 with a clear bimodal distribution, i.e. six samples showing values from 0.707377 to 0.710752 and ten samples with values between 0.714936 and 0.717800. Referring to the subdivision into different generations, it can be concluded that Generations 2 and 3 (the prehnite and laumontite generations) are characterised by a close relationship in that the co-precipitated calcites of these generations do not only show similarities in O and C isotope values, but also in Sr-isotope ratios and in a significantly higher strontium content than Generations 4 and 5 (Figures 4-74 and 4-75). Generation 4 and 5 calcites have largely uniform $^{87}Sr/^{86}Sr$ ratios that are significantly higher than those measured in Generation 2 and 3 samples. This may indicate a close relationship between Generation 4 and 5 as indicated for Generation 2 and 3. Generation 4 and 5 could therefore be part of two different prolonged events which are probably clearly separated in time. Another possibility is, however, that the hydrothermal fluids that gave rise to the calcites had very different compositions and therefore their Sr-isotope ratios were distinctly different. The groundwater analyses all show $^{87}Sr/^{86}Sr$ ratios < 0.717300 which means that there is only one calcite sample showing an overlap with the groundwater Sr-isotope interval.

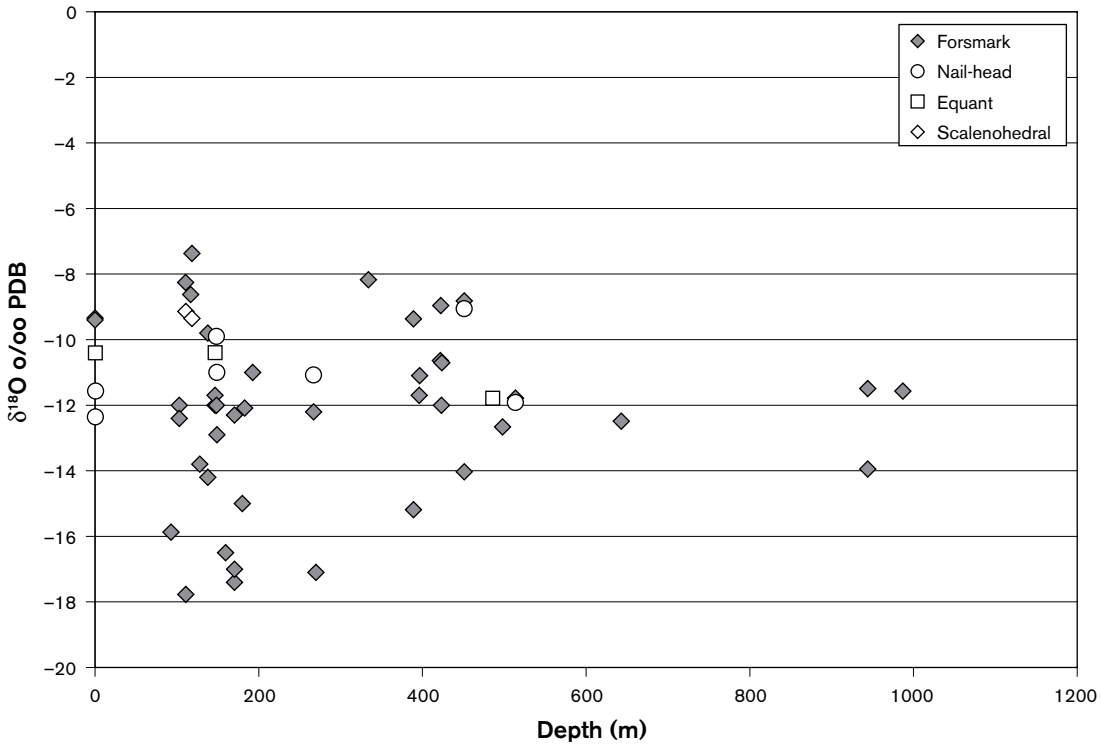

Figure 4-72. *$\delta^{18}O$ versus depth for fracture calcites from KFM0A1, KFM02A, KFM03A, KFM03B and the DS5 site. Crystal shapes distinguished when possible.*

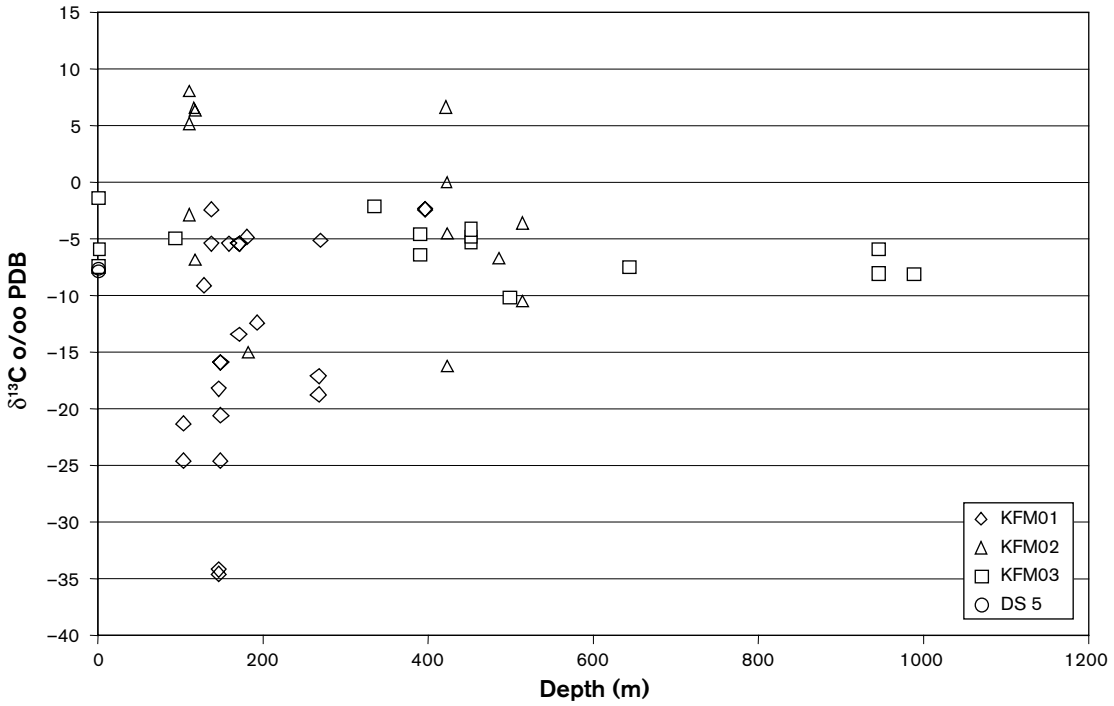

Figure 4-73. *$\delta^{13}C$ versus depth for fracture calcites from boreholes KFM0A, KFM02A, KFM03A, KFM03B and the DS5 site.*

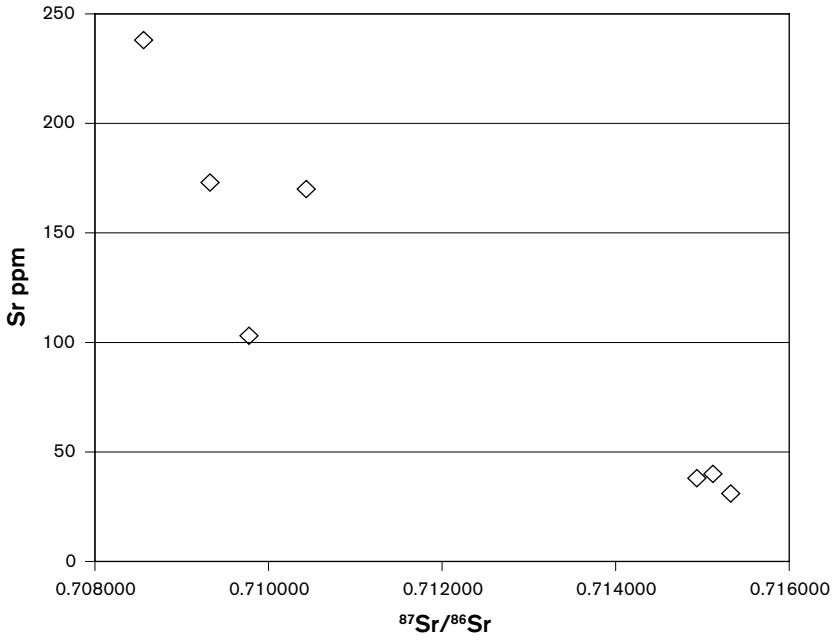

Figure 4-74. *$^{87}Sr/^{86}Sr$ versus Sr in fracture calcites from borehole KFM01A.*

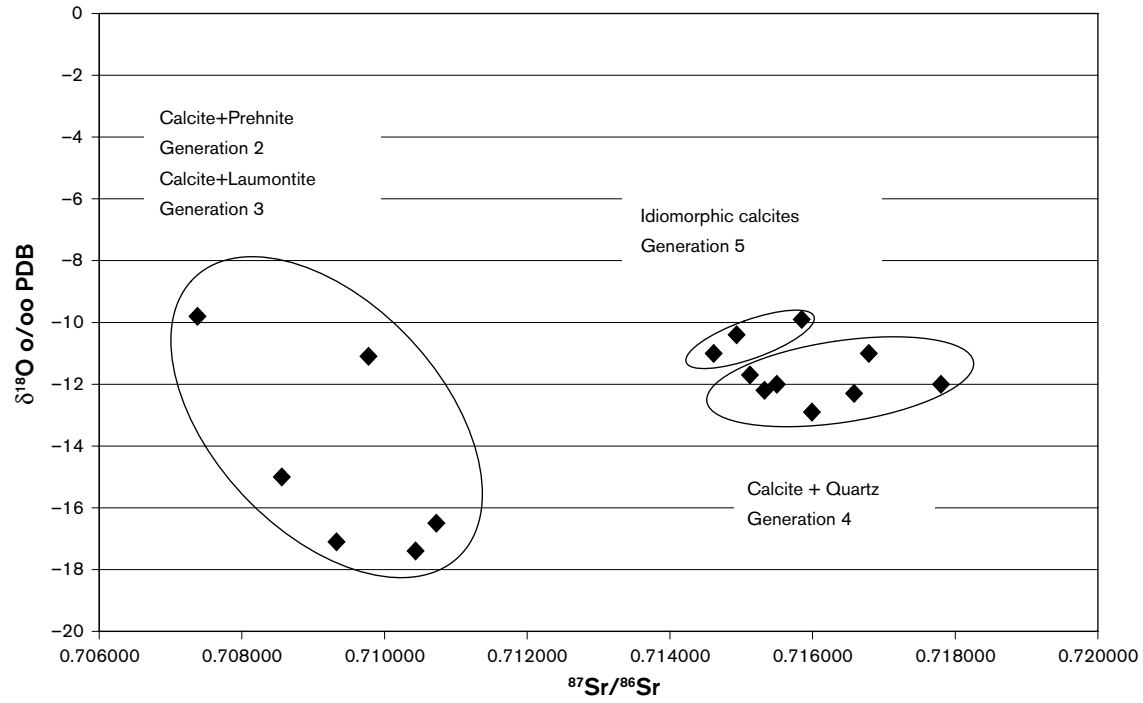

Figure 4-75. *$^{87}Sr/^{86}Sr$ versus $\delta^{18}O$ values in fracture calcites from borehole KFM01A.*

Trace element analyses have been carried out on seven calcite samples from which duplicates have been made on two samples (Sandström et al.; P-report, in press). These analyses are made on leachates from calcite samples and it can be suspected that minor amounts of contaminant minerals have dissolved as well, or that ion exchanged elements are released from clay minerals included in the calcite samples. This is, however, still the best way to gain information about the trace element contents in very small calcite samples.

The trace element contents are generally low (Figure 4-76), but some differences between Generation 3 calcites (Laumontite-generation) and 4 (quartz and adularia generation) can be seen. Generation 3 calcites are higher in Sr and Mg, lower in light REEs, and show mostly negative cerium anomalies. One sample from Generation 3 shows a significantly higher manganese value than the other samples analysed. The reason for this is at present not understood.

The negative cerium anomalies in the Generation 3 samples may have several explanations. One is that oxidation has occurred during the hydrothermal event causing immobilisation of cerium and in turn a negative cerium anomaly in the hydrothermal fluid responsible for the calcite precipitation.

In conclusion, calcites have been precipitated in open fractures on several occasions, commencing with the hydrothermal prehnite-laumontite generation. Taken all the stable isotope data into account there is strong support for these two generations to be part of the same prolonged event; the tailing in $\delta^{18}O$ for this group from –18 to at least –14‰ may be due to precipitation from a hydrothermal fluid during decreasing temperatures. The connection between the calcite in the prehnite and laumontite generations are in accordance with earlier observations from Finnsjön.

Calcite with extremely low $\delta^{13}C$ values has been produced during the event responsible for the quartz and analcime formation. These mineralisations must have been precipitated during lower temperatures than the preceding laumontite formation, although it is reasonable to assume that it was still hydrothermal (< 200°C is suggested). The very low $\delta^{13}C$ values are usually interpreted as due to in-situ microbial activity which implies that the temperature was not significantly above 100°C when the carbon isotope signature was modified. However, the temperature may have increased subsequently during a period of calcite precipitation. Based on Sr-isotope values this period is clearly separated from the prehnite-laumontite formation, either in time (the radiogenic ^{87}Sr is much higher in the latter generation), or the chemistry of the hydrothermal fluid was significantly different and preferred dissolution of K-Rb minerals occurred.

The euhedral crystals (mostly equant in shape) formed on top of the quartz-calcite-adularia coatings in some of the fractures, are possibly the latest phase of these events.

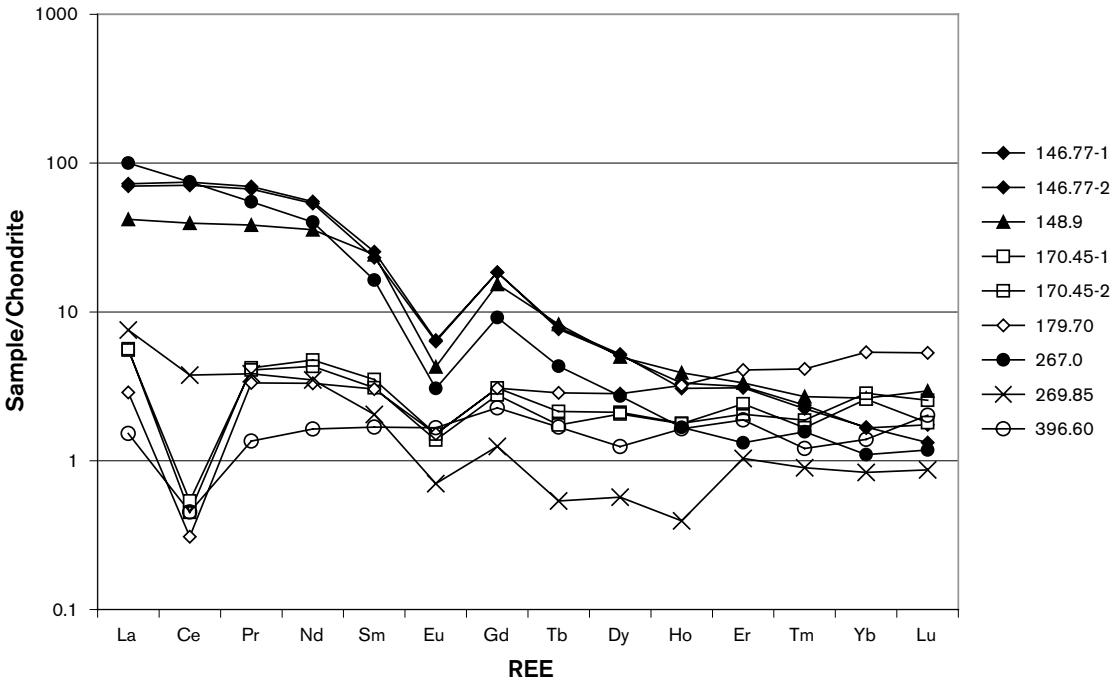

Figure 4-76. *Chondrite normalised REE patterns for fracture calcites from borehole KFM01A. Note that these analyses are made on leachates of calcite samples which contain small amounts of contaminant minerals.*

It has not been possible yet to relate several calcite precipitates to any specific fracture mineralisation event. For example, a group of calcites from borehole KFM02A (110–118 m) shows significantly positive $\delta^{13}C$ values (+6 to +8‰) and $\delta^{18}O$ values of –8 to –11‰. There is also a cluster of samples that may include relatively late (Quaternary) precipitates. More analyses are, therefore, needed in order to better identify this group.

4.7 Evidence of a Littorina signature

The Littorina stage in the postglacial evolution of the Baltic Sea commenced when the passage to the Atlantic Ocean opened through Öresund in the southern part of the Baltic Sea. The relatively high sea level together with the early stages of isostatic land uplift led to a successively increasing inflow of marine water into the Baltic Sea. Salinities twice as high as modern Baltic Sea have been estimated for a time period of about 2,000 years starting some 7,000 years ago (cf. description of the post glacial scenario and references therein). Based on shore displacement curves it is clear that the Forsmark area has been covered by the Littorina Sea for a long period of time (8,000 to 9,000 years) and the low topography implies that it reached several tens of kilometres further inland for a considerable part of that time. The present meteoric recharge stage following uplift and emergence has only prevailed for less than 1,000 years such that any flushing out of the Littorina Sea component is relatively limited. Strong evidence of a Littorina Sea water signature can therefore be expected in groundwaters at Forsmark which is also confirmed by the hydrochemical interpretations.

The Simpevarp/Laxemar area, in contrast, was only partly covered by the Littorina Sea. Due to the topography of the area and the on-going isotstatic land uplift, the Laxemar area was probably influenced only to a small degree, whereas the Simpevarp peninsula was covered for several thousands of years until eventual emergence during uplift initiated a recharge meteoric water system some 4,000 to 5,000 years ago. This recharge system effectively flushed out much of the Littorina Sea water.

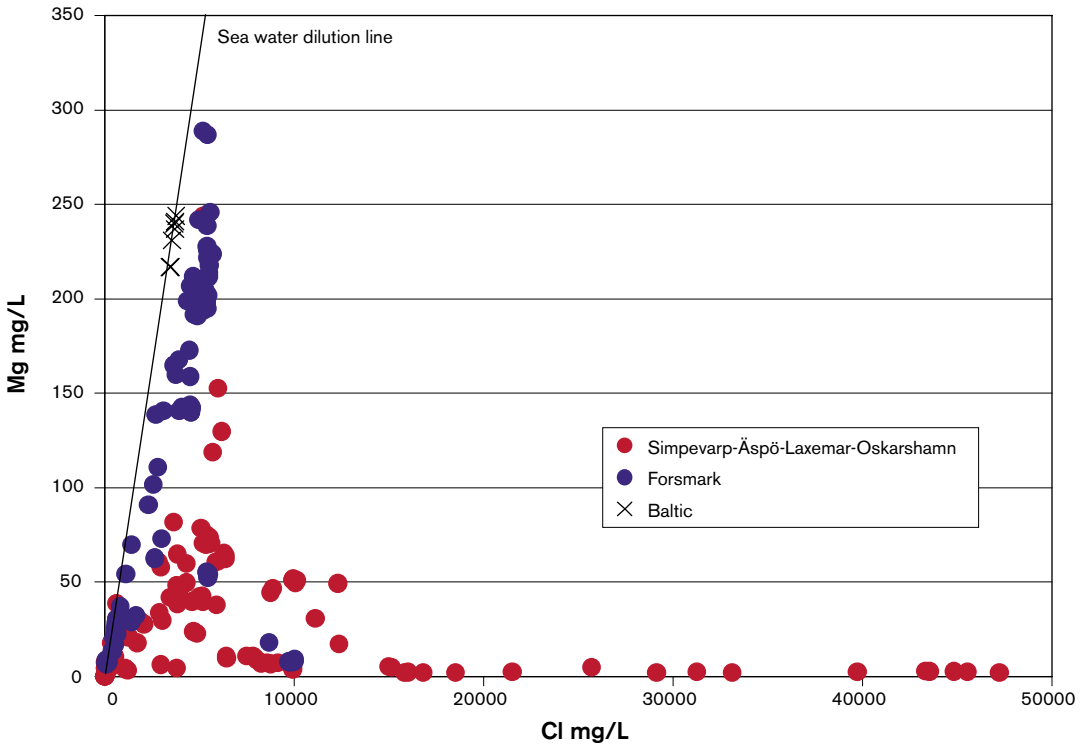

Figure 4-77. *Mg versus Cl for groundwaters from Forsmark and the Oskarshamn sites (Simpevarp-Äspö-Laxemar-Oskarshamn (KOV01)). Baltic Sea waters from Simpevarp and Forsmark are included for reference.*

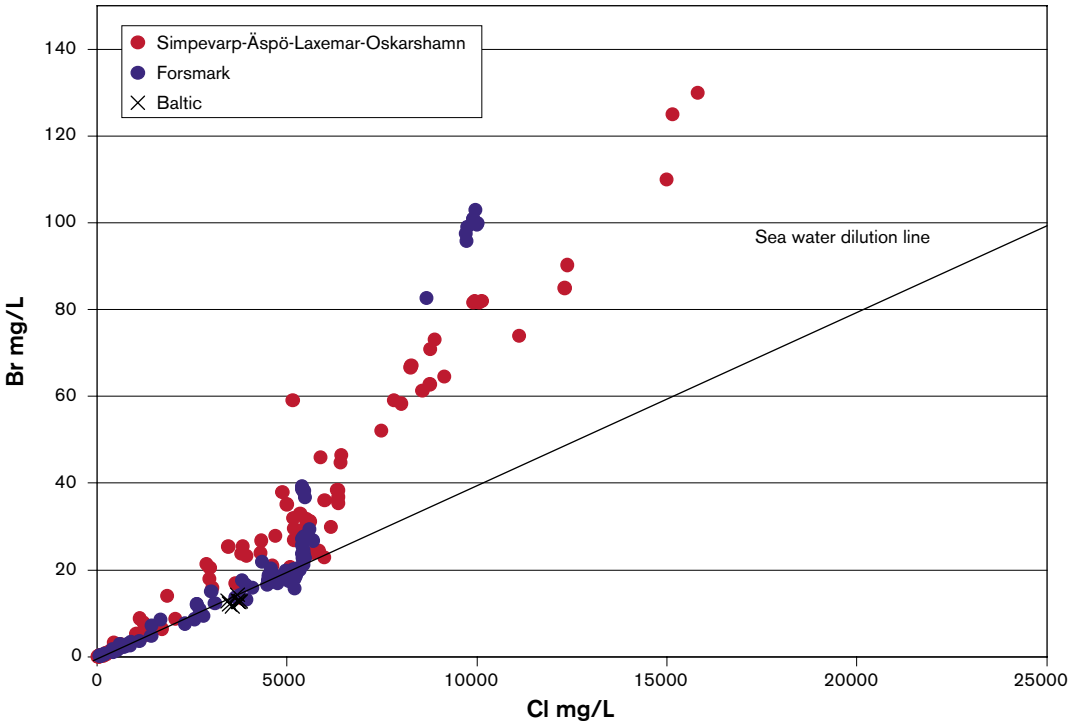

Figure 4-78. *Br versus Cl for groundwater samples from Forsmark and the Oskarshamn sites (Simpevarp-Äspö-Laxemar-Oskarshamn (KOV01)). Baltic Sea waters from Forsmark and Simpevarp are included for reference.*

Comparison of Forsmark data with the Simpevarp area (i.e. Äspö, Laxemar and Oskarshamn sites) indicates large differences in the character and origin of the groundwaters, especially for brackish groundwaters with chloride contents of around 4,000–6,000 mg/L Cl. This is exemplified in three plots showing chloride versus magnesium, bromide and $\delta^{18}O$ (Figures 4-77, 4-78 and 4-79).

The magnesium versus chloride plot (Figure 4-77) clearly shows the difference between the Forsmark and Simpevarp groundwaters characterised by chloride contents up to 5,500 mg/L Cl; characteristically the Forsmark samples closely follow the modern marine (Baltic Sea) trend. Those few groundwaters that plot within the Simpevarp area group are from greater depths in the bedrock and, as such, have been influenced by mixing with deeper non-marine saline groundwaters. A few samples from Äspö (KAS06 and HAS02; Figure 4-80) also show relatively high magnesium contents, although not as high as in the Forsmark groundwaters with similar chloride contents. Most of the Oskarshamn groundwaters show low magnesium values although small increases are observed for samples in the chloride interval 4,000–6,300 mg/L.

The bromide versus chloride plot (Figure 4-78) underlines the marine signature for most of the Forsmark groundwaters with salinities up to brackish values (~ 5,500 mg/L), with the exception of sample KFM03A: 638–644 m which shows a mixed origin (already commented upon in previous sections), whereas marine signatures only are obtained in a few of the Oskarshamn sub-area groundwaters. This observation is strengthened in the $\delta^{18}O$ versus chloride plot (Figure 4-79) which shows deviating groundwater trends for Forsmark and Simpevarp.

Generally, with a few exceptions, the brackish groundwaters up to 5,500 mg/L Cl at Forsmark show indications of a marine origin in terms of: a) Br/Cl ratios, b) Mg values ≥100 mg/L, and c) $\delta^{18}O$ values higher than meteoric waters (due to in-mixing of marine waters). In contrast, for the Äspö-Simpevarp-Laxemar samples these criteria are only fulfilled in samples from KAS06 and one sample in KSH03A. In both cases the groundwater samples have been collected from fracture zones outcropping close to the shoreline or under the Baltic Sea.

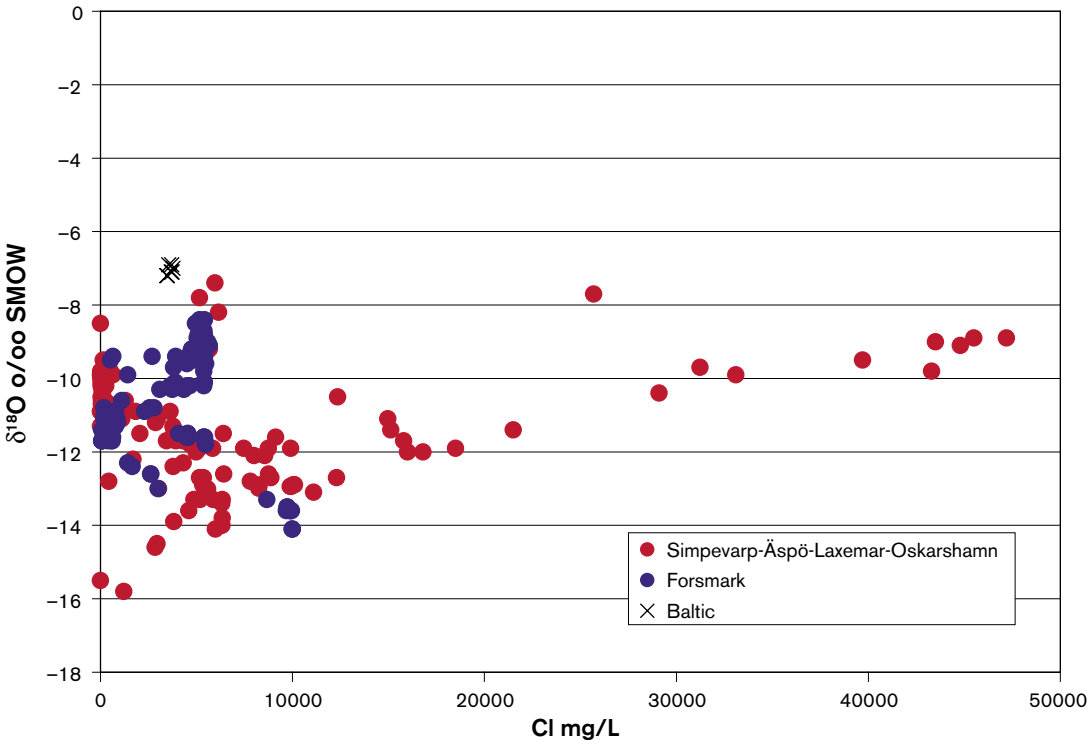

Figure 4-79. *$\delta^{18}O$ versus Cl for groundwaters from Forsmark and the Simpevarp sub-areas (Simpevarp-Äspö-Laxemar-Oskarshamn (KOV01)). Baltic Sea waters from the Simpevarp area are included for reference.*

The chloride content and $\delta^{18}O$ value for the Littorina Sea at maximum salinity is difficult to determine precisely. Interpretations of salinities based on fossil fauna together with $\delta^{18}O$ analyses of the fossils has resulted in suggested salinities around 6,500 mg/L Cl and $\delta^{18}O$ values ~ –4.5‰ SMOW /Donner et al. 1994; Pitkänen et al. 2004/. In Figure 4-80 (Cl versus $\delta^{18}O$) groundwaters from the Forsmark, SFR, and the Oskarshamn sub-areas which show Br/Cl ratio < 0.0045 and magnesium values > 100 mg/L are plotted. For comparison data from Olkiluoto /Pitkänen et al. 2004/ are included.

The top three mixing lines in Figure 4-80 represent Oceanic/Littorina/meteoric, Oceanic/Baltic (Simpevarp)/meteoric and Oceanic/Baltic (Forsmark)/meteoric. The sub-vertical mixing line represents Littorina/glacial. Most of the plotted groundwaters reflect mixtures of varying proportions comprising the four end-members: Glacial, Littorina Sea, Baltic Sea and Meteoric waters.

Assuming that the suggested Littorina Sea water is the product of simple mixing between Ocean Sea water and a meteoric component, then this meteoric water had heavier $\delta^{18}O$ values than present-day mixing processes that have given rise to the Baltic Sea close to Forsmark and Simpevarp (Figure 4-80). It is well known that climatic conditions were warmer during parts of the Littorina Sea period and therefore heavier $\delta^{18}O$ signatures in the meteoric water during that stage were probably the case. However, it is probable that both the salinity and $\delta^{18}O$ were variable during the entire Littorina Sea period such that none of the sampled groundwaters at any of the sites studied achieved a proper estimate of the Littorina Sea composition.

Based on the post-glacial scenario a successive replacement of the glacial water by the denser Littorina Sea water has occurred giving rise to the sub-vertical Littorina/glacial mixing line in Figure 4-80. As can be seen a number of waters from Forsmark and SFR cluster along this mixing line together with samples representing the brackish SO_4 type water from Olkiluoto, interpreted by /Pitkänen at al. 2003/ to represent large portions of Littorina water.

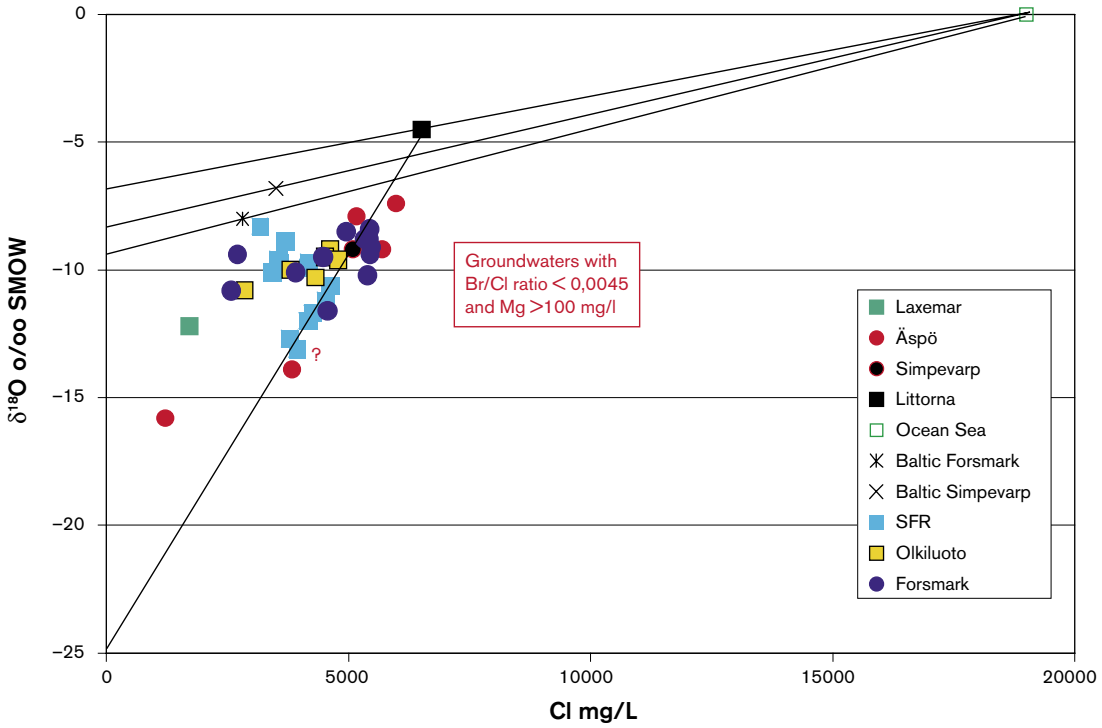

Figure 4-80. *$\delta^{18}O$ versus chloride content for potential marine groundwaters from Simpevarp, Äspö, Forsmark and Olkiluoto, the latter from /Pitkänen et al. 2004/. The top three mixing lines represent Oceanic/Littorina/meteoric, Oceanic/Baltic (Simpevarp)/meteoric and Oceanic/Baltic (Forsmark)/ meteoric. The sub-vertical mixing line represents Littorina/glacial. Most of the plotted groundwaters reflect mixtures of varying proportions comprising the four end-members: Glacial, Littorina Sea, Baltic Sea and Meteoric waters.*

From the Simpevarp area there are samples from KAS06 and also one sample from KSH03 that show a large component of Littorina Sea water. Weaker indications are also found in a KAS02 sample from 200 m depth were the magnesium content is low but the Br/Cl ratio is marine.

From Figure 4-80: 1) The uppermost heavier $\delta^{18}O$ values plot along the Oceanic Sea mixing line joining the Littorina Sea with precipitation values at that time of ~ 7‰ SMOW, and 2) The Littorina Sea water subsequently mixed with the older, dilute glacial meltwaters as it slowly descended into the bedrock. This has given rise to 'Littorina Sea' waters of varying chemical and isotopic composition. One such example is the narrow range of composition that characterises many of the SFR groundwaters which plot along the present-data mixing line shown in Figure 4-80.

In conclusion, of the groundwaters sampled in the cored boreholes KFM01A, KFM02A, KFM03A and KFM04A at the Forsmark area, six out of ten sampled sections plot along the Littorina/glacial mixing line. These waters represent depths ranging from 110 m in borehole KFM01A to 520 m in borehole KFM02A. Section 640 m in borehole KFM03A indicates a mixed origin comprising a Littorina/glacial and a deep saline component. Also the groundwaters sampled from KFM04A show inmixing of a deeper saline component based on the Br/Cl ratio, even though a large portion of Littorina Sea is present. Of the 17 percussion boreholes where chemical data are available, three show values that plot along the Littorina Sea mixing line; HFM08 (0–144 m), HFM 10 (0–150 m) and HFM19 (0–173 m). The others show inmixing of today's meteoric and/or modern Baltic Sea to various degrees with the Littorina Sea/glacial mixture. This is also the case for part of the SFR groundwaters; a number of these are approaching Baltic Sea values (Figure 4-80).

If applying simple regularity for the mixing between the glacial and Littorina Sea waters (and assuming that the suggested Littorina Sea and glacial end member values are at least approximately correct) than the glacial components in the Forsmark samples vary from 18 to 33%, and the highest portion of glacial water at 42% is found in the SFR groundwaters. This only concerns the glacial-Littorina mixing; the deep saline/glacial mixing which precedes this event is not addressed here.

5 Conclusions

5.1 Representativity

A detailed representativity evaluation, distinguishing between suitable (orange colour in the dataset) and less suitable (green colour in the dataset) for modelling purposes, resulted in 7 suitable and 25 less suitable groundwater samples from the cored and percussion boreholes. Because of the difficulty of constraining all possible influences on the hydrochemistry of the surface and near-surface Baltic Sea, Lake and Stream waters, and the shallow Soil Pipe groundwaters, a less rigorous representativity evaluation was carried out in these cases.

Precipitation waters have not undergone any representativity check *senso stricto*. As the main intention is to monitor $\delta^{18}O$, δD and tritium, since these parameters are used to identify modern meteoric groundwater components at depth, all isotope data available were used for this purpose. Disturbances, such as unpredictable annual and seasonal trends and possible evaporation, have not been evaluated in this present representativity check.

5.2 Main elements

- General depth trends show increasing TDS with depth; in particular the increase in Ca/Na and Br/Cl ratios.
- Three main depth-related hydrochemical subdivisions can be recognised: a) shallow (0–150 m) dilute groundwaters (< 1,000 mg/L Cl), b) intermediate (~ 150–600 m) brackish groundwaters (5,000–6,000 mg/L Cl), and c) deep (> 600 m) saline groundwaters (~ 10,000 mg/L Cl).
- The dilute shallow region is characterised mainly by Na-HCO_3-type groundwaters, but subordinate Na-HCO_3(SO_4) to Na(Ca)-HCO_3-Cl(SO_4) groundwater types also occur.
- The intermediate groundwater region is dominated by Na(Ca, Mg)-Cl(SO_4) to Na-Ca(Mg)-Cl(SO_4) groundwater types. A strong Littorina Sea signature is apparent in this brackish region.
- The deep groundwater region comprises Na-Ca-Cl to Ca-Na-Cl groundwater types.
- The marked deviation of the deep groundwater from all other groundwaters can be explained by increased mixing with an older deep saline component of a non-marine or non-marine/old marine origin. This is clearly shown by the Na/Ca/Mg and Br/Cl ratios versus Cl content. Only one deep groundwater sample so far exists, that from borehole KFM03A at 980–1,001 m. This borehole is characterised by fracture zones A4, A7 and B1 within the depth interval of 350–550 m. It would seem that this structural interval hydraulically separates brackish groundwaters partly of old and/or new marine origin, from deeper increasingly saline groundwaters of non-marine origin.
- Compared to other Fennoscandian sites, Forsmark shows close similarities with the nearby Finnsjön and SFR sites and also to the Olkiluoto site in Finland. The similarity with Olkiluoto, especially down to 500 m, is particularly relevant as the brackish groundwaters at this site also have a strong Littorina Sea signature.
- The Littorina Sea signature at Forsmark is indicated mainly by increases in Mg and SO_4, both of which decease rapidly after 500–600 m depth. A marine origin is further supported by the Br/Cl ratios. Although HCO_3 decreases markedly after 150 m depth, it persists at around the 100 mg/L level within the Littorina-type brackish groundwaters before dropping to very low values at depths greater than 500 m.

5.3 Isotopes

- The stable isotope data plot on or close to the Global Meteoric Water Line (GMWL) indicating a meteoric origin. Values range from $\delta^{18}O$ = –13.6 to –8.4‰ SMOW and δD = –98.5 to –66.1‰ SMOW with the most negative isotopic signatures (i.e. cold climate meteoric input) corresponding to the deepest groundwater sampled at 980–1,001 m.

- Plotting oxygen-18 against chloride further details the three distinct groups of groundwaters present at Forsmark: a) shallow, dilute groundwaters with a narrow range of $\delta^{18}O$ (–12 to –10‰ SMOW), close to present day precipitation, b) a wider range of values ($\delta^{18}O$ = –12 to –8‰ SMOW) for the more brackish groundwaters, the large variability in $\delta^{18}O$ is explained by mixing between glacial and Littorina Sea (characterised by heavier isotope values) groundwaters, and c) the deepest outlier ($\delta^{18}O$ = –13.6 SMOW) representing the most saline groundwater.
- One problem in using tritium for the interpretation of near-surface recharge/discharge is its variation in recharge water over time. This implies that near-surface groundwaters with values around 15 TU can be 100% recent, or a mixture of old meteoric (tritium free) water, and also a small portion (10%) of water from the sixties at the height of the atmospheric nuclear bomb tests.
- Below 200 m depth tritium values under 3 TU are detected for all samples. For the borehole sections sampled below 300 m there are samples with no detectable tritium but in two cases a few tritium units have been measured in the last sample in the time sequence prior to sampling. One of the near-surface samples KFM03A (0–46 m) shows a very high tritium content of 41 TU indicative of a significant portion of recharge from the sixties or seventies when tritium contents were much higher than at present. There is therefore the possibility that the observed tritium values in some of the deeper sampled borehole sections reflect some contamination by these tritium-enhanced waters entering into water-conducting fracture systems during open hole borehole activities.
- Tritium contents in surface and near-surface waters need to be carefully interpreted. For example, the measured tritium contents in the precipitation and Baltic Sea water at Forsmark may also contain some tritium locally produced by the nuclear power plants, i.e. that emitted as vapour to the atmosphere and that contained in the cooling water discharged to the Baltic Sea.
- The plot of tritium versus ^{14}C for surface waters from Forsmark shows that most Lake and Stream waters have higher ^{14}C values compared with Baltic Sea waters, whereas the tritium values range from 10–15 TU for all three water sources, although generally there is higher tritium in the Baltic Sea waters (due to reservoir effects).
- The tritium-free groundwaters from Forsmark show ^{14}C values in the range 14–25 pmC and these waters have generally low HCO_3 contents (< 150 mg/L) and $\delta^{13}C$ values between –10 and –5‰. A plot of ^{14}C (expressed as pmC) versus $\delta^{13}C$ ‰, shows that groundwaters from the percussion and cored boreholes indicate a mixing trend between: a) HCO_3-rich waters with low $\delta^{13}C$ and high ^{14}C content, and b) deeper groundwaters with lower HCO_3 contents, higher $\delta^{13}C$ values and lower ^{14}C.
- The groundwaters showing the lowest ^{14}C values have chloride contents ranging from 4,500–5,500 mg/L; these indicate marine signatures, i.e. they represent waters with a dominant Littorina Sea component. (Note: No ^{14}C analyses are available from the deep saline groundwaters). In terms of ‘relative age’, the measured pmC values indicate 11,000–16,000 years which is significantly older than the Littorina Sea period. This can be explained by an addition of older bicarbonate, probably by dissolution of older carbonate and/or mixing by glacial water (supported by low $\delta^{18}O$ in at least some of these groundwaters).
- The $\delta^{34}S$ data have a wide range (–11 to +30‰ CDT) indicating different sulphur sources for the dissolved SO_4. For the surface waters (Lake and Stream waters) the SO_4 content is usually below 35 mg/L and the $\delta^{34}S$ is relatively low but variable (–1 to +11‰ CDT) with most of the samples in the range 2 to 8‰ CDT. These relatively low values indicate atmospheric deposition and oxidation of sulphides in the overburden as being the origin for the SO_4. The Baltic Sea samples cluster around 20‰ CDT with some less saline Baltic samples showing lower $\delta^{34}S$ values resulting from inmixing of surface water.
- The deeper groundwaters show $\delta^{34}S$ values in the range +12 to +26‰ CDT where all samples with SO_4 contents greater than 250 mg/L show $\delta^{34}S$ values higher than +20‰ CDT. Such values are usually interpreted to result from sulphate reducing bacterial activity in the bedrock aquifer.
- The Cl versus $\delta^{34}S$ plot shows a clear trend with higher $\delta^{34}S$ values for groundwaters with higher salinities than present Baltic Sea waters (2,800 mg/L Cl). If the $\delta^{34}S$ values in the marine groundwaters are modified by sulphate reducing bacteria during closed conditions then a clear trend of more positive $\delta^{34}S$ values with decreasing sulphate content should be the result. This is not seen and therefore several processes need to be considered.

- The relatively few fracture calcites so far analysed for Sr-isotopes show values below 0.718 supporting that they are not precipitated from today's groundwater and that calcite dissolution has had little influence on the Sr-isotope ratios in the groundwater.
- Plotting $\delta^{37}Cl$ against chloride shows that most of the surface, near-surface and Baltic Sea waters have values within the range –0.28 to +0.34‰ SMOC. The former waters have the greatest spread (–06 to +2‰ SMOC) where most of the samples are within the interval –0.2 to +05‰ SMOC. The majority of the Baltic Sea samples values are close to 0‰ SMOC or slightly higher (up to +0.3‰ SMOC); a few samples show also lower values down to –0.6‰ SMOC.
- $\delta^{37}Cl$ in groundwaters from the cored and percussion boreholes are between –0.2 to +0.6‰ SMOC and demonstrate no relation with increasing chloride content. Given the analytical uncertainty of around ±2‰ SMOC, the groundwater values correspond to a slight emphasis on a water/rock origin.
- The presence of uranium in surface and near-surface waters is characterised by values between 0.05 and 28 µg/L. Large variations in uranium content in surface waters are common and are usually ascribed to various redox states and various contents of complexing agents, normally bicarbonate.
- Uranium versus bicarbonate for the waters shows no clear trend although there is a tendency of higher uranium contents in the surface and near-surface groundwaters associated with increasing bicarbonate up to 400 mg/L. For the few near-surface waters with higher bicarbonate contents the uranium tends to decrease, which may be due to very low redox potential in these waters caused by the microbial reactions producing the bicarbonate (probably to large extent sulphate reducers).
- Uranium versus chloride shows that the highest uranium contents are found in the waters with chloride values around 5,000–5,500 mg/L, i.e. the brackish groundwaters dominated by a Littorina Sea water component.
- These high but variable uranium contents at Forsmark are accompanied by increased ^{226}Ra and ^{222}Rn indicating that uranium and radium along the fracture pathways have been mobilised to various degrees by the slowly descending Littorina Sea waters. One possible scenario is that the glacial melt water is accompanied by oxidised uranium into the (near-surface?) fracture zones and subsequently easily remobilised by the reducing but bicarbonate (and DOC) rich Littorina Sea water. The mobilised uranium was then transported to greater depths during the density turnover. The reducing character of the Littorina Sea water is supported by, for example, the high Mn^{2+} contents (1–3 mg/L; resulting from Mn-reducing bacteria) recorded for most of the uranium-rich water samples.
- The primary origin of the oxidised and remobilised uranium may have been the uranium mineralisations found at several localites in Uppland. For example, pitchblende vein fillings in skarn have been documented only some kilometres from the Forsmark site.

5.4 Trace elements

Only a few data exist for the majority of groundwaters and even some of these are incomplete.

- Li, Rb and Cs (and to a lesser extent Y) from the cored and percussion boreholes show a sharp increase from low values (shallow surface to near-surface waters) to high values at approx. 100 m depth. This is followed by a levelling off (i.e. in the brackish groundwaters) until around 500 m when a decrease to moderate values occurs. Strontium, whilst reflecting a similar trend for the upper 500 m, increases significantly towards depth.
- La and Ce from the cored and percussion boreholes are close to detection apart from approx. 400–500 m depth when a significant peak can be observed.
- Shallow groundwaters from the Soil Pipes show a wide range of values for Ce, La and Y.

5.5 Calcites

Calcites have been precipitated in open fractures on several occasions, commencing with the hydrothermal prehnite-laumontite generation. Taken all the stable isotope data into account there is strong support for these two generations to be part of the same prolonged event; the tailing in $\delta^{18}O$ for this group from –18 to at least –14‰ may be due to precipitation from a hydrothermal fluid during decreasing temperatures and/or changes in water-rock ratio during a hydrothermal event. The connection between the calcite in the prehnite and laumontite generations are in accordance with earlier observations from Finnsjön.

Calcite with extremely low $\delta^{13}C$ values has been produced during the event responsible for the quartz and analcime formation partly as a late phase. These mineralisations must have been precipitated during lower temperatures than the preceding laumontite formation, although it is reasonable to assume that it was still hydrothermal (< 200°C is suggested). The very low $\delta^{13}C$ values are usually interpreted as due to in-situ microbial activity which implies that the temperature was not significantly above 100°C when the carbon isotope signature was modified. However, the temperature evolution during this period of fracture mineralisation is not yet known. Based on Sr-isotope values this period is clearly separated from the prehnite-laumontite formation, either in time (the radiogenic ^{87}Sr is much higher in the latter generation), or the chemistry of the hydrothermal fluid was significantly different and preferred dissolution of K-Rb minerals occurred.

The euhedral crystals (mostly equant in shape) formed on top of the quartz-calcite-adularia coatings in some of the fractures, are possibly the latest phase of these events.

It has not been possible yet to relate several calcite precipitates to any specific fracture mineralisation event. For example, a group of calcites from borehole KFM02A (110–118 m) shows significantly positive $\delta^{13}C$ values (+6 to +8‰) and $\delta^{18}O$ values of –8 to –11‰. There is also a cluster of samples that may include relatively late (Quaternary) fresh water precipitates. More analyses are therefore needed in order to better identify this group.

6 Visualisation of the Forsmark 1.2 data

Visualisation of the hydrogeochemical 1.2 evaluation is in the form of two vertical transects through the Forsmark site local model area, one oriented in a SW-NE direction and the other in a NW-SE direction (Figure 6-1). Their positions are based on topographical and hydrogeological criteria and the locations of the site characterisation boreholes (S. Follin, written comm. 2004). The vertical extent of the transects is to approx. 2,000 m to accommodate the known and suspected structural features.

The SW-NE transect was selected to approximate the main regional topographic gradient direction towards the Forsmark local model area. The final position of the transect was aligned to integrate boreholes KFM04A/B, KFM05A and KFM06A/B. The NW-SE transect was chosen parallel to the coastline to represent some of the groundwater flow directions diverted along several of the major gently dipping deformation zones; it was aligned to integrate boreholes KFM01A/B, KFM05A, KFM02A and KFM03A/B.

Note that boreholes KFM05A and KFM06A/B are not included in this present 1.2 hydrogeochemical model version.

The relationships of the chosen transects to the distribution of the major structural features are indicated in Figure 6-2. Transect SW-NE is sub-parallel to the dominant series of SW-NE trending steeply dipping deformation zones. Certain important structural features are, however, intersected by the transect including the sub-vertical NW-SE trending NW003A fracture and the low angle gently dipping A2 fracture. In contrast transect NW-SE intersects the series of SW-NE trending steeply dipping deformation zones together with a suite of gently dipping deformation zones (e.g. A1, A2, A3 etc) which increase in frequency towards the SE.

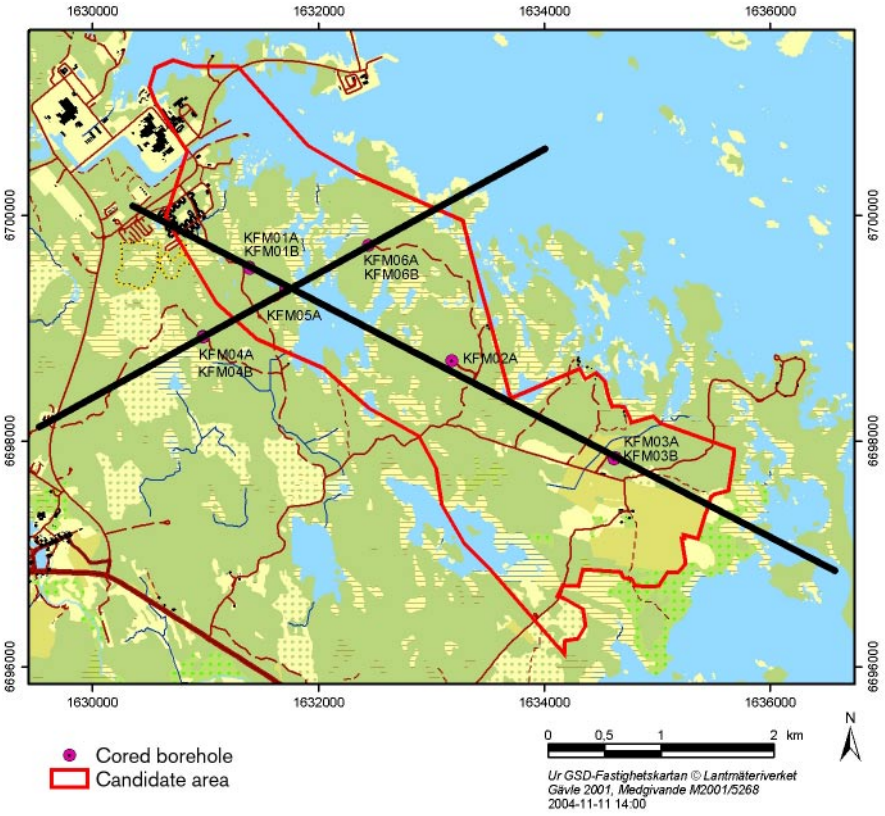

Figure 6-1. *Location of the selected vertical transects in relation to the major cored boreholes. The SW-NE transect reflects the regional topographic gradient direction towards the Forsmark local model area (U Brising, Sven Follin, written comm. 2004).*

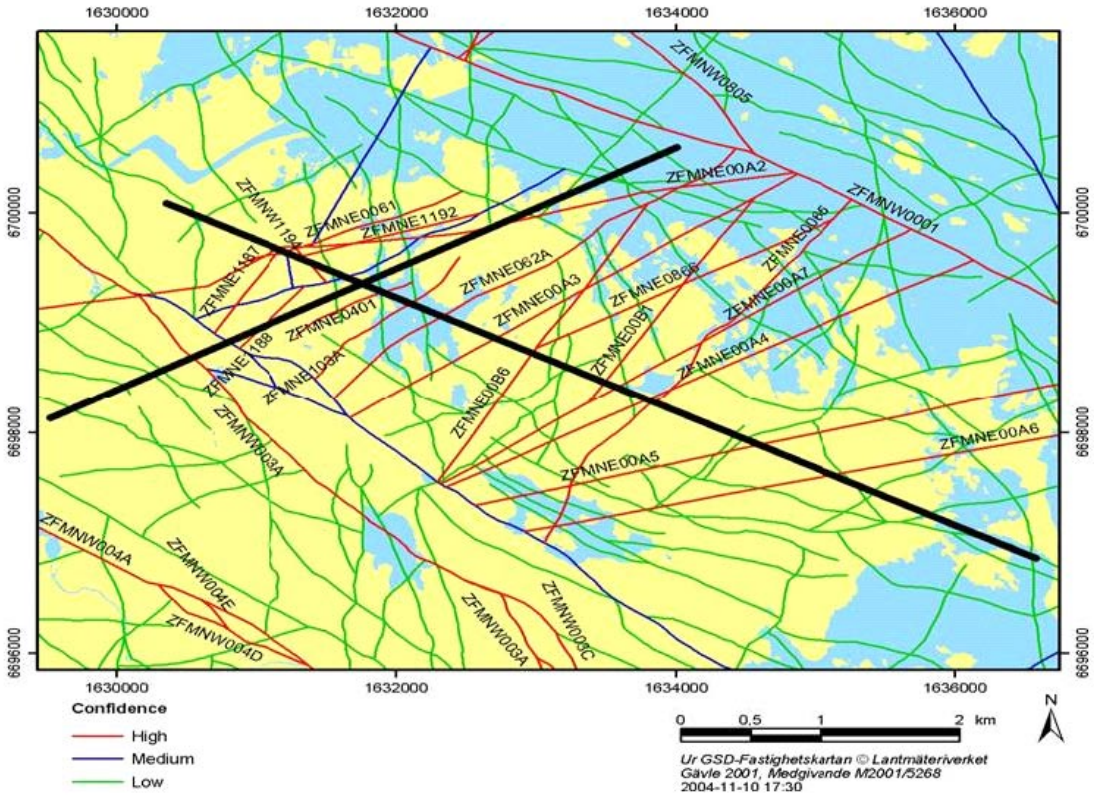

Figure 6-2. *Structural map of the region including and surrounding the Forsmark site. The SW-NE transect approximately follows the regional topographical gradient direction towards the investigated site. Transect NW-SE was chosen parallel to the coastline to represent some of the groundwater flow directions along several of the major gently dipping deformation zones (e.g. A1, A2 and A3) (S Follin, U Brising, written comm. 2004).*

Modelled 2-D versions of the vertical transects to 2,000 m were produced (Figures 6-3 and 6-5) showing the position of the main structures and the location (actual or extrapolated) of the boreholes. Using these modelled sections as a base, schematic manual versions then were produced to facilitate illustrating the most important deformation zones and their potential hydraulic impact on the groundwater flow. These tentative hydraulic conditions were then integrated with the results of the hydrogeochemical evaluation to help interpret the observed vertical and lateral changes in the groundwater chemistry (Figures 6-4 and 6-6).

Figure 6-3 shows for transect SW-NE the selected structures for further visualisation and the relationships of the boreholes (percussion and cored varieties) to these structures. The transect extends from close to the Eckarfjärden Deformation Zone in the SW to the Baltic Sea to the NE; the intercepted geology comprises mainly metagranitoid. Included in the transect is Bolundsfjärden Lake which is considered a discharge area. Structurally, intersected gently dipping deformation zones (B-series) increase in frequency towards the coast, with the A2 zone being a major feature within the characterised site area were the boreholes are located. As mentioned above, the transect is parallel or sub-parallel to the major system of SW-NE trending steeply dipping deformation zones which channel most of the groundwater flow towards the Forsmark local model area.

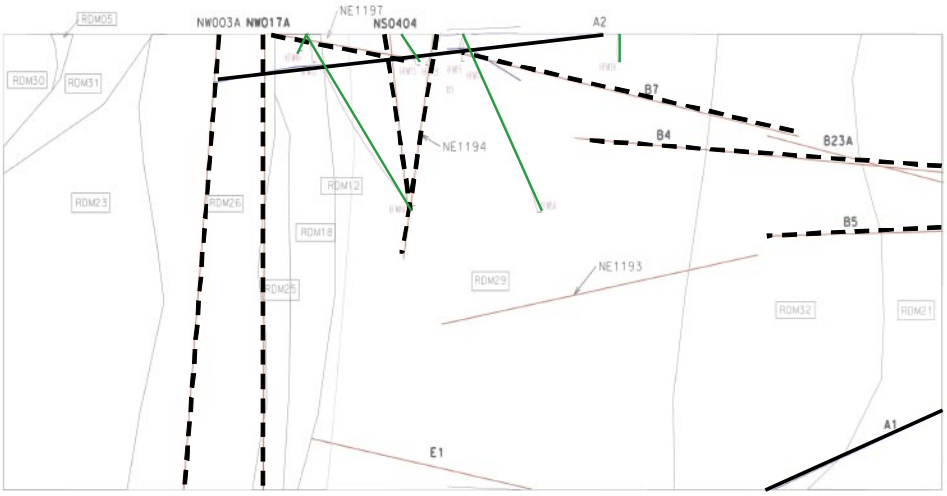

Figure 6-3. *Modelled 2-D version of the SW-NE vertical transect showing the intersected structures and the location (actual or extrapolated) of the boreholes used in the hydrogeochemical characterisation (A Simeonovz, written comm. 2004). Accentuated for further modelling (see Figure 6-4) are selected important structures (black hatch lines) and the borehole locations (percussion and cored in green).*

Figure 6-4 shows the further integration of the structural features with the main groundwater flow directions and their relative velocities, and the observed hydrochemistry along transect SW-NE. Groundwater data are limited to shallow depths (0–350 m). Two major groundwater types are indicated: 1) recent to young (0–5.6 TU) Na-HCO_3 type of meteoric origin ($\delta^{18}O$ = –11 to –9‰ SMOW; δD = –81.9 to –77.5‰ SMOW), and 2) old Na-Ca Cl(SO_4) type (Littorina Sea signature) of marine origin ($\delta^{18}O$ = –9.5 to –8.4‰ SMOW; δD = –84.4 to –66.1‰ SMOW). The lateral and vertical spatial extent of the Na-HCO_3 groundwater is uncertain due to a lack of data, but certainly the deeper, older Littorina Sea groundwater type lies close to the surface towards the SW in the near vicinity of the steeply dipping deformation zones NW003A and NW017A. These structures are believed to be discharging. Furthermore, close to Bolundsfjärden Lake the vertical extent of the Na-HCO_3 groundwater may be less than shown since this lake area is considered a zone influenced by discharge.

Figure 6-5 illustrates transect NW-SE, the selected structures for further visualisation and the relationships of the boreholes (percussion and cored varieties) to these structures. The transect extends from just south of the Forsmark nuclear power facility to the Baltic Sea coast to the SE; Bolundsfärben Lake (discharge zone) is incorporated in the transect.

Figure 6-5 shows that steeply dipping structures are more frequent to the NW of the transect and increasingly gently dipping structures dominate southeastwards to the Baltic Sea coast. The gently dipping A2 zone is observed once again to be an important feature in the Forsmark site providing a hydrostructural connection across the Forsmark local model area (S Follin, pers. comm. 2005). The intercepted geology comprises mainly metagranitoid.

Figure 6-6 shows the further integration of these features with the main groundwater flow directions and their relative velocities, and the observed hydrochemistry along the NW-SE transect.

The groundwater flow regimes at Forsmark are considered small scale and their vertical extent depends on local hydraulic conditions. Close to the Baltic Sea coastline where topographical variation is even less, groundwater flow penetration to depth will subsequently be less marked and such areas will tend to be characterised by groundwater discharge. The discharge groundwater flow along the steeply dipping deformation zones (Figure 6-6) is restricted to a vertical depth of around 500–600 m, increasing in rate towards the surface. In contrast, the discharge groundwater flow in the gently dipping deformation zones may extend down to 1,000 m depth, also increasing in rate towards the surface.

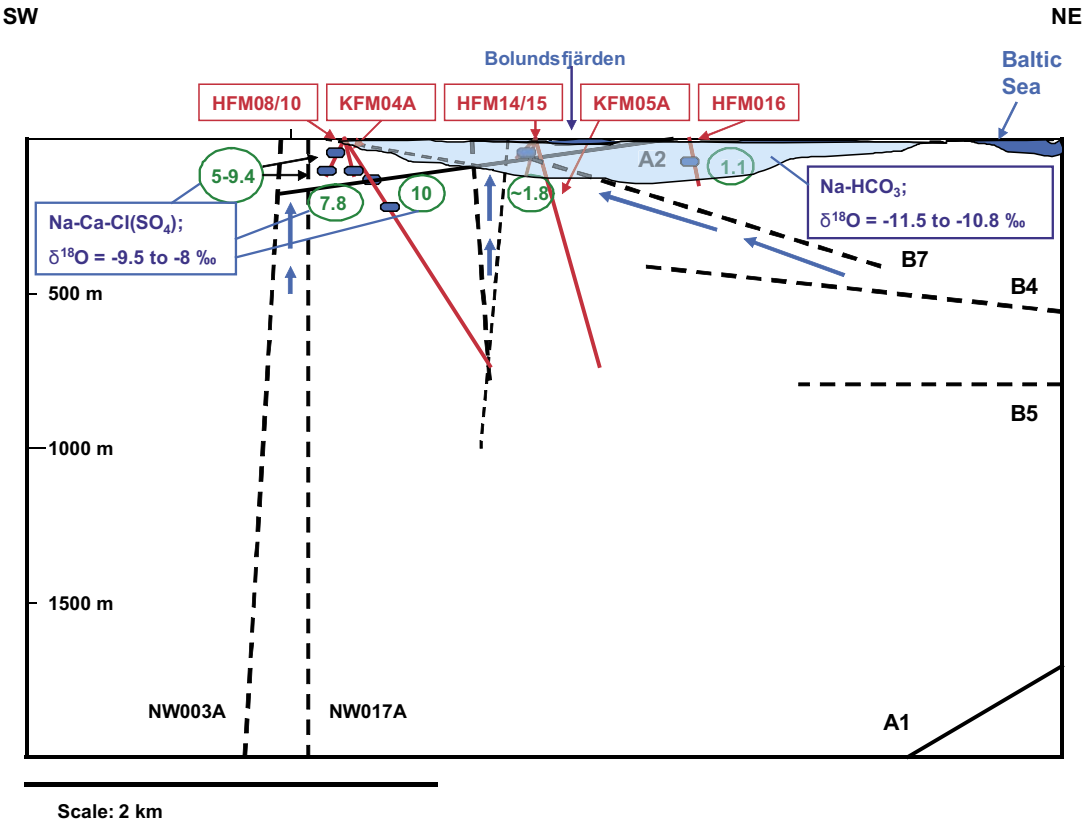

Figure 6-4. *Schematic 2-D model based on Figure 6-3 integrating the major structures, the major groundwater flow directions and the variation in groundwater chemistry from the sampled boreholes. Sampled borehole sections are indicated in blue, circled numbers refer to g/L TDS and orange infilled circles refer to groundwaters exhibiting a Littorina Sea signature. The blue arrows are estimated groundwater flow directions and their respective lengths reflect relative groundwater flow velocities (short = low flow; longer = greater flow).*

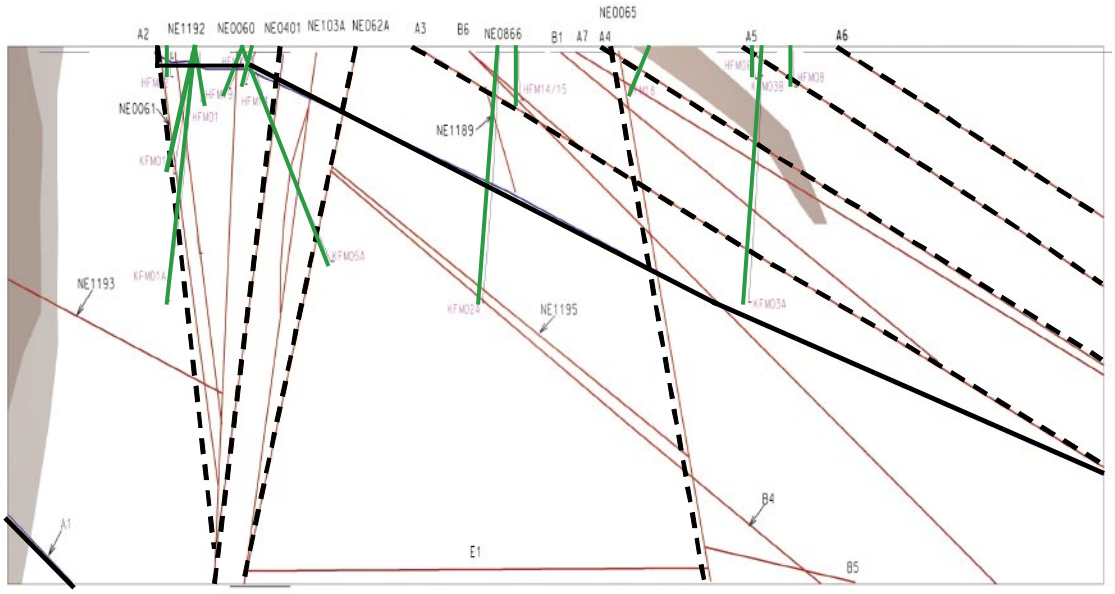

Figure 6-5. *Modelled 2-D version of the NW-SE vertical transect showing the intersected structures and the location (actual or extrapolated) of the boreholes used in the hydrogeochemical characterisation (A Simeonov, written comm. 2004). Accentuated for further modelling (see Figure 6-6) are the more important structures (solid and black hatch lines) and the borehole locations (percussion and cored types in green).*

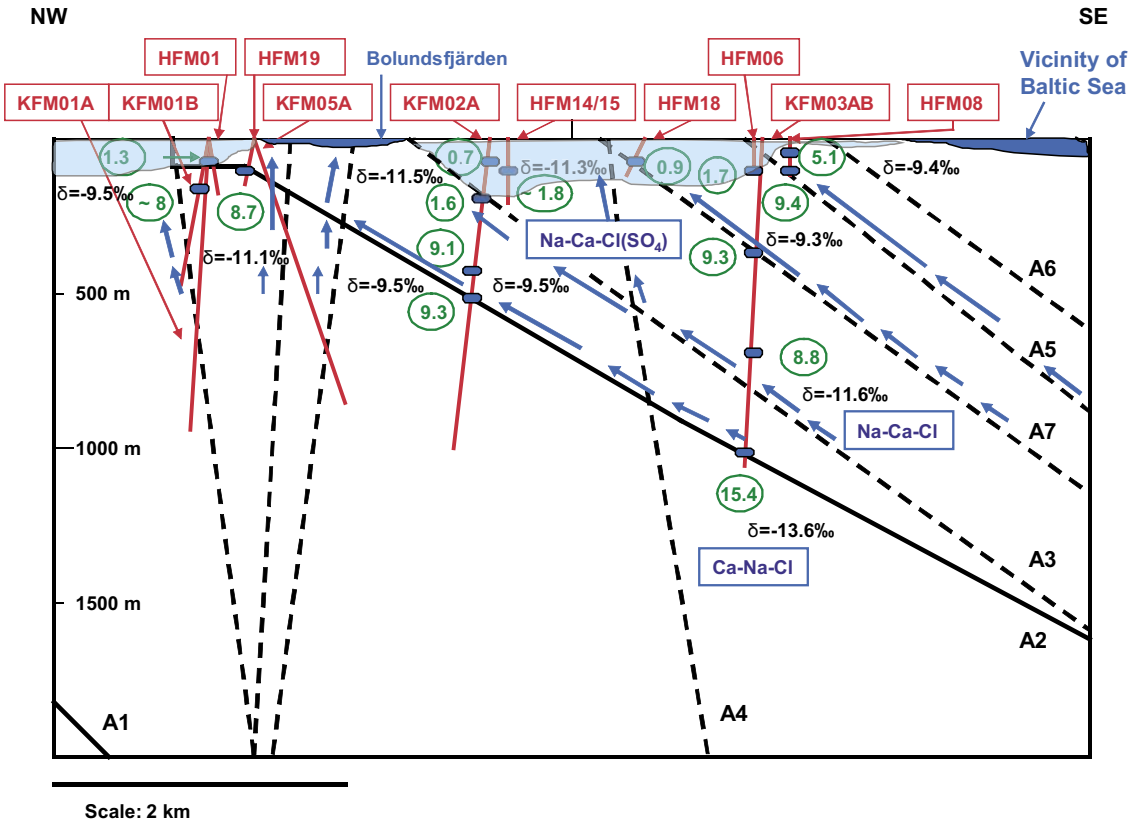

Figure 6-6. *Schematic 2-D model based on Figure 6-5 integrating the major structures, the major groundwater flow directions and the different groundwater chemistries. Sampled borehole sections are indicated in blue, circled numbers refer to g/L TDS and orange infilled circles refer to groundwaters exhibiting a Littorina Sea signature. The blue arrows are estimated groundwater flow directions and their respective lengths reflect relative groundwater flow velocities (short = low flow; longer = greater flow). The 'δ' values refer to* 'δ^{18}O = ‰ SMOW'.

Four main groundwater types are present. In addition to the recent to young Na-HCO_3 type groundwaters and old Na-Ca Cl(SO_4) type groundwaters (Littorina Sea signature) as already described above, there exist at greater depths (KFM03A; 645 m) an older meteoric Na-Ca-Cl type groundwater (~ 16 pmC) with a small glacial component (δ^{18}O = –11.6‰ SMOW; δD = –84.3‰ SMOW). At still greater depth (KFM03A: 990 m) the groundwater changes to a higher saline Ca-Na-Cl type characterised by an even greater glacial signature (δ^{18}O = –13.6‰ SMOW; δD = –98.5‰ SMOW). Although only one deep sample exists, the A2 sub-horizontal zone appears to form the boundary between the Na-Ca-Cl and Ca-Na-Cl groundwater types were borehole KFM03A is drilled.

The near-surface Na-HCO_3 groundwaters form a distinctive horizon at the centre of the transect which lenses out towards the SE Baltic Coast where discharge of deeper groundwater probably occurs. From Bolundsfjärden to the NW a less marked horizon is indicated but data are few. In addition, the influence of A2 on the groundwater chemistry is not clear at this near-surface locality.

Bordering the shallow Na-HCO_3 groundwaters, and extending from close to the surface (near the SE coast) to depths of around 500 m (along deformation zone A2), are the Littorina Sea type groundwaters. The upward (discharging) movement of these Littorina Sea type groundwaters below Bolundsfjärden Lake is supported by the soil pipe groundwater sample SFM0023 collected under Bolundsfjärden showing increased Mg and SO_4.(cf. Figure 1-27). Therefore, assuming that Bolundsfjärden Lake is a recharge area, which in Figure 6-6 may correspond to the intersection of the illustrated steeply dipping deformation zones (further connected to A2), then the distribution of the near-surface Na-HCO_3 groundwaters may be as indicated although a mixture of Na-HCO_3 and deeper Littorina Sea groundwaters would be more representative in the bedrock under Bolundsfjärden Lake.

7 References

Berg C, Nilsson A-C, 2004. Hydrochemical logging of KFM04A. Forsmark site investigation. SKB P-04-47, Svensk Kärnbränslehantering AB.

Byegård J, Ramebäck H, Widestrand H, 2002. Use of radon concentrations for estimation of fracture aperture. SKB Äspö HRL, ICR Report. (ICR 02-xxxx), Svensk Kärnbränslehantering AB.

Bäckblom G, Stanfors R, 1989. Interdisciplinary study of post-glacial faulting in the Lansjärv area, northern Sweden. SKB TR-89-31, Svensk Kärnbränslehantering AB.

Claesson L-Å, Nilsson G, 2004. Drilling of five percussion boreholes, HFM11–12 and HFM19, on different lineaments. Forsmark site investigation. SKB P-04-106, Svensk Kärnbränslehantering AB.

Donner J, Kankainen T, Karhu J A, 1994. Radiocarbon ages and stable isotope composition of Holocene shells in Finland. In T. Andrén (ed), Proceedings of the Conference The Baltic – past, present and future. Stockholm March 14–16, 1994. Stockholm University, Quaternaria A:7, 31–38.

Eriksson L, 2004. Miljörapport 2003. Utsläpp av radioaktiva ämnen. Forsmarks Kraftgrupp. Rep. Nr. FQ-2004-78.

Frape S K, Byrant G, Blomqvist R, Ruskeeniemi T, 1996. Evidence from stable chlorine isotopes for multiple sources of chloride in groundwaters from crystalline shield environments. In: Isotopes in Water Resources Management, 1996. IAEA-SM-336/24, Vol. 1, 19–30.

Hallbeck L, 2004. Forsmark Hydrogeochemical Site Description Model v. 1.2, December (Submitted).

Källgården J, Ludvigson J-E, Jönsson S, 2003. Pumping tests and flow logging. Boreholes KFM03A (0–100 m), HFM06, HFM07 and HFM08. Forsmark site investigation. SKB P-03-36, Svensk Kärnbränslehantering AB.

Ludvigson J-E, Jönsson S, Levén J, 2003a. Pumping tests and flow logging. Boreholes KFM01A (0–100 m), HFM01, HFM02 and HFM03. Forsmark site investigation. SKB P-03-33, Svensk Kärnbränslehantering AB.

Ludvigson J-E, Jönsson S, Svensson T, 2003b. Pumping tests and flow logging. Boreholes KFM02A (0–100 m), HFM04 and HFM05. Forsmark site investigation. SKB P-03-34, Svensk Kärnbränslehantering AB.

Ludvigson J-E, Jönsson S, Jönsson J, 2004a. Pumping tests and flow logging. Boreholes HFM11 and HFM12. Forsmark site investigation. SKB P-04-64, Svensk Kärnbränslehantering AB.

Ludvigson J-E, Jönsson S, Hjerne C, 2004b. Pumping tests and flow logging. Boreholes KFM06A (0–100 m) and HFM16. Forsmark site investigation. SKB P-04-65, Svensk Kärnbränslehantering AB.

Ludvigson J-E, Källgården J, Hjerne C, 2004c. Pumping tests and flow logging. Boreholes HFM17, HFM18 and HFM19. Forsmark site investigation. SKB P-04-72, Svensk Kärnbränslehantering AB.

Ludvigson J-E, Källgården J, Jönsson J, 2004d. Pumping tests and flow logging. Boreholes HFM09 and HFM10. Forsmark site investigation. SKB P-04-74, Svensk Kärnbränslehantering AB.

Milodowski A E, Gillespie m R, Pearce J M, Metcalfe R, 1998. In collaboration with the SKB EQUIP programme; Petrographic characterisation of calcites from Äspö and Laxemar deep boreholes by scanning electron microscopy, electron microprobe and cathodoluminescence petrography, WG/98/45C, British Geological Survey, Keyworth, Nottingham, UK.

Nilsson A-C, 2003a. Sampling and analyses of groundwater in percussion drilled boreholes and shallow monitoring wells at drillsite DS1. Results from the percussion boreholes HFM01, HFM02, HFM03, KFM01A (borehole section 0–100 m) and the monitoring wells SFM0001, SFM0002 and SFM0003. Forsmark site investigation. SKB P-03-47, Svensk Kärnbränslehantering AB.

Nilsson A-C, 2003b. Sampling and analyses of groundwater in percussion drilled boreholes and shallow monitoring wells at drillsite DS2. Results from the percussion boreholes HFM04, HFM05, KFM02A (borehole section 0–100 m) and the monitoring wells SFM0004 and SFM0005. Forsmark site investigation. SKB P-03-48, Svensk Kärnbränslehantering AB.

Nilsson A-C, 2003c. Sampling and analyses of groundwater in percussion drilled boreholes at drillsite DS3. Results from the percussion boreholes HFM06 and HFM08. Forsmark site investigation. SKB P-03-49, Svensk Kärnbränslehantering AB.

Nilsson P, Gustafsson C, 2003. Geophysical, radar and BIPS logging in boreholes HFM04, HFM05, and the percussion drilled part of KFM02A. Forsmark site investigation. SKB P-03-53, Svensk Kärnbränslehantering AB.

Nilsson D, 2004. Sampling and analyses of groundwater from percussion drilled boreholes. Results from the percussion boreholes HFM09 to HFM19 and the percussion drilled part of KFM06A. Forsmark site investigation. SKB P-04-92, Svensk Kärnbränslehantering AB.

O'Neil J R, Clayton R N, Mayeda T K, 1969. Oxygen isotope fractionation in divalent metal carbonates. J. Chem. Phys., 51 (12), 5547–5558.

Petersson J, Berglund J, Danielsson P, Wängnerud A, Tullborg E-L, Mattsson H, Thunehed H, Isaksson H, Lindroos H, 2004. Petrography, geochemistry, petrophysics and fracture mineralogy of boreholes KFM01A, KFM02A and KFM03A+B. SKB P-04-103, Svensk Kärnbränslehantering AB.

Pitkänen P, Luukkonen A, Ruotsalainen P, Leino-Forsman H, Vuorinen U, 1999. Geochemical modelling of groundwater evolution and residence time at the Olkiluoto site. Posiva Tech Rep. (98-10), Posiva, Helsinki, Finland.

Pitkänen P, Partamies S, Luukkonen A, 2004. hydrogeochemical interpretation of baseline groundwater conditions at the Olkiluoto site. Posiva Tech. Rep. (2003-07), Posiva, Helsinki.

Sandström B, Savolainen M, Tullborg E-L, 2004. Fracture mineralogy. Results from fracture minerals and wall rock alteration in boreholes KFM01A, KFM02A, KFM03A and KFM03B (In press).

SKB, 2004. Preliminary site description. Forsmark area – version 1.1. SKB R-04-15, Svensk Kärnbränslehantering AB.

Smellie J A T, Larsson N-Å, Wikberg P, Carlsson L, 1985. Hydrochemical investigations in crystalline bedrock in relation to existing hydraulic conditions: Experience from the SKB test-sites in Sweden. SKB TR-85-11, Svensk Kärnbränslehantering AB.

Smellie J A T, Larsson N-Å, Wikberg P, Puigdomenech I, Tullborg E-L, 1987. Hydrochemical investigations in crystalline bedrock in relation to existing hydraulic conditions: Klipperås test-site, Småland, southern Sweden. SKB TR-87-21, Svensk Kärnbränslehantering AB.

Smellie J A T, Wikberg P, 1989. Hydrochemical investigations at the Finnsjön site, central Sweden. J. Hydrol., 126, 147–169.

Smellie J, Laaksoharju M, Tullborg E-L, 2002. Hydrogeochemical site descriptive model – a strategy for the model development during site investigations. SKB R-02-49, Svensk Kärnbränslehantering AB.

Tullborg E-L, Larson S Å, 1982. Fissure fillings from Finnsjön and Studsvik, Sweden. Identification, chemistry and dating. SKB TR-82-20 (ISSN 0348-7504), Svensk Kärnbränslehantering AB.

Wacker P, Nilsson A-C, 2003. Hydrochemical logging and “clean up” pumping in KFM02A. Forsmark site investigation. SKB P-03-95, Svensk Kärnbränslehantering AB.

Wacker P, Bergelin A, Nilsson A-C, 2003. Complete hydrochemical characterisation in KFM01A. Results from two investigated sections, 110.1–120.8 and 176.8–183.9 metres. Forsmark site investigation. SKB P-03-94, Svensk Kärnbränslehantering AB.

Wacker P, Bergelin A, Nilsson A-C, 2004a. Hydrochemical characterisation in KFM02A. Results from three investigated sections, 106.5–126.5, 413.5–433.5 and 509.0–516.1 metres. Forsmark site investigation. SKB P-04-70, Svensk Kärnbränslehantering AB.

Wacker P, Bergelin A, Berg C, Nilsson A-C, 2004b. Hydrochemical characterisation in KFM03A. Results from six investigated borehole sections: 386.0–391.0 m, 448.0–453.0 m, 448.5–455.6 m, 639.0–646.1 m, 939.5–946.6 m, 980.0–1001.2 m. Forsmark site investigation. SKB P-04-108, Svensk Kärnbränslehantering AB.

Wacker P, Bergelin A, Berg C, Nilsson A-C, 2004c. Hydrochemical characterisation in KFM04A. Results from two investigated borehole sections, 230.5–237.6 and 354.0–361.1 metres. Forsmark site investigation. SKB P-04-109, Svensk Kärnbränslehantering AB.

Welin E, 1964. Uranium dissemination and vein fillings in iron ores of northern Uppland, central Sweden. GFF, 51–82.

Appendix 2

Explorative analyses of microbes, colloids and gases

Contribution to the model version 1.2

Lotta Hallbeck

Vita vegrandis

December 2004

Contents

1 Microbiology and microbial model

1.1 Introduction

To understand the present undisturbed conditions the following parameters are of interest for hydrogeochemical site description modelling: pH, Eh, S^{2-}, S^0, SO_4, HCO_3^-, HPO_4^{2-}, nitrogen species and TDS together with colloids, fulvic and humic acids, dissolved organic compounds and microorganisms. Further, for a full understanding it is necessary to be able to predict how the conditions will change during the construction of a repository and during the following phases of the storage of spent nuclear waste. This part of the report will deal with the microbial data available so far from the site investigation in the Forsmark area.

Microbial parameters of interest are the total number and the presence of different metabolic groups of microorganisms /Pedersen, 2001/. These data will indicate activity of specific microbial populations at a certain site and how they may affect the geochemistry. The groups cultured for the microbial part of the site investigation were iron-reducing bacteria (IRB), manganese-reducing bacteria (MRB), sulphate-reducing bacteria (SRB), auto- and heterotrophic methanogens and auto- and heterotrophic acetogens.

MPN, "most probable number of microorganisms", is a statistical cultivation method for numbering the most probable number of different cultivable metabolic groups of microorganisms /American Public Health Association, 1992/.

1.2 Available data

At the data freeze for model version 1.2, 30 June 2004, microbiological data from six depths in three boreholes KFM01A, KFM02A and KFM03A were available. Information of the MPN culturing in the different boreholes can be found in Table 1. In this report microbe data are analysed in comparison to chemistry and gas data of importance for the different microbial processes.

Table 1-1. The MPN of different metabolic groups tested with groundwater from six depths in the boreholes in Forsmark.

Metabolic group	KFM01A 115.4 m	KFM01A 180.4 m	KFM02A 512.5 m	KFM03A 642.6 m	KFM03A 943 m	KFM03A 990 m
Iron-reducing bacteria	analysed	analysed	analysed	analysed	analysed	analysed
Manganese-reducing bacteria	analysed	analysed	analysed	analysed	analysed	analysed
Sulphate-reducing bacteria	analysed	analysed	analysed	analysed	analysed	analysed
Autotrophic methanogens	not analysed	not analysed	analysed	analysed	analysed	analysed
Heterotrophic methanogens	not analysed	not analysed	analysed	analysed	analysed	analysed
Autotrophic acetogens	not analysed	not analysed	analysed	analysed	analysed	analysed
Heterotrophic acetogens	analysed	analysed	analysed	analysed	analysed	analysed

1.3 Evaluation of the microbial data

1.3.1 Total number of cells and total organic carbon, TOC

In Figure 1-1 it can be seen that the total numbers of cells at the six depths in the three boreholes were all below 10^5 ml^{-1} with the lowest number at 642.5 m in KFM03A with 2.1×10^4 ml^{-1}. These data are similar to the numbers found in boreholes in the Fennoscandian shield /Pedersen, 2001/. The TOC values follow the decreasing trend with depth also in agreement with earlier studies /Pedersen, 2001/.

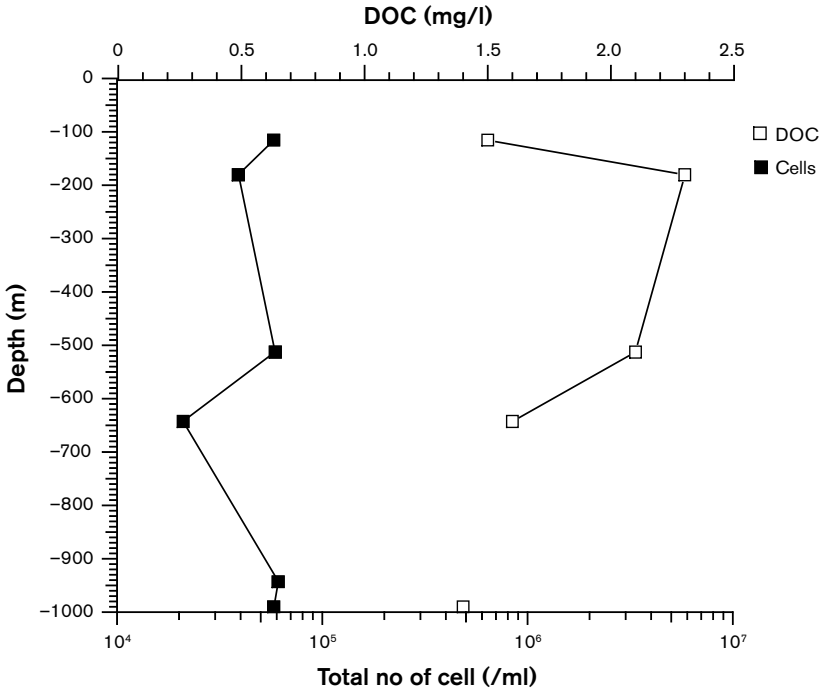

Figure 1-1. *Total number of cells and total organic carbon (TOC) at three depths in boreholes in Forsmark.*

During this phase of investigation the amount of humic and fulvic acids were determined by fractionation filtration. This determination showed that there were no organic acids in the fraction > 1,000 D but < 5,000 D. All of the organic fractions were smaller than 1,000 D /Wacker et al. 2003, 2004a,b/.

1.4 Redox potential in groundwater

Figure 1-2 shows the measured redox potentials in groundwater from the different depths in the three boreholes studied. The values were highest in the shallowest groundwater and reach the lowest value, –250 mV at 943 m in KFM03A. The redox values in combination with the microbial data will be discussed in section 1.12.

1.5 Iron-reducing bacteria, Fe^2 and Fe_{tot}

The highest amount of iron-reducing bacteria was found at 115.4 m in KFM01A with 4×10^3 per ml (Figure 1-3). In this figure it can also be seen that IRB also were found at 512.5 m in KFM02A and at 642.6 m in KFM03A but in numbers hundred times lower than at the shallowest depth. At the other levels sampled IRB were found only in trace amounts.

The presence of high numbers of IRB corresponds well with the measured redox potential, –174 mV at 115.4 m.

The high number of IRB implies that this group of organisms are of importance for the geochemistry in this area. Since most iron-reducing bacteria use partially oxidized organic matter, such as short organic acids, as energy- electron and carbon source they participate in the degradation of organic matter from the ground surface. It is not elucidated from where organic material at this depth comes from. Another source could be acetic acid produced by acetogens at deeper depths.

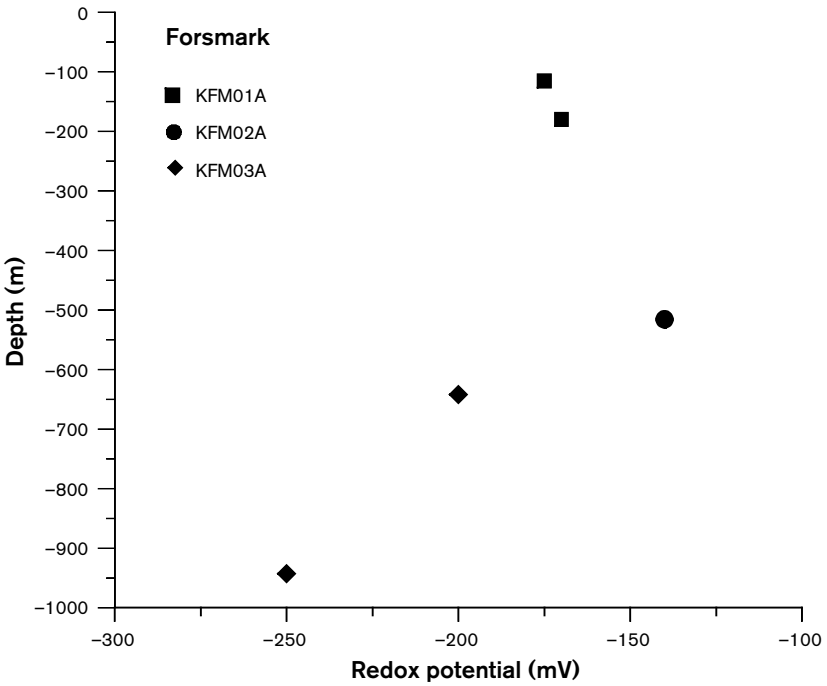

Figure 1-2. *Measured redox potentials at six depths in boreholes in the Forsmark area.*

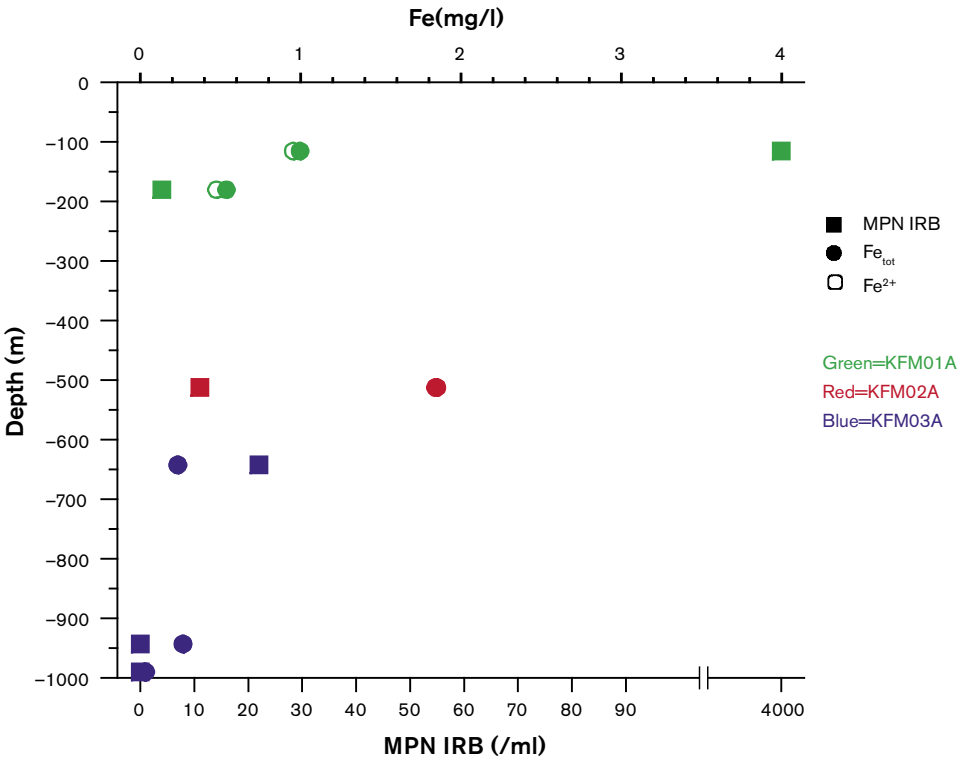

Figure 1-3. *Most probable number of cells (MPN) for iron-reducing bacteria (IRB) and Fe^{2+} and Fe_{tot} versus depths at six levels in boreholes in the Forsmark area.*

Iron in the groundwater is mostly in ferrous state and if sulphide is present some of the ferrous iron has precipitated as ferrous sulphide and sedimented out of the groundwater. Ferric state iron will probably be found as minerals on fracture surfaces.

1.6 Manganese-reducing bacteria and manganese

Figure 1-4 shows that the number of manganese-reducing bacteria (MRB) was high at 115.4 m in KFM01A together with the IRB as described in section 1.5. Manganese in solution is in the Mn^{2+} state due to the insolubility of MnO_2, the form that Mn(IV) will have in natural water within pH range 5–8. Also MRB are part of the ground water community that degrade organic matter from surface or utilise acetic acid produced by acetogens, and are therefore an important part of the process that lower the redox potential in ground water by oxidation of organic matter with oxidized manganese compounds.

1.7 Sulphate-reducing bacteria, sulphate and sulphide

The number of sulphate-reducing bacteria (SRB) was highest at 943 m in KFM03A with 5×10^3 ml^{-1} and this value corresponds to the low sulphate (Figure1-5). This correlation is value found in ground waters with high amounts of SRB. High amounts of sulphate were on the other hand found at depths with low numbers of SRB also this found in many environments including ground water in the Fennoscandian Shield. The hydrogen sulphide values were low at all depths, which may seem contradictory to the large number of SRB. One explanation for this could be formation and precipitation of pyrite in fractures.

1.8 Methanogens

In Figure1-6 the MPN numbers for the two different types of methanogens, autotrophic and heterotrophic, together with methane and hydrogen concentrations are plotted versus depth. There are unfortunately no data available for any type of methanogens from the two depths in KFM01A. The highest amount of methane in this investigation was found in KFM01A at 180.4 m. The MPN numbers from this depth were in general low and this could be explained by the lack of data of methanogens.

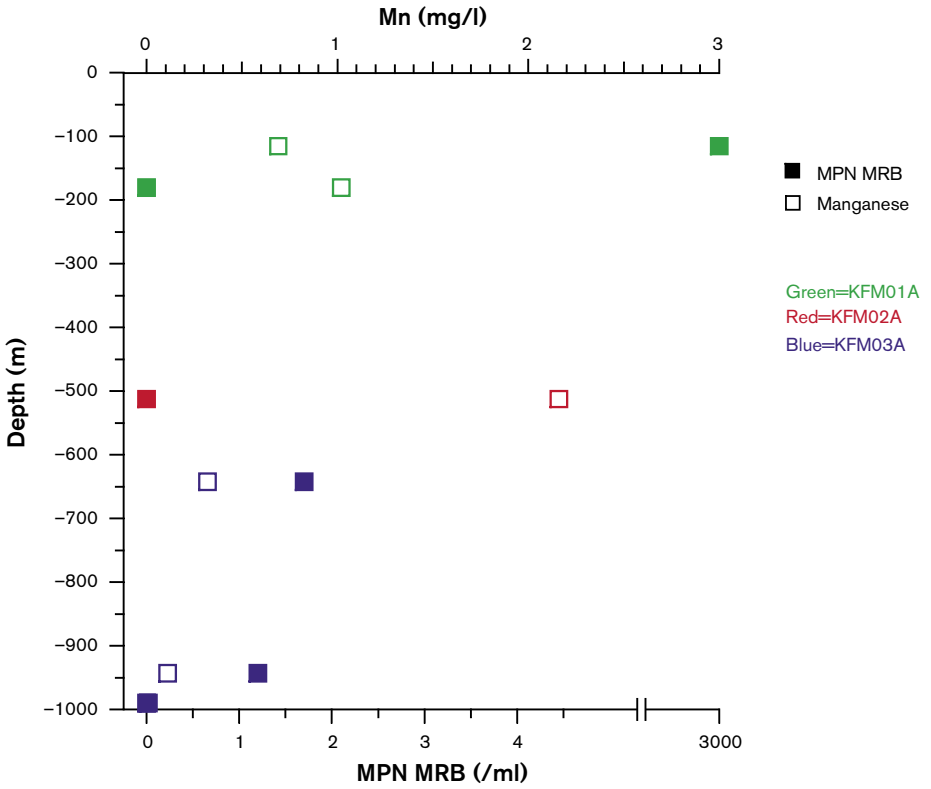

Figure 1-4. *Most probable number of cells (MPN) for manganese-reducing bacteria (MRB) and manganese versus depths at three levels in boreholes in the Forsmark area.*

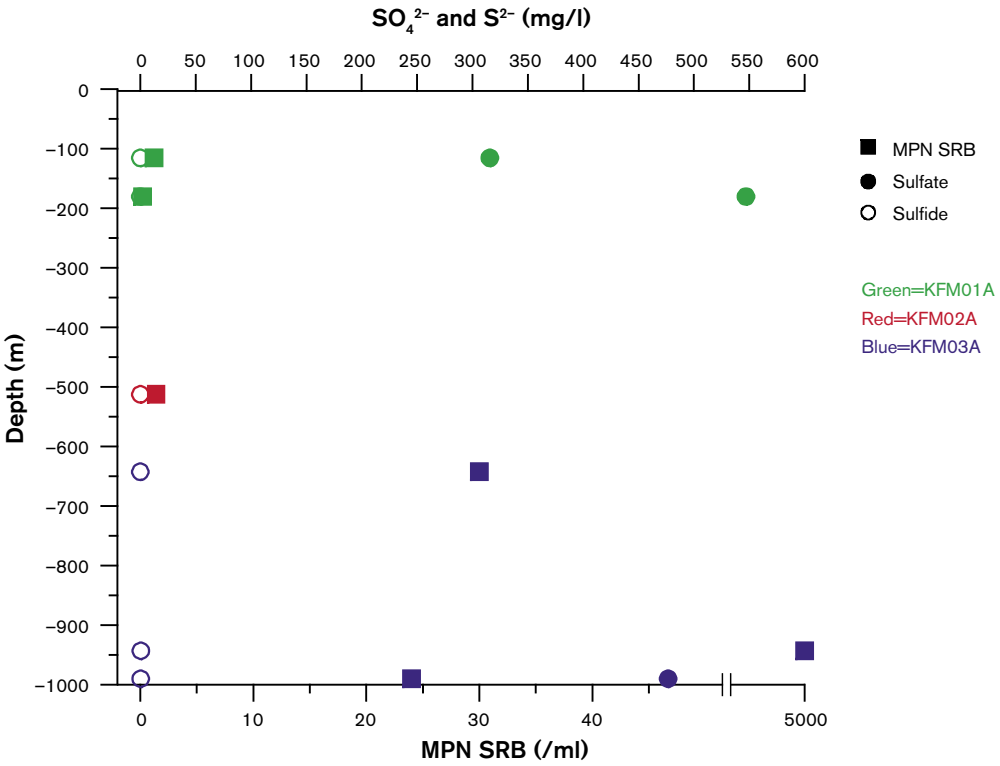

Figure 1-5. *Most probable number of cells (MPN) for sulphate-reducing bacteria (SRB), sulphate and sulphide versus depths at six levels in boreholes in the Forsmark area.*

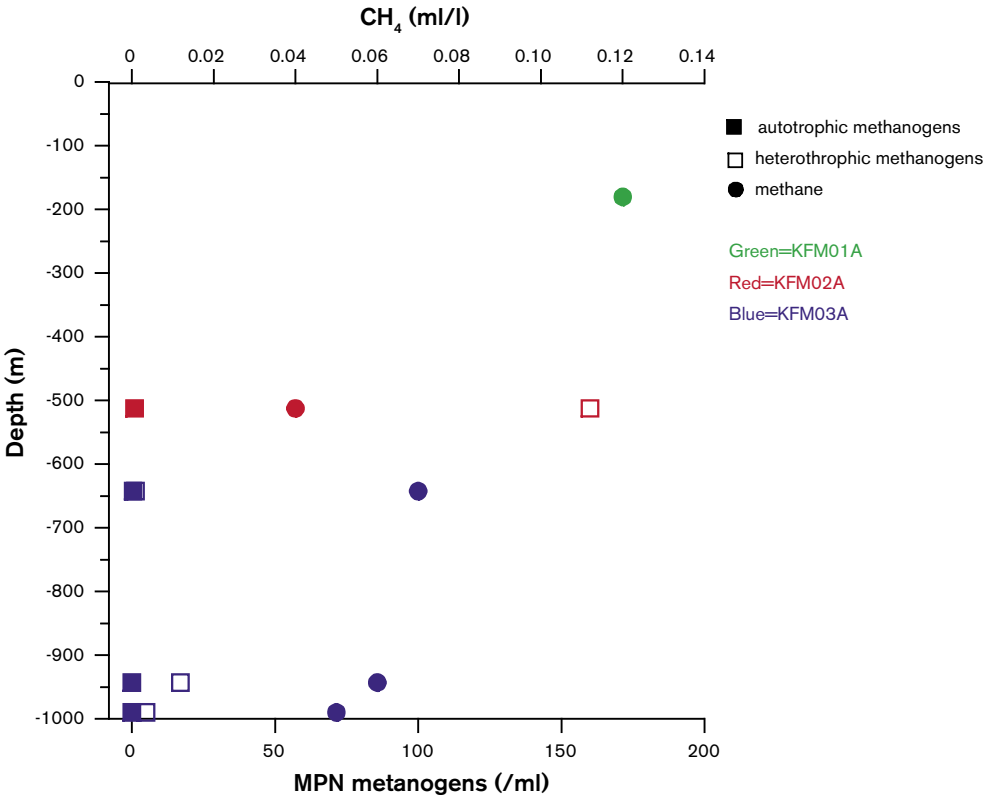

Figure 1-6. *Most probable number of cells (MPN) for auto- and heterotrophic methanogens,and methane versus depths in boreholes in the Forsmark area.*

The highest number of methanogens, heterotrophic methanogens, was found at 512,5 m in KFM02A with 160 ml l^{-1}. The amount of methane was here 0.04 ml l^{-1} corresponding to 2 µM (see also section 3.2.3). Autotrophic methanogens was present but only in trace amounts at this level and at 642.5 m in KFM03A.

There are no isotopic data available for the measured methane and, therefore, it is difficult to conclude the origin of the methane but the quota C1/C2+C3, see the part about hydrocarbons in 3.2.4, implies that it is a mixture of biogenic and abiogenic methane.

1.9 Acetogens

The result from acetogenic activity is production of acetate. In borehole KFM03A at 943 m depth there were high amounts of both auto- and heterotrophic acetogens (Figure 1-7). Especially the heterotrophs were numerous with 2.3×10^4 ml^{-1}. At the other depths there were only traces of acetogens. So far, there are no acetate data available; however, acetate could be an important parameter to measure in the future.

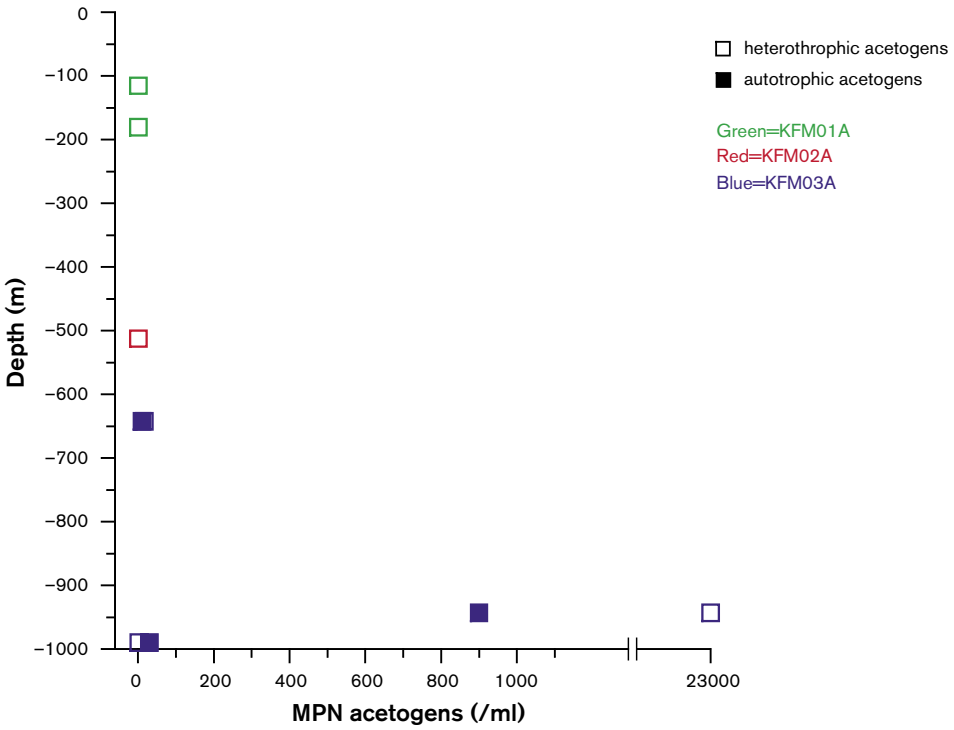

Figure 1-7. *Most probable numbers of cells (MPN) for auto- and heterotrophic acetogens versus depths at 6 depths in boreholes in the Forsmark area.*

1.10 Total number of cells versus MPN

From a comparison of the total number of cells found in groundwater from the six levels versus the MPN numbers obtained from culturing it can be seen that from most of the samples only a small percentage of the total numbers was possible to culture. Table 1-2 shows percentages from 0.015 up to 0.4 and this is in agreement what often is the result when the MPN method is applied to deep ground water. Interestingly the percentages for cultures from KFM01A, 115.4 m and KFM03A, 943 m, are extremely high with 12 and 48%, respectively. It should be taken in consideration that not all groups of microorganisms were included in the shallowest depth but still gave 115.4 m such high number. One explanation for this might be that the groundwater at 115.4 and 943 m were mixtures of different ground waters creating gradients for some of the chemical species promoting energy reactions in the cells.

In general, it can be concluded that even if the MPN numbers are too low, the proportion of the different metabolic groups registered is correct. This is supported by the agreement between cultured microorganisms and measured redox values (see section 1.12).

Table 1-2. The percentage of the total number of cells cultured with MPN in the analysed sections in boreholes in the Forsmark area.

Borehole (section, m)	Cells cultured (%)	
	MPN	Lower – upper 95% confidence limits
KMF01A (110–120,67)	12.0	3.5–48.3
KMF01A (176,8–183,9)	0.015	0.005–0.32
KMF02A (509–516)	0.29	0.11–0.96
KFM03A (448–453 m)	0.28	0.11–0.88
KFM03A (639–646 m)	0.40	0.16–1.2
KFM03A (938–944 m)	48	18–164
KFM03A (981–1,000 m)	0.16	0.06–0.57

1.11 Correlations

In the evaluation of data for different microorganisms, correlations between the presence of the microorganisms and one or more parameters involved in the metabolism of the respective microorganism should be tested for. In Figure 8 the MPN values for iron-, manganese- and sulphate-reducing bacteria together with methanogens are plotted versus ferrous iron, manganese, sulphate and methane, respectively.

There are no good correlations for IRB and MRB versus ferrous iron and manganese. Ferrous iron can precipitate as FeS and by that settle as solids. Figure 8c shows SRB versus sulphate and here a correlation with low sulphate and high numbers of SRB can be seen as a trend that is common for sulphate-reducing bacteria. The low sulphate values are possibly due to reduction by SRB to sulphide. If MPN for SRB were plotted versus produced sulphide it would show an opposite trend. However, low sulphide values indicate that the sulphide seems to be precipitated as iron sulphide (pyrite).

Unfortunately there were no data for methanogens at the level 180.4 m, KFM01A, where the highest methane concentration was found. For the available data no clear correlation can be seen (Figure 1-8d).

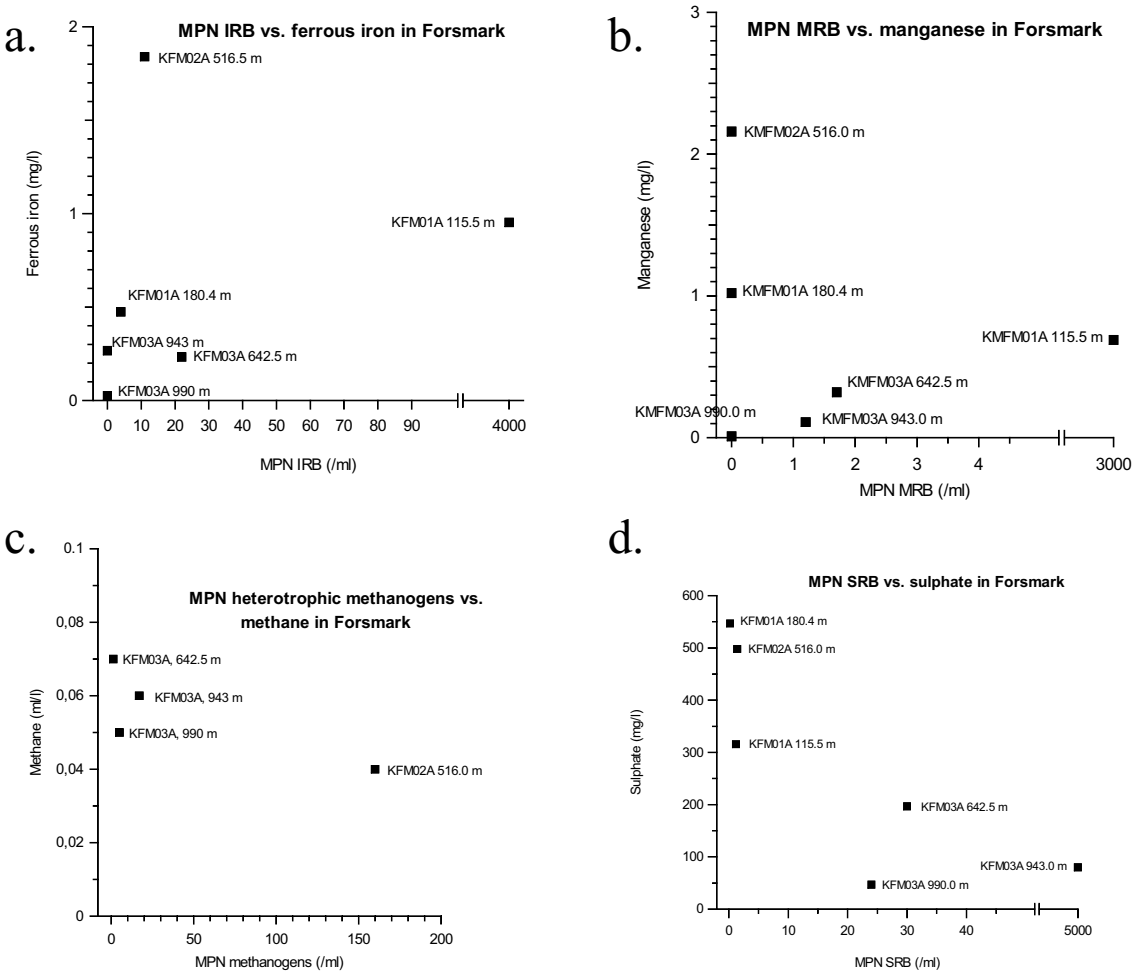

Figure 1-8. *MPN values for (a) IRB versus ferrous iron, (b) MRB versus manganese, (c) heterotrophic methanogens versus methane, (d) SRB versus sulphate in boreholes in the Forsmark area. Numbers in the figure indicate the borehole section centre.*

1.12 The microbial model

Figure 1-9 shows the distribution of the different microbial groups found at the six sampled levels in Forsmark and the measured redox potentials from Figure 1-2. The redox potential was from –140 to –250 mV. There is no obvious connection between measured redox potential and depth within this dataset.

To the right in Figure1-9 is a so-called redox ladder with different microbial respiration redox couples placed at their respective E_0'. The vertical red line in this figure marks the redox interval measured in Forsmark. These redox values coincide with where iron-, manganese and sulphate reducers, methanogens and acetogens can be found and correlate very well with the MPN results for this area.

Figure 1-10 shows the MPN numbers but in relation to depth. Here it can be seen that iron- and manganese reducers only were present at the shallow depth, above 300 metres. These groups were absent at lower depth where methanogens, acetogens and SRB dominated. It had to be remembered that there were no data of methanogens available from KFM01A, 115.4 and 180.4 m. The picture of the distribution over depth is therefore incomplete.

Figure 1-11 shows a redox model of the boreholes KFM01A, KFM02A and KFM03A including the 6 sampling levels. In the shallow levels in KFM01A, the iron- and manganese-reducing bacteria dominated and this correlated well with the measured redox values at this depth. Here the sulphate reducing bacteria were absent.

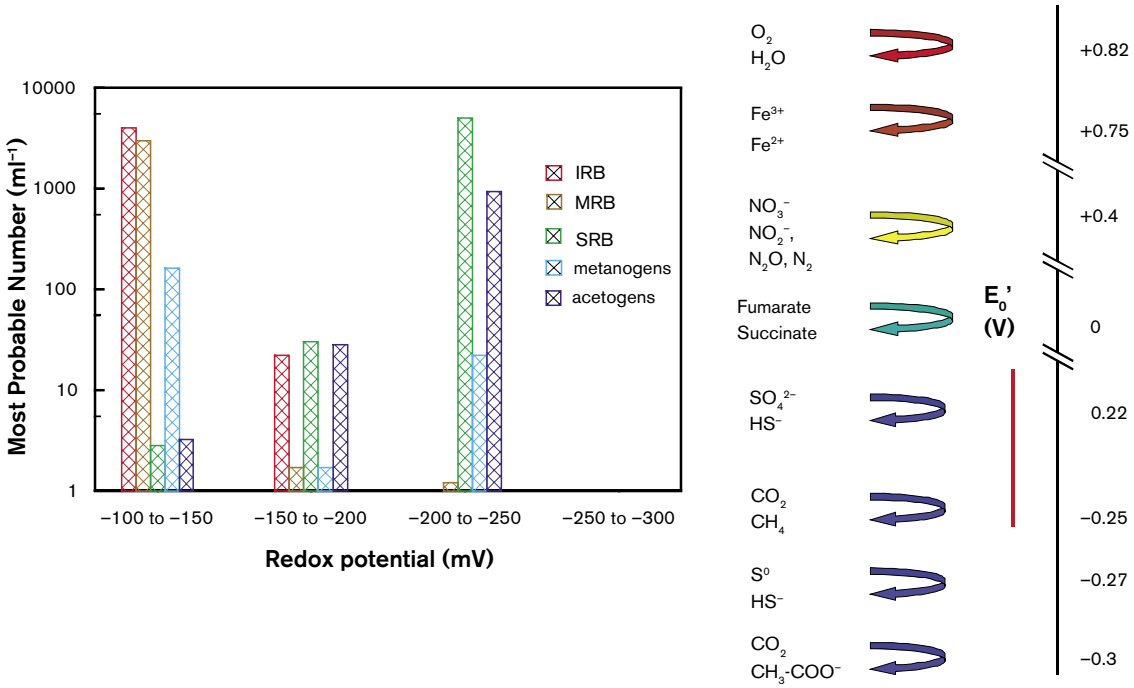

Figure 1-9. *The sum of the most probable number of microorganisms plotted versus intervals of redox values. The data are from sampling of groundwater in boreholes in the Forsmark area.*

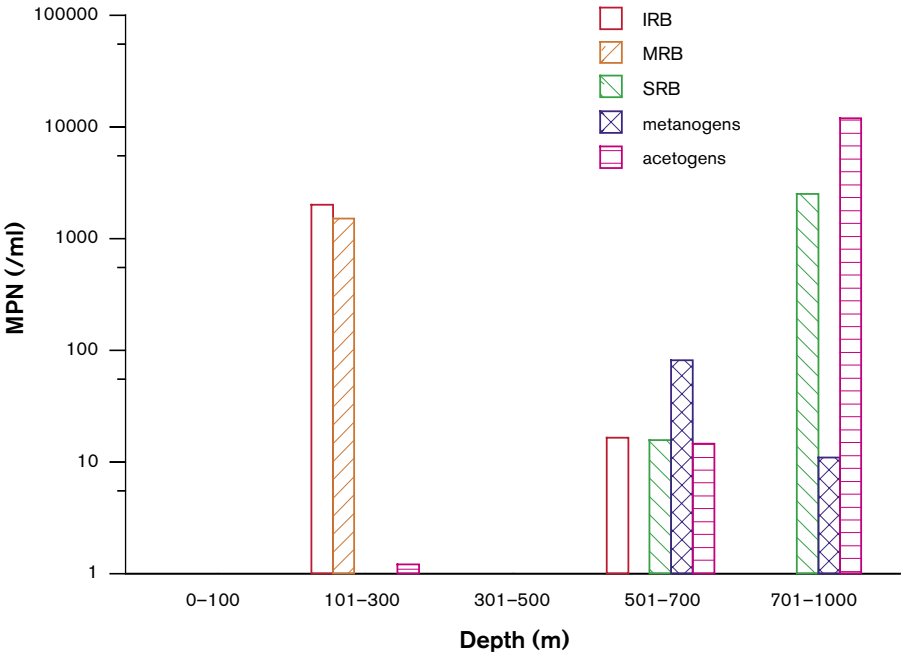

Figure 1-10. *The sums of most probable number (MPN) of microorganisms plotted versus depth intervals. Data come from sampling of groundwater in the Forsmark area.*

Sulphate-reducing bacteria, on the other hand dominated at the deepest levels, in KFM03A, together with acetogens. These two groups could have established a relation where SRBs utilise acetic acid produced by the acetogens. The same kind of relationship has been suggested by /Pitkänen et al. 2004/ to exist in deep groundwater in Olkiluoto but for methanogens and SRB. That sulphate-reducing bacteria can oxidise methane anaerobically with sulphate as electron acceptor has still to be proved but environmental studies suggest that this microbial reaction really exist.

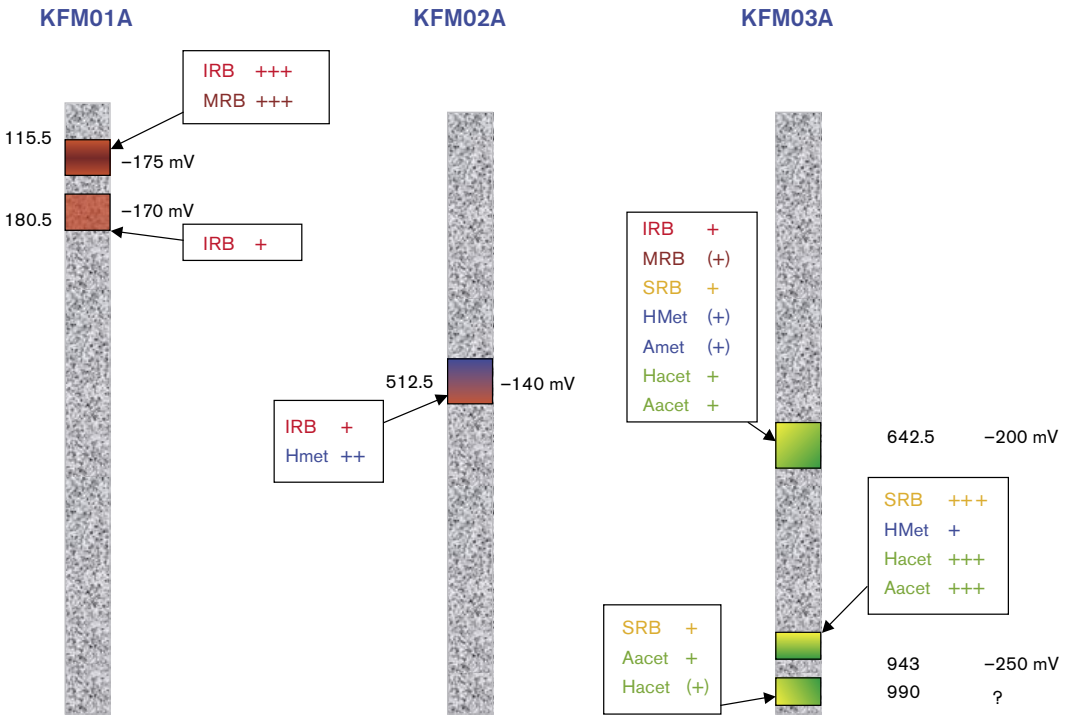

Figure 1-11. *Biogeochemical model of boreholes in the Forsmark area. This model is made with data available in SICADA 30 June 2004, the time for data freeze 1.2.*

At the intermediate levels the microbial populations seem to be more diverse and not dominated by any special group or groups, see KFM02A, 512.5 m and KFM03A, 642.5 m. If the flow in these sections is low and no mixture of water occurs the beneficial electrochemical gradients will not be establish and because that the activity of certain microbial groups will be lower.

1.13 Conclusions

- In this version three boreholes with six different depths were sampled and the dat were used in a descriptive model in two dimensions.
- Redox potentials in the boreholes differed from –140 mV to –250 mV.
- At the shallowest depths with the relatively high redox potential, iron- and manganese-reducing bacteria dominated.
- The number of methanogens was high at 512.5 m in KFM02A.
- Sulphate-reducing bacteria together with acetogens dominated at one of the deep levels, 943 m in KFM03A.
- The microbial species abundance and activity in borehole in the Forsmark seem to be in close correlation with the redox potential.
- High percentage of cultivable microorganisms with the MPN method was found at 115.4 m in KFM01A (iron-and manganese-reducing bacteria) and at 943 m in KFM03A (sulphate-reducing bacteria and acetogens).
- An explanation for the different amounts of cultivable cells could be differences in flow and mixing of groundwater at the sampled sites. Good mixing of two or more groundwater resulting in a gradient of different redox pairs would promote growth and activity of microorganisms with a suitable metabolism.

2 Colloids

2.1 Introduction

Particles in the size range 10^{-3} to 10^{-6} mm are regarded as colloids. Their small size prohibits them to settle which render them a potential to transport radionuclides in groundwater. The aim of the study of colloids in the site investigation of Forsmark 1.2, was to quantify and determine the composition of colloids in groundwater from boreholes. The results will be included in the modelling of the hydrochemistry at the site.

2.2 Methods

Two different methods were used. The first included filtering of the groundwater through a series of connected filters in a closed system under the pressure of argon. The filters had 0.2 and 0.05 µm pore size after a 0.4 µm prefilter. The mineral composition of the colloids on the filters was determined with ICP and the quantities of the analysed elements were recalculated in µg l^{-1} (ppb) considering the water flow (ml h^{-1}) registered through the filters. The elements analysed were calcium (Ca), iron (Fe), sulphur (S), manganese (Mn), aluminium (Al) and silicon (Si). The set of data includes samples from three boreholes KFM01A, KFM02A and KFM03A. Samples from KFM01A were taken 25 of February and, 1 and 7 of April 2003. KFM02A was sampled 24 of October 2003 and KFM03A was sampled 27 of April 2004. Sampling was made according to the activity plan AP PU 400-03-002.

The second method was a fractionation with a defined cut-off (pore-size) membrane filter concomitant with the analysis of organic colloids. Two different pore-sizes were used, 1,000 D and 5,000 D. The equipment and performance are described in SKB 431.043. The different fractions were analysed by ICP-AES. Several elements were determined but Fe, Si, Al and Mg only were considered important as colloid species.

2.2.1 Databases

The filtration data used were extracted from the file *All data Forsmark_1_2.xls* provided by Maria Gimeno at the Project Place. The data used here are compiled in Table 2-1. Data for the fractionation were obtain from P-reports /Wacker et al. 2003, 2004a,b/.

2.2.2 Evaluation of colloid data from the filtration method

During the evaluation of the primary data, a decision was taken to exclude silicon data from KFM01A 115.4 m in some of the figures, because they were extremely high probably due to a sampling artefact (see Table 2-1). All 0.05 and 0.2 µm filters were broken from borehole KFM02A. Because of this no total amount of colloid data are available from this borehole. All other data available were used in the evaluation.

In a report by /Laaksoharju et al. 1995/, calcium values calculated as calcite and sulphur values calculated as pyrite were both withdrawn from the total amount of colloids. In this presentation the same approach was used with the exception that the sulphur values are not recalculated as pyrite but are shown as sulphur.

Table 2-1. Calculated colloid phases (mean values of multiple samples) Forsmark 1.2 with sulphur as sulphur.

Borehole	KFM01A 115.435 m			KFM01A 180.35 m			KFM02A 512.54 m			KFM03A 450.5 m		
Pore Size (µm)	0.05	0.2	0.4	0.05	0.2	0.4	0.05	0.2	0.4	0.05	0.2	0.4
Cloride (mg l^{-1})	4,562.8	4,562.8	4,562.8	5,329.5	5,329.5	5,329.5	5,410	5,410	5,410	5,430	5,430	5,430
Colloid phase (µg l^{-1})												
Ca as Calcite $CaCO_3$	0.89	b.d.	1.36	0.21	0.10	0.14	–*	–	0.20	0.49	1.30	0.50
Fe as $Fe(OH)_3$	5.74	12.44	443.47	0.38	0.51	9.06	–	–	3.64	3.06	4.59	27.5
S as sulphur	61.25	b.d.	40.95	22.10	15.5	18.48	–	–	b.d.	30	72	16
Mn as Mn(OH)2	b.d.	b.d.	b.d.	b.d.	b.d.	b.d.	–	–	0.405	0.65	1.78	1.46
Al as K-Mg-Illite clay: $K_{0.6}Mg_{0.25}Al_{2.3}Si_{3.5}O_{10}(OH)_2$	71.36	14.9	29.45	10.39	8.30	20.21	–	–	2.90	2.5	2.5	172.2
Si as SiO_2	365.91	601.33	729.93	b.d.	b.d.	b.d.	–	–	b.d.	b.d.	b.d.	b.d.
Sum (ppb, (µg l^{-1}))	505.15	628.67	1,245.16	33.08	24.41	47.8			7.145	36.7	82.17	217.66
Sum omitting calcite	504.26	628.67	1,243.8	32.87	24.31	47.66			6.945	36.21	80.87	217.16
Sum omitting calcite and sulphur	443.01	628.67	1,202.85	10.77	8.81	29.18	–	–	6.945	6.21	8.87	201.16

*no data, broken filters

2.3 Colloids versus depth

In a valuation of the background values for colloids in groundwater, the amount of colloids versus depth is studied. It can be seen in Figure 2-1 that the amount of colloids were highest at the shallowest depth, 115,4 m. The lowest amount was found at 512,5 m depth. The average amount of colloids in this study was 46±50 µg l^{-1} and is in agreement with colloid studies from Switzerland (30±10 and 10±5 µg 1^{-1}) /Degueldre, 1994/ and Canada (300±300 µg 1^{-1}) /Vilks et al. 1991/ where they used the same approach as here /Laaksoharju et al. 1995/.

2.4 Colloids versus chloride

Figure 2-1 shows the amount of colloids versus chloride. In groundwater with a high chloride concentration the amount of colloids usually decreases because higher ion strength increases the precipitation of different solid particles. The chloride concentrations in this data set were relatively constant, around 5,000 mg l^{-1}. The highest amount of colloids was found in KFM01A, 115.4 m with the lowest chloride content, 4,562.8 mg l^{-1}.

2.5 Colloids versus iron

High iron concentrations in groundwater force the precipitation of other compounds by its ability for co-precipitation, which produces larger particles. Thus the amount of colloids will decrease with increasing iron concentration. Figure 2-3 shows the colloids versus the iron content in groundwater from KFM01A and KFM03A. Here it can be seen that the data correspond nicely with the theory with highest amount of colloids in water from 115.4 m in KFM01A.

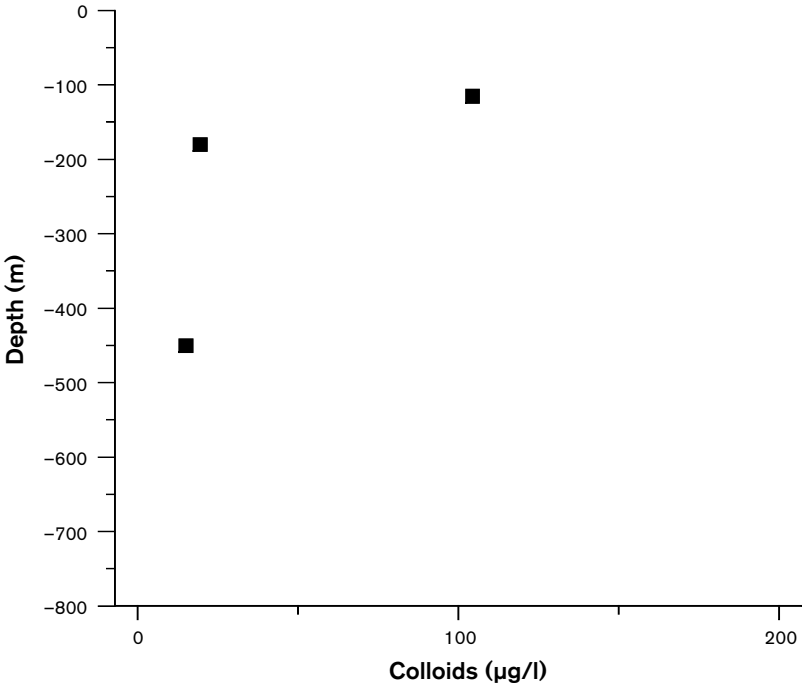

Figure 2-1. *Colloids (µg l^{-1}) plotted versus depth in samples from the boreholes KFM01A and KFM03A in the Forsmark area.*

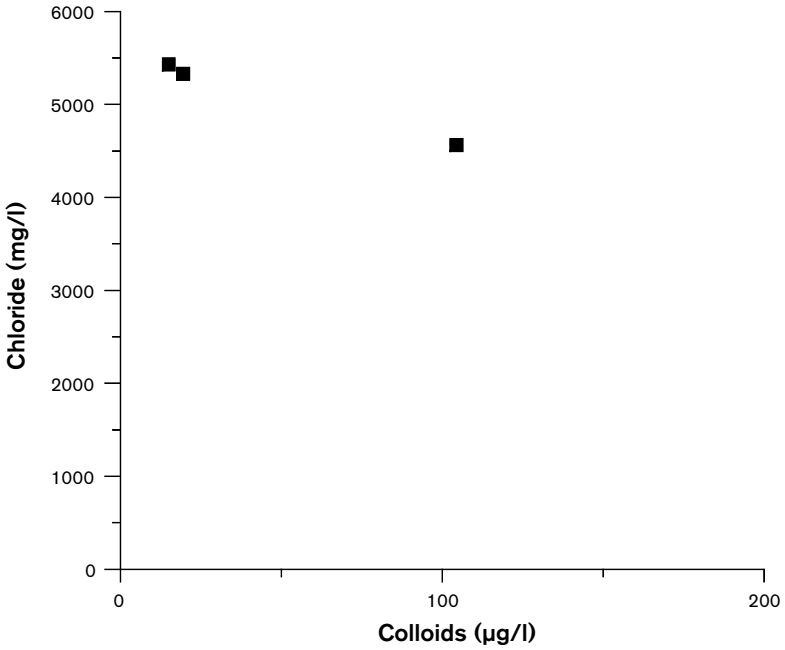

Figure 2-2. *Colloids (µg l^{-1}) plotted versus amount of chloride in the groundwater in samples from boreholes KFM01A and KFM03A in Forsmark.*

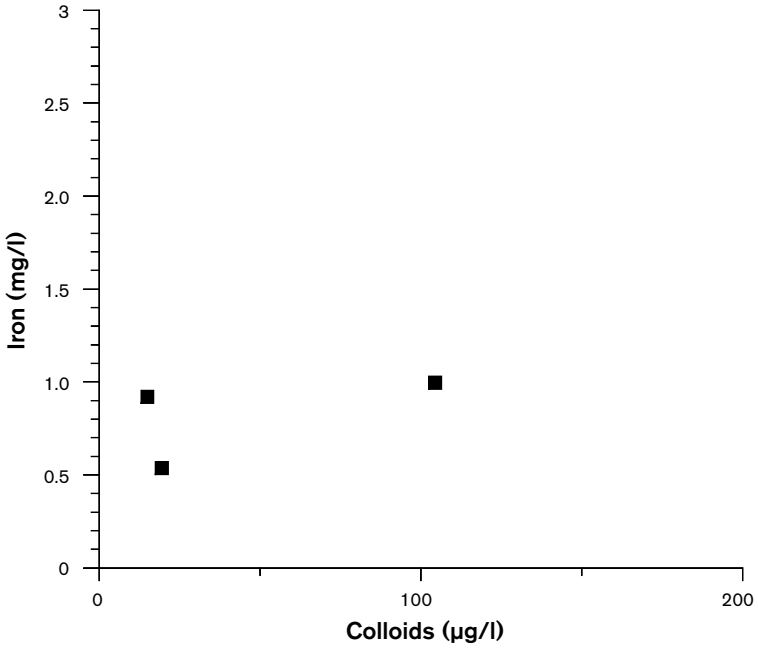

Figure 2-3. *Colloids (µg l^{-1}) plotted versus iron in groundwater in samples from the boreholes KFM01A and KFM03A in Forsmark.*

2.6 Composition of the colloids

The composition of the colloids has also been studied. Table 1 shows the values for the elements analysed, calcium (Ca), iron (Fe), sulphur (S), manganese (Mn), Aluminium (Al) and silica (Si), recalculated as colloid phases calcite, iron hydroxide, manganese dioxide, K-Mg-Illite clay and silica oxide. Sulphur was not recalculated to any other colloid phase.

Figure 2-4 shows the composition of the colloids sampled from different depths in the three boreholes. In this figure sulphur is shown. No data from KFM02A are shown because of broken filters. In Figure 2-5 on the other hand these values are removed. In both figures the calcite is omitted since it is considered as an artefact due to pressure changes during sampling.

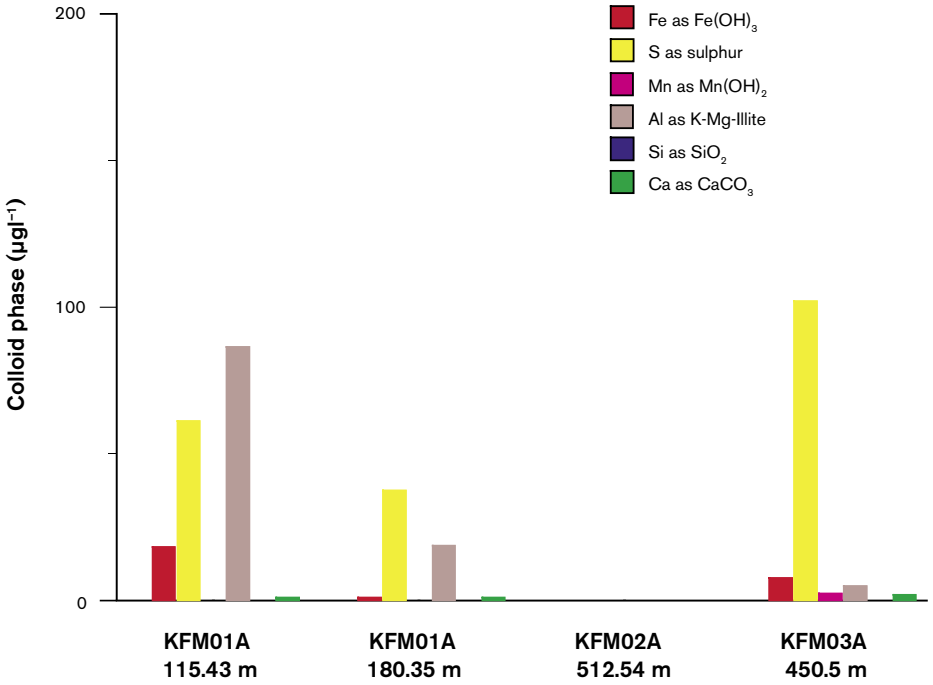

Figure 2-4. *The composition of colloids sampled from the boreholes KFM01A, KFM02A and KFM03A in the Forsmark area. Calcite is omitted in this figure and also the values of silica in borehole KFM01A, 115.4 m, see text above.*

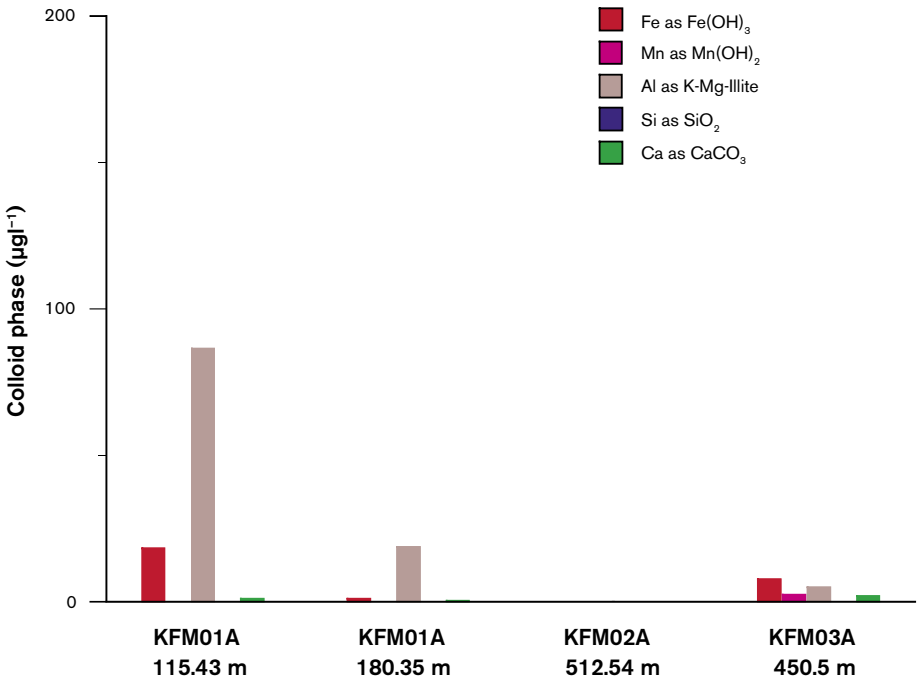

Figure 2-5. *The composition of colloids sampled from the boreholes KFM01A, KFM02A and KFM03A in the Forsmark area. Sulphur values are omitted in this figure and the values of silica in borehole KFM01A, 115.4 m, see text above.*

In Figures 2-4 and 2-5 it can be seen that manganese oxides were very rare in all of the three boreholes. Small amounts were found in KFM03A only. Iron oxides on the other hand were found in KFM01A. Also aluminium here represented as K-Mg-Illite was present at all sampling depths. This can also be an artefact from drilling of the boreholes. The amount of calcium was not high in these samples as can be seen by comparison of the two figures (Figure 2-4 and 2-5).

2.7 Compostiton of colloids – distribution of size

To understand the size distribution of the different colloid minerals colloids versus depth were plotted for each pore size of the filters, 0.05 and 0.2 (Figure 2-6). These figures show both all of colloid data available, also the silicon data from KFM01A, 115.4 m (Figure 2-6a–c). To increase the resolution for the lighter colloids Figures 2-6d–e were made and show the amount of colloids below 100 µgl^{-1}. As can be seen in these figures the silicon colloids were both small and large and heavy. Interesting to notice is that the amount of calcium colloids was low indicating small disturbance from the sampling. A question that appears is then if also the amount of sulphur is "real" colloids and not due to artefacts from sampling.

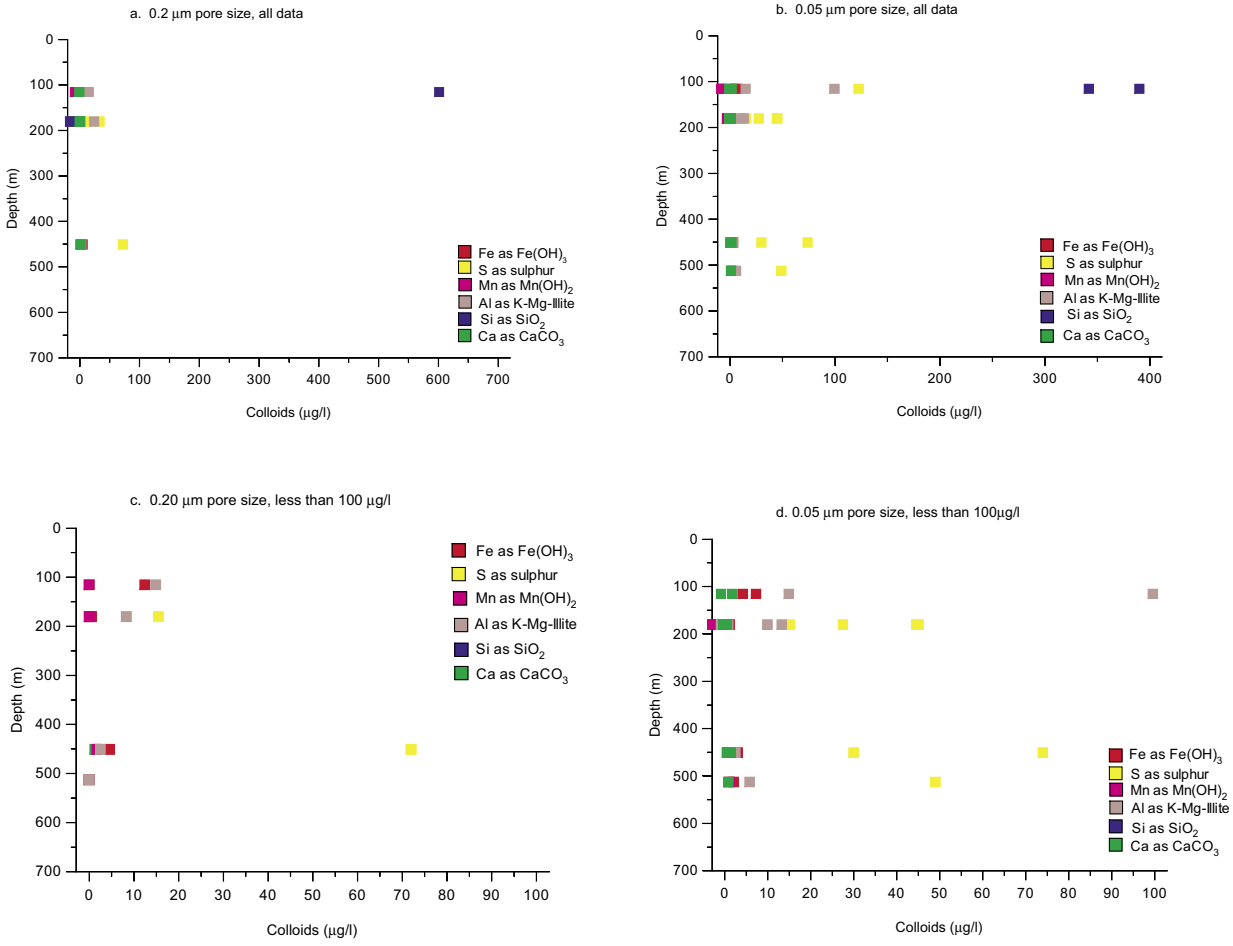

Figure 2-6. *Total amounts of colloids versus depth. Data from the Forsmark area. A–c all data are included, d–f amounts less than 100 µg l*$^{-}$.

2.8 Inorganic colloids – fractionation

The fractionation filtration was performed with sampled ground water from 10 sections in three boreholes with the following distribution: KFM01A, sections 110.1–120.8 m and 176.8–183.9 m, KFM02A, sections 106.5–126.5 m, 413.5–433.5, 509.0–516.1 m and in KFM03A, sections 386.0–391.0 m, 448.0–453.0 m, 448.5–455.6 m, 639.0–646.1 m and 980,0–1,001.2 m. With this method the calculated value > 1,000 D but < 5,000 D was considered as the colloid fraction.

All samples from the sections mentioned above showed values below the detection limit for the elements considered as important in colloid formation, iron, silicon and manganese. Measurable amounts were found in the fractions > 1,000 D but < 5,000 D. All data from the fraction filtration can be found in the P-reports for the boreholes /Wacker et al. 2003, 2004a,b/.

2.9 Conclusion

The filtration data available seems to agree with the amount of colloids earlier reported from Äspö and Bangombe /Laaksoharju et al. 1995; Pedersen, 1996/. The new sampling and filtering methods seemed to work well since the amounts of calcium carbonates were very low. This renders a rethinking of the sulphur colloids. They might be colloids present in ground water and then probably as iron sulphides. The silicon values from KFM01A, 115.4 m, on the other hand might be an artefact from sampling.

The fractionation data show that there should not be any colloids in the size < 1,000 D but < 5,000 D. This is in contradiction to the filtration results but might be the ones that are closer to the truth. There are no sulphur values reported from this method and it would be interesting to compare this with the filtration method since iron sulphides could be one explanation for the low sulphide values found in ground water even if SRBs (sulphate-reducing bacteria) were present (see section 1.7).

Data for the numbers of particles makes could increase the value of colloid analyse by making it possible to calculations of amounts binding sites for radionuclides in the different colloid fractions.

The comparison of the two methods, filtration and fractionation, needs to be further evaluated.

3 Gases

3.1 Introduction

Earlier studies of groundwater in the Fennoscandian shield have shown high amounts of dissolved gasses. If the sum of gas reaches above saturation gas bubbles may form. The surface of such bubbles can adsorb different compounds in the groundwater such as radionuclides. The bubbles will move rapidly in groundwater and can cause dispersion of radionuclides to large areas and especially to the ground surface. In a site investigation it is therefore of great importance to evaluate and include gas data in hydrogeochemical models.

Some gases are involved in microbiological reactions. These gases are methane, carbon dioxide and hydrogen. Methane is produced by methanogens in reduced environments and can be used as substrate by methanotrophic bacteria. Carbon dioxide is used as carbon source for autotrophic organisms and is the end product in microbial degradation. Hydrogen is energy and electron source for methanogens, acetogens and some other autotrophic microorganisms, i.e. sulphate reducers. It is also one of the end products in microbiological fermentation.

In this study up to 12 gases were analyzed: helium, argon, nitrogen, carbon dioxide, methane, carbon monoxide, oxygen, hydrogen, ethyne, ethene, ethane and propane. Gas content was analysed in ground water from 5 depth in 3 boreholes, KFM01A, KFM02A and KFM03A.

Table 1 shows the boreholes and depths from which data have been available for this report.

Table 3-1. Boreholes, depths, sampling dates and gas volumes available in SICADA for analysis in Forsmark model version 1.2.

Borehole	Depth centre (m)	Sampling date	Gas volume (ml l^{-1})
KFM01A	180.4	2003-03-31	57.8
KFM02A	512.5	2003-09-29 2003-10-21	83.2 73.5
KFM03A	452.1	2004-04-27	80.2
	642.5	2004-02-23	89.0
	943.0	2004-03-29	124,5
	990.6	2003-12-08	127.5

3.2 The dissolved gasses

3.2.1 Total volume of gas

Figure 3-1 shows the total volume of gas for all ground water samples. It shows an increasing amount of gas with depth with the highest volume, 127.5 ml l^{-1} the lowest level, 990.6 m in KFM03A. The shallowest ground water had 57.8 ml gas per litre. All of the data give a nice linear correlation.

3.2.2 Nitrogen and helium

Figure 3-2 shows that the amount of nitrogen, the dominating gas in all ground water, follows the trend of the total amount of gas, and increase with depth. This corresponds to the gas content in ground water in Olkiluoto, Finland that also showed an increasing trend with depth down to 1,100 m /Pitkänen et al. 2004/. The highest concentration found in the Forsmark investigation was at 990.5 m depth in KFM03A with 4.7 mM N_2 of ground water and the lowest was 2.4 mM at 180,4 m in KFM01A.

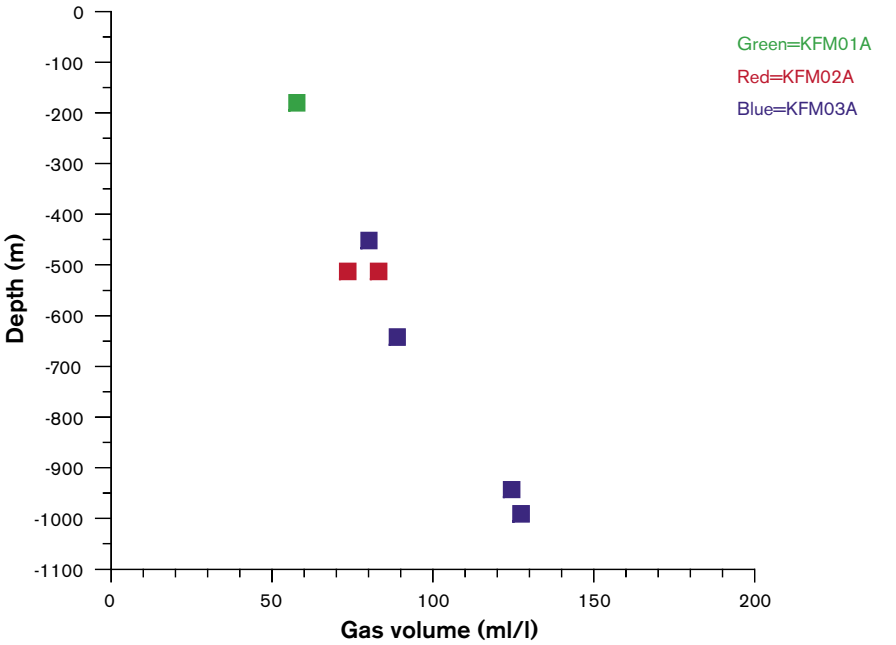

Figure 3-1. *Total volume of gas for samples from ground water in the Forsmark area.*

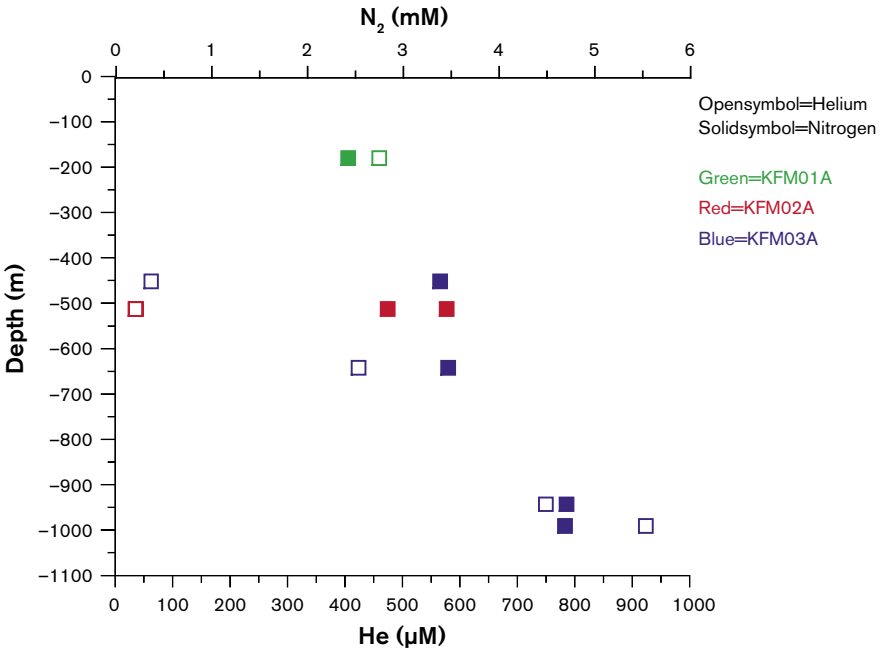

Figure 3-2. *The concentrations of nitrogen and helium plotted versus depth in samples from boreholes in the Forsmark area.*

Helium concentration in boreholes in the Forsmark area showed the same trend as nitrogen, increasing with depth. The concentration varied between 460 µM and 924 µM. The same trend was found in Olkiluoto ground water where helium concentrations following the nitrogen concentrations.

The origin of nitrogen and helium in groundwater is considered to be crustal degassing of the bedrock. Another source for helium can be radioactive decay, also this in the bedrock.

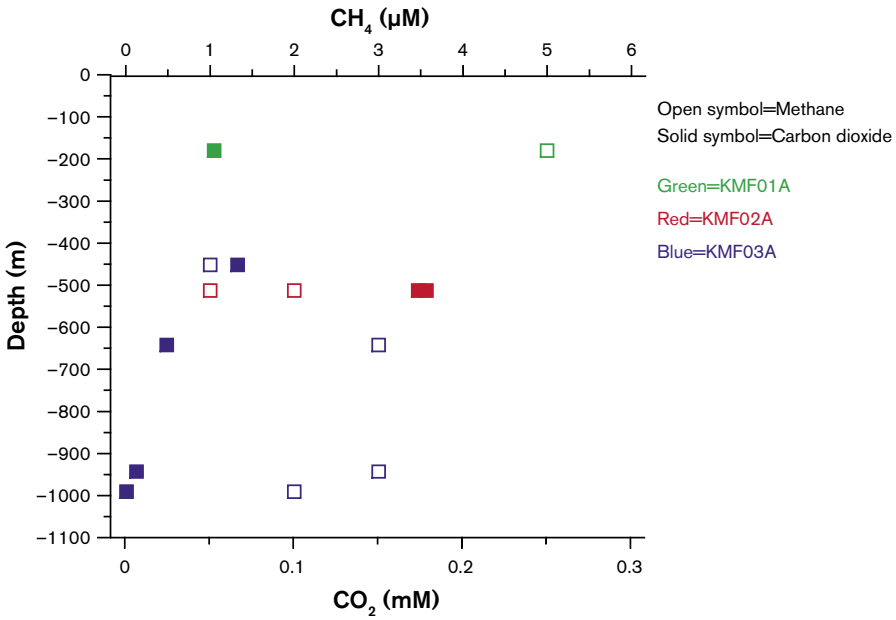

Figure 3-3. *Carbon dioxide and methane plotted versus depth in samples from boreholes in the Forsmark area.*

3.2.3 Carbon dioxide and methane

Carbon dioxide in groundwater is a dissociation product of dissolved carbonates from fractures in the bedrock. The carbon dioxide concentrations in samples from the Forsmark area showed a slight decreasing trend with depth. At 990.5 m the carbon dioxide concentration was very low with 0.001 mM. This pattern has also been observed for carbon dioxide concentrations in groundwater from the Olkiloto Site in Finland /Pitkänen et al. 2004/.

More or less the opposite trend was found for methane with increase with depth except for the shallowest ground water that showed the highest concentration with 5 µM.

The origin of methane in groundwater can be either biotic or abiotic. The biotic methane is produced by methanogenic Achaea, a group of prokaryotic organisms. They can utilize either C1-compounds or acetate. This is exemplified with acetate in Equation 1. They can also fixate carbon dioxide with hydrogen gas as energy and electron source (Eq. 2). The origin of their substrate can be biodegraded organic matter as in sea and lake sediments or composts. It can also be carbon dioxide and hydrogen with origin in the mantle /Apps and Van de Kamp, 1993/.

$$CH_3COOH \rightarrow CH_4 + CO_2 \qquad \text{(Eq.1)}$$

$$CO_2 + 4H_2 \rightarrow CH_4 + 2H_2O \qquad \text{(Eq.2)}$$

The abiogenic methane is produced in, for example, hydrothermal systems during water–rock interactions involving the Fischer-Tropsch synthesis reaction, which is the same as Eq.2 above. This methane can act as precursor for polymerisation to higher hydrocarbons such as short chain alkanes (see section 3.2.4).

The isotopic carbon signature of methane can reveal the source of the methane but there are no such data available in the SICADA but also calculation of the quota C1/C2+C3 will give evidence from where the methane originates (section 3.2.4).

3.2.4 Hydrocarbons

The data from 180.4 m depth in KFM01A was high compared to data from the other depths. The other data show an increase of hydrocarbon concentration with depth (Figure 3-4). The hydrocarbons come from a deep abiogenic source and move slowly by diffusion towards the surface. Calculating

the C1/(C2+C3) ratio can elucidate the source of the methane found. If this ratio is high, over 10^3, it is considered as microbiological methanogenesis, thermogenic and abiogenic methanogenesis will give a ratio around 10^1 /Sherwood-Lollar et al. 1993; Clark and Fritz, 1997; Whiticar, 1990/. The calculations for data fromKFM01A, KFM02A and KFM03A in Forsmark give ratios from 37 to 100. This indicates, referring to the theory above, that most of the methane originates from an abiogenic source, but it cannot be excluded that some of the methane has biogenic origin. To be conclusive in this statement, more HC data need to be generated together with stable isotope values for methane and hydrocarbons.

3.2.5 Hydrogen

Hydrogen is an important gas in several anaerobic microbial metabolisms such as methanogenesis and acetate production by acetogens. There are also autothrophic iron- and sulphate-reducing bacteria that can use hydrogen as energy and electron source concomitant with iron or sulphate reduction.

There are at least six possible processes in which crustal hydrogen is generated: (1) reaction between dissolved gases in the C-H-O-S system in magmas, especially in those with basaltic affinities; (2) decomposition of methane to carbon (graphite) and hydrogen at temperatures above 600°C; (3) reaction between CO_2, H_2O, and CH_4 at elevated temperatures in vapours; (4) radiolysis of water by radioactive isotopes of uranium, thorium and their decay daughters, and potassium; (5) cataclasis of silicates under stress in the presence of water; and (6) hydrolysis by ferrous minerals in mafic and ultramafic rocks /Apps and Van de Kamp, 1993/. It is important to explore the scale of these processes and the rates at which the produced hydrogen is becoming available for deep microbial ecosystems.

The hydrogen concentrations differ quite lot between the two measurements from the same depth at 512.5 m in KFM02A. A difference in the same range can be seen in data from two of the depths in KFM03A, 452.0 m and 642.5 m. Measurement of hydrogen is a complicated issue because of its tendency to diffuse through most materials. Most of the data are relatively low and this can be the explanation for these disagreeing values.

A comparison with hydrogen data from other sites in Sweden and Finland shows that the values from Forsmark are in the same range as they are /Pedersen, 2000/.

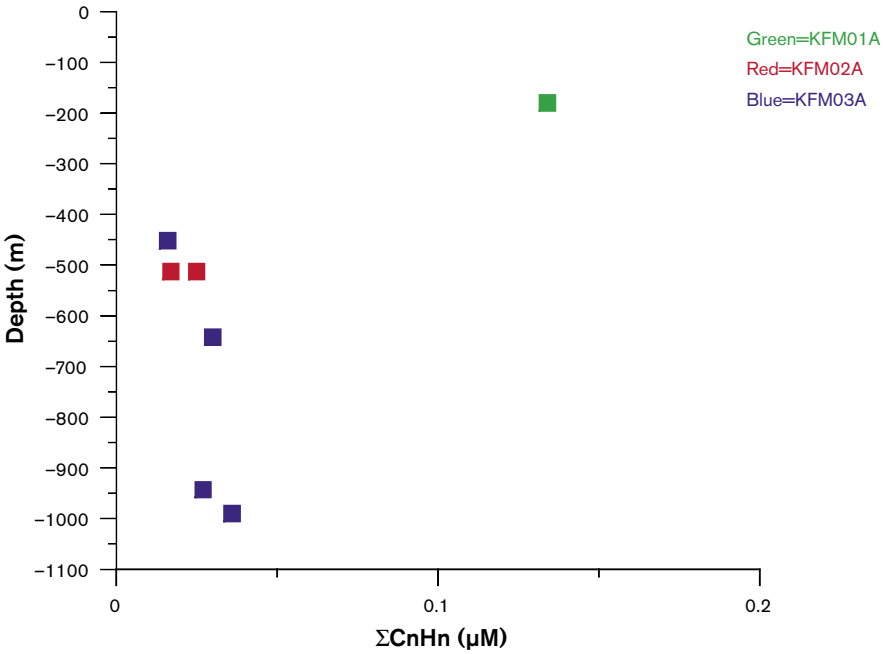

Figure 3-4. *Total concentrations of hydrocarbons, except methane, versus depth in boreholes in the Forsmark area.*

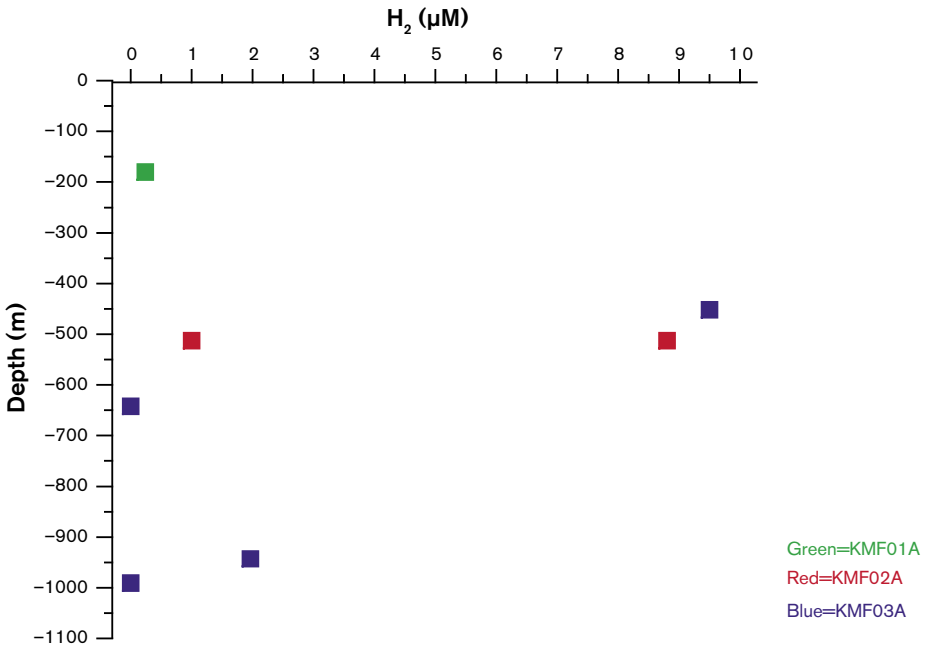

Figure 3-5. *Concentration of hydrogen in groundwater from bore holes in the Forsmark area.*

3.3 Conclusion

So far, the amounts of gas data are limited and exclude any considerable analysis of the impact of gases on geochemistry and microbiology but there is a clear trend with increasing volumes of gas towards depth.

The available gas data for the Forsmark area show that the gas content is in the same order of magnitude as in most of the Nordic sites studied.

The gases are probably mostly mantle-generated.

Gases are probably oversaturated in relation to atmospheric pressure but not at depth.

4 References

American Public Health Association, 1992. Estimation of bacterial density, 977–980. In: Standard methods for the examination of water and wastewater, 18th ed. American Public Health Association, Washington, D.C.

Apps J A, Van de Kamp P C, 1993. Energy gases of abiogenic origin in the Earth's crust. The future of energy gases. US Geological Survey Prof. Pap. 1570, 81–132.

Clark I, Fritz P, 1997. Environmental isotopes in hydrogeology. Lewis Publishers, Boca Raton, 328 p.

Degueldre C, 1994. Colloid properites in groundwaters from crystallineformation. PSI Bericht NP-94-21 Paul Scherrer Institute, Villigen, Switzerland

Laaksoharju M, Degueldre C, Skårman C, 1995. Studies of colloids and their importance for repository performance assessment. SKB TR-95-24, Svensk Kärnbränslehantering AB.

Pedersen K (ed), 1996. Bacteria, colloids and organic carbon in groundwater at the Bangombé site in the Oklo area. SKB TR-96-01, Svensk Kärnbränslehantering AB.

Pedersen, 2000. Exploration of deep intraterrestrial microbial life: current perspectives. FEMS Microbiology Letters 185, 9–16.

Pedersen K, 2001. Diversity and activity of microorganisms in deep igneous rock aquifers of the Fennoscandian Shield. In Subsurface microbiology and biogeochemistry. Fredrickson, J. K. & Fletcher, M., Eds. New York: Wiley-Liss Inc, 97–139.

Pitkänen P, Partamies S, Luukonen A, 2004. Hydrochemical interpretation of baseline groundwater conditions at the Olkiluoto site. POSIVA 2003-07, Posiva, Olkiluoto, Finland.

Sherwood-Lollar B, Frape S K, Weise S M, Fritz P, Macko S A, Welham J A, 1993. Abiogenic methaogenesis in crystalline rocks. Geochimica et cosmochemica Acta 57, 5087–5097.

Wacker P, Bergelin A, Nilsson A-C, 2003. Forsmark Site Investigation. Complete hydrochemical characterisation in KFM01A. SKB P-03-94, Svensk Kärnbränslehantering AB.

Wacker P, Bergelin A, Nilsson A-C, 2004a. Forsmark Site Investigation. Hydrochemical characterisation in KFM02A. SKB P-04-70, Svensk Kärnbränslehantering AB.

Wacker P, Bergelin A, Nilsson A-C, 2004b. Forsmark Site Investigation. Complete hydrochemical characterisation in KFM03A. SKB P-04-108, Svensk Kärnbränslehantering AB.

Whiticar M J, 1990. A geochemical perspective of natural gas and atmospheric methane. Organic Geochemistry 16, 531–547.

Vilks P, Miller H, Doern D, 1991. Natural colloids and suspended praticles in Whiteshell Research area, Manitoba, Canada, and their potential effect on radiocolloid formation. Applied Geochemistry 8, 565–574.

Appendix 3

PHREEQC modelling

Contribution to the model version 1.2

María J Gimeno, Luis F Auqué and Javier B Gómez
Department of Earth Sciences, University of Zaragoza

December 2004

Introduction

For this new site descriptive modelling phase in Forsmark (Forsmark 1.2), the chosen formalism has been to include all relevant data in the Forsmark area. The data included in this 1.2 data freeze contain all the information compiled in the previous phase (Forsmark 1.1) together with the specific data delivered in the 1.2 data freeze.

This fact frames phase Forsmark 1.2 in a different context from the previous work done for Forsmark 1.1. The contribution of the authors is now focussed on three main issues:

1. Evaluation of primary data. Here the main hydrogeochemical characters of the studied area are analysed as a whole. The analysis is performed following the same methodology used in the previous Forsmark 1.1 report (ion-ion plots). However, the internal structure of the chapter is different, now being divided according to compositional systems, that is, carbonate, sulphate and silica systems, integrating information on chemical contents together with some geochemical modelling results (SI calculations). This integrated presentation makes much easier the analysis of some specific aspects, facilitating the assessment of hypothesis and the proposal of suggestions.
2. Geochemical modelling. This activity has been centred in two aspects: (1) mass balance calculations with PHREEQC in order to obtain mixing proportions and main reactions, and comparison of the results with M4 (a modified version of M3 developed by the University of Zaragoza group); and (2) proposal of a preliminary conceptual model of reaction and mixing-reaction for aluminosilicate phases, already started in Simpevarp 1.2 /SKB, 2004/. Their study is particularly problematical but unavoidable due to their presence as fracture fillings in Forsmark.
3. Redox processes. Traditionally, the redox state control in the studied groundwaters has been assigned either to iron oxides/oxihydroxides or to sulphides, in most cases excluding each other. The analysis performed by the authors in Forsmark 1.1 (and Simpevarp 1.1, /Laaksoharju et al. 2004b/), suggests that the control is mainly exerted by the sulphidic system in detriment of the iron system. The increase in the number of samples from different depths, together with the comparison of the results obtained in Simpevarp 1.2, have allowed an in-depth re-evaluation of the problem.

Contents

1 State of knowledge at previous model version

The main findings from the 1.1 phase /Laaksoharju et al. 2004a/ can be summarised as follows.

Dilute surface waters, mostly represented by lake and stream samples, are usually characterised by very short residence times (days to some years) and high tritium and ^{14}C contents. Dilute, near-surface waters, mostly represented by soil-pipe waters, but also some discharging groundwater to surface lakes and streams, are probably characterised by longer residence times (months to several years). Despite this, similarly high tritium values are obtained for the surface-derived waters although ^{14}C (based only on very few samples) appears to be lower.

Based on their general geochemical characteristics and apparent age, two major groundwater types were defined in Forsmark 1.1: fresh waters with a bicarbonate imprint and low residence times (tritium values above detection limit), and brackish-marine waters with Cl contents up to 6,000 mg/L and longer residence times (tritium values below detection limit).

The chemistry of the first water type is mainly controlled by the chemistry of the recharge waters and, most important, by water-rock interaction processes. Locally, these waters can mix with water of marine origin, changing their chemical composition towards more chloride-rich compositions. Under these conditions the major water-rock interaction processes are organic matter decomposition, dissolution of the more soluble phases (such as calcite and sulphides), and the alteration of the granitic rock. Primary and secondary silicates and aluminosilicates are related by incongruent reactions which seem to control silica and aluminium contents and participate in the loss or gain of elements such as K, Mg and, to some extent, Na (through dissolution-precipitation or ion exchange).

Waters from the brackish-marine type have a longer residence time and a higher mixing proportion of older waters from different sources. Heterogeneous reaction processes are less important than in the first water type and can be described by the same set of minerals, with the only difference that calcite is precipitating instead of dissolving. Also, in some of these waters microbially-mediated reactions and dissolution-precipitation of Fe-mineral phases become important at controlling sulphate and iron contents, as well as the redox state of the system.

These brackish waters (with chloride contents of around 4,000–5,500 mg/L and $\delta^{18}O$ values between –10 and –12‰ SMOW) mainly represent Littorina Sea water or Littorina Sea/glacial water mixtures. The Littorina Sea water component (twice as saline as the present Baltic Sea water) has intruded into, and mixed with, glacial melt waters around 7,000–5,000 years ago. This glacial-Littorina mixture, when preserved in the bedrock, has mixed in some fractures with present Baltic Sea water and, during the last 1,000 years, probably also with meteoric water. Only in hydraulically favourable ‘pockets’ or ‘lenses/horizons’ has a stronger Littorina signature been recorded.

2 Evaluation of primary data

For this new site descriptive modelling phase (Forsmark 1.2), the dataset supplied by SICADA as Data Freeze 1.2, includes old (Data Freeze 1.1) and new (post-Data Freeze 1.1) samples. The number of samples included in this data freeze is shown in Appendix A[1], where the number of samples with complete chemical analysis and the number of representative samples is indicated.

The dataset consists of 1,131 water samples (Table A-1; Appendix A): Samples reflecting surface conditions (precipitation, streams, lakes and sea water) comprise a total of 735 samples. Of the remaining 396 samples, 84 samples are from percussion-drilled boreholes, 168 from core-drilled boreholes and 144 from shallow soil pipes; some of these borehole samples represent repeated sampling from the same isolated location or samples in a non-packered, open borehole (tube sampler; 50 samples).

From the total dataset only 171 surface samples and 210 groundwater samples were analysed for all major elements, stable isotopes and tritium at the time of Data Freeze 1.2. There are some samples with additional information, mainly on colloids, dissolved gasses and microbes, which are also shown in the table of chemical analysis (Appendix in this issue). This means that 33.7% of the samples could be used for a detailed evaluation concerning the origin of the waters. However, not all these samples have actually been used for the evaluation. According to the work done by Smellie and Tullborg (this issue) regarding the representativity of the groundwater samples, only 182 out of 381 samples with complete chemical analysis have been considered representative. How this dataset has been used in our modelling is listed in Appendix B.

Analysed data include the same set of parameters as in the previous stage (see table of chemical analysis; Appendix in this issue). The pH and conductivity values used in this report are the ones determined in the laboratory. There are no data for Eh and temperature for the surface waters but there are some continuous logging Eh, pH and temperature data from several boreholes at different depths. The selected Eh, pH and temperature values are also included in the table of chemical analysis (Appendix in this issue).

2.1 Representativity of the data

This analysis is presented in Smellie and Tullborg (this issue).

2.2 Explorative analysis

Following the same approach used in the previous stage (Forsmark 1.1), the evaluation of this new dataset starts with an explorative analysis of several groundwater variables. The evaluation already reported in version 1.1 will not be repeated here. However, all new observations and conclusions derived from the analysis of the whole available dataset will be clearly shown. Moreover, in this second stage the improved knowledge of the local and regional geology and mineralogy models, as well as the lessons learnt from Simpevarp 1.2 /SKB. 2004/, will serve as a background to interpret the evolution of the groundwaters.

[1] Table A-1 shows the number of samples included in the 1.2 data freeze. Table A-2 includes only the samples taken after 1.1 data freeze.

2.2.1 Evaluation of scatter plots for conservative and some non conservative elements

The hydrochemical data have been graphically displayed using X-Y plots to derive trends that may facilitate interpretation. Since chloride is generally conservative in normal groundwaters, its use is appropriate to study hydrochemical evolution trends when coupled to ions, ranging from conservative to non-conservative, to provide information on mixing, dilution, sources and sinks. Moreover, here chloride acts as a tracer of the main irreversible process operating in the system, which will be demonstrated below. Therefore, many of the X-Y plots involve chloride as one of the variables.

What follows is a preliminary evaluation of the various geochemical trends apparent in the Forsmark area groundwaters. The evaluation of the hydrogeochemical data uses all representative samples (and, in some cases, the whole data), both surface waters and groundwaters, in order to understand the overall large-scale dynamics and evolution of the system. However, in some cases, the evaluation will be focused only on the groundwater samples.

A general comparison of the Forsmark, Laxemar and Olkiluoto (Finland) chloride data versus depth has been made (Figure 2-1) in the same way as it was done in the previous phase. The Laxemar data show dilute groundwaters extending to around 1,000 m before a rapid increase in salinity to maximum values of around 47 g/L Cl at 1,700 m (see Simpevarp 1.2 report, /SKB, 2004/). Olkiluoto waters show an initial sharp increase in chloride at around 150 m, which levels off at 5 g/L Cl from 150 to 450 m. Then there is a relatively steady increase to maximum values of around 20 g/L Cl at 900 m depth (one maximum value of 44 g/L Cl was recorded).

The Forsmark data show a close similarity to the initial Olkiluoto trends as it was already observed in Forsmark 1.1 /Laaksoharju et al. 2004a/. The levelling off at 5 g/L Cl at Olkiluoto has been interpreted as possibly reflecting a Littorina seawater component /Pitkänen et al. 1999/. This may also be the case at Forsmark due to similarities in palaeoevolution at the two sites (we will come back to this hypothesis later on). However, in this new 1.2 phase, the Forsmark samples cover a wider range of depths and some new observations can be made. The levelling off at around 5 g/L Cl continues with increasing depth up to (at least) 700 m diverging from the Olkiluoto trend, which starts a steady increase below 450 m (Figure 2-1). Instead of that, Forsmark waters tend to follow the Laxemar trend, going towards increasing salinity values with increasing depth (Figure 2-2). This behaviour could be interpreted as reflecting the influence of more saline non-marine waters (Brine component), but the amount of data is still not enough to check whether groundwaters there will follow the same rapid increase in salinity with depth as in Laxemar.

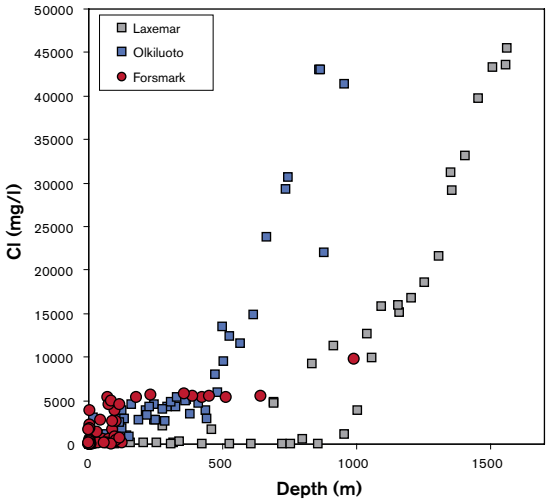

Figure 2-1. *Depth comparison of chloride between the Forsmark site and the Laxemar (KLX01 and KLX02) and Olkiluoto localities.*

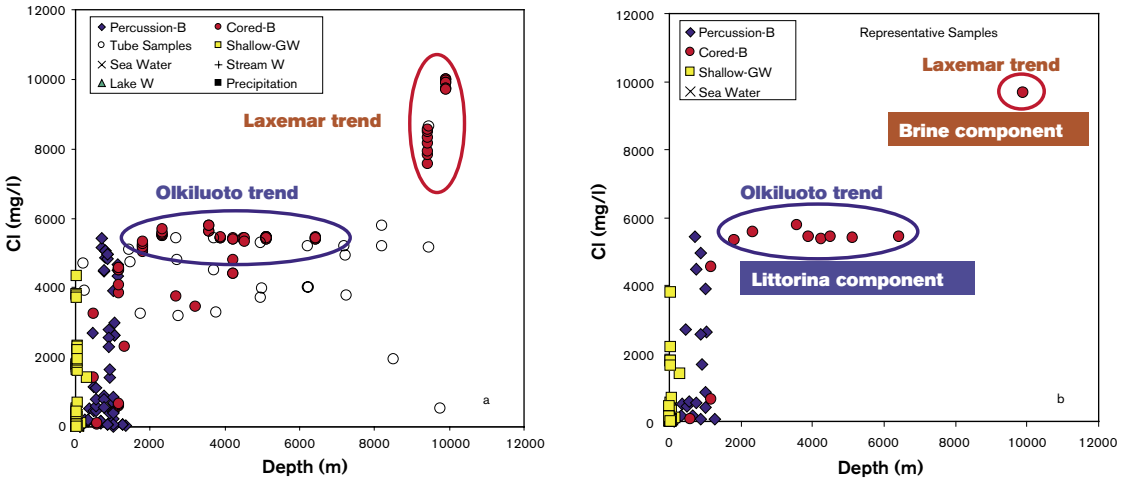

Figure 2-2. *Evolution of chloride with depth in the Forsmark area. (a) All the samples. (b) Representative samples.*

Bromide shows a linear increase with chloride, indicating a common geochemical origin for both (Figure 2-3a,b), but also with two different trends: the first one from shallow fresh groundwaters up to brackish waters at about 600 m depth, and the second represented by the more saline groundwaters. The first group (less saline groundwaters) has a rather homogeneous Br/Cl ratio, similar to sea water (Figure 2-3c,d), supporting a marine origin (or the influence of a marine component, Littorina in the plot) for these groundwaters. The more saline groundwaters have a higher bromide content than present Baltic or estimated Littorina Sea waters and their Br/Cl ratios (higher than sea water, Figure 2-3c,d) support a non-marine origin for the saline groundwaters (influence of a Brine component).

In this case, as in the rest of the plots vs. chloride, an interesting fact can be seen: Figure 2-2 above shows that chloride content of around 5,500 mg/L are maintained for a very wide range of depth (200 to 600 m); the effect of this constant Cl value is shown in the rest of the plots as a vertical grouping of samples with a similar Cl content but a wide range of content of the plotted element.

Sodium shows a positive correlation with chloride (Figure 2-4), which reflects that mixing is the main process controlling Na content. Again, the two trends already observed in previous plots are clearly visibly here. The deviation of groundwater samples from the sea water dilution line (SWDL in the plot) can be interpreted as mixing with more saline end members, Littorina-dominated in the first trend, and Brine-dominated in the second.

Potassium and magnesium contents in groundwaters (Figure 2-5 panels a,b and c,d respectively) show a very similar behaviour, slightly more scattered in the case of potassium but following the same trends, namely, a) an obvious modern Baltic Sea water dilution line; b) a clear borehole saline dilution line distinct from (a) and mainly defined by groundwaters with an important Littorina component; and c) a decreasing trend including groundwaters with higher contribution of a non marine saline end member.

The main difference with respect to the results obtained in the previous phase is represented by the trend shown by this last group (c), the groundwaters with a high contribution of a brine end member, which did not exist then because the depth range of the samples was narrower. Now we can see that the samples follow the same trend as in the other Swedish sites /Laaksoharju et al. 2004a/, evolving with depth towards higher salinity by mixing with a non marine saline component.

The Baltic Sea values cluster around 3,000 mg/L Cl which could be recommended to represent the Baltic Sea end-member composition at the Forsmark site (see discussion above). The plotted data show a large spread to more dilute mixing compositions, and extreme examples exist where only small amounts of Cl are present. These dilute samples represent some coastal Baltic Sea bay localities where there is a large fresh meteoric water input.

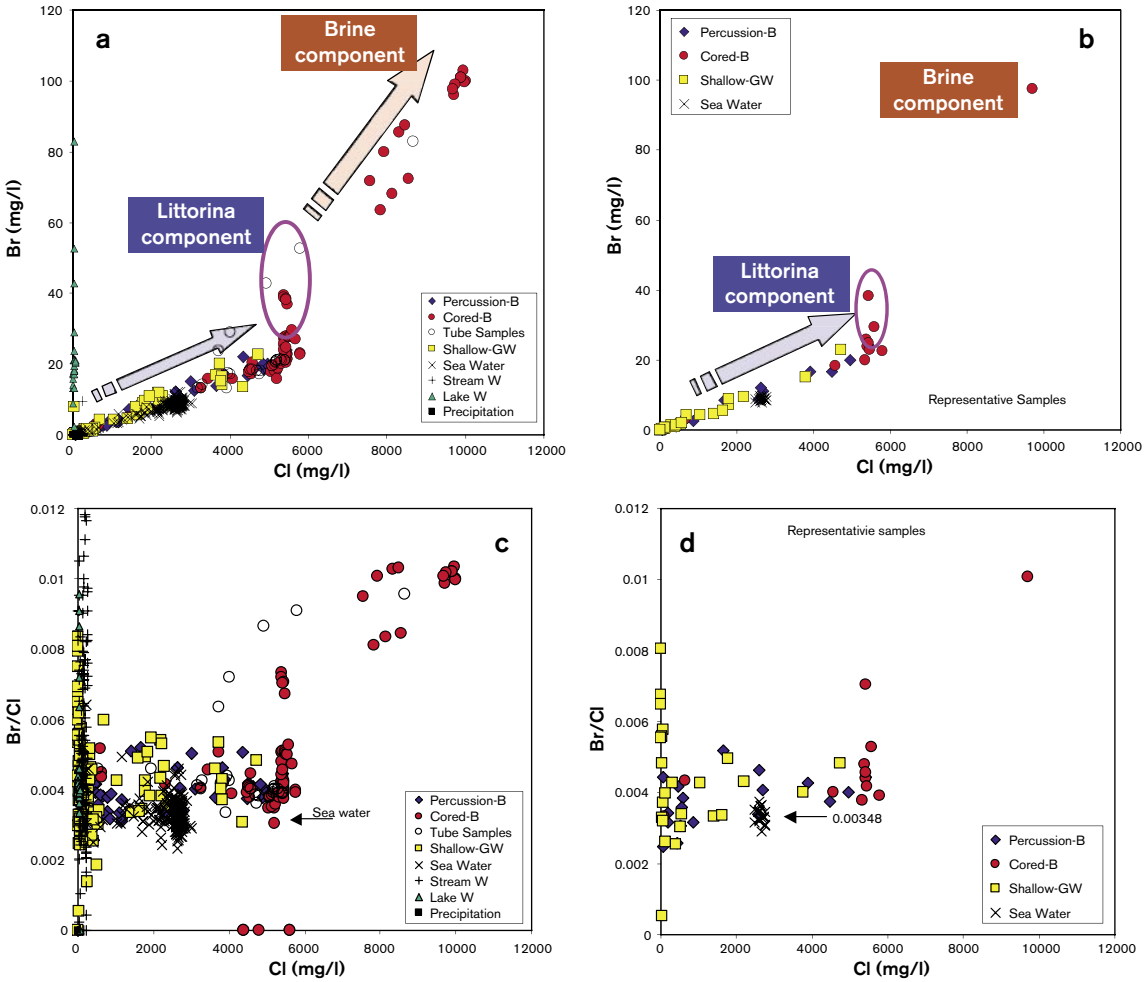

Figure 2-3. *Bromide vs. chloride in Forsmark waters: (a) full data set; (b) representative waters; (c) Br/Cl ratio for the full data set; (d) Br/Cl ratio for the representative samples. The labels "Littorina component" and "Brine component" indicate the contribution of these end members in the ground-waters. The actual position of these two end members is not shown because they lie outside the plot.*

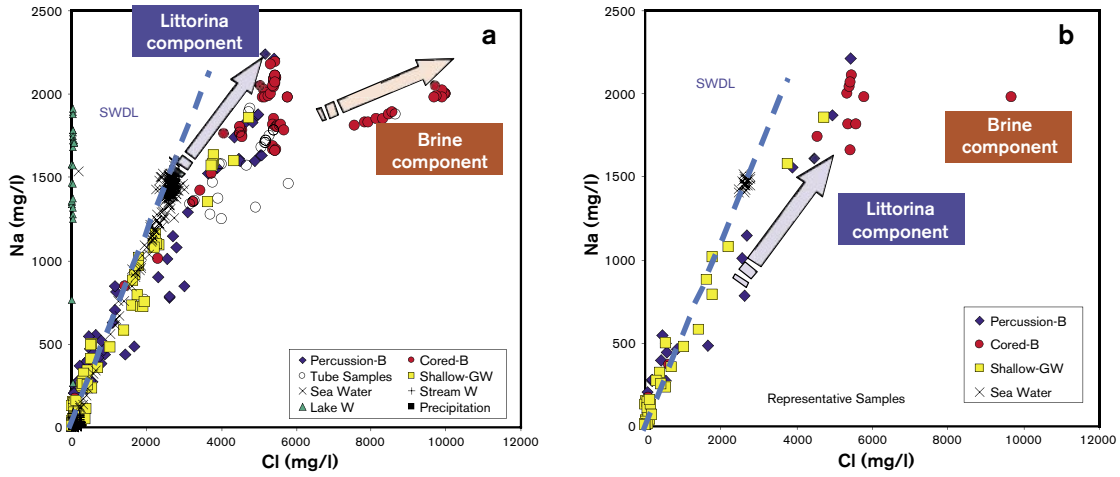

Figure 2-4. *Plot of Na vs Cl for Forsmark area. (a) Full data set. (b) Representative samples.*

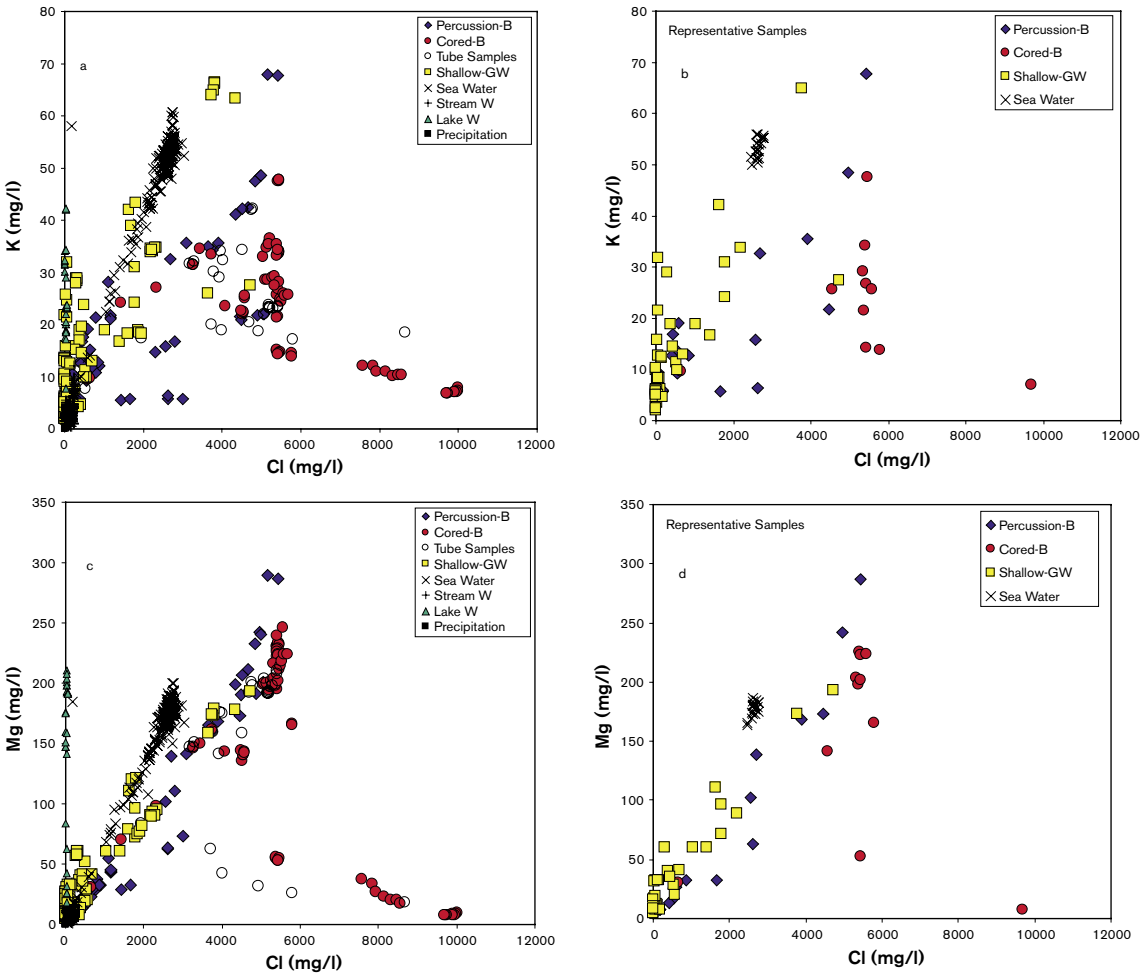

Figure 2-5. *Potassium (a and b) and magnesium (c and d) vs. chloride in water samples from Forsmark area. Full dataset (left) and only representative samples (right).*

Additionally, three different groups of soil pipe samples (shallow groundwaters) can be separated: (a) soil pipe waters plotting on the modern Baltic Sea water dilution line (Figure 2-5) indicating a certain contribution of this end member to their chemical content; (b) soil pipe waters plotting off the Baltic trend, with very little Cl but significant amounts of K and Mg. This may suggest either contact with an older marine water followed by cation exchange reactions and later flushing out of chloride, or simply water/rock interaction of recharge with minerals in the soil; (c) samples with high chloride contents (representative samples 8078 from PFM000009PW and 8252 from SFM0023, with 4,730 and 3,780 mg/L of chloride, respectively) and with a clear compositional affinity to deeper groundwaters representative of mixing with an older and more saline component (mainly Littorina). This last group of soil pipe samples could represent discharge zones.

2.2.2 Evaluation of scatter plots for the calcium carbonate system

Under this heading the evaluation of the main parameters controlling the carbonate system (pH, alkalinity, CO_2 and calcium) is included. Some PHREEQC modelling results (saturation indexes and pCO_2 values) are also included here in order to simplify the description and make the interpretation clearer.

Superficial fresh waters show a wide range of pH values as a consequence of their multiple origin (Figure 2-6a). The lowest values are associated with waters with a marked influence of atmospheric and biogenic CO_2; the highest values (up to 8.5 pH units) are associated with the most diluted groundwater. Overall this gives a decreasing trend with chloride when the rest of the groundwater samples are taken into account, although this trend inverts at depth, so that the more saline groundwaters have slighly higher values. Nevertheless, all these values are affected by uncertainties in pH measurements in the laboratory and there are not enough data from continuous logging pH measurements (apart from the analysis reported in phase 1.1) to check them.

Broadly speaking, the main features of the pH trend can be correlated with other Scandinavian sites with similar waters (e.g., Simpevarp area and Olkiluoto; /Laaksoharju et al. 2004b; Pitkänen et al. 1999/), also affected by uncertainties in pH.

Alkalinity (HCO_3^-) is, together with chloride and sulphate, the third major anion in the system, and is the most abundant in the non-saline waters. Its concentration increases in the shallower groundwaters (Figure 2-7a and b) as a result of atmospheric and biogenic CO_2 influence and/or calcite dissolution. The alkalinity content reaches equilibrium (or oversaturation) with calcite in the fresh groundwaters (Figures 2-8a and b) and then decreases dramatically with depth as it is consumed by calcite precipitation, whereas calcium keeps increasing as a result of mixing (Figure 2-7c and d).

As can be seen in Figure 2-7c and d, calcium shows the same two trends (one with an important Littorina component, and the other with a higher contribution of a brine component) as the rest of the cations. In general, it shows a good positive correlation with increasing chloride content, mainly in the most saline groundwaters, suggesting that mixing is the main process controlling the concentration of this element in Forsmark waters. In spite of the extent of reequilibrium with calcite affecting Ca, the high Ca content of the mixed waters (coming from saline end members) obliterates the effects of mass transfer with respect to this mineral. This fact justifies the quasi-conservative behaviour of calcium, at least in waters with chloride contents higher than 5,000 mg/L. Simple theoretical simulations of mixing between a brine end member and a dilute water, with and without calcite equilibrium, have shown the negligible influence of reequilibrium on the final dissolved calcium contents /Laaksoharju et al. 2004a/.

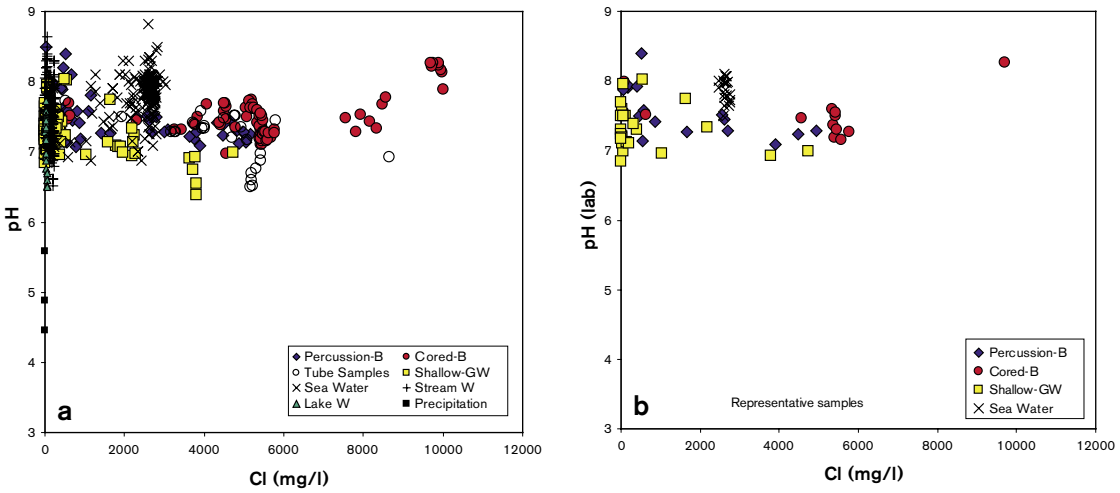

Figure 2-6. *pH vs. chloride content in mg/l (increasing with depth) in Forsmark waters. (a) All samples. (b) Representative samples.*

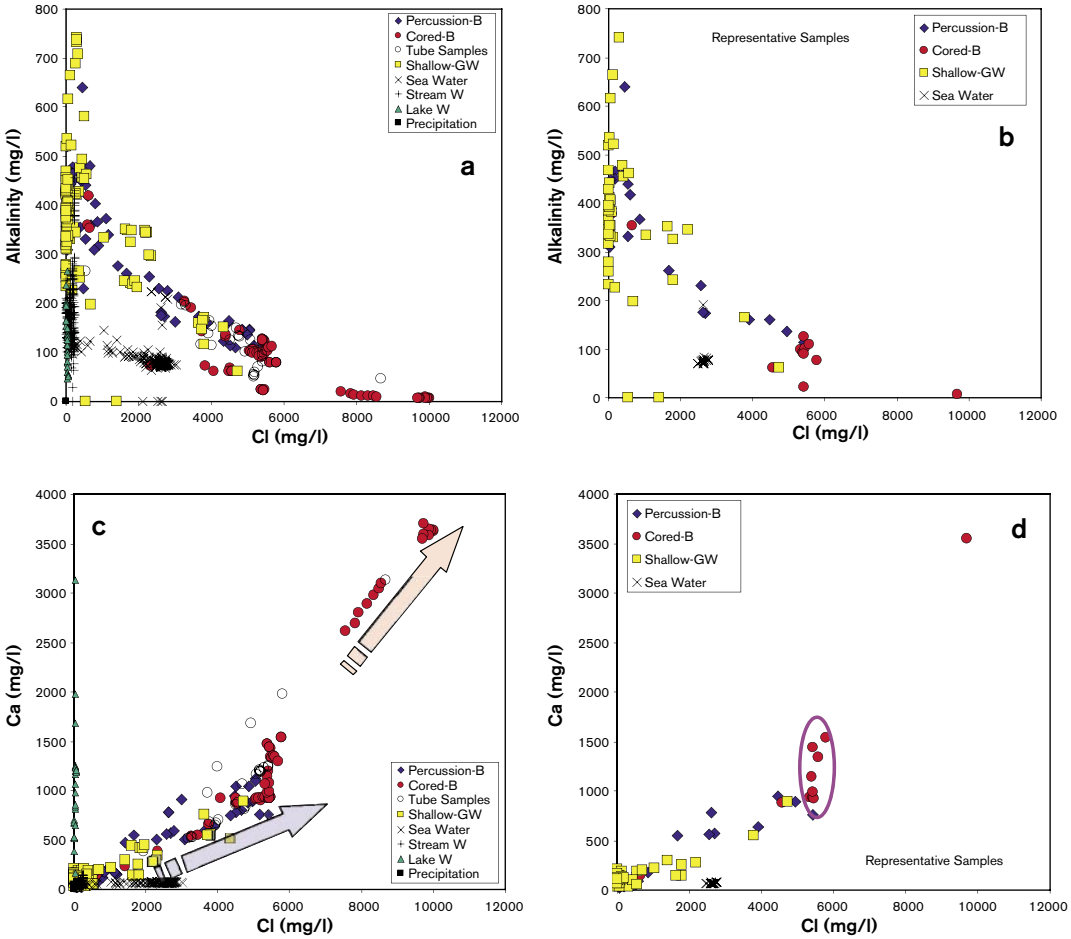

Figure 2-7. *Alkalinity and calcium vs. Cl in waters from Forsmark area. (a) Alkalinity evolution in all waters. (b) Alkalinity evolution in the representative waters. (c) Calcium content in all waters. (d) Calcium content in the representative waters.*

Figure 2-8 shows the calcite saturation index in the Forsmark waters. The alkalinity trend described above can be readily explained by looking at this plot. The uncertainty associated with the saturation index calculation (±0.5) is higher than that usually considered (±0.3). This is due to problems during the laboratory measurements of pH (CO_2 outgassing and ingassing), as was described in the report for the previous phase /Laaksoharju et al. 2004a/ and also in Simpevarp 1.2 report (Laaksoharju et al. in press).

As for CO_2, Figure 2-8 c and d show the trend of decreasing partial pressure as depth increases, reaching values well below the atmospheric in the more saline groundwaters.

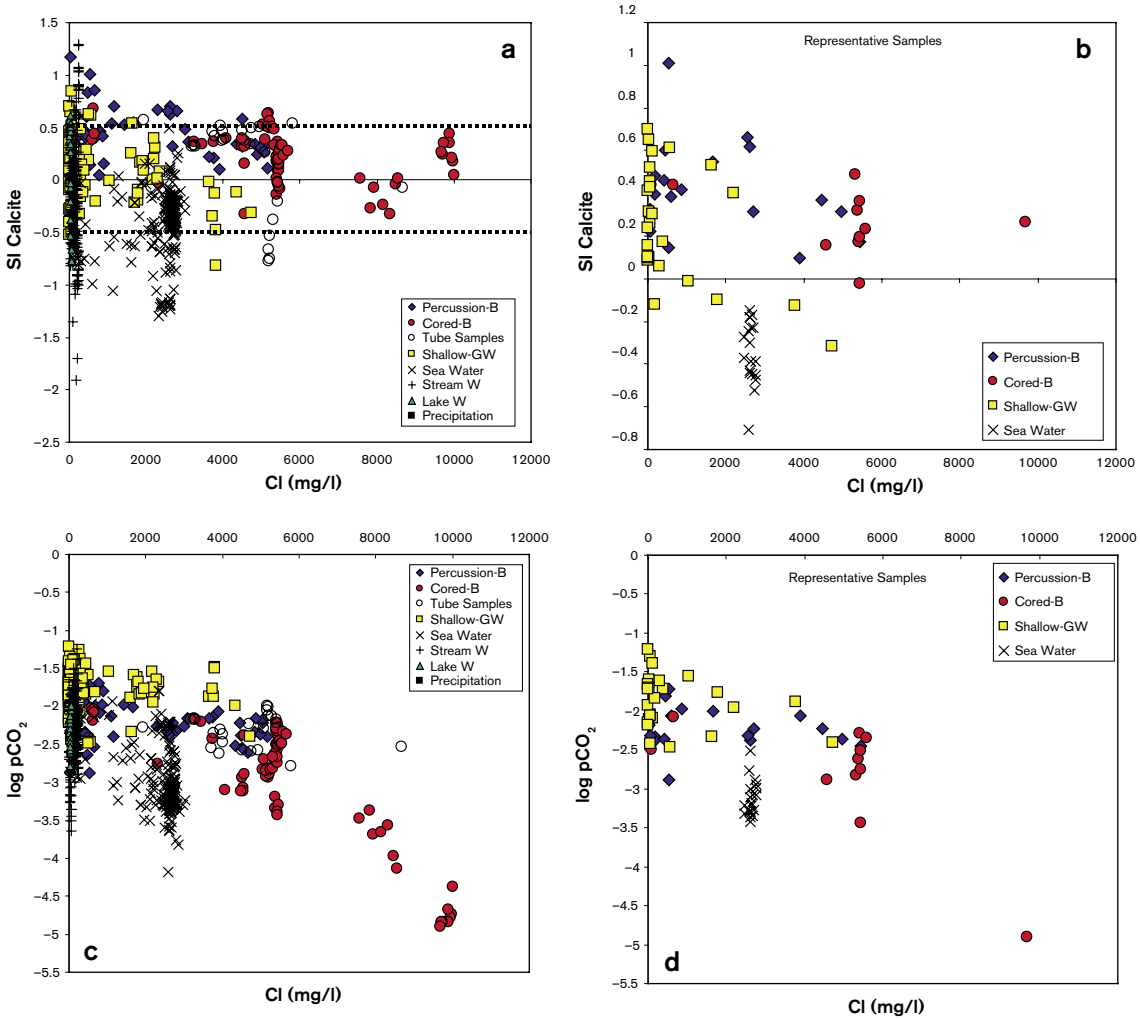

Figure 2-8. *Calculated calcite saturation indexes and partial pressure of CO2 against chloride for waters from Forsmark area. The dashed lines in panel a represent the uncertainty associated with SI calculations.(a) and (b) Calcite SI in all waters and in representative waters, respectively. (c) and (d) log pCO_2 in all waters and in the representative waters, respectively.*

2.2.3 Evaluation of scatter plots for the silica system

The content of dissolved SiO_2 in surface waters indicates a typical trend of weathering, while in groundwaters it has a narrower range of variation indicative of partial reequilibrium (Figure 2-9a,b). Also in this case, the range of silica contents is broken at Cl ~ 5,500 mg/L, where waters show different silica contents for the same chloride concentration. The general process evolves from an increase in dissolved SiO_2 by dissolution of silicates in surface waters and shallow groundwaters to a progressive decrease related to the participation of silica polymorphs and aluminosilicates which control dissolved silica as the residence time of the waters increases. This can be clearly seen in Figure 2-9c,d.

The weathering of rock-forming minerals is the main source of dissolved silica. Superficial waters have a variable degree of saturation with respect to silica phases (quartz and chalcedony), compatible with the weathering hypothesis, and a rather unclear control by secondary phases. This is a rough generalization, useful for this general description but it should be noted that surface waters come from diverse systems (streams, lakes and soil zones) involving contrasting processes (evaporation, biological uptake, etc; /Laaksoharju et al. 2004b/ that affect silica concentrations.

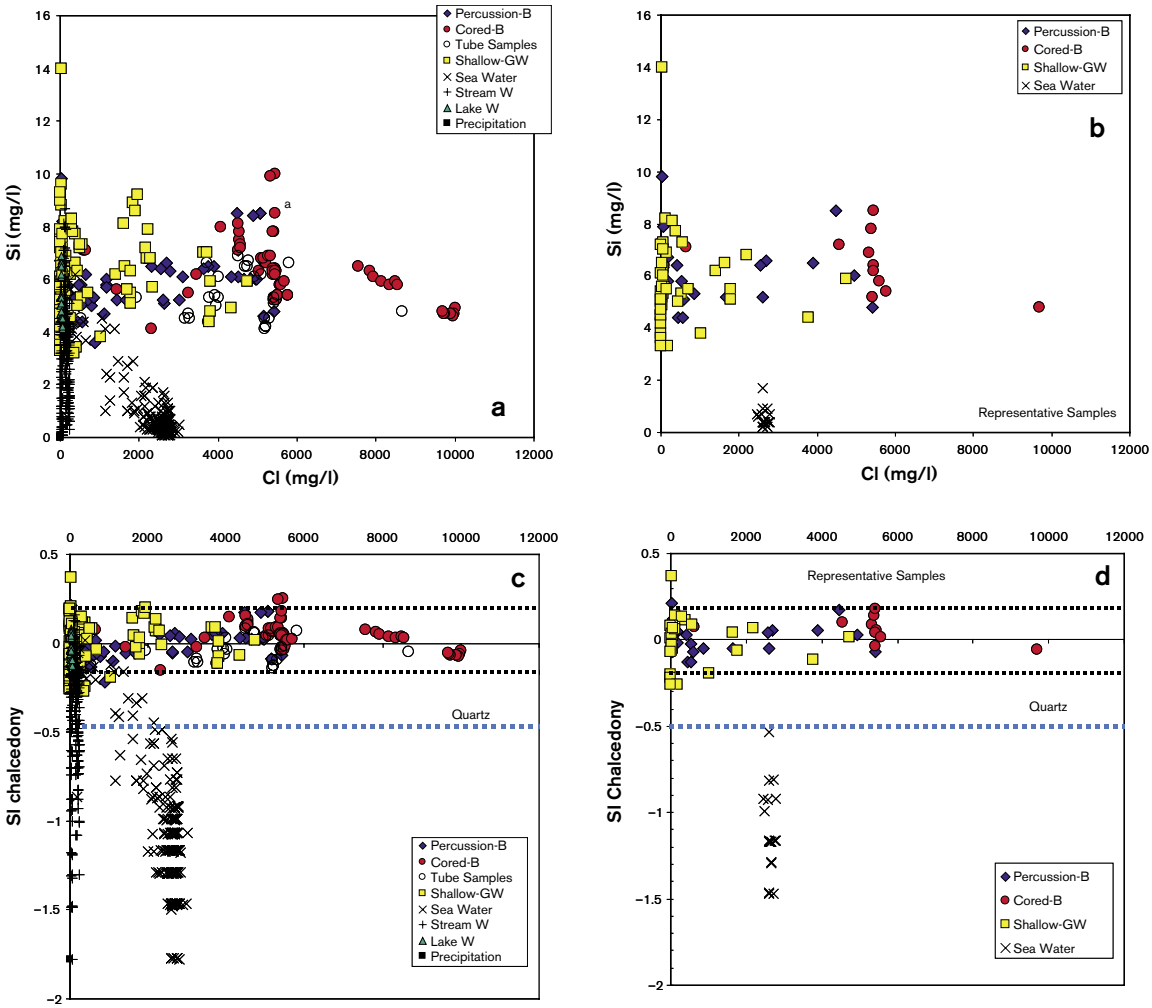

Figure 2-9. *(a) Plot of SiO2 vs.Cl for all Forsmark waters and for the representative waters (b). (c) Saturation indexes of chalcedony and quartz as a function of Cl in all Forsmark waters and in the representative waters (d). The dashed lines represent the uncertainty associated with SI calculations /Deutsch et al. 1982/.*

Groundwaters are oversaturated in quartz and close to equilibrium with chalcedony (Figure 2-9c,d). Saturation indices are relatively constant and independent of chloride content; this suggests that the groundwater has already reached, at least, an apparent equilibrium state associated with the formation of aluminosilicates or secondary siliceous phases like chalcedony, which seems to be controlling dissolved silica.

The lack of QA aluminium data for Simpevarp groundwaters precludes a speciation-solubility analysis of aluminosilicates. Therefore, activity diagrams were used to study the relationship between silicate minerals and their stability. This analysis will be discussed later (modelling part, 3.2).

2.2.4 Evaluation of scatter plots for the sulphate system

Figure 2-10a, showing SO_4 vs Cl, suggests three possible trends:

a) An obvious modern Baltic Sea water dilution line, including Sea water samples and some shallow groundwaters (soil pipes and percussion boreholes).

b) A borehole brackish groundwater dilution trend moving away from (a) towards very high sulphate values, suggesting, as in the previous phase, some Littorina influence /Laaksoharju et al. 2004a/. Some shallow groundwaters (soil pipe samples) are also included in this trend.

c) A decreasing SO_4 trend as chloride increases from 6,000 mg/L to more saline values. In general, these groundwater data lend support to the absence of a significant postglacial marine component, suggesting instead a mixing with deeper, more saline waters of non-marine origin.

There is even an additional low chloride-low sulphate dilution trend incorporating some shallow groundwaters and some Lake/Stream water. The greater scatter of sulphate at lower chloride levels may partly reflect some modern Baltic Sea water influence, some near-surface oxidation of sulphides, and also the variable effects of microbially mediated reactions (e.g. effect of sulphate-reducing bacteria) below and above the geosphere/biosphere interface.

Perhaps the most interesting aspect of Forsmark waters is their different evolution, as shown by the sulphate content, with respect to sulphate behaviour in the Simpevarp area /SKB, 2004/. Figure 2-10e shows the sulphate contents in waters from Simpevarp and Olkiluoto. Forsmark data are more limited in salinity than Olkiluoto data, but they appear to be following the same trend. In both cases, after an initial increase in sulphate (reaching the maximum values when salinity is around 5,000–6,000 mg/L of Cl) there is a clear decrease towards zero. On the contrary, for the same chloride content, sulphate concentration in the Simpevarp area is clearly higher (Figure 2-10e).

This contrasting behaviour must be related to the process controlling sulphate content in these waters. Analysing the saturation state of the groundwaters with respect to gypsum some conclusions can be drawn. This analysis was also carried out for Simpevarp and included in Simpevarp 1.2 report /SKB, 2004/. In both cases (Simpevarp 1.2 and Forsmark 1.2) the range of salinity in the samples has increased since previous datafreeze, and a more complete evolution can be observed.

Forsmark groundwaters are undersaturated in gypsum but they evolve towards equilibrium with it as chloride increases up to 6,000 mg/L (Figure 2-10c and d). Then, the more saline groundwaters evolve towards an even more undersaturated state than shallow groundwaters. The same behaviour can be seen in Olkiluoto groundwaters. However, in Simpevarp groundwaters the gypsum SI trend indicates a clear evolution towards equilibrium (Figure 2-10f) which is reached at chloride values of 10,000 mg/L and maintained even in the most saline waters /Laaksoharju et al. 2004b/.

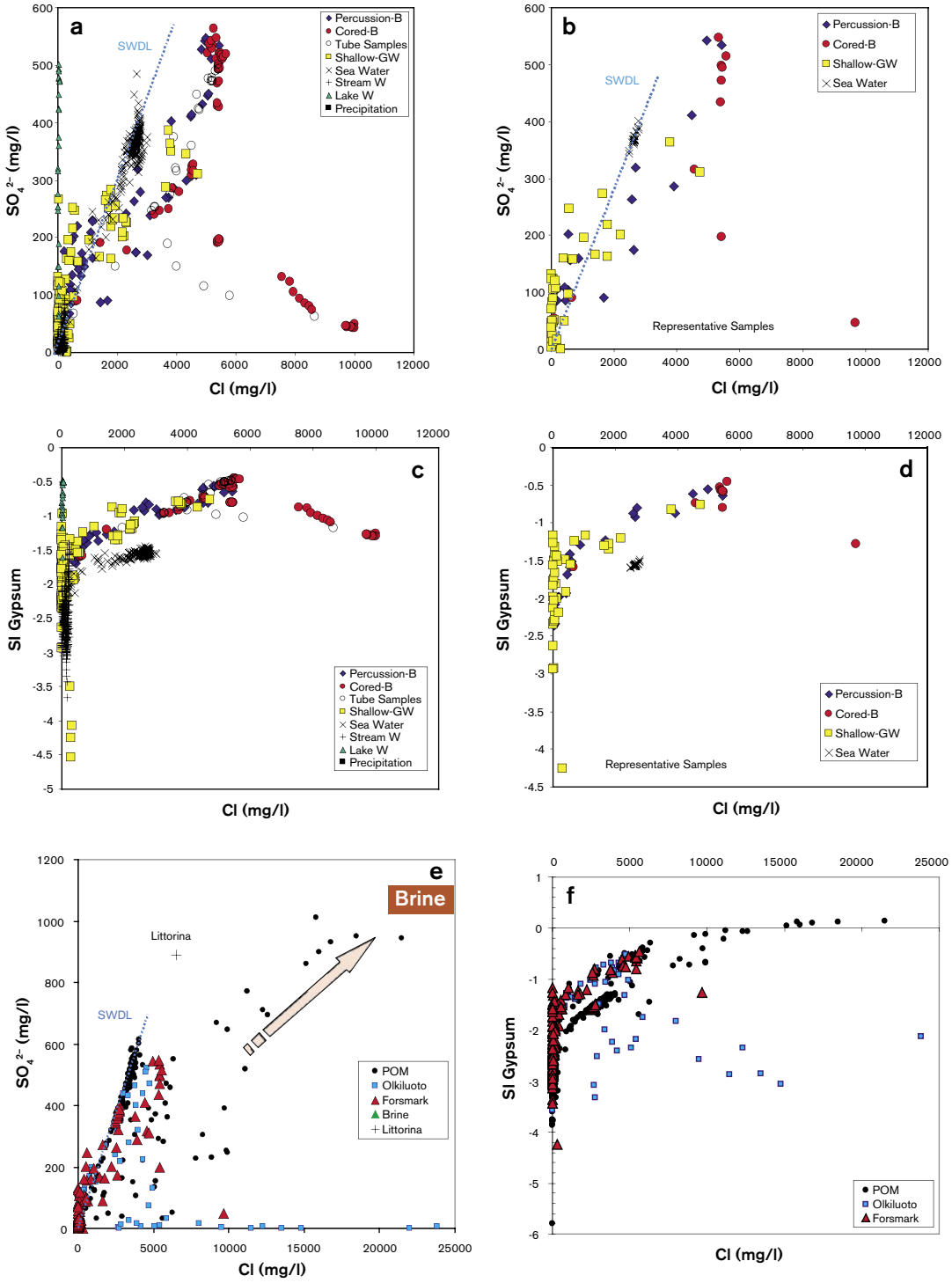

Figure 2-10. *(a) and (b)Plots of SO_4 vs Cl for all Forsmark waters and for the representative ones, respectively. (c) and (d) Plots of Gypsum saturation index vs Cl for all Forsmark waters and the representative ones, respectively. (e) and (f) Plots of SO_4 and Gipsum SI vs Cl comparing Forsmark data with samples from Simpevarp Area and Olkiluoto.*

3 Geochemical modelling

Geochemical modelling calculations are used to investigate the processes that control water composition at the Forsmark area.

Speciation-solubility calculations (some already described in section 2.2, "Explorative analysis"), mixing and mass balance and reaction-path modelling have been carried out with the geochemical code PHREEQC /Parkhurst and Appelo, 1999/ and the WATEQ4F thermodynamic database[2]. The principles of speciation-solubility calculations were described in previous reports /Laaksoharju et al. 2004a,b,c/ and will not be repeated here. The principles of mass balance and reaction-path calculations are briefly described below.

This chapter is divided into three sections: (a) mass balance and mixing calculations; (b) appraisal of the consequences of mixing and reaction for some problematic minerals in the aluminosilicate system; and (c) redox system modelling.

3.1 Mass balance and mixing calculations

In the previous evaluation of Forsmark groundwaters, presented in Chapter 2, two different trends were identified and ascribed to two representative mixing processes: the first one giving rise to Littorina-rich waters (already identified in Forsmark 1.1; /Laaksoharju et al. 2004a/), and the second producing waters with an important participation of a brine end member. Besides, the presence of very shallow groundwaters with compositional features representative of discharge zones of old groundwaters has now been identified as a separate group.

These three groups of samples have been processed through the mass balance capabilities of PHREEQC in order to check the hypothesis advanced above on the influence of the different end members on their chemistry[3]. Additionally, mixing proportions obtained by PHREEQC for selected samples have been compared with the results obtained with a modified version of M3, called M4, developed by the University of Zaragoza team[4], in order to validate the code.

3.1.1 Methodology

PHREEQC inverse modelling calculations follow the same methodology used in Forsmark 1.1 and Simpevarp 1.1 /Laaksoharju et al. 2004a,b/. All the calculations assume the presence of four end member waters (Brine, Littorina, Glacial and Precipitation, in common with M3 and M4 calculations), and try to predict mixing proportions and mass transfers due to reactions with a variable set of minerals. The elements used in the calculations are: Ca, Mg, Na, K, Si, HCO_3^-, Cl^-, SO_4^{2-}, Fe^{2+}, S^{2-}, ^{18}O and D.

The mineralogical study of boreholes KFM01B, KFM02A, KFM03A and KFM04A has identify the presence of a complex sequence of fracture fillings. Apart from widespread chlorite and calcite, phases such as epidote, prenhite, laumontite, adularia, albite, apophyllite, analcime, apatite, fluorite, hematites and pyrite have also been reported. Small amounts of coatings of high-surface-area smectite, interstratified clay minerals and illite have also been identified. Most of these minerals are common to other Swedish sites (e.g., Simpevarp area). Their presence validates the broad range of minerals considered in Forsmark 1.1 modelling /Laaksoharju et al. 2004a/, when no mineralogical information was available. Therefore, the number of feasible reacting phases is very high and, unfortunately, being most of them aluminosilicates, not well constrained in mass balance calculations due to the lack of dissolved Al data in the water samples.

[2] The selection of this thermodynamic database has already been justified in /Laaksoharju et al. 2004b/.

[3] The group of fresh non-saline waters was already identified and analysed in the previous phase (Forsmark 1.1; /Laaksoharju et al. 2004a/) and will not be presented here.

[4] Some additional comparisons between M3 and M4 are presented in /Gurban et al. 1998/, and Appendix C gives a summary of the code, together with a sensitivity analysis carried out with both synthetic and real samples.

Following the same methodology as in Forsmark 1.1 and Simpevarp 1.1 /Laarksoharju et al. 2004a,b/ the selected set of minerals includes calcite, SiO_2 phases, plagioclase, biotite, chlorite, different phyllosilicates (especially those identified in fracture fillings), sulphides (pyrite and monosulphides), $Fe(OH)_3$, CH_2O and various exchange reactions involving Na, Ca, Mg, and K. Additionally, different stoichiometries for biotite (phlogopite and Fe-biotite) chlorite (Mg and Fe chlorite) and smectites (Na and K smectite), and some more specific phases identified as fracture fillings have been added (e.g. adularia, laumontite) to assess their incidence in the mixing proportions.

The number of models obtained with such a broad type of reactions is high. However, this sensitivity analysis shows that variations in the reaction set do not produce significant changes in the calculated mixing proportions. Therefore, only a qualitative reference to the mass transfers for reactions a priori more kinetically favoured in this kind of systems, will be given.

As commented above, the samples selected for the mass balance calculations belong to three different groups:

1. Brackish-saline groundwaters (Cl = 4,500–5,500 mg/L) with an important Littorina signature. They are distributed at variable depths, from 110 to 184 m (samples 4538 and 4724) and from 450 to 643 m (samples 8016, 8017 and 8273).
2. The deepest groundwaters (represented by sample 8152 at 980–1,000 m depth), with an important Brine component.
3. Shallow groundwaters belonging to (probable) discharge zones (PFM000009PW sample 8078 and SFM0023 sample 8252).

3.1.1 Results

Table 3-1 summarises PHREEQC and M4 results, showing the good agreement between both approaches (see also Appendix C for an in-depth validation of M4). PHREEQC results give the maximum and minimun values among all the successful mixing models for each sample.

Samples of Group 1 have Littorina proportions ranging from 35 to 51% (only the two samples with the most extreme Littorina mixing proportion are shown in the table: 4538 and 8016). In detail, the sample with the lowest chloride content (4538) has a similar proportion of Littorina and Glacial end-members, while the other samples (represented in Table 3-1 by sample #8016) have a higher Littorina proportion (50%) and a much lower Glacial proportion. Brine percent is consistently low (< 5%) and Precipitation is in the range 20–23%. Therefore, this set of samples shows a clear Littorina contribution but, in some cases, Glacial proportions can also be important.

The only sample representative of Group 2 (the most saline groundwaters found in Forsmark, #8152), reveals an important Brine contribution (16.02%; cf. < 5% in Group 1 samples) and a lower (or null) participation of Littorina (< 9%). The most important contribution comes from the Glacial end member (48%). These values are consistent with the results obtained for other groundwaters at similar depths elsewhere in Sweden /SKB, 2004/ and correspond to waters representative of old (> 10,800 BP) mixing events with Brine and Glacial end-member waters, with little modifications by more recent mixing processes.

Finally, Group 3 samples (shallow groundwaters in discharge zones, #8078 and 8252) are characterized by a high Littorina percentage, similar in general to the value reported for Group 1 samples. The other end-members have also similar contributions to the ones in Group 1. Therefore, they could represent genuine discharge zones of old, deep groundwaters.

The main reaction processes associated to these mixing models include decomposition of organic matter; dissolution of plagioclase, biotite and $Fe(OH)_3$; precipitation of calcite, K- and Mg-phyllosilicates, silica (chalcedony), and sulphides; and ionic exchange between Na and Ca. Mass transfers associated with dissolution-precipitation reactions are small (< 0.1 mmol) and slightly higher for cation exchange processes (in the range of 1 mmol), specially for groundwaters with high Littorina signature.

Table 3-1. PHREEQC and M4 results for the groundwaters representative of three different trends in the Forsmark area.

	Sample	Code	Brine	Littorina	Glacial	Precipitation
Brackish-saline	4538 Cl = 4,563 mg/L Depth: 115 m	PHREEQC	3.8–5.1	27.9–35.2	27.8–31.6	29.4–39.0
		M4	2.6	35.7	40.8	20.8
	8016 Cl = 5,410 mg/L Depth: 512 m	PHREEQC	3.3–4.3	50–54	12.2–14.3	28.6–33.5
		M4	1.6	50.8	24.4	23.2
Saline	8152 Cl = 9,690 mg/L Depth: 990 m	PHREEQC	17.5–19.5	0–15	34–42	24–42
		M4	16.02	9.2	47.9	26.9
Discharge	8078 Cl = 4,730 mg/L Depth: 3 m	PHREEQC	3.5–4.8	30.5–38.5	27.2–32	28.2–33.5
		M4	2.7	39	39.4	18.9
	8252 Cl = 3,780 mg/L Depth: 3.8 m	PHREEQC	1.3–2.4	50.9–55	11.6–15.9	27.2–34
		M4	0	51.4	26.3	22.4

Reactions involving redox species are not well constrained in this type of calculations because the end members lack a proper redox characterisation. Nevertheless, most of the models obtained for Group 2 groundwaters predict a significant precipitation of sulphides (mass transfer rates similar to non-redox minerals). This result is consistent with the redox and microbiological character of these waters as discussed in Section 3.3.

3.1.2 Discusion

Brackish-saline groundwaters (with chloride around 5,000 mg/L) show an important Littorina signature, usually being the dominant end member, with mixing proportions around 45–50%. Locally, Littorina contribution is lower (35%) and then the Glacial end member becomes dominant (40%). These group of groundwaters are scattered in depth, from 100 to 500 m, and therefore deeper than previously assumed in Forsmark 1.1 iteration /Laaksoharju et al. 2004a/. At depths below 200 m, these brackish-saline groundwaters are located at the same level as the fresh-non saline groundwaters found in other boreholes. In fact, some soil pipe samples (Group 3 samples, < 3 m depth) show the same compositional characteristics and mixing proportions as the deeper brackish groundwaters, suggesting the existence in the system of discharge zones for these old, Littorina-dominated groundwaters.

The deepest saline groundwaters (1,000 m depth) show a clear Brine signature, a low (or null) Littorina contribution and a dominance of the Glacial end-member. These Group 2 groundwaters represent the remnant of a very old mixing process (Baltic Ice Lake Stage, > 10,800 BP) when glacial melt water flushed the bedrock and mixed with ancient Brine groundwaters. It can then be concluded that the forced introduction of glacial melt water in Forsmark reached at least a depth of 1,000 m.

3.2 The aluminosilicate system

As it has been commented on above, the mineralogical study of boreholes KFM01B, KFM02A, KFM03A and KFM04A have demonstrated the presence of a complex sequence of fracture fillings. Besides the granite rock-forming minerals, most fracture filling phases are aluminosilicate minerals with which waters have been in contact during their geochemical evolution. Therefore, they are important water-rock interaction phases. However, as already pointed out, the lack of aluminium data for Forsmark groundwaters precludes a speciation-solubility analysis, limiting the analysis to a graphical representation of stability diagrams.

The accuracy of the stability diagrams depends on pH and is therefore affected by uncertainties in its value. Uncertainties in the equilibrium constants of the aluminosilicates (especially the phyllosilicates) also affect the conclusions drawn from these diagrams and from the ensuing theoretical models based on them /e.g. Laaksoharju and Wallin, 1997; Trotignon et al. 1997, 1999/. As a consequence, the study of aluminosilicate phases has been restricted to those with low uncertainties, using thermodynamic data already tested and verified in comparable systems. That means that the "aluminosilicate system" as defined here reduces to the set adularia, albite, kaolinite, laumontite, prenhite and chlorite. The selected thermodynamic data are taken from /Grimaud et al. 1990/ at 15ºC in their study of Stripa groundwaters.

The following description includes a general evaluation of Forsmark groundwaters from their position in the stability diagrams and a discussion on the effects of mixing and reaction on the groundwaters' chemistry[5]. This discussion is illustrated by means of a theoretical equilibrium modelling. The origin of the saline groundwaters (Littorina and/or Brine end members) is not discussed here, and the model just assumes that they are already in the system, participating in the mixing process. Nevertheless, in the Simpevarp 1.2 report, the potential use of this modelling approach to predict the chemical characteristic of these old saline groundwaters is indicated.

3.2.1 Forsmark waters in the stability diagrams

Following the same procedure developed for Simpevarp 1.2 phase /SKB, 2004/, Forsmark waters have been plotted in different stability diagrams (see Appendix D). The set of thermodynamic data utilized to construct the stability diagrams was calibrated for Stripa groundwaters /Grimaud et al. 1990/, and the presentation and explanation of the original diagrams can be found in /SKB, 2004/.

The analysis of Forsmark waters uses the kaolinite-albite-adularia stability diagram because it is the most suitable for discriminating waters that have undergone mixing, and because many Fenoscandian groundwaters plot near the albite-adularia boundary line, suggesting a true or apparent equilibrium with both phases.

Figure 3-1 shows the diagram kaolinite-albite-adularia for the Forsmark waters. Green and blue arrows mark the two main trends that can be distinguished. *The first trend* (green arrows) starts inside the kaolinite stability field and evolves towards the kaolinite-adularia boundary. This trend is defined by modern surface waters and shallow groundwaters with low chloride contents and whose geochemical evolution is mainly the result of water-rock interaction.

The evolution path of these waters in the kaolinite field has a slope of around 2, similar to other weathering/alteration processes in granitic materials and represents the effects of a progressive dissolution of the rock forming minerals calcite, biotite, plagioclase, K-feldspars, etc. Along this process, partial reequilibria with phyllosilicates (represented by, e.g., kaolinite) can be reached. Ionic exchange and, in later stages, calcite precipitation can also take place. Waters close to or on the kaolinite-adularia boundary would correspond to the most evolved samples in this water-rock interaction process.

Some shallow groundwaters (soil pipes) and lake waters from Forsmark do not plot inside the kaolinite field, as expected, but inside the adularia stability field instead. Some of these samples (samples close to the adularia-albite limit, see below) show clear evidences of mixing with modern Baltic Sea, and even with another older marine (Littorina) and saline (non marine) end member (see also the discussion following Figures 2-3, 2-11, and Section 3.1). Therefore, they could be waters whose chemistry is not only controlled by water-rock interaction and plot together with groundwaters characterised by mixing. The rest of the soil pipe and lake samples plot in the adularia field further away from the adularia-albite limit. They have low chloride contents but anomalously high K, Mg, SO_4^{2-}, etc. (Figures 2-6 and 2-11). These samples could be the result of water-rock interaction in the detritic overburden or could even represent some kind of contribution from an old marine component, as they are geographically associated to what seems to be discharge zones in the system. More data would be needed to determine the origin of these waters.

[5] In this section different diagrams and computer simulations for Forsmark waters are presented, in some of the cases together with other sites (Stripa, Olkiluoto and Simpevarp area).

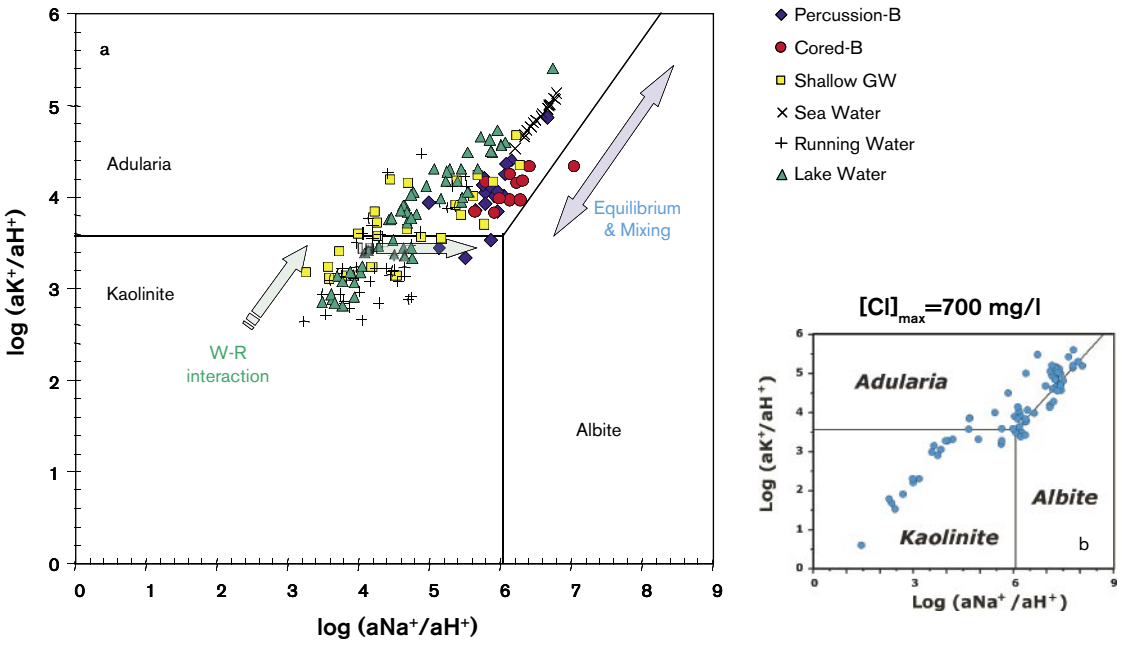

Figure 3-1. *Kaolinite-adularia-albite stability diagram for Forsmark representative surface and groundwaters (a) and for Stripa groundwaters (b).*

The second trend (blue arrow), followed by all Forsmark brackish and saline groundwaters, runs parallel to the adularia-albite limit, indicating an equilibrium (or near equilibrium) situation. This result is very similar to Stripa's (compare the figures and the scale) but with an important difference: maximum chloride content in Stripa reaches only 700 mg/L, whereas Forsmark groundwaters, plotted in the same position, have Cl contents up to 10,000 mg/L. The residence time of Stripa groundwaters has been estimated at roughly 100,000 years /Fontes et al. 1989/, meaning that water-rock interaction processes can only provide up to 700 mg/L of chloride in such a big time span. It is clear, therefore, that an additional source of salinity is needed to justify the existence of much younger waters with much higher chloride concentrations in Forsmark. This source of chlorine comes from mixing with a saline component of marine and/or non marine origin. And therefore, this points again to mixing as the key process controlling the chemistry of these waters, as it has been repeatedly reported in previous works /Laaksoharju and Wallin, 1997; Laaksoharju et al. 1999; Laaksoharju et al. 2004b/.

In Figure 3-2 Forsmark samples have been plotted together with those of Olkiluoto /Pitkänen et al. 2004/ and of Simpevarp area (Laaksoharju et al. in press). Olkiluoto waters occupy, in general, the same position as Forsmark waters[6] . Olkiluoto samples in the kaolinite stability field and on the kaolinite-adularia boundary correspond to subsurface or shallow groundwaters whose chemistry is controlled by water-rock interaction. Samples located on the adularia-albite boundary correspond to brackish and saline groundwaters characterised by having undergone complex mixing processes (between Meteoric, Littorina, Glacial and Saline end members, /Pitkänen et al. 2004/).

Results for Simpevarp groundwaters are similar, although in this case the number of samples in the adularia stability field is smaller than in the cases of Forsmark and Olkiluoto.

The position of the theoretical end members is also shown in Figure 3-2 (Brine, Littorina and Glacial; Meteoric is close to Glacial). It is fairly clear that the evolution path of these waters is the result of (a) reaction between the rock and diluted waters (surface and shallow groundwaters), (b) mixing in depth with more saline groundwaters in different proportions, as a function of location and residence time, and (c) the simultaneous interaction of these deep waters with the rock.

[6] Although not presented in the Appendix D, the same match is observed in diagrams AD-1 and AD-2.

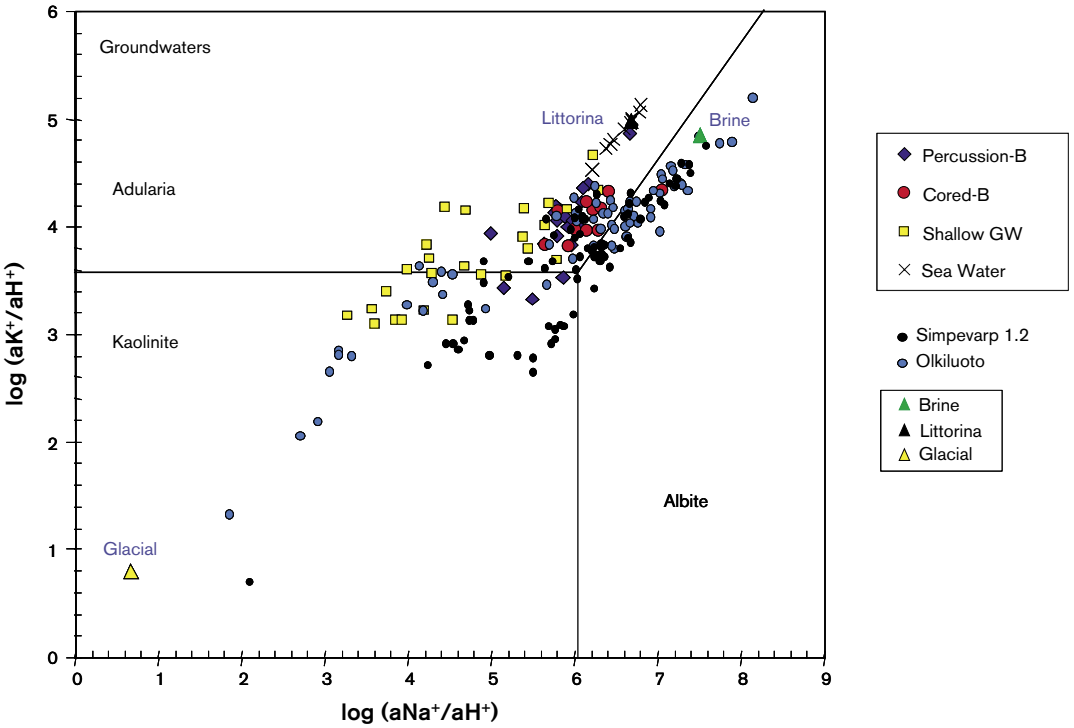

Figure 3-2. *Kaolinite-adularia-albite stability diagram. Together with the Forsmark representative groundwaters, the Olkiluoto /Pitkänen et al. 2004/ and Simpevarp area groundwaters, and also the theoretical end members (Brine, Littorina and Glacial) have been plotted in this diagram.*

An identical result has been found in Simpevarp 1.2 /SKB, 2004/. However, in this case there is an important number of samples located close to the adularia-albite boundary but inside the adularia field, showing a clear trend towards the Littorina end member. We will come back to this later.

3.2.2 Theoretical simulations based on the stability diagrams

As shown above, Forsmark, Simpevarp area and Olkiluto groundwaters on the adularia-albite boundary and inside the adularia stability field but close to the boundary include samples of broadly different salinities, chemical contents and depths, but reflecting an apparently similar equilibrium situation. In a first approximation, they could be interpreted as the result of different mixing episodes between different end members at different times during the site evolution. Alongside this main process, there would be re-equilibration periods (reaction with the rock) following the disequilibrium created by the successive mixing episodes.

The chemistry of the groundwaters is then the result of a complex sequence of mixing and reaction. Following the procedure developed in Simpevarp 1.2 report, a direct mixing and reaction calculation has been chosen in order to evaluate the relative contribution of the two processes.

The modelling performed in Simpevarp 1.2 was focused on the assessment of the oldest mixing episode between the saline and glacial end members (8,000–10,000 BC) and is entirely valid as an explanation of the more saline waters in Forsmark (see a detailed description in /Laaksoharju et al. 2004b/, and also Figure 3-4). Therefore, in this report the simulations will be focused on the next mixing episode, involving the previously mixed waters and a certain amount of Littorina Sea water end member.

The simulation flow chart is shown in Figure 3-3. From previously calculated (Simpevarp 1.2) mixing proportions between Brine and Glacial (the two extreme cases analysed: 63% Brine and 37% Glacial, 5% Brine and 95% Glacial), equilibrium with different mineral assemblages was imposed (“Reaction” in Figure 3-3). Equilibrium with calcite, chalcedony, albite, and adularia has been chosen here only as an example, but models with other mineral assemblages have also been run.

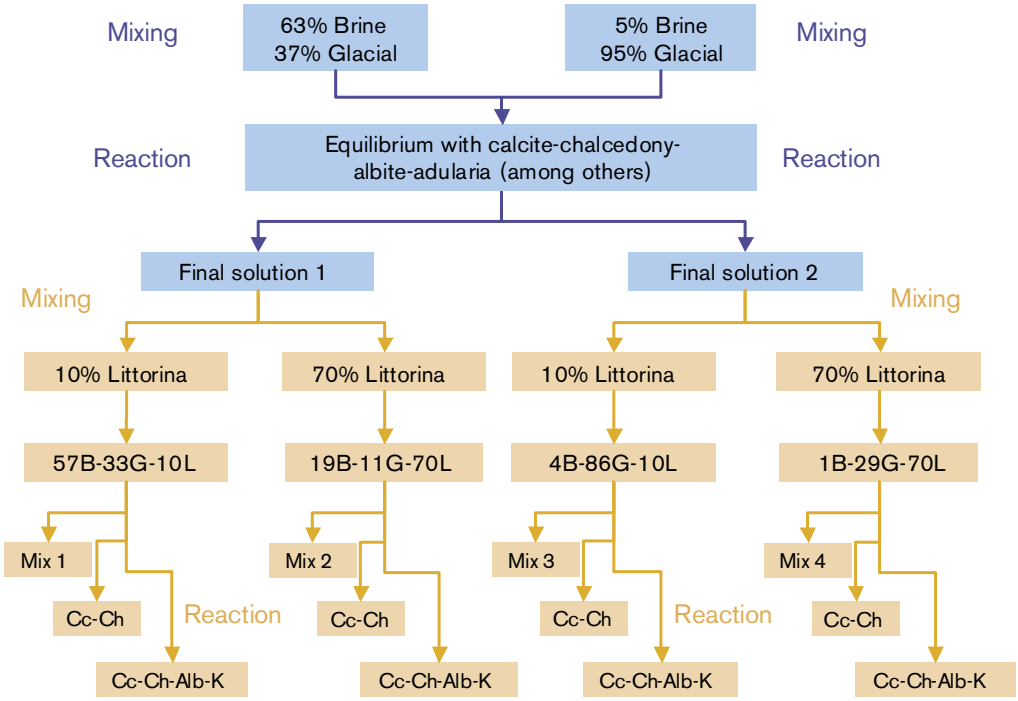

Figure 3-3. *Simulation procedure for the assessment of the mixing episode between Littorina and a saline groundwater (result of a previous mixing process between Brine and Glacial end members and the equilibrium with a mineral assemblage).*

The resulting water (final solutions 1 and 2 in Figure 3-3) was mixed with different proportions of Littorina (between two extreme cases: 10% and 70%). The new mixed waters are named Mix 1, 2, 3 and 4. The final step consists in imposing again an equilibrium with different mineral assemblages. The equilibria with calcite-chalcedony and calcite-chalcedony-albite-kaolinite have been chosen here as mere examples.

Figure 3-4 shows the location of final solutions 1 and 2 after mixing with Brine and Glacial and in equilibrium with the selected minerals (black squares and orange diamonds). They plot on the adularia-albite boundary very close together. They represent the final result of the simulations performed in Simpevarp 1.2 and the starting point of this new calculation.

The next modelling step (the first of the simulation presented here) is a mixing calculation. Each of the already calculated final solutions was mixed with the Littorina end member in two different proportions: 10% and 70%.The position of these mixed waters is plotted in the stability diagrams (Figure 3-5). After mixing, the equilibrium of the mixed waters with different combinations of calcite, chalcedony, albite, adularia and kaolinite was simulated in order to measure its effects on the final composition of the waters. Only selected results are shown in Figure 3-5.

The first theoretical mixing point (before reactions, Figure 3-5a) plots on the adularia-albite equilibrium boundary and, after reaction, the point simply moves along (and very close to) the equilibrium line. The other three theoretical mixing points plot inside the adularia field, progressively closer to the position of the Littorina end-member (Mix 4, Figure 3-5b). In the three cases, the reaction with different mineral assemblages show the same trend parallel to the albite-adularia boundary.

Figure 3-6 superimposes on the previous results the real water samples. As the four graphs show, mixing with Brine and Glacial is responsible (directly or indirectly) for most chemical variability (Littorina component is absent or in very low percentage) in the most saline waters (only one red cicle in the plots, close to the symbol of Mixing) from Forsmark (as it was demonstrated in Simpevarp 1.2; /SKB, 2004/). Water-rock interaction processes for this saline groundwaters can be approached by thermodynamic modelling using the same mineral assemblage considered in the Simpevarp area.

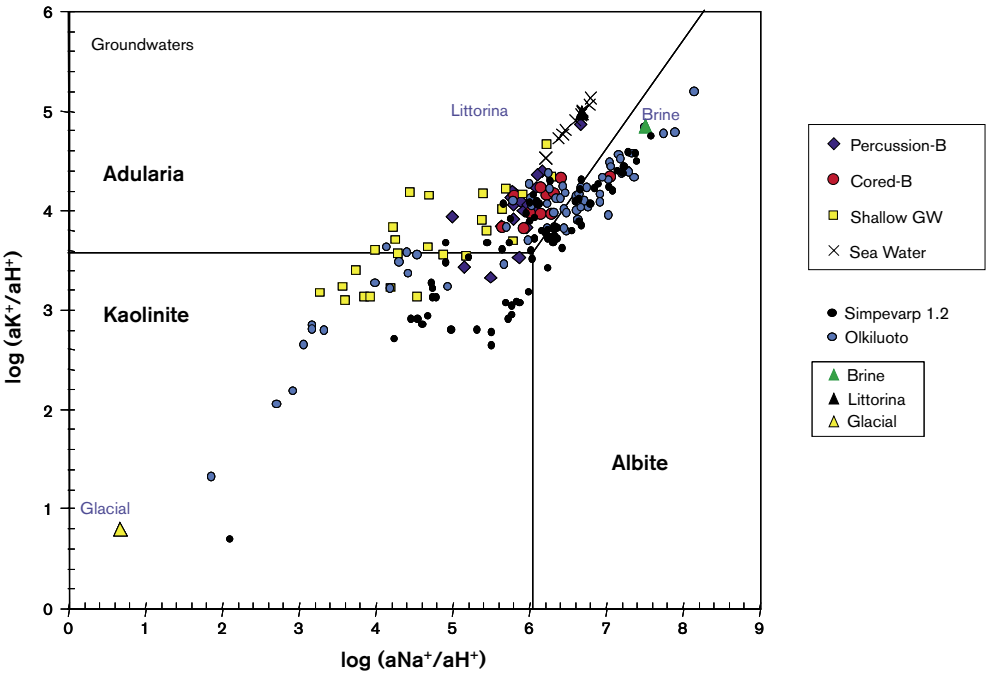

Figure 3-4. *Starting point for the simulation of the mixing episode between Littorina and a saline groundwater result of a previous mixing process between Brine and Glacial end members (Mix points in the plot), and the equilibrium with a mineral assemblage (C_Ch_Alb_Adu in the plot).*

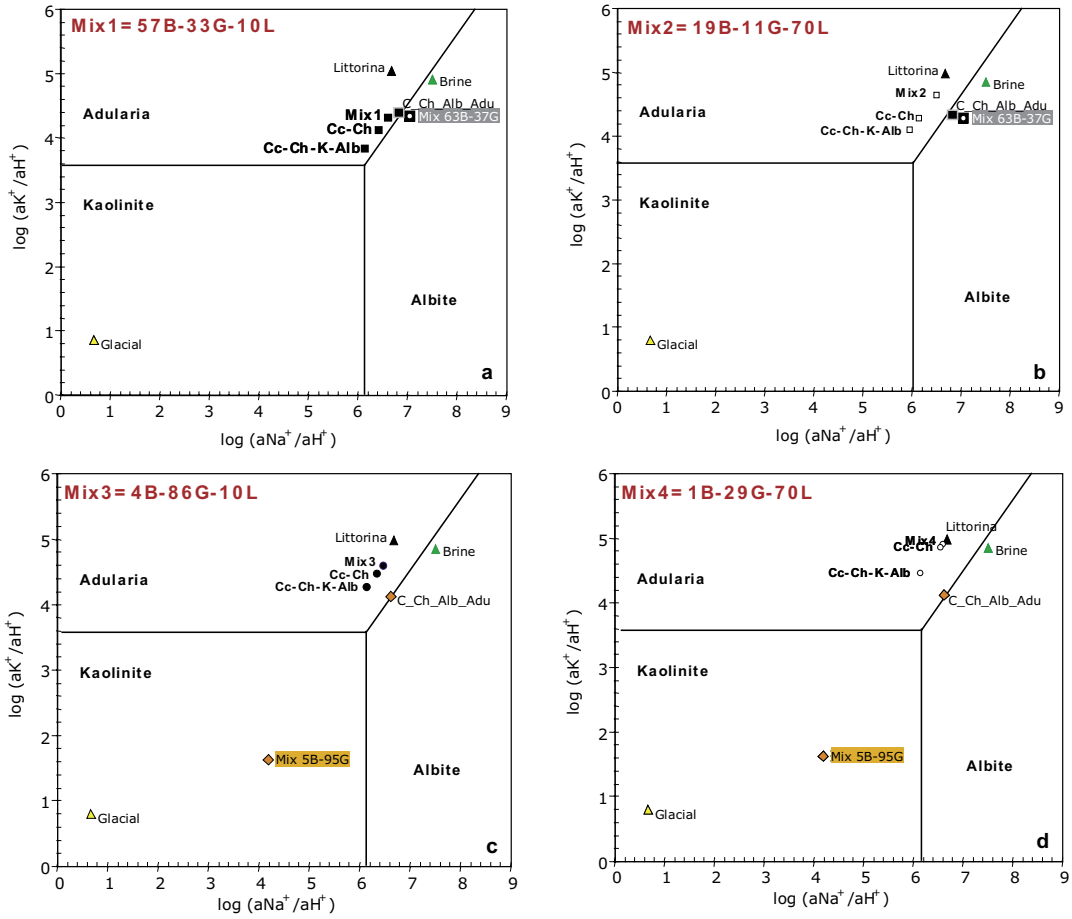

Figure 3-5. *Graphical representation of simulations in the kaolinite-adularia-albite stability diagram. Location of the calculated waters as a result of the different mixing proportions and different reequilibrium reactions (Cc: calcite; Ch: chalcedony; Alb: albite; K: kaolinite) (a) Mix 1, (b)Mix 2; (c) Mix 3; and (d) Mix 4.*

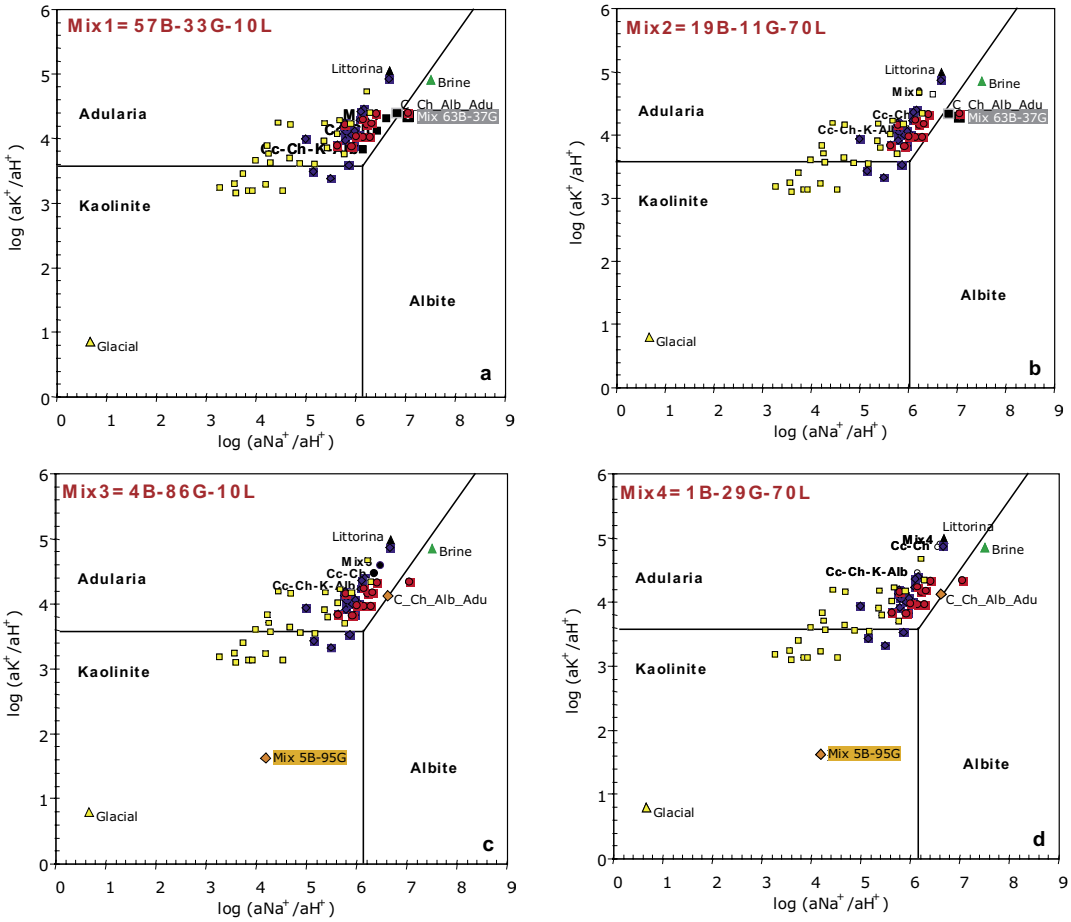

Figure 3-6. *Superposition of Forsmark groundwater samples on the stability diagram of Figure 3-5.*

As for the brackish-saline groundwaters with a Littorina signature, mixing with Littorina explains the position of the samples near the adularia-albite boundary, but inside the adularia field, for most of the equilibrium situations considered. If time since mixing with Littorina has been enough to reequilibrate the waters with the aluminosilicates, the samples will tend to concentrate on the albite-adularia boundary. In this case, even taking the maximum values considering an equilibrium albite-adularia (without kinetic limitations), the calculated mass transfers for both minerals are very low (< 1 mmol/L).

Table 3-2. Calculated mass transfers (mol/L) in the four mixing proportions analysed above. Only two examples are shown here: the equilibrium with calcite (Cc) and chalcedony (Ch), and the equilibrium with calcite, chalcedony, kaolinite (Kaol) and albite (Alb).

Mass Transfers	**90% (63Brine – 37Glacial) 10%Litt.**		**30% (63Brine – 37Glacial) 70%Litt.**		**90% (5Brine – 95Glacial) 10%Litt.**		**30% (5Brine – 95Glacial) 70%Litt**	
	57B+33G+10L		19B+11G+70L		4B+86G+10L		1B+29G+70L	
	Cc-Ch	Cc-Ch-Kaol-Alb	Cc-Ch	Cc-Ch-Kaol-Alb	Cc-Ch	Cc-Ch-Kaol-Alb	Cc-Ch	Cc-Ch-Kaol-Alb
Calcite (C)	$6.6\cdot10^{-6}$	$2.2\cdot10^{-4}$	$1.1\cdot10^{-4}$	$4.7\cdot10^{-4}$	$4.3\cdot10^{-6}$	$1.1\cdot10^{-4}$	$5.6\cdot10^{-6}$	$1.4\cdot10^{-3}$
Chalcedony (Ch)	$8.1\cdot10^{-6}$	$5.1\cdot10^{-4}$	$6.0\cdot10^{-5}$	$8.2\cdot10^{-4}$	$5.3\cdot10^{-6}$	$2.5\cdot10^{-4}$	$6.0\cdot10^{-5}$	$3.3\cdot10^{-3}$
Kaolinite (K)		$1.3\cdot10^{-4}$		$2.2\cdot10^{-4}$		$6.1\cdot10^{-5}$		$8.1\cdot10^{-4}$
Albite (Alb)		$2.5\cdot10^{-4}$		$4.4\cdot10^{-4}$		$1.2\cdot10^{-4}$		$1.6\cdot10^{-3}$

As a summary, these results indicate that re-equilibrium reaction processes are important in the control of some parameters such as pH (as well as Eh, and some minor-trace elements), moving the waters towards the adularia-albite boundary. However, the main compositional changes, and even the extent of re-equilibration processes[7], are controlled by the extent of the mixing process.

3.2.3 Uncertainties associated with the theoretical simulations

There are several kinds of uncertainties associated with the previous analysis. The first, already introduced above, involve the equilibrium constants selected to construct the stability diagrams and used in the modelling calculations. Only phases with low thermodynamic uncertainties (e.g. adularia and albite) have been included in the calculations. Laumontite and chlorite require a more detailed evaluation as they have either much higher thermodynamic uncertainties (laumontite) or a broad compositional variability in the system (chlorite). Mineral phases such as zeolites, smectite, illite or epidote are common as fracture fillings in this system and could contribute to the control of the chemical contents. However, they have not been considered in the calculations due to their high thermodynamic uncertainties (equilibrium solubility constants not well defined[8]).

The second type of uncertainty is associated with the ambiguity between the possible control by aluminosilicate dissolution-precipitation or by ionic exchange in clay minerals. This last process involving illite, smectites or zeolites could be an alternative way to express constraints on cations like K^+, Na^+ or Ca^{2+} in low temperature systems. The ionic exchange control on the groundwater composition can be especially effective in the most recent mixing event, with short interaction (reequilibrium) time with minerals. This is the reason for having considered ion exchange in the mass balance calculations described in Section 3.1.

Therefore, this uncertainty means that aluminosilicate dissolution-precipitation and ionic exchange in clay minerals can possibly result in the same water chemistry /SKB, 2004/.

3.3 Redox system modelling

In this section the results from the modelling of the redox state in the Forsmark area are presented. For Forsmark 1.2, the amount of suitable data for a redox study is slightly greater than for Forsmark 1.1 and, therefore, this study is somehow more complete. The two possibilities suggested in previous studies about the redox state of the groundwaters have been revisited, namely: (a) the iron system controls the redox state /Grenthe et al. 1992/; and (b) the sulphur system controls the redox state /e.g. Nordstrom and Puigdomenech, 1986/.

For this modelling exercise, only samples with enough redox data were selected. This includes Eh and pH[9] data from continuous logging, concentrations of Fe^{2+}, S^{2-} and CH_4, and microbiological information. The selection criteria have drastically reduced the number of suitable samples for the redox characterization of the system. In spite of this, the selected samples cover a wide range of depths (115 to 990 m; Figure 3-7) in three boreholes KFM01, KFM02 and KFM03. Moreover, most of them have continuous Eh logging, redox pair concentrations and even microbiological information (in some cases) and thus, a combination of these three data sets can be made.

The selected samples represent three different situations in the Forsmark groundwater system:

4. Most selected samples belong to the group of brackish-saline groundwaters (Cl = 4,500–5,500 mg/L) with an important Littorina signature. They are distributed at variable depths, from 110 to 184 m (samples 4538 and 4724) and from 450 to 643 m (samples 8016, 8017 and 8273).
5. Two samples from the deepest groundwaters (samples 8281 and 8152; 940 to 990 m) representative of the group with an important brine component.

[7] Calculated mass transfers for the same equilibrium situation change in more than one order of magnitude depending on the considered mixing proportions (Table 3-2).

[8] It is planned to carry on with this type of analysis, including additional aluminosilicate phases, when available data allow a more specific characterization.

[9] In order to minimize the pH uncertainty effects on the redox calculations /Laaksoharju et al. 2004a,b,c/.

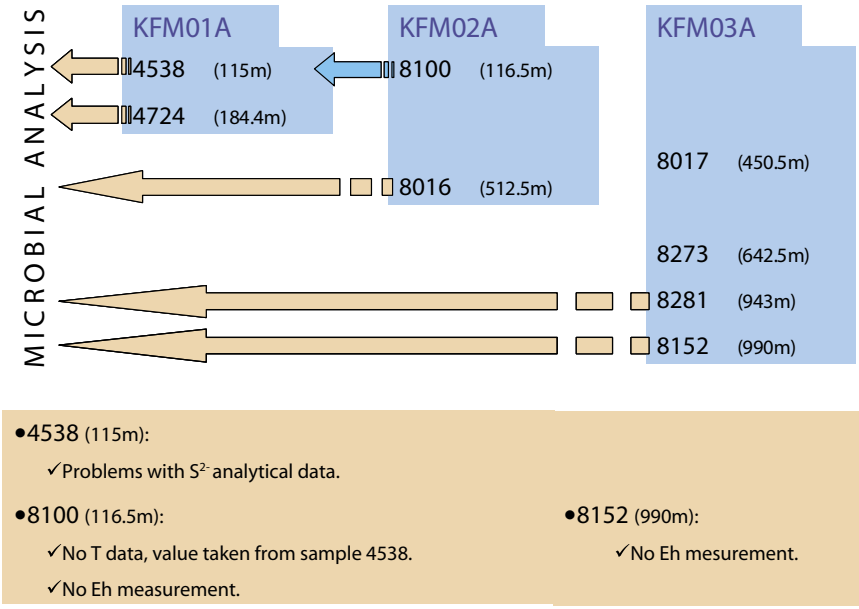

Figure 3-7. *Selected samples for the redox modelling indicating their depths and the kind of available information. The analytical problems in samples 4538 are detailed explained in Appendix D.*

6. Finally, sample 8100, representative of the fresh non-saline groundwaters (Cl = 642 mg/L, at 116 m depth), posibly with some marine contribution and without tritium.

The concentrations of the main redox elements in the selected samples are collected in Table 3-3 and plotted in Figure 3-8. Sulphide and iron concentrations do not show a clear trend with chloride and depth (Figure 3-8a,b). This is especially true for iron, mainly due to the wide range of concentrations in Littorina-rich groundwaters at around 5,500 mg/L of chloride. Although not shown, this also happens with the rest of the redox-sensitive elements, a feature in common with the non-redox elements, as described in Section 2.2.

Although the number of samples with both Fe^{2+} and S^{2-} is very limited, it seems that waters with higher Fe^{2+} concentrations tend to have low levels of S^{2-} and vice versa (Figure 3-8c). The deepest saline waters show the lowest Fe^{2+} concentrations and the maximium S^{2-} levels (although concentrations are low in absolute value). This inverse behaviour can be explained by changes in the dominant species or the component that buffers the redox system in different groundwater layers /Pitkänen et al. 1999/.

Speciation-solubility calculations show that the waters are oversaturated in pyrite and close to equilibrium with different iron monosulphides. Therefore, precipitation of iron sulphides can be an active process in the system, partially controlling the concentration of both elements in solution.

3.3.1 The redox pair calculations

Methodology

The calculations include the following redox pairs: dissolved SO_4^{2-}/S^{2-} and CH_4/CO_2, and the heterogeneous $Fe(OH)_3$ /Fe^{2+}, pyrrhotite (or FeS)/SO_4^{2-} pyrite/ SO_4^{2-} couples. As in previous reports /Laaksoharju et al. 2004a,b,c/ dissolved Fe^{3+}/Fe^{2+} and Fe^{3+}-clay/Fe^{2+}-clay /Banwart, 1999/ were also tested but the results are not presented here[10].

Iron oxides (including hematite) and oxihydroxides are common fracture filling minerals in the Forsmark area. Therefore, several calibrations were employed to model the redox potential with the $Fe(OH)_3/Fe^{2+}$ heterogeneous pair.

[10] Differences between total iron and Fe^{2+} concentrations are too small to obtain reliable figures with the Fe^{3+}/Fe^{2+} homogeneous redox couple, and calculated Eh values are always oxidizing. The Fe^{3+}-clay/Fe^{2+}-clay pair provides, in general, much more oxidizing values than any other redox couple or Eh measurements.

Table 3-3. Eh values for the selected samples in the Forsmark area. The potentiometrically measured values are shown for comparison with the values calculated with the different redox pairs. Additional information for each sample is also included.

Borehole	Sample	Depth (m)	T (ºC)	Fe^{2+} (mg(l)	S^{2-} (mg/l)	CH_4 (ml/l)	pH	Eh (mV)					
								Chemmac	SO_4^{2-}/S^{2-}	CH_4/CO_2	$Fe(OH)_3/Fe^{2+}$ Grenthe(1)	$Fe(OH)_3/Fe^{2+}$ microcrystalline	Pyrite/SO_4^{2-} (2) Pyrrotite/SO_4^{2-}
KFM01A	4538	115.5	6.9	0.953	0.01		7.65	–195	–190		–315	–130	–210
KFM01A	4724	184.4	7.57	0.475	–0.03	0.12	7.50	–188		–223	–273	–83	–205
KFM02A	8100	116.5	7.57	1.35	0.01		7.55		–195		–306	–94	–207
KFM02A	8016	512.5	11.35	1.84	0.01	0.04	7.00	–143	–164	–194	–221	–30	–175
KFM03A	8017	450.5	10.7	0.919	–0.03		7.50	–176			–289	–100	–205
KFM03A	8273	642.5	13.05	0.233		0.07	7.40	–196		–231	–233	–48	–197
KFM03A	8281	943	17.2	0.208	0.06	0.06	7.50	–245	–221	–247	–253	–62	–205
KFM03A	8152	990	18	0.026	0.03	0.05	8.00		–254	–283	–286	–98	–235

(1) “Original” Grenthe’s fit is included; correction for Fe^{2+} activity only provides differences of 30 mV.

(2) Average of Pyrite/SO_4^{2-} and FeS/SO_4^{2-} pairs calculated with WATEQ4F thermodynamic data.

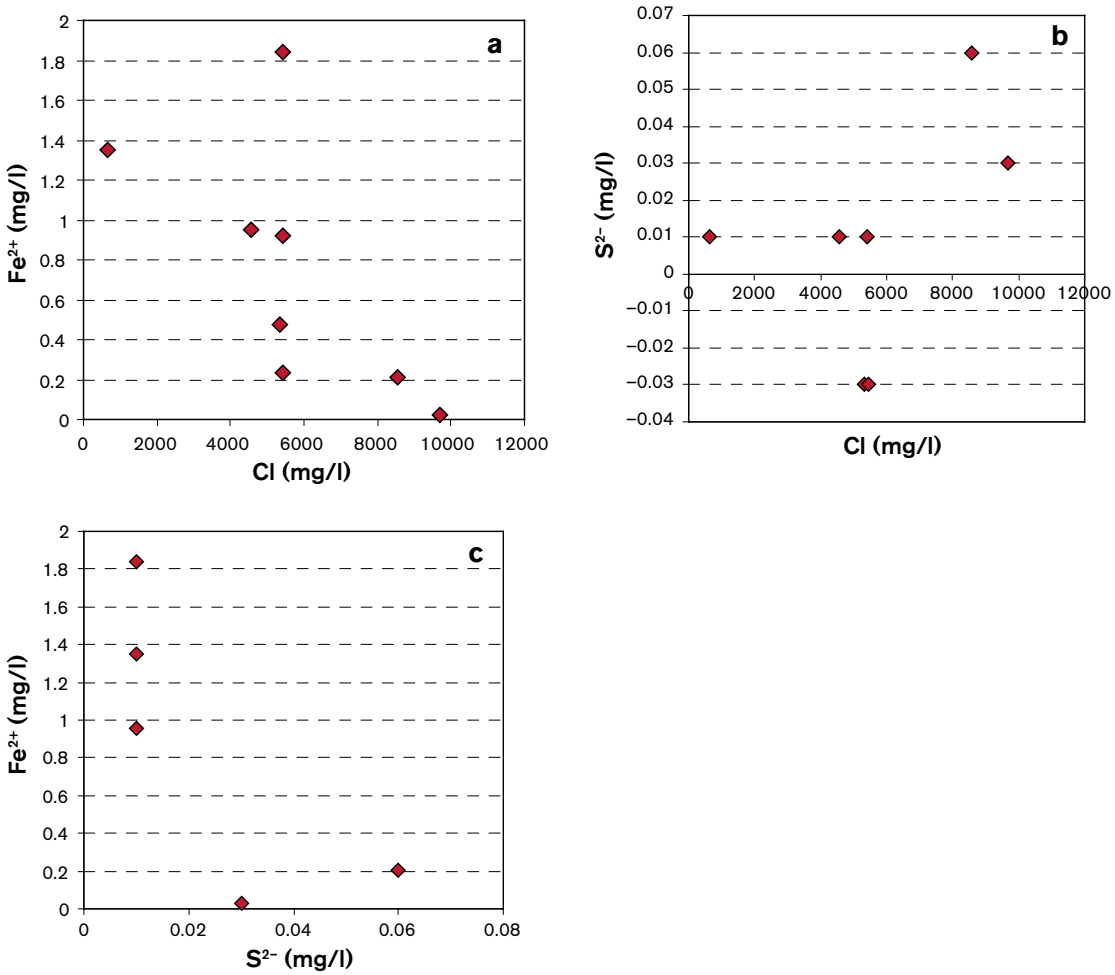

Figure 3-8. *Fe^{2+} and S^{2-} contents in the Forsmark groundwaters analysed for the redox state.*

1. *The calibration proposed by /Grenthe et al. 1992/.* According to these authors, Eh values in Swedish groundwaters can be estimated with the $Fe(OH)_{3(s)}$/ Fe^{2+} heterogeneous redox couple,

$$Fe(OH)_{3(s)} + 3H^+ + e^- \rightarrow Fe^{2+} + 3H_2O \quad (1)$$

by means of the equation

$$Eh = E^{0*} - 2.303\frac{RT}{F}\left(3pH + \log\left[Fe^{2+}\right]\right) \quad (2)$$

where E^{0*} = 707 ± 59 mV at 10 ºC (the average Swedish groundwater temperature), F is the Faraday constant (23.061 cal V^{-1} equivalent^{-1}), R is the gas constant (1.98717 cal deg^{-1} mol^{-1}) and T is the temperature (K). The E^{0*} value determined by /Grenthe et al. 1992/ is based on a fit of equation (1) to Eh, pH and Fe^{2+} data from SKB groundwaters from different sites. $Fe(OH)_3$ solubility product obtained from this fit is intermediate between freshly precipitated amorphous hydroxide and crystalline goethite. In fact, the solubility product is the one proposed by /Langmuir, 1997/ for lepidocrocite. Equation (2) is usually employed to estimate Eh values from pH and Fe^{2+} concentration data /e.g. Smellie and Laaksoharju, 1992/. For the fit, /Grenthe et al. 1992/ used Fe^{2+} concentration data corrected only for the $FeCO_3^0$ ion pair. But Fe^{2+} speciation is usually more complex than the simple correction made by these authors. Following /Glynn and Voss, 1999/, in this study two sets of Eh values were calculated with equation (1), one considering Fe^{2+} analytical data and the other considering the Fe^{2+} species' activities obtained from the speciation-solubility calculations with WATEQ4F database.

2. *The calibration suggested by /Bruno et al. 1999/* using the thermodynamic data for amorphous and microcrystalline $Fe(OH)_3$ in reaction (1).

The redox potential for the SO_4^{2-}/S^{2-} and CH_4/CO_2 homogeneous redox pairs was calculated by PHREEQC with WATEQ4F database. A sensitivity analysis was performed with the thermodynamic values included in LLNL database and in NAGRA database (release 26-Aug-2002; /Hummel et al. 2002/). The results indicate differences not greater than 30 mV for the calculated Eh.

The presence of pyrite as fracture filling mineral is also common in the Forsmark area. Pyrrothite or amorphous FeS have not been identified in the system, but these minerals are usually the precursors of pyrite formation. Pyrrothite can precipitate at hematite surface in the presence of sulphate-reducing bacteria /Neal et al. 2001/. Therefore, pyrite/SO_4^{2-} (using thermodynamic data from WATEQ4F and /Bruno et al. 1999/), pyrrothite/SO_4^{2-} (data from /Bruno et al. 1999/) and FeS_{ppt} (data from WATEQ4F) buffers were used to perform the redox calculations.

Results

The results are summarised in Table 3-3 and Figures 3-9 and 3-10. The Eh calculated with the $Fe(OH)_3/Fe^{2+}$ redox pair and Grenthe's calibration agrees reasonably well with the Eh values measured in the deepest samples[11]. The Eh calculated with the same redox pair for microcrystalline $Fe(OH)_3$ is much more oxidant (see Table 3-3). On the contrary, the microcrystalline phase gives better results in the shallower samples (4538), whereas Grenthe's calibration gives a much more reducing Eh value (Table 3-3 and Figure 3-10). This observation was already made in the previous phase (Forsmark 1.1, /Laaksoharju et al. 2004a/). In some samples (4724, 8100, 8016) none of the iron calibrations provide good results. This fact suggests that the groundwater redox state can be controlled by iron oxides and oxihydroxides with different degrees of crystallinity.

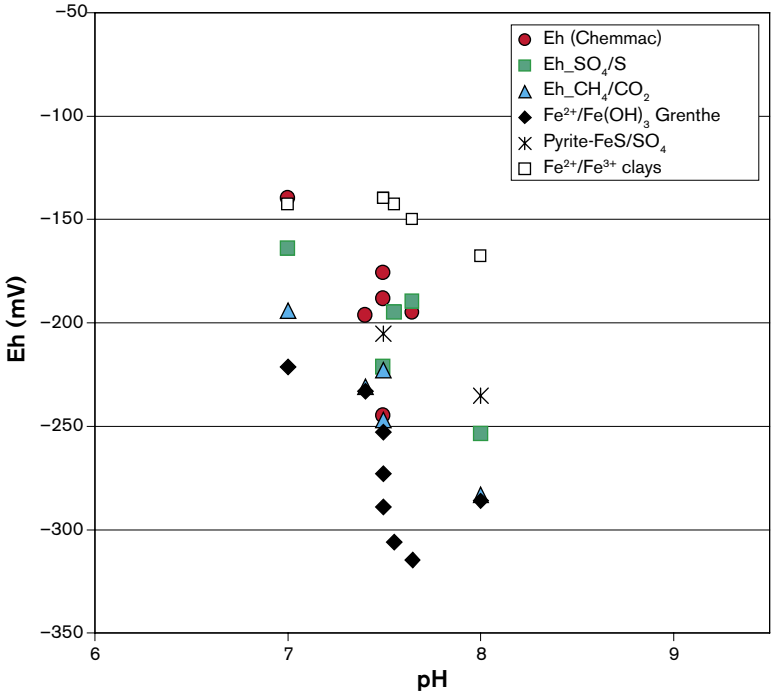

Figure 3-9. *Comparison of redox results for different redox pairs in the Forsmark selected groundwaters.*

[11] In the case of sample 8152, the result must be taken with caution. Fe^{2+} concentration in this sample (0.026 mg/L or $4.6 \cdot 10^{-7}$ mol/L) is below the lower limit (10^{-6} molar) for a successful Eh measurements when iron pairs control the redox potential /Grenthe et al. 1992/.

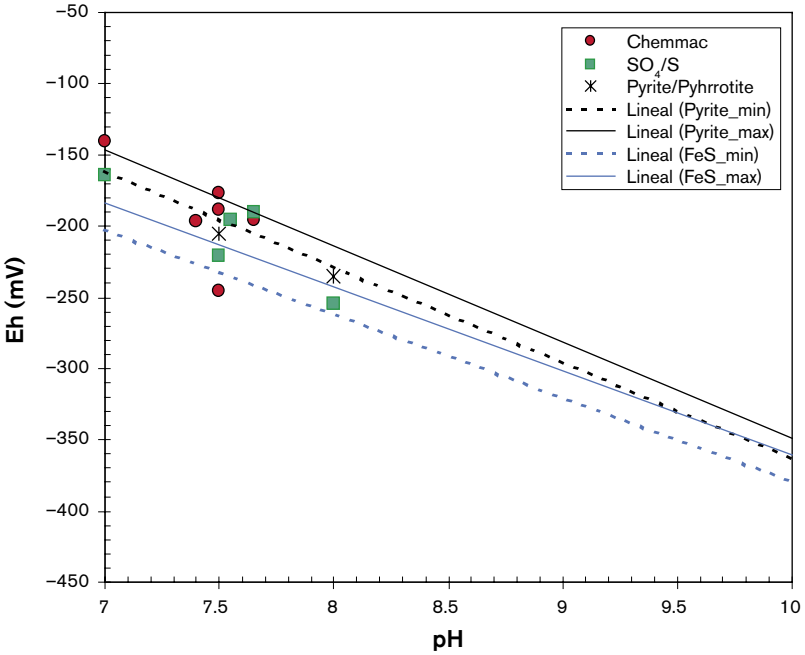

Figure 3-10. *Eh-pH diagram showing the calculated Eh values for the Forsmark samples. Potentionetrically measured values are shown as red circles. The Eh values from the SO_4^{2-}/S^{2-} redox pair are represented with green squares and the values obtained with the pyrite-pyhrrotite/SO_4^{2-} pair, with an asterisk. "Pyrite_min" and "Pyrite max" lines represent the equilibrium situation for the range of SO_4^{2-} and Fe^{2+} concentration found in Forsmark groundwaters. The same is valid for the FeS/SO_4^{2-} equilibrium.*

Except for a few samples, the different "sulphur system" redox pairs provide Eh values coincident with the potentiometrically measured Eh. The SO_4^{2-}/S^{2-} homogeneous redox pair gives Eh values similar to the ones obtained from the heterogeneous pairs (Pyrite/SO_4^{2-} and FeS/SO_4^{2-}; Figures 3-9 and 3-10) as calculated with WATEQ4F thermodynamic data. A sensitivity analysis carried out comparing these data to /Bruno et al. 1999/'s shows only minor differences.

As expected, Eh values obtained with the CH_4/CO_2 pair are very similar to those obtained with the SO_4^{2-}/S^{2-} pair (and to the remaining sulfur redox pairs). Therefore, they also agree well with the potentiometrically measured Eh.

Redox pairs results for samples without Eh measurements (8100 and 8152) are not so easy to interpret, but it seems that, in both cases, the sulfur redox pairs give coherent results. Moreover, Eh values from these pairs obtained for sample 8152 agree well with the ones from CH_4/CO_2.

There is an overall good agreement between the potentiometrically measured Eh and the values calculated with the heterogeneous sulphur pairs, the homogenous sulfur pair and the CH_4/CO_2 pair, even taken into account the low concentrations of S^{2-} and CH_4. Grenthe's calibration for $Fe(OH)_3/Fe^{2+}$ provides Eh values in good agreement with the measured Eh for the deepest waters but in the shallowest samples the iron system seems to be controlled by a microcrystalline hydroxide and not by an intermediate phase, as Grenthe's calibration assumes.

This suggests that the sulphur system is the main controller of the groundwater redox state, as reported previously /Nordstrom and Puigdomenech, 1986; Glynn and Voss, 1999; Laaksoharju et al. 2004a,b/, or at least that it is the most suitable (together with the CH_4/CO_2 redox pair) to characterize the redox state of these groundwaters. The variable results obtained with the $Fe(OH)_3/Fe^{2+}$ pair do not mean that the iron system does not participate in the redox control of these waters, but the variable crystallinity of the phases involved hinders a clear and general assessment.

Limitations of SO_4^{2-}/S^{2-} and CO_2/CH_4 pairs

The redox potential for the SO_4^{2-} redox pair can be calculated for waters with pH > 7 from the equation:

$$= \log K - \frac{9}{8} pH + \frac{1}{8} \log \frac{\left[SO_4^{2-}\right]}{\left[HS^-\right]}$$

As the reaction involve the transfer of 8 electrons, the change in the calculated redox potential amounts only to 1/8 pe unit (or 7 mV) for a tenfold change in the sulphate/sulphide ratio. Therefore, this pair is not very sensitive to changes in the concentration of S^{2-} for fixed SO_4^{2-} concentrations.

The same argument is valid for the CO_2/CH_4 pair, whose redox potential can be obtained from:

$$p\varepsilon = \log K - pH + \frac{1}{8} \log \frac{\left[CO_2\right]}{\left[CH_4\right]}$$

Besides, the log K values for both reactions are close enough to produce very similar Eh results. Therefore, the calculated Eh from these redox pairs is only meaningful when S^{2-} and CH_4 concentrations are reliable. This important condition seems to have not been fulfilled in the case of S^{2-} for sample 4538, as it has a different S^{2-} value in Data Freeze 1.1 and Data Freeze 1.2 (and the detection limit is not stated). A value of 0.01 mg/L has been selected for calculations with sample 4538.

The rest of S^{2-} and CH_4 concentrations are low, although apparently meaningful. Nevertheless, it is recommended to improve the detection limits, especially for S^{2-}, and to explicitly indicate them in future phases of this project.

In any case, it is always convenient to check the validity of the redox pair results comparing them with the information from the microbial studies and the potentiometric measured Eh values. In spite of the technical difficulties in obtaining reliable Eh values in the boreholes, SKB methodology is a valuable (and indispensable) element in the study of redox conditions.

3.3.2 Discusion

Microbial analysis (Hallbeck, this volume) of Forsmark groundwaters has identified Sulphate Reducing Bacteria (SRB) at depths from 642.5 m (sample 8273) to 990 m (sample 8152), and their number is specially high at 943 m, in sample 8281. At these depths the lowest values of SO_4^{2-} and the highest values of S^{2-} from all the analysed waters are found, which is consistent with the metabolic activity of SRB. However, there is no correlation between the number of SRB and dissolved sulphide; moreover, sulphide concentrations (0.03–0.06 mg/L) are too low for the high SRB number found and the expected intensity of the sulphate reduction process.

This fact, together with the low ferrous iron concentration, could indicate the presence of active iron-sulphide precipitation in fractures. This process can keep dissolved sulphide at the low levels detected, even though sulphate reduction might produce substantial amount of sulphide. And it can be active if a source of Fe^{2+} (iron oxyhydroxides) exists. This source can explain the low iron concentrations in samples at 642.5 and 943 m depth, but it has apparently been exhausted in the deepest groundwaters (at 990 m; Table 3-3).

In summary, most lines of evidence support that the sulphur system, microbiologically mediated, is the main redox controller in the deepest and more saline groundwaters.

On the other hand, Littorina-rich brackish-saline groundwaters show variable and very high iron contents, in agreement with what has been observed in similar groundwaters elsewhere (e.g. Olikiluoto; /Pitkänen et al. 1999/).

The microbial analysis only found trace amounts of SRB in samples 4538 and 8016 (115.5 and 512.5 m depth, respectively), but very high numbers of iron-reducing bacteria (IRB), mainly in sample 4538. However, there is no correlation between Fe^{2+} concentration and the number of IRB

in these groundwaters. Moreover, they show very low but detectable contents of dissolved S^{2-} and the $\delta^{34}S$ values are very homogeneous (around 25‰) and clearly higher than in present Baltic Sea, indicating that sulphate reduction has operated. These observations could support the existence of an iron-sulphide precipitation process in these groundwaters but not intense enough to effectively limit Fe^{2+} solubility. The question then arises as when did it happen?

The high Fe^{2+} concentration in these groundwaters and the main episode of sulphate reduction could have happened during Littorina seawater infiltration through sea bottom sediments during the Littorina stage. Sedimentological studies support the existence of sulphate reduction processes at that moment in the organic-rich sediments /e.g. Albi and Winterhalter, 2001/. Later on, the mixing of this Littorina seawater with pre-Littorina groundwaters was not able to provide enough organic carbon to keep the sulphate reduction process with the necessary intensity to completely reduce the high Fe^{2+} concentration in these waters /Pitkänen et al. 1999/. At present, sulphate reduction could be limited by the lack of nutrients or by competition with other organisms.

Finally, methanogens were found at 512.5 and 642.5 m depth but not in the deepest samples[12]. Besides, there are no isotopic data for the measured methane (Hallbeck, this volume) and, therefore an organic control on the CH_4/CO_2 redox pairs for Forsmark groundwaters cannot be established.

[12] Unfortunately no data for the shallowest depths are available.

4 Hydrogeochemical conceptual model

Groundwaters in the Forsmark area can be divided into three groups based on their salinity:

1. *Saline groundwaters* with a brine signature (only 1 representative sample: #8152). Mixing between Brine and Glacial end members is responsible, directly or indirectly, for most of their chemical content, especially for Cl concentrations higher than 7,000 mg/L. A Littorina component is absent or in a very low percentage. Their alkalinity is low, and controlled by equilibrium with calcite. pH is controlled by calcite equilibrium and, possibly, by reactions with aluminosilicate minerals. These old mixed waters tend, with time, to re-equilibrate with the complex mineral assemblage identified as fracture fillings in Forsmark. Both mass balance and thermodynamic calculations predict low reaction mass transfers between these waters and the aluminosilicates, although more work is needed due to the wide variety of aluminosilicates detected. Fast cation exchange reactions are also possible but, in groundwaters with long residence times, these exchange processes may cause irreversible changes in the clay minerals /Pitkänen et al. 1999/, favouring an apparent solubility control.

The redox state is mainly controlled by the sulphur system. The existence of active sulfate-reduction processes and sulphide precipitation is in agreement with the presence of high numbers of sulphate-reduction bacteria (SRB) detected in the microbiological analysis.

Finally, the high contribution of the Glacial end member points out that the forced introduction of glacial melt water in Forsmark reached at least a depth of 1,000 m. This penetration depth is higher than Olkiluoto's, but similar to the penetration depth reported in other Swedish sites /Puigdomenech, 2001/.

2. *Brackish-saline groundwaters* with an important and relatively constant Littorina component. They are widely distributed in the Forsmark area, from very shallow levels (discharge areas?) to 500 m depth. A combination of slow and fast chemical reactions have operated on the mixed waters. Calcite reequilibrium and Ca-Na exchange reactions are the kinetically most favoured processes. Reequilibrium with different aluminosilicates is also possible, although the mass transfers involved are low even when "forcing" pure equilibrium situations.

As in other Littorina-rich groundwaters /Pitkänen et al. 2004/, iron concentration is variable but usually high, while dissolved sulphide, although detectable, is in very low concentrations. This suggests that sulphate reduction is of minor importance (in agreement with microbial studies) and that iron does not have a strict solubility limit through sulphide precipitation. In this situation, the good results provided by the sulphur redox pairs in characterizing the redox state of these groundwaters deserve further attention.

The penetration depth of Littorina waters (500 m) is higher than presumed in previous work (Forsmark 1.1; /Laaksoharju et al. 2004a/, and slightly higher than the one deduced for Olkiluoto /Pitkänen et al. 1999, 2004/. However, this penetration depth appears to be similar to the calculated for the Äspö area /Puigdomenech, 2001/.

3. Non saline *groundwaters* in Forsmark cover a wide range of chloride concentrations and show different trends (Ca-Na-HCO_3, Na-HCO_3-Cl, Na-Cl-HCO_3, etc). The compositional characters of the most diluted groundwaters are controlled by weathering reactions (dissolution of calcite, plagioclase, biotite, sulphides, etc) induced by atmospheric and biologically produced dissolved gasses (CO_2 and O_2). More concentrated waters show an additional and variable mixing contribution with a marine component (some of them with a clear modern Baltic signature) that gradually promotes Na-Ca exchange and the precipitation of calcite.

5 References

Albi K, Winterhalter B, 2001. Authigenic mineralisation in the temporally anoxic Gotland Deep, the Baltic Sea. Baltica, 14, 74–83.

Banwart S A, 1999. Reduction of iron (III) minerals by natural organic matter in groundwater. Geochim. Cosmochim. Acta, **63**(19/20), 2919–2928.

Bruno J, Cera E, Grivé M, Rollin C, Ahonen L, Kaija J, Blomqvist R, El Aamrani F Z, Casas I, de Pablo J, 1999. Redox Processes in the Palmottu Uranium Deposit. Redox measurements and redox controls in the Palmottu System. (Technical Report), Quantisci, Barcelona, Spain, 76 p.

Deutsch W J, Jenne E A, Krupka K M, 1982. Solubility equilibria in basalt aquifers: The Columbia Plateau, Eastern Washington, USA. Chem. Geol. 36, 15–34.

Fontes J-Ch, Louvat D, Michelot J-L, 1989. Some constraints on geochemistry and environmental isotopes for the study of low fracture flows in crystalline rocks – The Stripa case. In: International Atomic Energy Agency (Eds.) Isotopes techniques in the study of the Hydrology of Fractured and Fissured Rocks. IAEA, Vienna, Austria.

Garrels R M, 1984. Montmorillonite/illite stability diagrams. Clays Clay Miner., **32**(3), 161–166.

Glynn P D, Voss C I, 1999. SITE-94. Geochemical characterization of Simpevarp ground waters near the Äspö Hard Rock laboratory. (Technical Report SKI R 96-29), SKI, Stockholm, Sweden 210 p.

Grenthe I, Stumm W, Laaksoharju M, Nilsson A C, Wikberg P, 1992. Redox potentials and redox reactions in deep groundwater systems. Chem. Geol., 98, 131–150.

Grimaud D, Beaucaire C, Michard G, 1990. Modelling of the evolution of ground waters in a granite system at low temperature: the Stripa ground waters, Sweden. Appl. Geochem., 5, 515–525.

Gurban I, Laaksoharju M, Ledoux E, Made B, Salignac A L, 1998. Indications of uranium transport around the reactor zone at Bagombé (Oklo). SKB TR-98-06, Svensk Kärnbränslehantering AB.

Helgeson H C, 1969. Thermodynamics of hydrothermal systems at elevated temperatures and pressures. Am. J. Sci., 267, 729–804.

Helgeson H C, Delaney J M, Nesbitt H W, Bird D K, 1978. Summary and critique of the thermodynamic properties of rock forming minerals. Am. J. Sci., 278, 229.

Hummel W, Berner U, Curti E, Pearson F J, Thoenen T, 2002. Nagra/PSI Chemical Thermodynamic Data Base 01/01. (Technical Report NTB 02-16), Nagra, Wettingen, Switzerland.

Laaksoharju M, Wallin B (ed), 1997. Evolution of the groundwater chemistry at the Äspö Hard Rock Laboratory. Proceedings of the second Äspö International Geochemistry Workshop, Äspö, Sweden, June 6–7, 1995. Svensk Kärnbränslehantering AB.

Laaksoharju M, Tullborg E L, Wikberg P, Wallin B, Smellie J, 1999. Hydrogeochemical conditions and evolution at the Äspö HRL, Sweden. Appl. Geochem., 14, 835–860.

Laaksoharju M, Gimeno M, Auqué L, Gómez J, Smellie J, Tullborg E-L, Gurban I, 2004a. Hydrogeochemical evaluation of the Forsmark site, model version 1.1. SKB R 04-05, 342 p, Svensk Kärnbränslehantering AB.

Laaksoharju M, Smellie J, Gimeno M, Auqué L, Gómez J, Tullborg E-L, Gurban I, 2004b. Hydrogeochemical evaluation of the Simpevarp area, model version 1.1. SKB R 04-16, Svensk Kärnbränslehantering AB.

Langmuir D, 1997. Aqueous Environmental Geochemistry. Prentice Hall, Upper Saddle River, NJ, USA, 600 p.

Neal A L, Techkarnjanaruk S, Dohnalkova A, McCready D, Peyton B M, Geesey G G, 2001. Iron sulfides and sulfur species produced at hematite surfaces in the presence of sulfate-reducing bacteria. Geochim. Cosmochim. Acta, 65(2), 223–235.

Nordstrom D K, Puigdomenech I, 1986. Redox chemistry of deep ground-waters in Sweden. SKB TR 86-03, Svensk Kärnbränslehantering AB.

Parkhurst D L, Appelo C A J, 1999. User´s guide to PHREEQC (Version 2) , a computer program for speciation, batch reaction, one dimensional transport, and inverse geochemical calculations. (Science Report WRRIR 99-4259), USGS, 312 p.

Pitkänen P, Luukkonen A, Ruotsalainen P, Leino-Forsman H, Vuorinen U, 1999. Geochemical modelling of groundwater evolution and residence time at the Olkilouto Site. (Technical Report POSIVA 98-10), POSIVA, Helsinki, Finland, 184 p.

Pitkänen P, Partamies S, Luukkonen A, 2004. Hydrogeochemical interpretation of baseline groundwater conditions at the Olkiluoto Site. (Technical Report POSIVA 2003-07), POSIVA, Helsinki, Finland, 159 p.

Puigdomenech I (ed), 2001. Hydrochemical stability of groundwaters surrounding a spent nuclear fuel repository in a 100,000 year perspective. SKB TR 01-28, 83 p, Svensk Kärnbränslehantering AB.

SKB, 2004. Hydrogeochemical evaluation for Simpevarp model version 1.2. SKB R-04-74, Svensk Kärnbränslehantering AB.

Smellie J A T, Laaksoharju M, 1992. The Äspö Hard Rock Laboratory: Final evaluation of the hydrogeochemical pre-investigations in relation to existing geologic and hydraulic conditions. SKB TR 92-31, 239 p, Svensk Kärnbränslehantering AB.

Trotignon L, Beaucaire C, Louvat D, Aranyossy J F, 1997. Equilibrium geochemical modelling of Äspö groundwaters: a sensitivity study to model parameters. In: Laaksoharju M and Wallin B (eds) Evolution of the groundwater chemistry at the Äspö Hard Rock Laboratory. (Report SKB 97-04) Svensk Kärnbränslehantering AB.

Trotignon L, Beaucaire C, Louvat D, Aranyossy J F, 1999. Equilibrium geochemical modelling of Äspö groundwaters: a sensitivity study of thermodynamic equilibrium constants. Appl Geochem, 14, 907–916.

Appendix A

Samples supplied in the 1.2 datafreeze

Table A-1. Number of samples supplied in the data freeze 1.2 for the Forsmark area (including samples from data freeze 1.1).

Type of Water	Type of sampling	ID code	Dates	Depths	Number of Samples				
					Total (Data Freeze 1.2)	With Major Elements (ME)	With ME & Stable isotopes	With ME, SI & Tritium	Representative
Ground Water	Packered	HFM01	2002	0–200	22 (1M)	4	2	2	1
		HFM02	2002	0–100	2	2	0	0	1
		HFM03	2002	0–26	2	1	1	1	1
		HFM04	2002	30–222	3	3	3	3	1
		HFM05	2002,03	0–200	8 (1M)	7	7	7	1
		HFM06	2003	0–111	4	4	4	4	1
		HFM08	2003	0–144	3	3	3	3	2
		HFM09	2003,04	0–50	4	4	2	2	1
		HFM10	2003,04	0–150	7 (1M)	5	4	4	1
		HFM11	2003	0–182	3	3	3	3	1
		HFM12	2003	0–210	3	3	3	3	1
		HFM13	2003,04	0–176	5	3	3	3	1
		HFM14	2003	0–151	3	3	3	3	1
		HFM15	2003	0–200	3	3	3	3	1
		HFM16	2003	0–133	3	3	1	1	1
		HFM17	2004	0–203	3	3	1	1	1
		HFM18	2004	0–173	3	3	1	1	1
	Packered	HFM19	2004	0–173	3	3	1	1	1
		KFM01A	2002	0–101	1	0	0	0	0
			2003	110–121	8 (1M,1C)	7	6	6	1
	Packered	KFM02	2003	177–184	10 (1G,1C)	9	9	9	1
			2003	1–100	1	1	0	0	0
			2002	18–100	2	2	2	2	1
			2003	107–127	3	3	3	3	1
			2003	105–159	1	1	0	0	0
			2003	250–291	1	1	0	0	0
			2003	249–396	1	1	0	0	0
			2003	417–426	3	0	0	0	0

Type of Water	Type of sampling	ID code	Dates	Depths	Number of Samples Total (Data Freeze 1.2)	With Major Elements (ME)	With ME & Stable isotopes	With ME, SI & Tritium	Representative
			2004	414–434	3	2	2	2	1
			2003	505–520	28	0	0	0	0
			2003	509–516	16 (2G,1M,1C)	11	3	3	1
	Tube (16)	KFM03 (48)	2003	100–1,000	16	8	0	0	0
	Packered (31)		2003	347–394	1	0	0	0	0
			2003	386–391	4	4	3	3	1
			2003,04	488–456	4 (1G,1M,1C)	4	2	2	1
			2004	639–646	6 (1G,1M,1C)	5	5	5	1
			2004	940–947	8 (1G,1M,1C)	7	0	0	0
			2003	980–1,001	8(1G,1M,1C)	8	8	8	1
	Tube	KFM04	2003	0–996	17	9	5	5	0
	Packered		2004	231–238	7	6	6	6	1
			2004	354–361	4	0	0	0	1
Shallow Groundwater	Tube		2003	0–995	17	9	3	3	0
	Private Wells	PFM***	2003		9	9	9	9	6
	Soil Pipes	SFM0001	2002,03,04	4–5	8	7	7	7	1
		SFM0002	2002,03,04	4–5	8	7	7	7	1
		SFM0003	2002,03,04	9–11	8	7	7	7	1
		SFM0005	2002,03,04	1–2	6	3	3	3	1
		SFM0006	2003,04	3–4	5	3	3	3	1
		SFM0007	2003		1	0	0	0	0
		SFM0008	2003,04	5–6	5	4	4	4	1
		SFM0009	2003,04	2–3	5	5	4	4	1
		SFM0010	2003	1–2	1	0	0	0	0
		SFM0011	2003	3–4	1	1	1	1	0
		SFM0012	2003,04	4–5	6	6	5	5	1
		SFM0013	2003	4–5	1	1	1	1	1
		SFM0014	2003	1–2	1	1	1	1	0
		SFM0015	2003,04	6–7	6	5	5	5	1
		SFM0016	2003	7–8	1	1	1	1	0
		SFM0017	2003	3–4	1	1	1	1	0
		SFM0018	2003	4–5	1	1	1	1	0

Type of Water	Type of sampling	ID code	Dates	Depths	Number of Samples Total (Data Freeze 1.2)	With Major Elements (ME)	With ME & Stable isotopes	With ME, SI & Tritium	Representative
		SFM0019	2003	3–4	1	1	1	1	0
		SFM0020	2003	2–3	1	1	1	1	0
		SFM0021	2003	1–2	0	0	0	0	0
		SFM0023	2003,04	3–4	5	4	4	4	1
		SFM0024	2003	2–2	3	3	3	3	1
		SFM0025	2003,04	5–6	5	4	4	4	0
		SFM0026	2003	15–16	1	1	1	1	0
		SFM0027	2003,04	6–7	5	4	4	4	1
		SFM0028	2003	6–7	1	1	1	1	0
		SFM0029	2003,04	6–7	4	3	3	3	1
		SFM0030	2003	3–4	1	1	1	1	0
		SFM0031	2003,04	3–4	4	4	3	3	1
		SFM0032	2003,04	2–3	5	4	4	4	1
		SFM0034	2003	1–2	1	1	1	1	0
		SFM0035	2003,04	1–2	3	0	0	0	0
		SFM0036	2003	1–2	1	1	1	1	0
		SFM0037	2003,04	1–2	4	3	3	3	1
		SFM0049	2003	3–4	1	1	1	1	0
		SFM0051	2003,04		4	3	3	3	1
		SFM0053	2003,04		4	3	3	3	1
		SFM0056	2003,04		4	3	3	3	1
		SFM0057	2003,04		4	3	2	2	1
		SFM0060	2004		1	1	1	1	1
Sea Water		SFM0074	2004		7	0	0	0	0
		PFM000062	2002,03,04		45	43	10	10	9
		PFM000063	2002,03,04		56	55	13	13	10
		PFM000064	2002,03,04		51	50	11	11	0
		PFM000065	2002,03,04		31	31	9	8	0
		PFM000082	2002,03,04		17	17	4	4	0
		PFM000083	2002,03		7	7	2	2	0
		PFM000084	2002,03		9	9	2	2	0
Running Water		PFM000153	2002		2	2	0	0	0
		PFM000066	2002,03,04		29	28	8	8	8

Type of Water	Type of sampling	ID code	Dates	Depths	Number of Samples Total (Data Freeze 1.2)	With Major Elements (ME)	With ME & Stable isotopes	With ME, SI & Tritium	Representative
		PFM000067	2002,03,04		39	38	11	9	9
		PFM000068	2002,03,04		36	35	9	9	9
		PFM000069	2002,03,04		36	36	6	6	6
		PFM000070	2002,03,04		30	29	9	7	7
		PFM000071	2002,03,04		27	26	4	3	3
		PFM000072	2002,03,04		34	33	9	9	9
Lake Water		PFM000073	2002,03,04		18	18	3	3	3
		PFM000074	2002,03,04		30	30	9	8	8
		PFM000086	2002		1	1	0	0	0
		PFM000087	2002,03,04		57	57	15	15	13
		PFM000097	2002,03,04		31	31	8	7	7
		PFM000107	2002,03,04		53	51	12	12	12
		PFM000117	2002,03,04		54	53	14	12	9
		PFM000127	2002,03		23	23	6	6	5
		PFM000135	2002,03,04		10	10	2	2	2
		PFM000151	2002		4	3	1	1	0
Precipitation		PFM002457	2002,03		5	4	4	4	0
Groundwaters		Deep GW	Percussion B.		84	60	45	45	19
			Cored B.	Packered	118	77	49	49	12
		Tube			50	26	8	8	0
Shallow GW					144	112	108	108	22
Total Groundwaters					396	275	210	210	53
Surface waters		Sea Water			218	214	51	50	19
		Running Water			249	243	59	54	54
		Lake Water			263	236	67	63	56
Precipitation					5	4	4	4	0
Total Surface waters					735	697	181	171	129
TOTAL					1,131	972	391	381	182

* (G) sample with dissolved gasses.
* (M) sample with microbial analysis.
* (C) sample with colloids.

Table A-7. Number of samples taken after data freeze 1.1 for the Forsmark area.

Type of Water	Type of sampling	ID code	Dates	Depths	Number of Samples New samples after Data Freeze 1.1	With Major Elements (ME)	With ME & Stable isotopes	With ME, SI & Tritium	Representative
Ground Water	Packered	HFM01	2002	0–200					
		HFM02	2002	0–100					
		HFM03	2002	0–26					
		HFM04	2002	30–222					
		HFM05	2002,03	0–200	2 (1M)	1	1	1	0
		HFM06	2003	0–111	1	1	1	1	0
		HFM08	2003	0–144					2
		HFM09	2003,04	0–50	4	4	2	2	1
		HFM10	2003,04	0–150	7 (1M)	5	4	4	1
		HFM11	2003	0–182	3	3	3	3	1
		HFM12	2003	0–210	3	3	3	3	1
		HFM13	2003,04	0–176	5	3	3	3	1
		HFM14	2003	0–151	3	3	3	3	1
		HFM15	2003	0–200	3	3	3	3	1
		HFM16	2003	0–133	3	3	1	1	1
		HFM17	2004	0–203	3	3	1	1	1
		HFM18	2004	0–173	3	3	1	1	1
	Packered	HFM19	2004	0–173	3	3	1	1	1
		KFM01A	2002	0–101					0
			2003	110–121					1
	Packered	KFM02	2003	177–184	10 (1G,1C)	9	9	9	1
			2003	1–100					
			2002	18–100					
			2003	107–127	3	3	3	3	1
			2003	105–159					
			2003	250–291					
			2003	249–396					
			2003	417–426	3	0	0	0	0
			2004	414–434	3	2	2	2	1
			2003	505–520	28	0	0	0	0

Type of Water	Type of sampling	ID code	Dates	Depths	Number of Samples New samples after Data Freeze 1.1	With Major Elements (ME)	With ME & Stable isotopes	With ME, SI & Tritium	Representative
			2003	509–516	16 (2G,1M,1C)	11	3	3	1
	Tube	KFM03	2003	100–1,000	16	8	0	0	0
	Packered		2003	347–394	1	0	0	0	0
			2003	386–391	4	4	3	3	1
			2003,04	488–456	4 (1G,1M,1C)	4	2	2	1
			2004	639–646	6 (1G,1M,1C)	5	5	5	1
			2004	940–947	8 (1G,1M,1C)	7	0	0	0
			2003	980–1,001	8(1G,1M,1C)	8	8	8	1
	Tube	KFM04	2003	0–996	17	9	5	5	0
	Packered		2004	231–238	7	6	6	6	1
			2004	354–361	4	0	0	0	1
Shallow Groundwater	Tube		2003	0–995	17	9	3	3	0
	Private Wells	PFM***	2003		9	9	9	9	6
	Soil Pipes	SFM0001	2003,04	4–5	6	5	5	5	0
		SFM0002	2003,04	4–5	5	4	4	4	0
		SFM0003	2003,04	9–11	5	4	4	4	0
		SFM0005	2003,04	1–2	5	2	2	2	0
		SFM0006	2003,04	3–4	5	3	3	3	1
		SFM0007	2003		1	0	0	0	0
		SFM0008	2003,04	5–6	5	4	4	4	1
		SFM0009	2003,04	2–3	5	5	4	4	1
		SFM0010	2003	1–2	1	0	0	0	0
		SFM0011	2003	3–4	1	1	1	1	0
		SFM0012	2003,04	4–5	6	6	5	5	1
		SFM0013	2003	4–5	1	1	1	1	1
		SFM0014	2003	1–2					
		SFM0015	2003,04	6–7	6	5	5	5	1
		SFM0016	2003	7–8	1	1	1	1	0
		SFM0017	2003	3–4	1	1	1	1	0
		SFM0018	2003	4–5	1	1	1	1	0
		SFM0019	2003	3–4	1	1	1	1	0
		SFM0020	2003	2–3	1	1	1	1	0

Type of Water	Type of sampling	ID code	Dates	Depths	Number of Samples New samples after Data Freeze 1.1	With Major Elements (ME)	With ME & Stable isotopes	With ME, SI & Tritium	Representative
		SFM0021	2003	1–2	0	0	0	0	0
		SFM0023	2003,04	3–4	5	4	4	4	1
		SFM0024	2003	2–2	3	3	3	3	1
		SFM0025	2003,04	5–6	5	4	4	4	0
		SFM0026	2003	15–16	1	1	1	1	0
		SFM0027	2003,04	6–7	5	4	4	4	1
		SFM0028	2003	6–7	1	1	1	1	0
		SFM0029	2003,04	6–7	4	3	3	3	1
		SFM0030	2003	3–4	1	1	1	1	0
		SFM0031	2003,04	3–4	4	4	3	3	1
		SFM0032	2003,04	2–3	5	4	4	4	1
		SFM0034	2003	1–2	1	1	1	1	0
		SFM0035	2003,04	1–2	3	0	0	0	0
		SFM0036	2003	1–2	1	1	1	1	0
		SFM0037	2003,04	1–2	4	3	3	3	1
		SFM0049	2003	3–4	1	1	1	1	0
		SFM0051	2003,04		4	3	3	3	1
		SFM0053	2003,04		4	3	3	3	1
		SFM0056	2003,04		4	3	3	3	1
		SFM0057	2003,04		4	3	2	2	1
		SFM0060	2004		1	1	1	1	1
Sea Water		SFM0074	2004		7	0	0	0	0
		PFM000062	2003,04		17	17	4	4	4
		PFM000063	2003,04		24	24	5	5	3
		PFM000064	2003,04		23	23	5	5	0
		PFM000065	2003,04		17	17	5	4	0
		PFM000082	2003,04		8	8	0	0	0
		PFM000083	2003		2	2	0	0	0
		PFM000084	2003		4	4	0	0	0
Running Water		PFM000153	2002						
		PFM000066	2003,04		17	17	4	4	4

Type of Water	Type of sampling	ID code	Dates	Depths	Number of Samples New samples after Data Freeze 1.1	With Major Elements (ME)	With ME & Stable isotopes	With ME, SI & Tritium	Representative
		PFM000067	2003,04		20	19	6	4	4
		PFM000068	2003,04		18	18	4	4	4
		PFM000069	2003,04		18	18	1	0	0
		PFM000070	2003,04		18	17	5	4	4
		PFM000071	2003,04		15	14	0	0	0
		PFM000072	2003,04		19	18	4	4	4
Lake Water		PFM000073	2003,04		11	11	2	2	2
		PFM000074	2003,04		18	18	5	4	4
		PFM000086	2002						
		PFM000087	2003,04		27	27	5	3	3
		PFM000097	2003,04		17	17	4	3	3
		PFM000107	2003,04		22	21	4	3	3
		PFM000117	2003,04		24	24	6	4	3
		PFM000127	2003		7	7	2	2	1
		PFM000135	2003,04		7	7	1	1	1
		PFM000151	2002						
Precipitation		PFM002457	2003		2	0	0	0	0
Groundwaters		Deep GW	Percussion B.		43	38	27	27	13
			Cored B.	Packered	105	59	41	41	11
		Tube			50	26	8	8	0
Shallow GW					134	102	98	98	24
Total Groundwaters					332	225	174	174	48
Surface waters		Sea Water			95	95	19	18	7
		Running Water			136	132	26	22	22
		Lake Water			122	121	27	20	18
Precipitation					2	0	0	0	0
Total Surface waters					335	348	72	60	47
TOTAL					667	573	246	234	95

Appendix B

How we used the data in our modelling

Table B-1. Available Forsmark site data and handling in model version 2.1. {Hydrochemical}.

Available site data		Utilized in model version 1.2		Not utilized in model version 1.2
Data specification	**Reference**	**Analysis/Modelling**	**cf. section**	**Motivation**
Cored borehole data				
KFM01A	Two representative samples with complete chemical and isotopic characterization: 4528,4724	Ion-ion plots Speciation-solubility calculations Redox pairs modelling		17 non representative samples only used in ion-ion plots
KFM02	Four representative packered samples with complete chemical and isotopic characterization: 4398,8100,8272,8016	Ion-ion plots Speciation-solubility calculations		71 non representative samples only used in ion-ion plots
	8100,8016	Redox pairs modelling		
KFM03	Four representative packered samples with complete chemical and isotopic characterization: 8012,8017,8273,8152	Ion-ion plots Speciation-solubility calculations		44 non representative samples only used in ion-ion plots
	8017,8273,8152,8281	Redox pairs modelling		
KFM04	Two representative samples with complete chemical and isotopic characterization: 8267,8287	Ion-ion plots Speciation-solubility calculations		26 non representative samples only used in ion-ion plots
Percussion hole data				
HFM01–HFM19	19 representative samples with complete chemical and isotopic characterization: 4116,4170,4167,4399,4964,4464,4535,4522,8335,4965,8038,8020,8129,8095,8127,8164,8246,8325,8247	Ion-ion plots Speciation-solubility calculations		65 non representative samples only used in ion-ion plots
Other borehole data				
PFM000001-7-8-9-10-39-2942-4778	Six representative sample with complete chemical and isotopic characterization: 8073,8046,8050,8078,4986,4987	Ion-ion plots Speciation-solubility calculations		3 non representative samples only used in ion-ion plots
Soil Pipes	19 representative sample with complete chemical and isotopic characterization: 4316,4220,4221,4432,4764,4812,4897,4921,4671,4922,8252,4918,4896,8237,4899,4894,4919,8091,8244	Ion-ion plots Speciation-solubility calculations		105 non representative samples only used in ion-ion plots
BAT Tubes	Three representative sample with complete chemical and isotopic characterization: 4855,4856,4857	Ion-ion plots Speciation-solubility calculations		9 non representative samples only used in ion-ion plots
Surface based data				
Rain				5 non representative samples not used in model version 1.2

Available site data		Utilized in model version 1.2		Not utilized in model version 1.2
Data specification	**Reference**	**Analysis/Modelling**	**cf. section**	**Motivation**
Sea Water	19 representative samples with complete chemical characterization: 4198,4229,4230,4322,4333,4763,4864,8048,8218,4195,4227,4228,4321,4324,4445,4450,4759,4862,8055	Ion-ion plots Speciation-solubility calculations		199 non representative samples only used in ion-ion plots
Running Water	54 representative samples with complete chemical characterization: 4045,4208,4223,4454,4771, 4869,8044,8224,4057,4204, 4242,4339,4459,4772,4822, 4868,8056,8216,4046,4213, 4238,4343,4457,4758,4872, 8060,8225,4055,4211,4244, 4342,4455,4819,4051,4210, 4240,4456,4776,4871,8059, 8221,4050,4209,4239,4460,4042,4214,4243,4345,4458,4769,4874,8049,8226,4043,4767,8229	Ion-ion plots Speciation-solubility calculations		195 non representative samples only used in ion-ion plots
Lake Water	56 representative samples with complete chemical characterization: 4202,4224,4337,4453,4770, 4821,4861,8045,8231,4060, 4061,4200,4201,4203,4222, 4327,4331,4442,4449,4860, 8047,8215,4056,4205,4245, 4452,4777,4820,4870,8217, 4058,4059,4206,4207,4233, 4234,4328,4444,4447,4757, 4866,8213,4048,4049,4217,4235,4440,4451,4774,4867,8210,4215,4216,4232,4241,8053,4443,8230	Ion-ion plots Speciation-solubility calculations		207 non representative samples only used in ion-ion plots

M4, a hyperspace version of M3

C.1 Calculation method

The proposed modification to M3 has a very simple rationale: instead of using only two of the principal components to calculate the mixing proportions, as M3 does, M4 (M3 Modified=M4) calculates them using as many principal components as end-members have been used minus one. This is equivalent to saying that the mixing proportions are computed in a space with N-1 dimensions, where N is the number of end-members. Working in hyperspace has the advantage of avoiding the uncertainties derived from the projection of the coordinates onto a plane before calculating the mixing ratios. This uncertainty grows with the number of end-members and can be high when working with end-members which plot close together in the plane defined by the first two principal components (the plane used by M3 to performed the calculations).

The mixing proportions are calculated from the principal component coordinates. The whole procedure is a simple coordinate transformation, from a N-1 Cartesian coordinate system (principal component coordinates) to a hyper-tetrahedral coordinate system (mixing proportions coordinates).

Figure C-1 shows how to compute the mixing proportions from the principal component coordinates for a 2D example (three en-members). The mixing proportions are denoted (ξ_1, ξ_2, ξ_3), and the Principal Component Analysis (PCA) coordinates (x,y). In Figure C-1 the red circle marks the location of the sample we want to compute the mixing proportions. From this circle we draw straight lines to the three vertices of the triangle. This operation subdivides the total triangle into three sub-triangles (one is coloured in blue) whose areas are A_1, A_2, A_3.

The area of the total triangle is $A= A_1+A_2+A_3$. From the knowledge of these areas it is straight-forward to compute the mixing proportions coordinates, which are the ratio of the area of each sub-triangle to the total area (see the expressions in Figure C-1). When coding this procedure, the required operations boil down to the computation of the determinant of a 3 × 3 coordinate matrix (one determinant for each coordinate):

$$\xi_1 = \frac{1}{2A}\begin{vmatrix} 1 & x & y \\ 1 & x_2 & y_2 \\ 1 & x_3 & y_3 \end{vmatrix}, \qquad \xi_2 = \frac{1}{2A}\begin{vmatrix} 1 & x_1 & y_1 \\ 1 & x & y \\ 1 & x_3 & y_3 \end{vmatrix}, \qquad \xi_3 = \frac{1}{2A}\begin{vmatrix} 1 & x_1 & y_1 \\ 1 & x_2 & y_2 \\ 1 & x & y \end{vmatrix}$$

where ξ_1, ξ_2, ξ_3 are the mixing proportions, (x, y) are the PCA coordinates of the point whose mixing proportions are being calculated, and (x_i, y_i) are the PCA coordinates of the end-members.

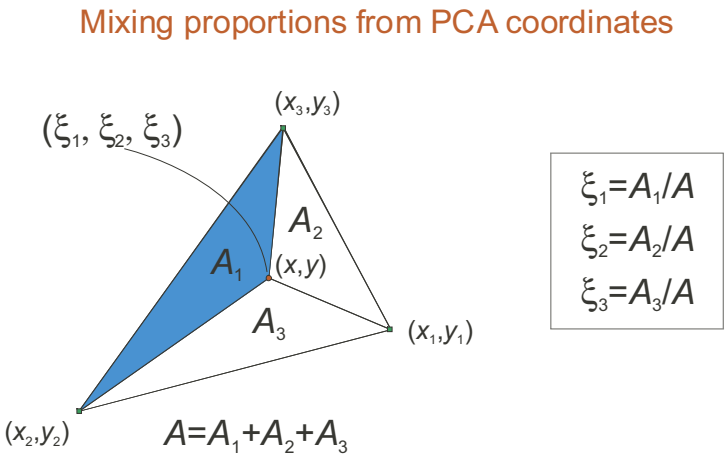

Figure C-1. *Calculation of the mixing proportion coordinates from the Principal Component Analysis (PCA) coordinates.*

For four end-members the polyhedron is a tetrahedron with four vertex, and the expressions for the mixing proportions are:

$$\xi_1 = \frac{1}{6A}\begin{vmatrix} 1 & x & y & z \\ 1 & x_2 & y_2 & z_2 \\ 1 & x_3 & y_3 & z_3 \\ 1 & x_4 & y_4 & z_4 \end{vmatrix}, \qquad \xi_2 = \frac{1}{6A}\begin{vmatrix} 1 & x_1 & y_1 & z_1 \\ 1 & x & y & z \\ 1 & x_3 & y_3 & z_3 \\ 1 & x_4 & y_4 & z_4 \end{vmatrix}, \qquad \xi_3 = \frac{1}{6A}\begin{vmatrix} 1 & x_1 & y_1 & z_1 \\ 1 & x_2 & y_2 & z_2 \\ 1 & x & y & z \\ 1 & x_4 & y_4 & z_4 \end{vmatrix}$$

$$\xi_4 = \frac{1}{6A}\begin{vmatrix} 1 & x_1 & y_1 & z_1 \\ 1 & x_2 & y_2 & z_2 \\ 1 & x_3 & y_3 & z_3 \\ 1 & x & y & z \end{vmatrix}.$$

The generalization of this procedure to any number of end-members is straightforward and the matrix whose determinant is to be computed is in general a d+1xd+1 coordinate matrix, where d is the dimensionality of the PCA space and d+1 the number of end-members:

$$\xi_1 = \frac{1}{d!A}\begin{vmatrix} 1 & x & y & z & \cdots & w \\ 1 & x_2 & y_2 & z_2 & \cdots & w_2 \\ 1 & x_3 & y_3 & z_3 & \cdots & w_3 \\ 1 & x_4 & y_4 & z_4 & \cdots & w_4 \\ \vdots & \vdots & \vdots & \vdots & \ddots & \vdots \\ 1 & x_{d+1} & y_{d+1} & z_{d+1} & \cdots & w_{d+1} \end{vmatrix}$$

and similar expressions for coordinates ξ_2, ξ_3, ..., ξ_{d+1}. The meaning of each row and column of the determinant is explained in Figure C-2.

C.2 Sensitivity analysis with synthetic samples

Mixing proportions. We have carried out a sensitivity analysis with synthetic samples to estimate the uncertainty associated with this new technique. 1,000 samples where generated by mixing a random amount of each of the four end-members Brine (Br), Glacial (Gl), Littorina (Lit), and Rain60 (R60), as shown in Figure C-3.

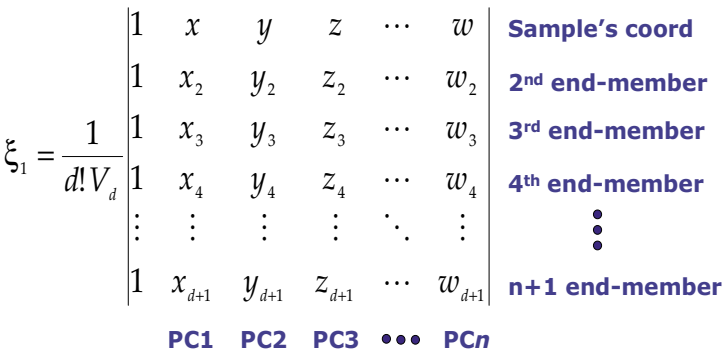

Figure C-2. *Meaning of the rows and columns of the determinant used to compute the proportion of the first end-member in a sample. The proportion of the other end-members is computed moving downwards the row containing the sample's coordinates.*

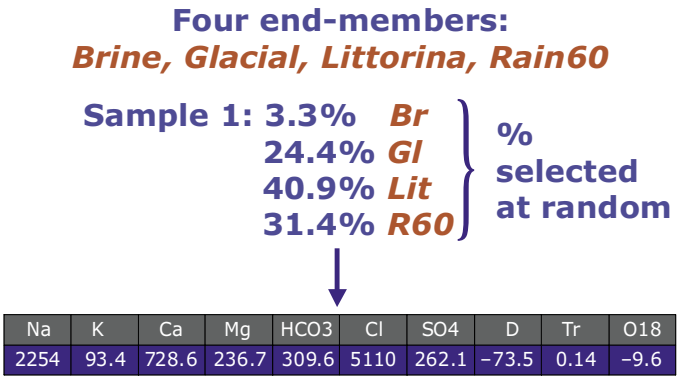

Na	K	Ca	Mg	HCO3	Cl	SO4	D	Tr	O18
2254	93.4	728.6	236.7	309.6	5110	262.1	−73.5	0.14	−9.6

Figure C-3. *Procedure to generate synthetic samples with known proportions of each end member. The example is applied to a four end-member case. Each end-member has a particular chemical composition (not shown) which is then multiplied by the randomly generated mixing proportion and summed to build the chemical composition of the synthetic sample.*

These samples where then fed into M4 to compute the mixing proportions and finally the squared difference of the known mixing proportions and the M4 mixing proportions were computed:

$$StdDev = [(Brine-Brine_{M4})^2 + (Litorina-Litorina_{M4})^2 + (Rain60-Rain60_{M4})^2 + (Glacial-Glacial_{M4})^2]^{1/2}.$$

In this expression Brine refers to the known mixing proportion and BrineM4 to the one calculated by M4. In Figure C-4, where the results are graphically presented, each of the 1,000 samples is colour-coded with respect to the standard deviation. Maximum deviation is of the order of 4% and the mean standard deviation for the 1,000 samples is 0.85%. As a comparison, the same sensitivity analysis with M3 gives a mean standard deviation of 17% when working with four end-members and of 23% with five end-members.

Chemical composition. How is the performance of M4 when predicting chemical compositions? Figure C-5 shows the predicted chlorine content for the 1,000 synthetic samples plotted against the known chlorine content. All the samples plot on the diagonal line demonstrating the good recovery capabilities of M4. The standard deviation is 0.27 mg/L in samples with an average Cl-content of 9,000 mg/L. As a comparison, M3 gives a standard deviation of 676 mg/L for the same data set.

End-member selection. Another extra bonus of M4 is the possibility of computing the "best combination of end-members". When the selection of end-members is good for the samples analysed, all of them should plot inside the hyper-volume defined by the end-members in the N-1-dimensional space. This is a generalization of the property of triangular coordinates: any point inside the triangle has *positive* triangular coordinates, and any point outside it has, at least, one *negative* coordinate. With this rule in mind, it is very simple to know which samples are inside the hyper-volume defined by the N end-members. Only these samples can be "explained" by the selected combination of end-members. The closer is this figure to the total number of samples, the better the combination is (in the sense that more samples can be explained as a mixing of the selected end-members). Figure C-6 is an example of the output for 119 samples from the Forsmark area. Each row is a combination of end-members selected from the set Brine, Littorina, Glacial, Rain60, Lake Water, Sea Sediment, and Baltic Sea, from two end-members to seven, and the value shown in the last column is the total number of samples with all the coordinates positive (i.e., the number of samples that plot inside the hyper-tetrahedron in N-1-dimensional space).

From this table it is simple to select the "most promising" combinations, in the sense that it is the combination of end-members that is able to explain, only by mixing, the highest percentage of samples. In the example below, combinations #38 (Glacial, Litorina, Lake Water) and #45 (Glacial, Lake Water, Baltic) are the best with three end-members; and combinations #58 (Brine, Glacial, Littorina, Lake water) and #65 (Brine, Glacial, Lake Water, Baltic) the best with four end-members. With five end-members only combination #101 (Brine, Glacial, Lake Water, Sea Sediment, Baltic) is rather good, explaining 95 out of 119 samples (80%). No combination with 6 or 7 end-members is able to explain more than 45% of the samples. Of course, the final selection of end-members will be based also in geochemical and hydrochemical clues.

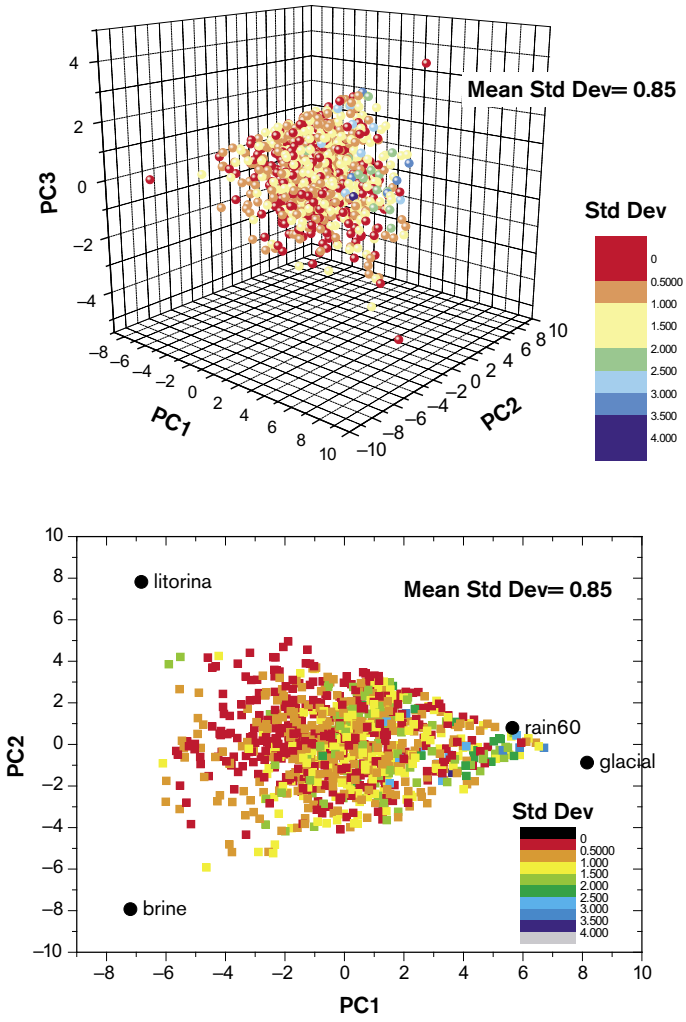

Figure C-4. *Difference between the known mixing proportions and the mixing proportions calculated by M4 for 1,000 synthetic samples and the four end-members Brine, Littorina, Rain60, and Glacial. Upper panel is a 3D view using three principal components and lower panel is the projection onto the PC1-PC2 plane, the one used by M3.*

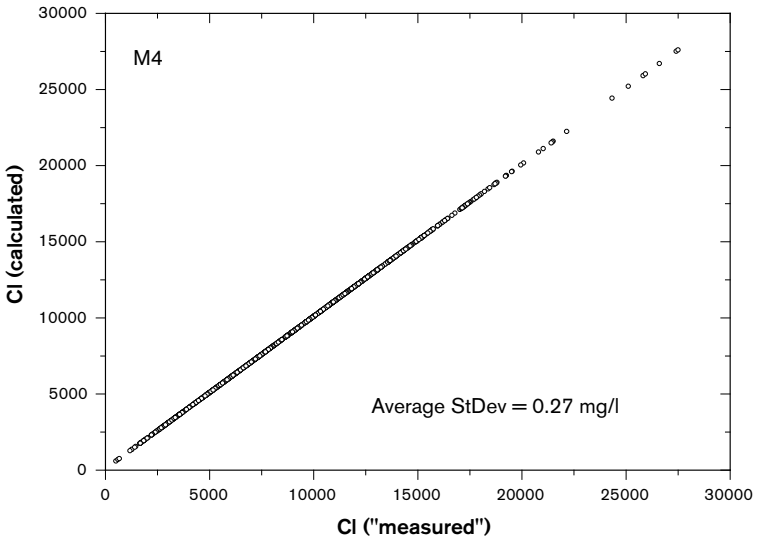

Figure C-5. *Predicted chlorine content (calculated) as a function of known chlorine content ("measured") for 1,000 synthetic samples. The average Cl-content of the samples is 9,000 mg/L and the standard deviation [(Clmeasured)2 – (Clcalculated)2]1/2 0.27 mg/L.*

1	Brine	Glacial	–	–	–	–	–	119
2	Brine	Litorina	–	–	–	–	–	0
3	Brine	Rain-60	–	–	–	–	–	119
4	Brine	Lake Water	–	–	–	–	–	52
5	Brine	Sediment	–	–	–	–	–	31
6	Brine	Baltic	–	–	–	–	–	0
7	Glacial	Litorina	–	–	–	–	–	119
8	Glacial	Rain-60	–	–	–	–	–	18
9	Glacial	Lake Water	–	–	–	–	–	86
10	Glacial	Sediment	–	–	–	–	–	115
11	Glacial	Baltic	–	–	–	–	–	119
12	Litorina	Rain-60	–	–	–	–	–	119
13	Litorina	Lake Water	–	–	–	–	–	49
14	Litorina	Sediment	–	–	–	–	–	26
15	Litorina	Baltic	–	–	–	–	–	0
16	Rain-60	Lake Water	–	–	–	–	–	72
17	Rain-60	Sediment	–	–	–	–	–	115
18	Rain-60	Baltic	–	–	–	–	–	119
19	Lake Water	Sediment	–	–	–	–	–	41
20	Lake Water	Baltic	–	–	–	–	–	49
21	Sediment	Baltic	–	–	–	–	–	29
22	Brine	Glacial	Litorina	–	–	–	–	4
23	Brine	Glacial	Rain-60	–	–	–	–	48
24	Brine	Glacial	Lake Water	–	–	–	–	92
25	Brine	Glacial	Sediment	–	–	–	–	4
26	Brine	Glacial	Baltic	–	–	–	–	34
27	Brine	Litorina	Rain-60	–	–	–	–	66
28	Brine	Litorina	Lake Water	–	–	–	–	30
29	Brine	Litorina	Sediment	–	–	–	–	4
30	Brine	Litorina	Baltic	–	–	–	–	0
31	Brine	Rain-60	Lake Water	–	–	–	–	58
32	Brine	Rain-60	Sediment	–	–	–	–	33
33	Brine	Rain-60	Baltic	–	–	–	–	64
34	Brine	Lake Water	Sediment	–	–	–	–	5
35	Brine	Lake Water	Baltic	–	–	–	–	30
36	Brine	Sediment	Baltic	–	–	–	–	29
37	Glacial	Litorina	Rain-60	–	–	–	–	84
38	Glacial	Litorina	Lake Water	–	–	–	–	115
39	Glacial	Litorina	Sediment	–	–	–	–	0
40	Glacial	Litorina	Baltic	–	–	–	–	25
41	Glacial	Rain-60	Lake Water	–	–	–	–	54
42	Glacial	Rain-60	Sediment	–	–	–	–	54
43	Glacial	Rain-60	Baltic	–	–	–	–	84
47	Litorina	Rain-60	Lake Water	–	–	–	–	36
48	Litorina	Rain-60	Sediment	–	–	–	–	38
49	Litorina	Rain-60	Baltic	–	–	–	–	1
50	Litorina	Lake Water	Sediment	–	–	–	–	30
51	Litorina	Lake Water	Baltic	–	–	–	–	1
52	Litorina	Sediment	Baltic	–	–	–	–	0
53	Rain-60	Lake Water	Sediment	–	–	–	–	48
54	Rain-60	Lake Water	Baltic	–	–	–	–	36
55	Rain-60	Sediment	Baltic	–	–	–	–	37
56	Lake Water	Sediment	Baltic	–	–	–	–	30
57	Brine	Glacial	Litorina	Rain-60	–	–	–	79
58	Brine	Glacial	Litorina	Lake Water	–	–	–	116
59	Brine	Glacial	Litorina	Sediment	–	–	–	1
60	Brine	Glacial	Litorina	Baltic	–	–	–	1
61	Brine	Glacial	Rain-60	Lake Water	–	–	–	16
62	Brine	Glacial	Rain-60	Sediment	–	–	–	50
63	Brine	Glacial	Rain-60	Baltic	–	–	–	65
64	Brine	Glacial	Lake Water	Sediment	–	–	–	88
65	Brine	Glacial	Lake Water	Baltic	–	–	–	116
66	Brine	Glacial	Sediment	Baltic	–	–	–	2
67	Brine	Litorina	Rain-60	Lake Water	–	–	–	47
68	Brine	Litorina	Rain-60	Sediment	–	–	–	51
69	Brine	Litorina	Rain-60	Baltic	–	–	–	3
70	Brine	Litorina	Lake Water	Sediment	–	–	–	34
71	Brine	Litorina	Lake Water	Baltic	–	–	–	1
72	Brine	Litorina	Sediment	Baltic	–	–	–	1
73	Brine	Rain-60	Lake Water	Sediment	–	–	–	34
74	Brine	Rain-60	Lake Water	Baltic	–	–	–	1

75	Brine	Rain-60	Sediment	Baltic	–	–	–	45
76	Brine	Lake Water	Sediment	Baltic	–	–	–	34
77	Glacial	Litorina	Rain-60	Lake Water	–	–	–	68
78	Glacial	Litorina	Rain-60	Sediment	–	–	–	2
79	Glacial	Litorina	Rain-60	Baltic	–	–	–	0
80	Glacial	Litorina	Lake Water	Sediment	–	–	–	18
81	Glacial	Litorina	Lake Water	Baltic	–	–	–	61
82	Glacial	Litorina	Sediment	Baltic	–	–	–	0
83	Glacial	Rain-60	Lake Water	Sediment	–	–	–	40
84	Glacial	Rain-60	Lake Water	Baltic	–	–	–	69
85	Glacial	Rain-60	Sediment	Baltic	–	–	–	12
86	Glacial	Lake Water	Sediment	Baltic	–	–	–	58
87	Litorina	Rain-60	Lake Water	Sediment	–	–	–	30
88	Litorina	Rain-60	Lake Water	Baltic	–	–	–	1
89	Litorina	Rain-60	Sediment	Baltic	–	–	–	0
90	Litorina	Lake Water	Sediment	Baltic	–	–	–	2
91	Rain-60	Lake Water	Sediment	Baltic	–	–	–	29
92	Brine	Glacial	Litorina	Rain-60	Lake Water	–	–	81
93	Brine	Glacial	Litorina	Rain-60	Sediment	–	–	8
94	Brine	Glacial	Litorina	Rain-60	Baltic	–	–	1
95	Brine	Glacial	Litorina	Lake Water	Sediment	–	–	29
96	Brine	Glacial	Litorina	Lake Water	Baltic	–	–	48
97	Brine	Glacial	Litorina	Sediment	Baltic	–	–	3
98	Brine	Glacial	Rain-60	Lake Water	Sediment	–	–	40
99	Brine	Glacial	Rain-60	Lake Water	Baltic	–	–	74
100	Brine	Glacial	Rain-60	Sediment	Baltic	–	–	23
101	Brine	Glacial	Lake Water	Sediment	Baltic	–	–	95
102	Brine	Litorina	Rain-60	Lake Water	Sediment	–	–	31
103	Brine	Litorina	Rain-60	Lake Water	Baltic	–	–	1
104	Brine	Litorina	Rain-60	Sediment	Baltic	–	–	0
105	Brine	Litorina	Lake Water	Sediment	Baltic	–	–	2
106	Brine	Rain-60	Lake Water	Sediment	Baltic	–	–	30
107	Glacial	Litorina	Rain-60	Lake Water	Sediment	–	–	33
108	Glacial	Litorina	Rain-60	Lake Water	Baltic	–	–	27
109	Glacial	Litorina	Rain-60	Sediment	Baltic	–	–	0
110	Glacial	Litorina	Lake Water	Sediment	Baltic	–	–	19
111	Glacial	Rain-60	Lake Water	Sediment	Baltic	–	–	32
112	Litorina	Rain-60	Lake Water	Sediment	Baltic	–	–	1
113	Brine	Glacial	Litorina	Rain-60	Lake Water	Sediment	–	36
114	Brine	Glacial	Litorina	Rain-60	Lake Water	Baltic	–	13
115	Brine	Glacial	Litorina	Rain-60	Sediment	Baltic	–	2
116	Brine	Glacial	Litorina	Lake Water	Sediment	Baltic	–	31
117	Brine	Glacial	Rain-60	Lake Water	Sediment	Baltic	–	57
118	Brine	Litorina	Rain-60	Lake Water	Sediment	Baltic	–	1
119	Glacial	Litorina	Rain-60	Lake Water	Sediment	Baltic	–	1
120	Brine	Glacial	Litorina	Rain-60	Lake Water	Sediment	Baltic	2

Figure C-6. *Number of samples than can be "explained" by each possible combination of end-members, from two to seven end-members. Samples from Forsmark.*

C.3 Sensitivity analysis with real samples

Two sensitivity analysis have been performed on real samples to assess M4 capabilities:
(1) a comparison of measured versus predicted concentrations for two conservative elements, and
(2) a comparison with the mixing proportions calculated with PRHEEQC.

Figure 7 shows measured chlorine and ^{18}O in 1,039 groundwater samples from several Swedish sites (including Forsmark, Simpevarp and Äspö) plotted against the predicted value as computed by M4. Six end-members has been used in the modelling: Brine, Littorina, Glacial, Rain60, Lake Water, and Sea Sediment. Cl and ^{18}O have been chosen because their behaviour is conservative and mostly influence by mixing without reaction. If the concentration of an element is controlled exclusively by mixing, then M4 should be able to predict its chemistry and the samples should plot on or near the diagonal line in Figure C-7. This is obviously the case for ^{18}O (most samples plot near the diagonal line), but not for Cl at low concentrations (< 1,000 mg/l), where the calculated value reaches a minimum of around 200 mg/l (some other processes, besides mixing should be invoked to interpret this behaviour).

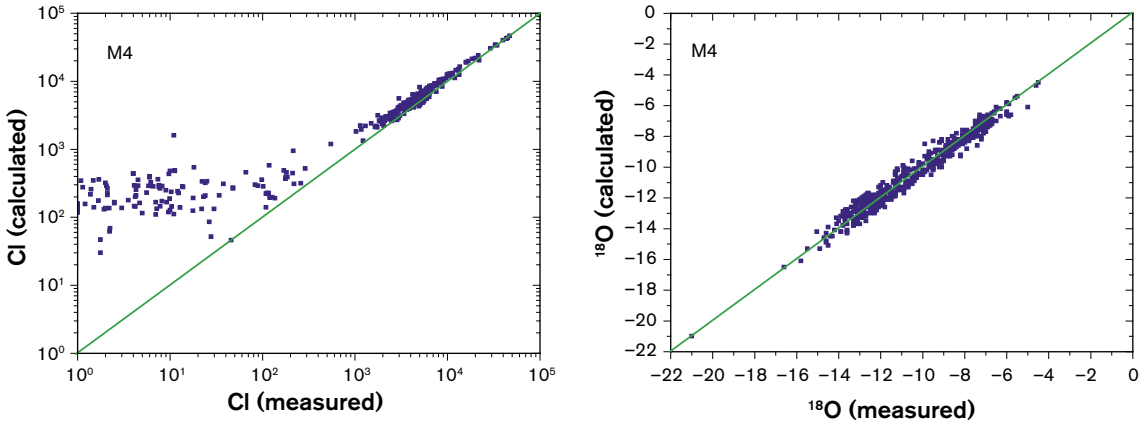

Figure C-7. *Measured versus calculated chlorine and 18O values for 1,039 groundwater samples from several Swedish sites.*

To further verify the validity of the M4 approach, it was applied to Forsmark 1.2 dataset. The calculations have been carried out with the same data set used for M3 modelling (Forsmark 1.2 Local Model) and using the same analytical data: Ca, Mg, Na, K, HCO_3^-, Cl^-, SO_4^{2-}, ^{18}O, D and tritium. An independent M4 run to select the best combination of end-members showed that the chosen end-member for M3 modelling (Brine, Glacial, Littorina and Precipitation) explain more than 90% of the samples, being the best four end-member combination. Therefore, all the calculations have been performed with these same end-members.

Once the mixing proportions of all the samples included in the Forsmark 1.2 Local Model were computed, several samples were selected to independently compute their mixing proportions using PHREEQC. The selected samples fall in three categories:

- KFM01A sample 4538 (at 110–120.67 m depth) and KFM02A sample 8016 (at 509–516 m depth) as representative of groundwaters with a clear Littorina signature.
- KFM03A samples 8152 (at 980–1,001 m depth) as representative of waters with the biggest brine contribution.
- PFM000009PW sample 8078 and SFM0023 sample 8252 as representative of shallow groundwaters in discharge zones.

Table C-1 shows the comparative results of a mixing calculation for three representative groundwater samples from Forsmark using M4 and PHREEQC. The procedure to compute mixing proportions with PHREEQC has been summarised elsewhere. Because PHREEQC calculation gives more than one feasible model for each sample, the numbers included in the table are for the models giving the maximum and minimum values for each mixing proportion. In both M4 and PHREEQC calculations the same four end-members (brine, littorina, glacial and precipitation) have been used. In most cases PHREEQC range brackets M4 value, supporting the validity of M4 approach to compute mixing proportions.

Table C-1. Comparative results of mixing proportions calculated with M4 and PHREEQC for three representative Forsmark groundwater samples.

	Sample	Code	Brine	Littorina	Glacial	Precipitation
Brackish-saline	4538 Cl = 4,563 mg/L Depth: 115 m	PHREEQC	3.8–5.1	27.9–35.2	27.8–31.6	29.4–39.0
		M4	2.6	35.7	40.8	20.8
	8016 Cl = 5,410 mg/L Depth: 512 m	PHREEQC	3.3–4.3	50–54	12.2–14.3	28.6–33.5
		M4	1.6	50.8	24.4	23.2
Saline	8152 Cl = 9,690 mg/L Depth: 990 m	PHREEQC	17.5–19.5	0–15	34–42	24–42
		M4	16.02	9.2	47.9	26.9
Discharge	8078 Cl = 4,730 mg/L Depth: 3 m	PHREEQC	3.5–4.8	30.5–38.5	27.2–32	28.2–33.5
		M4	2.7	39	39.4	18.9
	8252 Cl = 3,780 mg/L Depth: 3.8 m	PHREEQC	1.3–2.4	50.9–55	11.6–15.9	27.2–34
		M4	0	51.4	26.3	22.4

Appendix D

Stability diagrams

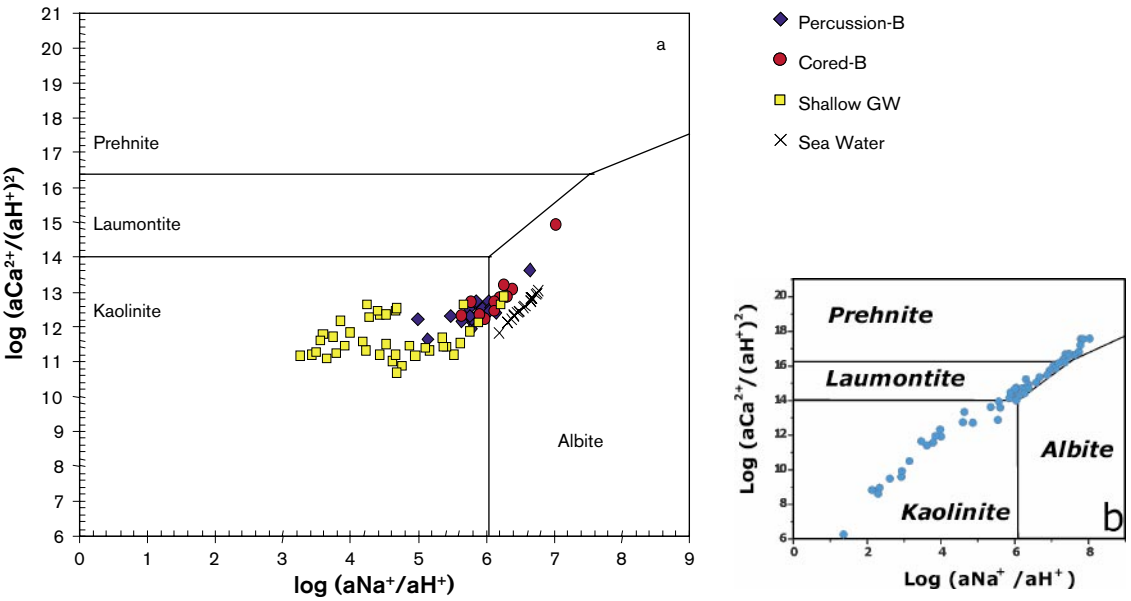

Figure AD-1. *Stability diagrams for kaolinite, Laumontite, Prehnite and albite in the representative waters from Forsmark area.*

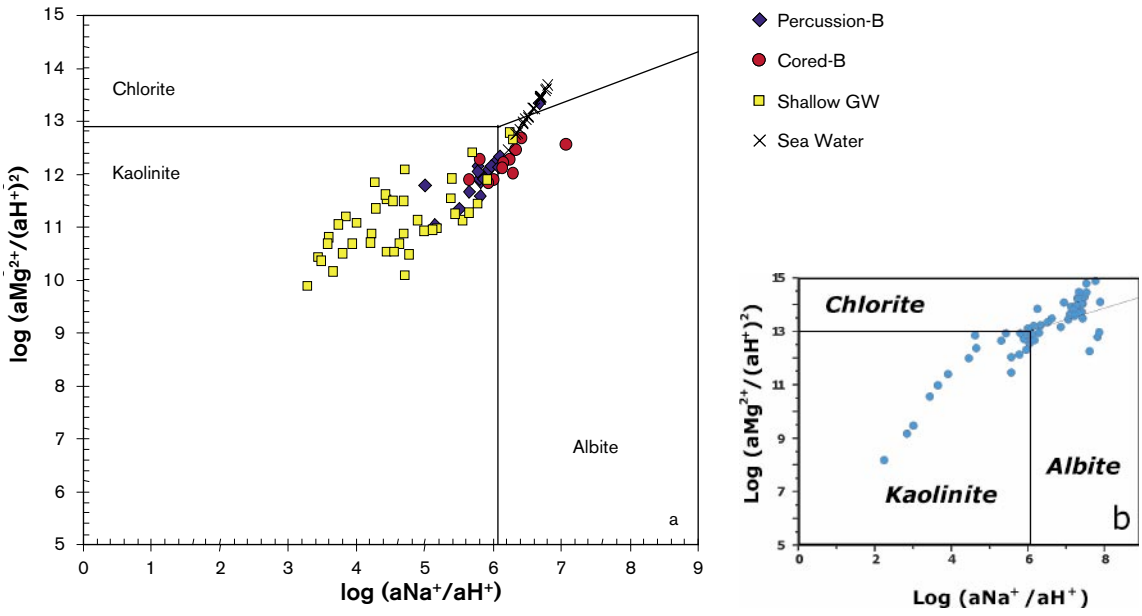

Figure AD-2. *Stability diagrams for kaolinite, chlorite and albite in the representative Forsmark waters (a) and in Stripa waters (b).*

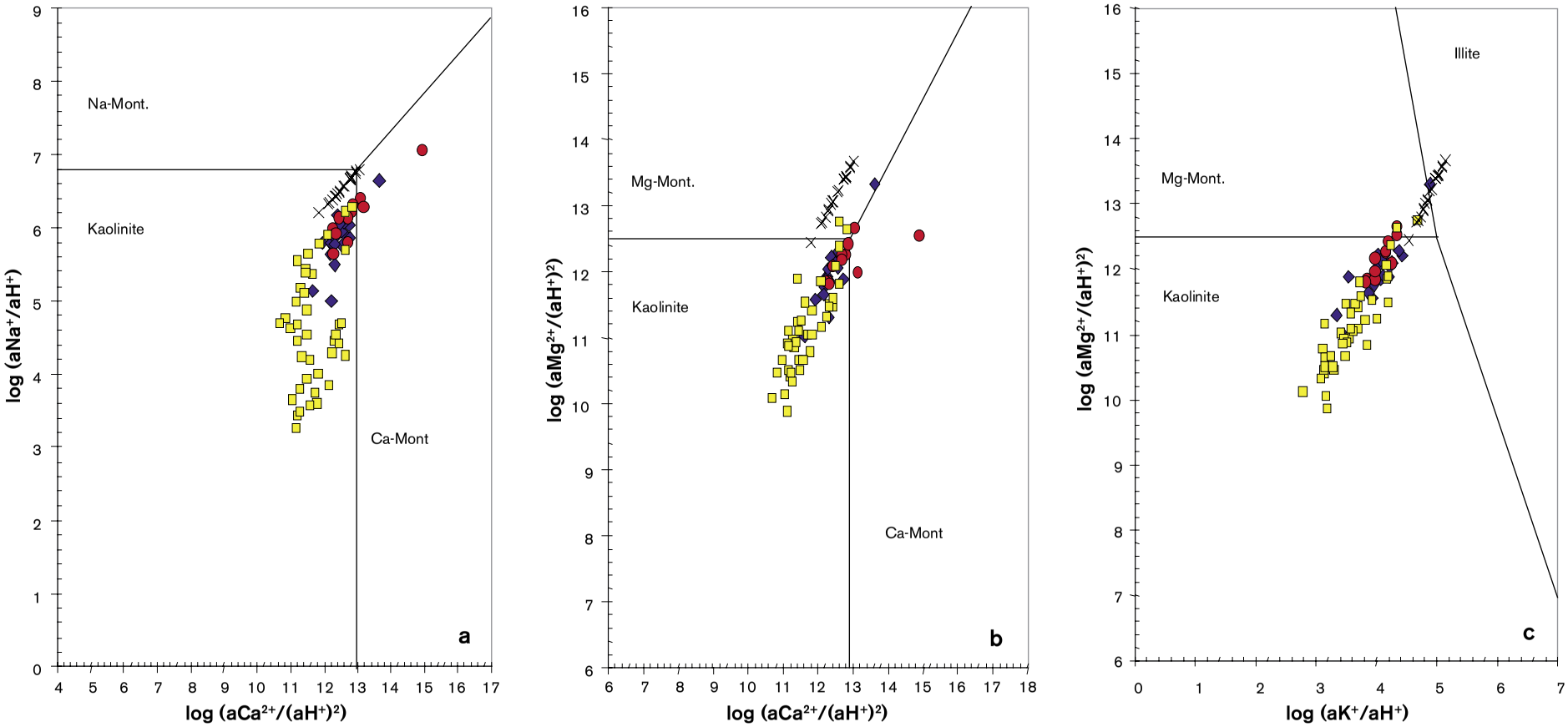

Figure AD-3. *Plot of the Forsmark representative waters in the aqueous activity diagrams for some aluminosilicate minerals at 7ºC, 1 bar. The field boundaries were calculated with data from /Helgeson, 1969/ and a logarithmic silica activity of −4. The legend in shown in next figure.*

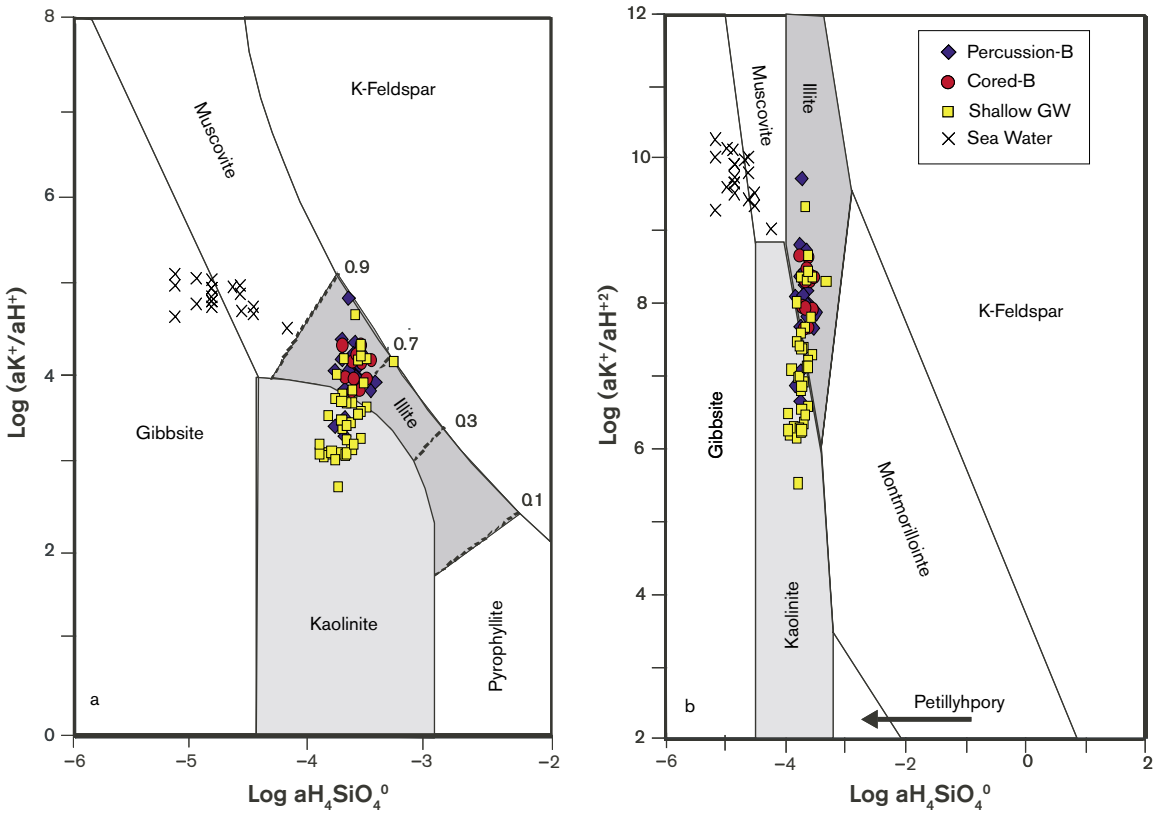

Figure AD-4. *Plot of the Forsmark representative waters in aqueous activity diagrams for some aluminosilicate minerals at 25°C, 1 bar, including illite. The field boundaries have been calculated with data from /Helgeson, 1969; and Helgeson et al. 1978/ in graph (a) and from /Garrels, 1984/ in graph (b). In graph (a) illite field is contoured to show the stability of different illite fractios in I/S.*

Appendix E

Analytical data for redox pairs calculations

When selecting the samples for the redox characterization, the main selection criteria has been the availability of analytical data for the redox elements Fe^{2+}, S^{2-} and CH_4. Special attention was paid to samples with CH_4 data as the redox pair CH_4/CO_2 was successfully applied in Simpevarp 1.2 /SKB, 2004/.

The quality of the analytical data was checked by comparing the concentration of the redox elements with their respective detection limits. The information about detection limits was not supplied with the 1.2 data freeze, thus, previous reports that include the same samples were consulted /Smellie and Laaksoharju, 1992; Laaksoharju et al. 1995/.

Aqueous redox-active species in Forsmark samples (see the table with the complete chemical analysis in this issue) are in sufficient concentrations for a successful Eh calculation. Total sulphide concentrations are low but above detection limit, with values between $3 \cdot 10^{-7}$ and $1.9 \cdot 10^{-6}$ mol/l; total iron concentrations are between $4.6 \cdot 10^{-7}$ and $3.3 \cdot 10^{-5}$ mol/l, above the theoretical lower limit of iron concentration for a successful Eh measurement if iron pairs control the redox potential (10^{-6} mol /l, /Grenthe et al. 1992/). Sample 4538 has a value of –0.03 mg/l in the S^{2-} column, indicating that its concentration is below detection limit. However, the same sample in 1.1 data freeze has very low, but apparently significative, S^{2-} values (between 0.01 and 0.02 mg/L). Also, /Wacker et al. 2003/ reported a sulphide value of 0.01 mg/L for this sample. There is no indication of the detection limit for this element, but in previous works a value of 0.01 mg/L has been reported. As a consequence, in this report a value of 0.01 mg/L has been chosen as the detection limit of sulphide.

Appendix 4

Water classification, M3 calculations and DIS modelling

Contribution to the model version 1.2

Ioana Gurban, 3D-Terra, Montreal

Marcus Laaksoharju, Geopoint AB, Stockholm

December 2004

Contents

1 Introduction

This paper presents the results of the water classification, mixing modelling, 3D visualisation and drilling impact study (DIS).

2 Water type classification

A classical geochemical evaluation and modelling tool AquaChem was used for water type classification of the Forsmark 1.2 samples. The aim of water classification is to simplify the groundwater information. First the data set was divided into different salinity classes. Except for sea waters, most surface waters and some groundwaters from percussion boreholes are fresh waters according to the classification used for Äspö groundwaters. The rest of the groundwaters are brackish (Cl < 5,000 mg/L), except for the deeper samples which are saline (> 5,000 mg/L). Most surface waters are of Ca-HCO_3 or Na-Ca-HCO_3 type and naturally the sea water is of Na-Cl type. The deeper groundwaters are mainly of Na-Ca-Cl type. These water classes are illustrated by using different standard plots in Figure 2-1 and the results are listed for all samples in Appendix 1.

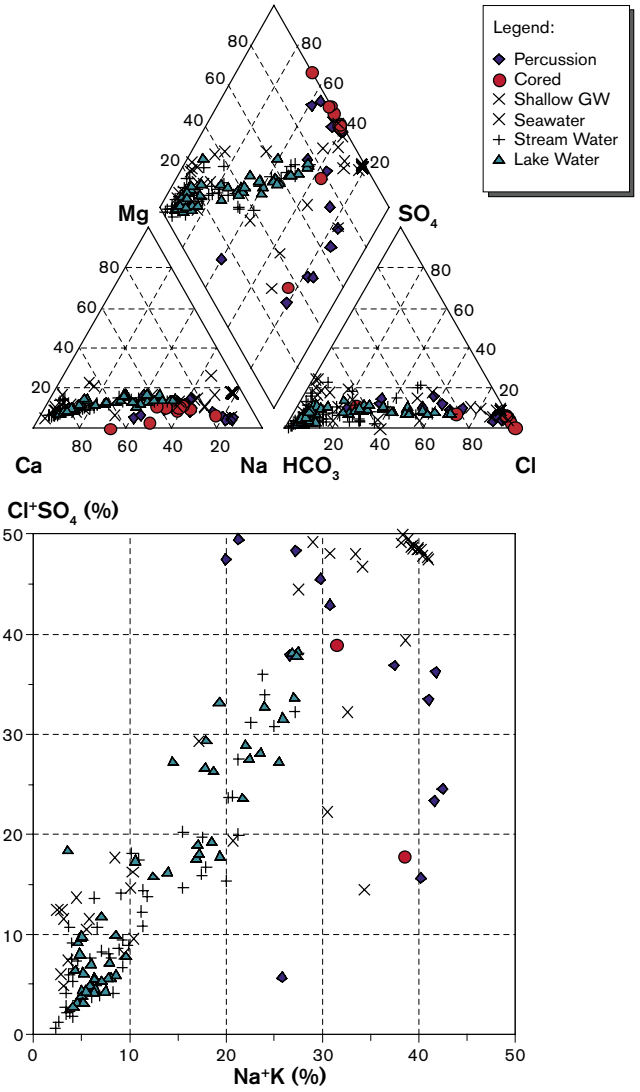

Figure 2-1. *Multicomponent plots used for classification of the data. From top to bottom: Piper plot and Ludwig-Langelier plot applied on all Forsmark data using AquaChem.*

3 Descriptive and quantitative modelling by using M3 code

3.1 M3 modelling

A challenge in groundwater modelling is to reveal the origin, mixing and reactions altering the groundwater samples. The groundwater modelling concept M3 (Multivariate Mixing and Mass-balance calculations) /Laaksoharju and Skårman, 1995; Laaksoharju et al. 1999b/ can be used for making judgment on this.

3.1.1 Introduction and model description

In M3 modelling the assumption is that the groundwater is always a result of mixing and reactions. M3 modelling uses a statistical method to analyse variations in groundwater compositions so that the mixing components, their proportions, and chemical reactions are revealed. The method quantifies the contribution to hydrochemical variations by mixing of groundwater masses in a flow system by comparing groundwater compositions to identified reference waters. Subsequently, contributions to variations in non-conservative solutes from reactions are calculated.

The M3 method has been tested, evaluated, compared with standard methods and modified over several years within domestic and international research programmes supported by the SKB. The main test and application site for the model has been the Äspö HRL /Laaksoharju and Wallin, 1997; Laaksoharju et al. 1999c/. Mixing seems to play an important role at many crystalline and sedimentary rock sites where M3 calculations have been applied such as in different Swedish sites /Laaksoharju et al. 1998/, Canada /Smellie and Karlsson, 1996/, Oklo in Gabon /Gurban et al. 1998/ and Palmottu in Finland /Laaksoharju et al. 1999a/.

The features of the M3 method are:

- It is a mathematical tool which can be used to evaluate groundwater field data, to help construct a conceptual model for the site and to support expert judgement for site characterisation.
- It uses the entire hydrochemical data set to construct a model of geochemical evolution, in contrast to a thermodynamic model that simulates reactions or predicts the reaction potential for a single water composition.
- The results of mixing calculations can be integrated with hydrodynamic models, either as a calibration tool or to define boundary conditions.
- Experience has shown that to construct a mixing model based on physical understanding can be complicated especially at site scale. M3 results can provide additional information of the major flow paths, flow directions and residence times of the different groundwater types which can be valuable in transport modelling.
- The numerical results of the modelling can be visualised and presented for non-expert use.

The M3 method consists of 4 steps where the first step is a standard principal component analysis (PCA), selection of reference waters, followed by calculations of mixing proportions, and finally mass balance calculations (for more details see /Laaksoharju et al. 1999b; Laaksoharju, 1999/).

In the present Forsmark 1.2 phase the version 1.1 /Laaksoharju et al. 2004/ is up-dated with the new available data. For Forsmark 1.2 phase, 2 models are constructed: at regional scale and at local scale. 367 samples from Forsmark 1.2 met the M3 criteria (data for major elements and isotopes) and were used in the M3 modelling. These samples were from boreholes (core and percussion), soil pipes (shallow and near surface groundwater), lake water, sea water, running water and precipitation. From the 367 samples available, 182 are considered representative from hydrochemical point of view and 185 non representative.

3.2 Regional model

The PCA applied to Forsmark data and all Nordic Sites data is illustrated in Figure 7. 367 samples from Forsmark site were used. Numerical values are listed in Appendix 2. Figure 3-1 shows a surface trend (winter – summer precipitation) and a marine trend showing possible Baltic Sea/ Litorina influences.

The reference waters used are:

- **Brine type of reference water:** Represents the sampled deep brine type (Cl = 47,000 mg/L) of water found in KLX02: 1,631–1,681 m /Laaksoharju et al. 1995/. An old age for the Brine is suggested by the measured ^{36}Cl values indicating a minimum residence time of 1.5 Ma for the Cl component /Laaksoharju and Wallin, 1997/.
- **Glacial reference water:** Represents a possible melt-water composition from the last glaciation > 13,000 BP. Modern sampled glacial melt water from Norway was used for the major elements and the $\delta^{18}O$ isotope value (−21‰ SMOW) was based on measured values of $\delta^{18}O$ in calcite surface deposits /Tullborg, 1984/. The $\delta^{2}H$ value (−158‰ SMOW) is a modelled value based on the equation ($\delta H = 8 \times \delta^{18}O + 10$) for the meteoric water line.
- **Littorina Water:** Represents modelled Litorina water (see Table 3-1).
- **Modified Sea water (Sea sediment):** Represents Baltic Sea affected by microbial sulphate reduction.
- **Precipitation water:** Corresponds to infiltration of meteoric water (the origin can be rain or snow) from 1960. Sampled modern meteoric water with a modelled high tritium (100 TU) content was used to represent precipitation from that period.

For groundwater analytical data see Table 3-1.

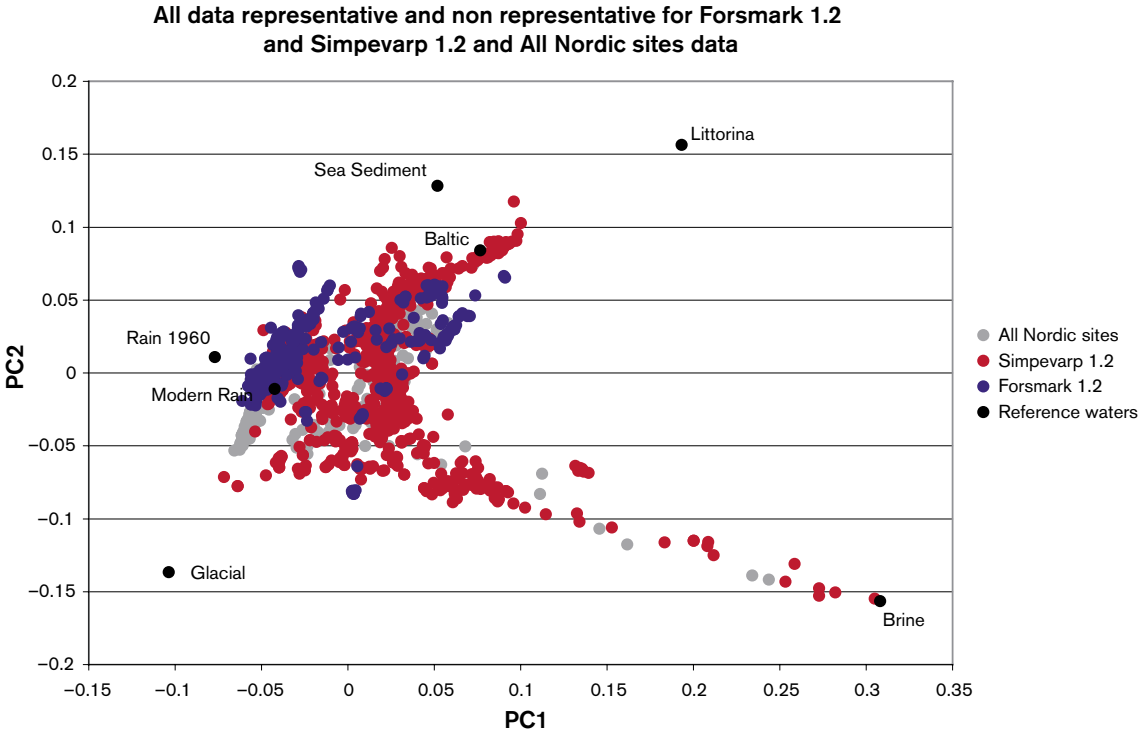

Figure 3-1. *The picture shows the principal components analysis and the identification of the reference waters. (Variance: First principal component: 0.39503, First and second principal components: 0.65743, First, second and third principal components: 0.76059). The figure shows the All Nordic sites data available (in grey circles), the Forsmark 1.2 representative and non representative data (in blue) and Simpevarp 1.2 representative and non representative data (in red). The Sea sediment, Littorina, Brine, Glacial and Rain60' reference waters are used as end members for the modeling.*

Table 3-1. Groundwater analytical or modelled data* used as reference waters in the M3 regional modelling for Forsmark.

	Cl (mg/L)	Na (mg/L)	K (mg/L)	Ca (mg/L)	Mg (mg/L)	HCO_3 (mg/L)	SO_4 (mg/L)	3H (TU)	δ^2H ‰	$\delta^{18}O$ ‰
Brine	47,200	8,500	45.5	19,300	2.12	14.1	906	0	–44.9	–8.9
Glacial	0.5	0.17	0.4	0.18	0.1	0.12	0.5	0	–158*	–21*
Littorina sea*	6,500	3,674	134	151	448	93	890	0	–38	–4.7
Sea Sediment	3,383	2,144	91.8	103	258	793	53.1	0	–61	–7
Baltic	3,760	1,960	95	234	93.7	90	325	20	–53.3	–5.9
Rain 1960	0.23	0.4	0.29	0.24	0.1	12.2	1.4	2,000	–80	–10.5
Modern Rain	0.23	0.4	0.29	0.24	0.1	12.2	1.4	20	–80	–10.5

The reference waters chosen are identification rows in Appendix 2:

- Brine (identification row 368).
- Littorina (identification row 370).
- Sea sediment (identification row 371).
- Rain’60 (identification row 373).
- Glacial (row 369).

The following six reactions have been considered, with comments on the qualitative outcomes of mixing and mass balance modeling with M3:

1. *Organic decomposition:* This reaction is detected in the unsaturated zone associated with Meteoric water. This process consumes oxygen and adds reducing capacity to the groundwater according to the reaction: $O_2 + CH_2O \rightarrow CO_2 + H_2O$. M3 reports a gain of HCO_3 as a result of this reaction.
2. *Organic redox reactions:* An important redox reaction is reduction of iron III minerals through oxidation of organic matter: $4Fe(III) + CH_2O + H_2O \rightarrow 4Fe^{2+} + 4H^+ + CO_2$. M3 reports a gain of Fe and HCO_3 as a result of this reaction. This reaction takes place in the shallow part of the bedrock associated with influx of Meteoric water.
3. *Inorganic redox reaction:* An example of an important inorganic redox reaction is sulphide oxidation in the soil and the fracture minerals containing pyrite according to the reaction: $HS^- + 2O_2 \rightarrow SO_4^{2-} + H^+$. M3 reports a gain of SO_4 as a result of this reaction. This reaction takes place in the shallow part of the bedrock associated with influx of Meteoric water.
4. *Dissolution and precipitation of calcite:* There is generally a dissolution of calcite in the upper part and precipitation in the lower part of the bedrock according to the reaction: $CO_2 + CaCO_3 \rightarrow Ca^{2+} + 2HCO_3^-$. M3 reports a gain or a loss of Ca and HCO_3 as a result of this reaction. This reaction can take place in any groundwater type.
5. *Ion exchange:* Cation exchange with Na/Ca is a common reaction in groundwater according to the reaction: $Na_2X_{(s)} + Ca^{2+} \rightarrow CaX_{(s)} + 2Na^+$, where X is a solid substrate such as a clay mineral. M3 reports a change in the Na/Ca ratios as a result of this reaction. This reaction can take place in any groundwater type.
6. *Sulphate reduction:* Microbes can reduce sulphate to sulphide using organic substances in natural groundwater as reducing agents according to the reaction: $SO_4^{2-} + 2(CH_2O) + OH^- \rightarrow HS^- + 2HCO_3^- + H_2O$. This reaction is of importance since it may cause corrosion of the copper capsules. Vigorous sulphate reduction is generally detected in association with marine sediments that provide the organic material and the favorable salinity interval for the microbes. M3 reports a loss of SO_4 and a gain of HCO_3 as a result of this reaction. This reaction modifies the seawater composition by increasing the HCO_3 content and decreasing the SO_4 content.

3.3 Local model

The local model was built with only data from the Forsmark site. The PCA applied on Forsmark data is illustrated in Figure 3-5 and 3-6. Figure 3-2 and 3-3 show a similar trend as Figure 2 but with a higher resolution.

The reference waters chosen are identification rows used in Appendix 2:

- Brine (identification row 368).
- Littorina (identification row 370).
- Sea sediment (identification row 371).
- Rain'60 (identification row 373).
- Glacial (row 369).

For groundwater analytical data see Table 3-1.

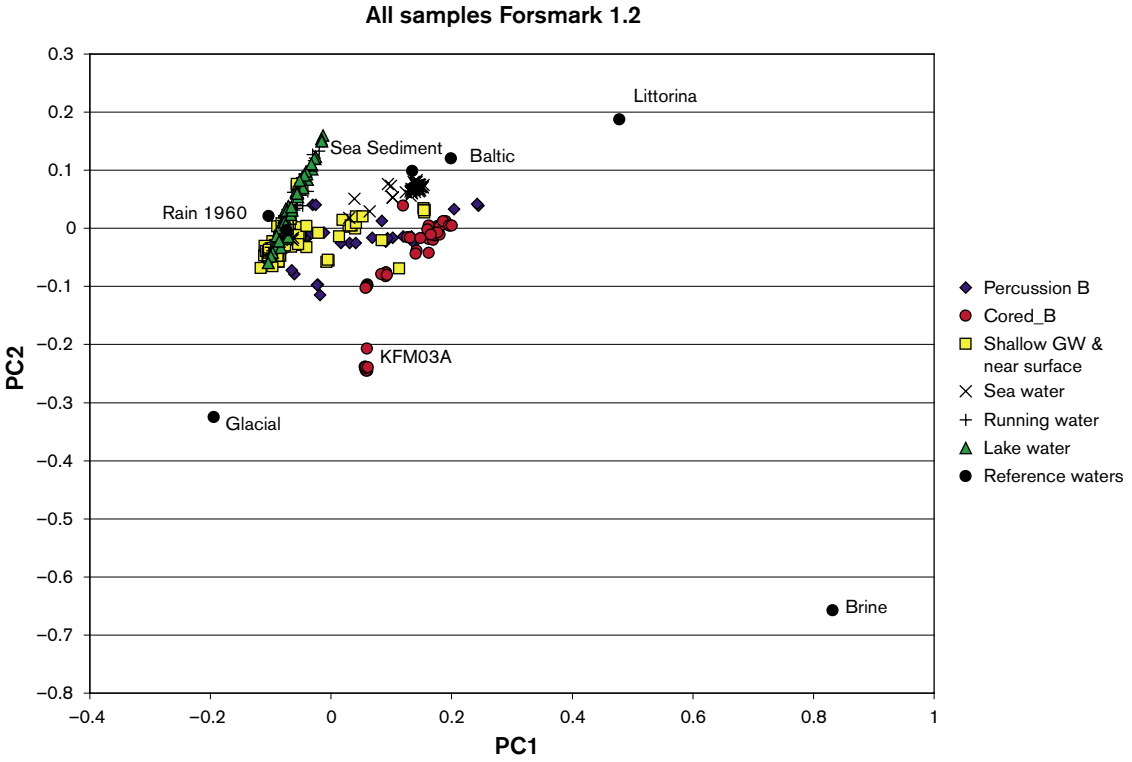

Figure 3-2. *The picture shows the PCA for the local model for Forsmark. The picture shows the principal components analysis and the identification of the reference waters. (Variance: First principal component: 0.46593, First and second principal components: 0.67811, First, second and third principal components: 0.79906). The picture shows the distribution of the boreholes (core and percussion), shallow and near surface groundwaters, lake water, sea water and running water. The Littorina, Brine, Glacial and Rain60' are used as reference waters for the modelling. In order to compare the results of the M3 modelling with the hydrogeological model it was decided to use the same reference waters as for the regional model.*

3.4 Alternative models

In order to better understand the data distribution and resolution, one other model was tested for the regional model. Figure 3-4 shows the distribution of All Nordic representative data, the Forsmark 1.2 and Simpevarp 1.2 representative data. Figures 3-1 and 3-4 show similar trends and data distribution. However, due to the fact that M3 is a statistical code it is better to include as many observations as possible in order to meet the M3 criteria.

3.5 Selected model

The local, regional and alternative models were analysed and compared. Due to the fact that the Forsmark 1.2 data do not include enough deep boreholes and to be able to compare the results with the hydrogeological model, the mixing proportions obtained from the regional model (Section 3.2) were used in the following analyses: visualisation along the boreholes and Tecplot 2D/3D visualisation. For the comparison of M3 and M4 codes, both local and regional models were used. The regional M4 model employs only 27% of the data employed by M3, it was therefore decided to make the M3/M4 comparison with the local scale model.

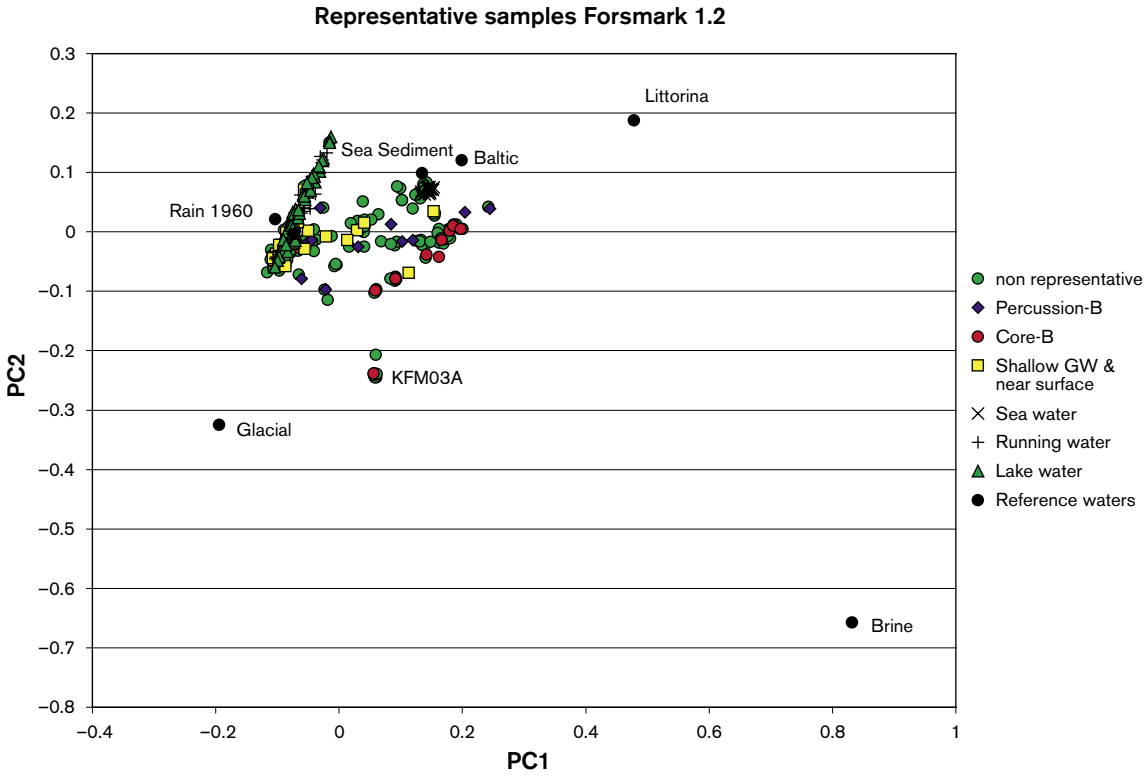

Figure 3-3. *The picture shows the PCA for the local model for Forsmark. The picture shows the principal components analysis and the identification of the reference waters. (Variance: First principal component: 0.46593, First and second principal components: 0.67811, First, second and third principal components: 0.79906). The picture shows the distribution of the representative data (182 samples), classified in boreholes (core and percussion), shallow and near surface groundwaters, lake water, sea water and running water and non-representative data(185 samples) represented in green.*

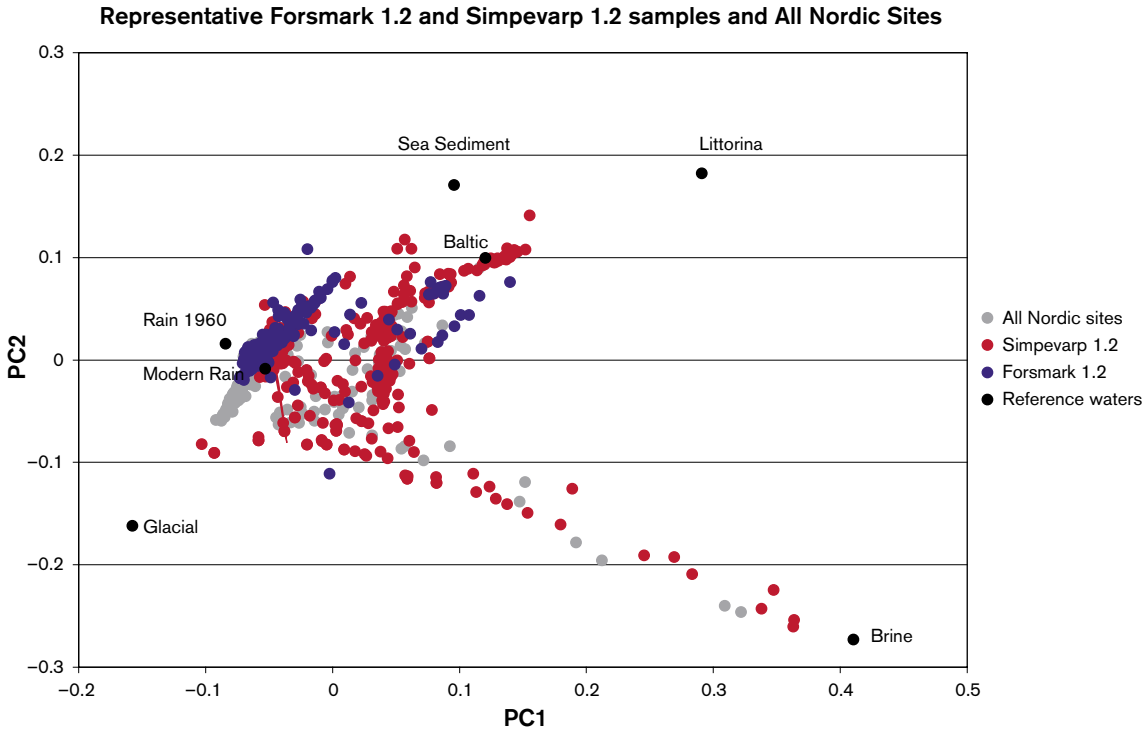

Figure 3-4. *The picture shows the principal components analysis and the identification of the reference waters. (Variance: First principal component: 0.4121, First and second principal components: 0.65696, First, second and third principal components: 0.76402). The figure shows only the representative All Nordic data (in grey circles), the Forsmark 1.2 representative data (in blue) and Simpevarp 1.2 representative data (in red). The Sea sediment, Littorina, Brine, Glacial and Rain60' reference waters are used as end members for the modelling.*

3.6 Scatter plots of M3 modelling results

The measured Cl content, the TDS (SumIons) and the calculated M3 mixing proportions are shown for various core boreholes within the modelling domain (see Figure 3-5 to 3-8 and Appendix 3). A mixing proportion of less than 10% is regarded as being under the detection limit of the method and is therefore shaded. The mixing proportions have an uncertainty range of ±0.1 mixing units. The purpose of the visualization is to compare the hydrochemical results (Cl, TDS, mixing proportions) with the hydrogeological results. Due to the fact that the hydrogeologists use only 4 reference waters (meteoric, glacial, brine and Littorina), the marine components (Littorina and Sea Sediment reference waters) were added together and named Marine water. Therefore the four reference waters presented in the following pictures are meteoric, glacial, brine and marine (marine water = Littorina + Sea sediment mixing proportions). The appendix 4 lists the Cl content, the TDS (SumIons) and M3 mixing proportions for all percussion and core boreholes available in Forsmark 1.2 data set. The representative samples are yellow labelled in the table. A red circle in the graphs indicates the representative samples.

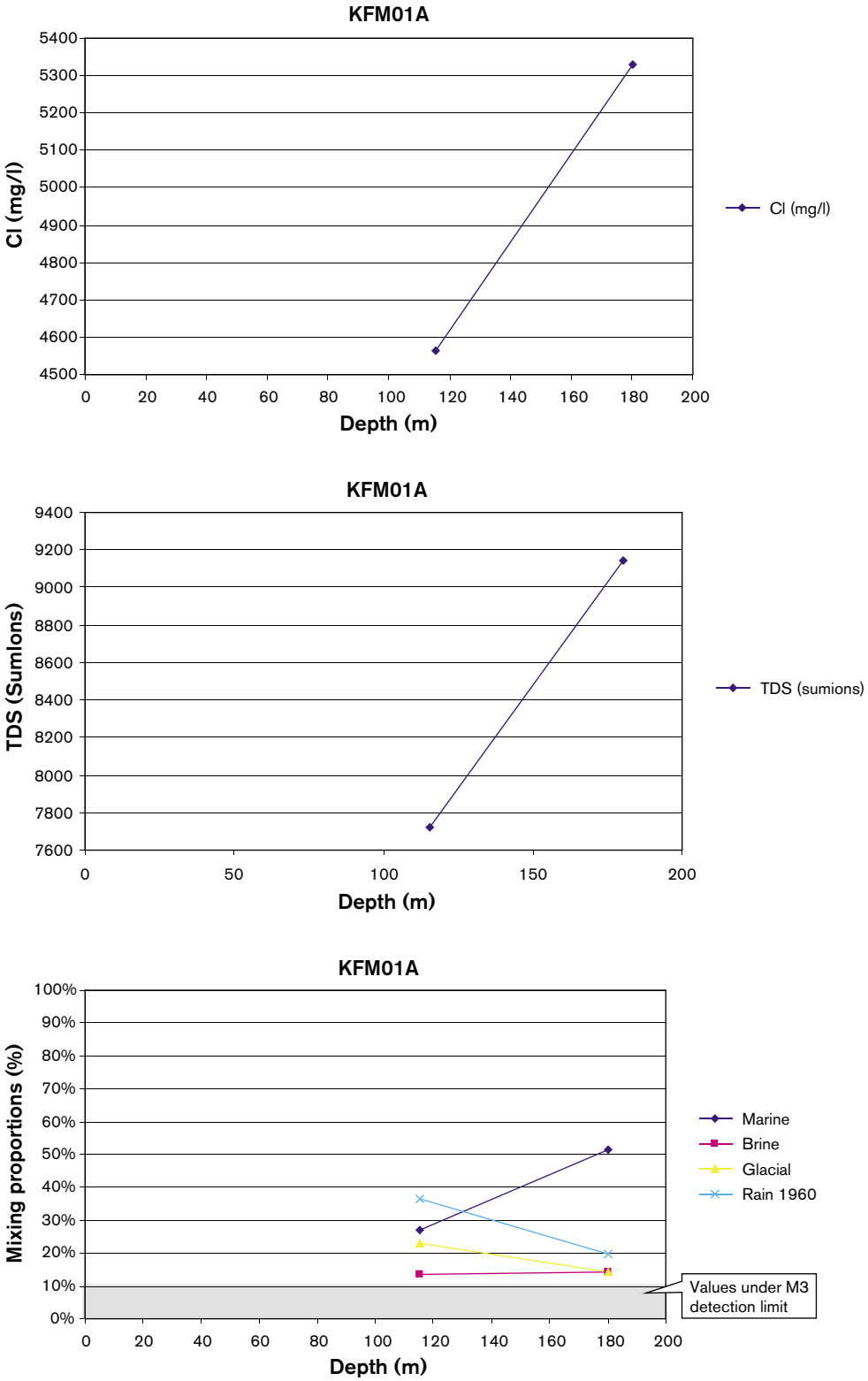

Figure 3-5. *The measured Cl content is shown in the uppermost figure, the TDS (Sum Ions) in the middle picture and the calculated M3 mixing proportions in the lowermost figure along borehole KFM01A.*

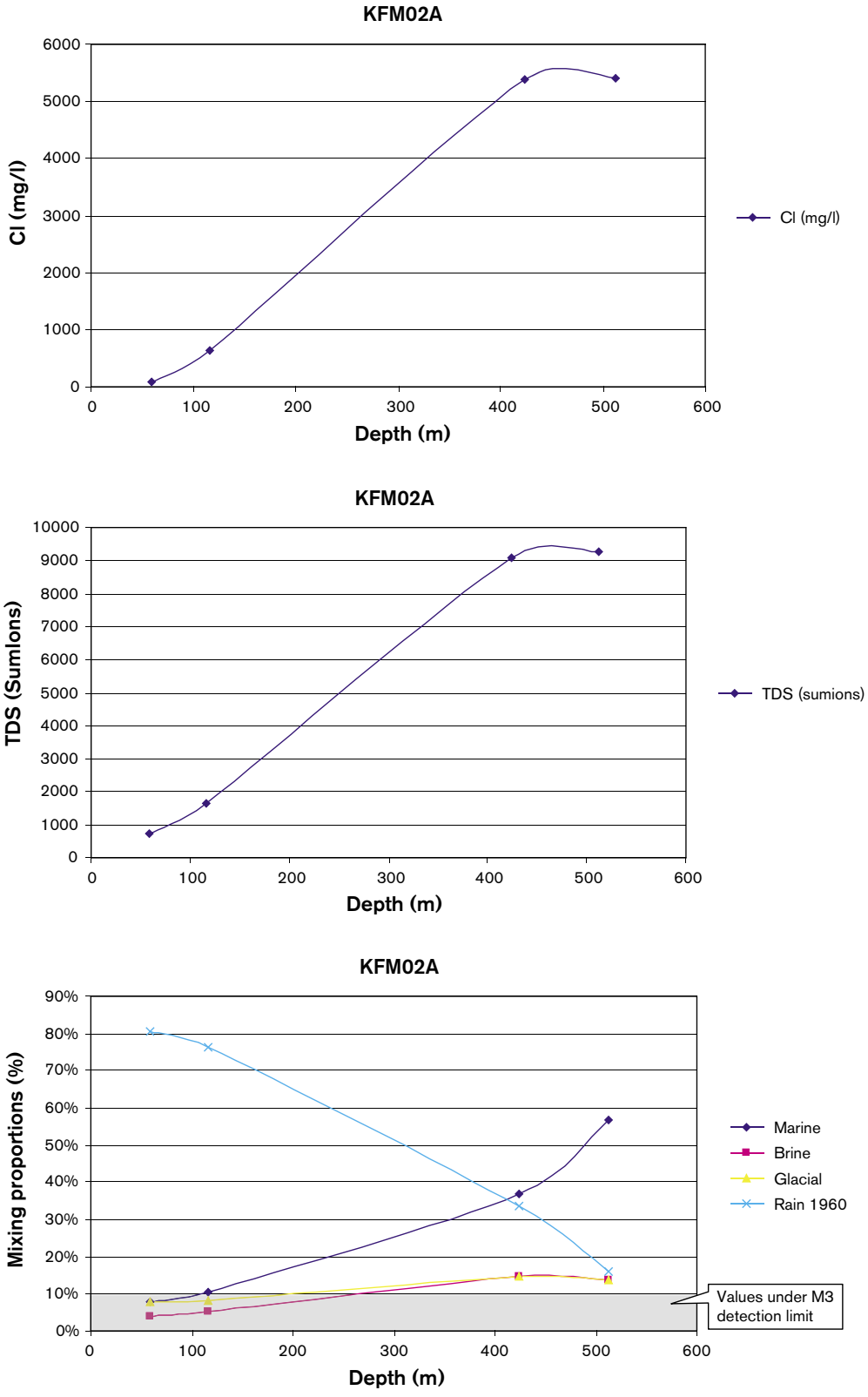

Figure 3-6. *The measured Cl content is shown in the uppermost figure, the TDS (Sum Ions) in the middle picture and the calculated M3 mixing proportions in the lowermost figure along borehole KFM02A.*

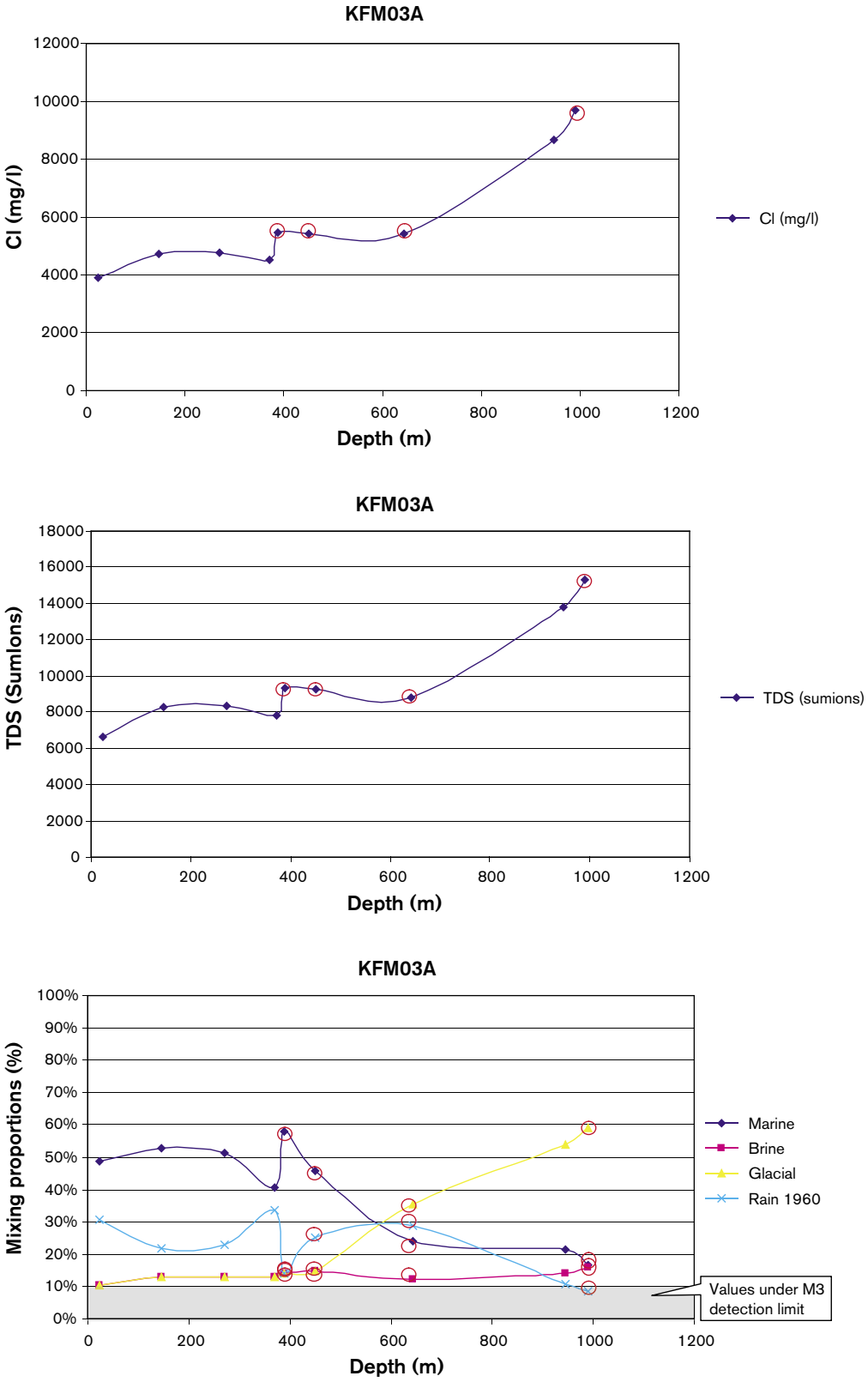

Figure 3-7. *The measured Cl content is shown in the uppermost figure, the TDS (Sum Ions) in the middle picture and the calculated M3 mixing proportions in the lowermost figure along borehole KFM03A.*

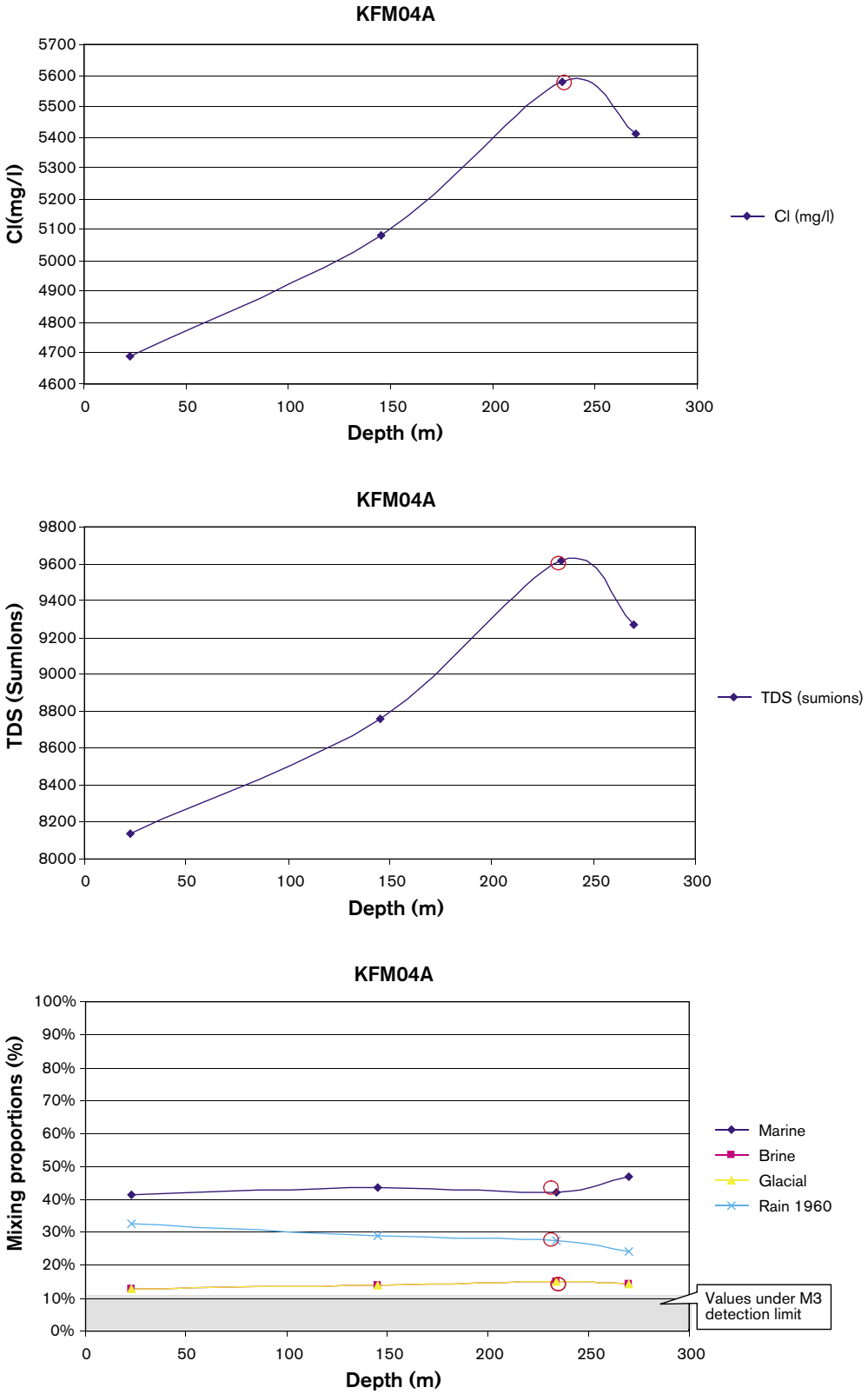

Figure 3-8. *The measured Cl content is shown in the uppermost figure, the TDS (Sum Ions) in the middle picture and the calculated M3 mixing proportions in the lowermost figure along borehole KFM04A.*

4 Site specific hydrogeochemical uncertainties

At every phase of the hydrogeochemical investigation programme – drilling, sampling, analysis, evaluation, modelling – uncertainties are introduced which have to be accounted for, addressed fully and clearly documented to provide confidence in the end result, whether it will be the site descriptive model or repository safety analysis and design /Smellie et al. 2002/. Handling the uncertainties involved in constructing a site descriptive model has been documented in detail by /Andersson et al. 2001/. The uncertainties can be conceptual uncertainties, data uncertainty, spatial variability of data, chosen scale, degree of confidence in the selected model, and error, precision, accuracy and bias in the predictions. Some of the identified uncertainties recognized during the Forsmark modelling exercise and during the DIS exercise are discussed below.

The following data uncertainties have been estimated, calculated or modelled:

- Drilling; may be ± 10–70%.
- Effects from drilling during sampling; is < 5%.
- Sampling; may be ± 10%.
- Influence associated with the uplifting of water; may be ± 10%.
- Sample handling and preparation; may be ± 5%.
- Analytical error associated with laboratory measurements; is ± 5%.
- Mean groundwater variability at Forsmark during groundwater sampling (first/last sample); is about 25%.
- The M3 model uncertainty; is ± 0.1 units within 90% confidence interval.

Conceptual errors can occur from e.g. the paleohydrogeological conceptual model. The influences and occurrences of old water end-members in the bedrock can only be indicated by using certain element or isotopic signatures. The uncertainty is therefore generally increasing with the age of the end-member. The relevance of an end-member participating in the groundwater formation can be tested by introducing alternative end-member compositions or by using hydrodynamic modeling to test if old water types can resign in the bedrock during prevailing hydrogeological conditions.

4.1 Model uncertainties

The following factors can cause uncertainties in M3 calculations:

- Input hydrochemical data errors originating from sampling errors caused by the effects from drilling, borehole activities, extensive pumping, hydraulic short-circuiting of the borehole and uplifting of water which changes the in-situ pH and Eh conditions of the sample, or as analytical errors.
- Conceptual errors such as wrong general assumptions, selecting wrong type/number of end-members and mixing samples that are not mixed.
- Methodological errors such as oversimplification, bias or non-linearity in the model, and the systematic uncertainty, which is attributable to use of the centre point to create a solution for the mixing model.

An example of a conceptual error is assuming that the groundwater composition is a good tracer for the flow system. The water composition is not necessarily a tracer of mixing directly related to flow since there is not a point source as there is when labelled water is used in a tracer test.

Another source of uncertainty in the mixing model is the loss of information in using only the first two principal components. The third principal component gathers generally around 10% of the groundwater information compared with the first and second principal components, which contain around 70% of the information. A sample could appear to be closer to a reference water in the 2D surface than in a 3D volume involving the third principal component. In the latest version of M3 the calculations can also be performed in 3D.

Uncertainty in mixing calculations is smaller near the boundary of the PCA polygon and larger near the center. The uncertainties have been handled in M3 by calculating an uncertainty of 0.1 mixing units (with a confidence interval of 90%) and stating that a mixing portion < 10% is under the detection limit of the method.

5 3D Visualisation of the samples location Cl, TDS and mixing proportions distribution with Tecplot

The 3D/2D visualization of the Cl, TDS and mixing proportions distribution in Forsmark was performed with Tecplot. The purpose of the visualization is to show the hydrochemical results (Cl, TDS, mixing proportions) and then to compare with the results from the hydrogeological modeling. In the Tecplot visualization the following reference waters: Marine, Rain 1960 (Meteoric), Glacial and Brine are shown.

The x, y, z coordinates represent the Easting, Northing and elevation of the midpoint of the sampling section in meters. The modeling domain was set according to the local model used in the hydrogeological modelling (Figure 5-1). The coordinates of the local model box are:

1627945.4	6701845.76	0
1630137.4	6704037.79	0
1636713.5	6697461.7	0
1634521.5	6695269.67	0
1627945.4	6701845.76	–1,100
1630137.4	6704037.79	–1,100
1636713.5	6697461.7	–1,100
1634521.5	6695269.67	–1,100

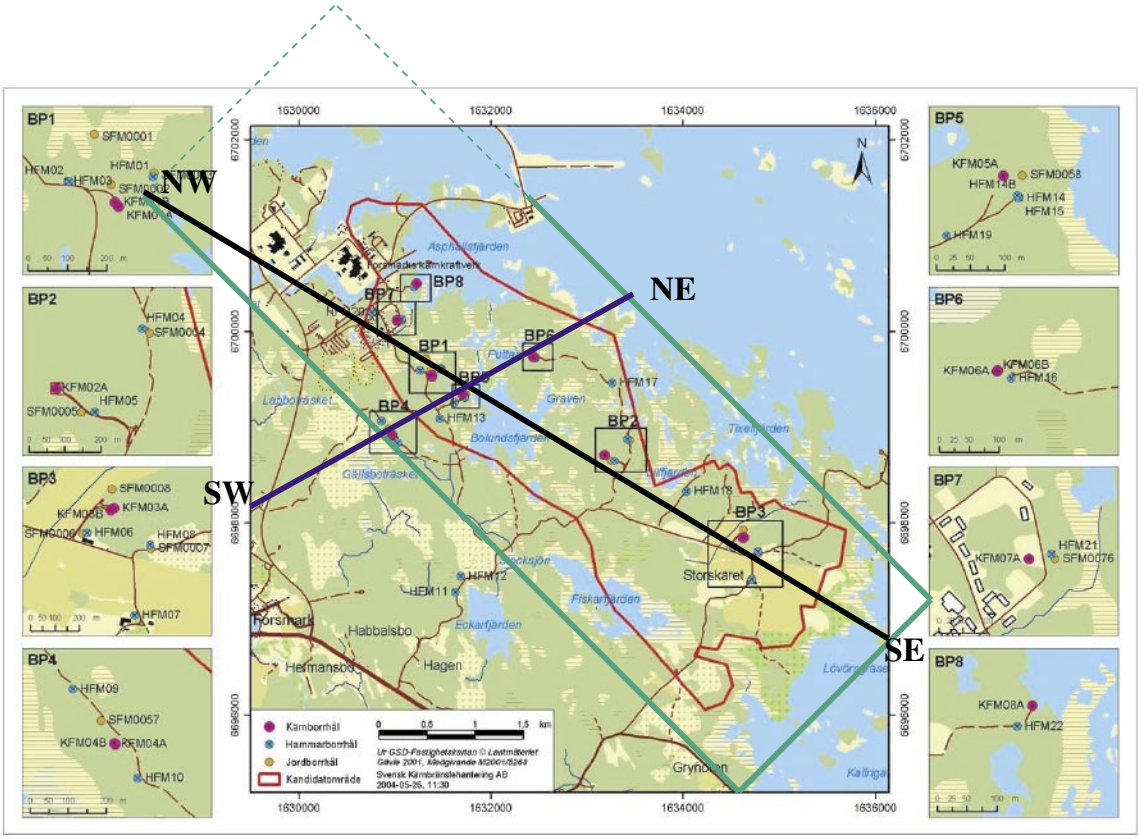

Figure 5-1. *3D/2D visualisation of the Cl sampling points in Forsmark. In black and blue are indicated the NW-SE and SW-NE vertical profiles.*

Figure 5-1 shows the locations of the sampling points used for M3 modelling. The z coordinate was not available for all the surface samples (sea, lake, streams, soil tubes). Therefore, the z coordinate was assumed to be 0. At the scale of the model, this represents an error smaller than 5%.

At the depth of –1,100 m the boundary conditions were given by the hydrodynamic model, and represent 50% brine mixing proportions, Cl = 23,600 mg/l and TDS = 40,120. Because lack of data at the model depth 1,100 m some control points were added for interpolational reason. These points also contain 50% brine, Cl = 23,600 mg/l and TDS = 40,120. The added points have the following coordinates: 1628000, 6701000; 1630000, 6702000; 1630000, 6700000; 1632000, 6701000; 1628000, 6699000; 1630000, 6697000; 1632000, 6698000; 1634000, 6697000; 1634000, 6699000; 1634000, 6702000; 1636000, 6700000; 1636000, 6698000.

The krigging method was used for the interpolation. From the modeling domain, two inclined vertical profiles were defined, one NW-SE which pass through KFM02A and KFM03A with a maximum of sampling points and another one with a SW-NE direction. The SW-NE profile passes through the KFM04 borehole. This profile will be analysed more in detail in the Forsmark 2.1 exercise when more data especially from KFM05 and KFM06 will be available. The coordinates of the profiles are:

NW-SE profile:

NW, X= 1627945.4; Y= 6701845.76

SE, X= 1636111; Y= 6696888

SW-NE profile:

SW, X= 1629520; Y= 6698129

NE, X= 1634006; Y= 6700595

The location of the sampling points used for the M3 modeling and the inclined vertical profiles are shown in Figures 5-2 to 5-7.

In the following pictures the mixing proportions presented are: Brine, Glacial, Rain 1960 (Meteoric) and Marine (Littorina + Sea Sediment mixing proportions). Figures 5-2 to 5-7 show the 2D and the 3D visualisation of all the available values (representative and non representative) based on the Forsmark 1.2 data set. Among the 336 available samples, some represent repeated sampling and have the same sampling location and the same x, y, z coordinates. Therefore, the representative samples or the latest samples in time series were selected when several samples were available for the same location. The 92 samples used for interpolation represent groundwater and surface data.

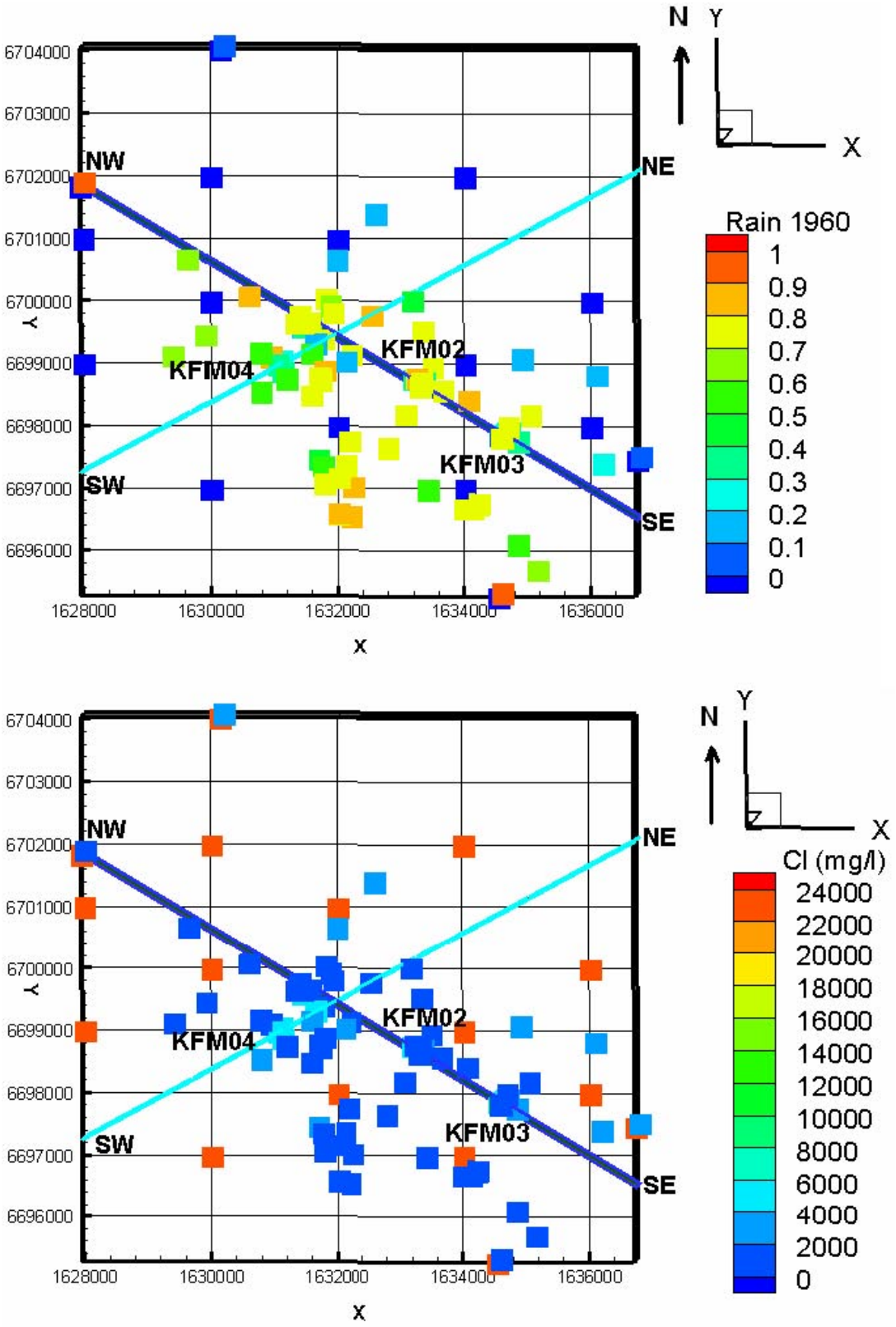

Figure 5-2. *2D visualisation (top view of the modelling box) of the Rain 1960 and the Cl distribution in Forsmark. The figures show the location of all the available samples (representative and non representative samples) and the location of the NW-SE and SW-NE inclined vertical profiles.*

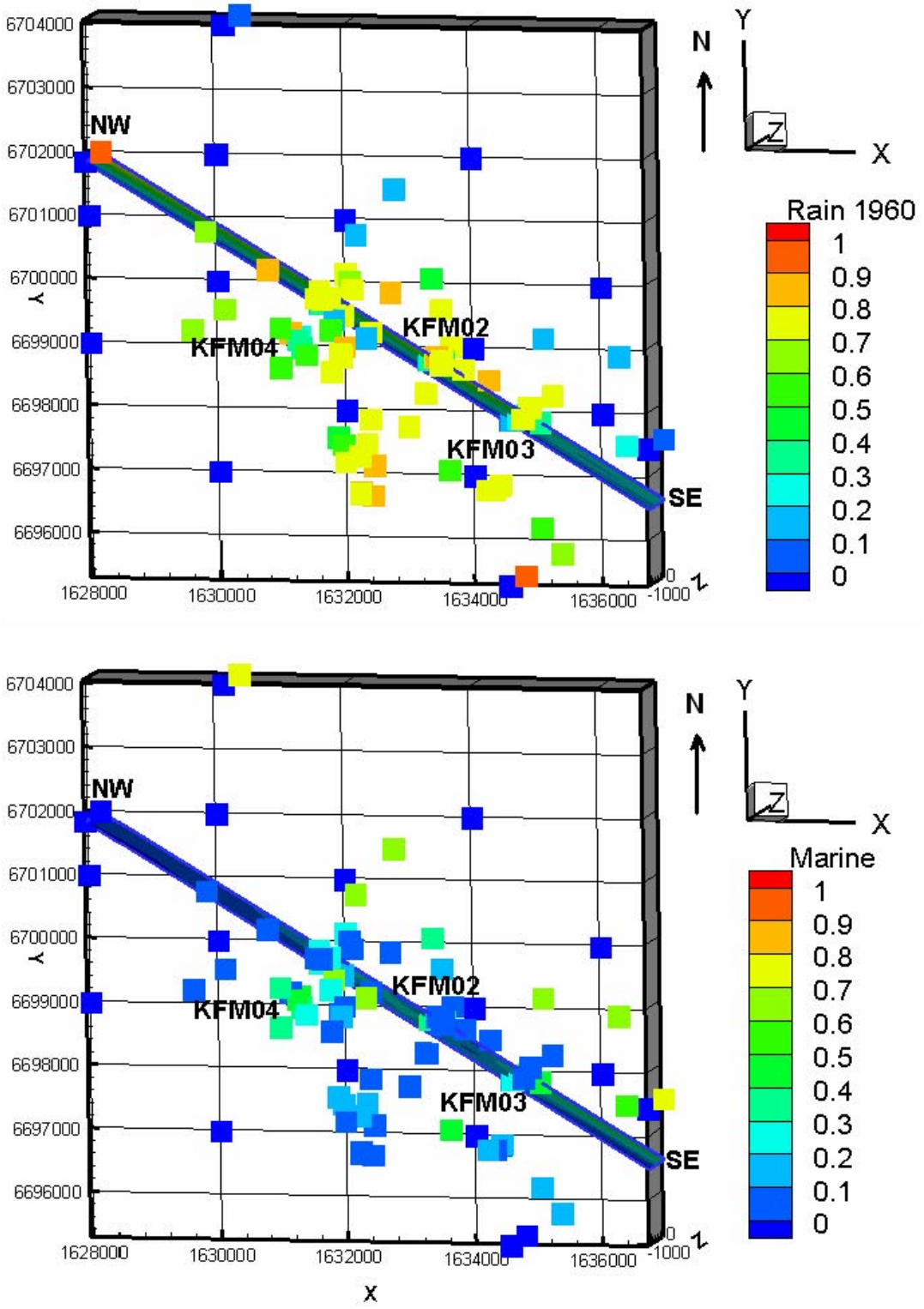

Figure 5-3. *2D/3D visualisation of the Rain 1960 and Marine distribution in Forsmark. The figure shows the location of all the available samples (representative and non representative samples) and the location of the NW-SE inclined vertical profile.*

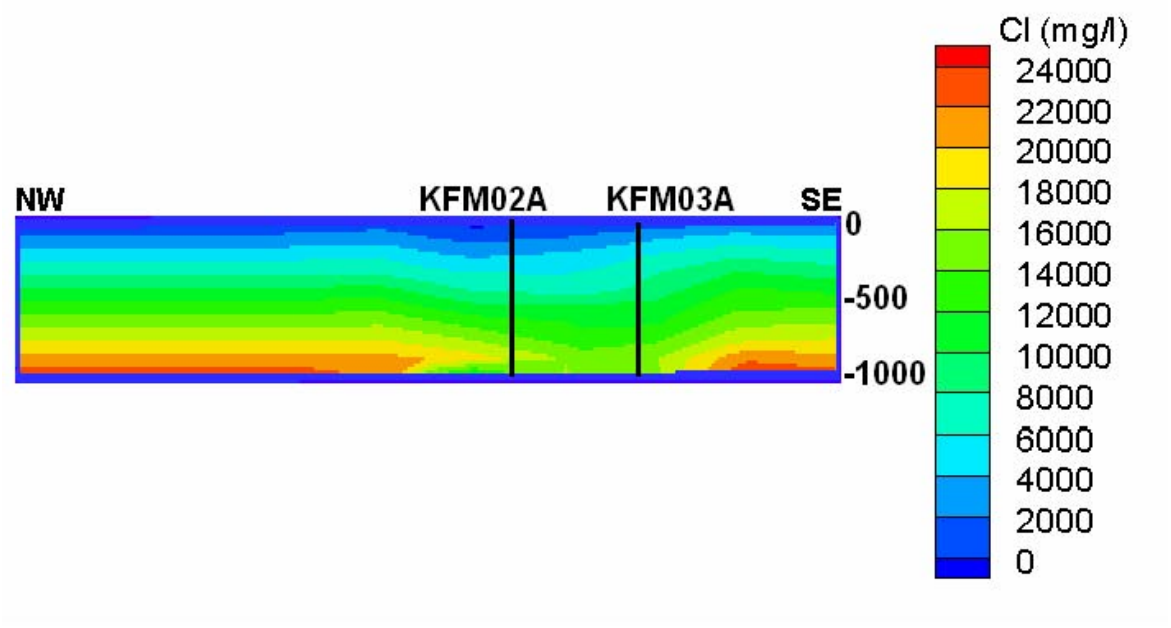

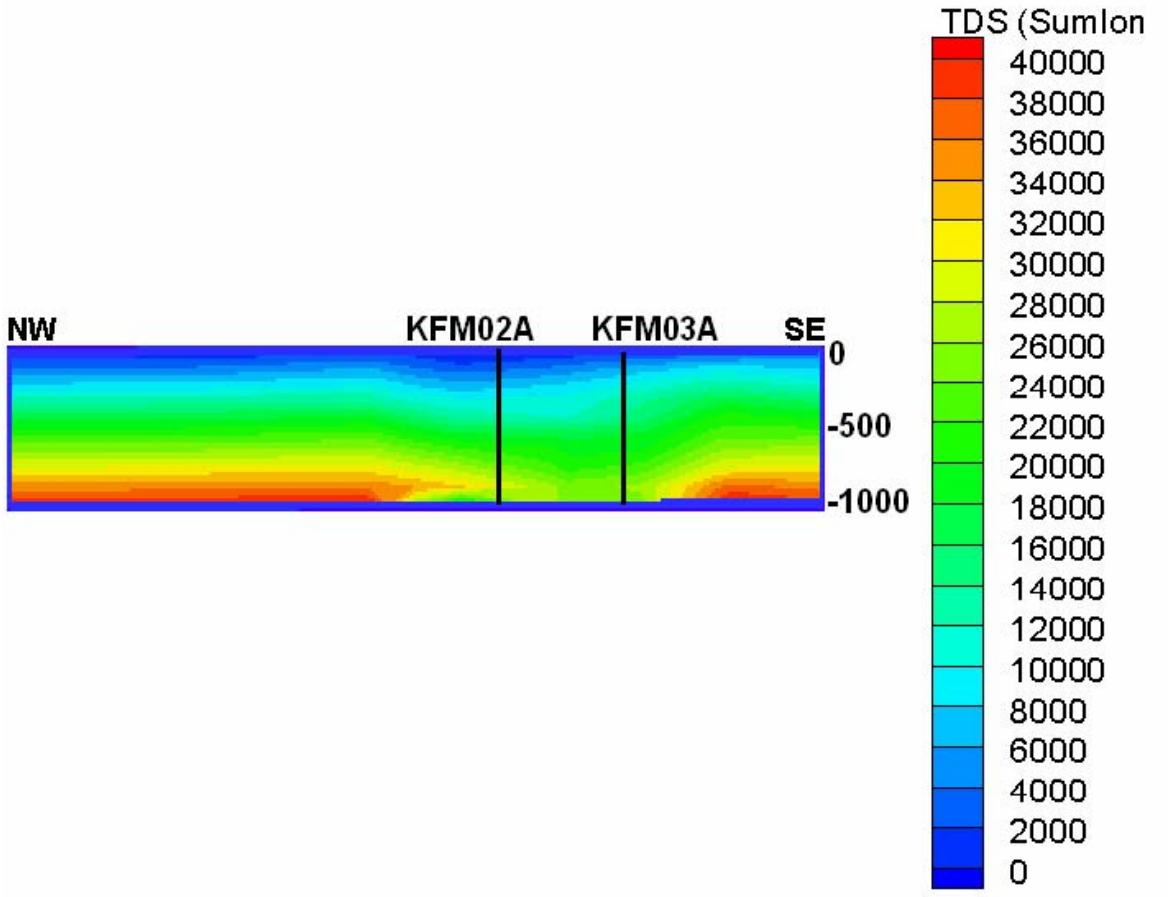

Figure 5-4. *3D visualisation of the Cl and TDS(SumIons) distribution in Forsmark. The figure shows the Cl and TDS distribution of all the available samples (representative and non representative samples) along the NW-SE inclined vertical profile. The depth scale is in metres. For visualisation purpose, the z scale is 2 times magnified compared with the length scale.*

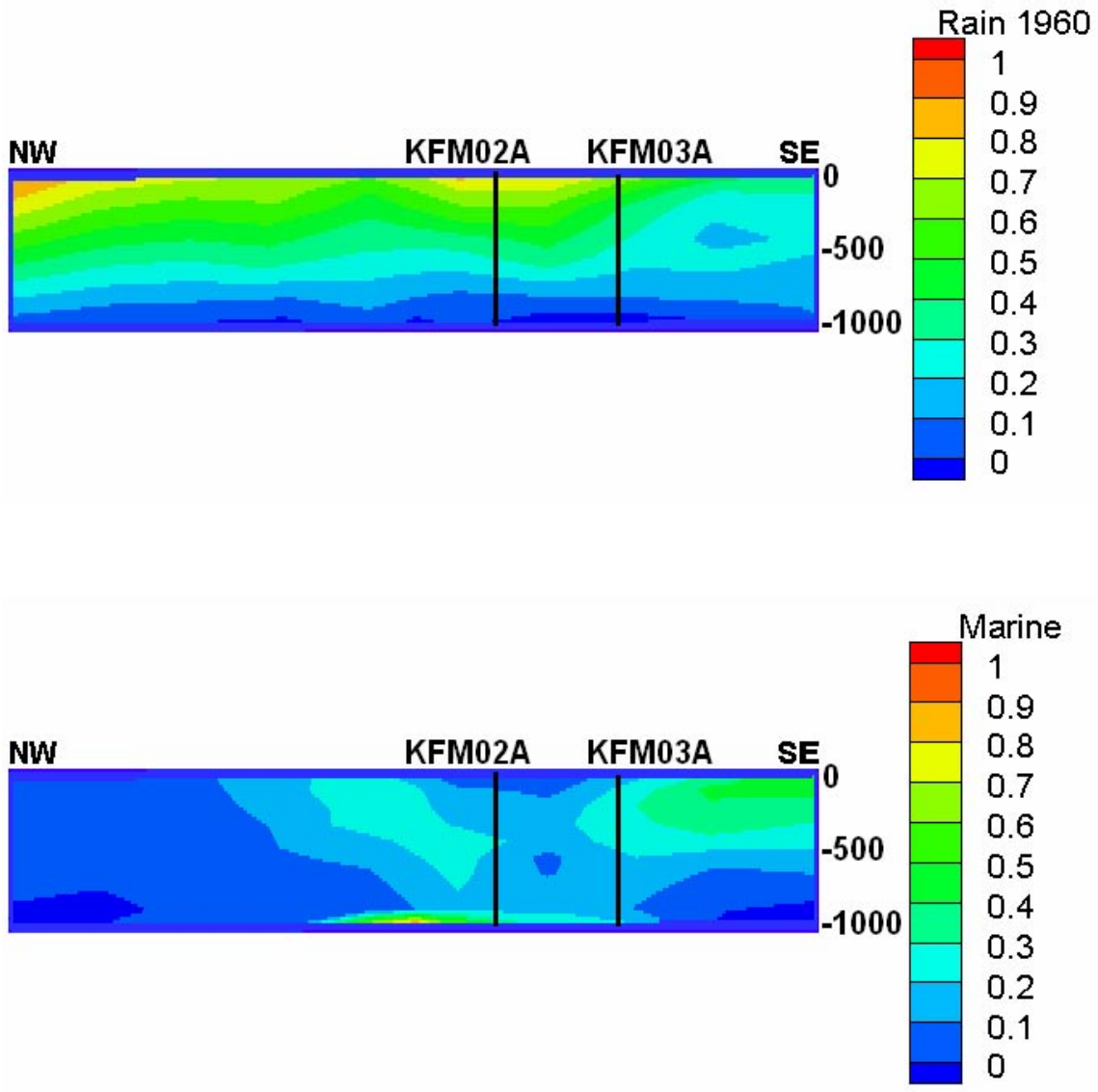

Figure 5-5. *3D visualisation of the Rain 1960 and Marine mixing proportions distribution in Forsmark. The figure shows the distribution of all the available samples (representative and non representative samples) along the NW-SE inclined vertical profile. The depth scale is in metres. For visualisation purpose, the z scale is 2 times magnified.*

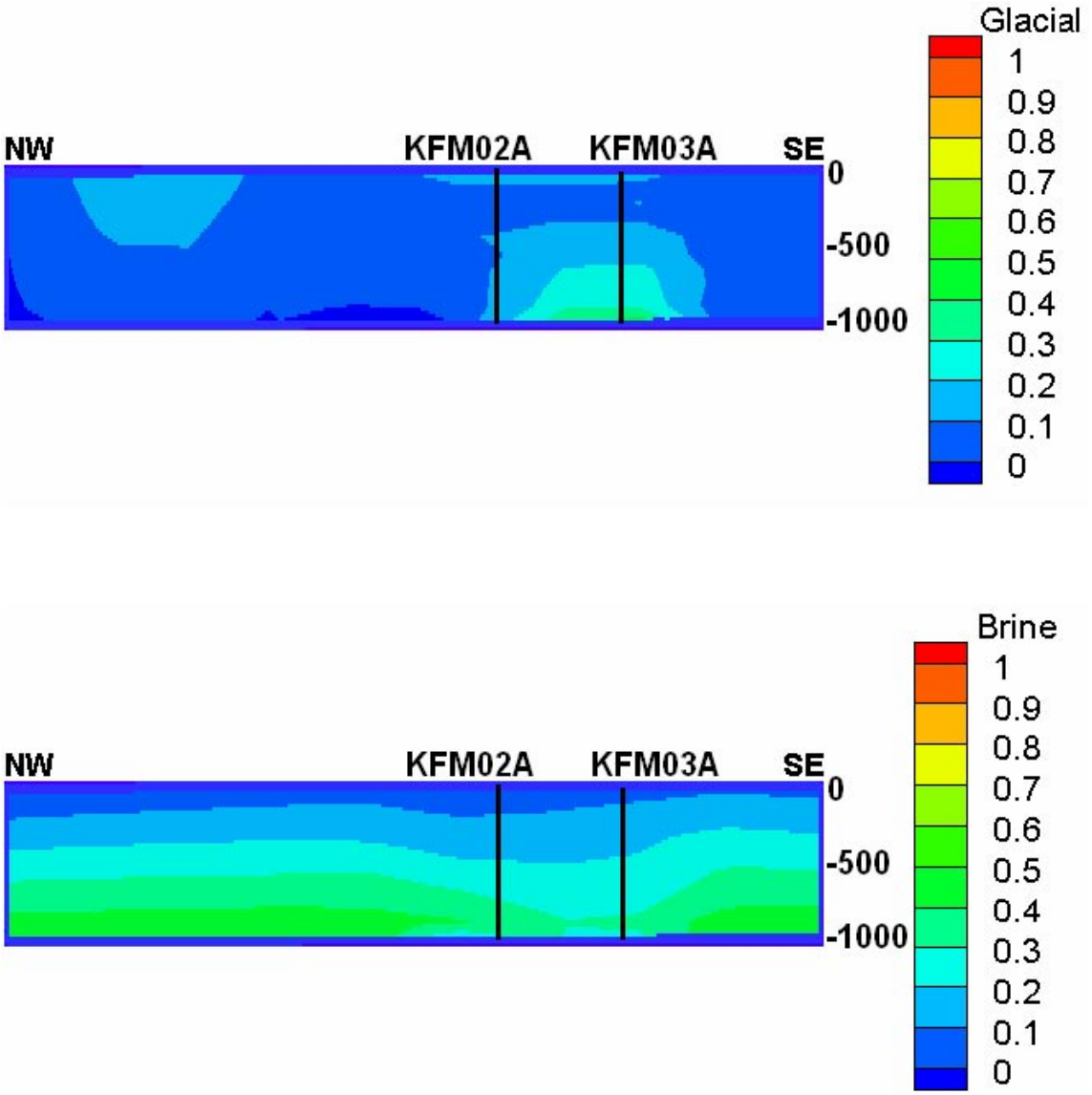

Figure 5-6. *3D visualisation of the Glacial and Brine mixing proportions distribution in Forsmark. The figure shows the distribution of all the available samples (representative and non representative samples) along the NW-SE inclined vertical profile. The depth scale is in metres. For visualisation purpose, the z scale is 2 times magnified.*

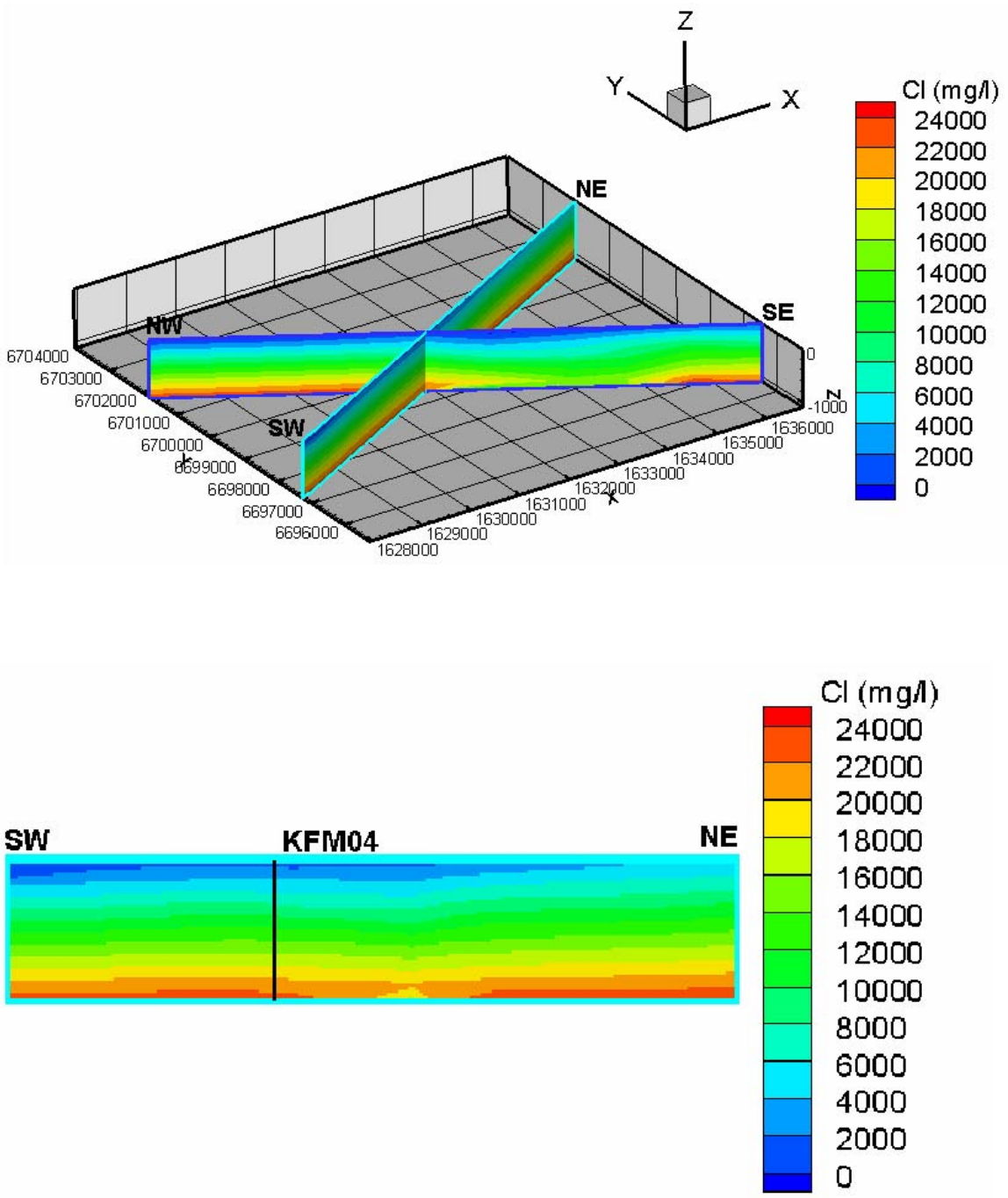

Figure 5-7. *3D visualisation of the Cl) distribution in Forsmark. The top figure shows the Cl distribution of all the available samples (representative and non representative samples) along the NW-SE and SW-NE inclined vertical profiles. The depth scale is in metres. The lower figure shows the Cl distribution along the SW-NE inclined vertical profile. Very few data points are available along this perpendicular profile to the coastline. For now, only some shallow samples points from KFM04 are available. This will be compared within Forsmark 2.1 exercise, with more data from KFM04, KFM05 and KFM06. For visualisation purpose, the z scale is 2 times magnified.*

6 Comparison between M3 and M4 codes

The Figures 6-1 and 6-2 show the comparison between the different mixing proportions calculated with the M3 and M4 codes. The M3 code is described in Chapter 3 of this report. The M4 code (M3 modified) is described in the report provided by the University of Zaragoza M4 performs the mixing calculations in multidimensional space and therefore the uncertainties associated with the mixing proportion calculations can be reduced. M3 and M4 codes were compared for the regional and local model. For the regional model M3 employs 347 samples and M4 only 95. Therefore it was decided at this stage to compare the M3 and M4 results for the local model. For the local model, M3 employs 295 samples and M4 employs 106 samples (Appendix 5). More comparisons between the codes will be done in the next phase of the project.

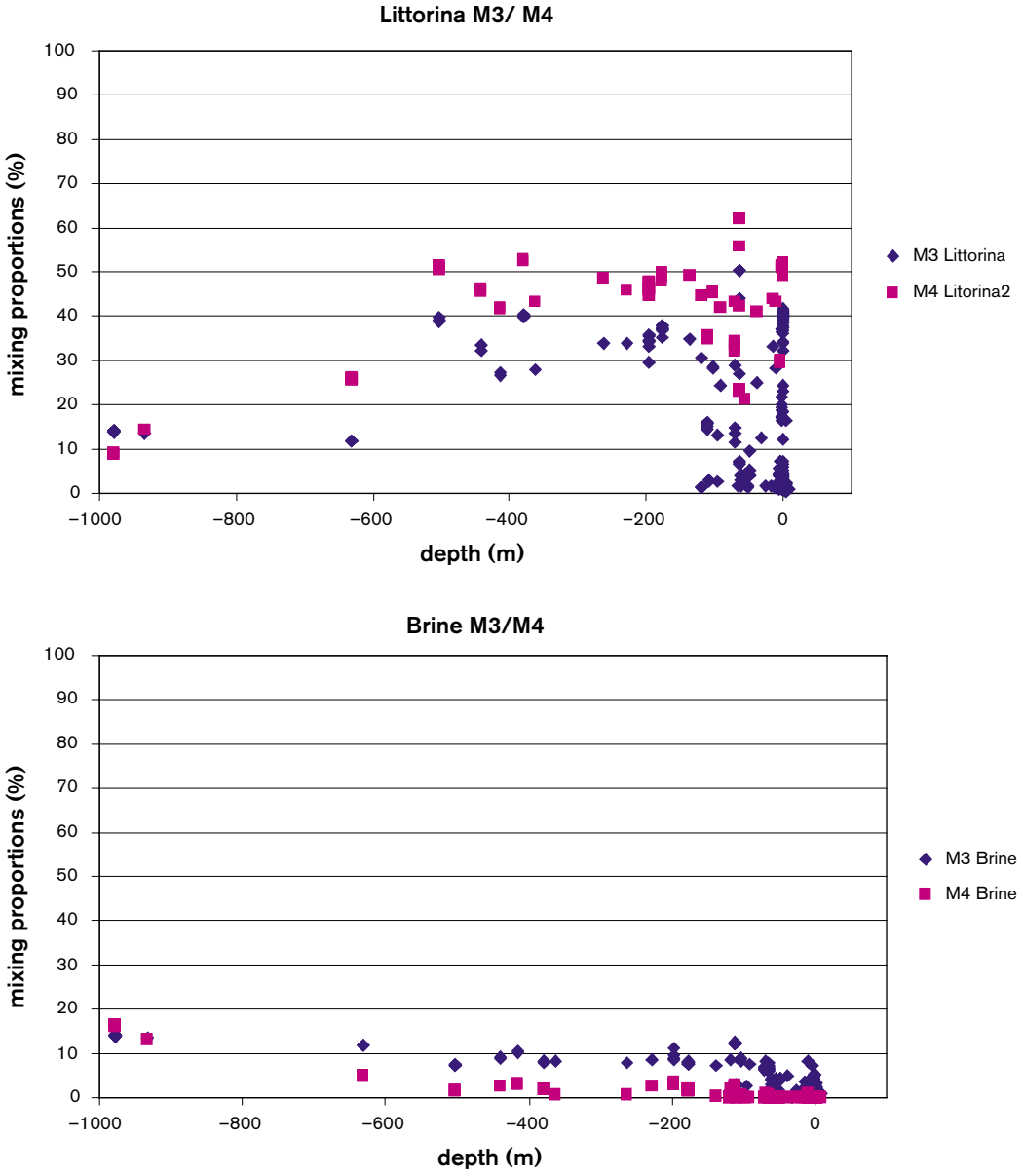

Figure 6-1. *Comparison of the Littorina and Brine mixing proportions obtained with M3 and M4 codes.*

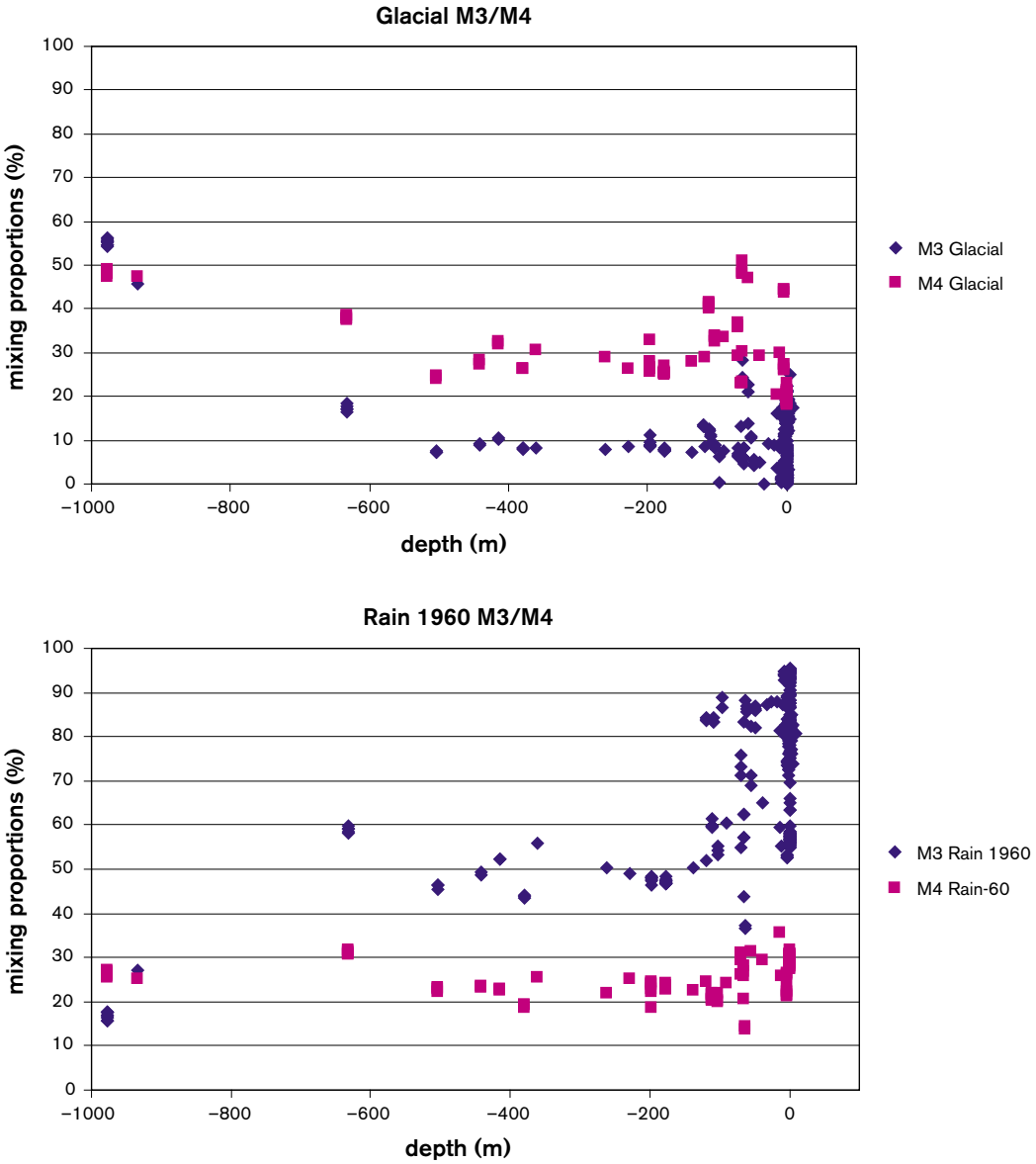

Figure 6-2. *Comparison of the Glacial and Rain 1960 mixing proportions obtained with M3 and M4 codes.*

The trend of the M3 and M4 mixing proportions is similar. M3 and M4 predict similar amount of Brine mixing proportions. M4 predicts slightly higher values for the Glacial and Littorina mixing proportions. M3 predicts higher values for the Rain 1960.

7 DIS (Drilling Impact Study) calculations for Forsmark

The Drilling Impact Study (DIS, /Gurban and Laaksoharju, 2003/) was used for evaluation of the borehole data for Forsmark. The DIS evaluates the impact of the drilling on the hydrochemistry. In the 1.1 phase the DIS calculations were applied on 2 sections (110.1–120.67 and 176.8–183.9) in KFM01. In the 1.2 phase the section 509–516.1 m in KFM02A is analysed.

The successful implementation of DIS evaluation required the availability of drilling data stored in SICADA and the results from DIFF (Differential Flow measurements). The DIS evaluation involved the compilation, calculation and interpretation of drilling data and DIFF measurements. The following data were analysed:

- Drilling water pumped in and out from the borehole during drilling operation.
- The drilled length versus time.
- Water pressure along the borehole during drilling.
- Uranine concentration in the drilling water pumped in and out from the borehole during drilling.
- The DIFF measurements performed in the borehole which measured the hydraulic conductivity along the borehole.

The evaluation work started by collecting data from the drilling and drilling related activities. The representativity of the drilling data and drilling related activities were judged and the data used for the DIS calculations were selected. The DIFF measurements provided the hydraulic conductivity of the fractures zones to be modeled.

As an example the Figures 7-1 to 7-3 show the results of the calculation steps used in the DIS modelling. The Figure 7-1 shows the accumulated drilling water volume pumped in and out from the borehole. Figure 7-2 shows the water pressure variation during of the section 509 to 516.1 m in KFM02A during drilling. Figure 7-3 shows the uranine concentration in the drilling water pumped in and out from the borehole.

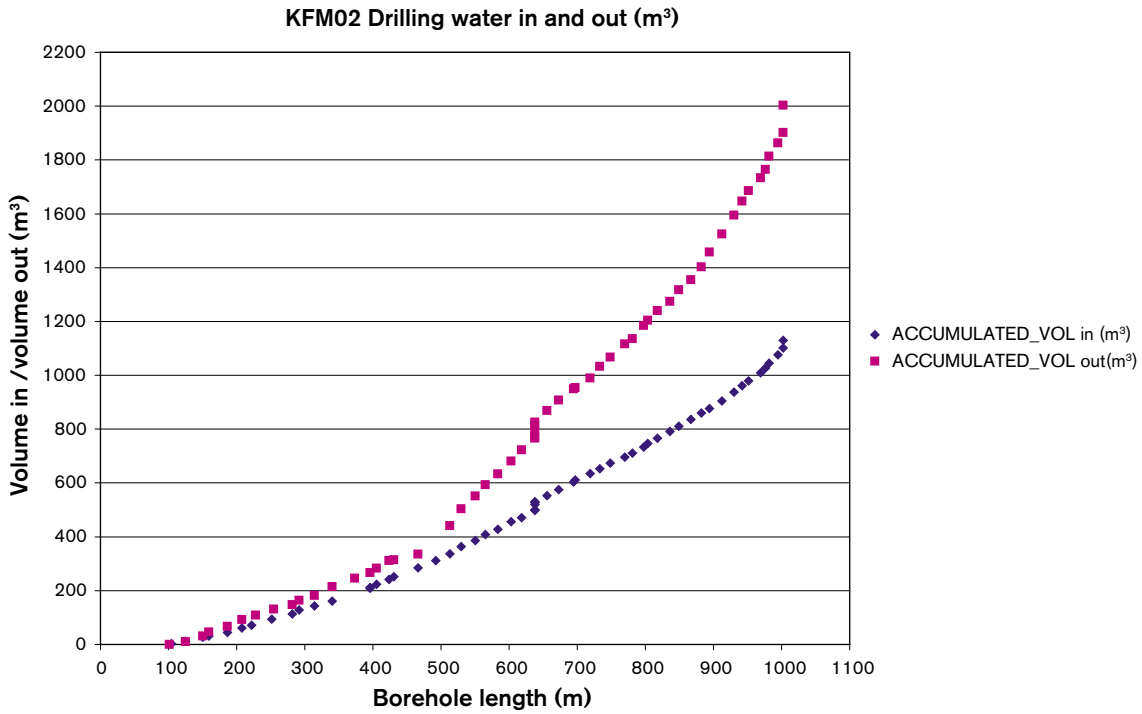

Figure 7-1. *The accumulated drilling water volume pumped in and out of KFM02A.*

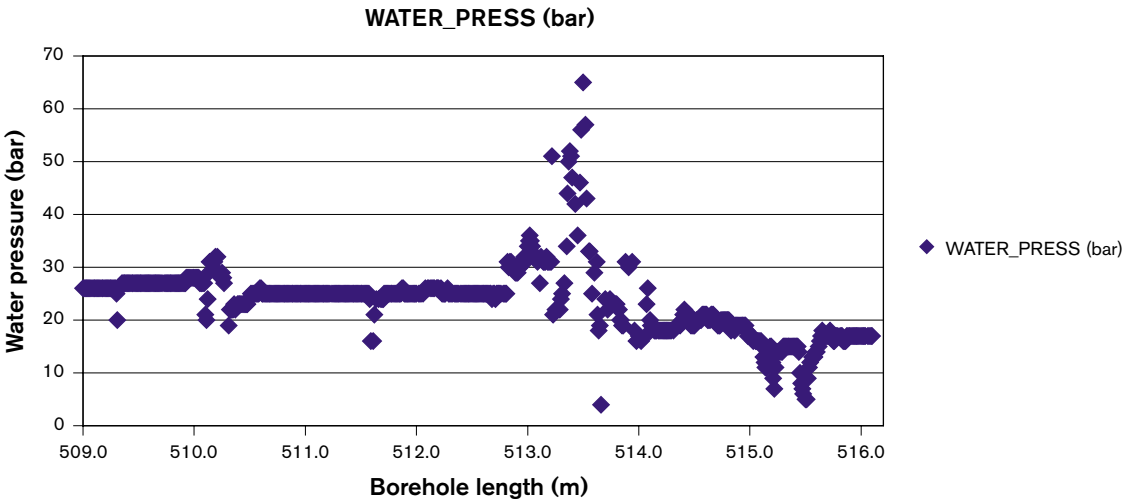

Figure 7-2. *Variation of water pressure in KFM02A when drilling the boreholesection 509 to 516.1 m.*

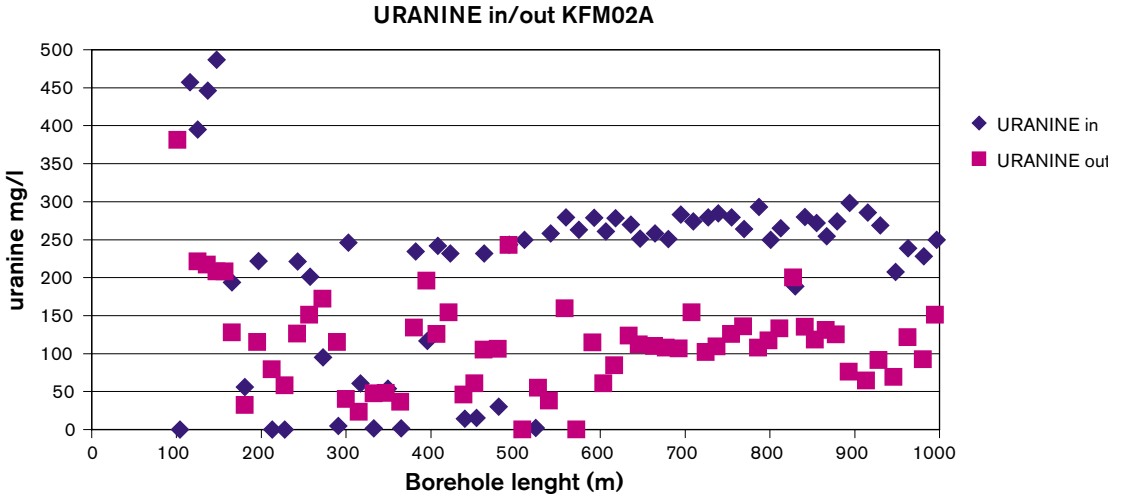

Figure 7-3. *Uranine concentration in the drilling water pumped in and out during the drilling of the borehole. "The addition of Uranine was done using the automatic dosing equipment which was controlled by a flow meter. After some initial problems the concentration was sufficiently constant although somewhat higher than the nominal value of 0.2 mg/l" /from Wacker et al. 2004/. The intention was to use 0.2 mg/l uranine in the flushing water, but in reality as in the graph shows this value may vary.*

The uranine concentration in the drilling water was analyzed (Figure 7-3). The readings for the drilling water pumped in and out from the borehole are unfortunately not recorded simultaneously. Sometimes the values are missing, which could be a malfunction of the dosing equipment or of the flow meter. This makes the interpretation more difficult. For example, at the depth 510 m the uranine concentration in the return water is 0. There are two possibilities: a malfunction of the flow meter or all the drilling water was left in the fracture.

7.1 Calculations of hydraulic permeability for individual fracture zone

This section explains how the hydraulic permeability for individual fracture zones can be calculated.

Calculations of hydraulic permeability for individual fracture zones by using data from KFM02A and comparison with the DIFF measurements:

- Calculation of the pressure:
  1. from the drill rig data: Δp maximum and Δp average
  2. by composing all the different pressures: h-drawdown+friction losses
- Calculation of the thickness of the section (Δe)
- Calculation of the effective drilling time
- Calculation of the flow in the fracture zone (considered the maximum flow which could penetrate the section):

  $Q = \Delta h \times K \times e$
- Calculation of the drilling water volume lost in the fracture from the on-line measurements:

  V lost = Vol in –Vol out
- Calculation of amount of drilling water remained in the fracture
- Calculation of the hydraulic permeability in the fracture Δ e:
  1. $K = \Delta V / \Delta t / (\Delta h \times e)$
  2. Comparison of $K_{calculated}$ with K_{DIFF}

By analysing the records from drilling, drilling related activities and DIFF measurements and by using the above methodology, the following results were obtained for the section 509–516.1 m in KFM01:

509–516.1 m

Δpressure max = 61 bar

Δpressure average = 23.7 bar

Drawdown average= not clear data in SICADA

Drawdown max= not clear data in SICADA

The time when the fracture was penetrated by the drilling was Δt = 30,585 s

The real time (without stops in the drilling activities) was Δt = 7,773 s

The uranine lost in the fracture is Δuranine= 0.25 mg/l.

The thickness of the section is Δe= 7.1 m.

The maximum hydraulic conductivity $K = 9.5 \times 10^{-7}$ m/s.

The average hydraulic Transmissivity $T = 9.5 \times 10^{-7}$ m/s × 5 + $8.94 \times 10^{-9} \times 2.1 = 4.8 \times 10^{-6}$ m^2/s

The error margin for the water pressure along borehole is +/–100 kPa.

The drawdown was measured in the borehole relative to the sea level. The sensor was not calibrated. The error margin is +/–2 m.

The average drilling water volume in the fracture during drilling (8.8 m^3) minus the average drilling water pumped out from the fracture during drilling (18.7 m^3) this section is negative (–9.9 m^3). Most probably formation water from more conductive upper sections were removed, but this hinders to calculate a water balance for this section based on the drilling water pumped in and out data. Therefore the drilling water, which contaminated this section will be calculated based only on the DIFF measurements and rig data.

7.2 Calculations based on DIFF measurements

By using the hydraulic conductivity K from the DIFF measurements, water pressure during drilling and the fracture thickness the flow of the fracture can be calculated.

The pressures were calculated with three methods: 1) average of the water pressure during drilling and mean value, 2) the maximum pressure difference between maximum and minimum recorded values and 3) by composing the different pressures during drilling: hydraulic charge, drawdown and friction losses. Two cases are presented:

1. the average value for the water pressure and transmissivity are used in the bellow calculations:

   $\mathbf{Qav = \Delta h \times K \times e = \Delta} p_{av\,(m)} \times K_{av} \times e = 237 \times (9.5 \times 10^{-7} \times 5 + 8.94\ 10^{-9} \times 2.1) = 1.13 \times 10^{-3}\ m^3/s$

2. the maximum value for the water pressure was used in the bellow calculation:

   $\mathbf{Qmax = \Delta h \times K \times e = \Delta} p_{max\,(m)} \times K_{max} \times e = 610 \times 9.5 \times 10^{-7} \times 7.1 = 0.4 \times 10^{-2}\ m^3/s$

For the maximum time of drilling of this section (30,585), the average drilling water volume which could penetrate the fracture Vav = 34.56 m^3, and the maximum drilling water volume which could penetrate the fracture Vmax = 125.85 m^3. By comparing with the drilling water pumped in the borehole during drilling, the Vav = 34.56 m^3 value is the most realistic. It is this value that will be used in the further calculation. It is important to note that the DIS calculations are made in the way to calculate the maximum possible amount of contamination of a fracture; it is important to correlate the calculations to the data available in order to predict realistic values. It is important to note also the different pressures that play a role during drilling: drilling water pressure, drawdown, friction losses. When these values are not completely known, it is preferable to use an average value for the water pressure. There are more than 20 variables from the drilling machine (rigg data), from the drilling water pumped in and out from the borehole, drawdown, friction losses, that have to be known, evaluated and compared.

By using the calculation scheme shown above, the DIS calculations show that the section was contaminated with Vav= 34.56 m^3 drilling water (the uranine concentration in the return water = 0). This drilling water was then mixed with the formation water. The uranine concentration in the return water was 0 mg/l. This can mean that all the drilling water was left in the fracture or that the flow meter was not working properly. The next reading on the flow meter, at the depth 526.8 was 55 mg/l. This means that 78% of the drilling water was left in the fracture.

The most extreme case being when the all drilling water was left in the fracture, the calculations are made according to this assumption. The drilling water was mixed with the formation water.

From the sampling reports (/Wacker et al. 2004a,b/, SKB P report in print), after pumping and removing a volume of 3.8 m^3, the drilling water concentration was 22%. The pumping continued (from an initial flushing water content of 14.5%), and after removing additional 205 m^3, the final flushing water content was 6%. The duration of the pumping, with some interruptions, was approximately 130 days. The amount of drilling water removed is approximately 22 m^3.

The DIS calculations show that the pumping should have continued for a longer time period in order to remove the 12.56 m^3 drilling water; this amount of drilling water mixed in a proportion of abaout 6% to the formation water represent a a volume of 209 m^3 to be removed from the formation in order to eliminate the flushing water content.

We recommend making DIS calculations during drilling and during sampling. However, for deeper sections the DIS calculations are more difficult. This is due to the contributions from the upper sections in the borehole, which may bias the calculations and make the interpretation more difficult.

8 Concluding remarks

This work represents the phase 1 of the hydrochemical evaluation of the Forsmark data. This comprises the explorative analyses (AquaChem), M3 modelling and alternative models, DIS (Drilling Impact Study) evaluation and 3D/2D visualisation of the data freeze for Forsmark 1.2. M3 modelling helped to summarize and understand the data. A comparison between M3 and M4 codes was presented. DIS evaluation helped to judge the representativity of the drilling and sampled data in the cored borehole KFM01. The visualisation helps to understand the distribution of the data at the site and represents a useful tool for comparison with the hydrodynamic model.

9 References

Andersson J, Christiansson R, Munier R, 2001. Djupförvarsteknik: Hantering av osäkerheter vid platsbeskrivande modeller. Tech. Doc. (TD-01-40), Svensk Kärnbränslehantering AB.

Gurban I, Laaksoharju M, Ledoux E, Made B, Salignac A L, 1998. Indications of uranium transport around the reactor zone at Bagombé (Oklo). SKB TR-98-06, Svensk Kärnbränslehantering AB.

Gurban I, Laaksoharju M, 2003. Drilling Impact Study (DIS); Evaluation of the influences of drilling, in special on the changes on groundwater parameters. SKB PIR-03-02, Svensk Kärnbränslehantering AB.

Laaksoharju M, Skårman C, 1995. Groundwater sampling and chemical characterisation of the HRL tunnel at Äspö, Sweden. SKB PR 25-95-29, Svensk Kärnbränslehantering AB.

Laaksoharju M, Smellie J, Nilsson A-C, Skårman C, 1995. Groundwater sampling and chemical characterisation of the Laxemar deep borehole KLX02. SKB TR 95-05, Svensk Kärnbränslehantering AB.

Laaksoharju M, Wallin B (eds), 1997. Evolution of the groundwater chemistry at the Äspö Hard Rock Laboratory. Proceedings of the second Äspö International Geochemistry Workshop, June 6–7, 1995. SKB International Co-operation Report ISRN SKB-ICR-91/04-SE. ISSN 1104-3210. Svensk Kärnbränslehantering AB.

Laaksoharju M, Gurban I, Skårman C, 1998. Summary of the hydrochemical conditions at Aberg, Beberg and Ceberg. SKB TR 98-03, Svensk Kärnbränslehantering AB.

Laaksoharju M, 1999. Groundwater Characterisation and Modelling: Problems, Facts and Possibilities. Dissertation TRITA-AMI-PHD 1031; ISSN 1400-1284; ISRN KTH/AMI/PHD 1031-SE; ISBN 91-7170-. Royal Institute of Technology, Stockholm, Sweden. SKB TR-99-42, Svensk Kärnbränslehantering AB.

Laaksoharju M, Gurban I, Andersson C, 1999a. Indications of the origin and evolution of the groundwater at Palmottu. The Palmottu NaturalAnalogue Project. SKB TR 99-03, Svensk Kärnbränslehantering AB.

Laaksoharju M, Skårman C, Skårman E, 1999b. Multivariate Mixing and Mass-balance (M3) calculations, a new tool for decoding hydrogeochemical information. Applied Geochemistry Vol. 14, #7, 1999, Elsevier Science Ltd., pp 861–871.

Laaksoharju M, Tullborg E-L, Wikberg P, Wallin B, Smellie J, 1999c. Hydrogeochemical conditions and evolution at Äspö HRL, Sweden. Applied Geochemistry Vol. 14, #7, 1999, Elsevier Science Ltd., pp 835–859.

Laaksoharju M (ed), Gimeno M, Auqué L, Gomez J, Smellie J, Tullborg E-L, Gurban I, 2004. Hydrogeochemical evaluation of the Forsmark site, version 1.1, SKB R 04-05, Svensk Kärnbränslehantering AB.

Smellie J, Karlsson F, 1996. A reappraisal of some Cigar-Lake issues of importance to performance assessment. SKB TR-96-08, Svensk Kärnbränslehantering AB.

Smellie et al. 2002. Hydrochemistry, Guidelines for evaluation and modelling. Draft SKB report.

Wacker P, Bergelin A, Nilsson A-C, 2004. Hydrochemical characterisation in KFM02A. Results from three investigated borehole sections; 106.5–126.5, 413.5–433.5 and 509.0–516.1 m. Forsmark site investigation. SKB P-04-70, Svensk Kärnbränslehantering AB.

Appendix 1

Water type classification of the Forsmark samples by using AquaChem

For data, please see attached CD!

Appendix 2

M3 mixing calculations for Forsmark 1.2 regional and local model: in dark blue the M3 regional modelling results and in light blue the local M3 modelling results; in yellow and light pink the representative samples

For data, please see attached CD!

Appendix 3

Visualisation of the Cl, TDS and M3 mixing proportions along the core boreholes available for Forsmark 1.2; in yellow the representative samples

For data, please see attached CD!

Appendix 4

Cl, TDS and M3 mixing proportions for the percussion and core boreholes available for Forsmark 1.2; in yellow are presented the representative samples

For data, please see attached CD!

Appendix 5

Comparison between the M3 and M4 mixing proportions for Forsmark 1.2

For data, please see attached CD!

Appendix 5

Coupled hydrogeological and solute transport modelling

Contribution to the model version 1.2

Jorge Molinero and Juan Ramón Raposo

Área de Ingeniería del Terreno

Universidade de Santiago de Compostela.

Escola Politécnica Superior. Lugo

December 2004

Contents

1 Introduction

This report constitutes the contribution of the University of Santiago de Compostela (USC) Team to the version 1.2 of the Hydrochemical Analysis of Forsmark site. The USC Team joined the HAG activities after model version 1.1. Then, results reported here correspond to the work performed during the period July–November of 2004.

The main objective is to perform a combined analysis of available hydrogeologic and hydrochemical information. At the present stage, the work has been focussed on the study of the shallow groundwater system and the present-day hydrogeologic conditions, following the recommendations made by the INSITE review to the model version 1.1.

The adopted approach follows a systematic methodology from data analyses to preliminary modelling of groundwater flow and solute transport. These preliminary models must be regarded as a tool for quantitative testing of different hypothesis and/or conditions rather than as accurate descriptions of the site.

The hydrogeologic and hydrochemical background of the Forsmark site is briefly summarized in Chapter 2. This background constitutes the starting point for the work reported here. Chapter 3 contains the analyses of available hydrogeologic and hydrochemical data for the shallow groundwater system. An attempt of hydrogeologic framework with definition of presumed recharge and discharge zones is included, as well as the consistency analysis of hydrochemical and isotopic data within this hydrogeologic framework. Chapter 4 deals with the main results of preliminary modelling of groundwater flow and solute transport. A qualitative but realistic description of the bedrock has been taken into account, according to available conceptual models. Computed results indicate that Quaternary sediments could be playing a relevant hydrogeologic role in Forsmark. This is the reason why groundwater flow through the Quaternary deposits has been further analysed and the main results are described in Chapter 5. Finally, Chapter 6 summarized the conclusions of the work.

2 Hydrogeological and hydrochemical background

2.1 Hydrogeology

Current knowledge of Forsmark hydrogeology is based mainly on SDM version 1.1 /SKB, 2004a/. Moreover, new hydrogeologic insights and unreported updates were regularly provided by hydrogeologists at the HAG meetings.

Figure 2-1 illustrates SKB's conceptual approach for hydrogeological modelling of groundwater flow through fractured crystalline bedrocks. From this conceptual point of view there is a division into 3 main hydraulic domains: (1) Hydraulic Soil Domains (HSD) which are used to represent shallowest quaternary deposits; (2) Hydraulic Conductor Domains (HCD) which are used to represent the main deterministic water-conducting fracture zones and; (3) Hydraulic Rock Domains (HRD) which are used to represent the mass of bedrock in between HCD.

The current interpretation of regional fracture network at Forsmark is available at SDM v1.1 report /SKB, 2004a/. According to the hydrogeological model, up to 166 fracture zones have been inferred, out of which 21 are of a high-confidence level /SKB, 2004a/.

Relevant qualitative facts about the hydrogeology of Forsmark can be summarized as follows:

1. Superficial bedrock id extensively fractured and their thickness varies in space.
2. High transmissivities were recorded in some percussion-drilled boreholes at shallow depths. The borehole information suggests that all of these fractures are either gently dipping or close to horizontal.
3. Down to a certain depth the bedrock is very low conductive. As an example, it is worth noting that overlapping difference flow logging conducted at KFM01A borehole shows that only 34 fractures, from a total of 1,517, were found to yield water. These 34 fractures were found between –105 and –365 masl.

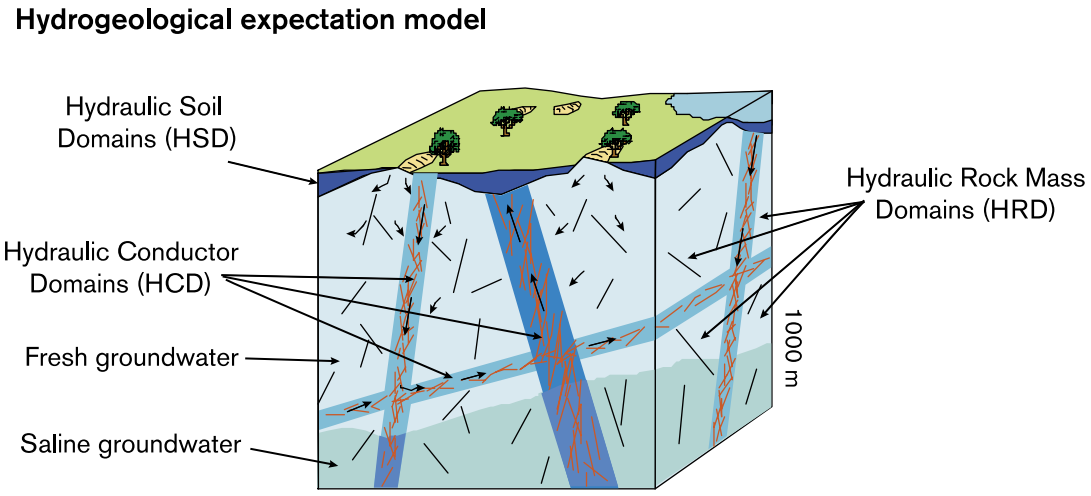

Figure 2-1. *SKB's conceptual approach for hydrogeological modelling of fractured crystalline bedrocks /from SKB, 2002/.*

2.2 Hydrogeochemistry

It is known that different pre- and postglacial events have affected the groundwater composition at the Forsmark area. However, the effects from the last glaciation and the subsequent land uplift are the most important events which are likely to affect the groundwater composition /Laaksoharju and Wallin, 1997/. The latest glacial event (Weichsel) reached its maximum approximately about 18,000 to 20,000 years ago /Ehlers, 1996/. The cyclic behaviour in the climate during the Quaternary Period imply that different groundwaters in the basement must have been modified and even replaced several times /Rhén et al. 1997/. Keeping in mind that most probably the events after the last glaciation have a dominant influence on the actual groundwater system, a working hypothesis and a conceptual model for this groundwater system was proposed by /Laaksoharju and Wallin, 1997/ and /Laaksoharju et al. 1999a/. This conceptual model of the postglacial scenario has been slightly updated recently /SKB, 2002/.

A hydrochemical mixing modelling approach, called M3 /Laaksoharju et al. 1999b/, has been applied at Forsmark /Laaksoharju et al. 2004/. M3 model assumes that chemical composition of groundwater samples are the result of a theoretical mixing between different end-members. Then, back-analyses of measured and computed groundwater compositions allows one to define deviations from the ideal mixing. Observed deviations from the ideal mixing can be attributed to the occurrence of geochemical processes. This approach has been proved very useful for deciphering hydrochemical signatures produced by the paleo-hydrogeological events in different sites of the the Fennoscandian Shield /Laaksoharju, 1999/. The application of M3 methodology to groundwater samples of Forsmark, pointed towards two main water types: (1) fresh, non-saline waters dominated by meteoric water and, (2) brackish-saline water affected by marine water, which in several cases show clear influences of Littorina Sea water.

Differences have been detected in the Forsmark groundwater with respect to Simpevarp water, especially concerning the clear signature of Littorina in many groundwater samples of Forsmark. It is worth noting that Forsmark area was covered by sea water until quite recently, 900 years AD, whereas the flushing of Laxemar-Simpevarp area started already at 3,500 years AD. This has been pointed as a possible reason to explain the higher Littorina influence found in Forsmark groundwater samples.

Both qualitative and quantitative geochemical modelling were performed within the activities of SDM version 1.1 /Gurban and Laaksoharju et al. 2004; Smellie and Tullborg, 2004; Gimeno et al. 2004/. Based on those modelling results, it was identified that major processes affecting the local chemistry of shallow fresh water are: organic matter decomposition, dissolution of more soluble phases such as calcite and sulphides and the alteration of the upper granitic bedrock. Locally, these waters can mix with marine components changing their chemical composition towards more chloride-rich members. Saline waters at Forsmark have been in contact with the bedrock for a long time, and this is why they are generally at chemical equilibrium with most minerals.

A preliminary hydrogeochemical conceptual visualization of the Forsmark site was presented in the HAG report v1.1 /Laaksoharju et al. 2004/. Figure 2-2 shows this integrated conceptual visualization of the Forsmark site, which constituted the conceptual “starting point” for the phase 1.2. This conceptual visualization is based not only on measured salinity values but on all relevant hydrochemical and isotopic data, as well as geological and hydrogeologic considerations.

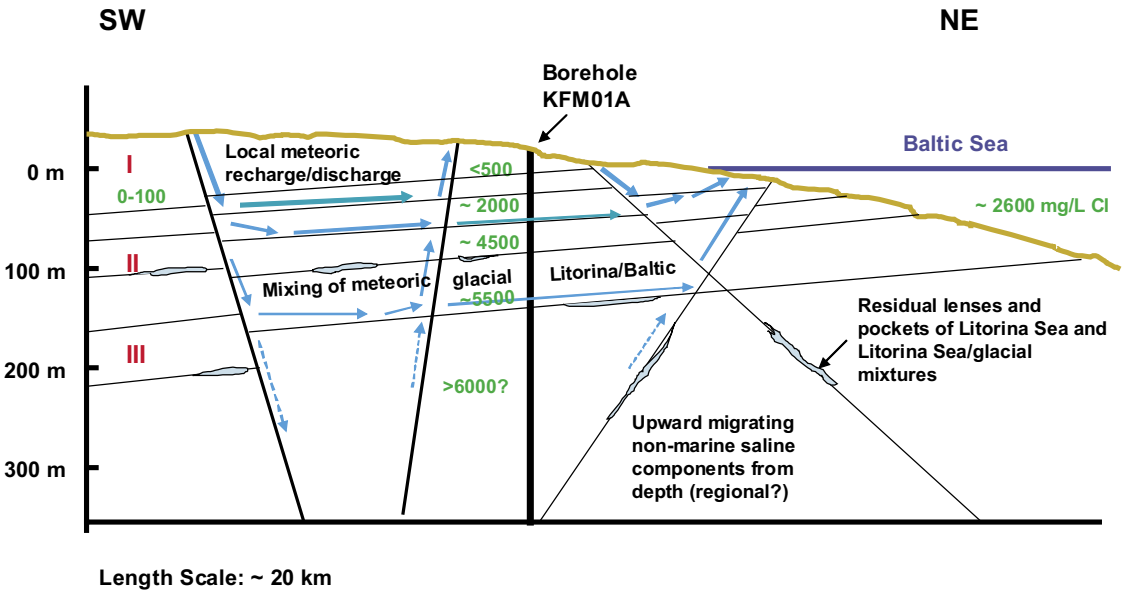

Figure 2-2. *HAG conceptual visualization of hydrogeochemical conditions of Forsmark site, at model stage 1.1 /from Laaksoharju et al. 2004/.*

2.3 Near surface hydrogeology

According to the report of Forsmark site description v1.1 (TR-04-15), The Forsmark area is characterised by a low relief with a small-scale topography and relatively shallow Quaternary deposits. This means that many small catchments with shallow groundwater flow systems are formed. The net precipitation (total rain minus evapotranspiration) has been estimated to approximately 200 mm/year. Groundwater levels are shallow. In recharge areas usually < 3 m below ground and in discharge areas < 1 m. The annual groundwater level fluctuations are assumed to be 2–3 m in recharge areas and < 1 m in discharge areas.

The Quaternary deposits, totally dominated by till, are less than 20 m thick and outcropping rock is frequent. From a hydrogeological point of view, the till can as a first assumption be divided into three layers with significant difference in hydraulic properties. An upper layer, strongly influenced by soil forming processes, with a relatively high hydraulic conductivity a second layer with hydraulic conductivities substantially lower, and a third layer (including the contact zone between the till and the bedrock) with a larger hydraulic conductivity (the geometric mean is reported as 1.18×10^{-5} m/s).

According to the preliminary conceptual model reported in TR-04-15, the lakes and main creeks are assumed to be important discharge areas. The wetlands can either be in direct

contact with the groundwater zone and constitute typical discharge areas or be separate systems with little or no contact with the groundwater zone. The available conceptual model concluded that only a small fraction of the total groundwater recharge will eventually reach below the uppermost permeable part of the bedrock, probably < 10%.

3 Hydrogeochemistry of shallow groundwater

3.1 Introduction

Hydrochemical and isotopic characterization has been performed in a number of shallow groundwater samples at Forsmark. There are two main types of shallow groundwater sampling points: (1) samples collected at soil pipes which correspond to near-surface groundwater circulating through the Quaternary deposits, and (2) samples collected at boreholes which correspond to granitic shallow groundwater. Figures 3-1 and 3-2 show maps with the location of available sampling points of shallow groundwater.

All the groundwater samples collected in soil pipes have been used in this study. However, only available groundwater samples collected in the first 100 m of the boreholes have been analysed, since the objective is to study the shallow hydrogeologic system. Deeper groundwater samples have been analysed in depth by other teams of the HAG. Available data from surface water and precipitation have been included in some plots for comparison, but it is worth noting that a deep analysis of these data is beyond the scope of the present work.

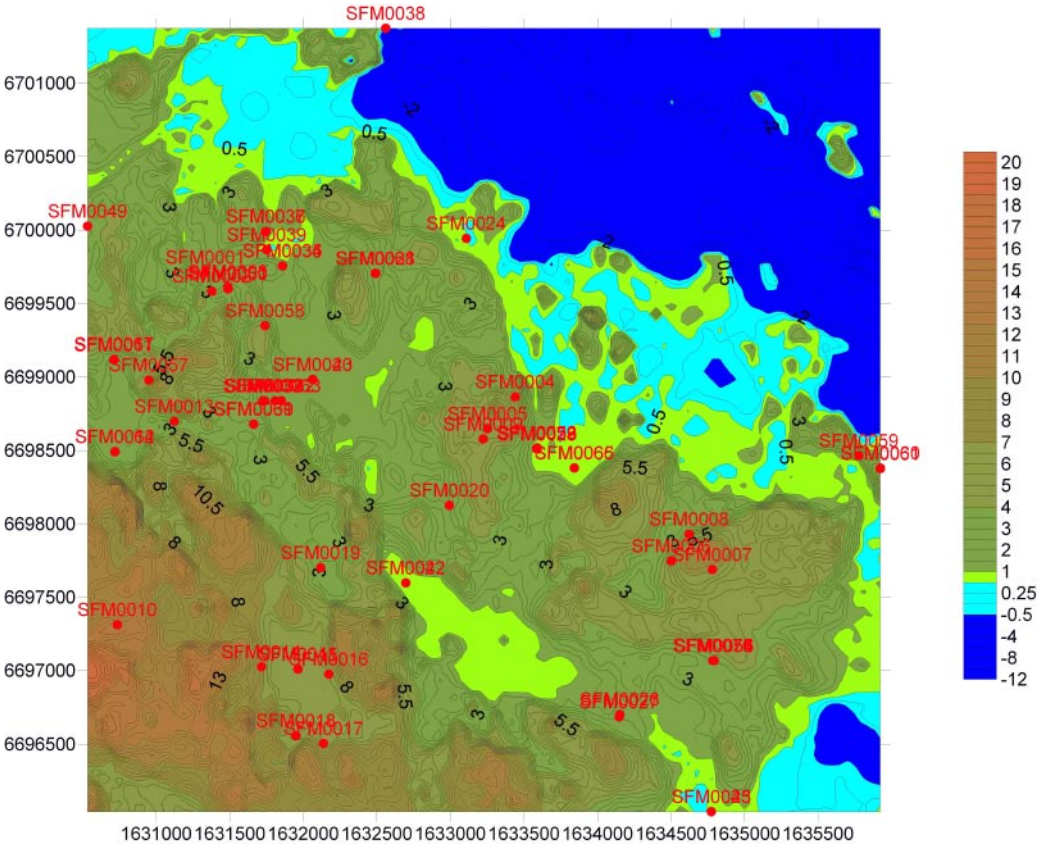

Figure 3-1. *Topographic map with the location of available sampling points in soil pipes (SFM groundwater samples). Values in the colour scale bar are in m.*

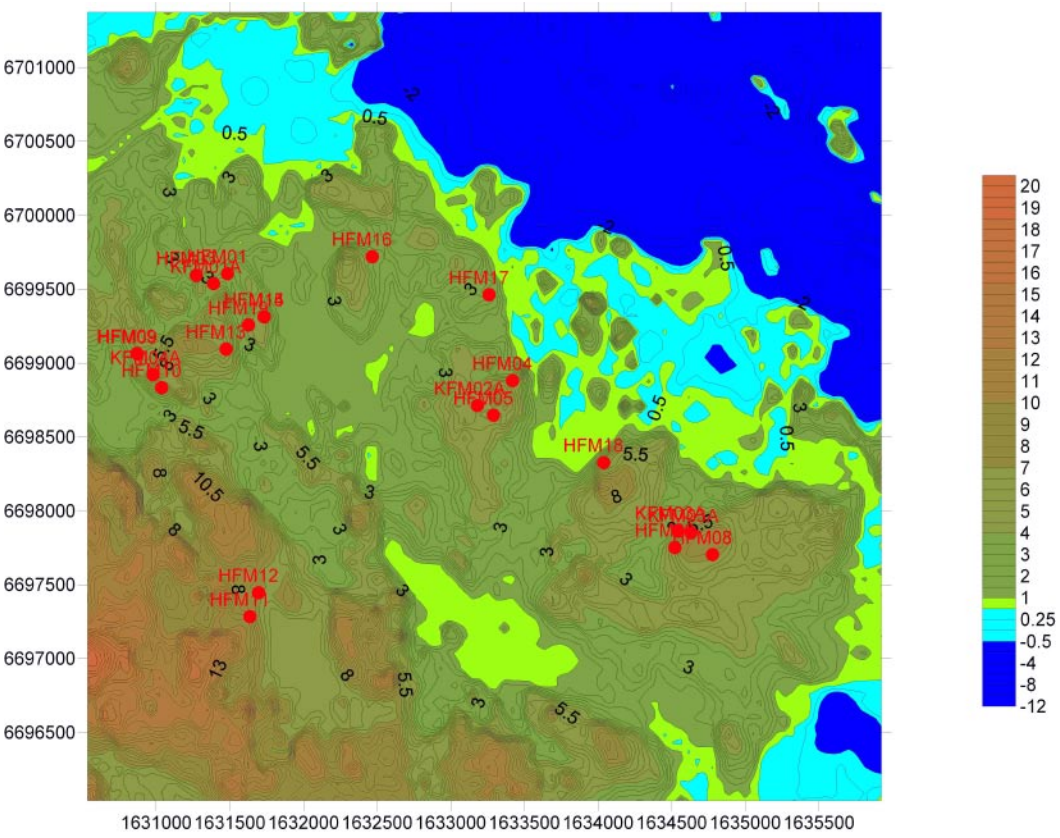

Figure 3-2. *Topographic map with the location of available sampling points in boreholes (HFM and KFM groundwater samples). Values in the colour scale bar are in m.*

3.2 Isotopic information

Isotopic characterization has been performed in a number of shallow groundwater samples at Simpevarp. Analysed environmental isotopes mainly include ^{14}C, ^{13}C, ^{3}H, ^{2}H, and ^{18}O.

Figure 3-3 shows a plot of ^{13}C versus ^{14}C in different types of waters at Forsmark. It can be seen that both marine and stream waters have ^{14}C contents around 100 pmC, but they have different values of ^{13}C deviations. ^{13}C contents of marine waters plot closer to 0‰ while stream waters tend to plot closer to –20‰ VPDB. Most lake water samples (surface lake water) plot in the same field as stream waters, but some of them show ^{13}C values similar to the values of Baltic Sea.

Shallow fresh groundwater samples of Forsmark plot in the middle of the graph in Figure 3-3. Samples of the Quaternary sediments (named near surface groundwater in the plot) clearly show higher ^{14}C contents than shallow groundwater in the granite (named fresh groundwater in the plot). With only 3 exceptions, all groundwater samples show a negative correlation of ^{13}C / ^{14}C.

It is worth noting that practically all surface waters have ^{14}C contents higher than 100 pmC. Even two near-surface groundwater samples collected in soil pipes have values higher than 100 pmC. This fact has been not observed (at least so clearly) in Simpevarp water samples.

Figure 3-4 shows measured values of Tritium at groundwater samples collected in the shallow hydrogeologic system of Forsmark. It can be seen at this figure that some of the groundwater samples plot above precipitation. These values could indicate an influence of recharge from the 1960s–1970s in the samples. On the other hand, the rest of groundwater samples have Tritium values which plot close to or below precipitation, probably corresponding to different mixtures of modern and submodern waters (understanding submoden water as recharged prior to 1952). It is worth noting that shallow groundwater samples collected in the boreholes (named fresh groundwaters in the graph) generally have lower tritium contents than soil pipes samples (named near surface groundwaters). Most of the shallow groundwater samples of the granitic boreholes are in the range from 2 to 8 TU.

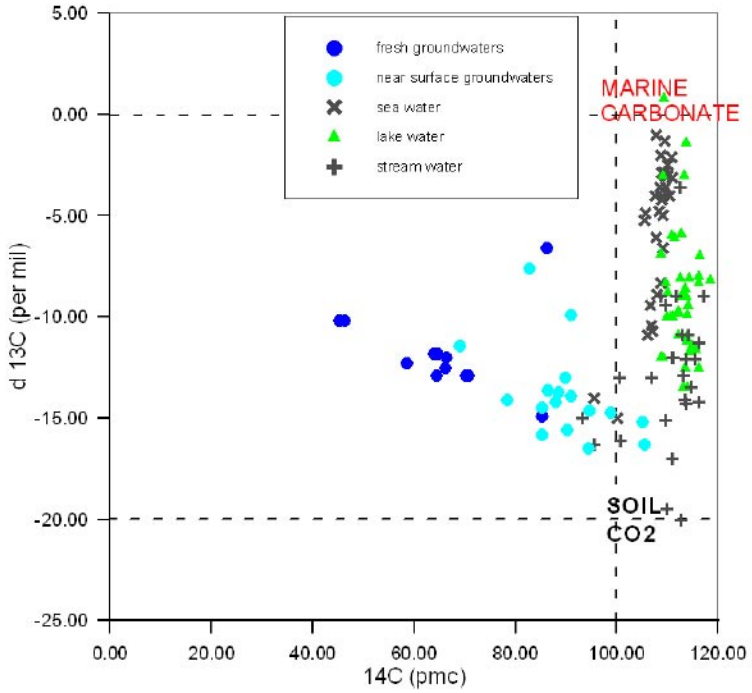

Figure 3-3. *^{14}C versus ^{13}C in different types of waters at Forsmark.*

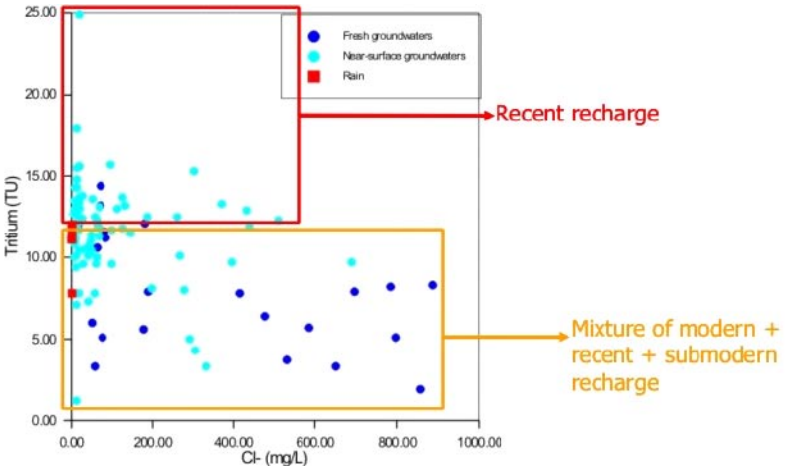

Figure 3-4. *Tritium versus chloride in shallow-fresh groundwater samples of Forsmark.*

3.3 Hydrochemical information

Figure 3-5 shows a Piper diagram containing all fresh groundwater samples (Cl^- < 1,000 mg/L) of Forsmark. In the first diagram (3-5 A) soil pipe samples have been highlighted in red colour. On the other hand, shallow borehole (granitic) samples have been highlighted in the second diagram (3-5 B).

One can see in Figure 3-5 that fresh groundwater samples of Forsmark plot along almost the whole range between chloride – bicarbonate and calcium – sodium hydrochemical facies. However, a relevant difference can be seen in the water samples depending whether the sampling point is a soil pipe or a borehole. Borehole samples are all of them Na-HCO_3,Cl type, while soil pipes samples can be either Ca-HCO_3 or Na-HCO_3, Cl type.

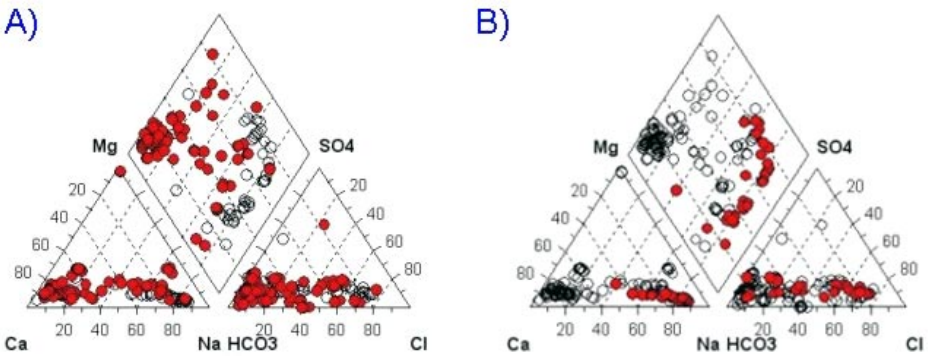

Figure 3-5. *Piper diagram with all fresh groundwater samples of Forsmark. A) soil pipes samples. B) shallow borehole samples.*

It can be expected that (at least) some soil pipe samples should correspond to recently infiltrated water (i.e., recharge water). On the other hand, borehole samples in the granite could represent older and hydrochemically more mature water. Figure 3-5 (A) is showing a water evolution tendency, where immature Ca-HCO_3 hydrochemical facies evolve to mature Na-HCO_3, Cl facies, probably due to cation exchange processes and mixing with older and more saline waters. However, water samples of the granitic boreholes only shows Na-HCO_3, Cl water types.

Figure 3-6 shows computed saturation indexes of calcite for soil pipe groundwater samples of Forsmark. Figures 3-7 shows computed saturation indexes of calcite for shallow groundwater samples collected in granitic boreholes in Forsmark. It is worth noting that, due to time constrains, saturation indexes have been computed only for a few samples. Then, not all the available water samples have been included in the graphs of Figures 3-6 and 3-7.

Figure 3-6 shows that selected groundwater samples in soil pipes are saturated or over-saturated with respect to calcite. This fact constitutes a relevant difference compared to Simpevarp, where almost all near surface groundwater samples were highly under-saturated with respect to this mineral phase. It is thought that this difference is because Quaternary deposits are much more abundant (and thicker) in Forsmark than in Simpevarp. In Formark, well developed Quaternary sediments cover more than 80% of the land area, and it has been reported /SKB, 2004a/ that these Quaternary sediments contain large amounts of calcite.

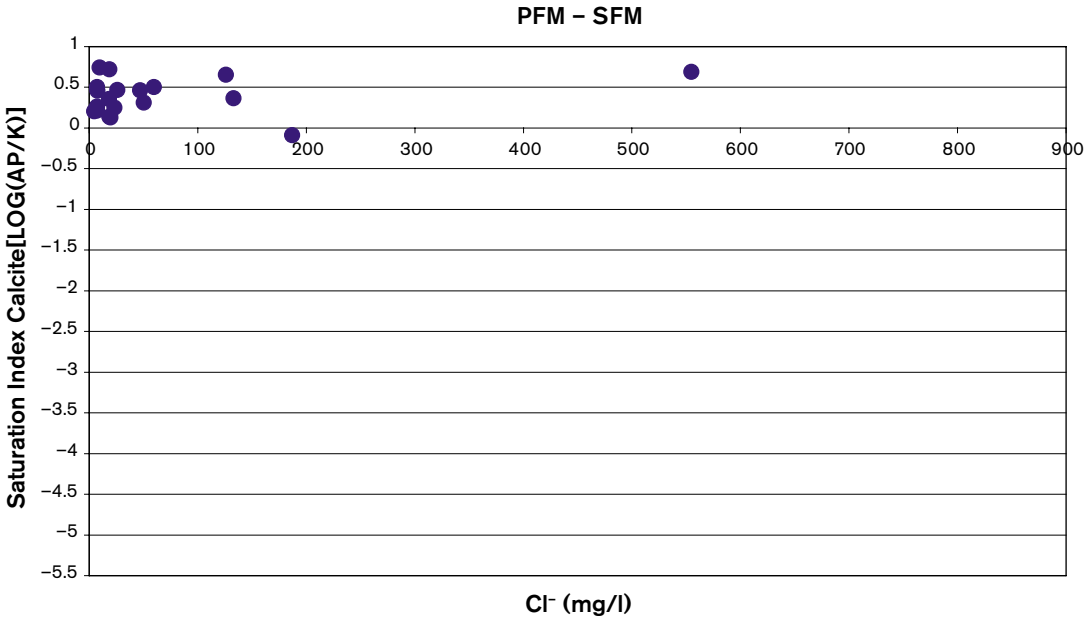

Figure 3-6. *Calcite saturation indexes versus chloride for soil pipe groundwater samples of Forsmark.*

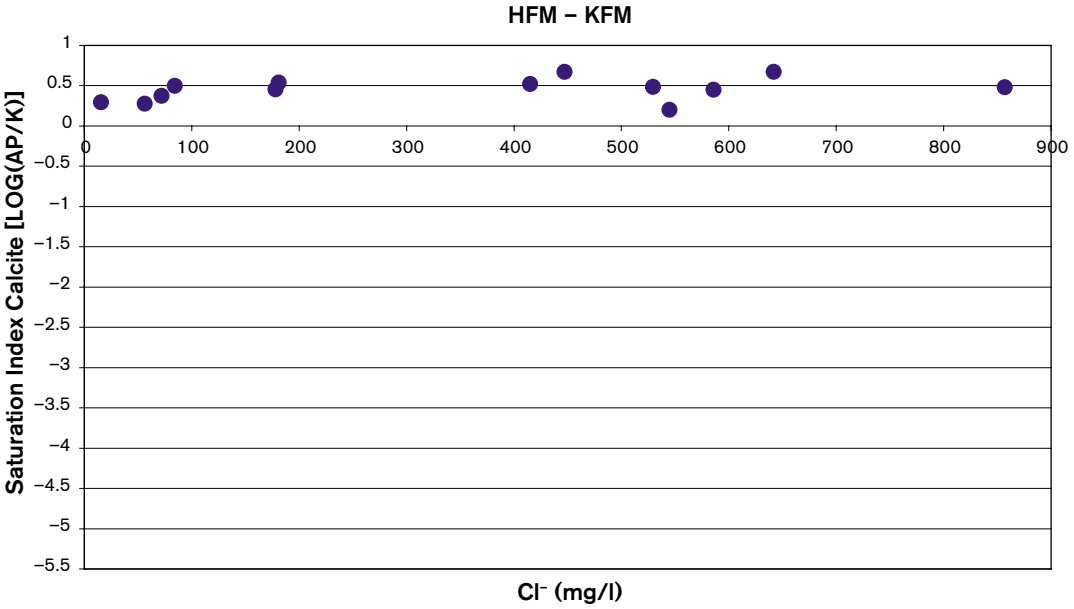

Figure 3-7. *Calcite saturation indexes versus chloride for shallow groundwater samples collected in boreholes at Forsmark.*

3.4 Hydrogeologic framework of hydrochemical observations

The working hypothesis is that meteoric water mainly reaches the shallow aquifer by distributed infiltration on the emerged lands, and then flows through both the Quaternary sediments and the granitic bedrock towards discharge zones, located mainly in the lakes and near the Baltic coastline. It has been hypothesized in the previous section that as groundwater moves through aquifers, its chemistry is altered by the effects of geochemical processes and, may be, mixing with older and more saline waters. Then, the hypothesis was that immature Ca-HCO_3 hydrochemical facies correspond to recently infiltrated water (i.e "recharge water"), which evolves to mature Na-HCO_3, Cl hydrochemical facies along flow paths. This hypothesis (which is based exclusively on hydrochemical considerations) should be consistent with the hydrogeologic framework of the Forsmark area.

Figure 3-8 shows the same piper diagram shown previously in Figure 3-5 (A), which contains all groundwater samples collected in soil pipes (Quaternary deposits). Now, different colours have been used to represent different hydrochemical facies (Figure 3-8). Blue colour has been used for Ca-HCO_3 water samples under the hypothesis that correspond to "recharge water". On the other hand, red colour has been used for Na-HCO_3, Cl water samples under the hypothesis that correspond to "discharge waters". A few water samples plotting in the middle of both groups have been coloured in yellow.

Figure 3-9 shows the spatial distribution of different soil pipes samples, which have been located on the topographic map.

It can be seen in Figure 3-9 that most of the red points, which correspond to the water samples assumed to be "discharge" water, are located under the lakes or Baltic estuaries, with only two exceptions which are located at local topographic minima. All the yellow points ("intermediate" hydrochemical facies) are located also close to the lakes or local topographic minima. On the other hand, blue points (Ca-HCO_3 water types) are distributed across the Forsmark site lands, most of them at (or close to) local topographic maxima. Figure 3-9 constitute a confirmation of the initial working hypothesis. Hydrochemical facies are different and can be used to detect local recharge and discharge areas of the Quaternary groundwater system. Figure 3-10 shows a very temptative map with presumably recharge (blue) and discharge (red) areas. This map has been elaborated only using hydrochemical data and topographic constrains, so it do not pretend to be a hydrogeologic map. Figure 3-10 could be useful to illustrate the working hypothesis that groundwater recharge in Forsmark is distributed across the site, whereas groundwater discharge is mainly concentrated in Lakes and Baltic coast line.

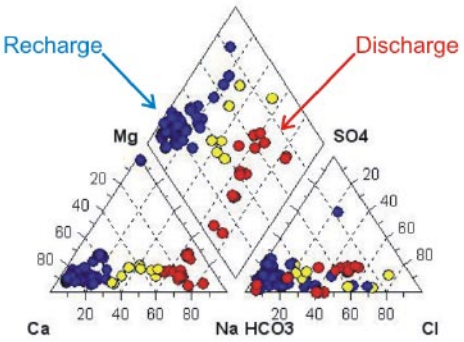

Figure 3-8. *Piper diagram with groundwater samples collected at soil pipes in Forsmark. Blue and red coloured samples are assumed to represent "recharge water" and "discharge water", respectively.*

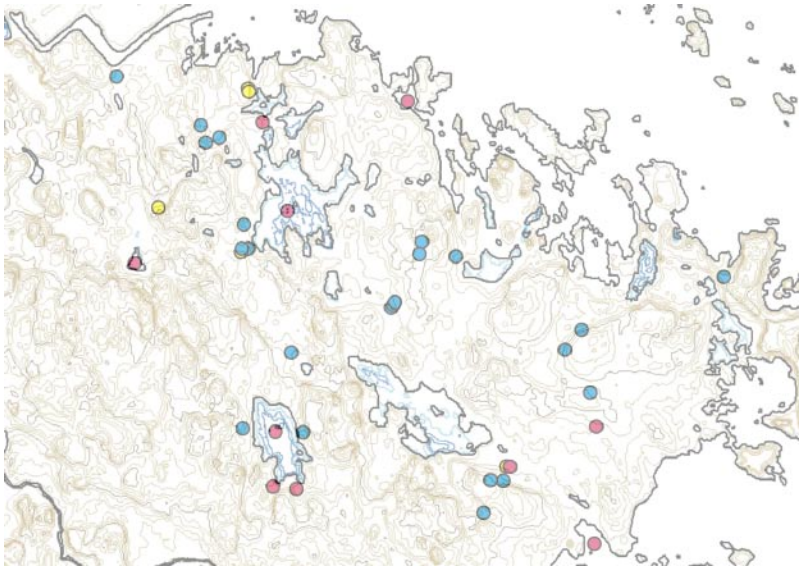

Figure 3-9. *Spatial distribution of the soil pipe groundwater samples shown in Figure 3-8, on the topographic map.*

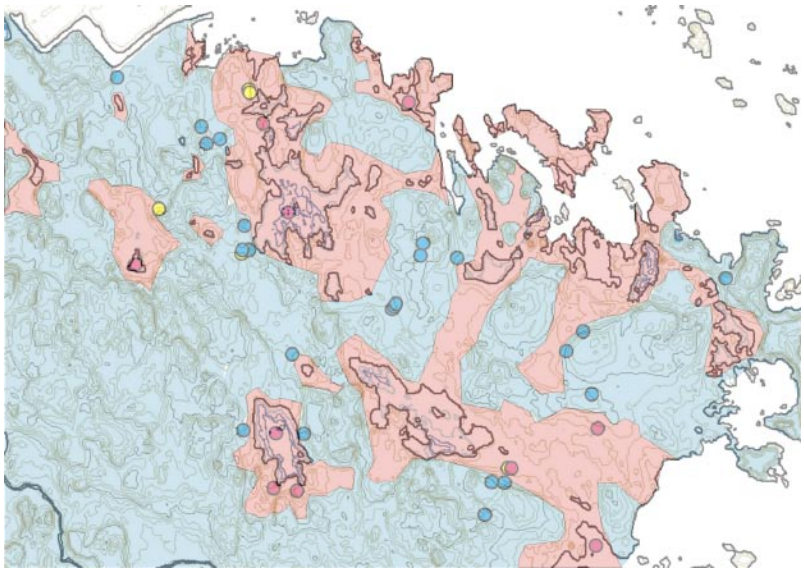

Figure 3-10. *A temptative mapping of presumably recharge (blue) and discharge (red) zones in Forsmark area. This map has been elaborated using only hydrochemical information of soil pipes and topographic constrains.*

It is worth noting that all shallow groundwater samples collected at (granitic) boreholes show Na-HCO_3, Cl hydrochemical facies, irrespectively if they are located in recharge or discharge zones. Then, shallow groundwater in the granitic bedrock of Forsmark represents meteoric water with residence time enough as to be noticeably altered by water-rock interaction processes, and/or by mixing with older and more saline relict waters.

Figure 3-11 shows a plot of tritium versus Cl^- only in those soil pipe samples (near surface groundwater) located at the presumably discharge zones shown in the map of Figure 3-10. It can be seen in Figure 3-11 that the lowest tritium contents are measured in soil pipes under 3 lakes (Bolundsfjärden, a small lake in SFM12 and Eckarfjärden). However, groundwater under these 3 lakes shows very different salinities. Near surface groundwater under Bolundsfjärden show Cl^- concentration values higher than the present Baltic sea water. By the contrary, shallow groundwater under Eckarfjärden shows Cl^- concentrations much lower (i.e. more diluted groundwater). Finally, shallow groundwater under the small lake in SFM12 shows an intermediate salinity.

It is worth noting that groundwater samples located under the Baltic Sea shows Cl^- contents lower than the sea water, which is consistent with the occurrence of local discharge of fresh groundwater under the sea.

The occurrence of brackish near surface groundwater under Bolundsfjärden and SFM12 could indicate the discharge of older groundwater under these lakes. However, other explanations are also possible, perhaps even more likely, such as the occurrence of relic ("trapped") marine water during earlier phases of shoreline displacement. Figure 3-12 shows measured time series of Cl^- in both surface water and groundwater under Bolundsfjärden. It can be noticed that surface lake water of this lake is highly diluted (< 50 mg/L of Cl^-), whereas groundwater a few meters below the lake show high chloride contents (4,000 mg/L of Cl^-).

Figure 3-13 shows a plot of $\delta^{18}O$ versus Cl^- in soil pipe samples located at the presumably discharge zones shown in the map of Figure 3-10. Littorina and average Baltic Sea values /Laaksoharju, 1999/ has been included in the plot. It can be seen in Figure 3-13 that near surface groundwater at presumably discharge zones plot along a hypothetical mixing line between Littorina water and fresh soil pipes water, with the exception of groundwater samples under Eckarfjärden. It is also noticeable that Baltic Sea water plots clearly out of this hypothetical mixing line.

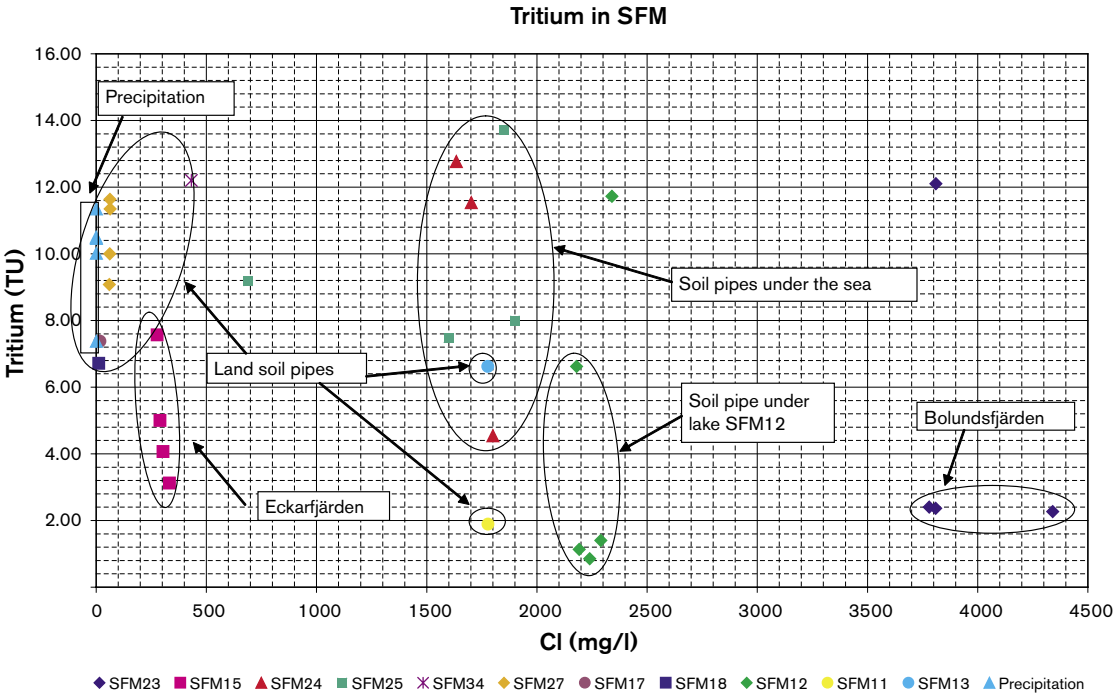

Figure 3-11. *Tritium versus Cl^- in soil pipe samples (near surface groundwater) located at the presumably discharge zones shown in the map of Figure 3-10.*

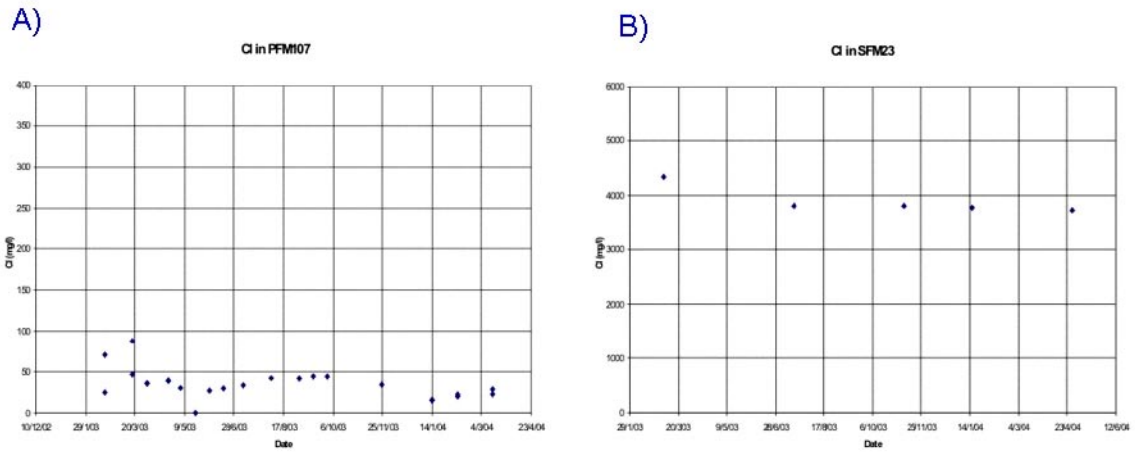

Figure 3-12. *Cl^- time series measured at Bolundsfjärden. A)surface (lake) water and B)Groundwater in soil pipe under the lake.*

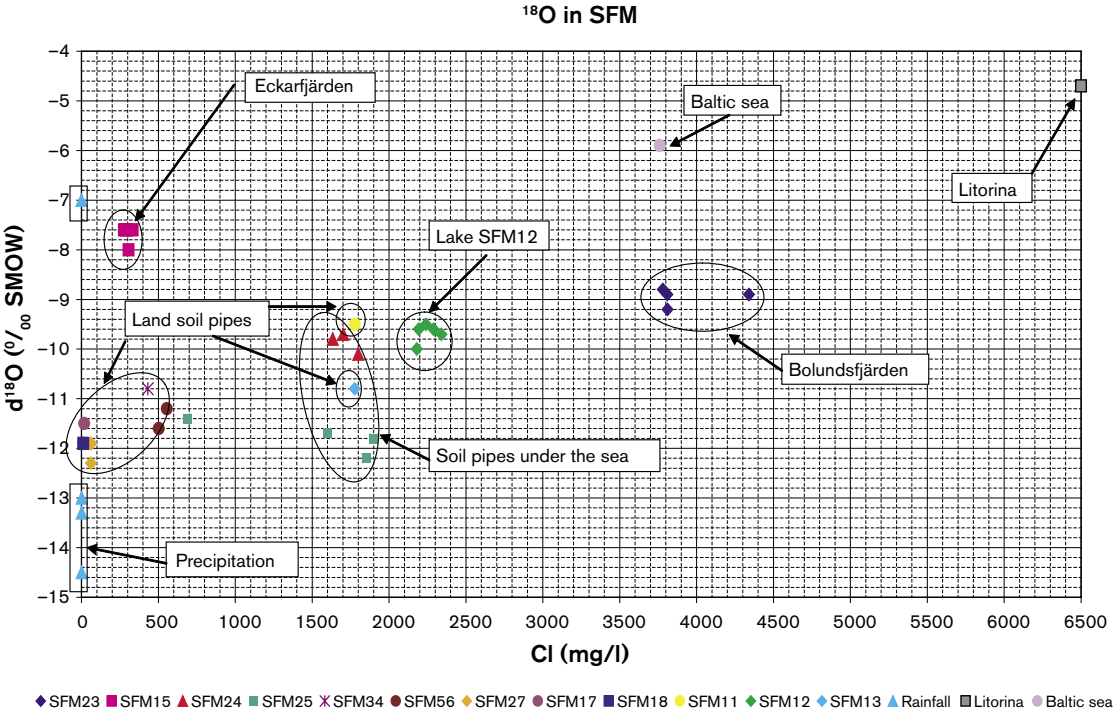

Figure 3-13. *^{18}O versus Cl^- in soil pipe samples (near surface groundwater) located at the presumably discharge zones shown in the map of Figure 3-10.*

The hydrochemical and isotopic patterns of the presumably discharge zones at Forsmark show differences between them. Some of the discharge zones may correspond exclusively to the discharge of very shallow and local groundwater systems, probably involving only flow through the Quaternary deposits. These very local systems show dilute groundwater and ^3H and ^{18}O values close to precipitation. On the other hand, there are other discharge zones which may represent the convergence of both very shallow and deeper flowlines in different proportions of flow rates. This could explain the different degree of mixing between meteoric and Littorina water. Bolundsfjärden, SFM11, SFM12 and SFM13 seem to be the discharge zones with higher Littorina influence.

Figure 3-14 shows a 3D view of the phreatic surface in Forsmark based on groundwater levels measured at soil pipes. Flow vector have been also included in the figure.

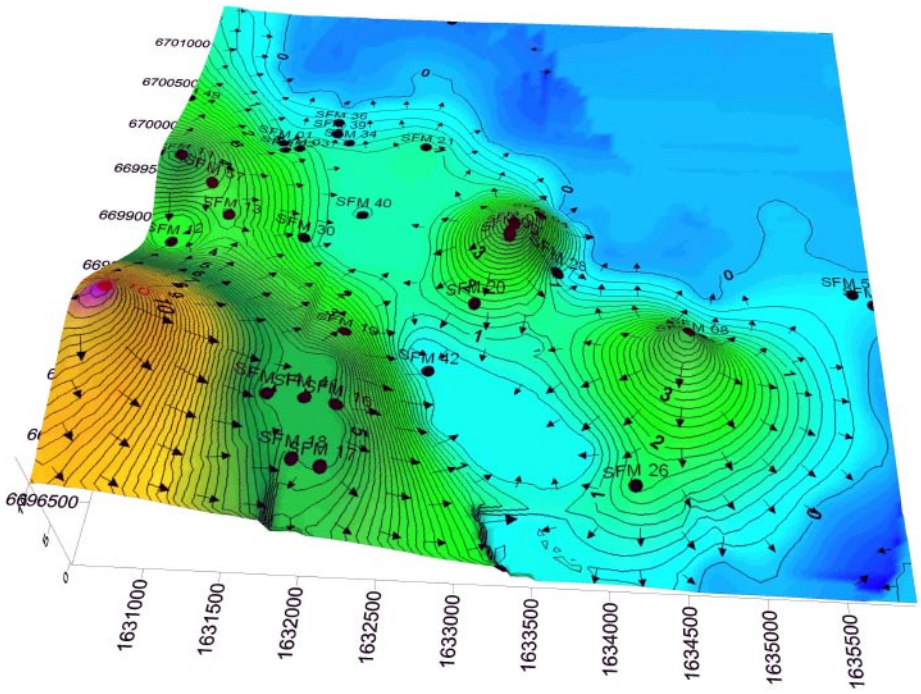

Figure 3-14. *3D view of groundwater heads measured at the soil pipes in Forsmark.*

Care must be taken looking at the map in Figure 3-14, since it has been constructed using a limited amount of data. However, it is thought that it provides a realistic view of the shallow groundwater system in Forsmark. A clear recharge zone is located in the south west corner of the domain, which coincides with the "inland direction". Moreover, other (3) local recharge zones can be clearly identified within the Forsmark site. The most apparent discharge zones coincides with the position of the 3 main lakes (Fiskarfjärden, Bolundsfjärden and Eckarfjärden), but also the discharge at SFM12 can be clearly identified (close to the left boundary in Figure 3-14). These hydrogeologic data fits with the hydrochemical interpretation proposed before.

Figure 3-15 shows the comparison between the piezometric map and ^{14}C measurements in shallow groundwater of Forsmark. Again, care must be taken analysing Figure 3-15 because the amount of ^{14}C data is still very limited. The kriging results based on so few data can indicate patterns that do not represent the real situation, and this is why sampling points have been always included in the maps. However, it can be seen that maximum values of ^{14}C correspond to main recharge zones, whereas the minimum values are located in the "alignment" of SFM12 (small lake), Eckarfjärden (SFM15) and SFM27 (close to the outlet of Fiskarfjärden).

Figure 3-16 shows the comparison between the piezometric map and Cl^- measurements in shallow groundwater of Forsmark (soil pipes). It can be seen that most of the near surface groundwater samples correspond to fresh water, but brackish discharge zones become evident at SFM12 (small lake), Bolundsfjärden (SFM23) and SFM025 (a soil pipe under the Baltic Sea and in front of Fiskarfjärden).

Figure 3-17 shows also the comparison between groundwater heads and (a) tritium and (b) ^{18}O contents. It can be seen in both figures that minimum tritium values and maximum $\delta^{18}O$ coincides with main groundwater discharge zones (Bolundsfjärden, Eckarfjärden and SFM12). However, it should be noticed that groundwater under Eckarfjärden shows very low Cl^- contents (see Figures 3-11, 3-13 and 3-16) which constitute a relevant difference with respect to the other two main discharge lakes.

Figure 3-18 shows the relationship of Ca/Na in soil pipe samples. It can be seen that maximum values of this cationic relationship coincides very well with the 3 main recharge zones. On the other hand, minimum values of Ca/Na relationship are measured under lakes (SFM12, Bolundsfjärden, Eckarfjärden and at the outlet of Fiskarfjärden).

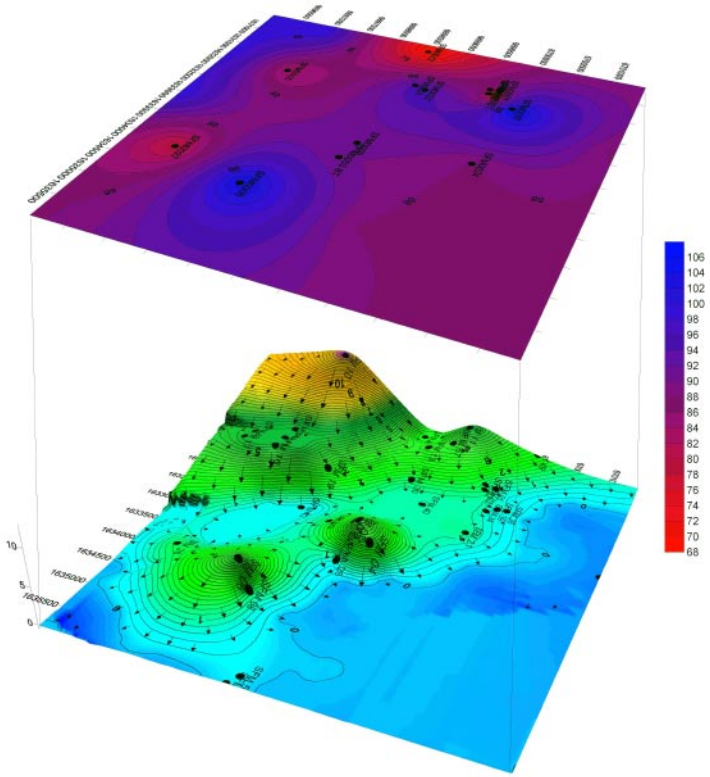

Figure 3-15. *3D view of groundwater heads (down) and ^{14}C measurements (up) at the soil pipes in Forsmark.*

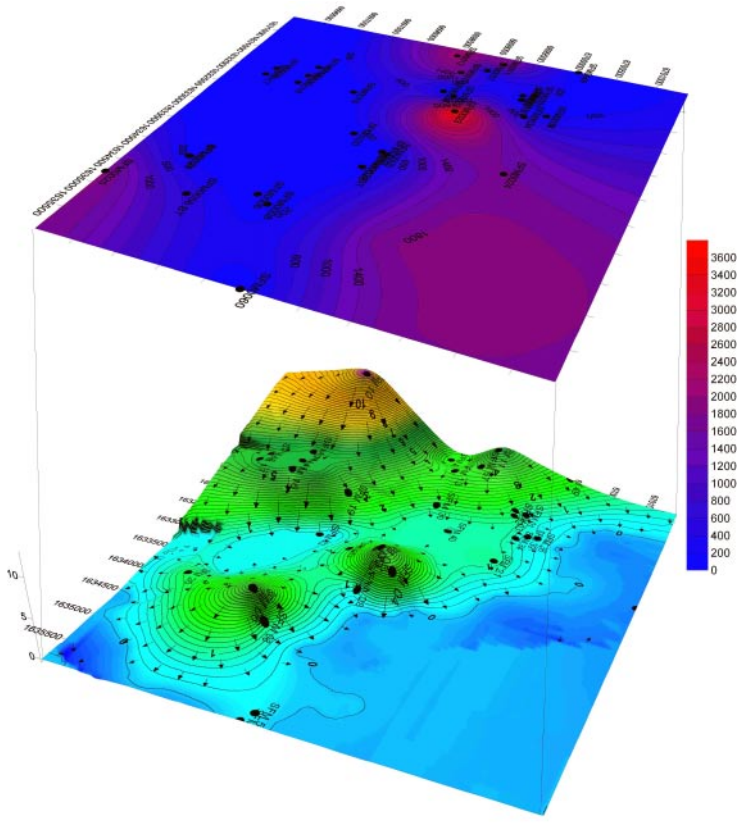

Figure 3-16. *3D view of groundwater heads (down) and Cl^- measurements (up) at the soil pipes in Forsmark.*

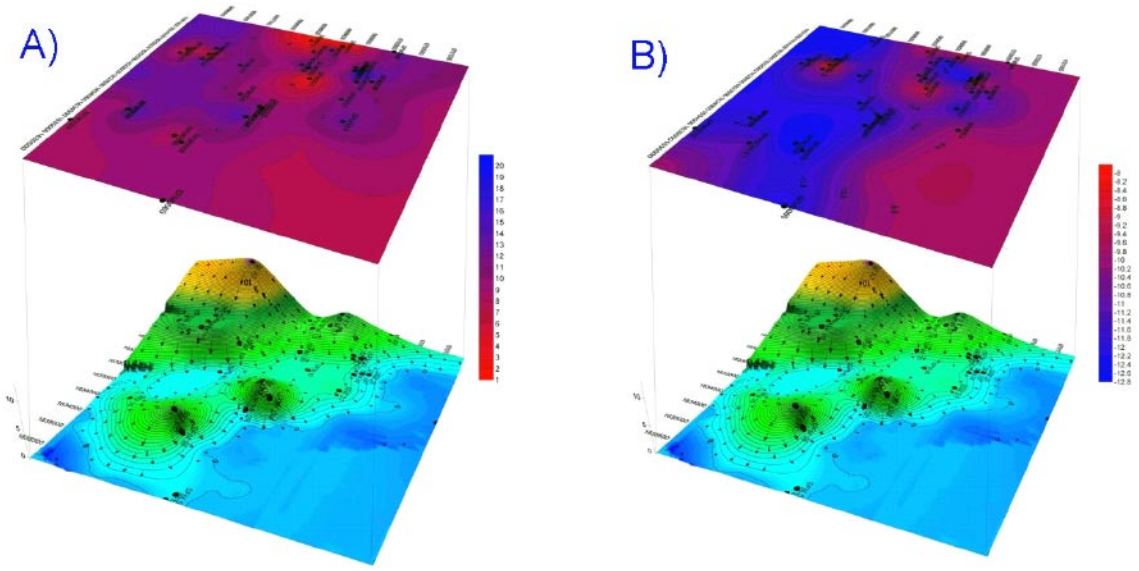

Figure 3-17. *3D view of groundwater heads and (A) tritium and (B) δ ^{18}O measured at the soil pipes in Forsmark.*

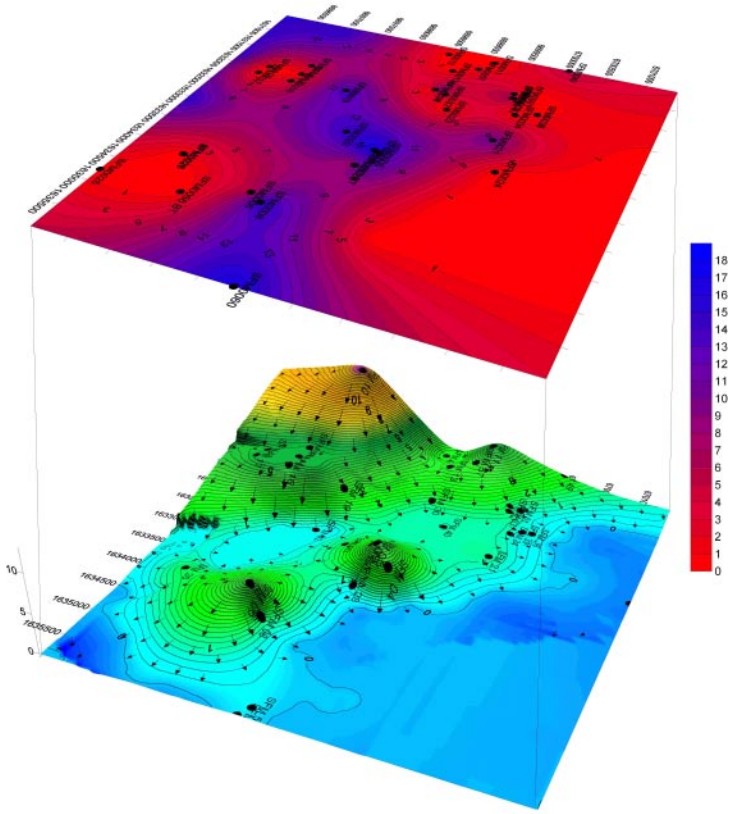

Figure 3-18. *3D view of groundwater heads and Ca/Na relationship measured at the soil pipes in Forsmark.*

A relevant matter now is to know whether the local flow systems detected in the subsurface of Forsmark influence or not the hydrogeologic behaviour at higher depths in the bedrock. Figure 3-19 shows the relationship of Ca/Na in water samples collected at the first 100 m of the granitic boreholes. It can be seen that the influence of local recharge and discharge zones is not so clearly reflected as in the soil pipes (Figure 3-19). The Ca/Na relationship distribution in the upper zone of the bedrock, displays parallel to the coastline, but small disturbances under SFM12 and Bolundsjärden can be still recognised (see Figure 3-19).

Figure 3-20 shows Cl^- measurements in the first 100 m of the granitic bedrock. It can be stated that groundwater in the first 100 m of the bedrock is slightly more saline than in the Quaternary layers. Maximum Cl^- values measured in the shallow bedrock are close to 5,000 mg/L, and are located near to the maximum values of salinities measured in the soil pipes (zone between Bolundsfjärden and SFM12). It is worth noting that two salinity maxima are observed under two of the recharge zones identified in the Quaternary aquifer (the two recharge zones located between Fiskafjärden and the Baltic coast; see Figure 3-20), which could be an indication of the local (shallow) character of these particular recharge zones. Changes in salinity distribution between the Quaternary sediments and the first 100 m of the bedrock can be observed by comparing Figures 3-16 and 3-20.

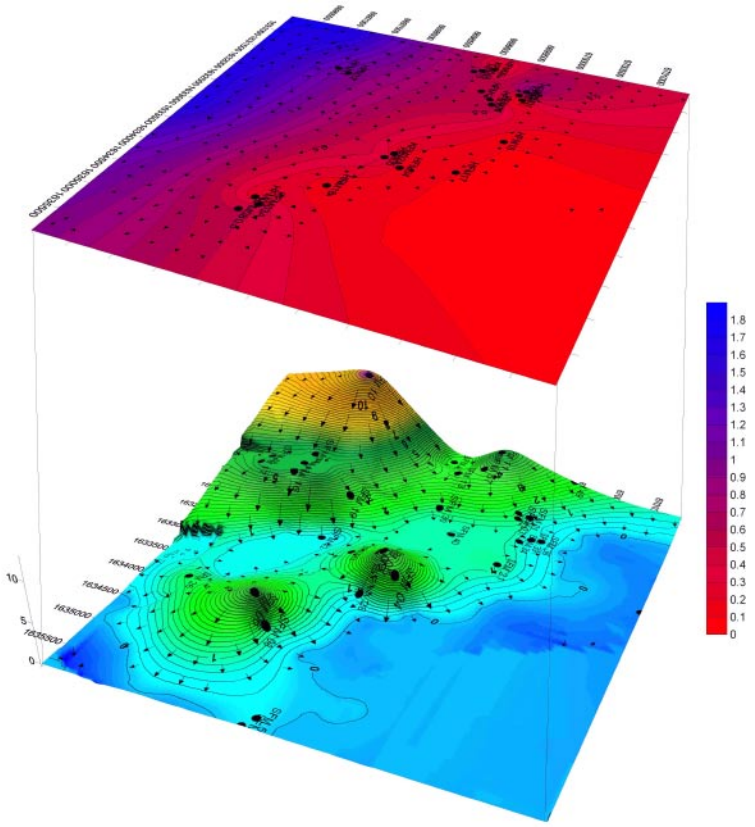

Figure 3-19. *3D view of groundwater heads and Ca/Na relationship measured at the first 100 m of the granitic boreholes in Forsmark.*

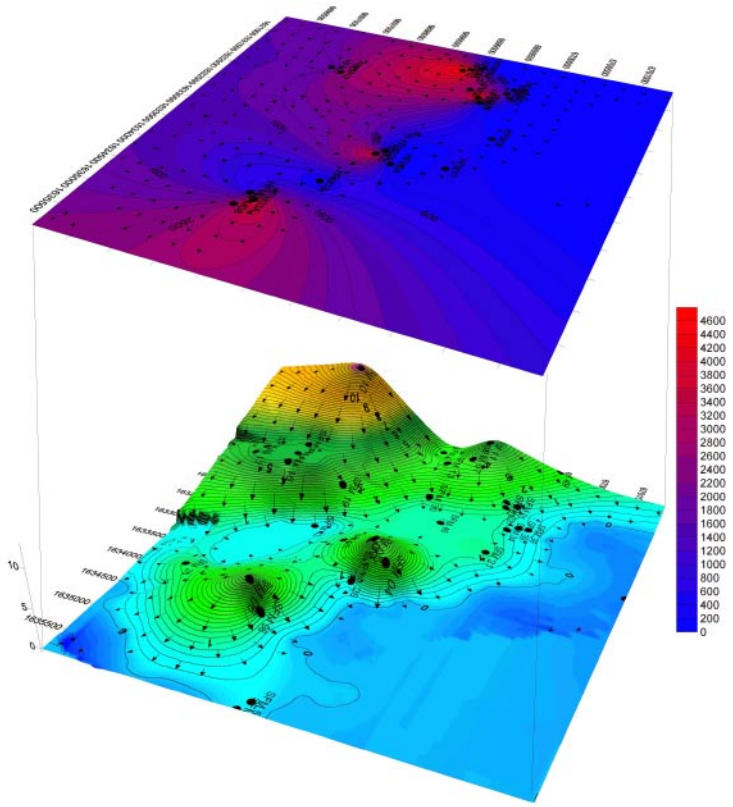

Figure 3-20. *3D view of groundwater heads (down) and Cl^- measurements (up) at the first 100 m of the granitic bedrock in Forsmark.*

4 Numerical modelling of groundwater flow and solute transport

4.1 Conceptual model and assumptions

The main objective of this model is to perform a preliminary analysis of the consistency between current hydrogeologic and hydrochemical knowledge in Forsmark. It should be noticed that a reliable transport model requires sound conceptual models of both hydrogeology and hydrochemistry. At the present time, the status of hydrogeological and hydrochemical modelling is still preliminary, with limited amount of data. Then, the work described here should be regarded as a first attempt to model groundwater flow and solute transport which will be subjected to further improvement, linked to the availability of new data and conceptual developments along the planned strategy for site descriptive modelling.

The conceptual model of Forsmark area is based on the results presented in /Laaksoharju et al. 2004/. The model domain covers a 2D profile similar to the conceptual visualization provided by SDM model v1.1 (see Figure 2-2). Bedrock properties are represented by effective parameters, according to an Equivalent Porous Media Approach. The 2D profile has a total length of 7 km, from the local topographic maximum (SW) to the Baltic Sea (NE) (Figure 4-1).

The model domain extends to a depth of 1 km. The spatial discretization was performed by means of triangular finite elements. The numerical mesh consists on 1,818 nodes and 3,400 elements (Figure 4-2).

Bottom and lateral boundary conditions are assumed to be Neumann type with zero flow-rate (impervious boundary). Top boundary is divided into Baltic Sea (1 km) and emerged lands (6 km). Baltic sea boundary condition is assumed to be Dirichlet type, with a prescribed head of 0 m.a.s.l. On the other hand, a flow-rate (recharge) of 10 mm/year is prescribed on the emerged lands. This value corresponds exactly to the same value used in the Simpevarp model /Molinero and Raposo, 2004/ and is consistent with calibrated and proposed values at Äspö and Laxemar areas /Rhèn et al. 1997; Banwart et al. 1999; Molinero et al. 2002; Molinero and Samper, 2004/.

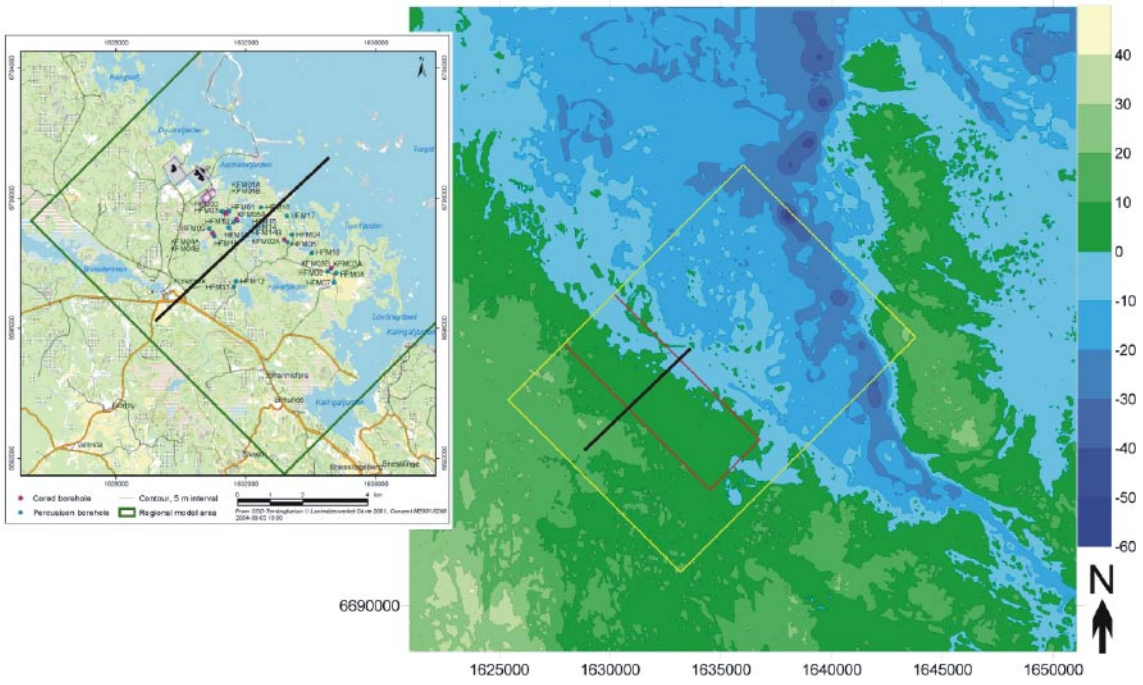

Figure 4-1. *Geographic location of the 2D profile selected for numerical modelling.*

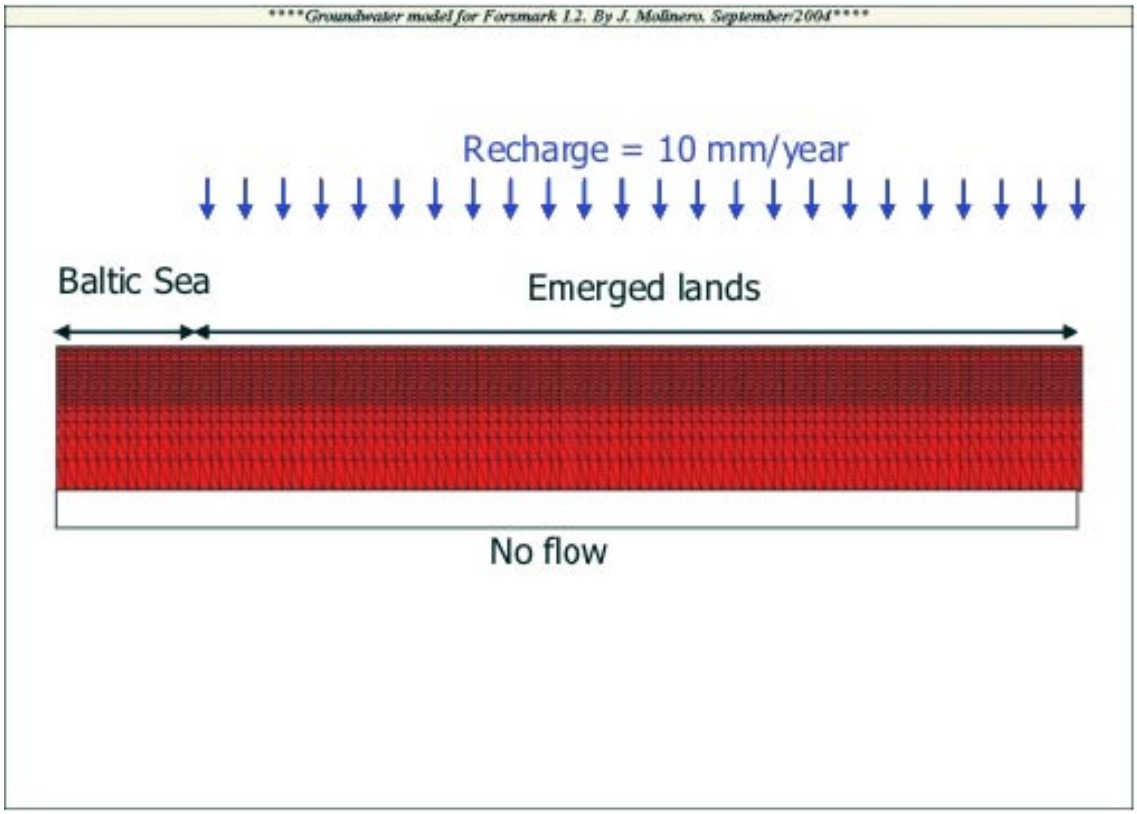

Figure 4-2. *Sketch of spatial discretization used for the numerical model. Finite element mesh consists on 1,818 nodes and 3,400 triangular elements. Lateral boundary conditions assume no flow across the boundaries. The assumptions for the upper boundary are explained in the figure.*

According to available borehole information most fractures are either gently dipping or close to horizontal, and the most conductive ones have been found between –100 and –350 masl, approximately. Down to this depth the bedrock is very low conductive. On the other hand, it is known that pseudo-vertical fracture zones conforms a large-scale fracture network of hydraulic conductor domains. This conceptual visualization of hydrogeologic properties has been translated to the numerical model by means of 4 different material zones: (1) shallow granite ($K = 10^{-7}$ m/s); (2) intermediate granite ($K = 5 \times 10^{-7}$ m/s); (3) deep granite ($K = 10^{-9}$ m/s); and (4) pseudo-vertical fracture zones ($K = 10^{-6}$ m/s). Figure 4-3 shows the material zones distribution in the numerical model.

The finite element mesh was generated with GEOSTAR, the basic pre and postprocessor of the COSMOS/M finite element package /SRAC, 1998/. This program is an interactive CAD like graphic geometric modelling system with a powerful mesh generator for finite elements.

The numerical solver used for flow and transport simulations was CORE^{2D} /Samper et al. 2000/. This code solves for variably saturated groundwater flow, heat transport and multi-component reactive solute transport.

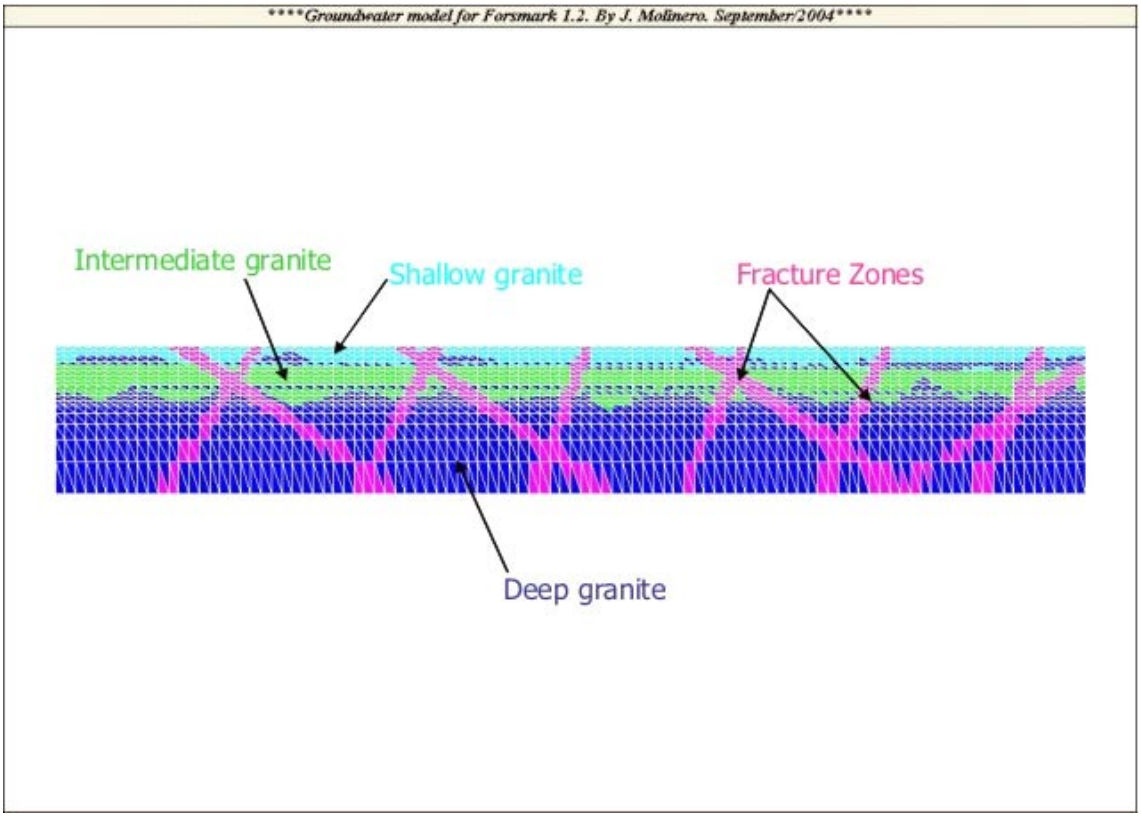

Figure 4-3. *Material zones distribution in the numerical model. Granite heterogeneity is based on the available borehole information at Forsmark. Fracture zones are inspired on the "conceptual visualization" shown in Figure 2-2.*

4.2 Groundwater flow and conservative solute transport

A groundwater flow simulation was performed using the boundary conditions and parameters described in the previous section. Figure 4-4 shows the computed groundwater head distribution in the modelled domain.

Figure 4-4 shows the effect of the heterogeneity in computed groundwater heads. It is worth noting that the existence of "pseudo-vertical" fracture zones generates local groundwater flow systems (see upper-right part of the model in Figure 4-4). This is consistent with the conceptual visualization shown in Figure 2-2 /Laaksoharju et al. 2004/; see Figure 2-2). Computed groundwater heads in high-conductive fracture zones are lower than in the vicinities (shallow granite). Then, fracture zones act as discharge zones in these local groundwater systems. The surface area between fracture zones become local recharge areas (see Figures 4-3 and 4-4). It is worth noting that the occurrence of this "local systems" can be produced without topographic constrains (the model do not consider the local topography) but only considering realistic heterogeneity in the granite.

The most relevant parameters for solute transport modelling are: (1) kinematic porosity and (2) dispersivity. At the present stage of S.I. there is no tracer test available at Forsmark. Then, transport parameters must be based on expert judgement and knowledge of similar granitic areas (i.e. Äspö). Hydrogeologic model version 1.1 is the most useful reference available for our work. Version 1.1 hydrogeologic model adopt a kinematic porosity of 10^{-5} in rock domains between fracture zones /SKB, 2004a/. Then, the same value has been used in this work. Longitudinal and transverse dispersivity has been set equal to 300 m and 100 m, respectively.

It is known that Forsmark region raised above sea level from 1,000 to 500 years ago. Previously, Forsmark region was covered by sea water during, at least, 9,000 years (known as the Littorina sea stage). At that time, it is thought that dense brackish seawater was able to penetrate the bedrock.

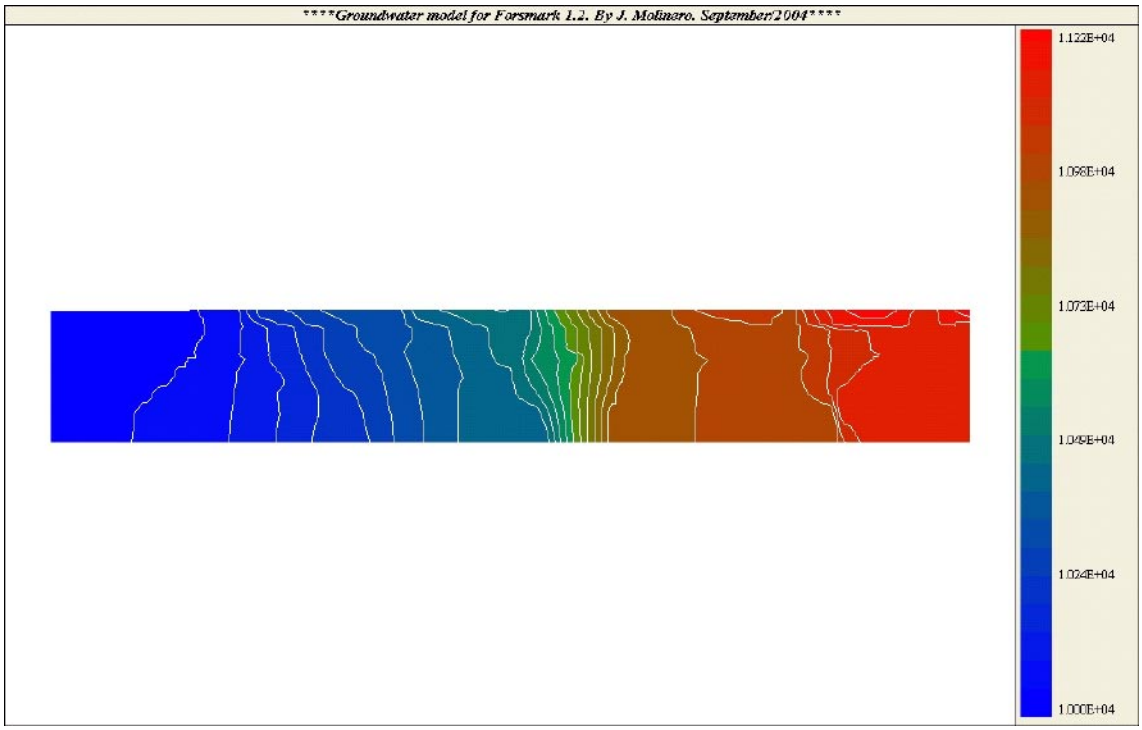

Figure 4-4. *Computed groundwater head distribution with the base run. Computed results are in decimetres. Model parameters and boundary conditions coincide with the conceptual model described in the previous section.*

Then, it can be expected that infiltration of meteoric water during the last 500–1,000 years has been continuously flushing out older and more saline groundwater in the shallow granitic aquifer. The main objective of the present solute transport modelling was to simulate the flushing of saline groundwater by fresh meteoric water.

The simulated situation is ideally simplified for illustrative purposes. A homogeneous field of unity concentration is assumed as initial condition. Then, the groundwater flow and solute transport model was run, using the same parameters and boundary conditions described above. The concentration of recharge water at the top boundary was set equal to 10^{-6}, in order to represent fresh meteoric water. Figure 4-5 shows computed results at 4 simulation times: 6, 42, 100 and 500 years.

Figure 4-5 shows computed results with the conservative transport model. It can be seen that meteoric water penetrates very deep after 500 years of simulated time. As expected, the penetration of meteoric water is still larger along fracture zones, reaching the bottom boundary of the model (1,000 m).

It is worth noting that computed results shown in Figure 4-5 do not reproduce qualitative trends of salinity and mixing fractions determined at Forsmark site, since computed results shows practically 100% of meteoric water reaching up to 500 m depth in the granite. As was shown in Chapter 3, measured salinity of shallow groundwater samples is relatively high. Chloride contents up to 4,000 mg/L have been measured in groundwater samples collected a few meters below the ground surface, and evidences of Littorina water have been detected in several shallow groundwater samples. Then, it can be stated that the current numerical model is overestimating the amount of meteoric water entering through the top boundary.

It can be stated that the hydrogeologic model contains 2 main assumptions which influence the computed depth of meteoric water penetration. On one hand, the effects of water density changes are neglected in the groundwater simulations. On the other hand, it is assumed that granitic bedrock is impervious at a depth of 1,000 m. Figure 4-6 shows groundwater head distribution computed with a new model run, using a different boundary condition on the bottom of the model domain.

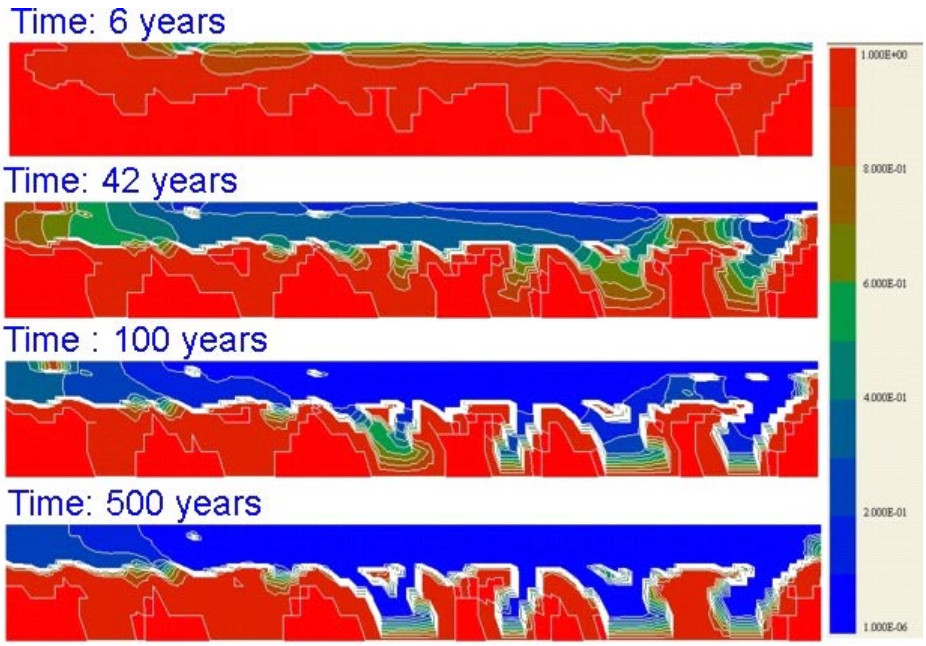

Figure 4-5. *Computed concentrations at: a) 6 years; b) 42 years, c) 100 years, and d) 500 years. After 500 years, meteoric water penetrates up to depths of 500 m in the granite and 1,000 m in fracture zones.*

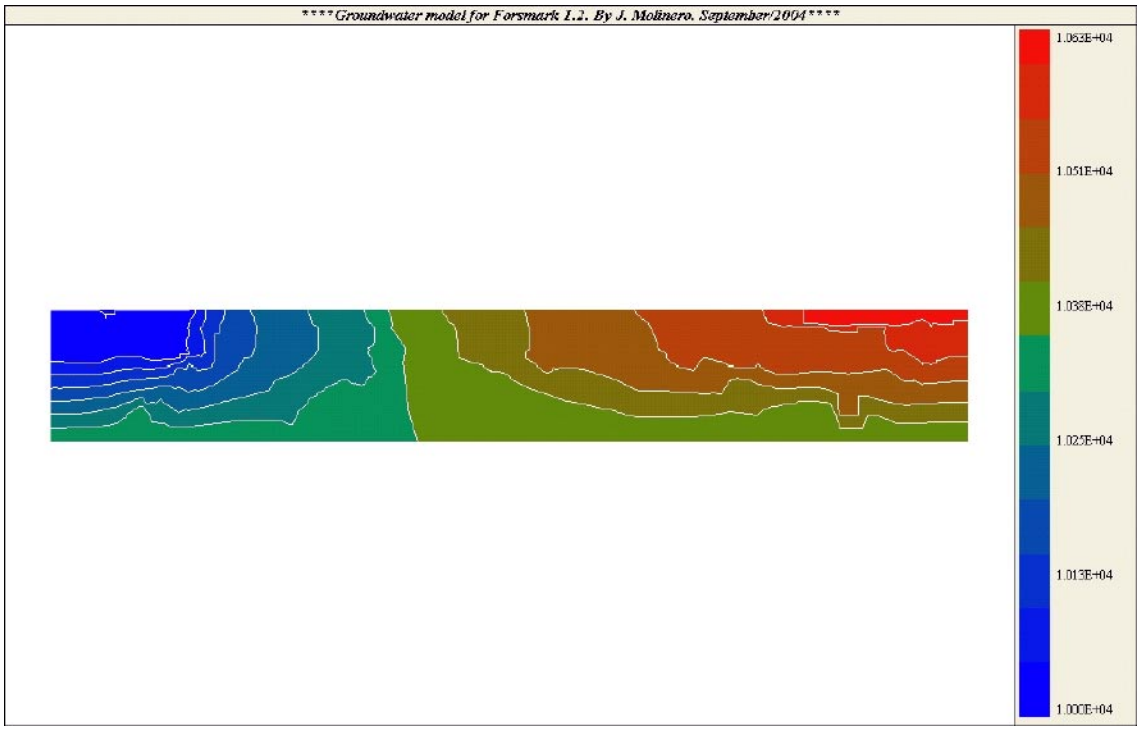

Figure 4-6*. Computed groundwater head distribution using a Dirichlet condition on the bottom boundary. Computed results are in decimetres.*

A Dirichlet-type boundary condition has been prescribed in order to simulate the occurrence of flow lines deeper than 1 km (i.e crossing through the bottom boundary).

Figure 4-7 shows computed results for conservative transport using the "new" bottom boundary condition described above. It can be seen that the depth of meteoric water penetration is also very deep, with almost 100% fresh water at the first 500 m of the granitic bedrock.

The flow rate prescribed in the top boundary of the model is 10 mm/year, which was the same value used in the Simpevarp modelling. Several runs were performed in order to evaluate the sensitivity of model results with respect to recharge flow rate. Figure 4-8 shows computed results using recharge flow rates of 1 mm/year and 2 mm/year, respectively.

Figure 4-8 shows that computed results using lower recharge values on the top boundary are more consistent with measured salinity in Forsmark. As expected, the simulated penetration of meteoric water is much shorter by using a recharge value of 1 mm/year (Figure 4-8a). In this scenario, 100% of meteoric water is only computed at very shallow depths under inland surface close to the water divide (upper-right corner in Figure 4-8a). The rest of shallow granite shows meteoric water proportions between 20% (near the sea) and 100% (Figure 4-8a). Computed results using a recharge value of 2 mm/year shows a little larger penetration of meteoric water into the shallow granite, ranging between 40% close to the sea (upper left in Figure 4-8b) to 100% inland.

According to these model results, it seems that the presence of shallow Littorina signatures at Forsmark could be explained by decreasing recharge flow rates in the granitic top surface. The recharge value should be on the order of 5–10 times shorter than the recharge in other Swedish sites such as Simpevarp, Laxemar or Äspö.

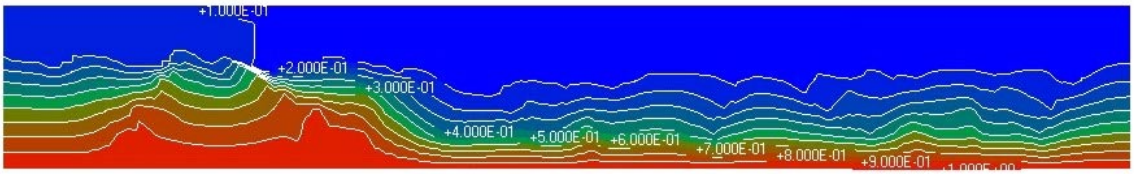

Figure 4-7*. Computed concentrations after 500 years, using the flow field shown in Figure 4-6.*

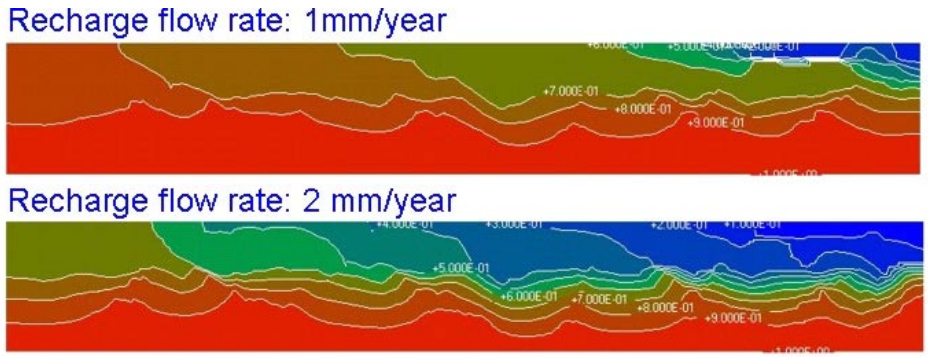

Figure 4-8*. Computed concentrations at 500 years, using different values of recharge flow rate: a) 1 mm/ year; b) 2 mm/year.*

4.3 Tritium transport

Tritium has become a standard tool for the definition and study of modern groundwater systems. The era of thermonuclear bomb testing in the atmosphere (1951–1976), provide the tritium input signal that defines modern water. Due to its natural decay, pre-bomb tritium input cannot be normally detected. Then, tritium-free groundwater is considered "sub-modern" or old water /Clark and Fritz, 1997/. Tritium evolution within the Forsmark aquifer can be simulated as a natural tracer test. The behaviour is not conservative since it is affected by radioactive decay, with a half-life of 12.43 years. In order to set up a model of groundwater flow and tritium transport, the input function of this environmental tracer is needed. There is an excellent time series of tritium levels in precipitation measured at Ottawa, Ontario, which has become a classical reference for hydrogeologists. However, such a good time characterization of rain water is not available in other places. Figure 4-9 shows the Ottawa time series of tritium levels in rain water, as well as discrete values from 4 places in Sweden. All these data have been downloaded from the Isotope Hydrology Information System (the ISOHIS database; http://isohis.iaea.org) provided by the IAEA. It can be seen (Figure 4-9) that, even with relevant latitude difference, the Ottawa time series can be adopted as an appropriate description for atmospheric tritium in Sweden. Figure 4-9 also shows a step-wise function representing a "smoothed" tritium evolution. This step-wise function has been used as the tritium input signal for the numerical model of tritium transport at Forsmark.

Figure 4-10 shows a sketch of the model domain and boundary conditions used for the tritium transport model. The numerical model keeps all the parameters and conditions used in the groundwater flow and conservative transport model described in the previous section. The only difference is that a time-function is linked to the concentration of the recharge water in the upper boundary (Figure 4-10). This time function allows reproducing the tritium input function shown in Figure 4-9.

Initial conditions of tritium contents have been generated by a long-term run of the model, since year 0 to year 1950. Precipitation before 1950 is assumed to have a constant tritium content of 15 TU.

Figure 4-11 shows a comparison of computed tritium contents (at simulated year 2004) using different recharge values on the top boundary. As expected, computed tritium concentrations are also highly sensitive to variations on the recharge flow rate prescribed in the top of the granite.

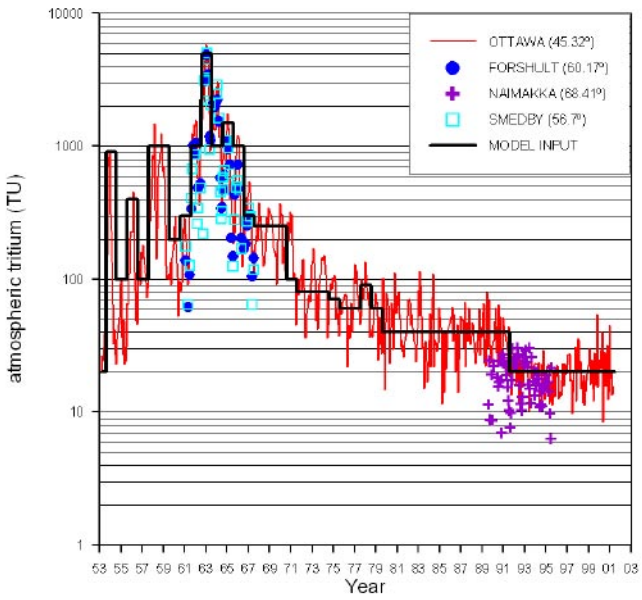

Figure 4-9. *Evolution of atmospheric tritium at Ottawa and 4 locations in Sweden (data from the ISOHIS database, /IAEA, 2001/). Step-wise function used as the model input signal is shown in solid black line.*

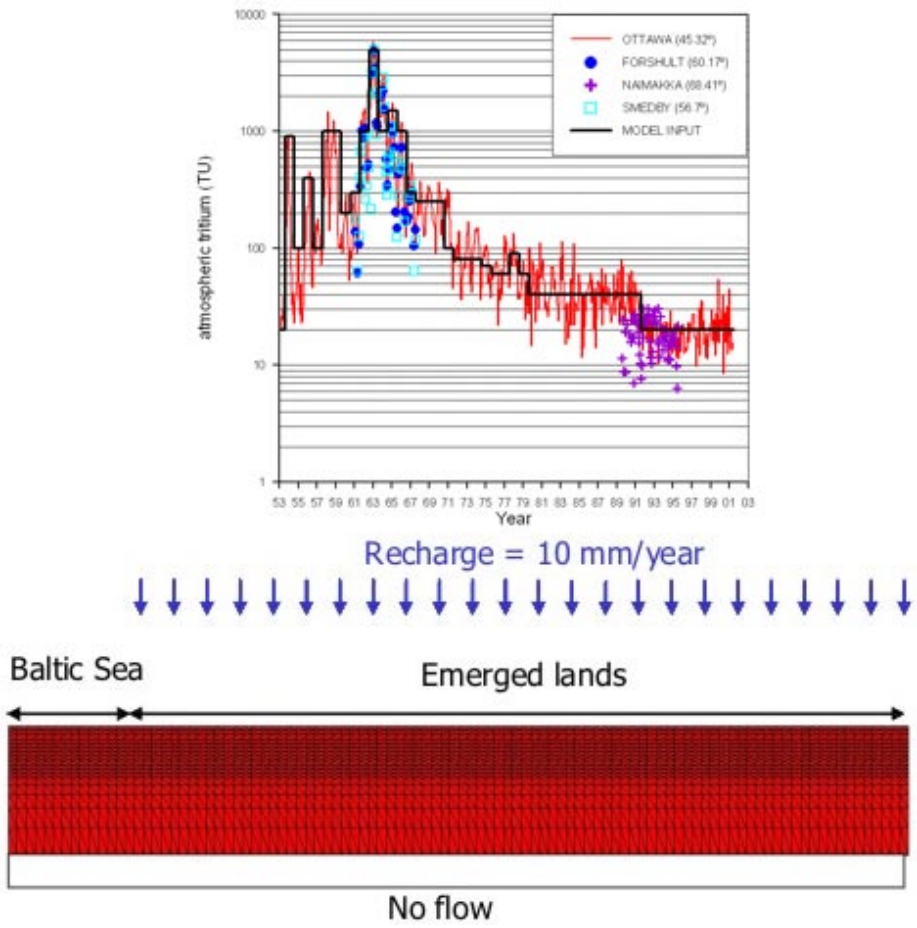

Figure 4-10. *Sketch of the boundary condition used to represent the input of tritium in the model.*

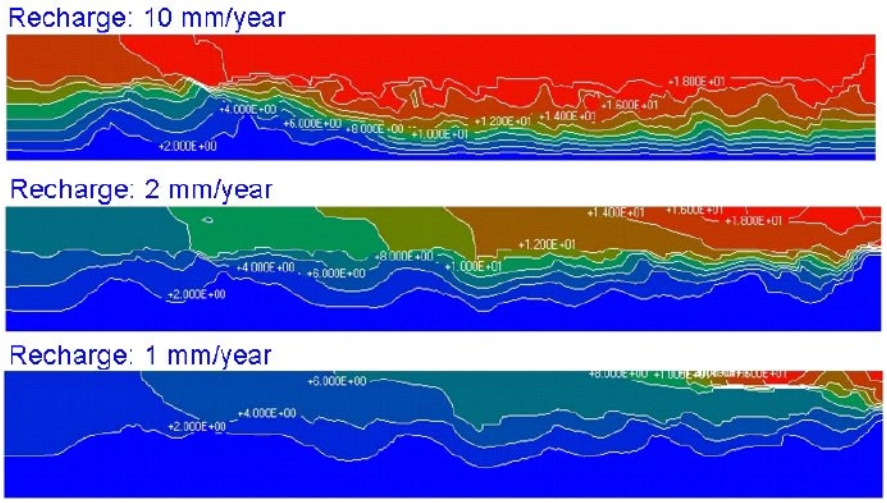

Figure 4-11. *Computed tritium concentrations (simulated year 2004) using different values of recharge flow rate: a) 10 mm/year, b) 2 mm/year, and c) 1 mm/year.*

Computed tritium contents are consistent with previously computed results of salinity. Using a recharge flow rate of 10 mm/year leads to a large penetration of meteoric water with high tritium contents. In this case, almost the first 500 m of the model domain contain water with 18–20 TU (Figure 4-11a). It has been already shown that this is not the case of shallow groundwater in Forsmark, where most of the water samples collected in the first 100 m have tritium contents in the range from 2 to 8 TU. It is worth noting that computed tritium contents in the shallow granite (in the equivalent positions to Forsmark site) are in the range from 6 to 14 TU when a recharge flow rate of 2 mm/year is prescribed (Figure 4-11b). Finally, it can be seen that using a recharge value of 1 mm/year leads to computed tritium contents in the range from 2 to 10 TU.

In summary, both measured salinity and tritium contents could be "qualitatively" reproduced only by reducing the effective recharge flow rate on the upper boundary of the model. Computed results suggest that effective recharge flow rates on the upper granitic surface of Forsmark could be much shorter than expected. The "calibrated" effective recharge is as low as 1–2 mm/year. Water recharge into the granitic bedrock is specifically analysed and modelled in the next Chapter.

5 Modelling water recharge into the bedrock

5.1 Conceptual model and hypotheses

The main objective of this chapter is to analyse the effective water recharge actually reaching the upper surface of the granitic bedrock in Forsmark. As pointed in the previous chapter, initial numerical modelling of groundwater flow and solute transport failed at reproducing (qualitatively) measured trend of salinity and tritium. It has been found that it is needed to decrease the initial guess of recharge flow rate in order to compute consistent meteoric water penetration into the bedrock. This initial guess of recharge was the same value used in Simpevarp, which at the same time was based on available knowledge of Laxemar and Äspö.

Then, the first step was trying to find a plausible explanation to support a lower effective recharge in Forsmark than in Laxemar or Äspö granitic bedrock. The magnitude of groundwater recharge into aquifers depends on several factors. Recharge is assumed to be the result of a water budget from the total precipitation to the final amount of water actually reaching the aquifer. Several methodologies have been developed for groundwater recharge evaluation ranging from either classical or more sophisticated water budget models to pure chemical mass balance of conservative tracers.

There is no major difference in mean annual precipitation between Forsmark and Laxemar areas, neither in mean annual temperature. Both parameters are relatively homogeneous in the south half of the Swedish Baltic Coast. Then, net precipitation (i.e. total precipitation minus actual evapotranspiration) should be also similar. This consideration has been written in the SDM v1.1 reports of both sites /SKB, 2004a,b/. These reports estimate that annual net precipitation is about 200 mm/year in both sites.

Other relevant factor affecting the groundwater recharge is the topography. High slopes usually favour run-off and the consequent decrease of infiltration and aquifer recharge. By the contrary, flat terrains usually favour the increase of groundwater recharge. In the case of Forsmark and Laxemar/Simpevarp, both sites are characterised by flat topography in general. It seems that Forsmark topography is even flatter than Simpevarp, which do not help to explain a shorter recharge flow rate value in Forsmark.

Finally, groundwater recharge also depends strongly on the nature (thickness, permeability, etc) and use (forest, agricultural, urban etc) of the soil cover and/or overburden units over the aquifer. Figure 5-1 shows the maps of Quaternary deposits in Forsmark.

Looking at Figure 5-1 it can be noticed that Quaternary deposits are very extensive in Forsmark. According to Forsmark SDM v1.1 report /SKB, 2004a/ Quaternary deposits occupy 82% of the land area. By the contrary, in the case of Simpevarp only 29% of the land area is cover by Quaternary deposits /SKB, 2004b/. Then, the bedrock in Forsmark is naturally covered by Quaternary layers. Then, a plausible working hypothesis is that Quaternary deposits in Forsmark could be preventing (limiting) meteoric water penetration into the bedrock, thus allowing the permanence of older groundwater at shallow depths in the bedrock (such as Littorina water).

Reported thickness of the Quaternary deposits in Forsmark varied between 20 and 0 m. From a stratigraphic point of view the Quaternary deposits consists of two main components:

1. Glacial deposits which were deposited either directly from the inland ice or from the water derived from the melting. This deposits include till, glaciofluvial sand and gravel, and varved glacial clay.
2. Post-glacial deposits which were formed after the ice had melted and retreated from the area. These deposits include sand, clay and organic deposits such as peat and gyttja.

Figure 5-2 shows two details of Quaternary deposits at Forsmark /SKB, 2004a/.

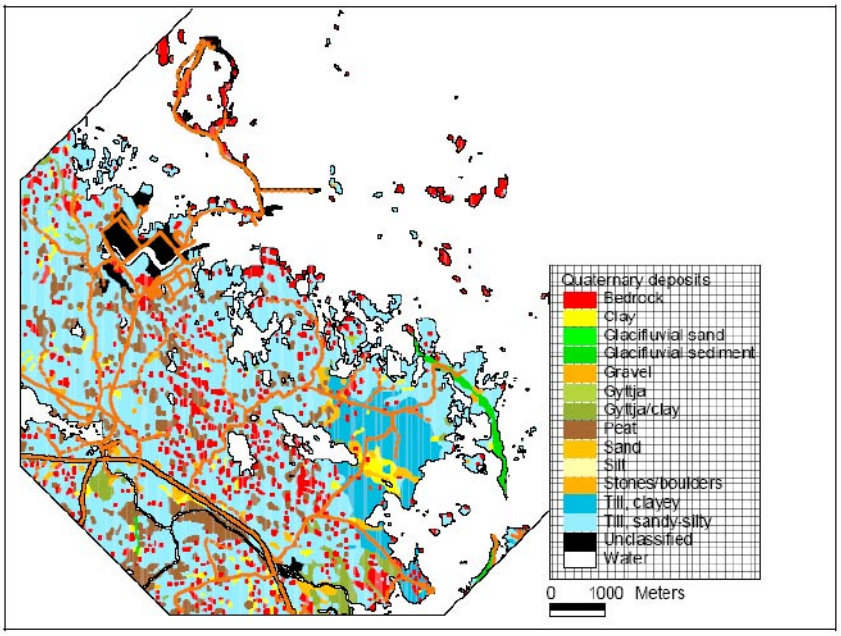

Figure 5-1. *Maps showing the distribution of Quaternary deposits in Forsmark. Red colour indicates areas with direct outcrop of bedrock or quaternary thickness less than 0.5 m. Other colours indicate different units of well developed Quaternary sediments. (Taken from TR-04-08).*

Figure 5-2. *Details of Quaternary deposits at Forsmark outcrops /from SKB, 2004a/.*

With respect to the hydrogeologic behaviour of the Quaternary deposits, it is known that groundwater levels in the soil pipes (i.e. mainly crossing the Quaternary deposits) are very shallow. Usually groundwater levels are less than 3 m deep in recharge areas and less than 1 m deep in discharge areas. Also based on the current knowledge it seems reasonable to work with a conceptual 3-layer model of the Quaternary /SKB, 2004a/: (1) an upper layer with a hydraulic conductivity of 10^{-5}–10^{-4} m/s, (2) a second layer down to approximately 1 m above the bedrock contact with a hydraulic conductivity of 10^{-8}–10^{-6} m/s, and (3) a third layer down to the bedrock with a hydraulic conductivity of 10^{-8}–10^{-4} m/s (with a geometric mean value of 1.18×10^{-5} m/s).

According to /SKB, 2004a/ the groundwater recharge over the Quaternary can be set equal to net precipitation (200 mm/year, approx.). Saturated overland flow appears in discharge areas where the groundwater level reaches the ground level. Figure 5-3 shows a sketch of the conceptual model of groundwater flow through the Quaternary deposits.

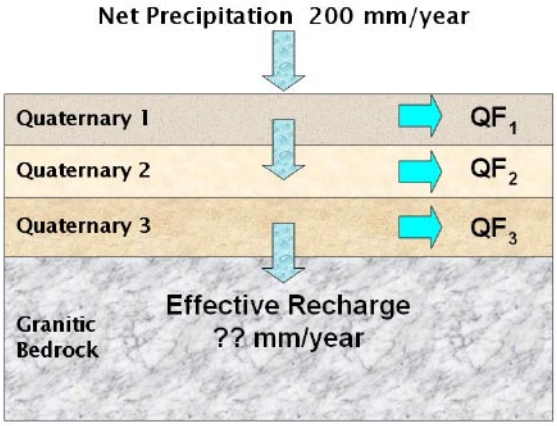

Figure 5-3. *Conceptual model of the hydrogeologic behaviour of the Quaternary deposits overlying the granitic bedrock at Forsmark.*

5.2 Numerical modelling of groundwater flow through the Quaternary deposits

A groundwater flow numerical model has been performed in order to evaluate the effective recharge into the granitic bedrock. The numerical model is based on the conceptual model, parameters and hypotheses shown in the previous section.

The model domain consists on a 2D profile from a local topographic maximum to a local discharge area (lake, swamp or estuary). The total length of the domain has been set equal to 1 km. 3 layers has been used to represent the Quaternary deposits: (a) layer #1 from 0 to 2 m depth with a hydraulic conductivity of 5×10^{-5} m/s, (b) layer #2 from 2 to 8 m depth with a hydraulic conductivity of 10^{-7} m/s and, (c) layer #3 from 8 to 10 m depth with a hydraulic conductivity of 10^{-5} m/s. Down to the bottom of the Quaternary, the granitic bedrock is assumed to extend to a total depth of 100 m, with a constant hydraulic conductivity of 10^{-8} m/s (the average order of magnitude found in Forsmark boreholes at a depth of 0–100 m).

The model domain has been discretized by means of quadrangular finite elements. Figure 5-4 shows a view of the finite element mesh and the material zones used for parameterization.

The numerical solver used for flow simulations was SUTRA /Voss, 1984/. This code solves for saturated-unsaturated, fluid-density-dependent ground-water flow with energy or solute transport. Source files and several documentation of the code is distributed by USGS (http://water.usgs.gov/software/sutra.html).

Boundary conditions include: (1) no flow (Neumann type) at the lateral and bottom boundaries, (2) prescribed flow rate recharge (Neumann type) of 200 mm/year at the recharge zone (900 m of the total length), and (3) prescribed head (Dirichlet type) of 0 m.a.s.l. at the discharge zone (100 m at the upper-left side of the domain).

Figure 5-5 shows computed groundwater velocities with the base run of the model.

It can be seen in Figure 5-5 that groundwater flows from the emerged land (recharge area) to the discharge zone in the upper-left boundary. Most of the water flows through the first and third layers of the Quaternary deposits (Figure 5-5). Down to the interface between Quaternary and granitic bedrock groundwater velocities are very small, indicating that effective recharge into the granite must be also very low.

Computed water budget shows that the total amount of water crossing through the Quaternary – bedrock interface is only 1 mm/year. The rest of the infiltrated water circulates through the Quaternary deposits. Figure 5-6 illustrates the water budget computed with the numerical model. It is worth remarking that these results have been computed using average hydraulic conductivity values reported in SDM v1.1 /SKB, 2004a/.

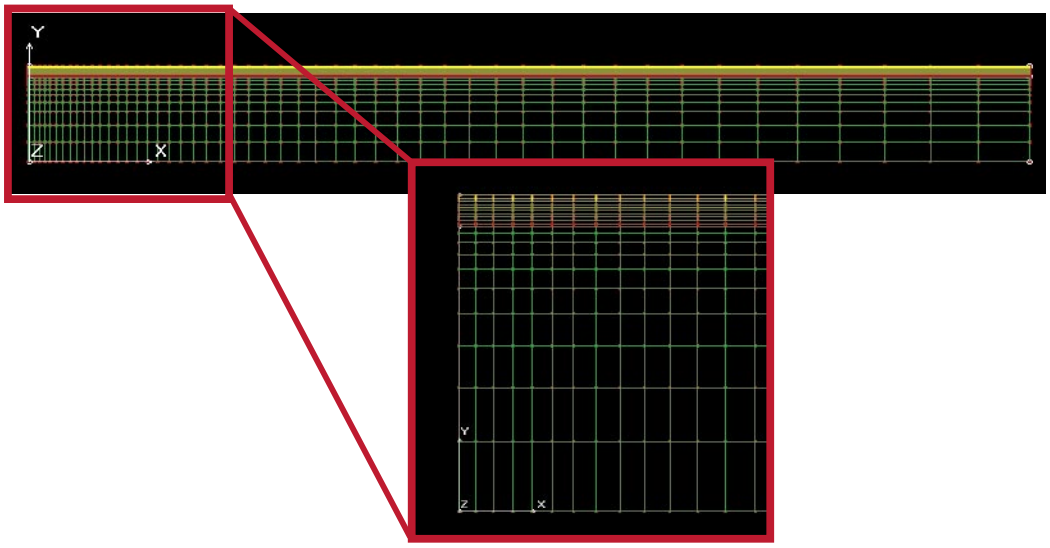

Figure 5-4. *Finite elements mesh used for numerical modelling of groundwater flow through the Quaternary deposits.*

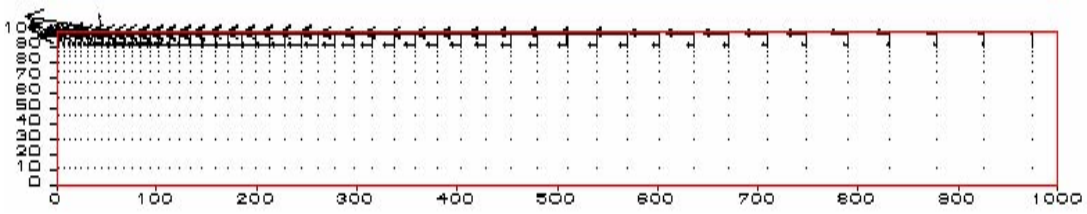

Figure 5-5. *Groundwater velocity field computed with the base run of the numerical model.*

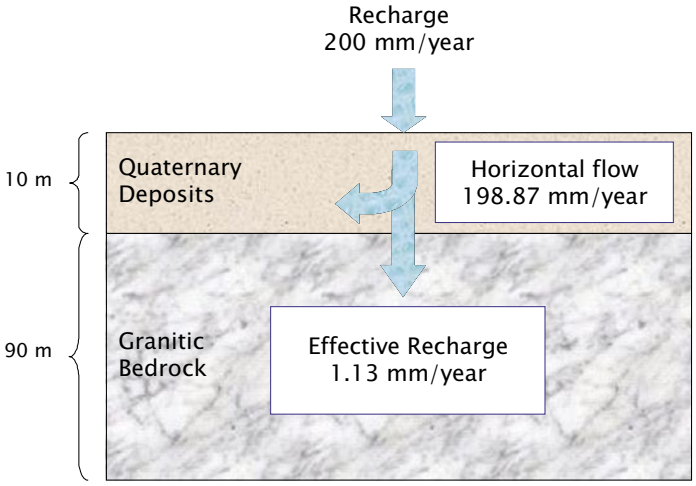

Figure 5-6. *Water budget computed with the base run (mean K-values of soil layers) of the numerical model. Computed effective recharge into the bedrock is only 1 mm/year.*

Computed results shown in Figures 5-5 and 5-6 provide quantitative support to the hypothesis of having a very small effective recharge at Forsmark. Then, it is thought that the Quaternary deposits of Forsmark are playing a very important hydrogeologic role, by limiting the amount of meteoric water penetration, and thus limiting the flushing of older groundwater in the shallow bedrock. This hypothesis provides a plausible explanation for the permanence of Littorina signatures which have been found in several Forsmark groundwater samples, even at very shallow depths.

6 Conclusions

Based on the current knowledge, a preliminary hydrogeologic conceptual model of the shallow groundwater system in Forsmark is proposed.

Well developed Quaternary deposits occupy more than 80% of the emerged lands in Forsmark. These Quaternary deposits can be conceptualized as a 3-layer hydrogeologic domain, with the first and third layer being highly conductive. Quaternary sediments may play a significant role since most of the infiltrated water could flow through the conductive layers to discharge zones, mainly located al lakes and the Baltic coast line. With this hypothesis, the effective recharge into the granitic bedrock is estimated to be shorter than in other investigated sites such as Simpevarp and Laxemar, where the presence of Quaternary overburden is less important.

Based on numerical modelling, and using average values of reported hydraulic conductivity, effective recharge actually reaching the granitic bedrock has been estimated to be on the order of 1 mm/year. By using this recharge flow rate, meteoric water penetration and tritium contents can be qualitatively reproduced in larger-scale numerical models.

The hydrogeologic behaviour of the Quaternary overburden in Forsmark provides a plausible explanation for the evidences of Littorina signatures found in several groundwater samples, even at very shallow depths. Other (and complementary) explanations can be related with the flat topography, as well as with the fact that the Forsmark site has emerged over the sea level more recently than other investigated sites.

Contrarily to what was observed at Simpevarp, near-surface groundwater in Forsmark is at saturation, even over-saturated, with respect to calcite. This provides additional support to the hydrogeologic role of the Quaternary sediments, where large amounts of calcite have been reported (up to 20%).

Hydrochemical and isotopic patterns observed in soil pipe samples are consistent with field data of phreatic level. Water samples collected in recharge zones (with the highest phreatic levels) are Ca-HCO_3 type, show high tritium and low $\delta^{18}O$ values, compared to water samples collected at discharge zones. The latter are Na-HCO_3, Cl type and show lower tritium contents and higher $\delta^{18}O$ values. ^{14}C data are also consistent with this trend, with the highest pmC values in the recharge zones and the lowest in the discharge zones. However, hydrochemical and isotopic differences have been detected between the presumed discharge zones.

Shallow groundwater under Bolundsfjärden shows the highest salinity (4,000 mg/L of Cl^-, approx.) and low tritium values (2 TU, approx.). Whether this indicates the discharge of deeper groundwater should be further investigated. Other explanations are possible such as the presence of "trapped" relict water not yet flushed out (due to low permeability bedrock, quasi-stagnant water pockets, etc).

The rest of the presumably discharge zones seems to display along a theoretical mixing line between Littorina and recent-fresh groundwater. The most relevant ones are a small lake (SFM12), soil pipes under the Baltic Sea (SFM15 and 24) and other soil pipes at (or close to) topographical minima. The convergence of both very local (shallow) and deeper flow lines, in different proportions of flow rates, could explain the different degree of apparent mixing. Again, other explanations are possible and should be investigated in future stages of the S.I. programme.

Eckarfjärden has been also identified as a groundwater discharge zone. However, hydrochemical and isotopic signatures show significant differences compared to the rest of the discharge zones. Groundwater under this lake is diluted and has relatively low tritium values (3–5 TU) but, according to $\delta^{18}O$-Cl plot, this shallow groundwater is the only one which seems to be out of the theoretical mixing line with Littorina water. It is interesting that this lake is the one located more distant to the coast and close to a pronounced topographical slope-change. The absence of information inland makes difficult to establish reliable hypotheses to explain the hydrochemistry of this discharge zone.

Down to the Quaternary-bedrock interface groundwater is more saline, with maximum values of about 5,000 mg/L which coincide in the same area than brackish water in the Quaternary soil pipes, pointing towards the occurrence of deep groundwater discharge in these areas. On the other hand, some local recharge areas of the near-surface groundwater system (Quaternary) are not clearly reflected in the hydrochemical signatures of shallow bedrock groundwater.

7 References

Banwart S, Gustafsson E, Laaksoharju M, 1999. Hydrological and reactive processes during rapid recharge to fracture zones. The Äspö large scale redox experiment. App. Geoch. 14, 873–892.

Clark I, Fritz P, 1997. Environmental Isotopes in Hydrogeology. Lewis Publishers. Boca Raton, Florida. 328 pp.

Ehlers J, 1996. Quaternary and glacial geology. John Willey & Sons. New York. 578 pp.

Gimeno M J, Auqué L, Gómez L, 2004. Explorative analyses and mass balance modelling. In: Hydrochemical evaluation of the Forsmark site, model version 1.1. Appendix 2. SKB R-04-05, Svensk Kärnbränslehantering AB.

Gurban I, Laaksoharju M, 2004. Explorative análisis, M3 calculations and DIS modelling. In: Hydrochemical evaluation of the Forsmark site, model version 1.1. Appendix 3. SKB R-04-05, Svensk Kärnbränslehantering AB.

IAEA, 2001. Isotope Hydrology Information System. The ISOHIS database. http://isohis.iaea.org

Laaksoharju M, Wallin B, 1997. Evolution of the groundwater chemistry at the Äspö Hard Rock Laboratory. Proceedings of the second Äspö International Geochemistry Workshop, June 6–7, 1995. SKB, International Cooperation Report 97-04, Svensk Kärnbränslehantering AB.

Laaksoharju M, 1999. Groundwater characterisation and modelling: problems, facts and possibilities. Ph.D. dissertation. Department of Civil and Environmental Engineering. Royal Institute of Technology (KTH) Stockholm.

Laaksoharju M, Tullborg E-L, Wikberg P, Wallin B, Smellie J, 1999a. Hydrogeochemical conditions and evolution at the Äspö HRL, Sweeden. App. Geoch. 14, 835–860.

Laaksoharju M, Skarman C, Skarman E, 1999b. Multivariate mixing and mass balance (M3) calculations, a new tool for decoding hydrogeochemical information. App. Geoch. 14, 861–872.

Laaksoharju, 2004. s 367 (2 ggr), 368 (bildtext), 382, 384

Laaksoharju M (ed), Smellie J, Gimeno M J, Auqué L, Gómez L, Tullborg E-L, Gurban I, 2004. Hydrogeochemical evaluation of the Forsmark site, model version 1.1. SKB R-04-05, Svensk Kärnbränslehantering AB.

Molinero J, Samper J, Juanes R, 2002. Numerical modeling of the transient hydrogeological response produced by tunnel construction in fractured bedrocks. Engineering Geology, 64, 369–386.

Molinero J, Samper J, 2004. Modeling Groundwater Flow and Solute Transport in Fracture Zones: Conceptual and Numerical Models of the Redox Zone Experiment at Äspö (Sweden). Journal of Hydraulic Research, 42, 157–172.

Molinero J, Raposo J, 2004. Coupled hydrogeological and reactive transport model. In: Hydrochemical evaluation of the Simpevarp area, version 1.2. In progress.

Rhén I, Gustafson G, Stanfors R, Wikberg P, 1997. Models based on site characterization 1986–1995. SKB TR 97-06, Svensk Kärnbränslehantering AB.

Samper J, Delgado J, Juncosa R, Montenegro L, 2000. CORE^{2D} v 2.0: A Code for non-isothermal water flow and reactive solute transport. User's manual.ENRESA Technical report 06/2000.

SKB, 2002. Simpevarp – site descriptive model version 0. SKB R-02-35, Svensk Kärnbränslehantering AB.

SKB, 2004a. Preliminary site description. Forsmark area – version 1.1. SKB R-04-15, Svensk Kärnbränslehantering AB.

SKB, 2004b. Simpevarp – site descriptive model v 1.1 (Draft provided by M. Laaksoharju). Svensk Kärnbränslehantering AB.

Smellie J, Tullborg E-L, 2004. Explorative analysis, expert judgement and modelling. In: Hydrochemical evaluation of the Forsmark site, model version 1.1. Appendix 1. SKB R-04-05, Svensk Kärnbränslehantering AB.

SRAC – Structural Research and Analysis Corporation, 1998. COSMOS/M. A Complete Finite Element Analysis System. USER'S GUIDE.

Voss C I, 1984. SUTRA – A finite element simulation model for saturated-unsaturated fluid density dependent groundwater flow with energy transport or chemically reactive single species solute transport, USGS Water Resources Investigation Report, 84-4269.

Appendix 6

Groundwater data from Forsmark

For data, please see the attached CD!

Appendix 7

Groundwater data from Nordic sites

For data, please see the attached CD!

Appendix 8

The use of the data in the modelling work

For information, please see the attached CD!